PNL-10821
UC-510

Screening the Hanford Tanks for Trapped Gas

Paul Whitney

October 1995

Prepared for the U.S. Department of Energy
under Contract DE-AC06-76RLO 1830

Pacific Northwest Laboratory
Richland, Washington 99352

DISCLAIMER

PACIFIC NORTHWEST LABORATORY
operated by
BATTELLE MEMORIAL INSTITUTE
for the
UNITED STATES DEPARTMENT OF ENERGY
under Contract DE-AC06-76RLO 1830

DISCLAIMER

Portions of this document may be illegible in electronic image products. Images are produced from the best available original document.

Summary

The Hanford Site is home to 177 large, underground nuclear waste storage tanks. Hydrogen gas is generated within the waste in these tanks. The flammable gas watch list of tanks with potential for hydrogen or other flammable gas accumulation currently includes 25 of the 177 tanks.

This document presents the results of a screening of Hanford's nuclear waste storage tanks for the presence of gas trapped in the waste. The method used for the screening is to look for an inverse correlation between waste level measurements and ambient atmospheric pressure. If the waste level in a tank decreases with an increase in ambient atmospheric pressure, then the compressibility may be attributed to gas trapped within the waste. In this report, this methodology is not used to estimate the volume of gas trapped in the waste.

The waste level measurements used in this study were made primarily to monitor the tanks for leaks and intrusions. Four measurement devices are widely used in these tanks. Three of these measure the level of the waste surface. The remaining device measures from within a well embedded in the waste, thereby monitoring the liquid level even if the liquid level is below a dry waste crust.

In the past, a steady rise in waste level has been taken as an indicator of trapped gas. This indicator is not part of the screening calculation described in this report; however, a possible explanation for the rise is given by the mathematical relation between atmospheric pressure and waste level used to support the screening calculation.

The screening was applied to data from each measurement device in each tank. If any of these data for a single tank indicated trapped gas, that tank was flagged by this screening process. A total of 58 of the 177 Hanford tanks were flagged as containing trapped gas, including 21 of the 25 tanks currently on the flammable gas watch list.

Acronyms and Abbreviations

AP	Atmospheric pressure
CASS	Computer Automated Surveillance System
CI	Confidence interval
DLM	Dynamic linear model
DWL	Detrended waste level
ENRAF	ENRAF 854 ATG level detector manufactured by ENRAF Incorporated
FIC	Tank waste surface level gauge made by the Food Instrument Company
ILL	Interstitial liquid level
MT	Manual tape, a tank waste surface level gauge
Neutron ILL	Interstitial liquid level measurement based on neutron loggings taken within the tank waste
SACS	Surveillance Analysis Computer System, the database in which the tank waste level data are stored
WL	Waste level; tank waste surface level, as well as tank waste liquid level

Contents

Figures

Tables

1 Introduction

The Hanford Site is home to 177 large, underground nuclear waste storage tanks. Numerous safety and environmental concerns relate to these tanks; one safety concern is the propensity for some of the tanks to generate and periodically release flammable gases in quantities sufficient to ignite the tank headspace. Currently, 25 of the 177 tanks are believed to have this potential and are listed on the flammable gas watch list. Hanlon (1994) lists these tanks and provides general information about the Hanford tanks. Hopkins (1994) provides more details about the issue of flammable gas in the Hanford waste tanks.

This report documents a screening of all 177 Hanford tanks for the existence of trapped gas, using tank waste level data and local weather data. In this report, the term "trapped gas" refers to gas phase material within the tank waste. The method used is to look for an inverse correlation between waste level measurements and ambient atmospheric pressure. If the waste level in a tank decreases with an increase in ambient atmospheric pressure, then the compressibility may be attributed to gas trapped within the waste. In this report, this methodology is not used to estimate the volume of gas trapped in the waste.

The data used for the screening were all the tank waste level data available in the Surveillance Analysis Computer System (SACS) database since 1981, along with atmospheric pressure data available over the same time span from the Hanford Meteorological Station. The waste level measurements were made primarily to monitor the tanks for leaks and intrusions.

The general approach to the screening is described in Section 2. Section 3 summarizes the types and amounts of available data on tank waste level and atmospheric pressure. This description includes more details about the measurements and a table showing the quantity of each type of data for each tank. Section 4 describes the screening methodology, both computationally and in a model that explains how the quantity being calculated is related to trapped gas. Section 5 presents the results of the screening calculation. The key summaries of the screening calculation are Table 2, which appears in Section 5, and the summary plots of the data for each tank and level measuring instrument, which are collected in the appendix.

2 Approach

Similarities observed in the fluctuations of waste level measurements for tanks, even when the tanks are in different farms, were the impetus for the search for an external, common cause. Whitney documents that the common fluctuations in waste level are related to changes in atmospheric pressure (AP).[1] The relationship between tank waste level and headspace pressure was also observed for Tank SY–101, and used to estimate the amount of gas contained in that tank's waste (Allemann et al. 1994). The expected relationship is that increased pressure compresses the gas in the waste, thereby decreasing the waste level.

Figure 1 exhibits how tank waste level (WL) and atmospheric pressure are related in Tank S–102, a tank on the flammable gas watch list. The figure shows two months of daily surface level measurements. During this time, the waste level was rising. The fluctuations in waste level visibly track the fluctuations in reciprocal atmospheric pressure. Figure 2 is similar, but instead of comparing waste level with atmospheric pressure, compares atmospheric pressure with the residuals from a linear fit to waste level versus time. The residuals from a linear fit of waste level to time are referred to in this report as "detrended waste level" (DWL). The correspondence between the detrended waste level and reciprocal atmospheric pressure shown in the figure is remarkable. This relationship between detrended waste level and atmospheric pressure is the basis for the screening of Hanford tanks for trapped gas, as presented in this report. Figure 3 shows the same data as Figure 2; the time order is ignored, and the paired measurements, detrended waste level and atmospheric pressure, are plotted. Linear fits such as the one shown in this plot are used to indicate trapped gas. In particular, the slope of the line is an estimate of the derivative $d\mathrm{DWL}/d\mathrm{AP}$, the size of the response of waste level to changes in atmospheric pressure. The quantity $d\mathrm{DWL}/d\mathrm{AP}$ is directly related to the amount of gas in the tank waste, as shown by Equations (5) and (7) in Section 4.2.1.

An earlier screening[1] failed to detect trapped gas in Tank SY–101, a tank viewed as the worst case of all the tanks on the flammable gas watch list. Two reasons for this failure were 1) the rise in level due to the increased volume of trapped gas masked the relation between surface level (as opposed to detrended surface level) and atmospheric pressure; and 2) the large jumps in liquid level in this tank, due to gas releases, also masked the relation between surface level and atmospheric pressure. The first problem is handled in this report by using detrended surface level data instead of the raw surface level data. The second problem is addressed in this report by using an algorithm called the multi-state dynamic linear model (DLM) to detect large changes in the tank level measurements. This algorithm and other steps in preprocessing the level data are described in Section 4.

[1] Whitney, P. 1994. *Preliminary Study of the Relationship Between Atmospheric Pressure and Surface Level in Hanford Tanks.* Letter report to Westinghouse Hanford Company from Pacific Northwest Laboratory.

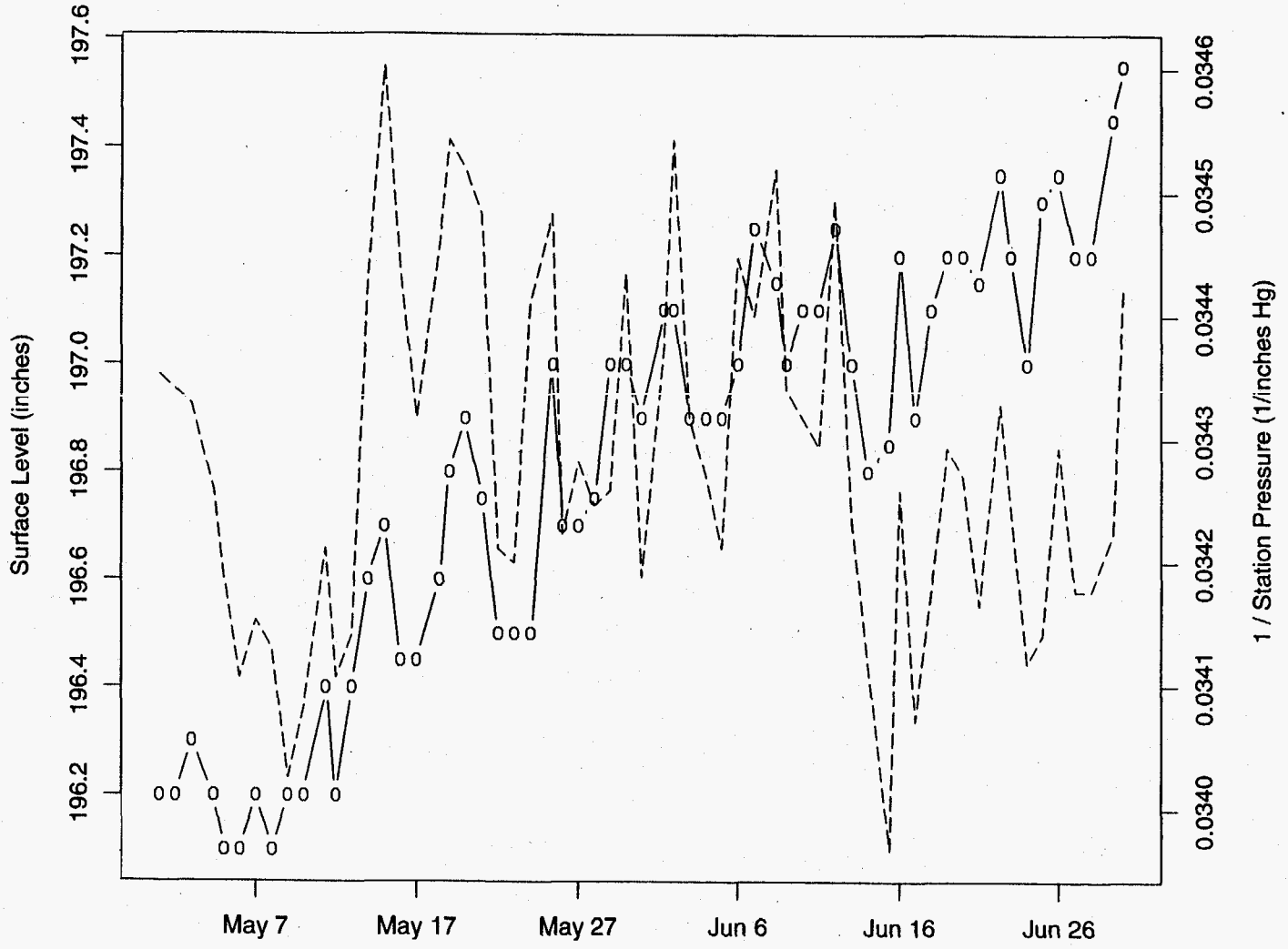

Figure 1: Tank waste surface level compared with atmospheric pressure for Tank S–102 for two months in 1981. The circles mark FIC surface level measurements; the dashed line traces reciprocal atmospheric pressure, sampled at the same time as the FIC measurement.

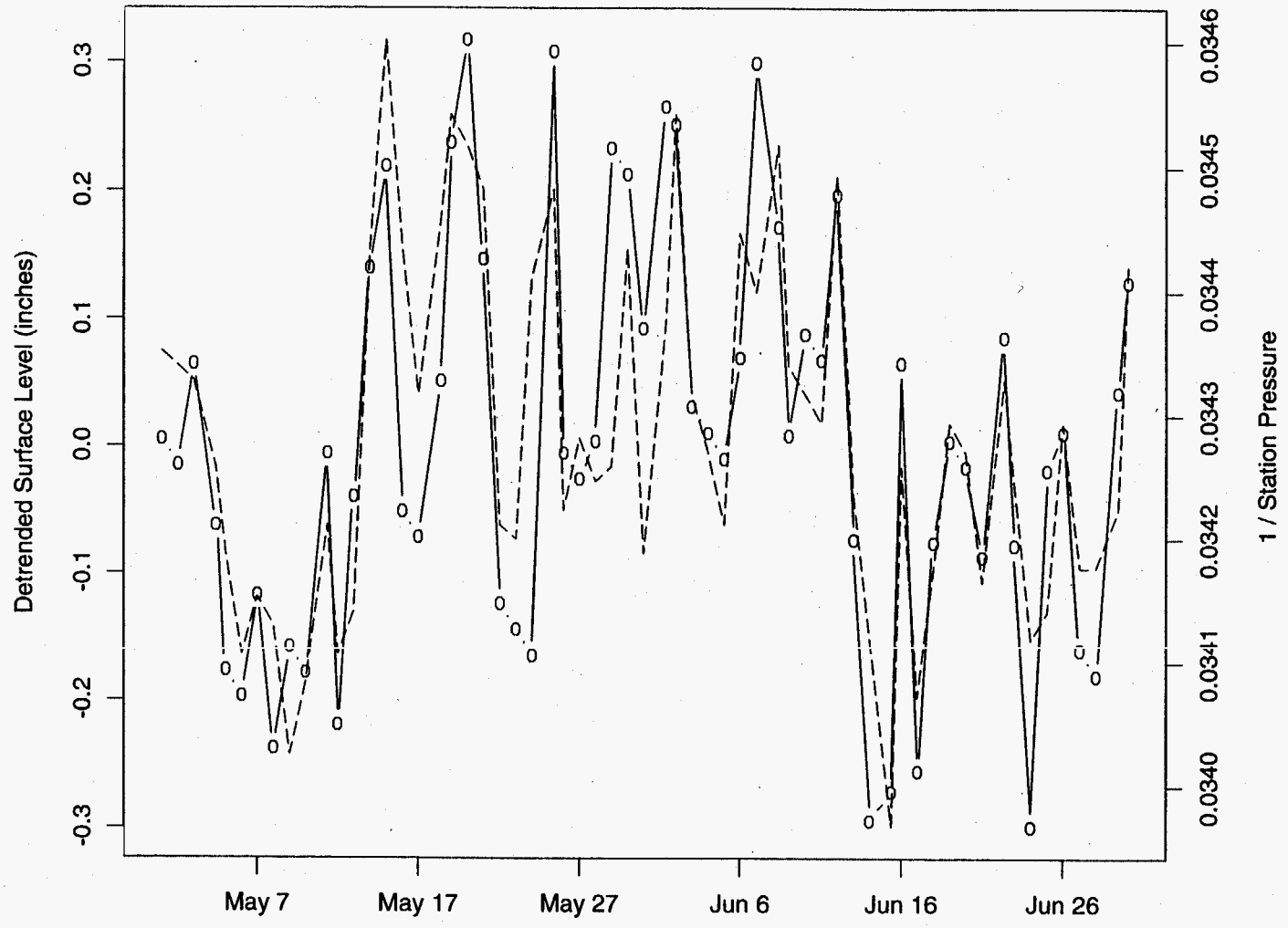

Figure 2: Detrended tank waste surface level compared with atmospheric pressure for Tank S–102 for two months in 1981. The circles mark detrended FIC surface level measurements; the dashed line traces reciprocal atmospheric pressure, sampled at the same time as the FIC measurements.

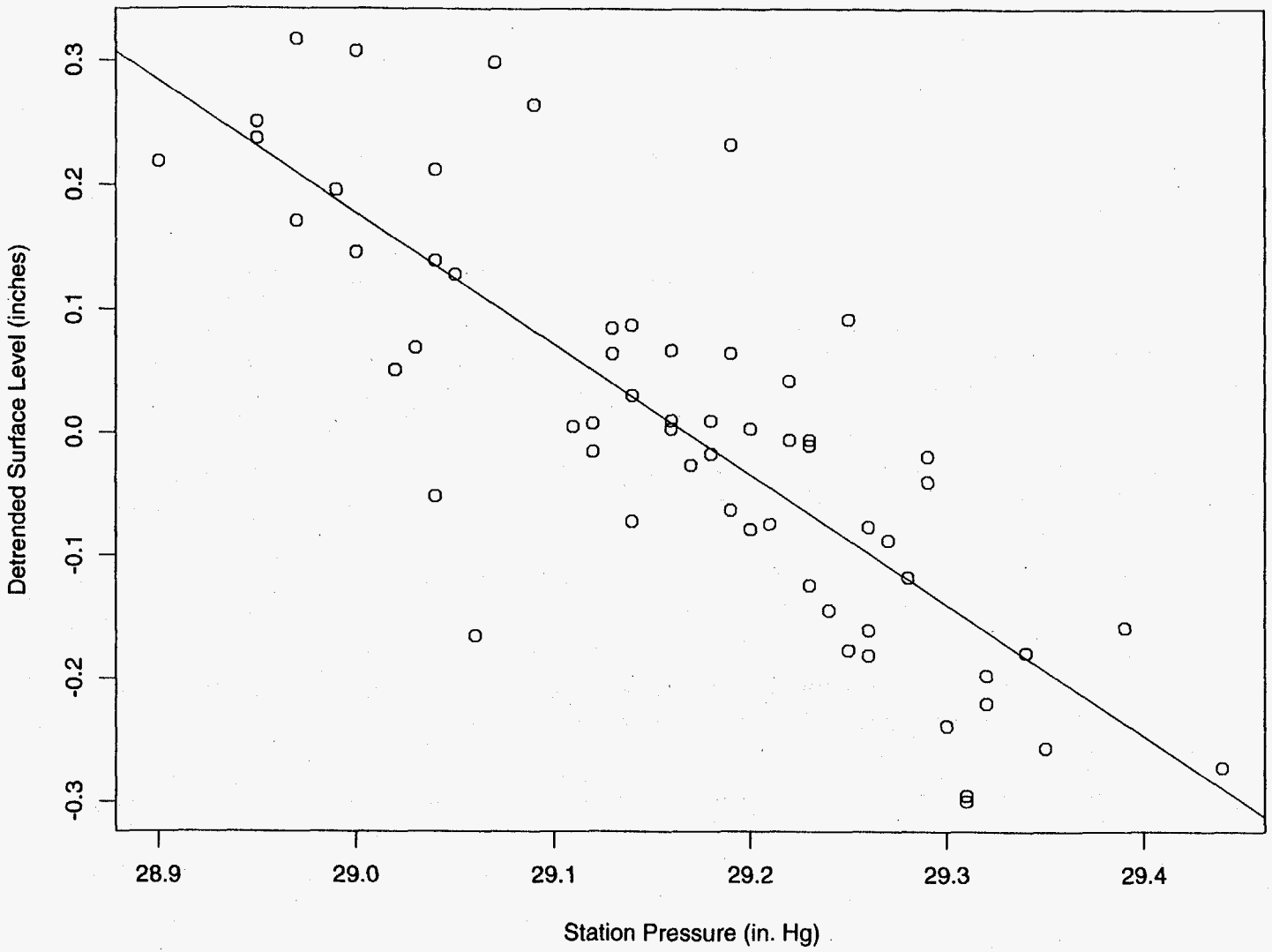

Figure 3: Detrended tank waste surface level versus atmospheric pressure for Tank S–102. The data in this plot are the same as shown in Figure 2. The line on the plot is a linear least squares fit of detrended tank waste surface level to atmospheric pressure. The slope of the linear fit, estimated $d\mathrm{DWL}/d\mathrm{AP}$, is the quantitative basis for the screening described in this report.

3 Data

Two types of data are used in the screening calculations, tank waste level data and ambient atmospheric pressure data. The measurement processes and sources for level data are described in Section 3.1; Section 3.2 presents an overview of the atmospheric pressure data taken at the Hanford Meteorological Station (HMS).

3.1 Tank Waste Level Data

Tank waste level measurements are made in the Hanford tanks to monitor for leaks and intrusions. Four measurement devices are widely used in these tanks. Three of these measure the level of the waste surface; they are referred to as the FIC (made by the Food Instrument Company), manual tape (MT), and ENRAF (not an acronym, but the capitalized name of the manufacturer). The remaining device measures from within a well embedded in the waste, thereby monitoring the liquid level even if the liquid level is below a dry waste crust. This measurement is referred to as `Neutron ILL`. It's typical that, for any extended time period, only one of the surface level instruments is used in a tank. The current deployment of these devices in the Hanford tank farms is described for each tank in Hanlon (1994).

All of the waste level measurements used in this report were retrieved from the Surveillance Analysis Computer System (SACS) database (Glasscock 1993). The level data on which this report is based represent a complete dump of the waste level measurements in the SACS database as of March 3, 1995. Table 1 summarizes the data available from this dump. The initial date for the data in the dump was January 1, 1981. The table shows, in the column labeled `# Obs.`, how many measurements (if any) of each type are available for each tank. The count does not include measurements marked "Suspect" in the SACS database; a waste level measurement is marked "Suspect" in SACS when it is judged to be far from the main trend of the data. The time span of the measurements is noted in the columns labeled `From` and `To`. The waste level data are shown in the plots contained in the appendix.

The FIC and manual tape, both of which are plummets on the ends of steel tapes, are lowered into the tank from the ground level. Both detect the waste surface by indicating the level at which an electrical circuit is completed. The plummet for the manual tape is lowered manually, and the level measurement is recorded to the nearest quarter-inch.

The FIC plummet is mechanically controlled, and the level measurement can be recorded by a data acquisition system to the nearest tenth-inch. Some of the FICs are read by the Computer Automated Surveillance System (CASS) data acquisition system (Spurling 1991); the rest are read manually. The manual readout on the FIC, similar to a car odometer, can be read to slightly better resolution than available through CASS.

The FIC is often deployed so that the plummet is suspended just slightly above the waste surface. The plummet is lowered every minute, and a reading is available through CASS. One of these measurements per day is recorded in the SACS database.

The ENRAF gauge detects the waste surface by the change in buoyancy of a weight on the end of a wire, as the weight encounters the liquid or solid waste surface. Daily measurements for this device are recorded in the SACS database. References providing more details on these devices are Brewster et al.[2] and Peters and Park (1993).

[2]Brewster, M., E. Eschbach, and Z. Antoniak. 1995. *Uncertainty Status of Selected Instruments in Tank 241-SY-101*. Letter Report PNLMIT:013095, Pacific Northwest Laboratory, Richland, Washington.

`Neutron ILL` measurements are made in some of the Hanford tanks; see (Stong 1986) for a description of this measurement. The neutron probe takes measurements of the waste from within a four-inch-diameter tube installed in the tank; the tube extends from ground level almost to the bottom of the tank. The tube is referred to as a liquid observation well. Currently, 58 Hanford tanks have working liquid observation wells. The neutron logging produces a vertical profile of the tank waste (at least at the location of the liquid observation well), and the liquid level can be estimated from the logging, even if the liquid level is below the waste surface level.

For some tanks, the apparently large number of observations and intervals is misleading because of transfer of contents between tanks. For instance, the data for the double shell Tank AP-101 (page 87) show that the tank has recently lost much of its contents due to a transfer to another tank. So, even though the table reports 2175 FIC measurements from September 1986 through March 1995, the number of measurements that describe current conditions is actually much less. Furthermore, *tank transfer events were not taken into account in the automatic screening calculation.* Other tanks to examine in this context include all the other double-shell tanks and all the single-shell tanks that have been pumped. A list of the single-shell tanks that have been pumped is given in Table I-1 of Hanlon (1994). Tanks that are flagged by the screening process and have had some transfer of contents are listed in Section 5.

Table 1: Level data availability by tank

Tank	FIC			ENRAF			MT			Neutron ILL		
	From	To	# Obs.	From	To	# Obs.	From	To	# Obs.	From	To	# Obs.
A-101	Jan 81	May 82	71	–	–	–	Jan 81	Jan 95	1092	Mar 86	Mar 95	108
A-102	Jan 81	Jan 95	711	–	–	–	–	–	–	–	–	–
A-103	Jan 81	Mar 95	2088	–	–	–	Jan 81	May 82	73	Mar 86	Mar 95	153
A-104	–	–	–	–	–	–	Jan 81	Jan 95	650	–	–	–
A-105	–	–	–	–	–	–	Jan 81	Jan 95	656	–	–	–
A-106	Jan 81	Jan 95	184	–	–	–	–	–	–	–	–	–
AN-101	Oct 81	Mar 95	2520	–	–	–	Mar 93	Mar 95	4	–	–	–
AN-102	Oct 81	Mar 95	2490	–	–	–	–	–	–	–	–	–
AN-103	Oct 81	Mar 95	2422	–	–	–	–	–	–	–	–	–
AN-104	Oct 81	Mar 95	2484	–	–	–	–	–	–	–	–	–
AN-105	Oct 81	Mar 95	2436	–	–	–	–	–	–	–	–	–
AN-106	Oct 81	Mar 95	2420	–	–	–	–	–	–	–	–	–
AN-107	Oct 81	Mar 95	2433	–	–	–	–	–	–	–	–	–
AP-101	Sep 86	Mar 95	2175	–	–	–	Sep 86	Feb 95	2107	–	–	–
AP-102	Sep 86	Mar 93	1447	–	–	–	Sep 86	Mar 95	2043	–	–	–
AP-103	Sep 86	Mar 95	1966	–	–	–	Sep 86	Feb 95	2149	–	–	–
AP-104	Sep 86	Mar 95	2144	–	–	–	Sep 86	Feb 95	1573	–	–	–
AP-105	Sep 86	Mar 95	2156	–	–	–	Sep 86	Feb 95	2141	–	–	–
AP-106	Sep 86	Mar 95	2180	–	–	–	Sep 86	Feb 95	2102	–	–	–
AP-107	Sep 86	Mar 95	2273	–	–	–	Aug 89	Feb 95	1871	–	–	–
AP-108	Aug 86	Mar 95	2999	–	–	–	Aug 86	Feb 95	3068	–	–	–
AW-101	Jan 81	Mar 95	1726	–	–	–	Jan 81	Mar 95	2527	–	–	–
AW-102	Jan 81	Mar 95	2089	–	–	–	May 83	Feb 95	2448	–	–	–
AW-103	Jan 81	Mar 95	1674	–	–	–	May 83	Feb 95	2200	–	–	–
AW-104	Mar 81	Mar 95	2460	–	–	–	May 83	Feb 95	2213	–	–	–
AW-105	Jan 81	Mar 95	1726	–	–	–	May 83	Feb 95	2766	–	–	–
AW-106	Jan 81	Feb 95	2328	–	–	–	May 83	Mar 95	2470	–	–	–
AX-101	Jan 81	Jan 95	275	–	–	–	–	–	–	Mar 86	Mar 95	114
AX-102	–	–	–	–	–	–	Jan 81	Jan 95	2237	–	–	–
AX-103	Jan 81	Jan 95	510	–	–	–	–	–	–	–	–	–
AX-104	–	–	–	–	–	–	Jan 81	Jan 95	658	–	–	–
AY-101	Jan 81	Aug 90	644	–	–	–	Jan 81	Mar 95	2470	–	–	–
AY-102	Jan 81	Mar 95	2367	–	–	–	Jan 81	Feb 95	2250	–	–	–
AZ-101	Jan 81	Feb 89	421	–	–	–	Jan 81	Mar 95	2325	–	–	–
AZ-102	Jan 81	Mar 95	917	–	–	–	Jan 81	Feb 95	2324	–	–	–
B-101	Jan 81	Jan 95	192	–	–	–	–	–	–	–	–	–
B-102	Jan 81	Feb 95	1767	–	–	–	Jan 81	Jan 83	106	–	–	–
B-103	Jan 81	Jan 95	597	–	–	–	–	–	–	–	–	–
B-104	–	–	–	–	–	–	Jan 81	Jan 95	315	Mar 86	Mar 95	106
B-105	–	–	–	–	–	–	Jan 81	Jan 95	681	Mar 86	Nov 94	100
B-106	Dec 80	Mar 95	3053	–	–	–	–	–	–	–	–	–
B-107	–	–	–	–	–	–	Jan 81	Jan 95	944	–	–	–
B-108	Jan 81	Jan 95	454	–	–	–	–	–	–	–	–	–
B-109	–	–	–	–	–	–	Jan 81	Jan 95	347	–	–	–
B-110	–	–	–	–	–	–	Jan 81	Jan 95	634	Nov 94	Mar 95	31
B-111	Jan 81	Jan 95	320	–	–	–	–	–	–	Nov 94	Mar 95	29
B-112	Jan 81	Mar 95	1614	–	–	–	Jan 81	Feb 83	109	–	–	–
B-201	–	–	–	–	–	–	Jan 81	Mar 95	1106	–	–	–
B-202	–	–	–	–	–	–	Jan 81	Mar 95	1363	–	–	–
B-203	–	–	–	–	–	–	Jan 81	Mar 95	833	–	–	–
B-204	–	–	–	–	–	–	Jan 81	Mar 95	1321	–	–	–
BX-101	–	–	–	–	–	–	Jan 81	Mar 95	746	–	–	–
BX-102	–	–	–	–	–	–	Jan 81	Jan 95	853	–	–	–
BX-103	Jan 81	Mar 95	1794	–	–	–	–	–	–	–	–	–
BX-104	Jan 81	Mar 95	1504	–	–	–	Jan 81	Jan 83	104	–	–	–
BX-105	Jan 81	Jan 95	538	–	–	–	Jan 81	Jan 83	105	–	–	–
BX-106	Jan 81	Jul 94	1415	Jul 94	Mar 95	371	Jan 81	Jan 83	106	–	–	–
BX-107	Jan 81	Mar 95	1315	–	–	–	–	–	–	–	–	–
BX-108	–	–	–	–	–	–	Jan 81	Jan 95	209	–	–	–
BX-109	Jan 81	Mar 95	1432	–	–	–	–	–	–	–	–	–
BX-110	–	–	–	–	–	–	Jan 81	Jan 95	1147	–	–	–
BX-111	–	–	–	–	–	–	Jan 81	Jan 95	1488	Mar 86	Mar 95	115
BX-112	Jan 81	Mar 95	2049	–	–	–	Jan 81	May 83	114	–	–	–
BY-101	Sep 88	Sep 88	1	–	–	–	Jan 81	Jan 95	781	Jul 86	Mar 95	114
BY-102	–	–	–	–	–	–	Jan 81	Mar 95	1791	Jul 86	Mar 95	121
BY-103	–	–	–	–	–	–	Jan 81	Jan 95	1262	Apr 86	Mar 95	129
BY-104	–	–	–	–	–	–	Jan 81	Jan 95	968	Apr 86	Mar 95	118
BY-105	–	–	–	–	–	–	Jan 81	Jan 95	1261	Mar 86	Mar 95	117
BY-106	–	–	–	–	–	–	Jan 81	Jan 95	1272	Jul 86	Mar 95	112
BY-107	–	–	–	–	–	–	Jan 81	Jan 95	864	Nov 86	Mar 95	100
BY-108	–	–	–	–	–	–	Jan 81	Jan 95	969	–	–	–
BY-109	Jan 81	Mar 95	1640	Oct 94	Oct 94	3	–	–	–	Mar 86	Mar 95	116
BY-110	–	–	–	–	–	–	Jan 81	Jan 95	978	Jul 86	Mar 95	106
BY-111	–	–	–	–	–	–	Jan 81	Jan 95	969	Mar 86	Mar 95	113
BY-112	–	–	–	–	–	–	Jan 81	Jan 95	964	Jul 86	Mar 95	69
C-101	–	–	–	–	–	–	Jan 81	Jan 95	803	–	–	–
C-102	Jan 81	Jan 95	656	–	–	–	–	–	–	–	–	–
C-103	Jan 81	Jul 94	2112	Aug 94	Mar 95	203	–	–	–	–	–	–
C-104	Jan 81	Jan 95	2040	–	–	–	Jan 81	Apr 81	15	–	–	–
C-105	Jan 81	Mar 95	2371	–	–	–	Jan 81	Jul 82	78	–	–	–
C-106	Jan 81	Feb 95	2441	Sep 94	Mar 95	174	–	–	–	–	–	–
C-107	Jan 81	Mar 95	2041	–	–	–	Jan 81	Jan 81	3	–	–	–
C-108	–	–	–	–	–	–	Jan 81	Jan 95	678	–	–	–
C-109	–	–	–	–	–	–	Jan 81	Jan 95	853	–	–	–
C-110	–	–	–	–	–	–	Jan 81	Mar 95	1683	–	–	–
C-111	–	–	–	–	–	–	Jan 81	Jan 95	873	–	–	–
C-112	–	–	–	–	–	–	Jan 81	Jan 95	1223	–	–	–
C-201	–	–	–	–	–	–	Jan 81	Jan 95	655	–	–	–

Table 1: *(continued)*

Tank	FIC			ENRAF			MT			Neutron ILL		
	From	To	# Obs.	From	To	# Obs.	From	To	# Obs.	From	To	# Obs.
C-202	–	–	–	–	–	–	Jan 81	Oct 94	655	–	–	–
C-203	–	–	–	–	–	–	Jan 81	Jan 95	657	–	–	–
C-204	–	–	–	–	–	–	Jan 81	Jan 95	841	–	–	–
S-101	Jan 81	Jan 95	1603	–	–	–	Jan 81	Jun 81	181	Mar 86	Mar 95	113
S-102	Jan 81	Mar 95	3323	–	–	–	Jan 81	Jun 81	178	Mar 86	Mar 95	101
S-103	Jan 81	May 94	1832	May 94	Mar 95	285	Jan 81	Jun 81	26	Mar 86	Mar 95	102
S-104	–	–	–	–	–	–	Jan 81	Jan 95	706	Oct 94	Mar 95	33
S-105	Jan 81	Jul 91	656	–	–	–	Jan 81	Jun 81	44	Mar 86	Mar 95	110
S-106	Jan 81	Jun 94	2000	Jun 94	Mar 95	252	Jan 81	Jun 81	26	Mar 86	Mar 95	111
S-107	Jan 81	Jun 94	2035	Jun 94	Mar 95	271	Jan 81	Jun 81	26	–	–	–
S-108	Jan 81	Jan 95	748	–	–	–	Jan 81	Jul 94	650	Mar 86	Mar 95	104
S-109	Jan 81	Jan 95	785	–	–	–	Jan 81	Jun 81	26	Mar 86	Mar 95	106
S-110	Jan 81	Apr 94	1171	–	–	–	Jan 81	Jun 81	26	Mar 86	Feb 95	106
S-111	Jan 81	Aug 94	1970	Aug 94	Mar 95	201	Jan 81	Jun 81	181	Mar 86	Mar 95	108
S-112	Jan 81	Apr 94	796	–	–	–	Jan 81	Dec 81	29	Mar 86	Mar 95	106
SX-101	Jan 81	Jan 95	219	–	–	–	Jan 81	Jan 85	506	Mar 86	Mar 95	110
SX-102	Jan 81	Jan 95	261	–	–	–	Jan 81	Aug 83	419	Mar 86	Mar 95	127
SX-103	Jan 81	Jan 95	1490	–	–	–	Jan 81	Jan 85	297	Mar 86	Mar 95	119
SX-104	Jan 81	Jan 95	523	–	–	–	Jan 81	May 82	301	Mar 86	Sep 91	34
SX-105	Jan 81	Jan 95	288	–	–	–	Jan 81	May 84	478	Mar 86	Mar 95	126
SX-106	Jan 81	Aug 94	1805	Aug 94	Mar 95	201	Jan 81	Jan 85	209	Mar 86	Mar 95	207
SX-107	–	–	–	–	–	–	Jan 81	Oct 94	820	–	–	–
SX-108	–	–	–	–	–	–	Jan 81	Jan 95	805	–	–	–
SX-109	–	–	–	–	–	–	Jan 81	Jan 95	758	–	–	–
SX-110	–	–	–	–	–	–	Jan 81	Jan 95	867	–	–	–
SX-111	–	–	–	–	–	–	Jan 81	Jan 95	850	–	–	–
SX-112	–	–	–	–	–	–	Jan 81	Jan 95	847	–	–	–
SX-113	–	–	–	–	–	–	Jan 81	Jan 95	850	–	–	–
SX-114	–	–	–	–	–	–	Jan 81	Jan 95	853	–	–	–
SX-115	–	–	–	–	–	–	Jan 81	Jan 95	851	–	–	–
SY-101	Jan 81	Mar 95	4816	Dec 94	Feb 95	75	Jan 81	Feb 95	1890	–	–	–
SY-102	Jan 81	Jun 94	1517	Jun 94	Mar 95	252	Jan 81	Jan 95	2498	–	–	–
SY-103	Jan 81	Jul 94	2091	Jul 94	Mar 95	242	Jan 81	Jan 95	1352	–	–	–
T-101	Jan 81	Jan 95	1046	–	–	–	Jan 81	Jan 94	145	–	–	–
T-102	Jan 81	Jun 94	692	Jun 94	Mar 95	411	–	–	–	–	–	–
T-103	Jan 81	Jan 95	619	–	–	–	–	–	–	–	–	–
T-104	–	–	–	–	–	–	Jan 81	Jan 95	1563	Mar 86	Feb 95	108
T-105	Jan 81	Jan 95	202	–	–	–	Jan 81	Nov 93	167	–	–	–
T-106	Jan 81	Jan 95	228	–	–	–	–	–	–	–	–	–
T-107	Jan 81	Jul 94	1715	Jun 94	Mar 95	418	–	–	–	–	–	–
T-108	–	–	–	–	–	–	Jan 81	Mar 95	1277	–	–	–
T-109	Jan 81	Apr 94	253	Sep 94	Mar 95	171	–	–	–	–	–	–
T-110	Jan 81	Feb 95	947	–	–	–	Jan 81	Jan 81	1	Mar 86	Feb 95	107
T-111	Jan 81	Mar 95	1673	–	–	–	–	–	–	Mar 86	Feb 95	104
T-112	Jan 81	Mar 95	1120	–	–	–	–	–	–	–	–	–
T-201	–	–	–	–	–	–	Jan 81	Mar 95	1297	–	–	–
T-202	–	–	–	–	–	–	Jan 81	Mar 95	1131	–	–	–
T-203	–	–	–	–	–	–	Jan 81	Jan 95	824	–	–	–
T-204	–	–	–	–	–	–	Jan 81	Mar 95	1242	–	–	–
TX-101	Jan 81	Mar 95	1803	–	–	–	–	–	–	–	–	–
TX-102	–	–	–	–	–	–	Jan 81	Jan 95	218	Mar 86	Mar 95	101
TX-103	Jan 81	Oct 94	179	–	–	–	–	–	–	–	–	–
TX-104	Jan 81	Jan 95	582	–	–	–	–	–	–	–	–	–
TX-105	–	–	–	–	–	–	Jan 81	Jan 95	221	–	–	–
TX-106	–	–	–	–	–	–	Jan 81	Jan 95	247	Mar 86	Mar 95	101
TX-107	Dec 80	Jan 95	2001	–	–	–	–	–	–	–	–	–
TX-108	Jan 81	Jan 95	232	–	–	–	–	–	–	Apr 86	Jul 94	61
TX-109	Jan 81	Jan 95	174	–	–	–	–	–	–	Mar 86	Mar 95	102
TX-110	–	–	–	–	–	–	Jan 81	Jan 95	251	Mar 86	Mar 95	102
TX-111	–	–	–	–	–	–	Jan 81	Jan 95	219	Mar 86	Mar 95	105
TX-112	–	–	–	–	–	–	Jan 81	Jan 95	251	Mar 86	Mar 95	117
TX-113	Jan 95	Jan 95	1	–	–	–	Jan 81	Oct 94	220	Mar 86	Mar 95	110
TX-114	–	–	–	–	–	–	Jan 81	Jan 95	220	Mar 86	Mar 95	105
TX-115	–	–	–	–	–	–	Jan 81	Jan 95	248	Mar 86	Mar 95	111
TX-116	–	–	–	–	–	–	Jan 81	Jan 95	231	–	–	–
TX-117	–	–	–	–	–	–	Jan 81	Jan 95	236	Mar 86	Mar 95	99
TX-118	Jan 81	Jan 95	223	–	–	–	–	–	–	Mar 86	Mar 95	108
TY-101	Jan 81	Jan 95	219	–	–	–	–	–	–	–	–	–
TY-102	Jan 81	Mar 95	1936	–	–	–	–	–	–	–	–	–
TY-103	Jan 81	Jan 95	238	–	–	–	–	–	–	Mar 86	Mar 95	104
TY-104	Jan 81	Mar 95	1432	–	–	–	–	–	–	–	–	–
TY-105	–	–	–	–	–	–	Jan 81	Jan 95	225	–	–	–
TY-106	–	–	–	–	–	–	Jan 81	Jan 95	399	–	–	–
U-101	–	–	–	–	–	–	Jan 81	Mar 95	593	–	–	–
U-102	Jan 81	Jan 95	237	–	–	–	Jan 95	Jan 95	1	Mar 86	Feb 95	100
U-103	Jan 81	Jul 94	1934	Jul 94	Mar 95	229	–	–	–	Mar 86	Feb 95	106
U-104	–	–	–	–	–	–	Jan 81	Jan 95	209	–	–	–
U-105	Jan 81	Jul 94	1336	Jul 94	Mar 95	215	Jan 81	Sep 85	245	Mar 86	Feb 95	102
U-106	Jan 81	Aug 94	1973	Aug 94	Mar 95	212	–	–	–	Mar 86	Feb 95	98
U-107	Jan 81	Jul 94	3117	Jul 94	Mar 95	220	–	–	–	Mar 86	Feb 95	97
U-108	Jan 81	Jan 95	218	–	–	–	–	–	–	Mar 86	Feb 95	98
U-109	Dec 80	Jul 94	3063	Jul 94	Mar 95	226	–	–	–	Mar 86	Feb 95	104
U-110	Jan 81	Jan 95	199	–	–	–	–	–	–	–	–	–
U-111	Jan 81	Jan 95	247	–	–	–	–	–	–	Mar 86	Feb 95	102
U-112	–	–	–	–	–	–	Jan 81	Jan 95	208	–	–	–
U-201	–	–	–	–	–	–	Jan 81	Mar 95	804	–	–	–
U-202	–	–	–	–	–	–	Jan 81	Mar 95	772	–	–	–
U-203	–	–	–	–	–	–	Jan 81	Jan 95	206	–	–	–
U-204	–	–	–	–	–	–	Jan 81	Mar 95	764	–	–	–

3.2 Hanford Meteorological Station Data

The Hanford Meteorological Station is the source of atmospheric pressure data used in this study. This weather station is located between the 200 East and 200 West areas on the Hanford Site (Hoitink and Burk 1994). The atmospheric pressure measurements used are single hourly measurements (not hourly averages of finer time resolution measurements). The data, including instrumentation and format of computer files, are described in Andrews and Buck (1987).

Figure 4 shows the hourly atmospheric pressure measurements from the HMS from 1979 through 1984. The plot shows that atmospheric pressure demonstrates seasonal behavior. Figure 5 shows the trend in the hourly atmospheric pressure measurements; the trend was obtained by smoothing the hourly atmospheric pressure measurements with a local weighted average. Note that, except for the winters of 1982 and 1983, the atmospheric pressure trend in Figure 5 has a seasonal component. The peak-to-peak amplitude of the seasonal effect is about 0.3 inch Hg. Comparing Figures 4 and 5 shows that the trend has a much smaller range than the raw atmospheric pressure data.

Seasonality in the variability of atmospheric pressure is shown in Figure 6. This figure shows the magnitude of the residuals of the observed atmospheric pressure from the trend. A range of typical values in the winter is 0.8, while a typical summer range is about 0.4 inches Hg.

Figures 7 and 8 show the hourly atmospheric pressure data, month by month, for 1992. The atmospheric pressure measurement range is again observed to be larger during the winter than in the summer. An interesting feature of the atmospheric pressure during the summer is the diurnal cycle. The amplitude of the cycle is observed to be between 0.1 and 0.2 inches Hg.

A major assumption in the screening process is that changes in atmospheric pressure are transferred to the tank headspace nearly instantaneously.

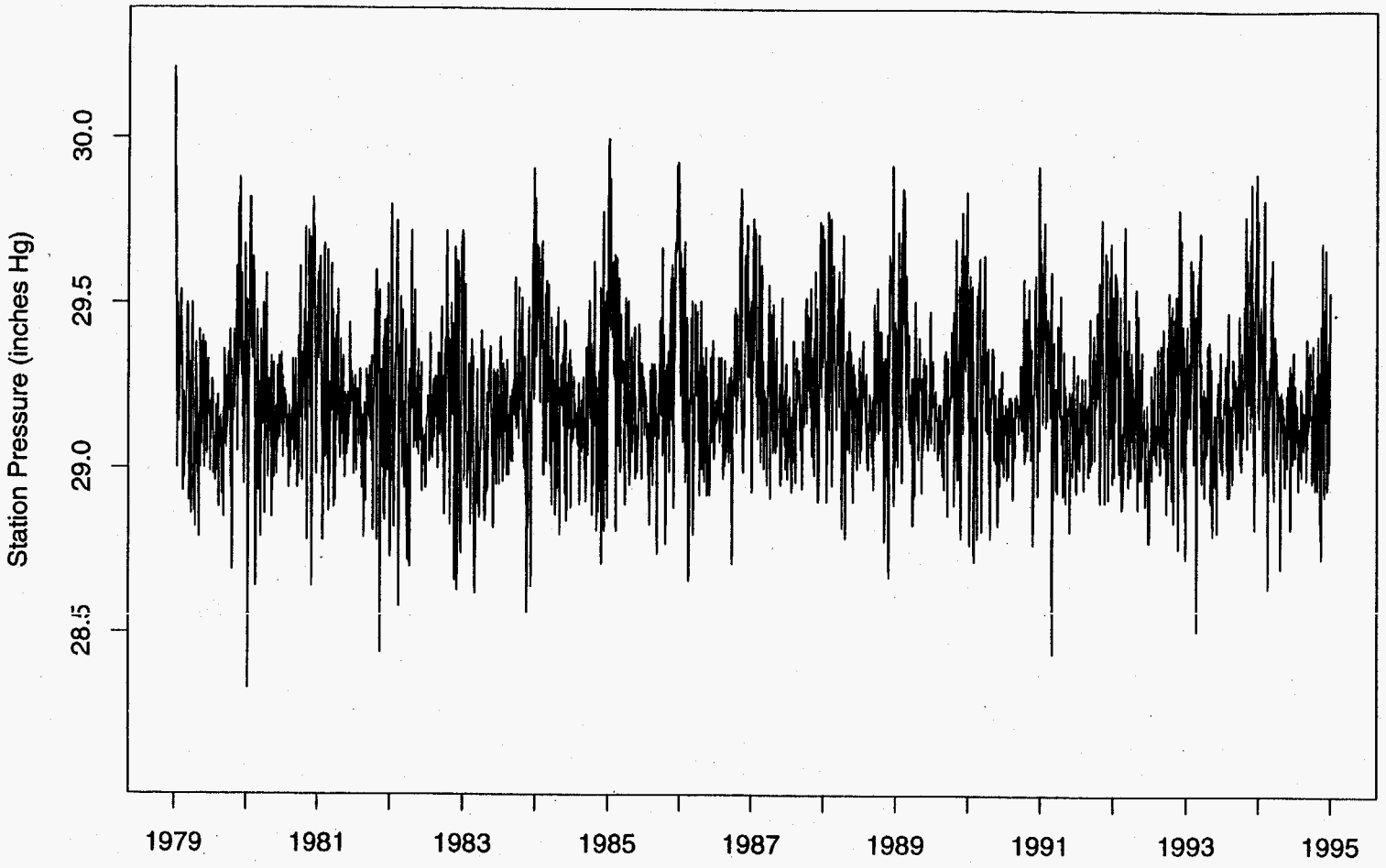

Figure 4: Hourly atmospheric pressure data for the Hanford Meteorological Station from 1979 through 1994, inclusive. The tick marks on the x-axis mark the beginning of each year.

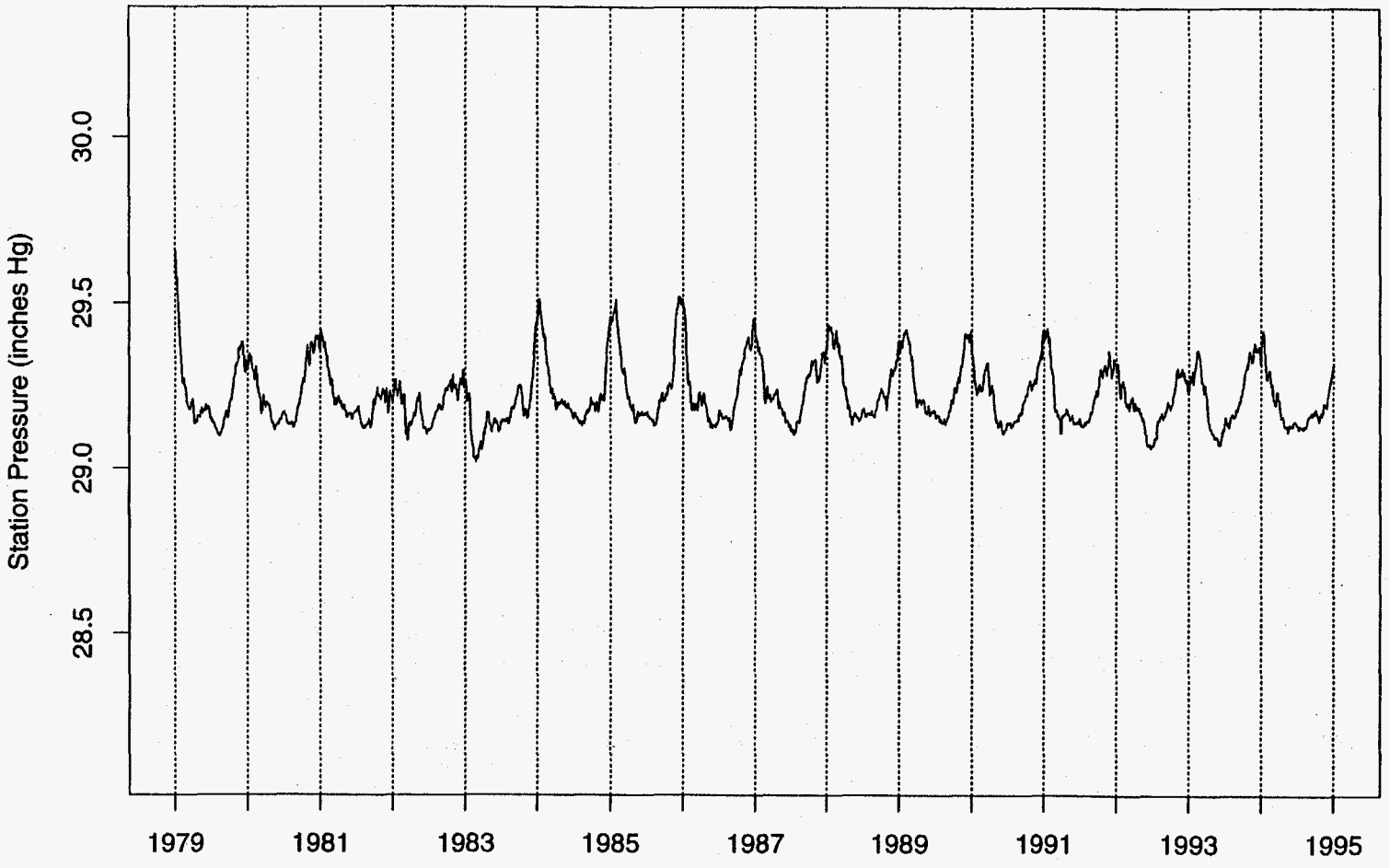

Figure 5: Trend in hourly atmospheric pressure data from the Hanford Meteorological Station from 1979 through 1994. The plot shows that atmospheric pressure tends to be higher during the winter than the summer. The vertical axis scale on this plot is the same as in Figure 4.

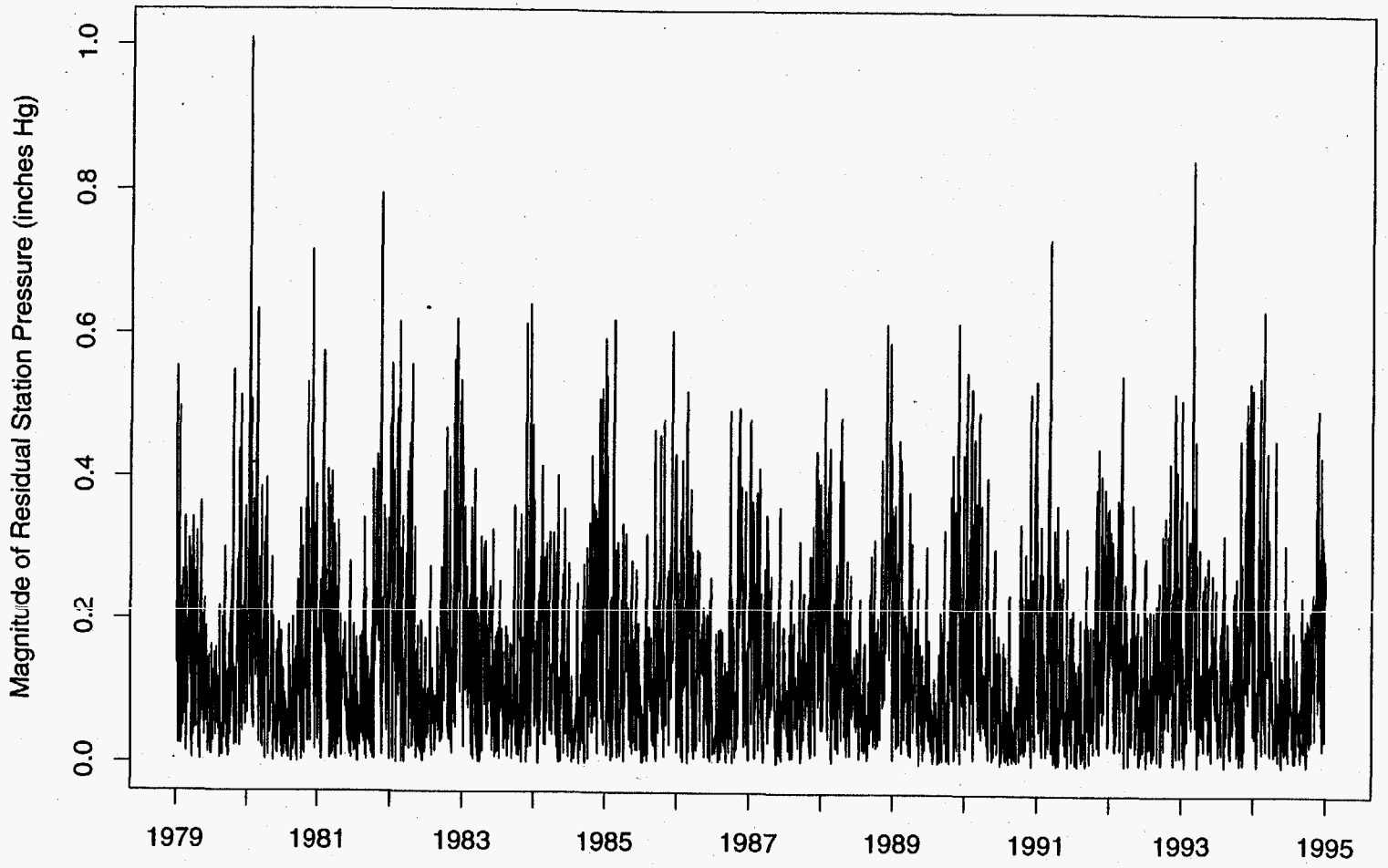

Figure 6: Absolute value of the residual of atmospheric pressure from the trend. While "inky," the plot shows that even after accounting for the trend in atmospheric pressure, a seasonality exists in the variation.

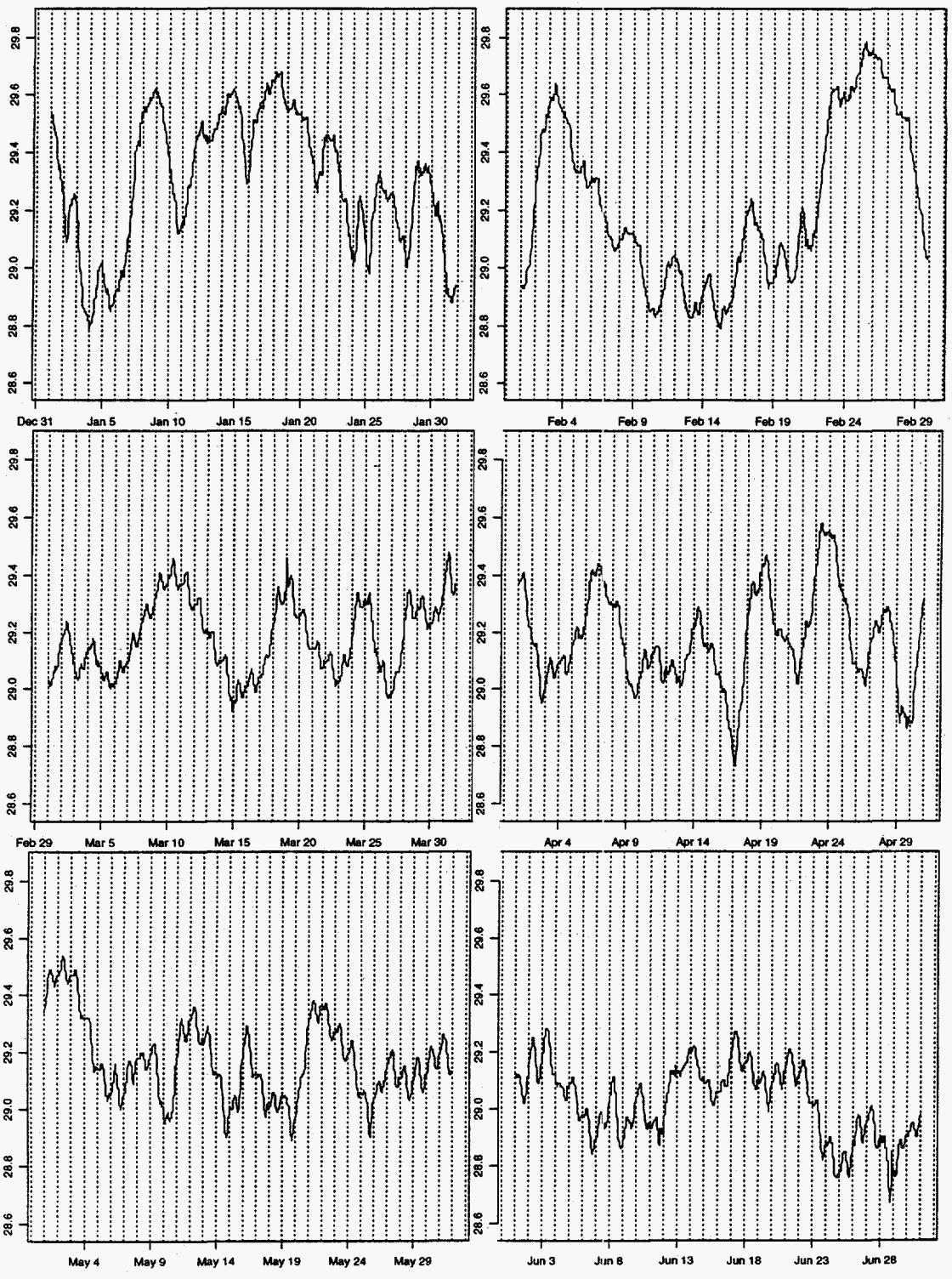

Figure 7: Hourly atmospheric pressure (inches Hg) during the first six months of 1992. The dashed vertical lines are drawn at midnight of each day.

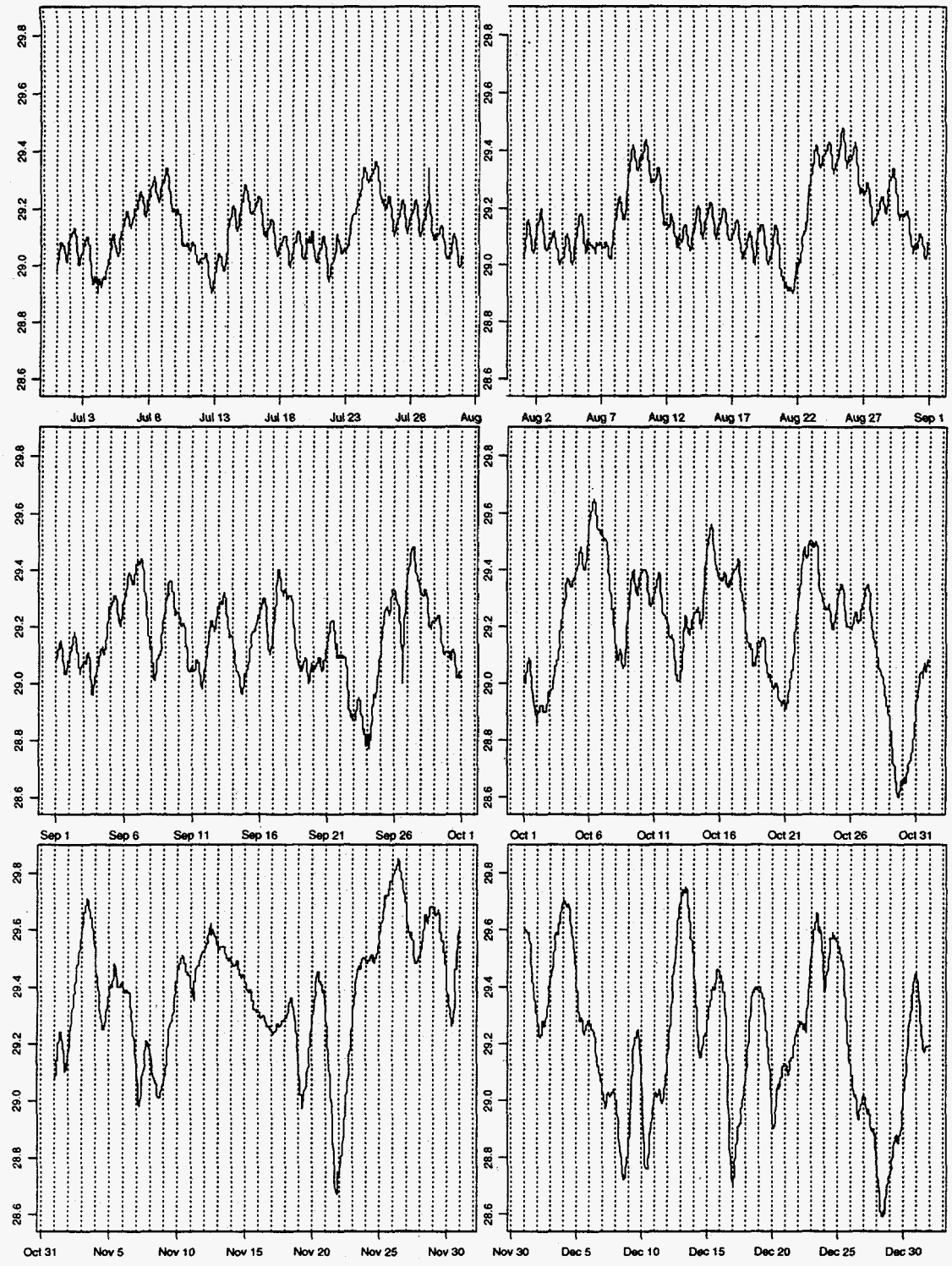

Figure 8: Hourly atmospheric pressure (inches Hg) during the last six months of 1992. The dashed vertical lines are drawn at midnight of each day.

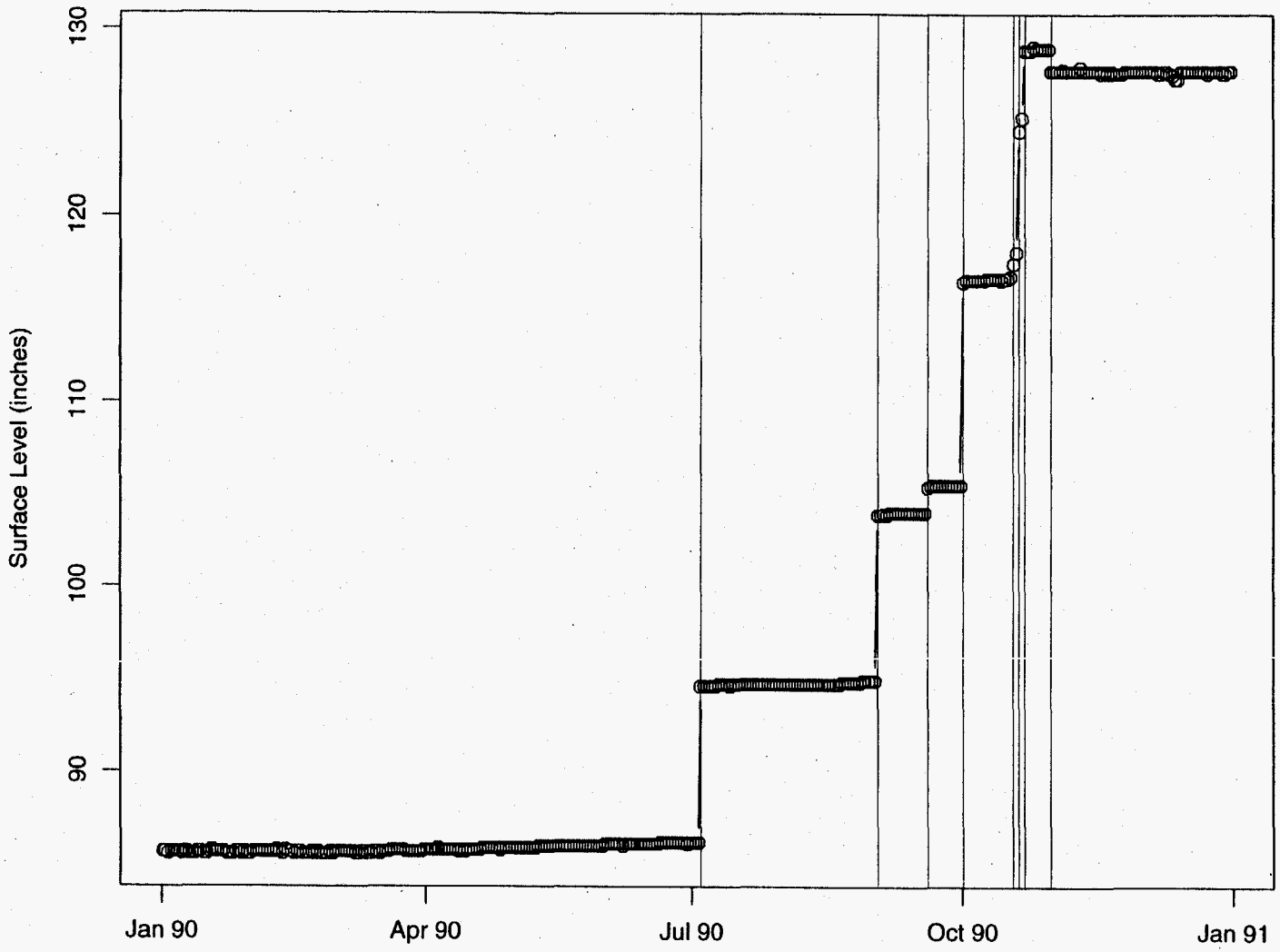

Figure 9: Tank AN–101 FIC waste level measurements from 1-1-90 through 12-31-90. Breaks estimated by the multi-state DLM are shown by the vertical lines.

4 Methodology

The methodology used in this report is based on relating the fluctuations in atmospheric pressure to corresponding fluctuations in tank waste level. When the tank waste contains trapped gas, the expected relationship is that increased atmospheric pressure compresses the gas trapped in the waste, thereby decreasing the waste level.

The screening calculation has three steps:

1. The level data are scanned for rapid changes in waste level and rapid rates of change in waste level. The times of these events are used as boundaries of time intervals. These intervals are further refined into shorter time intervals to block out potential "low frequency" effects in waste level, such as those caused by temperature changes.

2. For each time interval, the level data and atmospheric pressure data are examined as demonstrated in Figures 1-3. The key output of this step is the slope of the line relating detrended waste level to atmospheric pressure; see Figure 3 for an example.

3. The proportion of negative slopes is used to decide whether the tank waste contains trapped gas. A large proportion of negative slopes indicates trapped gas.

Step 1 is described in Section 4.1; Step 2 is outlined in Section 4.2; and Section 4.3 describes how the calculations from all the intervals are combined to decide whether trapped gas is indicated for a tank. A model that connects the slope estimate from the linear regression in Step 2 with the amount of trapped gas in the tank waste is presented in Section 4.2.1.

4.1 Preprocessing the Waste Level Data

Many of the Hanford tanks have had material removed or added during the time period of this study. These events produce large jumps in the level data plots. Other events that can lead to an abrupt change in the waste level measurements include gas release events and certain instrument maintenance operations, such as flushing waste buildup on an FIC. If a time interval in one of the Step 2 calculations were to contain one of these jumps, the calculation would be useless for deciding whether the waste contains trapped gas. Accordingly, a jump detector known as the multi-state dynamic linear model (DLM) was applied to the data to identify time intervals that were free of large level changes. The DLM also identifies point which are isolated away from the main body of data; these outlying points were removed from the analysis. The application of this algorithm to Hanford waste tank level data is described by Whitney et al.[3] General references for this procedure are Gordon and Smith (1988, 1990) and West and Harrison (1989).

Figure 9 shows the result of applying the DLM to FIC surface level data for Tank AN–101 for 1990. The waste level data stair-step up during the time period shown. The vertical lines are drawn at times where the multi-state DLM detected a jump.

A far less clean set of data, so far as the application of the multi-state DLM goes, are the FIC waste level measurements for Tank S–102, shown in Figure 10. Points marked with an "X" were identified as outliers by the DLM and removed from the data (for example, one point in 1984 and several in 1988 and 1989). The vertical lines again mark breaks identified by the DLM procedure. The lines marking breaks near January 1990 and January 1991 may be cases where the procedure failed; during this time of year the swings in atmospheric pressure are largest, and the effect of these

[3]Whitney, P., S. Sain, and T. Miley. 1995. *Applicability of Multi-State Modeling to Monitoring Hanford Waste Tank Surface Levels.* Letter Report to Westinghouse Hanford Company from Pacific Northwest Laboratory.

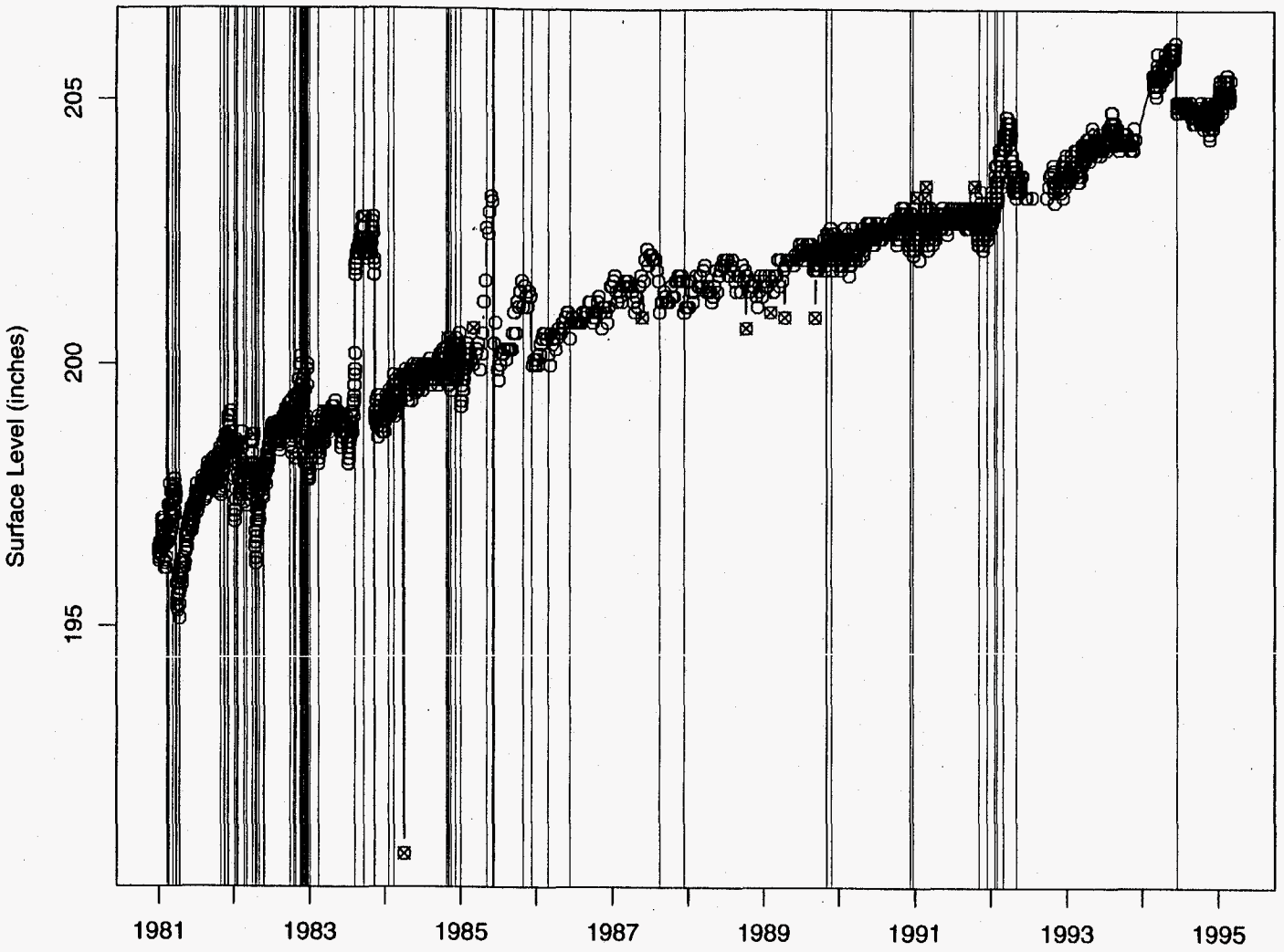

Figure 10: Tank S–102 FIC measurements with breaks and transients marked by vertical lines and Xs, respectively.

swings on waste level (for this tank) may have been large enough to mislead the procedure. Also, note the tendency for the algorithm to detect jumps in winter months, when the largest atmospheric pressure swings tend to occur. Figure 11 zooms in on the time period from January 1981 through August 7, 1981. The procedure correctly identifies the large jump in late March. Without further analysis, it's not clear whether the other identifications represent real level changes or not.

If the preprocessing mistakenly labels breaks caused by atmospheric pressure changes, the expected effect is less accurate estimates of the slope parameter. However, such an error is not expected to bias the slope estimate; since a single point is not expected to have a significant effect on the slope estimate. A potential fix for this problem is to integrate the physical modeling into the multi-state DLM. This is recommended work.

After the multi-state DLM has been used to identify breaks in the data, and outliers have been deleted, the remaining intervals of "steady state" data are broken up into approximately 60-day sub-intervals. The rationale for the 60-day intervals is to block out "low frequency" effects in waste level, such as those due to temperature changes. Otherwise, the 60-day criterion is arbitrary.

Intervals containing fewer than eight observations were not considered further in this study. Note that the proposed procedure requires at least three observations in each interval; if there were only two, the detrended waste levels would always be zero, and any relation between level and pressure would be hidden. Also, eight observations correspond to about two months of weekly data, and weekly level data is commonly available for the Hanford tanks. Otherwise, the eight-observation criterion is also arbitrary.

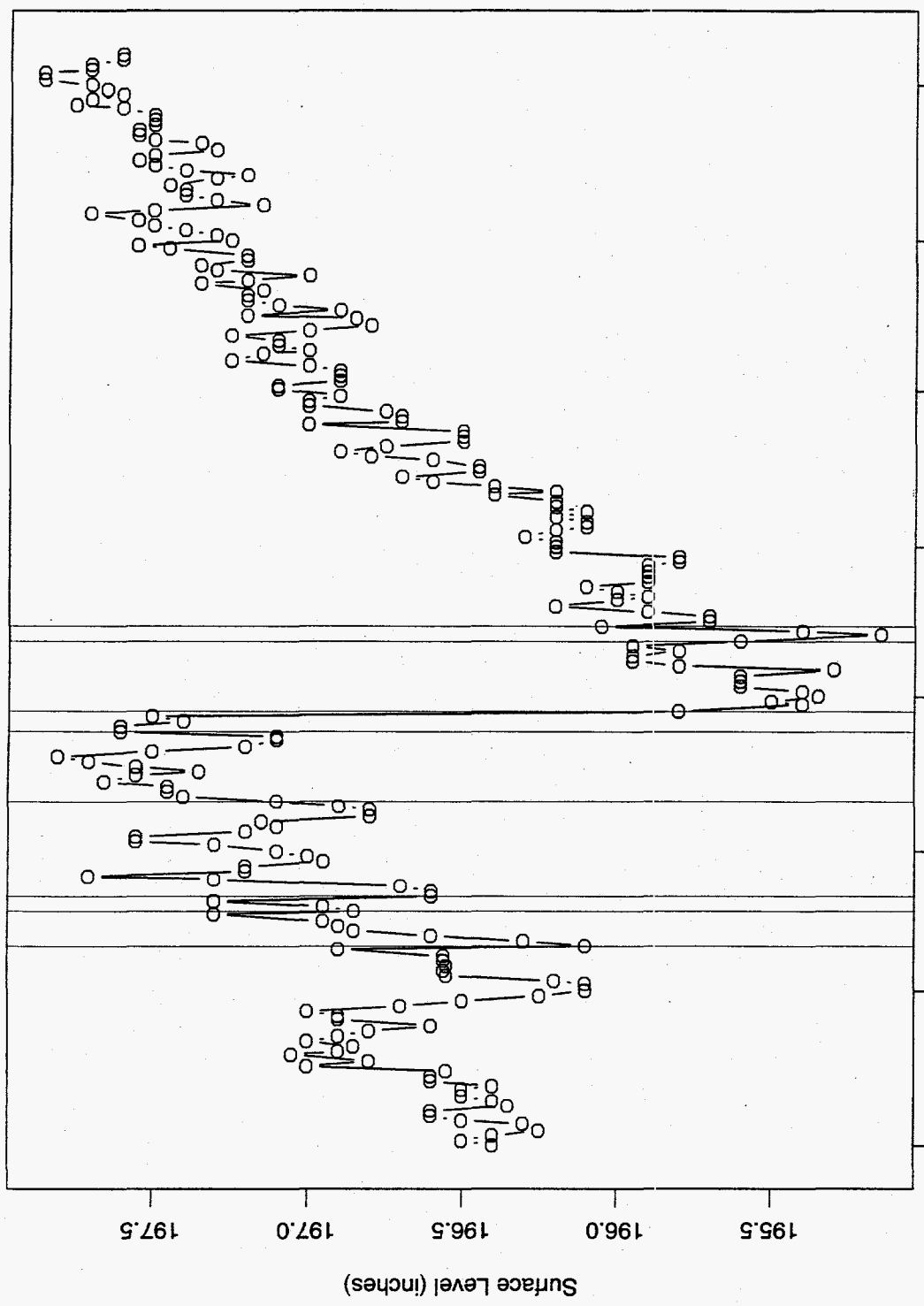

Figure 11: Tank S-102 FIC measurements with breaks marked by vertical lines. FIC data from 1-1-81 through 8-7-81.

4.2 Estimating the Response of Waste Level to Fluctuations in Atmospheric Pressure

This section describes the second step in the screening calculation. Section 4.2.1 describes a model which suggests why this screening process indicates trapped gas. Limitations of the screening process are pointed out in Section 4.2.2.

The inputs to a single calculation of the slope estimate are the tank level and atmospheric pressure data, and a time interval (output from preprocessing). The key operations in Step 2 of the screening process are:

(a) Select the waste level data from SACS for the tank and instrument (FIC, manual tape, ENRAF or Neutron ILL) during the selected time interval. The data quality flag in SACS was used to omit "suspect" measurements.

(b) Select the atmospheric pressure data taken at the same time as the waste level data identified in Step 2a. The time of a waste level measurement is recorded to the nearest minute in SACS, while the atmospheric pressure data are recorded hourly. Match the times by truncating the minutes in the waste level measurement's time stamp.

(c) Fit a straight line to waste level versus time via least squares regression.

(d) Calculate the residuals from the line obtained in Step 2c. These residuals are the detrended waste level (DWL).

(e) Compare tank waste level and atmospheric pressure.

   i. Regress waste level on atmospheric pressure (using data identified in Steps 2a and 2b). Return the slope estimate and its standard error.

   ii. Regress detrended waste level on atmospheric pressure (using data identified in Steps 2d and 2b). Return the slope estimate and its standard error.

   These two slopes are the key outputs of Step 2 and are used in the screening calculation described in Section 4.3.

   It's often the case, especially for manual tape data and less often for FIC data, that all the waste level measurements over a time interval are identical. In this case the slope estimate and the standard error of the slope estimate are recorded as zero. Figure 97 on page 138 of this document shows many instances of this situation.

   Two regressions are done at this step to gauge the effect of detrending. For instance, the FIC and MT screening summary for Tank SY–101 in Table 2 on page 32 shows that without detrending the tank is not flagged; with detrending it is. We would expect the first regression to produce a better slope estimate than the second in cases where there is no trend in the surface level.

4.2.1 Modeling Support for the Screening Calculation

This section relates a model of gas trapped in the waste to the linear regressions in Step 2. The model is essentially an application of Boyle's law to the waste and gas configuration shown in Figure 12. Additionally, the effects of a constant rate of gas accumulation on the tank waste surface level and on the surface level's response to changes in atmospheric pressure are demonstrated.

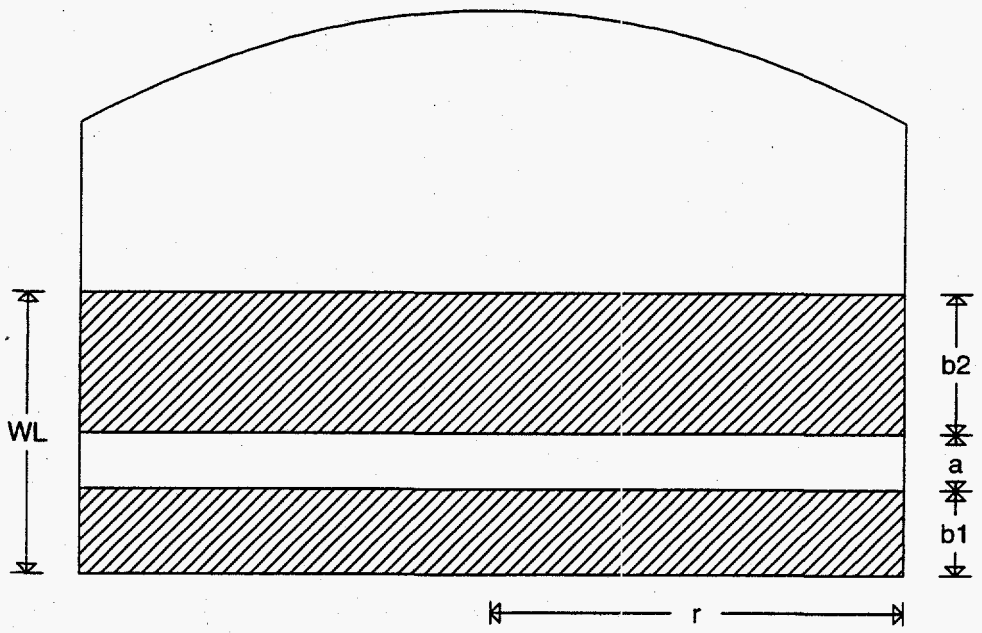

Figure 12: Hypothetical tank with a layer of trapped gas; represented as a cross-section of a tank and its contents. The dark layers represent liquid or solid tank waste. The layer sandwiched between the dark layers represents the trapped gas.

The following notation is used in the mathematical development and in Figure 12:

WL Measured in-tank waste level.

AP Ambient atmospheric pressure.

a Height of the trapped gas layer; this quantity is marked in Figure 12.

b Height of the tank waste.

r Radius of the tank; for the larger Hanford tanks, this value is 37.5 feet.

V Volume of the trapped gas in the tank.

P Average pressure exerted on the trapped gas.

The total pressure exerted on the trapped gas is a combination of the burden of the waste above the gas and the atmospheric pressure.

δ Fluctuations in pressure applied to the trapped gas that is due to changes in ambient atmospheric pressure. It's convenient to think of δ as a quantity that fluctuates about zero.

c Constant in Boyle's law. The quantity c satisfies

$$(P+\delta)V = c \tag{1}$$

Note that if P is expressed in units of atmospheres, then c is interpreted as the volume of the trapped gas at standard pressure.

From Figure 12, $\mathrm{WL} = a + b$ and $b = b_1 + b_2$ and $V = \pi r^2 a$. Rearranging Equation (1) and substituting for WL and V gives

$$\mathrm{WL} = b + \frac{c}{\pi r^2 (P+\delta)} = b + \frac{c}{\pi r^2 P}\,\frac{1}{1+(\delta/P)} \tag{2}$$

The fluctuations δ are always much smaller than P, so the geometric expansion can be used to give the approximation

$$b + \frac{c}{\pi r^2 P}\,\frac{1}{1+(\delta/P)} \approx b + \frac{c}{\pi r^2 P}\left(1 - \frac{\delta}{P}\right) \tag{3}$$

Equation (3) can be rearranged to give

$$\mathrm{WL} = b + \frac{c}{\pi r^2 P} - \frac{c}{\pi r^2 P^2}\delta = b + \frac{c}{\pi r^2 P} + \frac{c}{\pi r^2 P^2} - \frac{c}{\pi r^2 P^2}\mathrm{AP} \tag{4}$$

Equation (4) shows how $d\mathrm{WL}/d\mathrm{AP}$ can be used to estimate the amount of gas trapped in the tank. Since

$$\frac{d\mathrm{WL}}{d\mathrm{AP}} = -\frac{c}{\pi r^2 P^2}$$

the amount of gas, c, is estimated as

$$c = -\pi r^2 P^2 \frac{d\mathrm{WL}}{d\mathrm{AP}} \tag{5}$$

Equation (5) requires that the average pressure applied to the trapped gas be provided. This equation is also available from the development in Section 2.2 of Allemann et al. (1994).

Next, assume that gas is generated at a constant rate. In particular, assume that the volume of trapped gas at standard pressure of 1 atmosphere satisfies

$$c = V_0 + \alpha t$$

where V_0 is the volume of trapped gas at time $t = 0$, and α is the generation rate (volume per unit time). Subscripting WL and δ to reflect the time-varying nature of the tank level and atmospheric pressure, Equation (4) becomes

$$\mathrm{WL}_t = b + \frac{V_0 + \alpha t}{\pi r^2 P} - \delta_t \left(\frac{V_0 + \alpha t}{\pi r^2 P^2} \right) = \left[b + \frac{V_0}{\pi r^2 P} \right] + \left[\frac{\alpha}{\pi r^2 P} \right] t - \delta_t \left(\frac{V_0 + \alpha t}{\pi r^2 P^2} \right) \tag{6}$$

This equation, together with our assumptions on δ_t, means that a linear regression of WL_t on time, like that in Step 2c of the screening calculation, yields intercept and slope estimates which are, approximately, $\left[b + \frac{V_0}{\pi r^2 P} \right]$ and $\left[\frac{\alpha}{\pi r^2 P} \right]$, respectively. Equation (6) directly relates the slope of the overall linear trend to the rate of gas generation.

The residuals from a linear regression of WL_t against time constitute the detrended waste level. The residuals satisfy

$$-\delta_t \left(\frac{V_0 + \alpha t}{\pi r^2 P^2} \right) \approx \mathrm{DWL}_t$$

Now $\mathrm{AP}_t = 1 + \delta_t$, or $-\delta_t = 1 - \mathrm{AP}_t$, so

$$\mathrm{DWL}_t \approx (1 - \mathrm{AP}_t) \left(\frac{V_0 + \alpha t}{\pi r^2 P^2} \right)$$

and

$$\frac{d\mathrm{DWL}}{d\mathrm{AP}} \approx -\frac{V_0 + \alpha t}{\pi r^2 P^2}$$

This expression can be rearranged as

$$V_0 + \alpha t \approx -\pi r^2 P^2 \frac{d\mathrm{DWL}}{d\mathrm{AP}} \tag{7}$$

which is identical to Equation (5).

The magnitude of this estimate of $d\mathrm{DWL}/d\mathrm{AP}$ is related to the amount of gas trapped in the waste. Figure 13 shows waste level data for Tank SY–101. The two-stage linear fits (Steps 2c, 2d and 2e of Section 4.2) are applied for three time ranges, producing estimates of $d\mathrm{DWL}/d\mathrm{AP}$; these three estimates are shown on the plot. The fact that the magnitudes of the slopes increase as the waste level rises further supports the use of this screening statistic as an indicator of trapped gas. The model (see Equation (6)) implies that the larger the amount of gas, the larger the magnitude of the level response to pressure fluctuations. That the slopes are increasingly negative with the increasing surface level is consistent with this model; however, the magnitudes of the 95% confidence intervals for these slope estimates are sufficiently large that one cannot definitely conclude that $d\mathrm{DWL}/d\mathrm{AP}$ has changed significantly from the first interval to the third.

4.2.2 Limitations of the Slope Estimates

While there are both empirically based and model-based reasons to use the slope from Step 2 in the screening calculation to detect trapped gas, the following qualifications should be kept in mind:

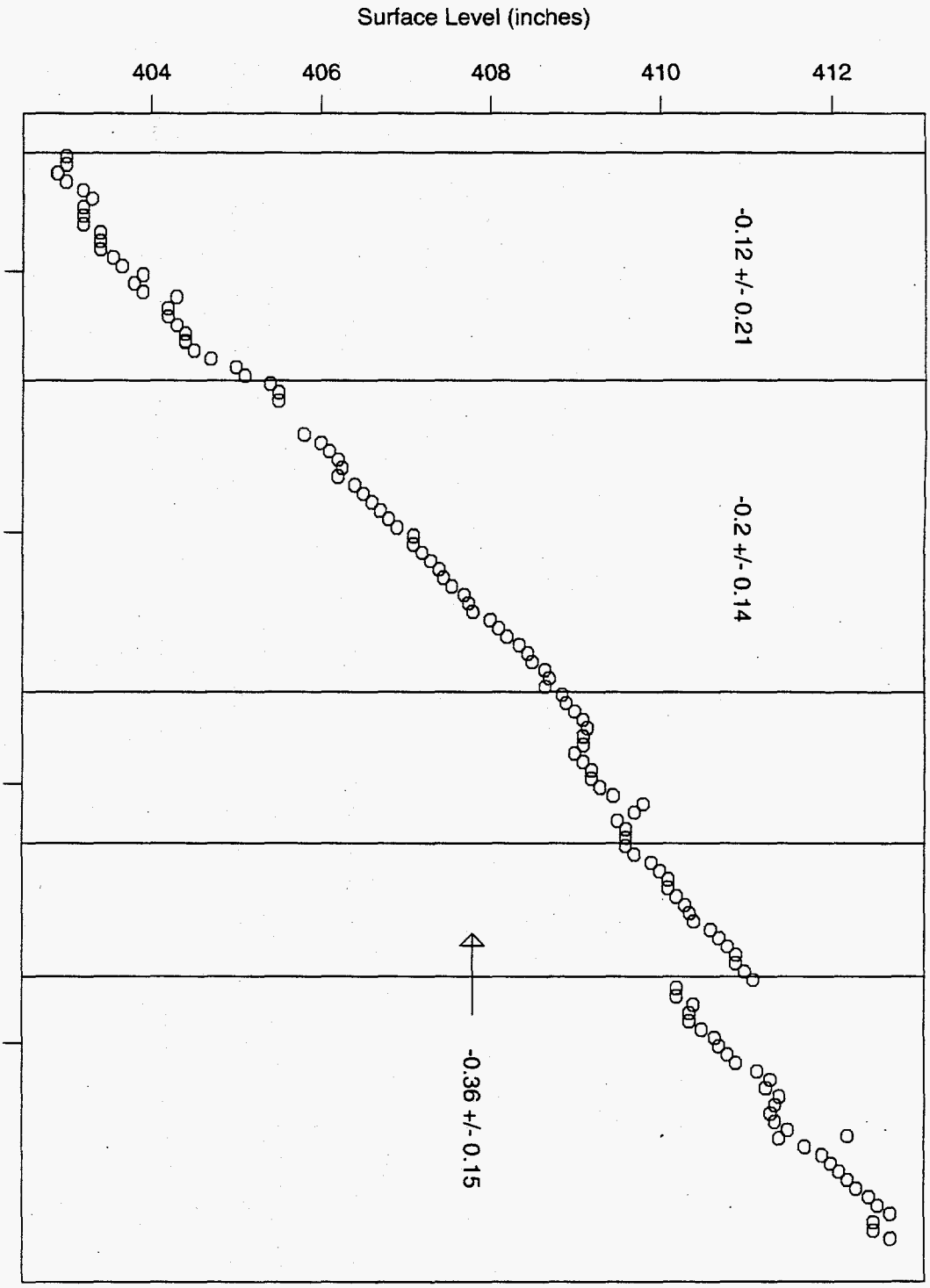

Figure 13: Tank SY-101 FIC data and dDWL/dAP estimates with 95% confidence intervals.

- The screening statistic does not make most efficient use of the available information. For instance, the two distinct regressions might be combined into a single one,

$$\mathrm{WL}_t = a + bt + c\mathrm{AP}_t$$

While there would be a slight efficiency advantage in working with just one regression, the approach as implemented in this report conforms more closely to the data analysis presented in Section 2 and the modeling presented in Section 4.2.1.

- The modeling and Step 2 calculation of $d\mathrm{DWL}/d\mathrm{AP}$ assume that pressure is known perfectly. An alternative model of the tank waste that incorporates the measurement error in atmospheric pressure (but ignores the detrending of surface level) is

$$\begin{aligned} \mathrm{wl} &= a - \frac{c}{\pi r^2 P^2}\,\mathrm{ap} \\ \mathrm{WL} &= \mathrm{wl} + \epsilon_{\mathrm{wl}} \\ \mathrm{AP} &= \mathrm{ap} + \epsilon_{\mathrm{ap}} \end{aligned} \tag{8}$$

where WL and AP are the observed waste level and corresponding atmospheric pressure; and wl and ap are the same quantities without observational error (compare the first equation with Equation (4)). In the context of this alternative model, Step 2 would ideally result in an estimate of the quantity $-c/(\pi r^2 P^2)$ in Equation (8). As discussed in Fuller (1987), the ordinary least squares estimate (calculated in Step 2) is biased in this alternative model. The least squares estimate is, in the context of Equation (8), unbiased for

$$\frac{\sigma^2_{\mathrm{e.ap}}}{\sigma^2_{\mathrm{e.ap}} + \sigma^2_{\mathrm{ap}}}\,\frac{-c}{\pi r^2 P^2} \tag{9}$$

where $\sigma^2_{\mathrm{e.ap}}$ is the error variance of the atmospheric pressure measurements, and σ^2_{ap} is the variance of the "true" atmospheric pressure. The quantity multiplying $-c/(\pi r^2 P^2)$ in Equation (9) is always less than 1; therefore, *any of the slope estimates reported in this document are expected to result in under-estimates of trapped gas volumes.* However, for detecting the existence of trapped gas, the quantities used in this report work well under the model described by Equation (8).

The modeling in this section merely supports the screening calculation as it currently stands. The work can and should be used to further refine the screening calculation, especially regarding the connection between a rise in waste level and an increase in magnitude of $d\mathrm{DWL}/d\mathrm{AP}$.

4.3 The Screening Calculation

The previous subsections described the screening process as breaking the waste level data into time intervals and calculating slopes $d\mathrm{DWL}/d\mathrm{AP}$ for those time intervals. This subsection describes how the information from those calculations is used to flag a tank as one that contains trapped gas.

The assumptions that drive the flagging are:

1. In the absence of trapped gas, an equal number of positive and negative $d\mathrm{DWL}/d\mathrm{AP}$ estimates will (tend to) be calculated; in the presence of trapped gas, the $d\mathrm{DWL}/d\mathrm{AP}$ estimates will tend to be negative.

2. The measurements in each interval are stochastically independent.

The flagging is done by evaluating the proportion of intervals for which the calculated slopes are negative. The tank is flagged as containing trapped gas when this proportion is so large as to be highly unlikely if the tank does not contain trapped gas. Specifically, if this proportion is enough larger than 0.5 that the probability of seeing that many negative slopes is less than 0.05, then the tank is flagged. See the discussion in Section 5, as well as Table 2.

Thus, the detection of trapped gas is based on the proportion of negative dDWL/dAP estimates. Formally, the flagging is a statistical test of hypothesis about a proportion, and is described in numerous references, including Ross (1987) and Fleiss (1981). The hypothesis test decides between

H_0: Proportion of negative slopes = 0.5
and
H_1: Proportion of negative slopes > 0.5

where, as described in Assumption 1, H_1 corresponds to the tank waste containing trapped gas and H_0 to the tank waste not containing trapped gas.

Note that there are 305 tank/instrument combinations leading to a screening calculation in this report. For a 95% confidence level, the expected number of "false positives" is $305 \times 0.05 = 15.25$ (so that each test has a 0.05 chance of mistakenly deciding H_1 when H_0 is true; in statistics references, 0.05 is referred to as the "size" of the hypothesis test). A "false positive" refers to mistakenly flagging a tank as containing trapped gas. Running the tests at size=0.01 instead of 0.05 would result in fewer false positives; $305 \times 0.01 = 3.05$. It turns out that using this "size" would have resulted in flagging 45 tanks (instead of 58); see Table 2. Setting the size of the test to 0.01 results in fewer false positives, but has a larger chance of missing some tanks which contain trapped gas.

Alternative Methods of Setting the Indicator Flag

The following options were considered for flagging the tanks based on the estimated slopes, but were rejected for the reasons described below.

An alternative procedure for flagging a tank is to look for a 95% confidence interval (CI) for the estimated slope below zero. That is, if a tank has one or more CIs completely below zero, flag the tank. One problem with this procedure is that too many false positives are possible. This procedure detects or flags 150 tanks, based on the calculations done for this report. A further problem with this procedure is that, for weekly tank level and pressure measurements, insufficient data may be available to detect a significant amount of gas.

Yet another option is to consider the proportion of 95% CIs entirely below zero. If the observed proportion is large enough, flag the tank. This amounts to the hypothesis test

H_0: Proportion of negative CIs = 0.025
and
H_1: Proportion of negative CIs > 0.025

This procedure also results in about 15.25 false positives. The first test is preferable to this one because of the additional overhead in statistical assumptions driving the choice of 0.025.

While no tanks have been flagged in this report based on either of the two alternative procedures *and neither of the above procedures is preferable to that described above*, the results from these procedures may be obtained from Table 4, which appears in the next section.

5 Screening Calculation Results

This section discusses the results of the screening process. The flagging of tanks based on the screening calculation is described in Section 5.1, a ranking of the tanks based on the calculated slopes is presented in Section 5.2, and the quality of the correlation (of detrended waste level with atmospheric pressure) is summarized in Section 5.3.

5.1 Flagging the Tanks

This section presents the results of applying the screening calculation to the available data for all tank and instrument combinations. As discussed earlier, detection of trapped gas is based on the number of negative estimates of dDWL/dAP. A tank is flagged as having trapped gas if any tank/instrument screening results in an excessively large proportion of negative slopes. Table 2 summarizes these calculations. Table 3 lists the 58 tanks that were flagged by this screening process. Finally, Table 4 is structured like Table 2, and includes sufficient information to perform the screening based on the two alternative procedures discussed in Section 4.3 (These results were not used to derive the list of 58 tanks in Table 3).

For each tank and instrument combination, the number of time intervals for which the slope could be calculated (from Step 2) is shown in the column labeled `# Ints`. The columns labeled `Raw` and `Detrended`, show the number of intervals for which the calculated slope is negative, based on the raw (Step 2e.i) and detrended (Step 2e.ii) observations of the waste level, respectively. In the same two columns, each of these negative slope counts is followed by a number in parentheses, which is the probability of observing the indicated number of negative slopes (or more) out of the total number of intervals, *if, in fact, the chances are 50-50 that the slope is negative.* A tank is flagged if either of these numbers (in parentheses) is less than 0.05.

For the manual tape data (MT column), the large number of high probabilities is due to the many "hard zeroes" in the regressions. That is, the manual tape measurements were the same for many intervals, so the estimates of dDWL/dAP and the corresponding standard errors are reported as zero. These zeroes inflate the probabilities in the tables and do not imply that dDWL/dAP tends to be positive for manual tape waste level measurements.

Note that the screening procedure based on negative slopes requires at least five time intervals to detect trapped gas. Since ENRAF data have not been taken for very long, they do not include many useful time intervals. Despite this problem, two tanks were "caught" by the screening procedure with ENRAF data, S–106 and S–111. For purposes of this screening exercise, the issue is fairly innocuous, since the FIC data provide good information and coverage of the tanks currently monitored with the ENRAF. There are numerous "fixes" for this particular procedural defect. For instance, one could reduce the target number of days in an interval from 60 to 30 or 15, thereby increasing the number of intervals. Another alternative would be to look at the test based on the proportion of negative confidence intervals for the slopes (the second alternate method in Section 4.3). For the ENRAF measurements, the tanks that would be flagged by this alternative are BX–106, C–103, S–107, T–102, T–107, T–109, U–106 and U–109.

Fourteen tanks were flagged based upon the `Neutron ILL` data alone — a surprising result considering its low measurement accuracy and the small number of intervals available.

Table 3 lists the tanks that were flagged by the screening procedure (as indicated by the word "gas"), and the type of measurement that led to flagging. The characters "ng" (no gas) mean that there were data of that particular type for the tank and that the screening calculation did not flag the tank. A dash means either that no data was available, or that not enough data was available to do a screening calculation.

Four tanks on the flammable gas watch list were not caught by this screening procedure: AX–101, S–112, SX–109, and T–110. Of these tanks, T–110 has a sinusoidal surface level measurement pattern that is unique among the Hanford tanks (see page 289 of this report). Tank SX–109 is on the watch list because its headspace is connected to other tanks on the flammable gas watch list. Tank S–112 FIC surface level measurements (see page 236) show neither the rise associated with a flammable gas watch list tank nor the response of waste level to changes in atmospheric pressure; however, the liquid level measurements are rising, as shown by the ILL data (see page 235). For Tank AX–101, the SACS database does not have enough data to suggest a reason for the flagging failure.

Some of the flagged tanks have seen recent tank transfer activity. For instance, Tank AW–106 is flagged because of manual tape level data. However, the plot of AW–106 manual tape data (see page 104) shows that the tank has recently been drawn down significantly. The FIC data for this tank (see page 103) show the same transfer record and also indicate that the tank contained trapped gas back in the early 1990s. A more refined analysis than the screening calculation in this report is required to decide the *current* status of Tank AW–106.

The other tanks in Table 3 with transfer events are A–103, AP–105, AP–107, BX–104, BX–107, BY–102, BY–103, BY–109, C–107, SX–104, T–111, TX–107, TY–102, and TY–103. Additional work is required to determine the current state of these tanks.

Table 2: *(continued)*

Tank	FIC			ENRAF			MT			Neutron ILL		
	# Ints.	Raw	Detrended	# Ints.	Raw	Detrended	# Ints.	Raw	Detrended	# Ints.	Raw	Detrended
BX-111	–	–	–	–	–	–	84	44(0.372)	43(0.457)	8	4(0.637)	4(0.637)
BX-112	79	48(0.036)	56(0.000)	–	–	–	10	5(0.623)	5(0.623)	–	–	–
BY-101	–	–	–	–	–	–	23	9(0.895)	9(0.895)	8	7(0.035)	7(0.035)
BY-102	–	–	–	–	–	–	82	58(0.000)	60(0.000)	7	4(0.500)	2(0.938)
BY-103	–	–	–	–	–	–	75	44(0.083)	46(0.032)	9	5(0.500)	4(0.746)
BY-104	–	–	–	–	–	–	36	15(0.879)	15(0.879)	8	3(0.855)	4(0.637)
BY-105	–	–	–	–	–	–	67	30(0.836)	28(0.929)	8	7(0.035)	6(0.145)
BY-106	–	–	–	–	–	–	74	44(0.065)	43(0.100)	8	5(0.363)	5(0.363)
BY-107	–	–	–	–	–	–	27	9(0.974)	9(0.974)	7	5(0.227)	4(0.500)
BY-108	–	–	–	–	–	–	36	16(0.797)	19(0.434)	–	–	–
BY-109	82	72(0.000)	73(0.000)	–	–	–	–	–	–	8	5(0.363)	5(0.363)
BY-110	–	–	–	–	–	–	35	19(0.368)	21(0.155)	8	5(0.363)	5(0.363)
BY-111	–	–	–	–	–	–	35	13(0.955)	14(0.912)	7	5(0.227)	4(0.500)
BY-112	–	–	–	–	–	–	35	18(0.500)	18(0.500)	4	1(0.938)	1(0.938)
C-101	–	–	–	–	–	–	30	11(0.951)	10(0.979)	–	–	–
C-102	65	35(0.310)	34(0.402)	–	–	–	–	–	–	–	–	–
C-103	81	36(0.867)	39(0.672)	5	3(0.500)	3(0.500)	–	–	–	–	–	–
C-104	80	51(0.009)	52(0.005)	–	–	–	1	1(0.500)	0(1.000)	–	–	–
C-105	70	40(0.141)	42(0.060)	–	–	–	6	6(0.016)	4(0.344)	–	–	–
C-106	53	30(0.205)	31(0.136)	5	3(0.500)	4(0.187)	–	–	–	–	–	–
C-107	81	61(0.000)	63(0.000)	–	–	–	–	–	–	–	–	–
C-108	–	–	–	–	–	–	28	12(0.828)	11(0.908)	–	–	–
C-109	–	–	–	–	–	–	30	4(1.000)	6(1.000)	–	–	–
C-110	–	–	–	–	–	–	83	38(0.810)	34(0.961)	–	–	–
C-111	–	–	–	–	–	–	31	5(1.000)	6(1.000)	–	–	–
C-112	–	–	–	–	–	–	69	26(0.985)	26(0.985)	–	–	–
C-201	–	–	–	–	–	–	26	7(0.995)	9(0.962)	–	–	–
C-202	–	–	–	–	–	–	26	7(0.995)	4(1.000)	–	–	–
C-203	–	–	–	–	–	–	26	16(0.163)	12(0.721)	–	–	–
C-204	–	–	–	–	–	–	30	13(0.819)	14(0.708)	–	–	–
S-101	29	25(0.000)	27(0.000)	–	–	–	3	3(0.125)	2(0.500)	8	5(0.363)	6(0.145)
S-102	95	95(0.000)	94(0.000)	–	–	–	2	2(0.250)	2(0.250)	7	6(0.062)	6(0.062)
S-103	74	68(0.000)	73(0.000)	4	4(0.062)	4(0.062)	2	2(0.250)	2(0.250)	8	5(0.363)	5(0.363)
S-104	–	–	–	–	–	–	31	10(0.985)	10(0.985)	2	0(1.000)	0(1.000)
S-105	46	26(0.231)	23(0.559)	–	–	–	2	1(0.750)	1(0.750)	8	7(0.035)	7(0.035)
S-106	80	79(0.000)	78(0.000)	5	5(0.031)	5(0.031)	2	1(0.750)	2(0.250)	8	5(0.363)	7(0.035)
S-107	79	69(0.000)	72(0.000)	3	1(0.875)	3(0.125)	2	1(0.750)	1(0.750)	–	–	–
S-108	41	19(0.734)	16(0.941)	–	–	–	60	21(0.993)	20(0.997)	8	4(0.637)	4(0.637)
S-109	55	29(0.394)	29(0.394)	–	–	–	2	0(1.000)	1(0.750)	8	8(0.004)	8(0.004)
S-110	65	35(0.310)	36(0.229)	–	–	–	2	2(0.250)	1(0.750)	7	4(0.500)	4(0.500)
S-111	76	75(0.000)	75(0.000)	6	6(0.016)	5(0.109)	3	1(0.875)	1(0.875)	8	6(0.145)	6(0.145)
S-112	59	20(0.996)	23(0.966)	–	–	–	2	1(0.750)	1(0.750)	7	6(0.062)	6(0.062)
SX-101	20	14(0.058)	16(0.006)	–	–	–	23	13(0.339)	17(0.017)	8	4(0.637)	5(0.363)
SX-102	23	21(0.000)	21(0.000)	–	–	–	12	7(0.387)	8(0.194)	8	2(0.965)	4(0.637)
SX-103	61	58(0.000)	61(0.000)	–	–	–	22	17(0.008)	15(0.067)	8	5(0.363)	5(0.363)
SX-104	42	30(0.004)	35(0.000)	–	–	–	11	6(0.500)	4(0.887)	–	–	–
SX-105	27	21(0.003)	24(0.000)	–	–	–	17	3(0.999)	1(1.000)	9	6(0.254)	6(0.254)
SX-106	53	43(0.000)	51(0.000)	3	3(0.125)	3(0.125)	21	7(0.961)	8(0.905)	10	9(0.011)	7(0.172)
SX-107	–	–	–	–	–	–	30	5(1.000)	5(1.000)	–	–	–
SX-108	–	–	–	–	–	–	28	0(1.000)	0(1.000)	–	–	–
SX-109	–	–	–	–	–	–	29	3(1.000)	2(1.000)	–	–	–
SX-110	–	–	–	–	–	–	29	4(1.000)	3(1.000)	–	–	–
SX-111	–	–	–	–	–	–	28	3(1.000)	3(1.000)	–	–	–
SX-112	–	–	–	–	–	–	28	4(1.000)	4(1.000)	–	–	–
SX-113	–	–	–	–	–	–	30	8(0.997)	7(0.999)	–	–	–
SX-114	–	–	–	–	–	–	30	5(1.000)	4(1.000)	–	–	–
SX-115	–	–	–	–	–	–	32	4(1.000)	4(1.000)	–	–	–
SY-101	72	43(0.062)	54(0.000)	3	2(0.500)	3(0.125)	51	26(0.500)	33(0.024)	–	–	–
SY-102	35	18(0.500)	21(0.155)	3	3(0.125)	2(0.500)	36	22(0.121)	22(0.121)	–	–	–
SY-103	58	39(0.006)	43(0.000)	4	3(0.312)	4(0.062)	68	35(0.452)	35(0.452)	–	–	–

Table 2: Proportion of negative estimates of dDWL/dAP by tank and instrument

Tank	FIC			ENRAF			MT			Neutron ILL		
	# Ints.	Raw	Detrended	# Ints.	Raw	Detrended	# Ints.	Raw	Detrended	# Ints.	Raw	Detrended
A-101	5	5(0.031)	5(0.031)	–	–	–	61	41(0.005)	39(0.020)	7	6(0.062)	6(0.062)
A-102	53	27(0.500)	27(0.500)	–	–	–	–	–	–	–	–	–
A-103	49	36(0.001)	39(0.000)	–	–	–	7	5(0.227)	4(0.500)	10	7(0.172)	5(0.623)
A-104	–	–	–	–	–	–	20	7(0.942)	6(0.979)	–	–	–
A-105	–	–	–	–	–	–	21	8(0.905)	9(0.808)	–	–	–
A-106	16	9(0.402)	10(0.227)	–	–	–	–	–	–	–	–	–
AN-101	60	29(0.651)	31(0.449)	–	–	–	–	–	–	–	–	–
AN-102	70	33(0.725)	37(0.360)	–	–	–	–	–	–	–	–	–
AN-103	64	52(0.000)	54(0.000)	–	–	–	–	–	–	–	–	–
AN-104	75	45(0.053)	57(0.000)	–	–	–	–	–	–	–	–	–
AN-105	68	49(0.000)	53(0.000)	–	–	–	–	–	–	–	–	–
AN-106	76	33(0.897)	40(0.366)	–	–	–	–	–	–	–	–	–
AN-107	77	37(0.676)	40(0.410)	–	–	–	–	–	–	–	–	–
AP-101	46	23(0.559)	21(0.769)	–	–	–	50	23(0.760)	25(0.556)	–	–	–
AP-102	32	17(0.430)	21(0.055)	–	–	–	38	20(0.436)	18(0.686)	–	–	–
AP-103	40	17(0.866)	21(0.437)	–	–	–	43	26(0.111)	25(0.180)	–	–	–
AP-104	47	22(0.720)	19(0.928)	–	–	–	39	19(0.625)	19(0.625)	–	–	–
AP-105	46	30(0.027)	32(0.006)	–	–	–	47	27(0.191)	28(0.121)	–	–	–
AP-106	46	21(0.769)	23(0.559)	–	–	–	49	27(0.284)	23(0.716)	–	–	–
AP-107	47	32(0.009)	30(0.039)	–	–	–	32	19(0.189)	19(0.189)	–	–	–
AP-108	60	30(0.551)	28(0.741)	–	–	–	56	32(0.175)	27(0.656)	–	–	–
AW-101	42	22(0.439)	30(0.004)	–	–	–	53	32(0.084)	28(0.392)	–	–	–
AW-102	43	21(0.620)	19(0.820)	–	–	–	33	14(0.852)	16(0.636)	–	–	–
AW-103	45	26(0.186)	37(0.000)	–	–	–	44	29(0.024)	22(0.560)	–	–	–
AW-104	62	40(0.015)	46(0.000)	–	–	–	52	28(0.339)	28(0.339)	–	–	–
AW-105	48	24(0.557)	22(0.765)	–	–	–	63	33(0.401)	32(0.500)	–	–	–
AW-106	55	25(0.791)	33(0.089)	–	–	–	49	29(0.126)	32(0.022)	–	–	–
AX-101	19	12(0.180)	12(0.180)	–	–	–	–	–	–	7	3(0.773)	3(0.773)
AX-102	–	–	–	–	–	–	55	22(0.948)	19(0.993)	–	–	–
AX-103	47	32(0.009)	31(0.020)	–	–	–	–	–	–	–	–	–
AX-104	–	–	–	–	–	–	23	10(0.798)	8(0.953)	–	–	–
AY-101	33	21(0.081)	17(0.500)	–	–	–	53	31(0.136)	34(0.027)	–	–	–
AY-102	73	29(0.970)	28(0.983)	–	–	–	60	33(0.259)	29(0.651)	–	–	–
AZ-101	35	21(0.155)	19(0.368)	–	–	–	58	38(0.012)	32(0.256)	–	–	–
AZ-102	31	15(0.640)	16(0.500)	–	–	–	85	42(0.586)	45(0.332)	–	–	–
B-101	18	7(0.881)	9(0.593)	–	–	–	–	–	–	–	–	–
B-102	58	28(0.653)	30(0.448)	–	–	–	11	3(0.967)	4(0.887)	–	–	–
B-103	34	16(0.696)	14(0.885)	–	–	–	–	–	–	–	–	–
B-104	–	–	–	–	–	–	29	10(0.969)	10(0.969)	8	4(0.637)	5(0.363)
B-105	–	–	–	–	–	–	32	7(1.000)	7(1.000)	6	2(0.891)	2(0.891)
B-106	60	30(0.551)	25(0.922)	–	–	–	–	–	–	–	–	–
B-107	–	–	–	–	–	–	42	18(0.860)	18(0.860)	–	–	–
B-108	36	21(0.203)	19(0.434)	–	–	–	–	–	–	–	–	–
B-109	–	–	–	–	–	–	31	7(1.000)	6(1.000)	–	–	–
B-110	–	–	–	–	–	–	32	11(0.975)	11(0.975)	2	2(0.250)	2(0.250)
B-111	29	12(0.868)	16(0.356)	–	–	–	–	–	–	2	1(0.750)	1(0.750)
B-112	57	27(0.702)	27(0.702)	–	–	–	11	6(0.500)	7(0.274)	–	–	–
B-201	–	–	–	–	–	–	37	11(0.996)	12(0.990)	–	–	–
B-202	–	–	–	–	–	–	48	14(0.999)	13(1.000)	–	–	–
B-203	–	–	–	–	–	–	35	11(0.992)	13(0.955)	–	–	–
B-204	–	–	–	–	–	–	44	10(1.000)	11(1.000)	–	–	–
BX-101	–	–	–	–	–	–	27	14(0.500)	13(0.649)	–	–	–
BX-102	–	–	–	–	–	–	31	7(1.000)	7(1.000)	–	–	–
BX-103	50	18(0.984)	18(0.984)	–	–	–	–	–	–	–	–	–
BX-104	69	46(0.004)	45(0.008)	–	–	–	11	3(0.967)	3(0.967)	–	–	–
BX-105	22	9(0.857)	9(0.857)	–	–	–	12	7(0.387)	8(0.194)	–	–	–
BX-106	78	40(0.455)	40(0.455)	3	2(0.500)	2(0.500)	12	2(0.997)	2(0.997)	–	–	–
BX-107	73	59(0.000)	59(0.000)	–	–	–	–	–	–	–	–	–
BX-108	–	–	–	–	–	–	18	6(0.952)	7(0.881)	–	–	–
BX-109	55	28(0.500)	29(0.394)	–	–	–	–	–	–	–	–	–
BX-110	–	–	–	–	–	–	43	17(0.937)	16(0.967)	–	–	–

Table 2: *(continued)*

Tank	FIC			ENRAF			MT			Neutron ILL		
	# Ints.	Raw	Detrended	# Ints.	Raw	Detrended	# Ints.	Raw	Detrended	# Ints.	Raw	Detrended
T-101	69	30(0.886)	31(0.832)	–	–	–	3	1(0.875)	1(0.875)	–	–	–
T-102	30	13(0.819)	12(0.900)	4	1(0.938)	1(0.938)	–	–	–	–	–	–
T-103	23	12(0.500)	13(0.339)	–	–	–	–	–	–	–	–	–
T-104	–	–	–	–	–	–	76	30(0.975)	33(0.897)	8	5(0.363)	5(0.363)
T-105	22	8(0.933)	7(0.974)	–	–	–	2	2(0.250)	2(0.250)	–	–	–
T-106	21	8(0.905)	7(0.961)	–	–	–	–	–	–	–	–	–
T-107	77	48(0.020)	56(0.000)	4	4(0.062)	4(0.062)	–	–	–	–	–	–
T-108	–	–	–	–	–	–	36	9(0.999)	12(0.986)	–	–	–
T-109	21	12(0.332)	11(0.500)	2	1(0.750)	1(0.750)	–	–	–	–	–	–
T-110	65	37(0.161)	36(0.229)	–	–	–	–	–	–	7	3(0.773)	3(0.773)
T-111	80	44(0.217)	51(0.009)	–	–	–	–	–	–	7	4(0.500)	4(0.500)
T-112	40	12(0.997)	11(0.999)	–	–	–	–	–	–	–	–	–
T-201	–	–	–	–	–	–	40	11(0.999)	11(0.999)	–	–	–
T-202	–	–	–	–	–	–	34	10(0.995)	8(1.000)	–	–	–
T-203	–	–	–	–	–	–	29	9(0.988)	12(0.868)	–	–	–
T-204	–	–	–	–	–	–	37	9(1.000)	8(1.000)	–	–	–
TX-101	55	30(0.295)	31(0.209)	–	–	–	–	–	–	–	–	–
TX-102	–	–	–	–	–	–	11	9(0.033)	7(0.274)	7	5(0.227)	5(0.227)
TX-103	14	8(0.395)	9(0.212)	–	–	–	–	–	–	–	–	–
TX-104	25	15(0.212)	13(0.500)	–	–	–	–	–	–	–	–	–
TX-105	–	–	–	–	–	–	18	9(0.593)	11(0.240)	–	–	–
TX-106	–	–	–	–	–	–	15	7(0.696)	5(0.941)	7	5(0.227)	6(0.062)
TX-107	43	22(0.500)	29(0.016)	–	–	–	–	–	–	–	–	–
TX-108	19	6(0.968)	6(0.968)	–	–	–	–	–	–	2	2(0.250)	1(0.750)
TX-109	16	10(0.227)	7(0.773)	–	–	–	–	–	–	8	4(0.637)	3(0.855)
TX-110	–	–	–	–	–	–	15	11(0.059)	9(0.304)	8	5(0.363)	4(0.637)
TX-111	–	–	–	–	–	–	16	13(0.011)	8(0.598)	8	7(0.035)	7(0.035)
TX-112	–	–	–	–	–	–	16	10(0.227)	13(0.011)	8	8(0.004)	8(0.004)
TX-113	–	–	–	–	–	–	17	6(0.928)	6(0.928)	8	6(0.145)	7(0.035)
TX-114	–	–	–	–	–	–	12	7(0.387)	8(0.194)	8	4(0.637)	5(0.363)
TX-115	–	–	–	–	–	–	15	4(0.982)	4(0.982)	8	7(0.035)	8(0.004)
TX-116	–	–	–	–	–	–	18	7(0.881)	7(0.881)	–	–	–
TX-117	–	–	–	–	–	–	16	6(0.895)	6(0.895)	6	2(0.891)	3(0.656)
TX-118	14	9(0.212)	9(0.212)	–	–	–	–	–	–	9	4(0.746)	4(0.746)
TY-101	18	8(0.760)	8(0.760)	–	–	–	–	–	–	–	–	–
TY-102	50	31(0.059)	35(0.003)	–	–	–	–	–	–	–	–	–
TY-103	20	12(0.252)	15(0.021)	–	–	–	–	–	–	8	1(0.996)	2(0.965)
TY-104	48	26(0.333)	27(0.235)	–	–	–	–	–	–	–	–	–
TY-105	–	–	–	–	–	–	17	6(0.928)	7(0.834)	–	–	–
TY-106	–	–	–	–	–	–	21	10(0.668)	10(0.668)	–	–	–
U-101	–	–	–	–	–	–	25	8(0.978)	6(0.998)	–	–	–
U-102	21	18(0.001)	19(0.000)	–	–	–	–	–	–	8	7(0.035)	7(0.035)
U-103	79	78(0.000)	79(0.000)	4	4(0.062)	4(0.062)	–	–	–	8	7(0.035)	7(0.035)
U-104	–	–	–	–	–	–	17	4(0.994)	4(0.994)	–	–	–
U-105	63	56(0.000)	54(0.000)	3	3(0.125)	3(0.125)	28	20(0.018)	18(0.092)	7	6(0.062)	5(0.227)
U-106	81	54(0.002)	54(0.002)	3	1(0.875)	2(0.500)	–	–	–	8	6(0.145)	7(0.035)
U-107	79	78(0.000)	79(0.000)	4	4(0.062)	4(0.062)	–	–	–	7	6(0.062)	7(0.008)
U-108	22	21(0.000)	21(0.000)	–	–	–	–	–	–	8	6(0.145)	6(0.145)
U-109	81	81(0.000)	81(0.000)	2	2(0.250)	2(0.250)	–	–	–	8	5(0.363)	5(0.363)
U-110	19	9(0.676)	8(0.820)	–	–	–	–	–	–	–	–	–
U-111	18	10(0.407)	11(0.240)	–	–	–	–	–	–	7	5(0.227)	5(0.227)
U-112	–	–	–	–	–	–	18	4(0.996)	5(0.985)	–	–	–
U-201	–	–	–	–	–	–	30	12(0.900)	12(0.900)	–	–	–
U-202	–	–	–	–	–	–	27	8(0.990)	7(0.997)	–	–	–
U-203	–	–	–	–	–	–	18	6(0.952)	7(0.881)	–	–	–
U-204	–	–	–	–	–	–	28	15(0.425)	15(0.425)	–	–	–

Table 3: Tanks flagged by the screening calculation. Tank/instruments combinations are marked "gas", "ng" and "–" according to whether the tank/instrument was flagged as containing trapped gas, not flagged or there was insufficient data for the screening to proceed, respectively. An asterisk indicates tanks currently on the flammable gas watch list.

Tank	FIC	MT	ENRAF	Neutron ILL
A–101*	gas	gas	–	ng
A–103	gas	ng	–	ng
AN–103*	gas	–	–	–
AN–104*	gas	–	–	–
AN–105*	gas	–	–	–
AP–105	gas	ng	–	–
AP–107	gas	ng	–	–
AW–101*	gas	ng	–	–
AW–103	gas	gas	–	–
AW–104	gas	ng	–	–
AW–106	ng	gas	–	–
AX–103*	gas	–	–	–
AY–101	ng	gas	–	–
AZ–101	ng	gas	–	–
BX–104	gas	ng	–	–
BX–107	gas	–	–	–
BX–112	gas	ng	–	–
BY–101	–	ng	–	gas
BY–102	–	gas	–	ng
BY–103	–	gas	–	ng
BY–105	–	ng	–	gas
BY–109	gas	–	ng	ng
C–104	gas	ng	–	–
C–105	ng	gas	–	–
C–107	gas	–	–	–
S–101	gas	ng	–	ng
S–102*	gas	ng	–	ng
S–103	gas	ng	ng	ng
S–105	ng	ng	–	gas
S–106	gas	ng	gas	gas
S–107	gas	ng	ng	–
S–109	ng	ng	–	gas
S–111*	gas	ng	gas	ng
SX–101*	gas	gas	–	ng
SX–102*	gas	ng	–	ng
SX–103*	gas	gas	–	ng
SX–104*	gas	ng	–	ng
SX–105*	gas	ng	–	ng
SX–106*	gas	ng	ng	gas
SY–101*	gas	gas	ng	–
SY–103*	gas	ng	ng	–
T–107	gas	–	ng	–
T–111	gas	–	–	ng
TX–102	–	gas	–	ng
TX–107	gas	–	–	–
TX–111	–	gas	–	gas
TX–112	–	gas	–	gas
TX–113	–	ng	–	gas
TX–115	–	ng	–	gas
TY–102	gas	–	–	–
TY–103	gas	–	–	ng
U–102	gas	–	–	gas
U–103*	gas	–	ng	gas
U–105*	gas	gas	ng	ng
U–106	gas	–	ng	gas
U–107*	gas	–	ng	gas
U–108*	gas	–	–	ng
U–109*	gas	–	ng	ng

Table 4: Proportion of negative confidence intervals for the dDWL/dAP estimates by tank and instrument

Tank	FIC			ENRAF			MT			Neutron ILL		
	# Ints.	Raw	Detrended	# Ints.	Raw	Detrended	# Ints.	Raw	Detrended	# Ints.	Raw	Detrended
A-101	5	0(1.000)	1(0.119)	–	–	–	61	5(0.018)	6(0.004)	7	0(1.000)	0(1.000)
A-102	53	3(0.147)	2(0.383)	–	–	–	–	–	–	–	–	–
A-103	49	19(0.000)	20(0.000)	–	–	–	7	0(1.000)	1(0.162)	10	0(1.000)	0(1.000)
A-104	–	–	–	–	–	–	20	1(0.397)	0(1.000)	–	–	–
A-105	–	–	–	–	–	–	21	0(1.000)	0(1.000)	–	–	–
A-106	16	0(1.000)	1(0.333)	–	–	–	–	–	–	–	–	–
AN-101	60	5(0.017)	3(0.190)	–	–	–	–	–	–	–	–	–
AN-102	70	3(0.255)	3(0.255)	–	–	–	–	–	–	–	–	–
AN-103	64	33(0.000)	35(0.000)	–	–	–	–	–	–	–	–	–
AN-104	75	15(0.000)	24(0.000)	–	–	–	–	–	–	–	–	–
AN-105	68	18(0.000)	24(0.000)	–	–	–	–	–	–	–	–	–
AN-106	76	6(0.012)	6(0.012)	–	–	–	–	–	–	–	–	–
AN-107	77	4(0.127)	5(0.044)	–	–	–	–	–	–	–	–	–
AP-101	46	4(0.028)	2(0.320)	–	–	–	50	0(1.000)	2(0.356)	–	–	–
AP-102	32	2(0.190)	2(0.190)	–	–	–	38	4(0.015)	4(0.015)	–	–	–
AP-103	40	2(0.264)	4(0.017)	–	–	–	43	5(0.004)	1(0.663)	–	–	–
AP-104	47	4(0.030)	2(0.329)	–	–	–	39	7(0.000)	3(0.073)	–	–	–
AP-105	46	5(0.006)	10(0.000)	–	–	–	47	6(0.001)	4(0.030)	–	–	–
AP-106	46	3(0.108)	1(0.688)	–	–	–	49	6(0.001)	4(0.034)	–	–	–
AP-107	47	9(0.000)	5(0.006)	–	–	–	32	5(0.001)	4(0.008)	–	–	–
AP-108	60	2(0.444)	2(0.444)	–	–	–	56	7(0.000)	5(0.013)	–	–	–
AW-101	42	10(0.000)	15(0.000)	–	–	–	53	7(0.000)	5(0.010)	–	–	–
AW-102	43	3(0.092)	5(0.004)	–	–	–	33	3(0.049)	4(0.009)	–	–	–
AW-103	45	8(0.000)	13(0.000)	–	–	–	44	3(0.097)	4(0.024)	–	–	–
AW-104	62	18(0.000)	19(0.000)	–	–	–	52	3(0.141)	3(0.141)	–	–	–
AW-105	48	4(0.032)	8(0.000)	–	–	–	63	4(0.073)	6(0.005)	–	–	–
AW-106	55	7(0.000)	13(0.000)	–	–	–	49	4(0.034)	8(0.000)	–	–	–
AX-101	19	3(0.011)	2(0.081)	–	–	–	–	–	–	7	0(1.000)	0(1.000)
AX-102	–	–	–	–	–	–	55	1(0.752)	2(0.401)	–	–	–
AX-103	47	4(0.030)	3(0.113)	–	–	–	–	–	–	–	–	–
AX-104	–	–	–	–	–	–	23	1(0.441)	0(1.000)	–	–	–
AY-101	33	1(0.566)	2(0.199)	–	–	–	53	4(0.043)	2(0.383)	–	–	–
AY-102	73	8(0.000)	8(0.000)	–	–	–	60	6(0.004)	2(0.444)	–	–	–
AZ-101	35	1(0.588)	1(0.588)	–	–	–	58	9(0.000)	3(0.177)	–	–	–
AZ-102	31	2(0.181)	0(1.000)	–	–	–	85	9(0.000)	5(0.062)	–	–	–
B-101	18	2(0.073)	0(1.000)	–	–	–	–	–	–	–	–	–
B-102	58	4(0.057)	4(0.057)	–	–	–	11	0(1.000)	0(1.000)	–	–	–
B-103	34	1(0.577)	2(0.209)	–	–	–	–	–	–	–	–	–
B-104	–	–	–	–	–	–	29	0(1.000)	0(1.000)	8	0(1.000)	1(0.183)
B-105	–	–	–	–	–	–	32	1(0.555)	1(0.555)	6	0(1.000)	0(1.000)
B-106	60	4(0.063)	4(0.063)	–	–	–	–	–	–	–	–	–
B-107	–	–	–	–	–	–	42	1(0.655)	1(0.655)	–	–	–
B-108	36	2(0.227)	2(0.227)	–	–	–	–	–	–	–	–	–
B-109	–	–	–	–	–	–	31	2(0.181)	2(0.181)	–	–	–
B-110	–	–	–	–	–	–	32	0(1.000)	0(1.000)	2	0(1.000)	0(1.000)
B-111	29	2(0.163)	1(0.520)	–	–	–	–	–	–	2	0(1.000)	0(1.000)
B-112	57	6(0.003)	5(0.014)	–	–	–	11	0(1.000)	0(1.000)	–	–	–
B-201	–	–	–	–	–	–	37	0(1.000)	0(1.000)	–	–	–
B-202	–	–	–	–	–	–	48	0(1.000)	1(0.703)	–	–	–
B-203	–	–	–	–	–	–	35	0(1.000)	0(1.000)	–	–	–
B-204	–	–	–	–	–	–	44	0(1.000)	0(1.000)	–	–	–
BX-101	–	–	–	–	–	–	27	2(0.146)	3(0.029)	–	–	–
BX-102	–	–	–	–	–	–	31	0(1.000)	1(0.544)	–	–	–
BX-103	50	2(0.356)	2(0.356)	–	–	–	–	–	–	–	–	–
BX-104	69	18(0.000)	18(0.000)	–	–	–	11	2(0.030)	1(0.243)	–	–	–
BX-105	22	1(0.427)	1(0.427)	–	–	–	12	0(1.000)	0(1.000)	–	–	–
BX-106	78	4(0.132)	3(0.310)	3	1(0.073)	0(1.000)	12	0(1.000)	0(1.000)	–	–	–
BX-107	73	30(0.000)	32(0.000)	–	–	–	–	–	–	–	–	–
BX-108	–	–	–	–	–	–	18	0(1.000)	0(1.000)	–	–	–
BX-109	55	8(0.000)	12(0.000)	–	–	–	–	–	–	–	–	–
BX-110	–	–	–	–	–	–	43	6(0.001)	4(0.022)	–	–	–

Table 4: *(continued)*

Tank	FIC			ENRAF			MT			Neutron ILL		
	# Ints.	Raw	Detrended	# Ints.	Raw	Detrended	# Ints.	Raw	Detrended	# Ints.	Raw	Detrended
BX-111	–	–	–	–	–	–	84	2(0.624)	6(0.019)	8	1(0.183)	0(1.000)
BX-112	79	19(0.000)	26(0.000)	–	–	–	10	0(1.000)	0(1.000)	–	–	–
BY-101	–	–	–	–	–	–	23	0(1.000)	0(1.000)	8	3(0.001)	2(0.016)
BY-102	–	–	–	–	–	–	82	12(0.000)	11(0.000)	7	0(1.000)	0(1.000)
BY-103	–	–	–	–	–	–	75	4(0.119)	3(0.289)	9	0(1.000)	0(1.000)
BY-104	–	–	–	–	–	–	36	0(1.000)	0(1.000)	8	0(1.000)	0(1.000)
BY-105	–	–	–	–	–	–	67	1(0.817)	2(0.502)	8	1(0.183)	1(0.183)
BY-106	–	–	–	–	–	–	74	5(0.038)	4(0.114)	8	0(1.000)	0(1.000)
BY-107	–	–	–	–	–	–	27	1(0.495)	1(0.495)	7	0(1.000)	1(0.162)
BY-108	–	–	–	–	–	–	36	5(0.002)	6(0.000)	–	–	–
BY-109	82	48(0.000)	49(0.000)	–	–	–	–	–	–	8	0(1.000)	0(1.000)
BY-110	–	–	–	–	–	–	35	1(0.588)	1(0.588)	8	0(1.000)	0(1.000)
BY-111	–	–	–	–	–	–	35	1(0.588)	1(0.588)	7	0(1.000)	1(0.162)
BY-112	–	–	–	–	–	–	35	4(0.011)	5(0.002)	4	0(1.000)	0(1.000)
C-101	–	–	–	–	–	–	30	1(0.532)	0(1.000)	–	–	–
C-102	65	1(0.807)	3(0.222)	–	–	–	–	–	–	–	–	–
C-103	81	8(0.001)	7(0.004)	5	1(0.119)	0(1.000)	–	–	–	–	–	–
C-104	80	9(0.000)	9(0.000)	–	–	–	1	0(1.000)	0(1.000)	–	–	–
C-105	70	11(0.000)	7(0.002)	–	–	–	6	0(1.000)	0(1.000)	–	–	–
C-106	53	5(0.010)	5(0.010)	5	3(0.000)	1(0.119)	–	–	–	–	–	–
C-107	81	19(0.000)	20(0.000)	–	–	–	–	–	–	–	–	–
C-108	–	–	–	–	–	–	28	1(0.508)	0(1.000)	–	–	–
C-109	–	–	–	–	–	–	30	0(1.000)	0(1.000)	–	–	–
C-110	–	–	–	–	–	–	83	2(0.617)	3(0.344)	–	–	–
C-111	–	–	–	–	–	–	31	0(1.000)	0(1.000)	–	–	–
C-112	–	–	–	–	–	–	69	1(0.826)	2(0.517)	–	–	–
C-201	–	–	–	–	–	–	26	1(0.482)	0(1.000)	–	–	–
C-202	–	–	–	–	–	–	26	0(1.000)	0(1.000)	–	–	–
C-203	–	–	–	–	–	–	26	3(0.026)	1(0.482)	–	–	–
C-204	–	–	–	–	–	–	30	0(1.000)	0(1.000)	–	–	–
S-101	29	20(0.000)	21(0.000)	–	–	–	3	0(1.000)	1(0.073)	8	0(1.000)	1(0.183)
S-102	95	76(0.000)	76(0.000)	–	–	–	2	2(0.001)	2(0.001)	7	0(1.000)	0(1.000)
S-103	74	47(0.000)	46(0.000)	4	4(0.000)	4(0.000)	2	1(0.049)	0(1.000)	8	1(0.183)	1(0.183)
S-104	–	–	–	–	–	–	31	1(0.544)	0(1.000)	2	0(1.000)	0(1.000)
S-105	46	1(0.688)	1(0.688)	–	–	–	2	1(0.049)	0(1.000)	8	0(1.000)	0(1.000)
S-106	80	65(0.000)	52(0.000)	5	5(0.000)	4(0.000)	2	0(1.000)	0(1.000)	8	2(0.016)	2(0.016)
S-107	79	25(0.000)	27(0.000)	3	0(1.000)	2(0.002)	2	0(1.000)	0(1.000)	–	–	–
S-108	41	3(0.083)	3(0.083)	–	–	–	60	2(0.444)	2(0.444)	8	0(1.000)	0(1.000)
S-109	55	1(0.752)	3(0.159)	–	–	–	2	0(1.000)	0(1.000)	8	1(0.183)	1(0.183)
S-110	65	4(0.080)	4(0.080)	–	–	–	2	0(1.000)	1(0.049)	7	1(0.162)	1(0.162)
S-111	76	68(0.000)	65(0.000)	6	4(0.000)	3(0.000)	3	0(1.000)	0(1.000)	8	0(1.000)	0(1.000)
S-112	59	2(0.436)	2(0.436)	–	–	–	2	0(1.000)	0(1.000)	7	1(0.162)	1(0.162)
SX-101	20	4(0.001)	4(0.001)	–	–	–	23	1(0.441)	1(0.441)	8	0(1.000)	0(1.000)
SX-102	23	13(0.000)	13(0.000)	–	–	–	12	2(0.035)	2(0.035)	8	0(1.000)	0(1.000)
SX-103	61	46(0.000)	38(0.000)	–	–	–	22	4(0.002)	4(0.002)	8	1(0.183)	1(0.183)
SX-104	42	6(0.001)	12(0.000)	–	–	–	11	1(0.243)	0(1.000)	–	–	–
SX-105	27	7(0.000)	9(0.000)	–	–	–	17	1(0.350)	0(1.000)	9	1(0.204)	0(1.000)
SX-106	53	27(0.000)	35(0.000)	3	3(0.000)	3(0.000)	21	0(1.000)	0(1.000)	10	2(0.025)	1(0.224)
SX-107	–	–	–	–	–	–	30	1(0.532)	1(0.532)	–	–	–
SX-108	–	–	–	–	–	–	28	0(1.000)	0(1.000)	–	–	–
SX-109	–	–	–	–	–	–	29	0(1.000)	0(1.000)	–	–	–
SX-110	–	–	–	–	–	–	29	1(0.520)	1(0.520)	–	–	–
SX-111	–	–	–	–	–	–	28	1(0.508)	0(1.000)	–	–	–
SX-112	–	–	–	–	–	–	28	0(1.000)	1(0.508)	–	–	–
SX-113	–	–	–	–	–	–	30	2(0.172)	1(0.532)	–	–	–
SX-114	–	–	–	–	–	–	30	0(1.000)	0(1.000)	–	–	–
SX-115	–	–	–	–	–	–	32	0(1.000)	0(1.000)	–	–	–
SY-101	72	20(0.000)	23(0.000)	3	2(0.002)	3(0.000)	51	5(0.009)	10(0.000)	–	–	–
SY-102	35	6(0.000)	3(0.057)	3	1(0.073)	1(0.073)	36	6(0.000)	2(0.227)	–	–	–
SY-103	58	6(0.003)	14(0.000)	4	2(0.004)	4(0.000)	68	3(0.242)	5(0.028)	–	–	–

Table 4: *(continued)*

Tank	FIC			ENRAF			MT			Neutron ILL		
	# Ints.	Raw	Detrended	# Ints.	Raw	Detrended	# Ints.	Raw	Detrended	# Ints.	Raw	Detrended
T-101	69	2(0.517)	1(0.826)	–	–	–	3	0(1.000)	0(1.000)	–	–	–
T-102	30	4(0.006)	4(0.006)	4	0(1.000)	1(0.096)	–	–	–	–	–	–
T-103	23	3(0.019)	2(0.112)	–	–	–	–	–	–	–	–	–
T-104	–	–	–	–	–	–	76	6(0.012)	4(0.123)	8	1(0.183)	1(0.183)
T-105	22	2(0.104)	2(0.104)	–	–	–	2	0(1.000)	0(1.000)	–	–	–
T-106	21	2(0.096)	1(0.412)	–	–	–	–	–	–	–	–	–
T-107	77	13(0.000)	11(0.000)	4	1(0.096)	0(1.000)	–	–	–	–	–	–
T-108	–	–	–	–	–	–	36	2(0.227)	2(0.227)	–	–	–
T-109	21	0(1.000)	1(0.412)	2	0(1.000)	0(1.000)	–	–	–	–	–	–
T-110	65	5(0.023)	2(0.486)	–	–	–	–	–	–	7	1(0.162)	1(0.162)
T-111	80	10(0.000)	6(0.015)	–	–	–	–	–	–	7	0(1.000)	0(1.000)
T-112	40	1(0.637)	0(1.000)	–	–	–	–	–	–	–	–	–
T-201	–	–	–	–	–	–	40	0(1.000)	0(1.000)	–	–	–
T-202	–	–	–	–	–	–	34	0(1.000)	0(1.000)	–	–	–
T-203	–	–	–	–	–	–	29	1(0.520)	0(1.000)	–	–	–
T-204	–	–	–	–	–	–	37	0(1.000)	0(1.000)	–	–	–
TX-101	55	6(0.002)	7(0.000)	–	–	–	–	–	–	–	–	–
TX-102	–	–	–	–	–	–	11	0(1.000)	1(0.243)	7	1(0.162)	1(0.162)
TX-103	14	1(0.298)	2(0.047)	–	–	–	–	–	–	–	–	–
TX-104	25	2(0.129)	2(0.129)	–	–	–	–	–	–	–	–	–
TX-105	–	–	–	–	–	–	18	0(1.000)	0(1.000)	–	–	–
TX-106	–	–	–	–	–	–	15	1(0.316)	1(0.316)	7	1(0.162)	1(0.162)
TX-107	43	7(0.000)	6(0.001)	–	–	–	–	–	–	–	–	–
TX-108	19	0(1.000)	0(1.000)	–	–	–	–	–	–	2	0(1.000)	0(1.000)
TX-109	16	0(1.000)	0(1.000)	–	–	–	–	–	–	8	1(0.183)	1(0.183)
TX-110	–	–	–	–	–	–	15	1(0.316)	0(1.000)	8	0(1.000)	0(1.000)
TX-111	–	–	–	–	–	–	16	0(1.000)	0(1.000)	8	4(0.000)	3(0.001)
TX-112	–	–	–	–	–	–	16	1(0.333)	1(0.333)	8	4(0.000)	4(0.000)
TX-113	–	–	–	–	–	–	17	0(1.000)	0(1.000)	8	0(1.000)	1(0.183)
TX-114	–	–	–	–	–	–	12	1(0.262)	1(0.262)	8	0(1.000)	0(1.000)
TX-115	–	–	–	–	–	–	15	0(1.000)	0(1.000)	8	1(0.183)	1(0.183)
TX-116	–	–	–	–	–	–	18	0(1.000)	0(1.000)	–	–	–
TX-117	–	–	–	–	–	–	16	0(1.000)	0(1.000)	6	0(1.000)	0(1.000)
TX-118	14	1(0.298)	2(0.047)	–	–	–	–	–	–	9	0(1.000)	0(1.000)
TY-101	18	0(1.000)	0(1.000)	–	–	–	–	–	–	–	–	–
TY-102	50	19(0.000)	18(0.000)	–	–	–	–	–	–	–	–	–
TY-103	20	0(1.000)	3(0.013)	–	–	–	–	–	–	8	0(1.000)	0(1.000)
TY-104	48	10(0.000)	10(0.000)	–	–	–	–	–	–	–	–	–
TY-105	–	–	–	–	–	–	17	1(0.350)	0(1.000)	–	–	–
TY-106	–	–	–	–	–	–	21	2(0.096)	1(0.412)	–	–	–
U-101	–	–	–	–	–	–	25	1(0.469)	1(0.469)	–	–	–
U-102	21	7(0.000)	7(0.000)	–	–	–	–	–	–	8	1(0.183)	1(0.183)
U-103	79	63(0.000)	60(0.000)	4	4(0.000)	4(0.000)	–	–	–	8	0(1.000)	1(0.183)
U-104	–	–	–	–	–	–	17	1(0.350)	1(0.350)	–	–	–
U-105	63	29(0.000)	24(0.000)	3	3(0.000)	3(0.000)	28	3(0.032)	2(0.154)	7	0(1.000)	0(1.000)
U-106	81	13(0.000)	16(0.000)	3	0(1.000)	0(1.000)	–	–	–	8	2(0.016)	2(0.016)
U-107	79	67(0.000)	65(0.000)	4	4(0.000)	4(0.000)	–	–	–	7	0(1.000)	0(1.000)
U-108	22	11(0.000)	14(0.000)	–	–	–	–	–	–	8	0(1.000)	0(1.000)
U-109	81	68(0.000)	69(0.000)	2	0(1.000)	0(1.000)	–	–	–	8	1(0.183)	1(0.183)
U-110	19	0(1.000)	0(1.000)	–	–	–	–	–	–	–	–	–
U-111	18	0(1.000)	3(0.010)	–	–	–	–	–	–	7	1(0.162)	1(0.162)
U-112	–	–	–	–	–	–	18	0(1.000)	0(1.000)	–	–	–
U-201	–	–	–	–	–	–	30	2(0.172)	2(0.172)	–	–	–
U-202	–	–	–	–	–	–	27	0(1.000)	0(1.000)	–	–	–
U-203	–	–	–	–	–	–	18	0(1.000)	0(1.000)	–	–	–
U-204	–	–	–	–	–	–	28	2(0.154)	3(0.032)	–	–	–

5.2 Ranking the Tanks

A ranking of the tanks for degree of flammable gas hazard would be useful. Unfortunately, the information base supporting this document is insufficient for such a calculation. Indeed, the summaries presented in this document are, by themselves, not sufficient to estimate the amount of trapped gas in the tank waste; much less the explosive potential. The additional information and analyses needed to rank the tanks by degree of hazard would include density of tank waste, distribution of the gas in the tank, gas composition, tank headspace volume, headspace ventilation rates, probability of a gas release event (GRE), probability of an ignition and the amount of gas released in each GRE. This list is, no doubt, incomplete.

Accordingly, this subsection presents a less ambitious ranking of the tanks; the objective of the ranking presented is to order the tanks by the magnitude of the dDWL/dAP estimates.

There are many ways to order or rank the tanks on the basis of the regression summaries provided in this report. For instance, the means or medians of the estimated slopes could be used to rank the tanks. A potential difficulty with using the mean or median is that the uncertainty associated with each slope estimate is not directly reflected in these quantities. A natural way to incorporate the uncertainty information is to build a distributional summary of slope estimates; the summary may or may not explicitly incorporate the standard errors of the estimates. Then the distributional summaries would need to be ordered according to some scoring procedure.

Recapping the ranking procedure to take uncertainty into account: a distributional summary of the slope estimates is created for each combination of tank and instrument; then, a "probability score" is determined for each combination by comparing the summary distribution with a reference distribution; and finally, the tank/instrument combinations are sorted according to that score.

The distributional summary is calculated as

$$\frac{1}{n}\sum_{i=1}^{n}\phi((x-\hat{\beta}_i)/s_{\hat{\beta}_i}) \tag{10}$$

where $\phi(\cdot)$ is the density function of the standard Gaussian distribution[4], $\hat{\beta}$ is the slope estimate for the interval, $s_{\hat{\beta}}$ is the standard error of the slope estimate and x is a dummy-variable.

Letting $\boldsymbol{X}$ denote a quantity with the distribution of the calculated slopes for a particular tank/instrument combination, then the numerical quantity used to order the tanks is the probability that a slope randomly selected from $\boldsymbol{X}$ is less than a randomly selected value from a Gaussian distribution centered at zero with a standard deviation of 1. Centering the reference distribution around zero results in the interpretation that probabilities less than 0.5 suggest that the tank has trapped gas; however, no strict cutoffs are suggested here, nor does the author currently have a strategy for recommending a cutoff.

The probability that $\boldsymbol{X}$ is less than a value drawn from the reference distribution can be calculated as

$$\frac{1}{n}\sum_{i=1}^{n}\Phi\left(-\frac{\hat{\beta}_i}{\sqrt{s_{\hat{\beta}_i}^2+1}}\right)$$

where Φ is the cumulative distribution function of the standard Gaussian[5]. These probability scores have been calculated for the available data, and are presented in Table 5. The tanks are listed in ascending order of the resulting probability scores; *note that the lower the score the better*

[4] $\phi(x) = \exp\{-x^2/2\}/\sqrt{2\pi}$

[5] $\Phi(x) = \int_{-\infty}^{x}\phi(y)dy$

the indication of trapped gas. These probability scores take into account the magnitude of the slope estimates as well as their uncertainties.

The ordering shown in Table 5 is generally consistent with the flagging of the tanks described previously: tanks with a preponderance of negative slopes, as measured by the numerical score, are the same as the flagged tanks. The flagged tanks do not match this ordering precisely, since the flagging was based on the proportion of negative slopes *without regard to the magnitudes of the slopes*, while this ranking incorporates the sizes of the negative slopes and their uncertainties.

Among the early entries in Table 5, the discrepancies between this ranking and the flagged tanks are mostly tanks with ENRAF measurements; as discussed previously, the ENRAF data did not result in many flaggings since there were not enough intervals of measurements. The other notable discrepancy is the S-102 MT combination; this data did not result in a flag because it includes only two intervals, which are insufficient for a screening determination.

Table 5: Tank/instrument rankings according to slope distributions. The rankings are based on the probability that one of the estimated slope distributions is less than a value drawn from a reference distribution. Tanks marked with an asterisk are on the current Flammable Gas Watchlist. Tanks marked with a dagger are flagged by the screening procedure described in Section 4 of this report.

Tank	Instrument	Score
S-102 *	MT	0.231
S-106 †	FIC	0.237
SX-105 * †	FIC	0.267
SX-102 * †	FIC	0.276
S-102 * †	FIC	0.280
SX-103 * †	FIC	0.283
S-111 * †	FIC	0.308
S-106 †	ENRAF	0.334
SX-104 * †	FIC	0.350
SY-101 *	ENRAF	0.352
SX-106 * †	FIC	0.362
S-103 †	FIC	0.367
U-103 * †	FIC	0.370
AN-103 * †	FIC	0.371
SX-106 *	ENRAF	0.378
TX-102 †	MT	0.379
U-103 *	ENRAF	0.382
SY-101 * †	FIC	0.389
S-103	ENRAF	0.389
U-108 * †	FIC	0.391
U-109 * †	FIC	0.392
BY-109 †	FIC	0.392
A-101 * †	FIC	0.396
S-111 * †	ENRAF	0.399
U-107 * †	FIC	0.403
TX-112 †	Neutron ILL	0.404
U-107 *	ENRAF	0.404
U-105 *	ENRAF	0.410
SY-103 *	ENRAF	0.414
S-109 †	Neutron ILL	0.415
U-105 * †	FIC	0.416
TX-112 †	MT	0.422
S-112 *	Neutron ILL	0.431
U-102 †	FIC	0.432
SX-101 * †	FIC	0.434
TX-115 †	Neutron ILL	0.439
S-101 †	FIC	0.440
A-103 †	FIC	0.441
SX-103 * †	MT	0.441
S-112 *	MT	0.443
BY-102 †	MT	0.444
A-101 * †	MT	0.444
TX-110	MT	0.444
U-102 †	Neutron ILL	0.447
TX-111 †	Neutron ILL	0.448
S-106	MT	0.448
S-107 †	FIC	0.449
BY-101 †	Neutron ILL	0.449
SX-101 * †	MT	0.451
S-101	MT	0.451
SY-103 * †	FIC	0.454

Tank	Instrument	Score
AN-105 * †	FIC	0.455
SY-102	FIC	0.457
BX-107 †	FIC	0.457
C-106	ENRAF	0.459
U-105 * †	MT	0.460
BY-108	MT	0.460
AN-104 * †	FIC	0.460
S-103	MT	0.461
U-111	FIC	0.461
AW-106 †	MT	0.463
SY-102	MT	0.464
U-204	MT	0.465
BY-112	MT	0.466
TX-106	Neutron ILL	0.466
SX-102 *	MT	0.467
S-106 †	Neutron ILL	0.467
TY-103 †	FIC	0.467
TX-108	Neutron ILL	0.467
BY-106	MT	0.468
C-107 †	FIC	0.468
SY-101 * †	MT	0.468
TX-113 †	Neutron ILL	0.468
S-110	MT	0.469
TX-118	FIC	0.469
BY-105 †	Neutron ILL	0.470
AP-102	FIC	0.471
AW-101 * †	FIC	0.472
S-107	ENRAF	0.472
C-104 †	FIC	0.473
AW-102	MT	0.473
U-106 †	Neutron ILL	0.473
BY-103 †	MT	0.474
TY-106	MT	0.475
U-105 *	Neutron ILL	0.475
TX-106	MT	0.475
BY-104	MT	0.476
A-103	MT	0.476
BX-105	MT	0.477
AW-103 †	FIC	0.477
AZ-101	FIC	0.477
S-110	Neutron ILL	0.477
BX-112 †	FIC	0.478
AP-105	MT	0.478
AW-104 †	FIC	0.479
AY-101 †	MT	0.479
AY-101	FIC	0.479
BY-107	MT	0.480
S-102 *	Neutron ILL	0.480
AX-103 * †	FIC	0.480
AP-103	MT	0.480
TX-102	Neutron ILL	0.481

(continued on next page)

Table 5: *(continued)*

Tank	Instrument	Score
B–104	MT	0.481
SY–103 *	MT	0.481
SX–106 * †	Neutron ILL	0.481
C–203	MT	0.481
BX–109	FIC	0.481
A–106	FIC	0.481
U–109 *	ENRAF	0.482
T–107 †	FIC	0.483
B–108	FIC	0.483
S–105 †	Neutron ILL	0.483
S–103	Neutron ILL	0.483
U–106 †	FIC	0.483
TX–114	MT	0.483
TX–111 †	MT	0.483
AZ–101 †	MT	0.484
C–105 †	MT	0.484
BX–104 †	FIC	0.484
U–202	MT	0.485
TX–117	MT	0.485
T–109	FIC	0.485
TX–109	FIC	0.486
BY–111	Neutron ILL	0.486
S–111 *	Neutron ILL	0.486
C–110	MT	0.486
AP–106	MT	0.486
B–111	FIC	0.487
A–101 *	Neutron ILL	0.487
U–107 * †	Neutron ILL	0.487
AP–101	MT	0.487
U–110	FIC	0.487
S–107	MT	0.487
T–110 *	FIC	0.488
T–103	FIC	0.488
TX–104	FIC	0.489
U–111	Neutron ILL	0.489
AP–104	MT	0.489
BX–110	MT	0.489
TY–104	FIC	0.489
AP–108	MT	0.490
SY–102	ENRAF	0.490
AP–105 †	FIC	0.490
TX–108	FIC	0.490
U–201	MT	0.491
S–110	FIC	0.491
BX–111	MT	0.491
AP–107	MT	0.491
BX–105	FIC	0.491
TY–102 †	FIC	0.491
B–110	Neutron ILL	0.491
T–101	MT	0.491
C–103	ENRAF	0.492

Tank	Instrument	Score
TY–105	MT	0.492
C–102	FIC	0.492
SX–110	MT	0.492
TX–101	FIC	0.492
AW–104	MT	0.492
C–108	MT	0.493
AW–106	FIC	0.493
U–103 * †	Neutron ILL	0.493
B–101	FIC	0.493
AW–101 *	MT	0.493
T–111 †	FIC	0.493
TX–114	Neutron ILL	0.493
AX–101 *	FIC	0.494
BY–110	MT	0.494
S–109	FIC	0.494
BY–111	MT	0.494
AP–102	MT	0.494
B–203	MT	0.494
SX–104 *	MT	0.494
TX–116	MT	0.494
T–102	FIC	0.494
AN–106	FIC	0.494
U–108 *	Neutron ILL	0.495
BY–110	Neutron ILL	0.495
U–106	ENRAF	0.495
TX–103	FIC	0.495
C–109	MT	0.495
C–105	FIC	0.495
C–112	MT	0.496
B–112	FIC	0.496
SX–103 *	Neutron ILL	0.496
B–106	FIC	0.496
T–107	ENRAF	0.496
T–101	FIC	0.496
C–103	FIC	0.496
SX–107	MT	0.496
U–101	MT	0.496
S–101	Neutron ILL	0.496
T–105	MT	0.497
SX–115	MT	0.497
AX–104	MT	0.497
B–107	MT	0.497
AP–107 †	FIC	0.497
AW–105	FIC	0.497
B–104	Neutron ILL	0.498
S–105	FIC	0.498
BY–102	Neutron ILL	0.498
TX–110	Neutron ILL	0.498
BX–106	ENRAF	0.498
BX–106	FIC	0.498
C–106	FIC	0.498

(continued on next page)

Table 5: *(continued)*

Tank	Instrument	Score
AP-101	FIC	0.498
B-112	MT	0.499
AN-102	FIC	0.499
SX-102 *	Neutron ILL	0.499
BY-103	Neutron ILL	0.499
B-102	FIC	0.499
BX-112	MT	0.499
B-103	FIC	0.499
S-111 *	MT	0.499
AN-107	FIC	0.499
T-104	MT	0.499
U-109 *	Neutron ILL	0.499
SX-114	MT	0.499
BX-108	MT	0.500
S-104	MT	0.500
SX-108	MT	0.500
AX-101 *	Neutron ILL	0.500
SX-109 *	MT	0.500
SX-113	MT	0.500
T-109	ENRAF	0.500
T-104	Neutron ILL	0.500
BX-103	FIC	0.501
T-203	MT	0.501
TX-105	MT	0.501
TX-107 †	FIC	0.501
U-112	MT	0.501
SX-111	MT	0.501
T-110 *	Neutron ILL	0.502
TX-118	Neutron ILL	0.502
A-103	Neutron ILL	0.502
C-111	MT	0.502
B-111	Neutron ILL	0.502
AZ-102	MT	0.502
AZ-102	FIC	0.503
AX-102	MT	0.503
SX-105 *	Neutron ILL	0.503
AP-108	FIC	0.503
AN-101	FIC	0.503
AW-103 †	MT	0.504
T-106	FIC	0.504
A-102	FIC	0.504
T-111	Neutron ILL	0.505
AP-104	FIC	0.505
SX-106 *	MT	0.505
C-201	MT	0.505
TX-109	Neutron ILL	0.505
AW-105	MT	0.505
AY-102	MT	0.506
AP-106	FIC	0.506
T-201	MT	0.506
B-204	MT	0.506

Tank	Instrument	Score
T-105	FIC	0.507
T-102	ENRAF	0.507
AP-103	FIC	0.507
BX-101	MT	0.507
T-112	FIC	0.507
TX-115	MT	0.507
TX-113	MT	0.508
T-204	MT	0.508
BY-112	Neutron ILL	0.509
C-101	MT	0.509
BY-105	MT	0.509
BX-111	Neutron ILL	0.509
TY-101	FIC	0.509
B-201	MT	0.510
S-108	FIC	0.510
C-204	MT	0.510
A-105	MT	0.510
B-102	MT	0.511
B-202	MT	0.511
BY-107	Neutron ILL	0.511
S-112 *	FIC	0.511
T-108	MT	0.512
SX-101 *	Neutron ILL	0.513
U-203	MT	0.514
TX-117	Neutron ILL	0.514
BX-102	MT	0.514
SX-112	MT	0.515
C-202	MT	0.515
S-108	Neutron ILL	0.515
S-108	MT	0.515
BY-106	Neutron ILL	0.516
B-110	MT	0.516
BY-101	MT	0.516
TY-103	Neutron ILL	0.516
BY-109	Neutron ILL	0.517
B-109	MT	0.518
S-104	Neutron ILL	0.518
BY-104	Neutron ILL	0.518
S-105	MT	0.521
B-105	MT	0.521
T-202	MT	0.522
BX-104	MT	0.524
U-104	MT	0.525
SX-105 *	MT	0.527
A-104	MT	0.531
BX-106	MT	0.534
S-109	MT	0.538
AW-102	FIC	0.540
C-104	MT	0.541
AY-102	FIC	0.542
B-105	Neutron ILL	0.564

5.3 Summary of the Quality of the Linear Regressions

This subsection presents an evaluation of the "quality" of the individual regressions performed in Step 2.e.ii of the screening calculation. A measure of how well a linear regression describes the relationship between a pair of variables (in this case, detrended waste level and atmospheric pressure) is the square of the correlation coefficient of the two. This quantity, commonly referred to as R^2, has the properties:

- $0 \leq R^2 \leq 1$
- $R^2 = 1$ exactly when the relationship between the two quantities is perfectly linear.

Thus, R^2 values close to 1 indicate a strong linear relationship between the two measurements. As an example, $R^2 = 0.66$ for the data in Figure 3.

There are numerous regressions, and thus numerous values of R^2, for each tank/instrument combination. To summarize these values, a single display of boxplots was created for each tank/instrument combination, as shown in Figures 15 through 18. Each boxplot is constructed from a five-number summary of the R^2 values available for that tank/instrument combination. The five numbers are the minimum, lower quartile, median, upper quartile, and the maximum. These five numbers divide the R^2 values into 4 sequential blocks, each containing 1/4 of the total number of values. Figure 14 shows how these 5 numbers partition a set of numbers; the graphic at the bottom of the figure is called a "boxplot".

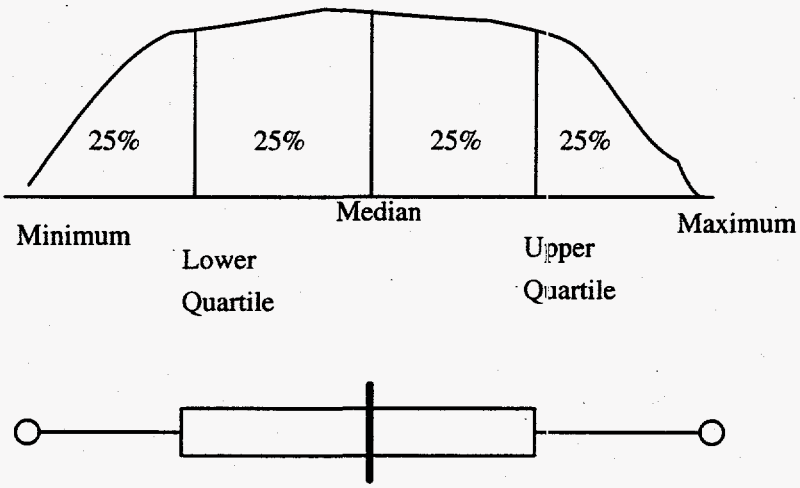

Figure 14: R^2 boxplot parameters

In a boxplot, the minimum and maximum data values are indicated by the open-circles at the extreme ends of the graphic; the value of the median is indicated by the the vertical line; and the rectangle between the minimum and maximum (the rectangle also brackets the median) begins at the lower quartile and ends at the upper quartile; this rectangle spans the middle 50% of the R^2 values. So, looking at the boxplot at the bottom of the first page of Figure 15, we see that the minimum R^2 for the regressions for Tank S–108 was 0, the maximum was about 0.3, and the median is $\sim$0.08. A full 25% of the R^2 values were between 0 and $\sim$.03.

Figures 15, 16, 17 and 18 show boxplots of the R^2 values for tanks with FIC, ENRAF, MT and Neutron ILL level measurements, respectively. In each figure, the tanks are sorted according

to ascending median value of R^2. Note that with this ordering, tanks which were flagged in this screening tend to appear at the end of the figure. A tank name is marked with an asterisk if it is currently on the flammable gas watch list and is marked with a dagger if it was flagged by the screening procedure *for that particular instrument.*

In a comparison of the boxplots across instruments, the MT regressions appear to be almost uniformly poor, even for tanks that are currently on the flammable gas watch list. In particular, 4 of the 125 tanks evaluated using manual tape have a median R^2 greater than 0.2 (see page 49) while 23 of the 102 tanks evaluated using FIC measurements have a median R^2 greater than 0.2 (see page 46). This suggests that tanks monitored primarily with MT may not be effectively screened by the procedure described in this report. The boxplots for the regressions based on the FIC show that the regressions with high R^2 values correspond with tanks that were flagged.

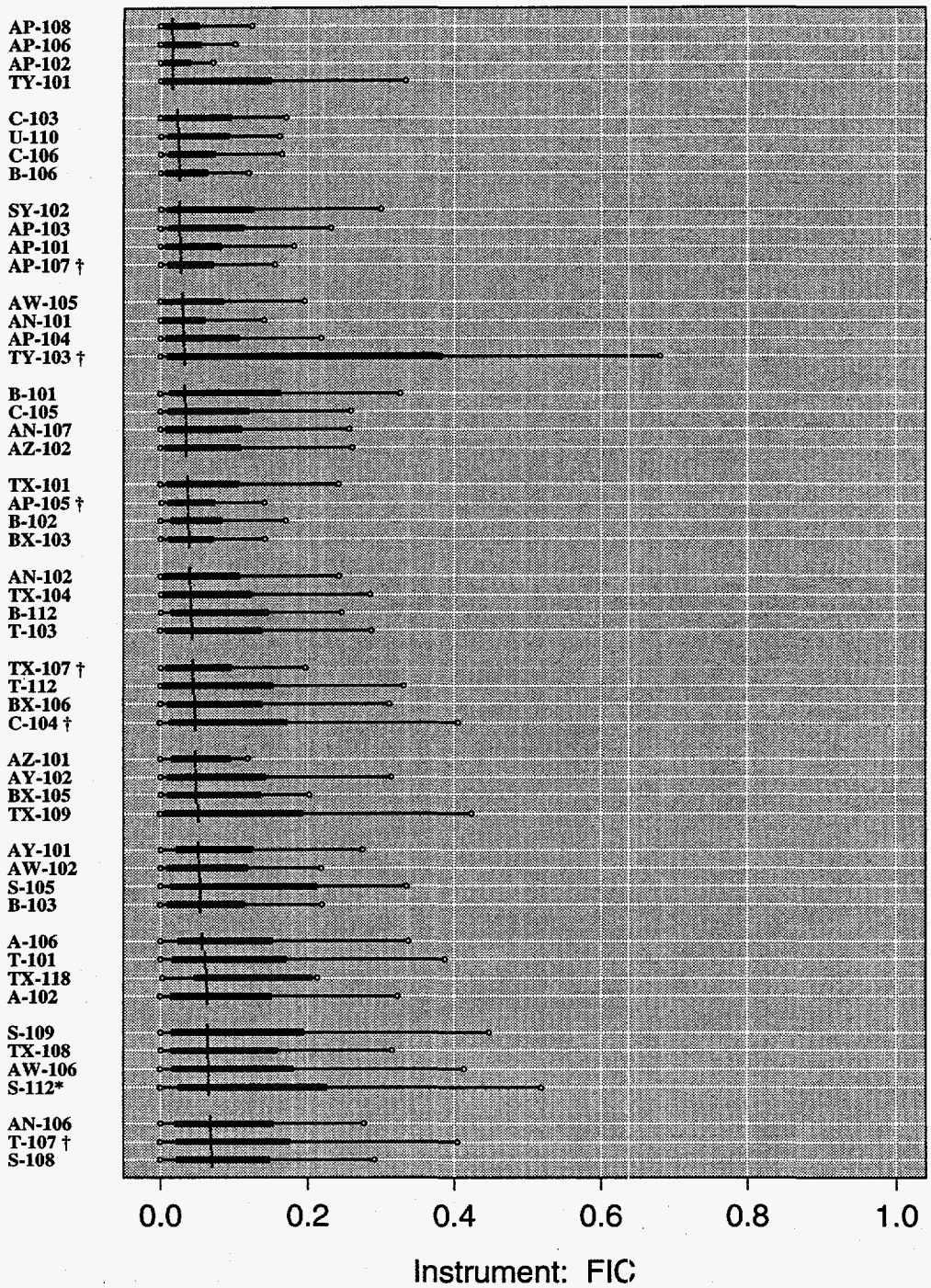

(continued on next page)

Figure 15: Summary of the FIC regressions

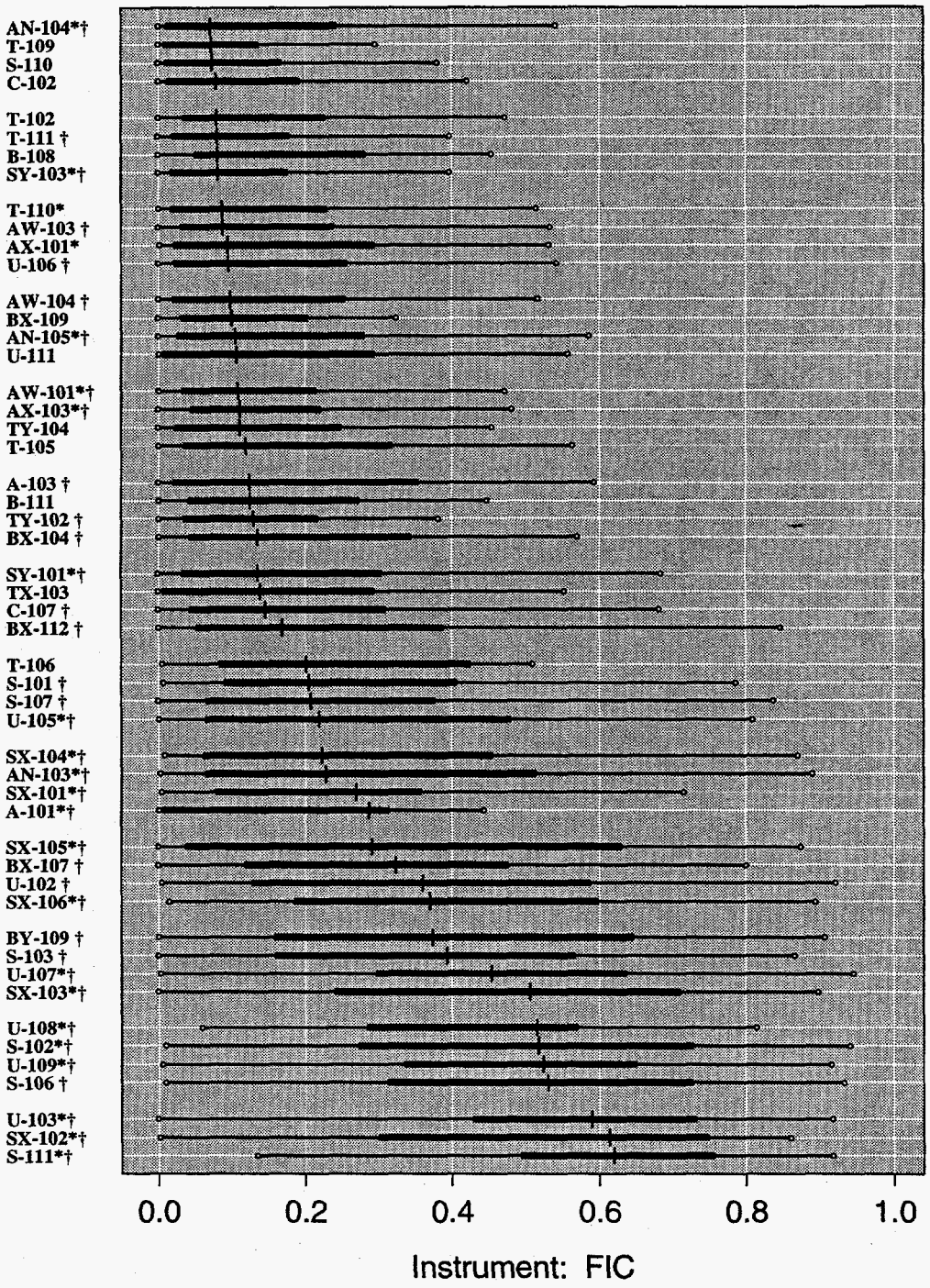

Figure 15: *(continued)*

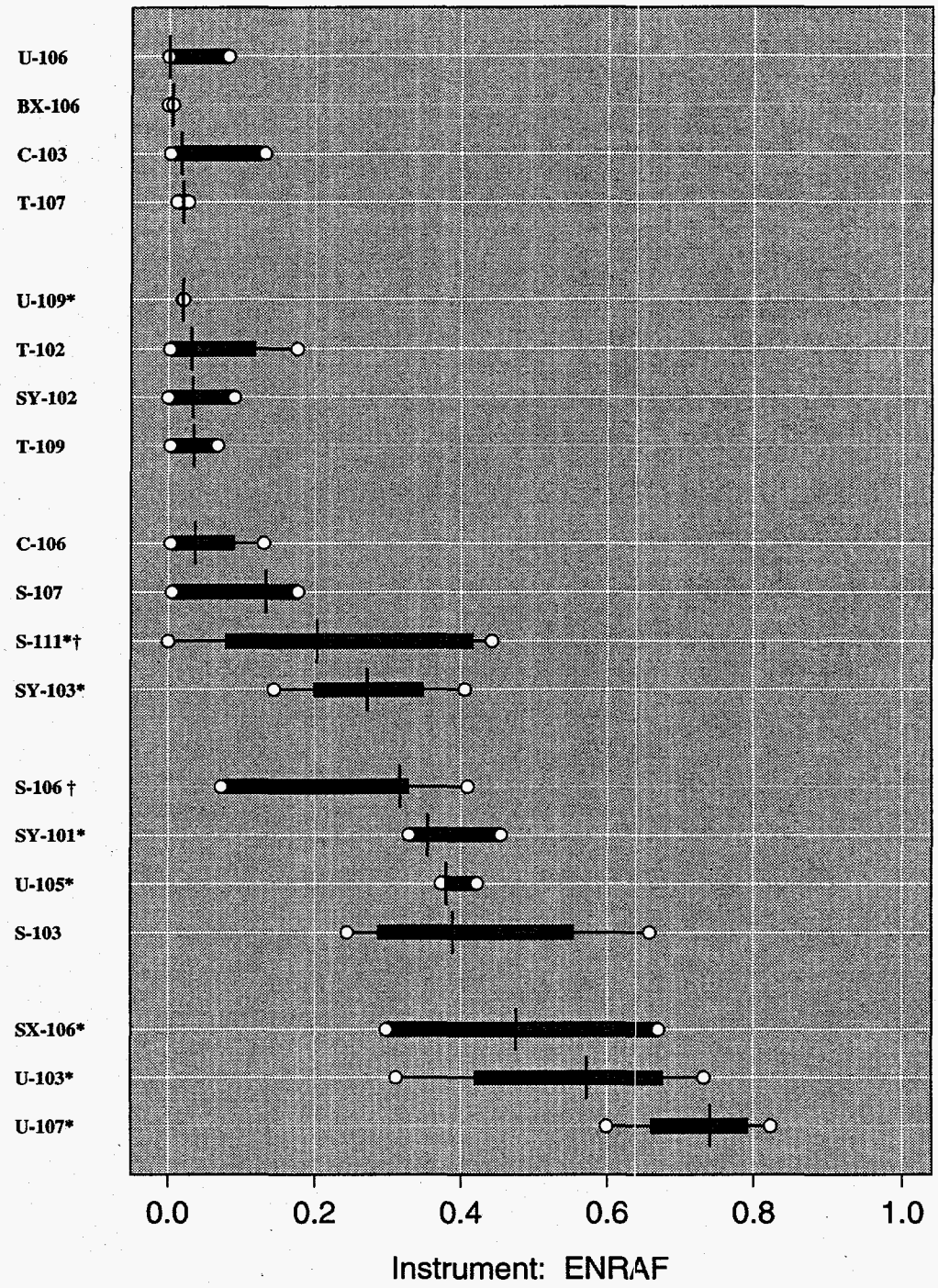

Figure 16: Summary of the ENRAF regressions

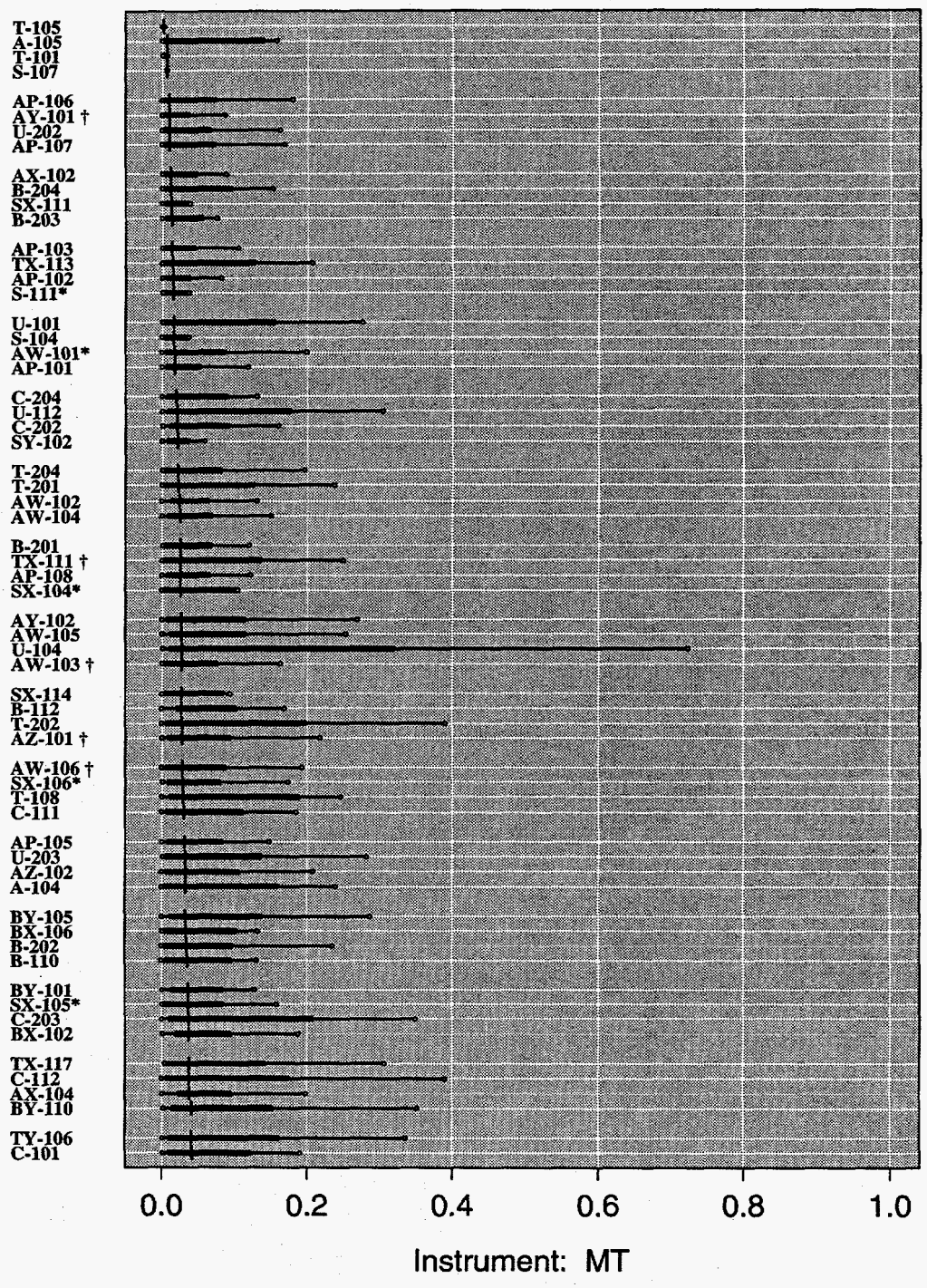

(continued on next page)

Figure 17: Summary of the MT regressions

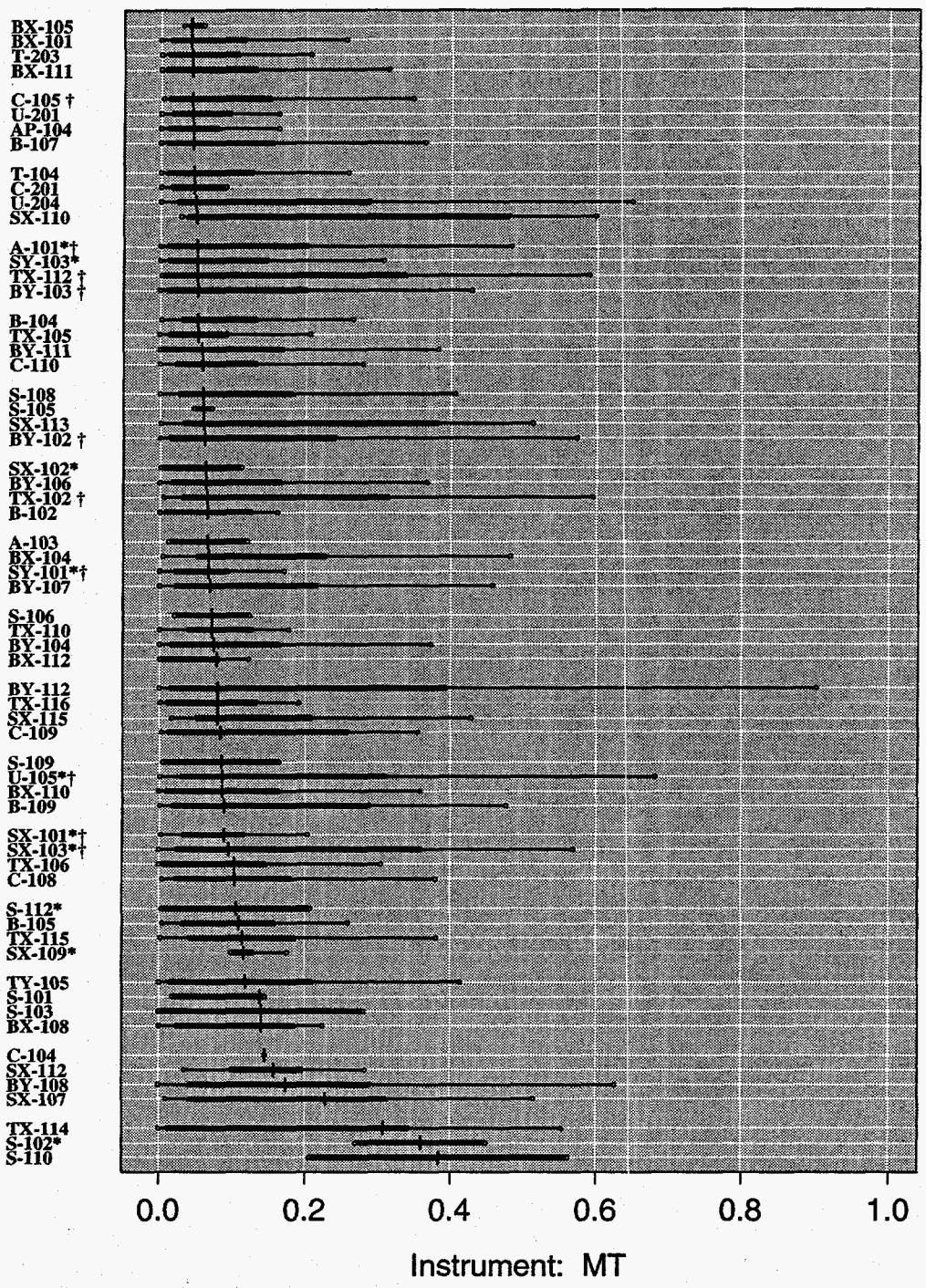

Figure 17: *(continued)*

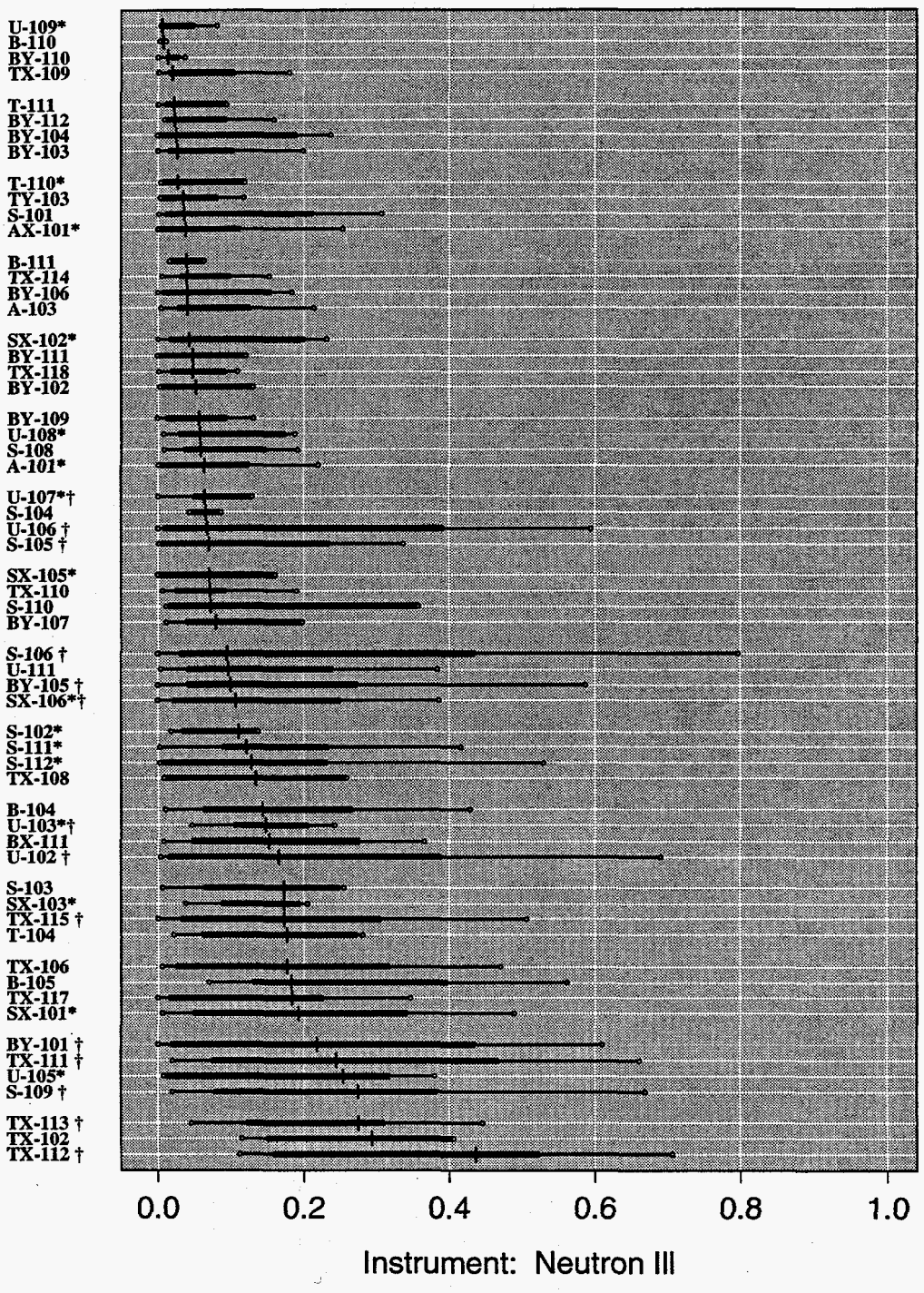

Figure 18: Summary of the Neutron ILL regressions

6 Recommendations

This section lists recommendations based on work described in this report; briefly, the recommendations are

- Extend modeling and methodology to estimate or bound the amount of gas trapped in the tank waste.
- Determine to what extent the data quality and quantity were adequate to detect significant quantities of trapped gas.
- Examine whether the observed waste level rise, common to many of the Hanford tanks, is consistent with the magnitude of level response to pressure fluctuations.
- Integrate the physical modeling with the multi-state dynamic linear model.
- Explain the magnitudes of the slope estimates in terms of waste types.

Each of the suggested activities has the potential for contributing to the understanding of the safety of the Hanford tanks. Discussion of each of these recommendations follows.

- Extend modeling and methodology to estimate or bound the amount of gas trapped in the tank waste.

  The quantity $d\text{DWL}/d\text{AP}$ has been linked to the volume of gas in the waste; this volume directly concerns tank safety, as discussed in Hopkins (1994) and in Nichols (1994). There are known sources of systematic errors in the estimates of gas volume that would be obtained using $d\text{DWL}/d\text{AP}$ and Equations (5) and (7). These are:

  1. Tank gas configuration

     Entrainment as small bubbles or in stiff sludge can potentially "hide" gas from the detection method described in this report. It's unclear how to bound or account for such entrainment with the data and models described in this report.
  2. Observation error in atmospheric pressure fluctuations.

     Equation (8) shows how $d\text{DWL}/d\text{AP}$ can result in an underestimate of the amount of trapped gas. A component of this error can be eliminated by estimating the time lag between the measurement at HMS and the transfer of the effect to the tank headspace. The time lag can be estimated from the cross correlation between measurements of tank level and atmospheric pressure.
  3. Trend in atmospheric pressure.

     Atmospheric pressure trends can be corrected for by using a variation on the regression procedure in this paper, viz., do not detrend, and use very short time intervals. This effect may not be significant, since the variation in atmospheric pressure is large compared with any trend.

- Determine to what extent the data quality and quantity were adequate to detect significant quantities of trapped gas.

  Even though there are some waste level data for each Hanford tank, an important and unfinished part of this screening task is to calculate for each tank whether there is enough level data to reliably detect a significant quantity of trapped gas. Such a calculation is possible and highly recommended.

  As discussed in Section 5.3, the quality of the regressions in the screening calculations using MT data were almost uniformly poor. Examining Table 2, we see that the screening for SY-101 using MT data was barely significant (since the probability in parentheses is 0.024, just slightly less than 0.05). This suggests that tanks primarily monitored via MT data may not have been adequately examined by the screening in this report.

- Examine whether the observed waste level rise, common to many of the Hanford tanks, is consistent with the magnitude of level response to pressure fluctuations.

  A proposed explanation for the steady waste level rise in tanks such as S-102 and U-105 is an increasing amount of trapped gas. The modeling in Section 4.2.1 suggests that if the growth is due to increasing amounts of gas, then the dDWL/dAP estimates should become increasingly negative. Examining the plots in the appendix (see for instance Figure 302 on page 343), it's not clear that this relationship between waste level and dDWL/dAP exists. A more detailed investigation is required to settle this question.

- Integrate the physical modeling with the multi-state DLM.

  The multi-state DLM was used in this report to detect large changes in waste level; the algorithm can be modified to incorporate the ideal gas law relation between trapped gas volume, pressure and temperature. The result would be a candidate algorithm for

  1. Detecting GREs based on tank waste level and tank temperature data.

     Whether or not a tank experiences GREs is a criterion for evaluating whether the tank is "safe" or not. Currently, many of the Hanford tanks have hydrogen monitors in place; however, before 1995 none of the Hanford single shell tanks were routinely monitored for hydrogen. The proposed algorithm could be used to examine the historical level data for GREs.

  2. Correcting tank waste level for pressure and temperature.

     An output of the algorithm would be tank waste level corrected for temperature and atmospheric pressure fluctuations. If temperature and pressure significantly affect tank waste level; then modeling their effect would result in a more precise view of a tank's contents. In this case, the algorithm would result in improved leak/intrusion detection.

     Given that seasonal variations in atmospheric pressure amount to $\sim$0.4 inches Hg and typical values of dDWL/dAP for flammable gas watch list tanks are 0.2 to 0.5, a variation of .08 to .20 inches in level could be attributed to seasonal variations in atmospheric pressure. It would be interesting to compare the seasonality of waste level in some of the Hanford tanks with the seasonality of atmospheric pressure; good candidates for this experiment can be found in the S and U tank farms.

- Explain the magnitudes of slope estimates in terms of waste types.

  The two components of this activity are 1) obtaining a single, representative slope estimate for each tank and 2) attempting to predict this slope estimate based on waste level and waste type (as in Hanlon [1994]). One use of such a model would be to extrapolate estimates of the amount of trapped gas to tanks for which the waste level data are insufficient for the screening process described here. The results of this exercise may also be helpful in determining the characteristics of tank wastes that generate and trap gas.

7 References

Allemann, R., Z. Antoniak, W. Chvala, L. Efferding, J. Fadeff, J. Friley, W. Gregory, J. Hudson, J. Irwin, N. Kirch, T. Michener, F. Panisko, C. Stewart, and B. Wise. 1994. *Mitigation of Tank 241-SY-101 by Pump Mixing: Results of Testing Phases A and B.* PNL-9423, Pacific Northwest Laboratory, Richland, Washington.

Andrews, G., and J. Buck. 1987. *Hanford Meteorological Station Computer Codes, Volume 6 - The SFC Computer Code.* PNL-6279 Vol. 6, Pacific Northwest Laboratory, Richland, Washington.

Fleiss, J. L. 1981. *Statistical Methods for Rates and Proportions.* Wiley Series in Probability and Mathematical Statistics, 2nd edition. John Wiley & Sons, New York.

Fuller, W. A. 1987. *Measurement Error Models.* Wiley Series in Probability and Mathematical Statistics. John Wiley & Sons, New York.

Glasscock, J. 1993. *Surveillance Analysis Computer System Temperature Database Software Requirements Specification.* WHC-SD-WM-CSRS-007 Rev. 1a, Westinghouse Hanford Company, Richland, Washington.

Gordon, K., and A. Smith. 1988. "Modeling and Monitoring Discontinuous Changes in Time Series." *Bayesian Analysis of Time Series and Dynamic Models*, Spall, J., editor. Marcel Dekker, Inc., New York.

Gordon, K., and A. Smith. 1990. "Modeling and Monitoring Biomedical Time Series." *JASA*, 85(410):328–337.

Hanlon, B. 1994. *Waste Tank Summary for Month Ending September 30, 1994.* WHC-EP-0182-78, Westinghouse Hanford Company, Richland, Washington.

Hoitink, D., and K. Burk. 1994. *Climatological Data Summary 1993 with Historical Data.* PNL-9809, Pacific Northwest Laboratory, Richland, Washington.

Hopkins, J. 1994. *Proposed Criteria for Flammable Gas Watch List Tanks.* WHC-EP-0702 Rev. 0, Westinghouse Hanford Company, Richland, Washington.

Nichols, B., S. Eisenhawer, and J. Spore. 1994. *Bounding Gas Release Calculations of Flammable Gas Watch List Single-Shell Tanks.* LA-UR-94-1323, Los Alamos National Laboratory. Los Alamos, New Mexico.

Peters, T., and W. Park. 1993. *Evaluation of Methods to Measure Surface Level in Waste Storage Tanks: Second Test Sequence.* PNL-8839, Pacific Northwest Laboratory, Richland, Washington.

Ross, S. M. 1987. *Introduction to Probability and Statistics for Engineers and Scientists.* Wiley Series in Probability and Mathematical Statistics. John Wiley & Sons, New York.

Spurling, D. 1991. *Software Requirements Specification: CASS Central Facility.* WHC-SD-SFR-003 Rev 0, Westinghouse Hanford Company, Richland, Washington.

Stong, F. 1986. *Drywell Van In-Tank Liquid Observations Well Surveillance Data Interpretation.* SD-WM-TI-237, Rockwell Hanford Operations, Richland, Washington.

West, M., and J. Harrison. 1989. *Bayesian Forecasting and Dynamic Models.* Springer-Verlag, New York.

Appendix A

Summary Plots for Each Tank and Instrument

A Summary Plots for Each Tank and Instrument

This Appendix presents two plots for each screened combination of tank and instrument. Each figure includes:

1. A plot of the level data versus time
2. A plot of the estimated dDWL/dAP versus time

The two plots use the same x-axis, although a time scale is shown only for the second plot. The error bars in the second plot are for 95% confidence intervals on the slope estimates. This plot may not show the complete error bars, nor all of the dDWL/dAP estimates, because the y-axis range was restricted to -2 to 1 units, covering most of the range of interest.

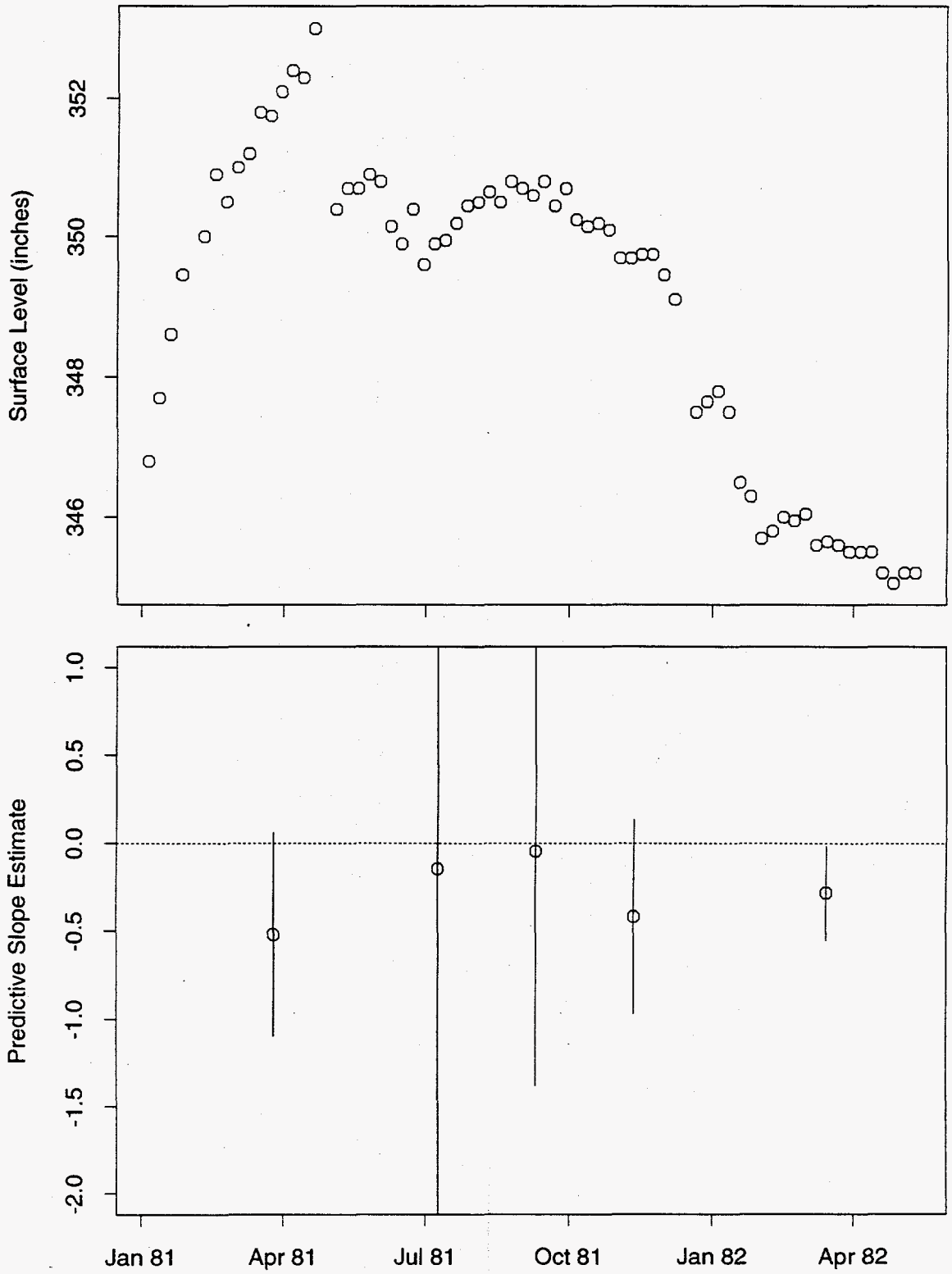

Figure 19: Tank A–101 FIC Data

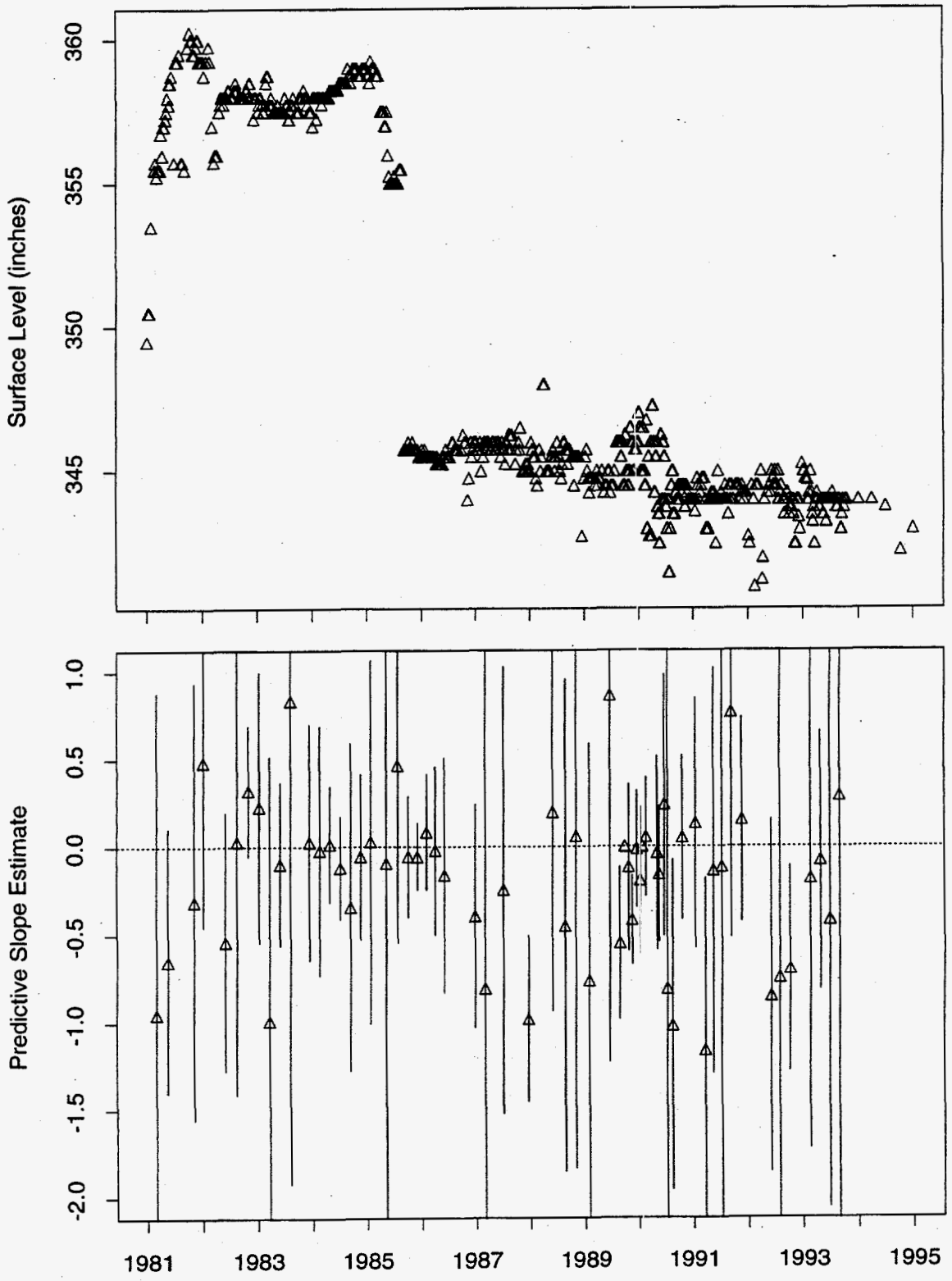

Figure 20: Tank A–101 MT Data

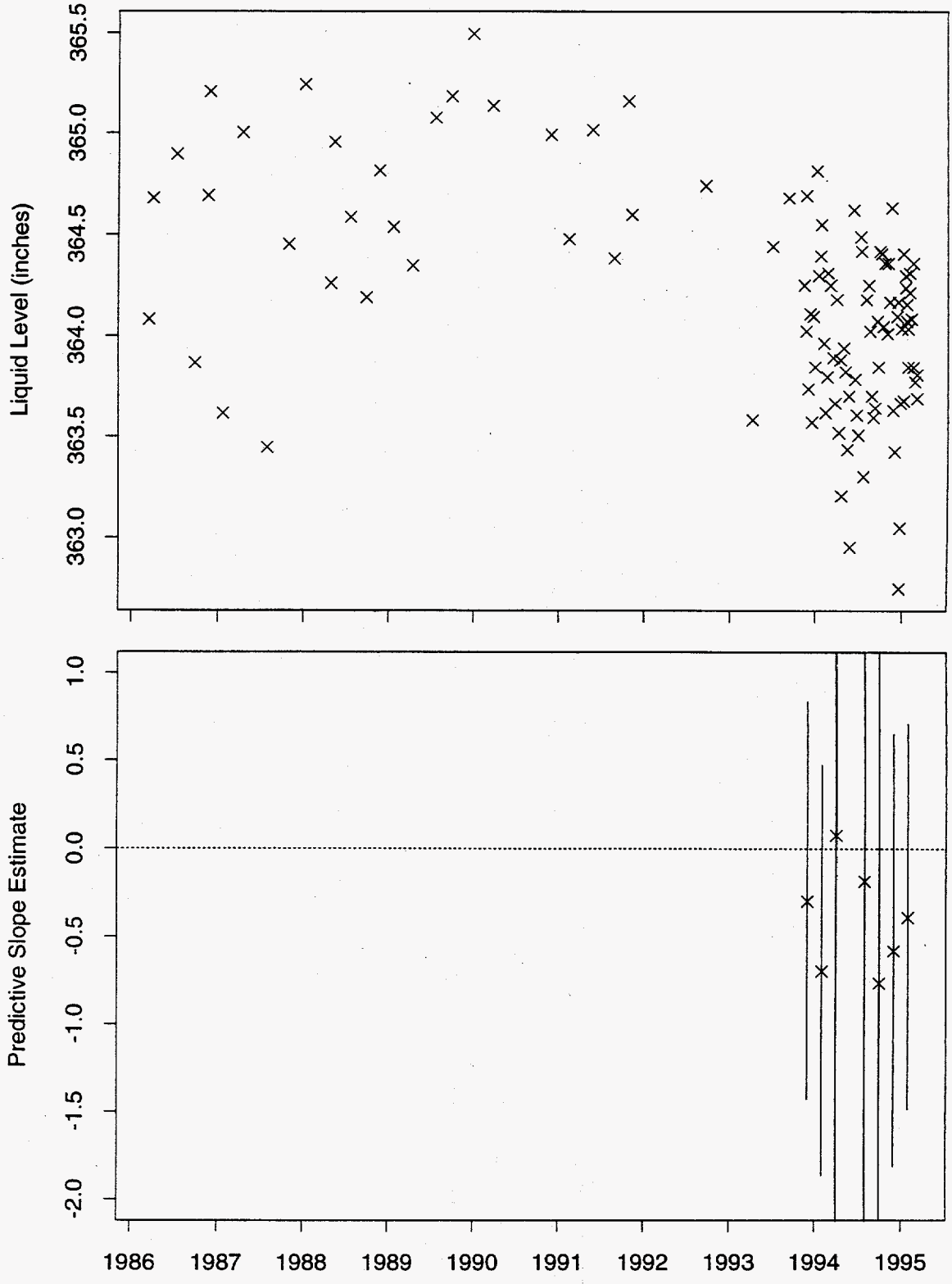

Figure 21: Tank A–101 Neutron ILL Data

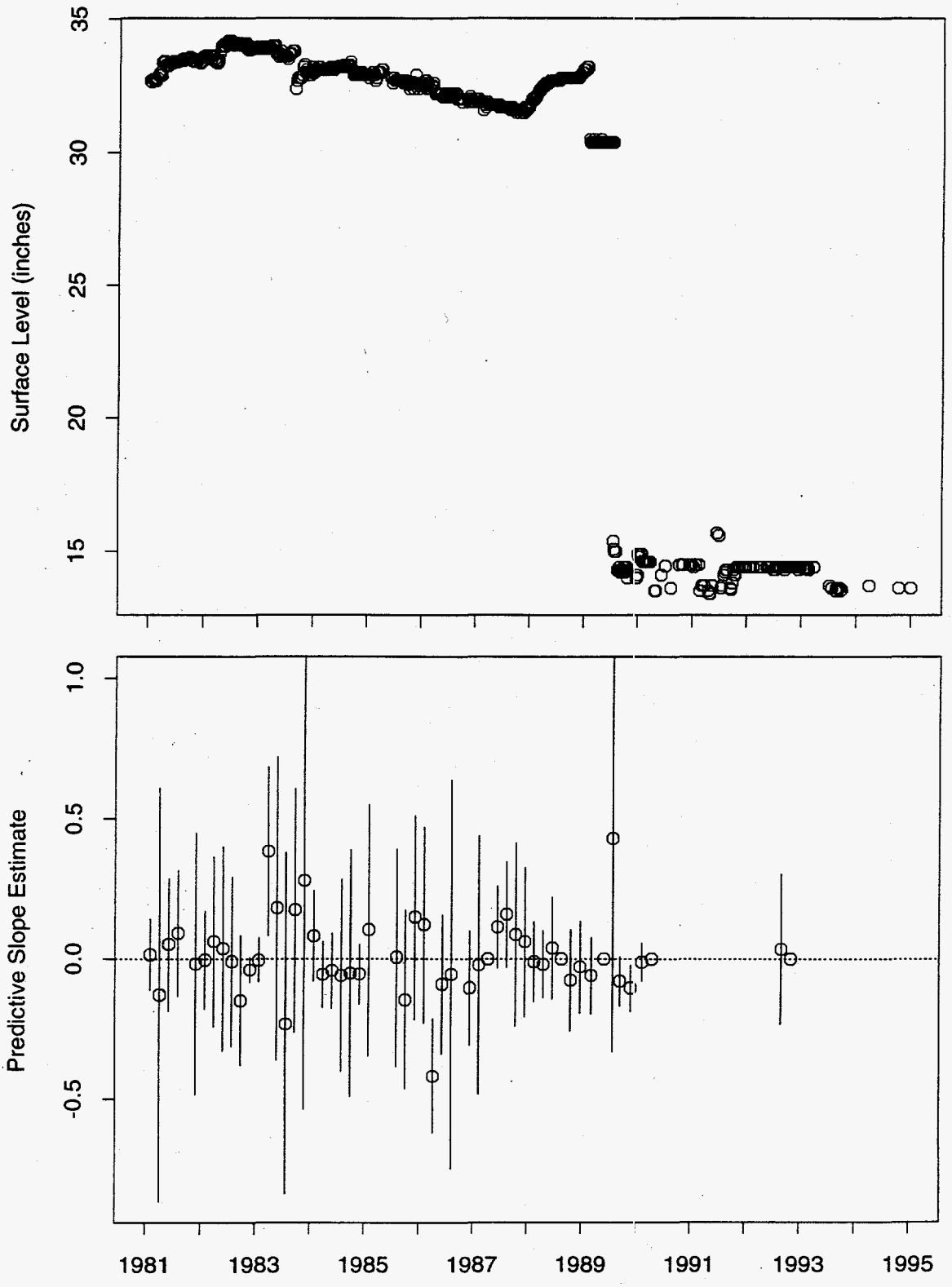

Figure 22: Tank A–102 FIC Data

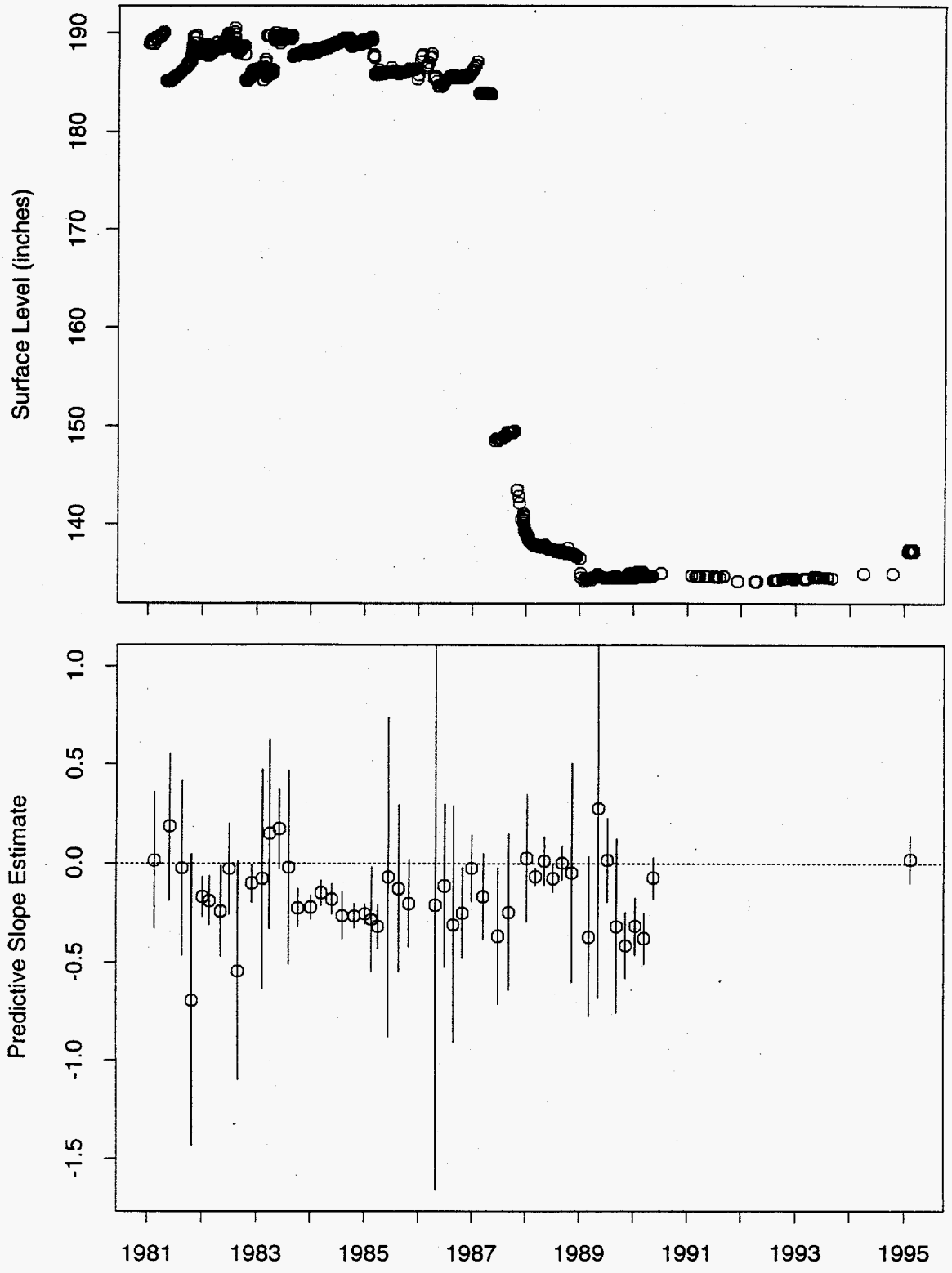

Figure 23: Tank A–103 FIC Data

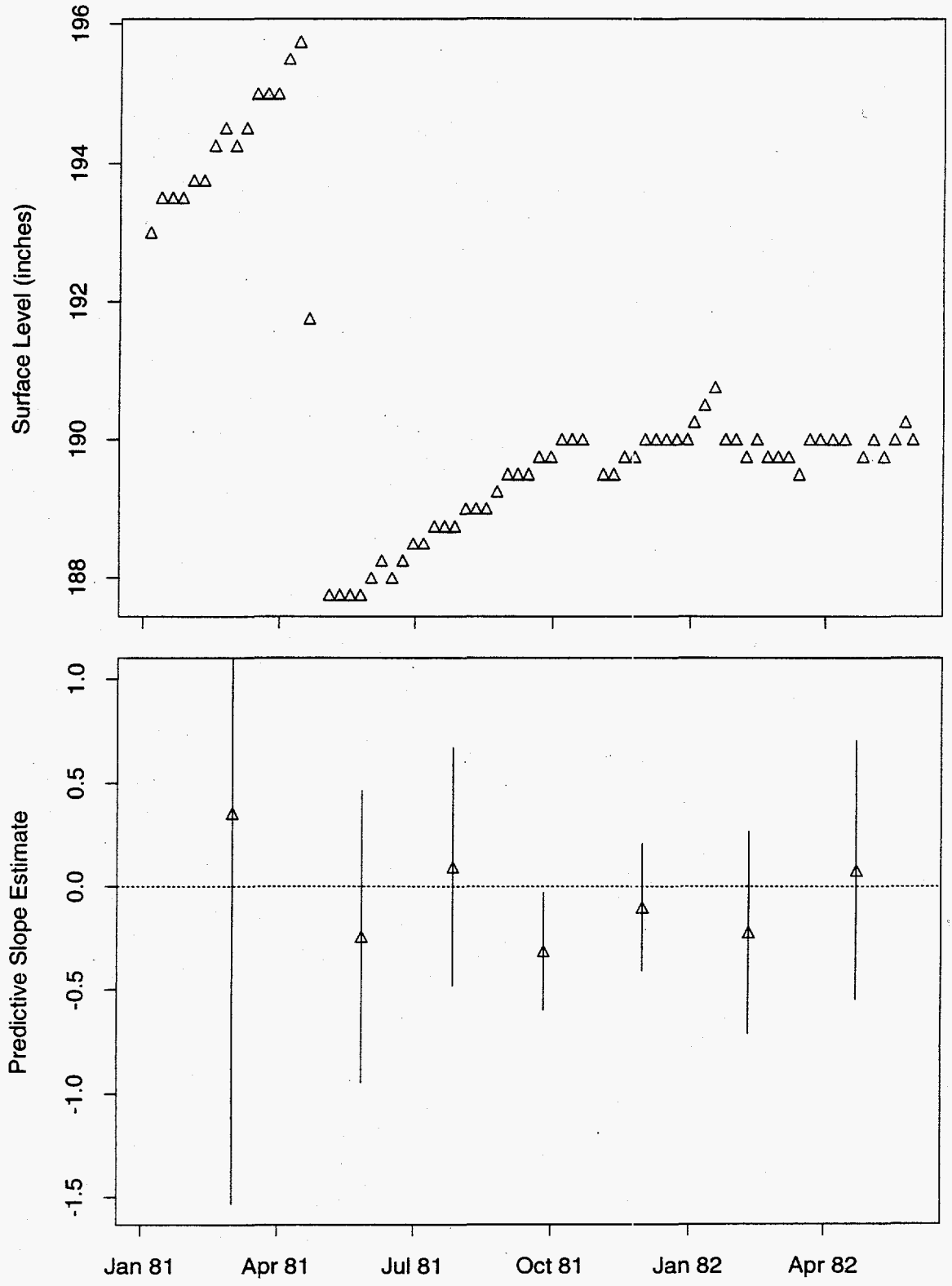

Figure 24: Tank A–103 MT Data

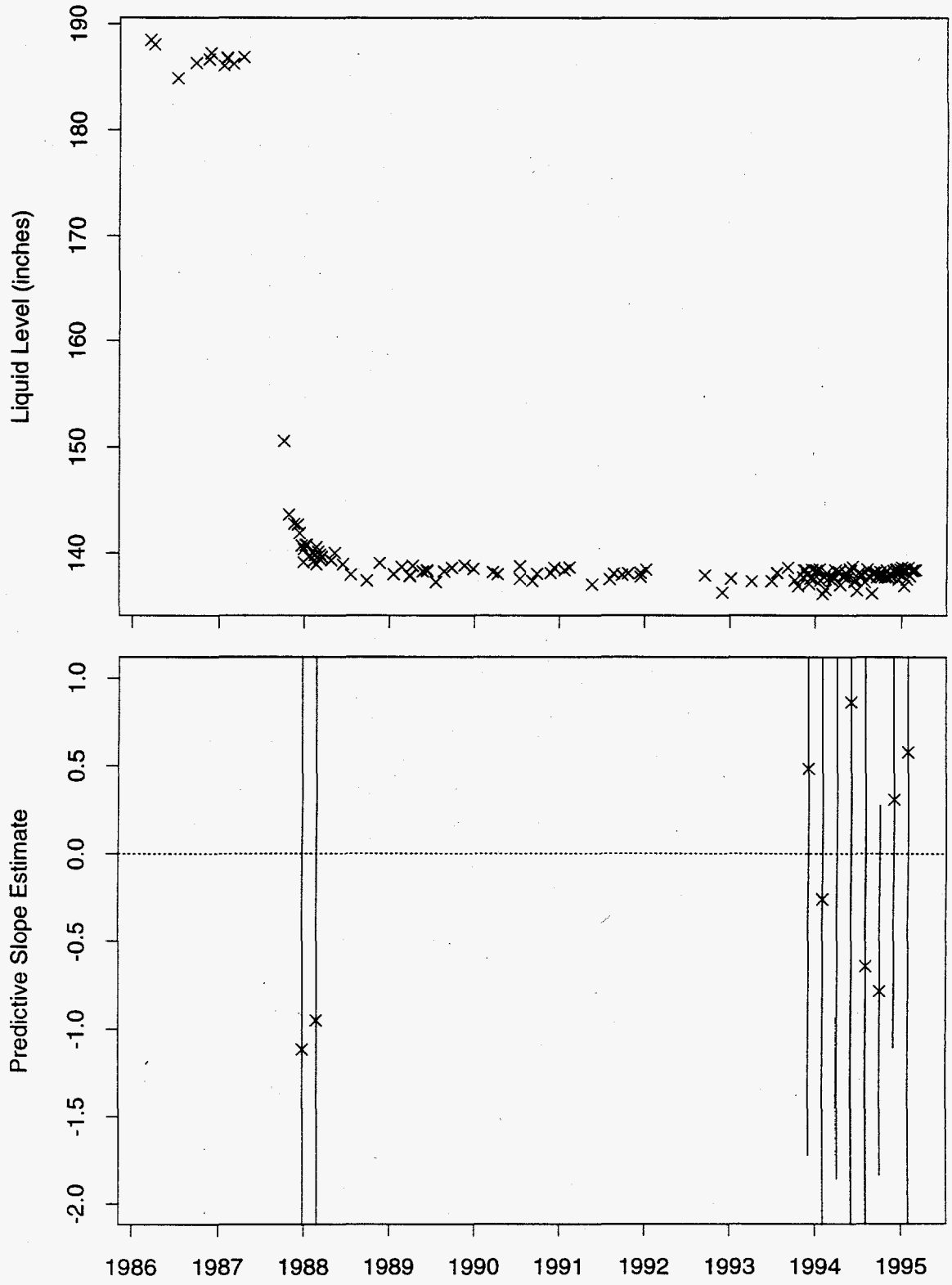

Figure 25: Tank A–103 Neutron ILL Data

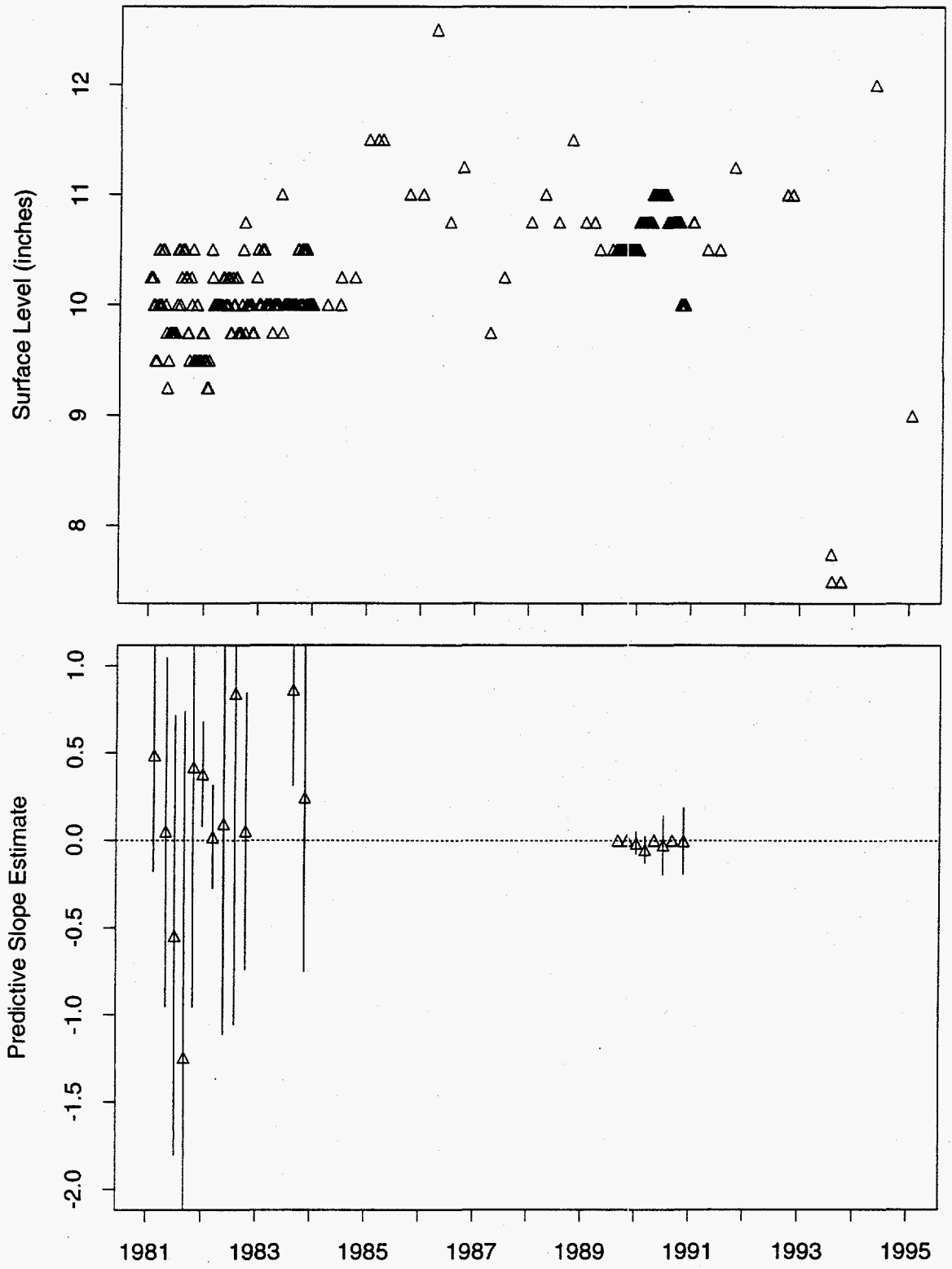

Figure 26: Tank A–104 MT Data

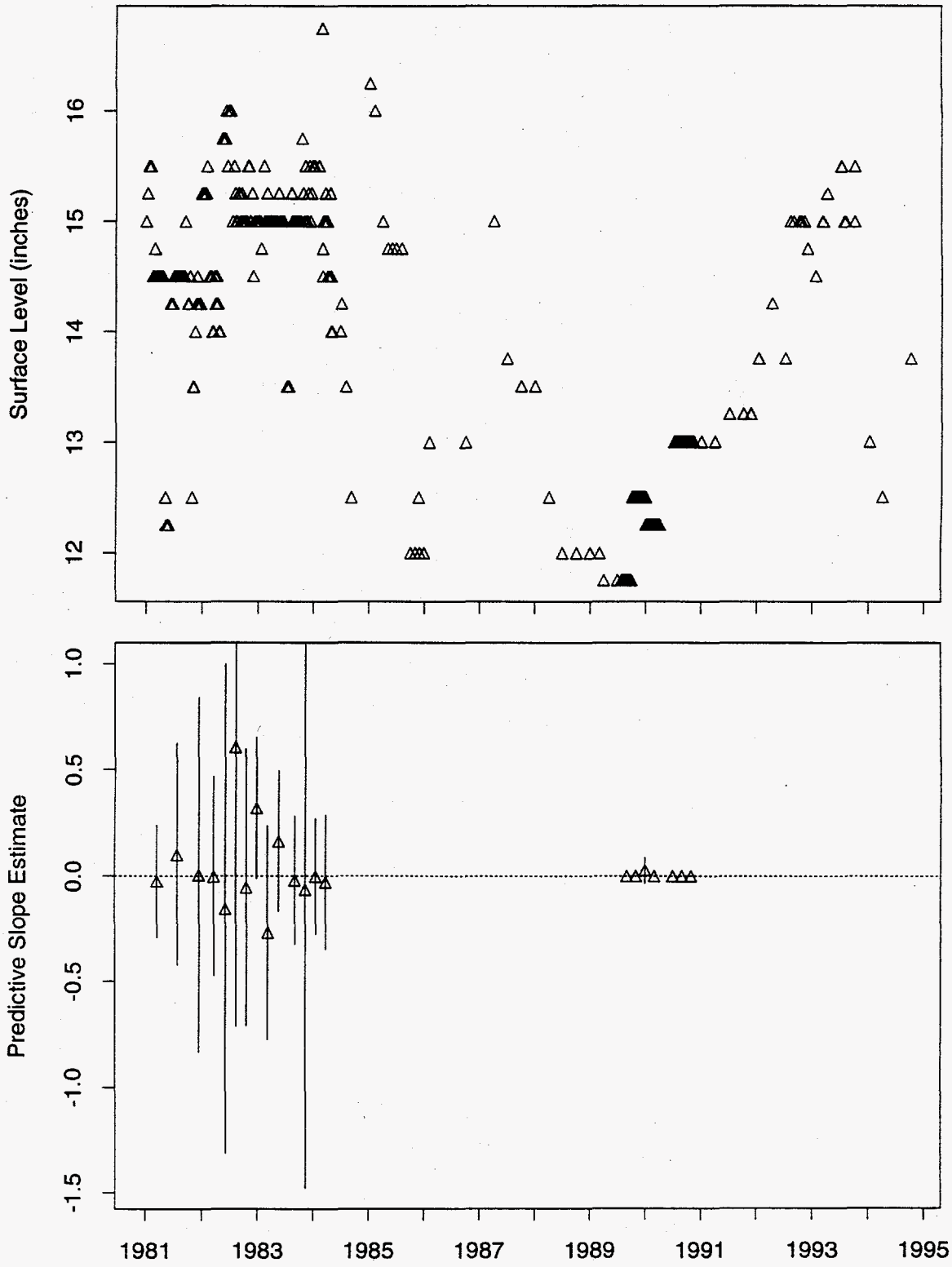

Figure 27: Tank A–105 MT Data

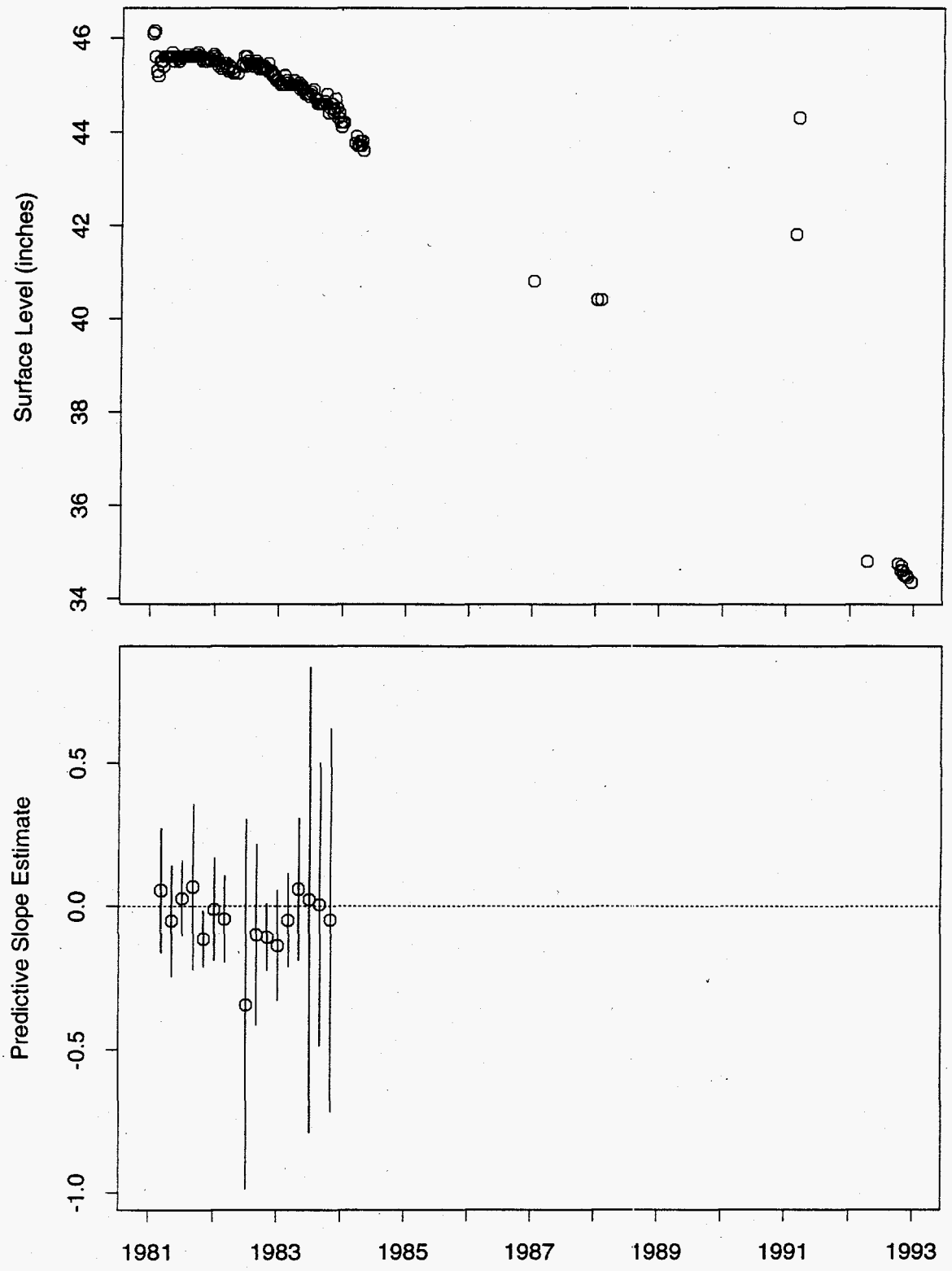

Figure 28: Tank A-106 FIC Data

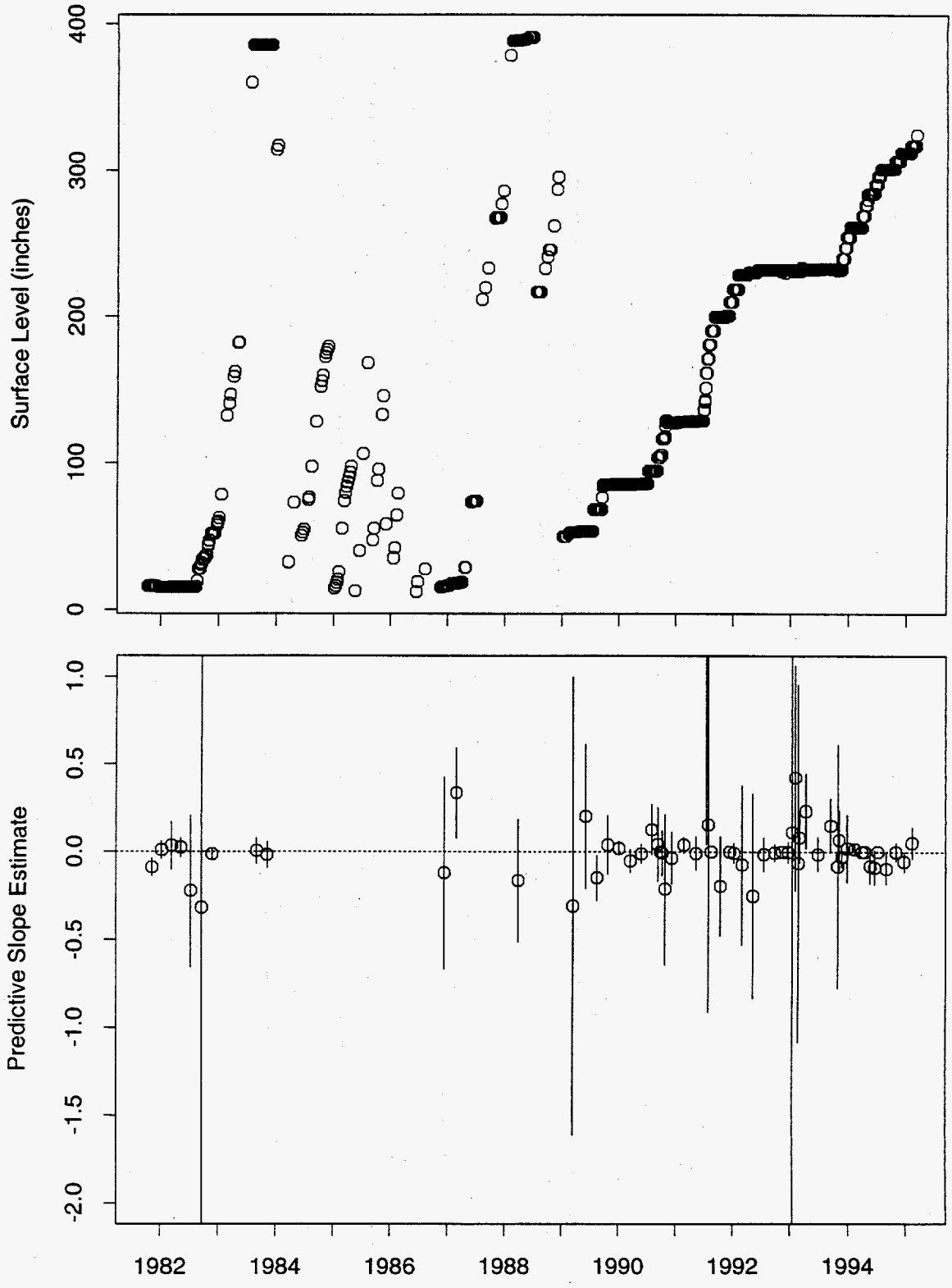

Figure 29: Tank AN–101 FIC Data

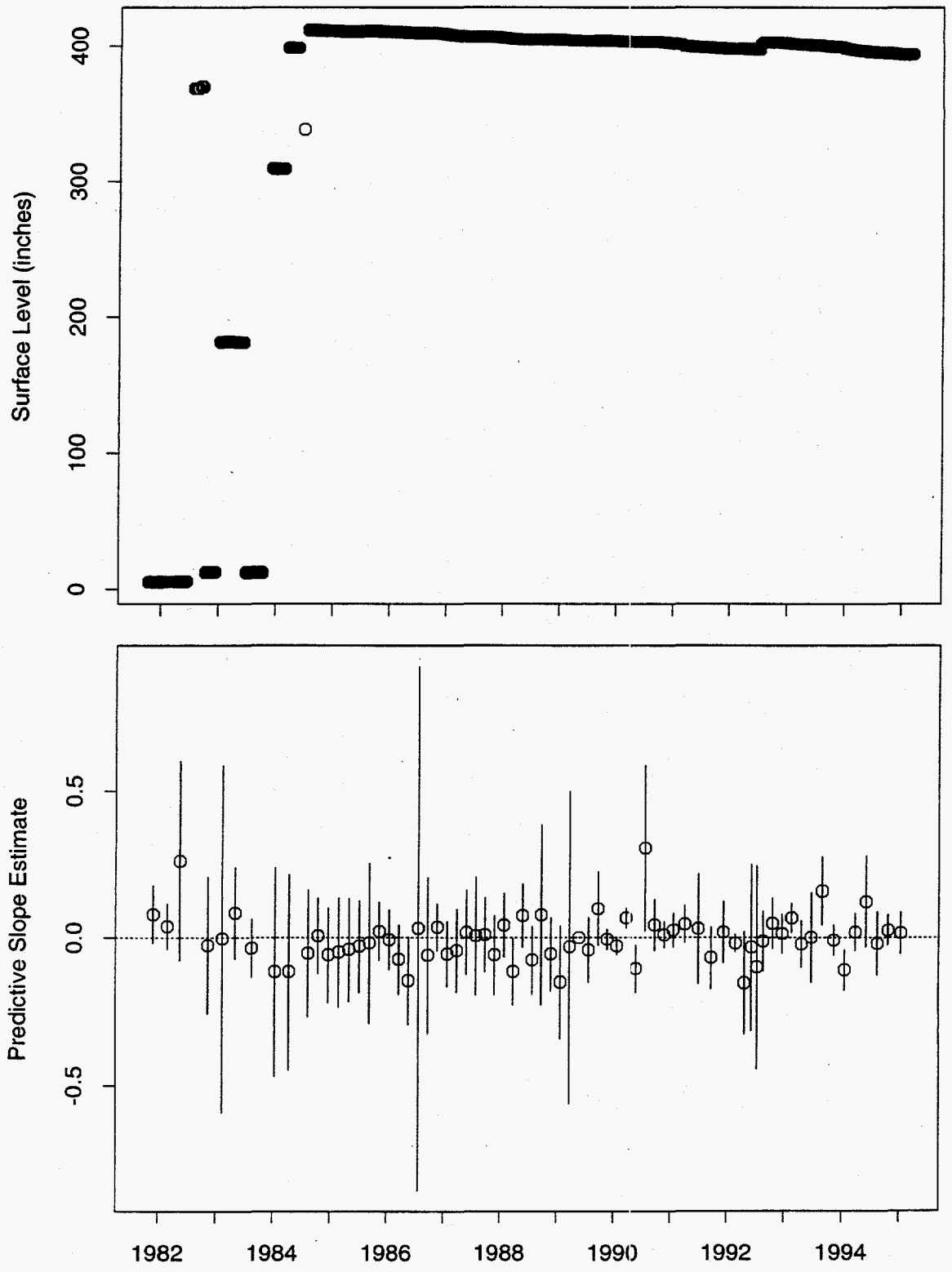

Figure 30: Tank AN–102 FIC Data

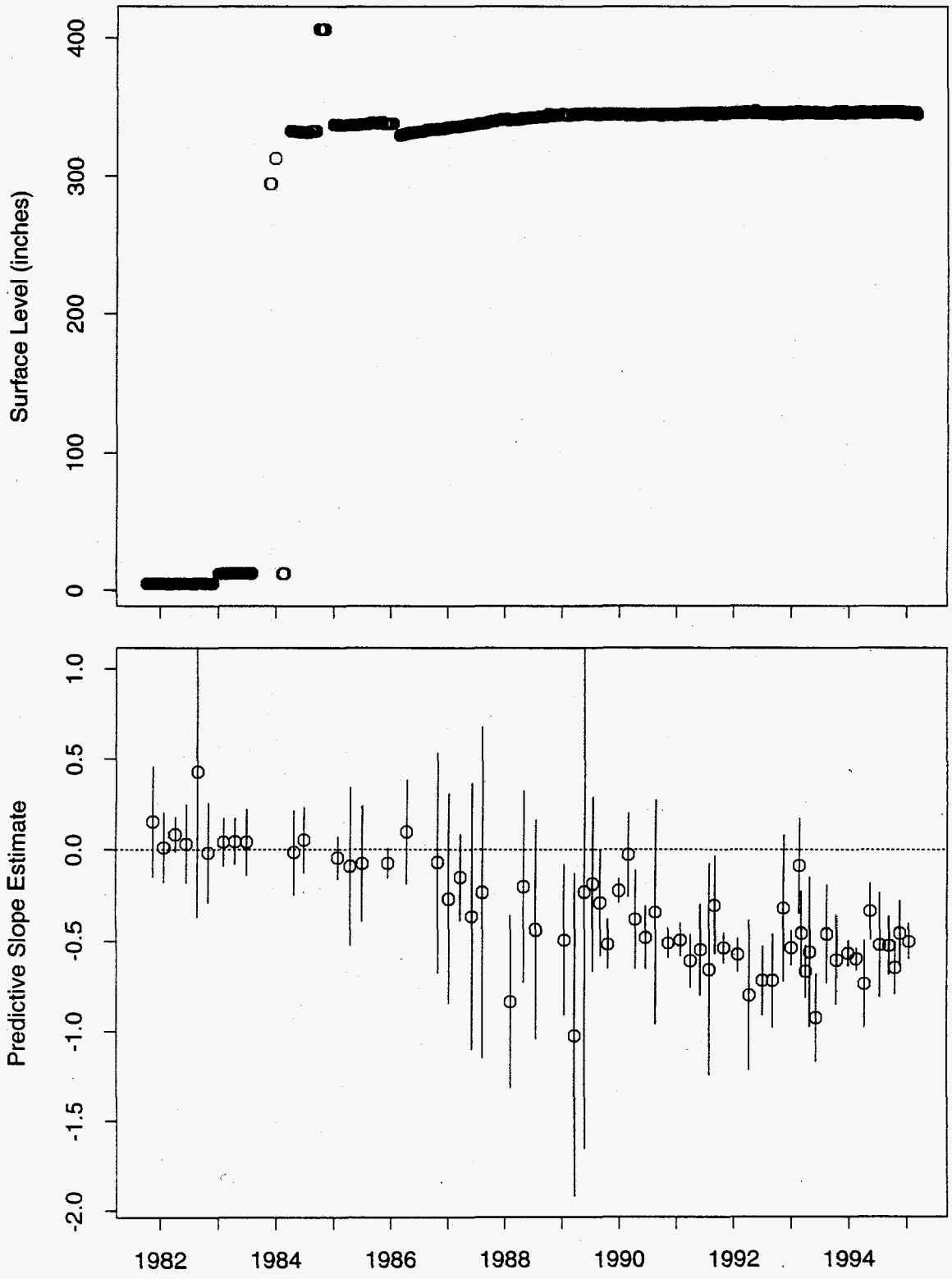

Figure 31: Tank AN–103 FIC Data

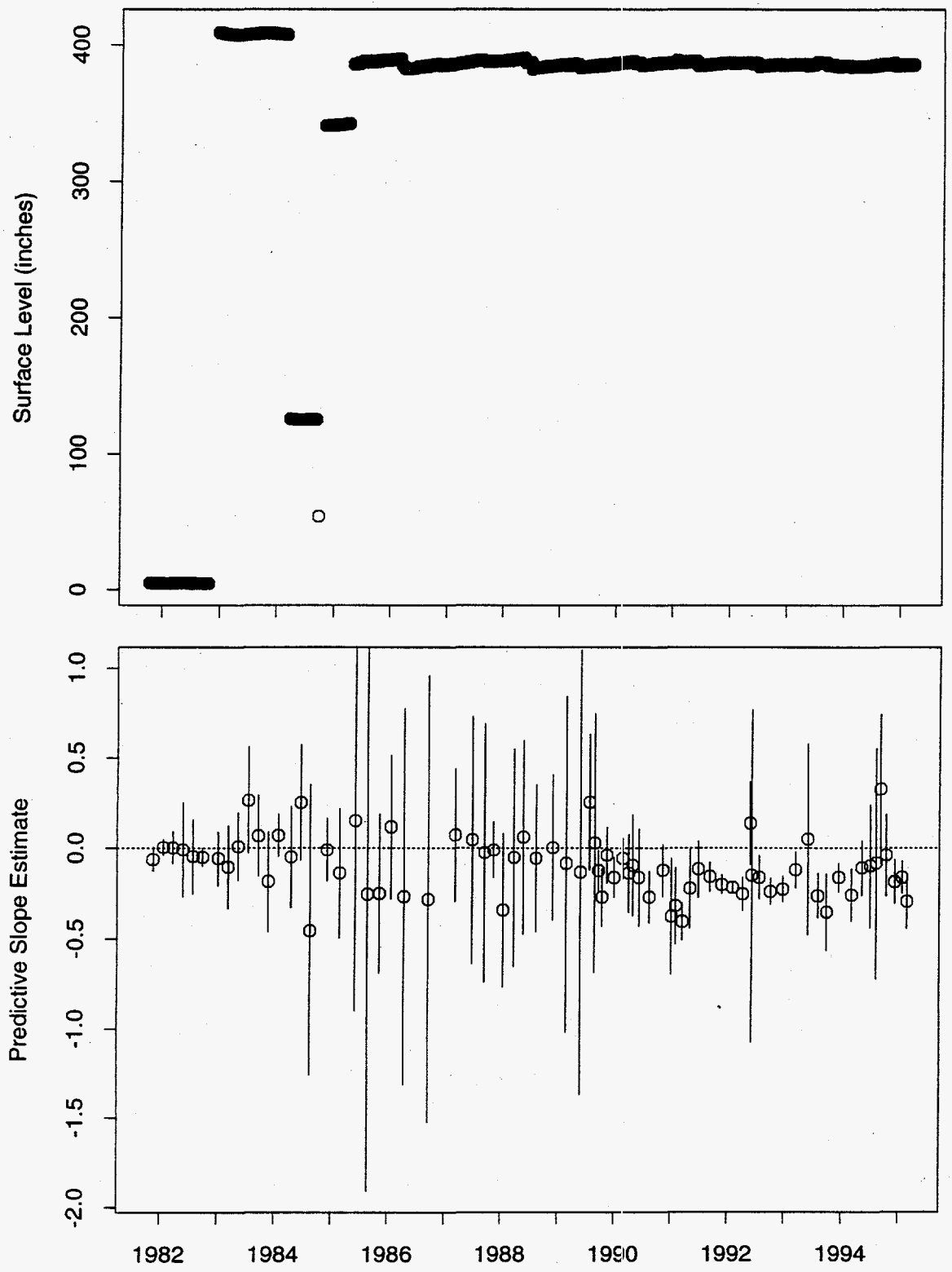

Figure 32: Tank AN–104 FIC Data

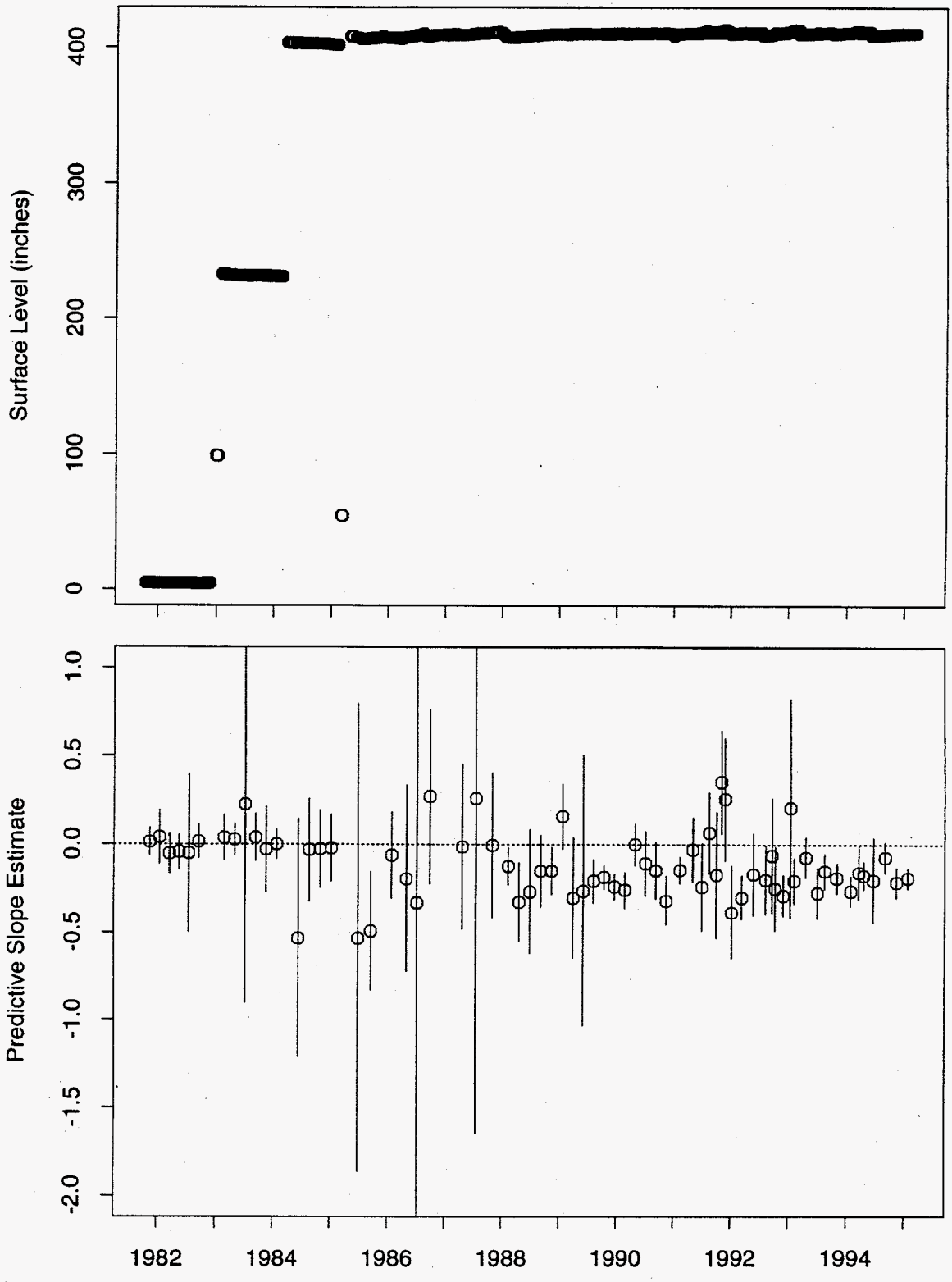

Figure 33: Tank AN–105 FIC Data

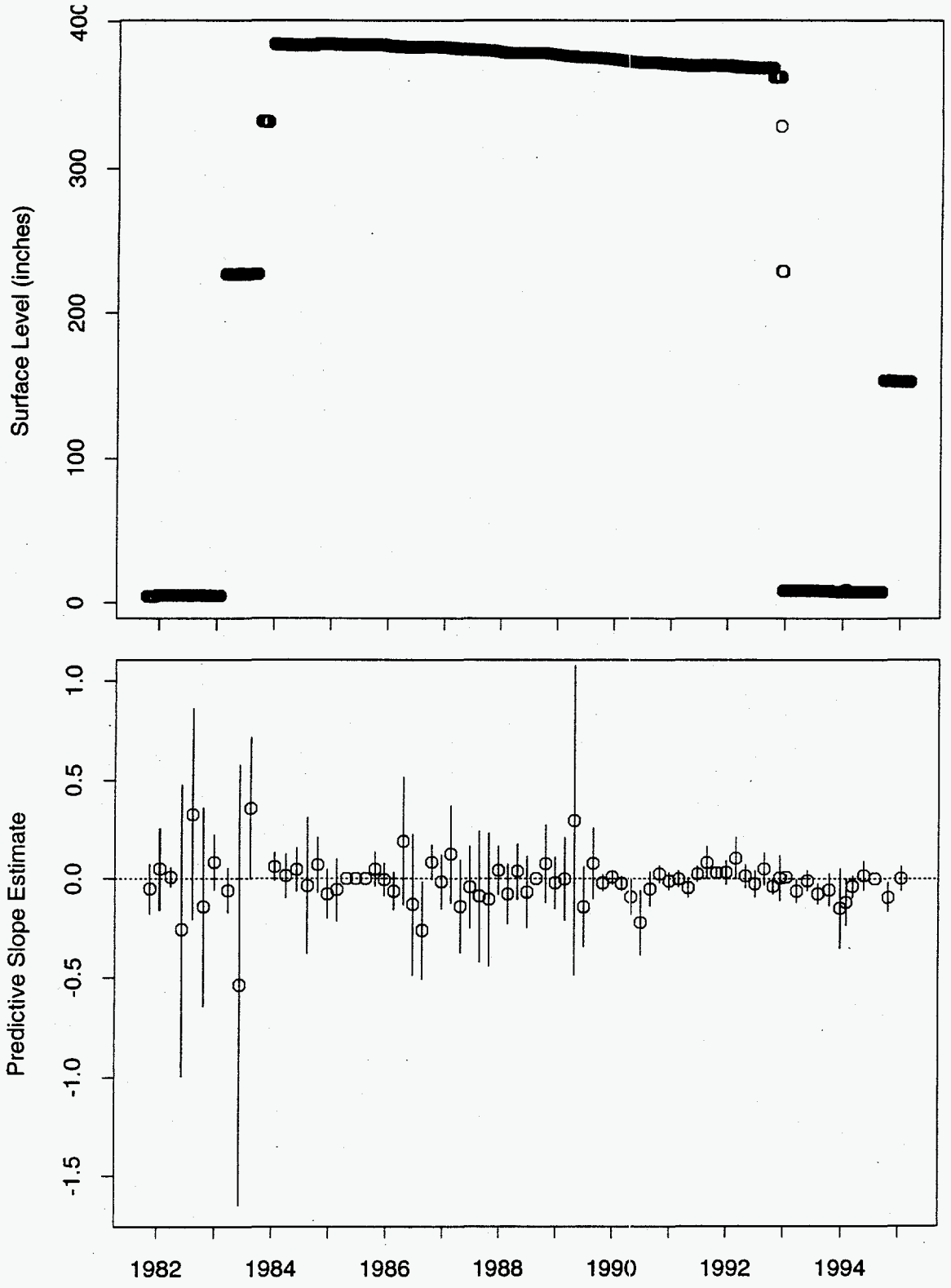

Figure 34: Tank AN–106 FIC Data

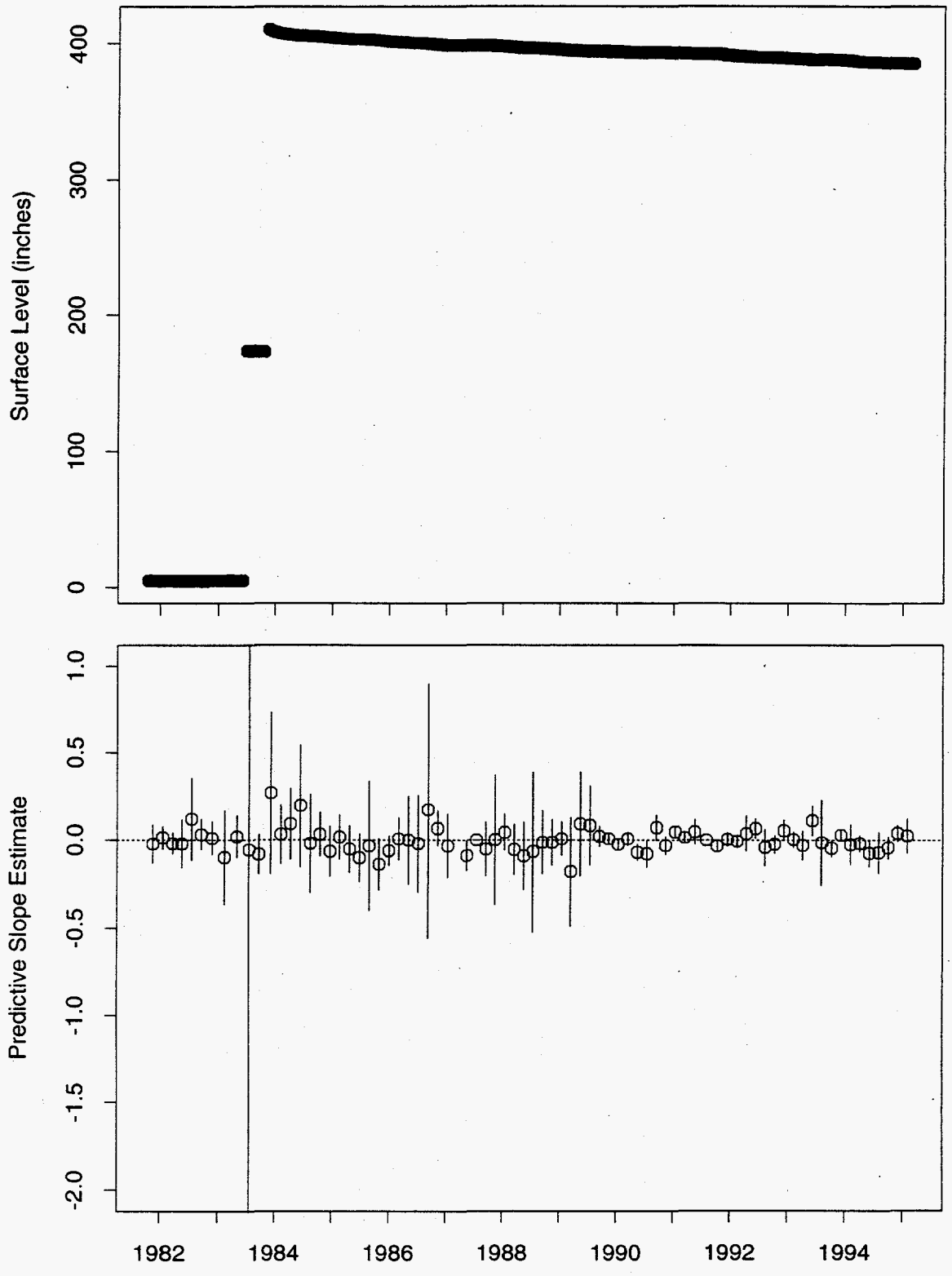

Figure 35: Tank AN–107 FIC Data

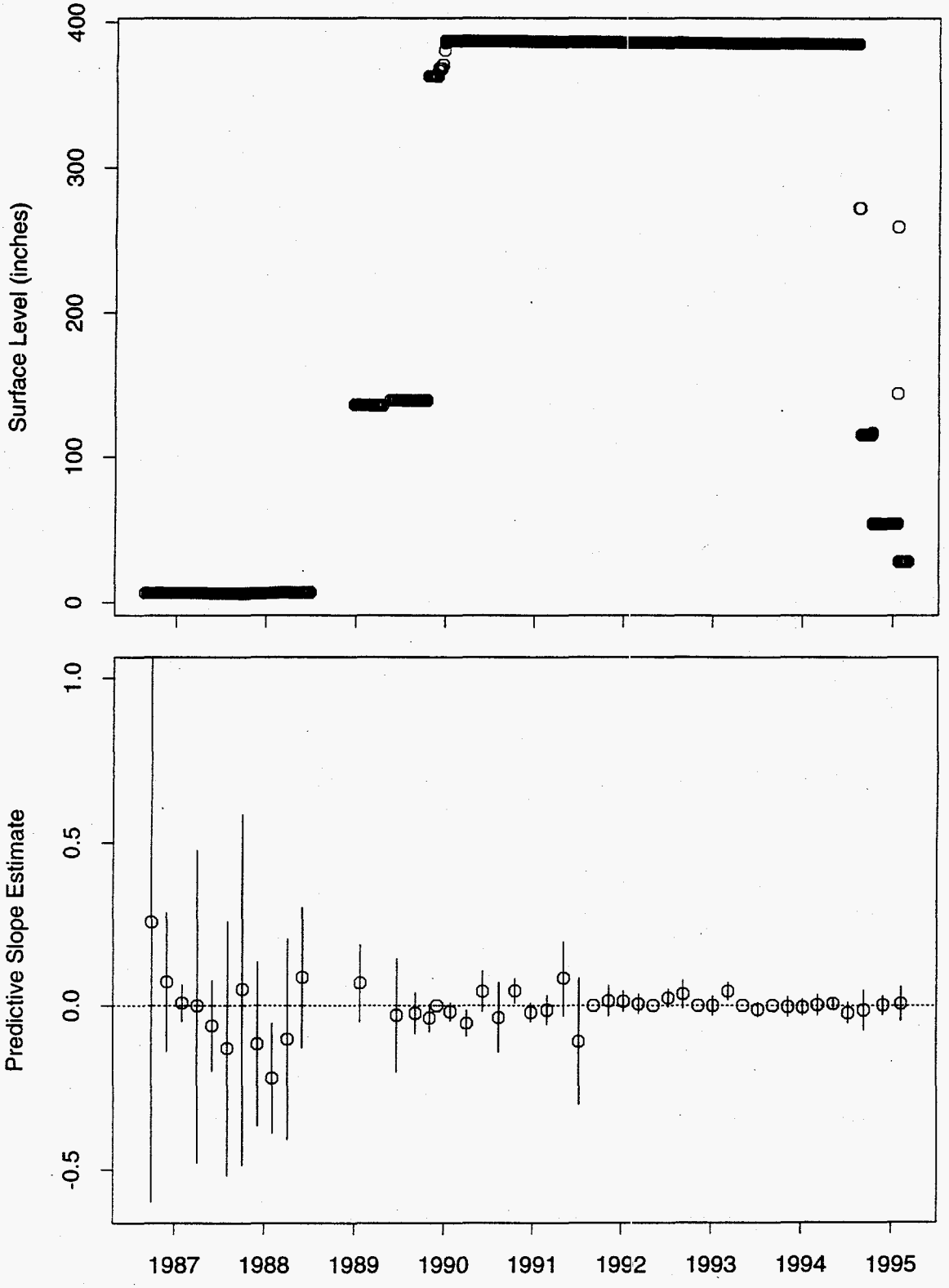

Figure 36: Tank AP–101 FIC Data

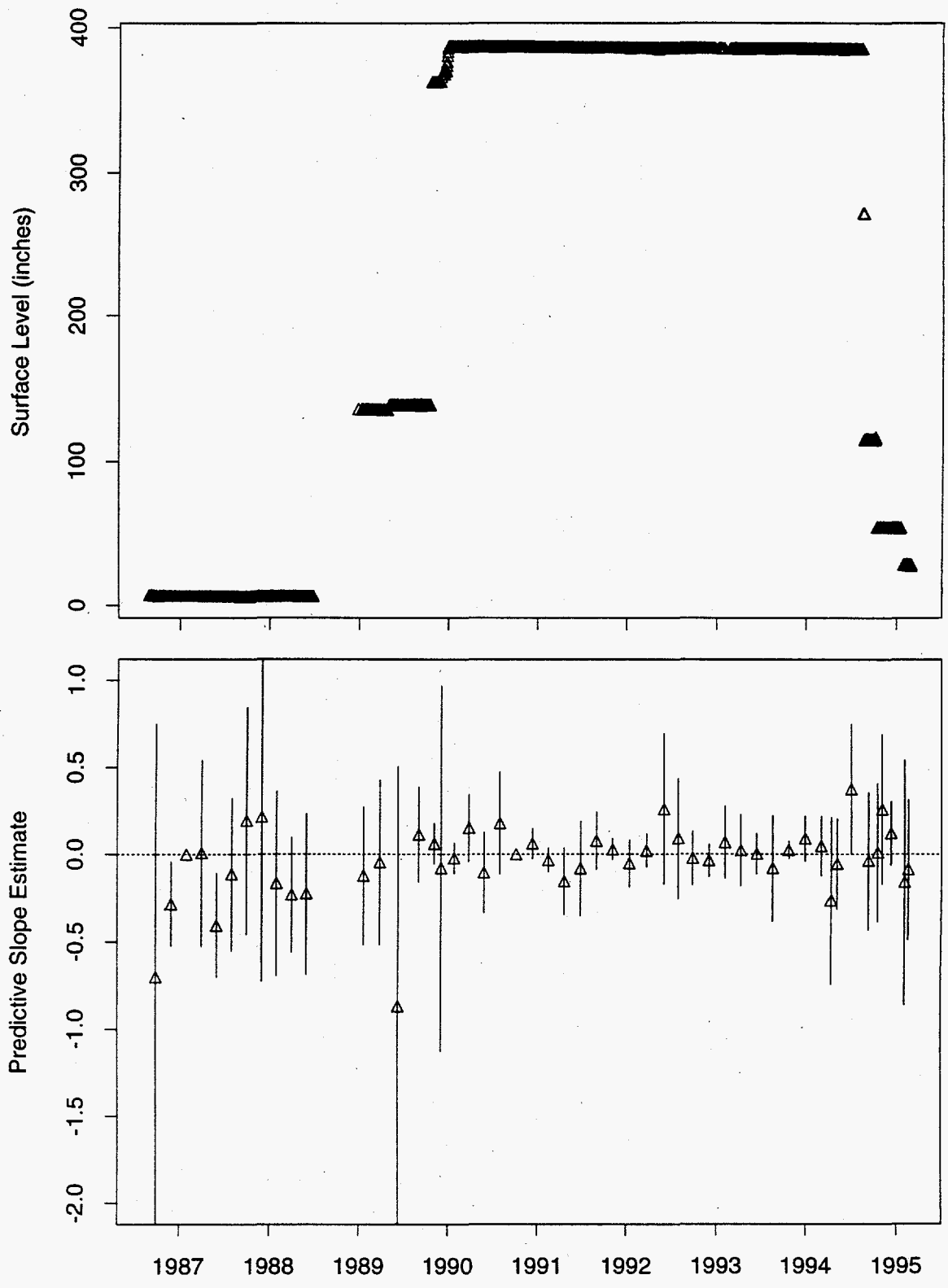

Figure 37: Tank AP–101 MT Data

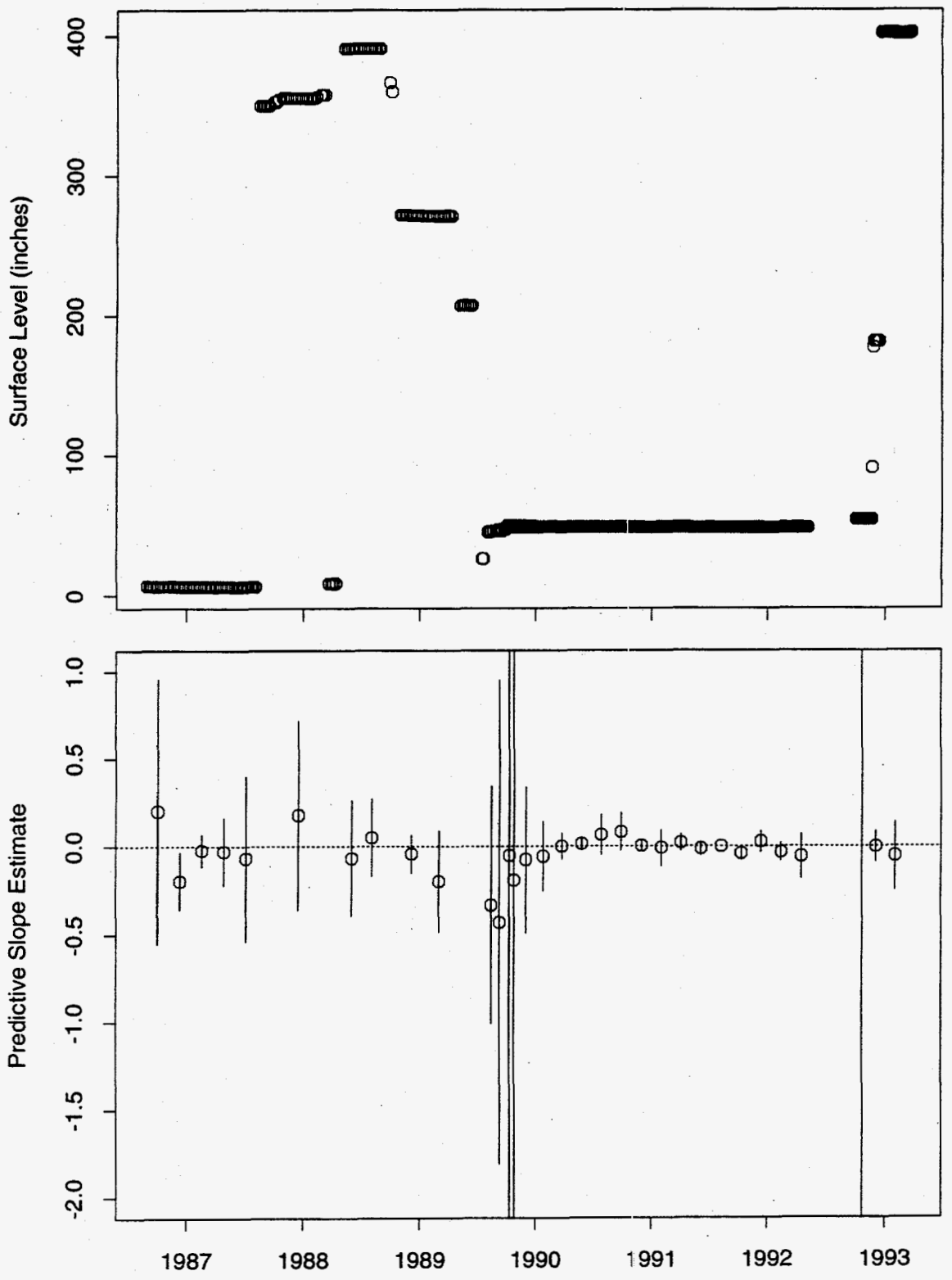

Figure 38: Tank AP–102 FIC Data

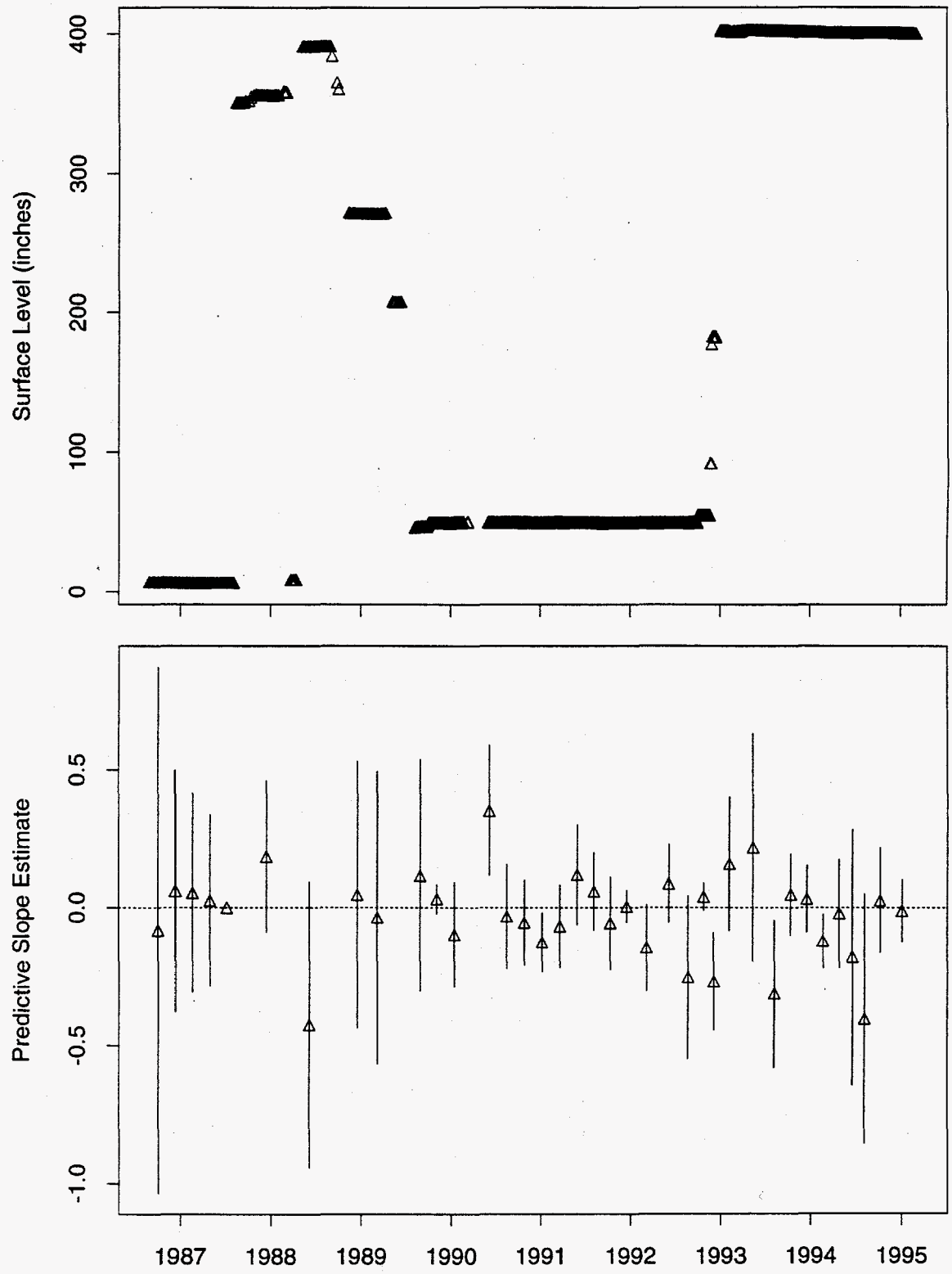

Figure 39: Tank AP–102 MT Data

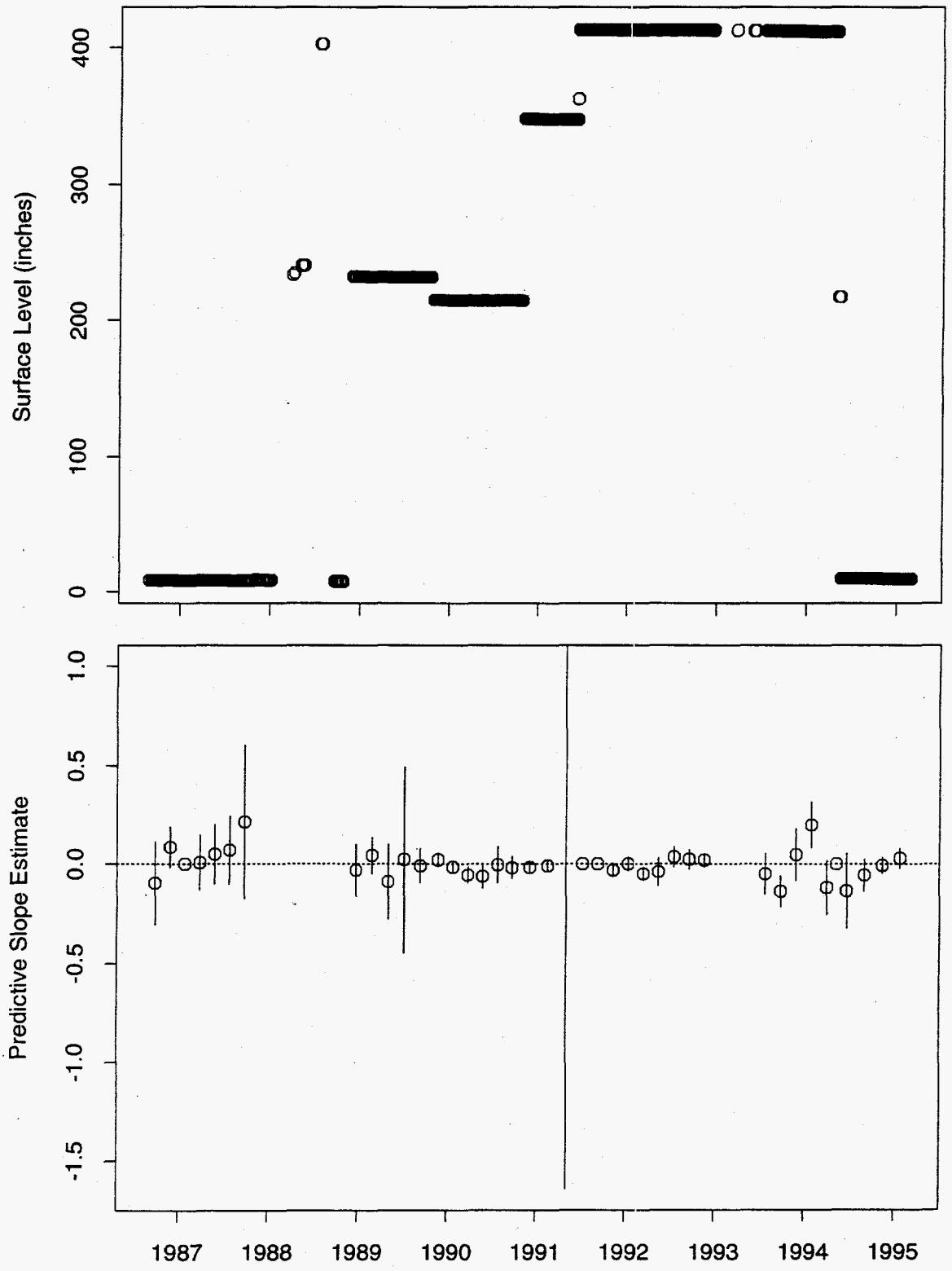

Figure 40: Tank AP–103 FIC Data

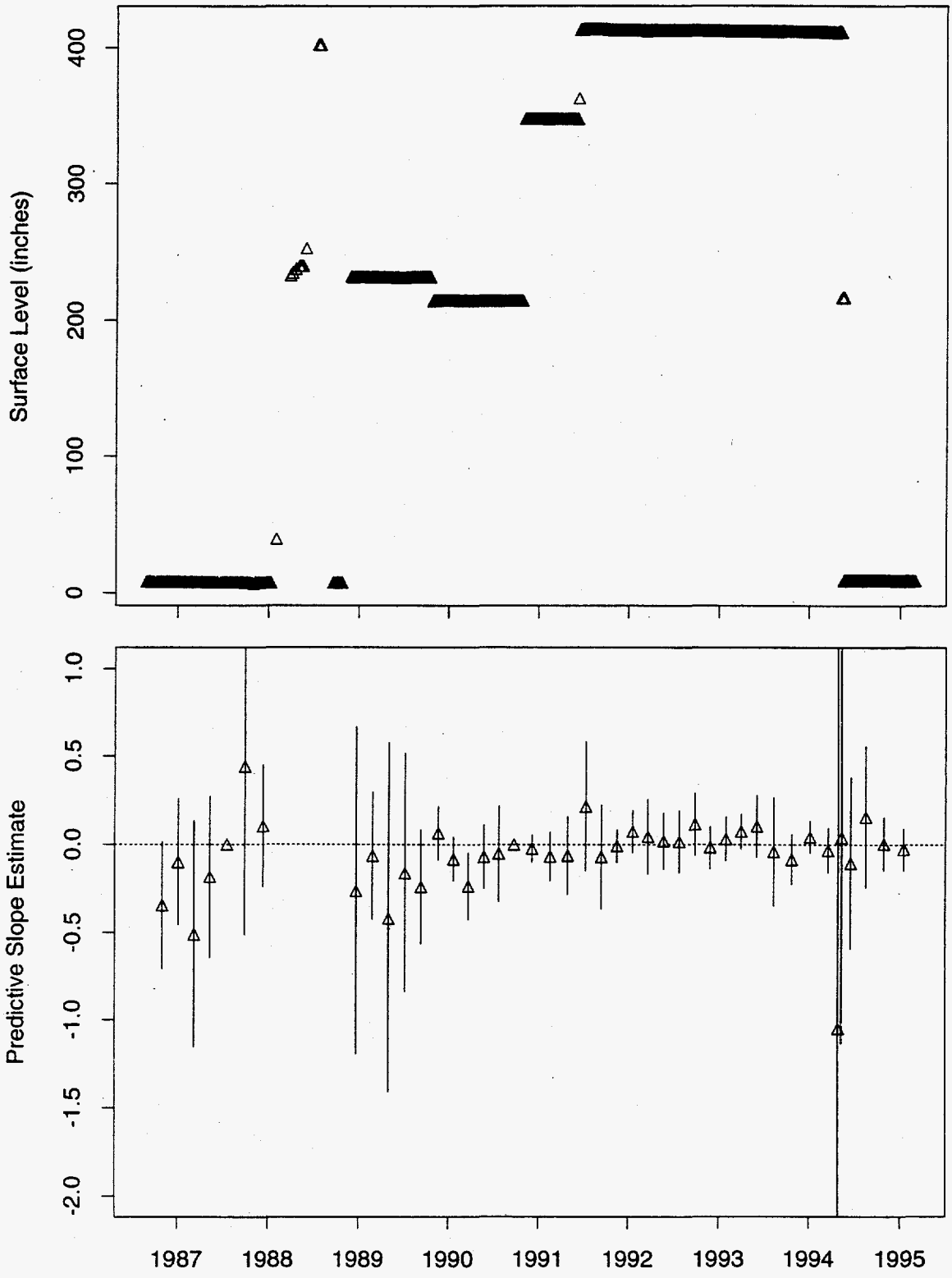

Figure 41: Tank AP-103 MT Data

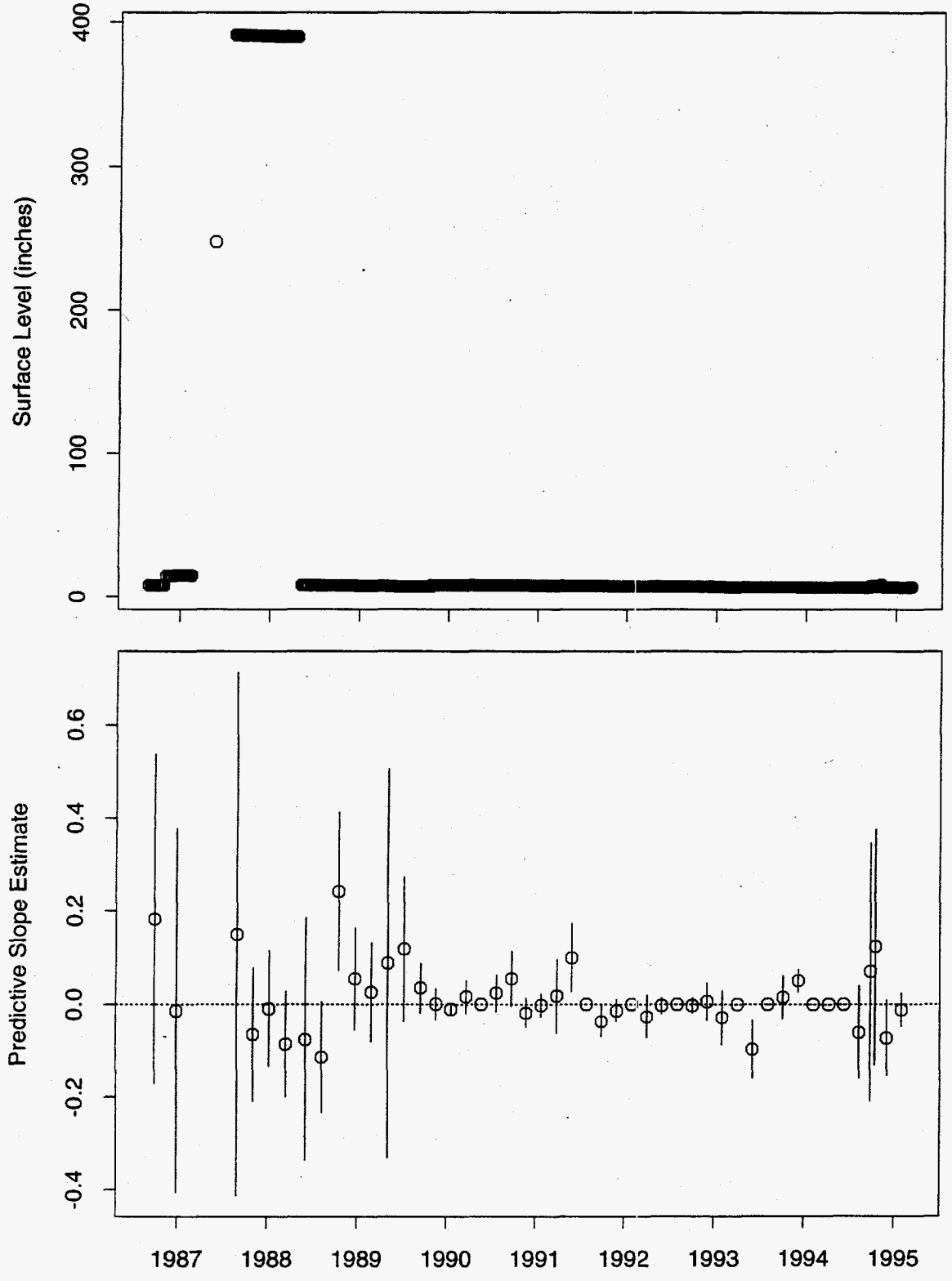

Figure 42: Tank AP–104 FIC Data

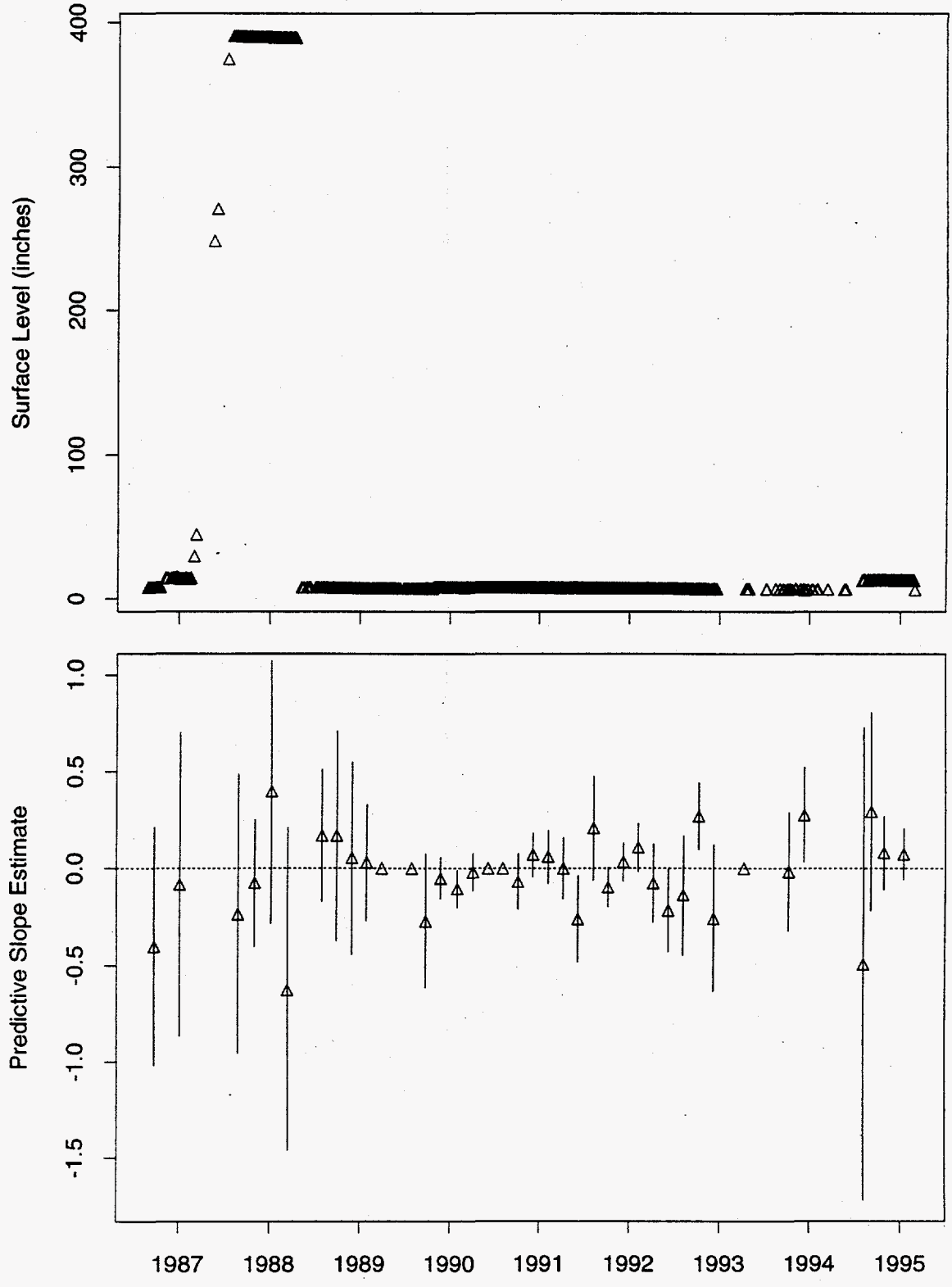

Figure 43: Tank AP–104 MT Data

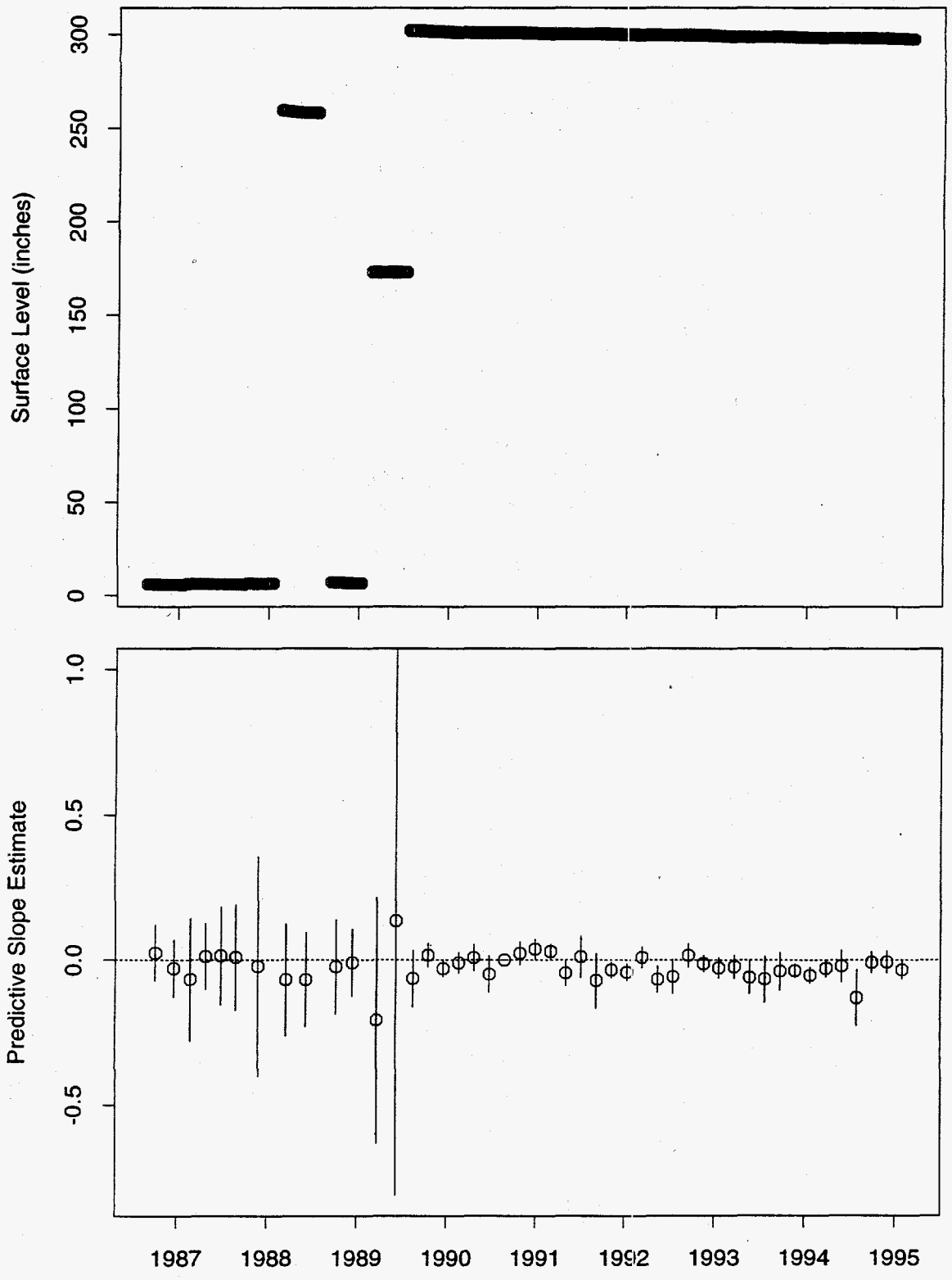

Figure 44: Tank AP–105 FIC Data

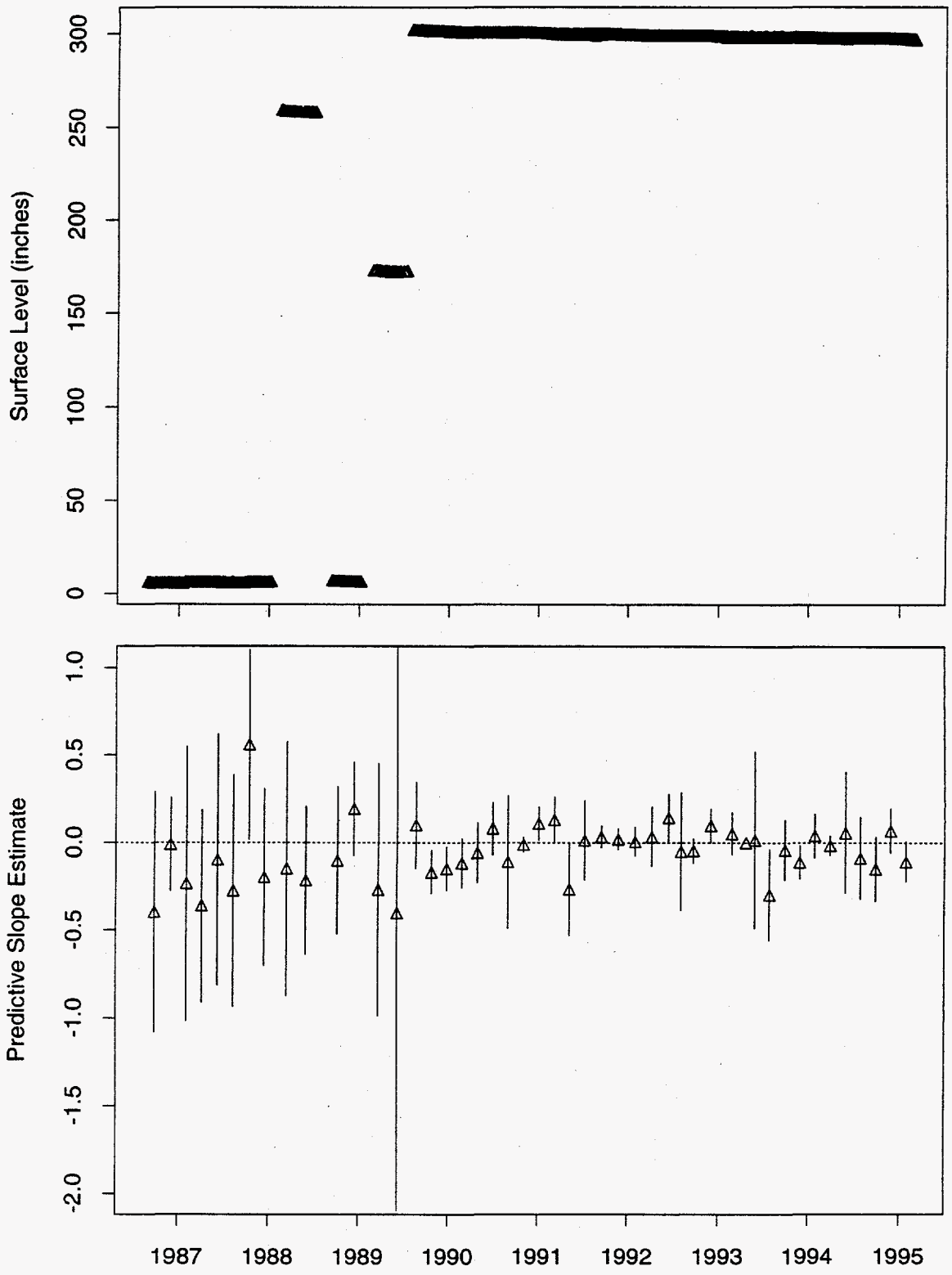

Figure 45: Tank AP–105 MT Data

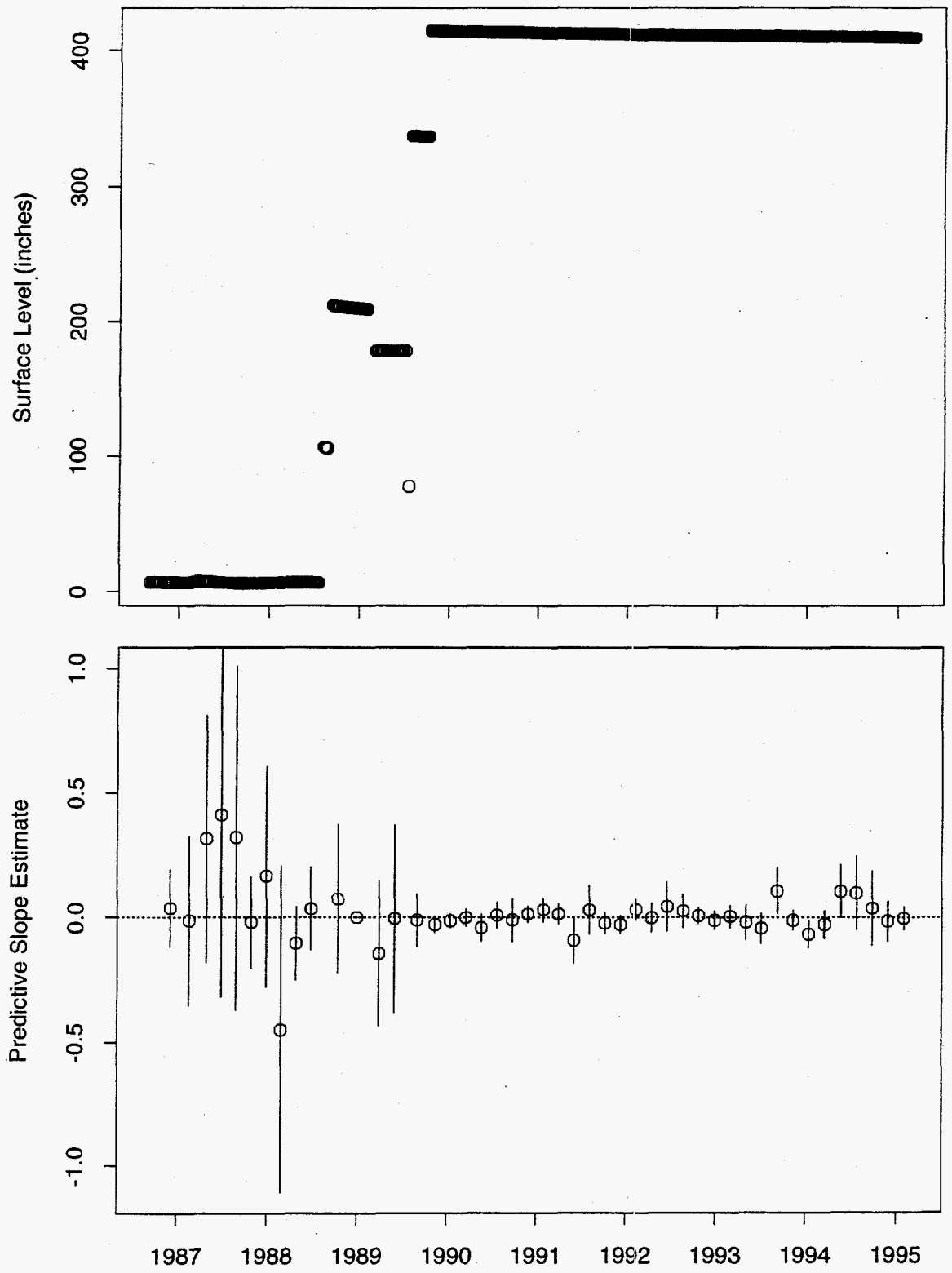

Figure 46: Tank AP–106 FIC Data

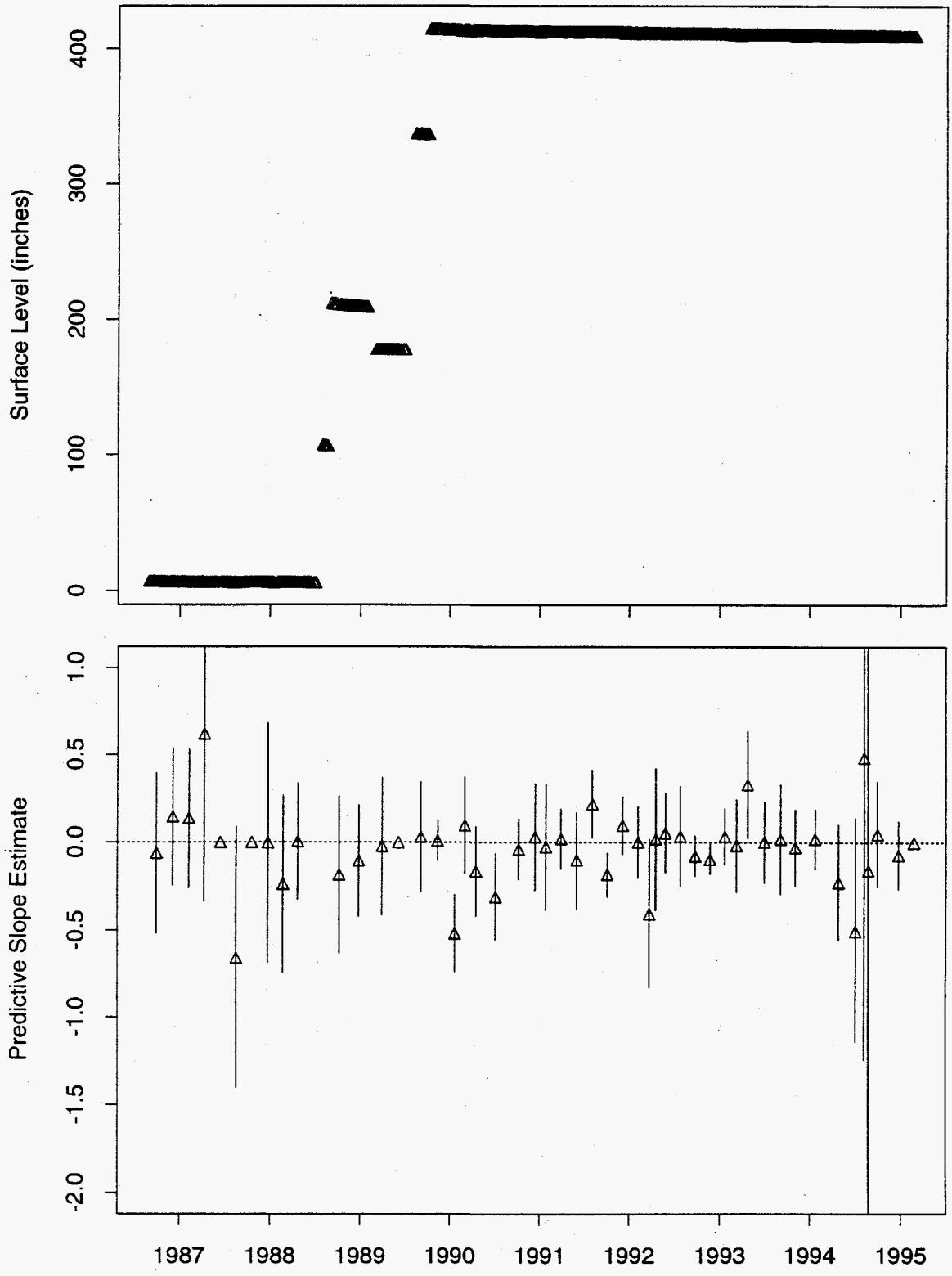

Figure 47: Tank AP–106 MT Data

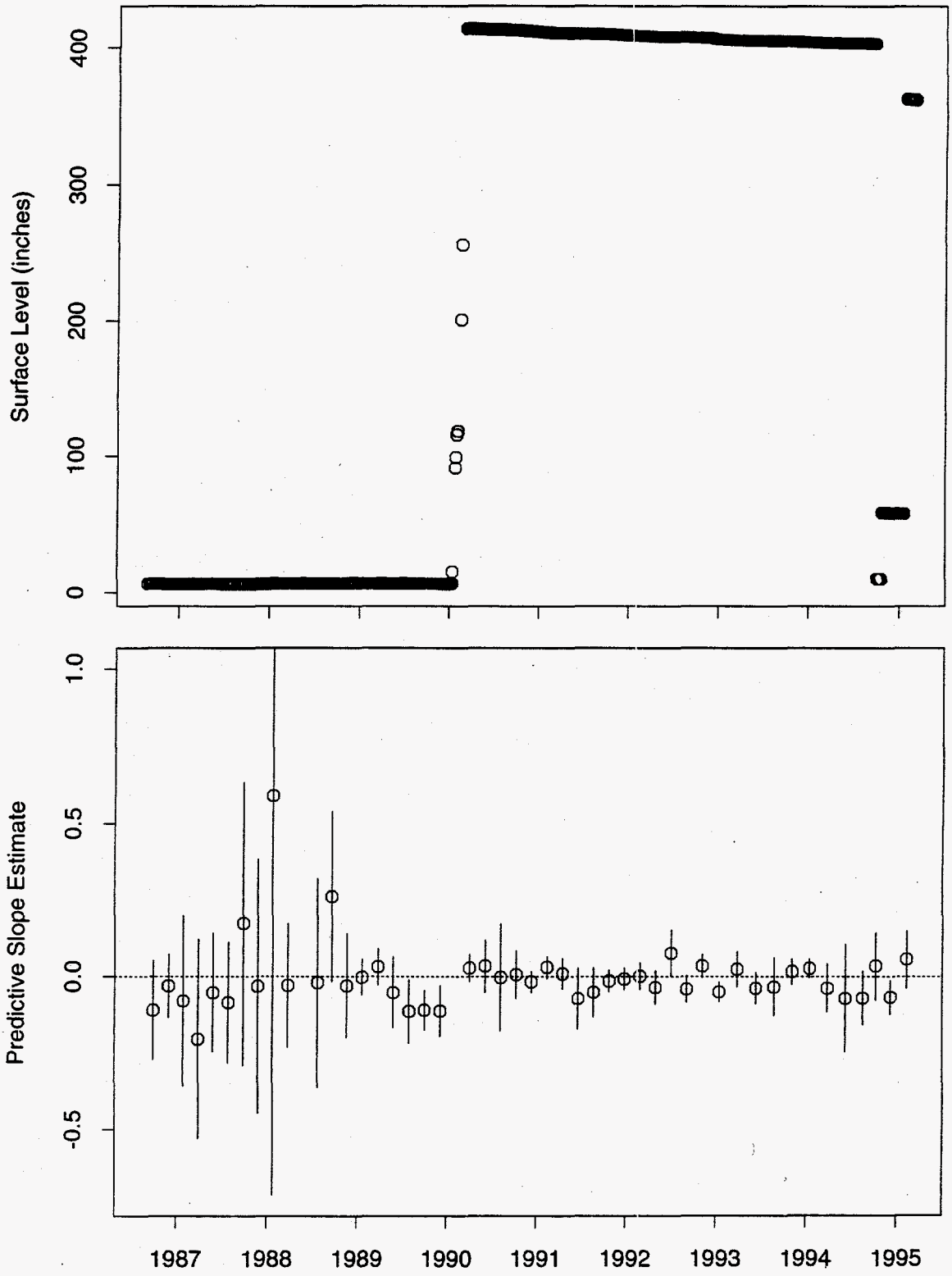

Figure 48: Tank AP–107 FIC Data

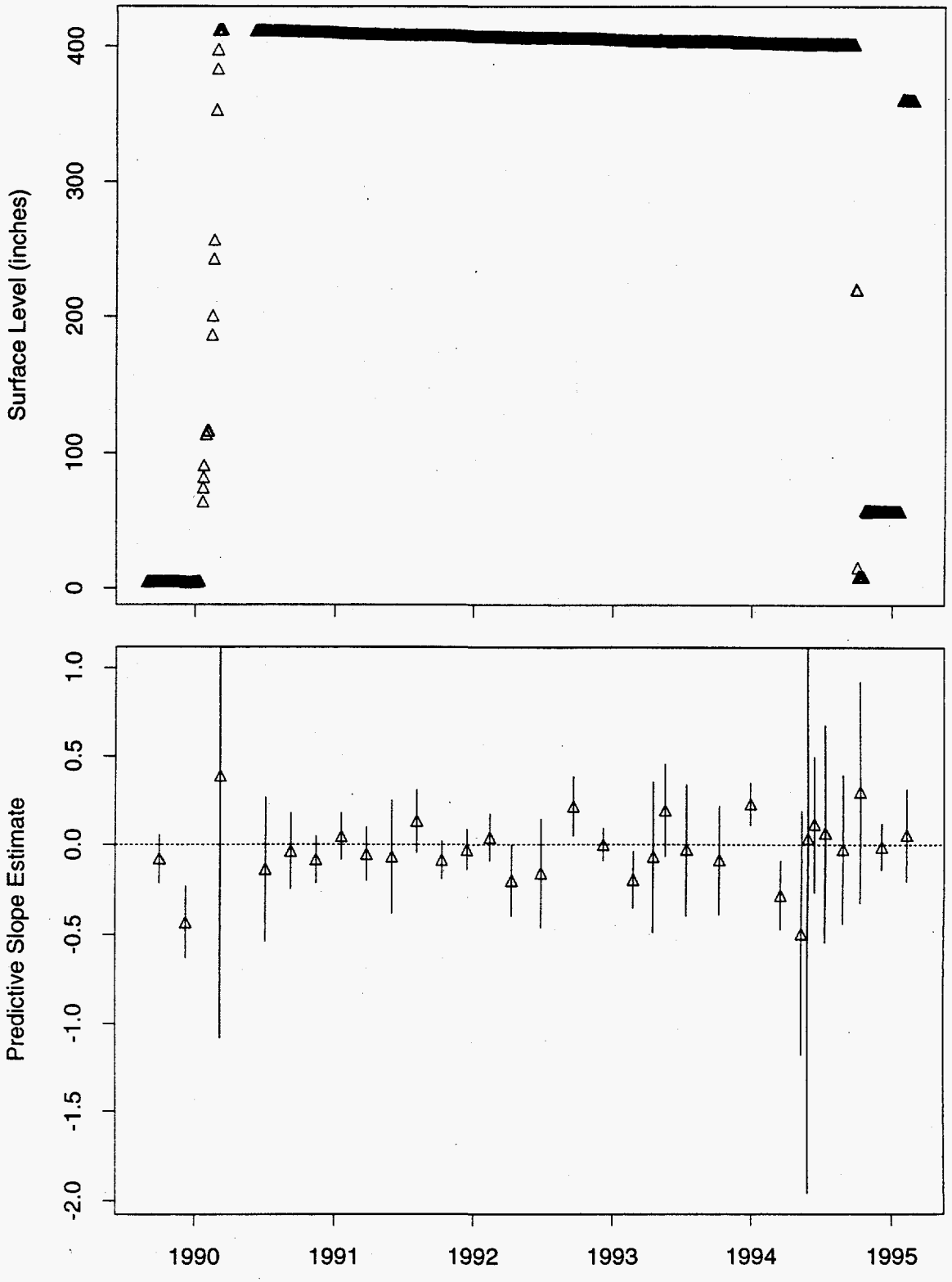

Figure 49: Tank AP–107 MT Data

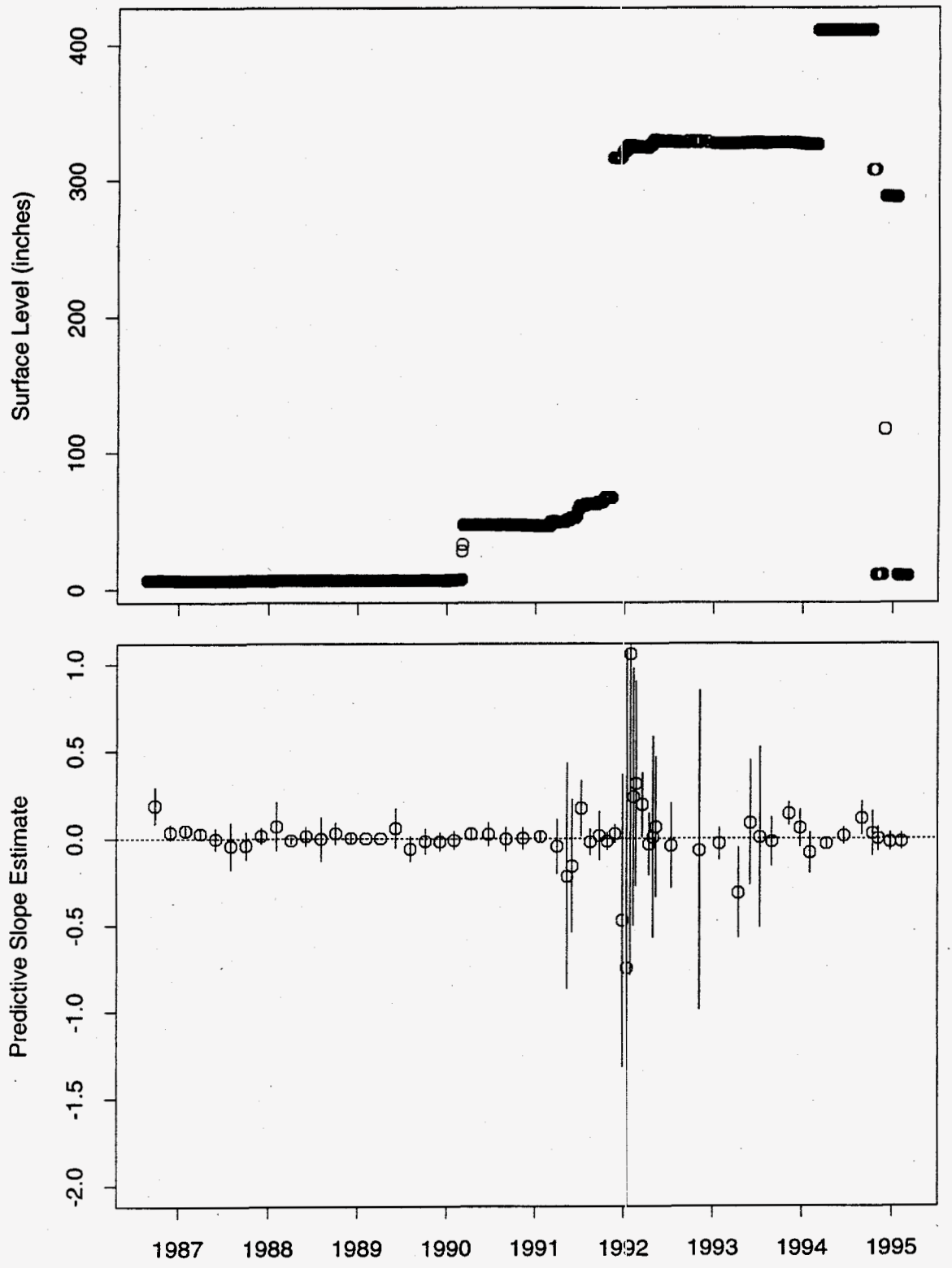

Figure 50: Tank AP–108 FIC Data

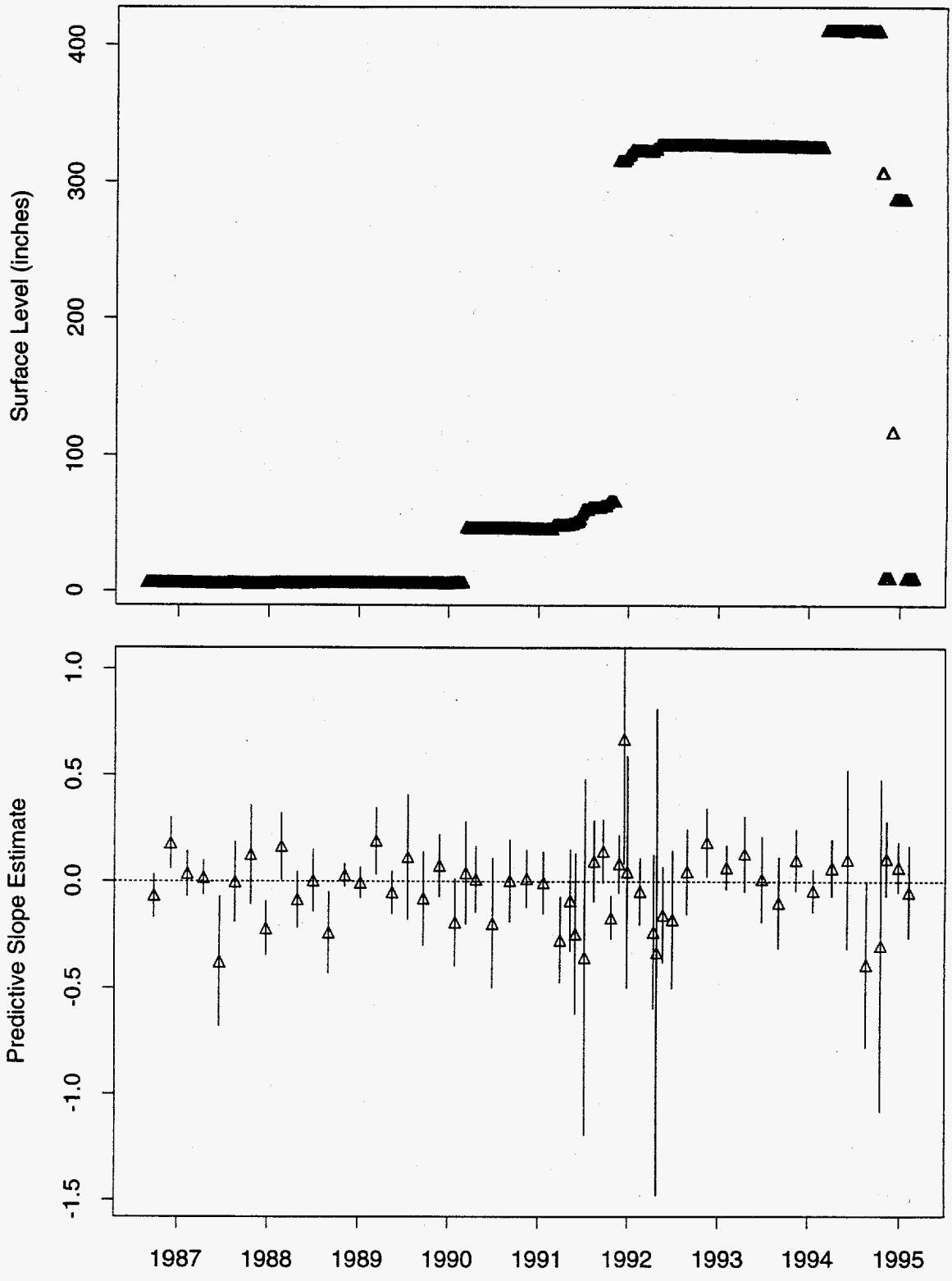

Figure 51: Tank AP–108 MT Data

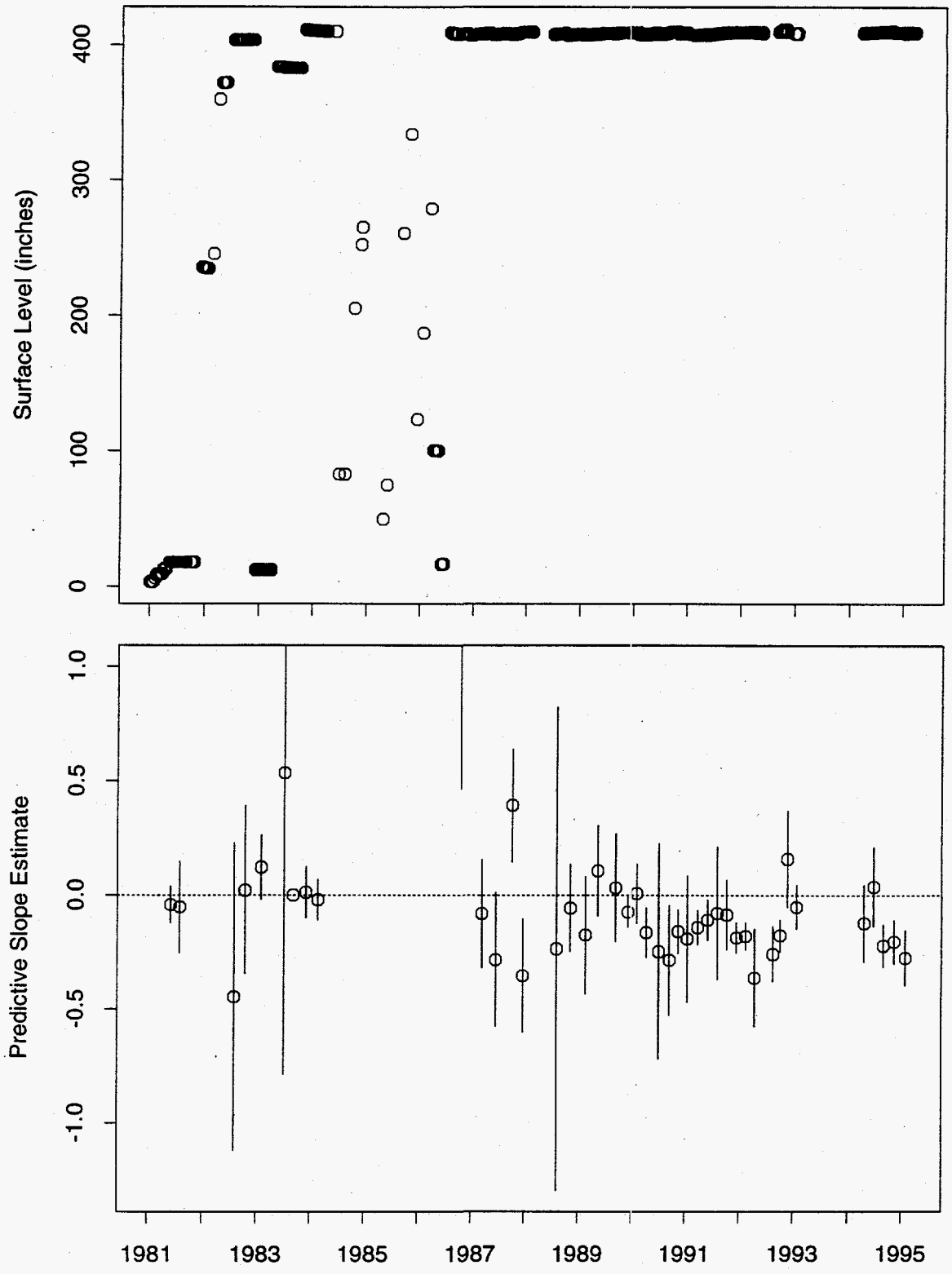

Figure 52: Tank AW–101 FIC Data

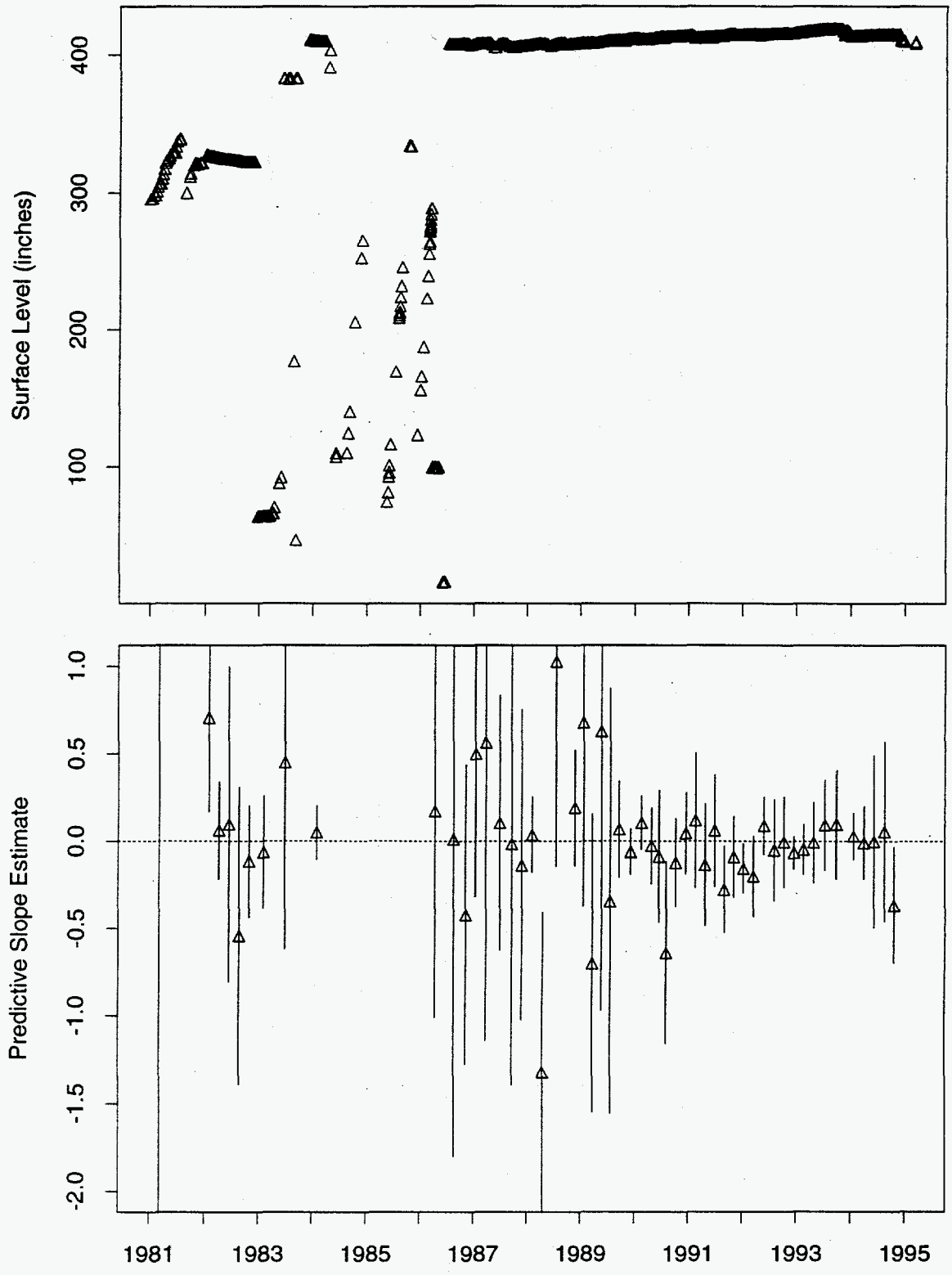

Figure 53: Tank AW–101 MT Data

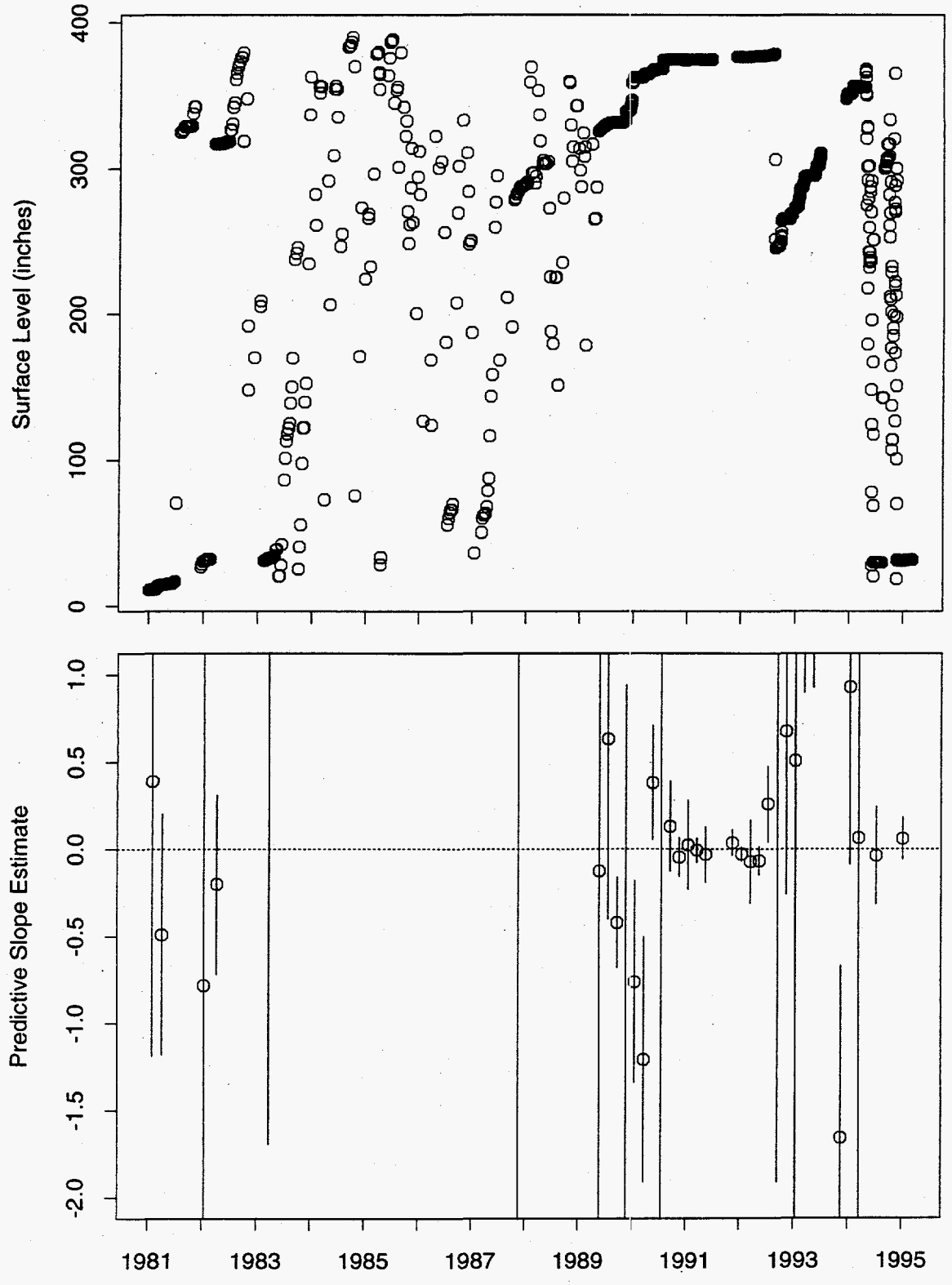

Figure 54: Tank AW-102 FIC Data

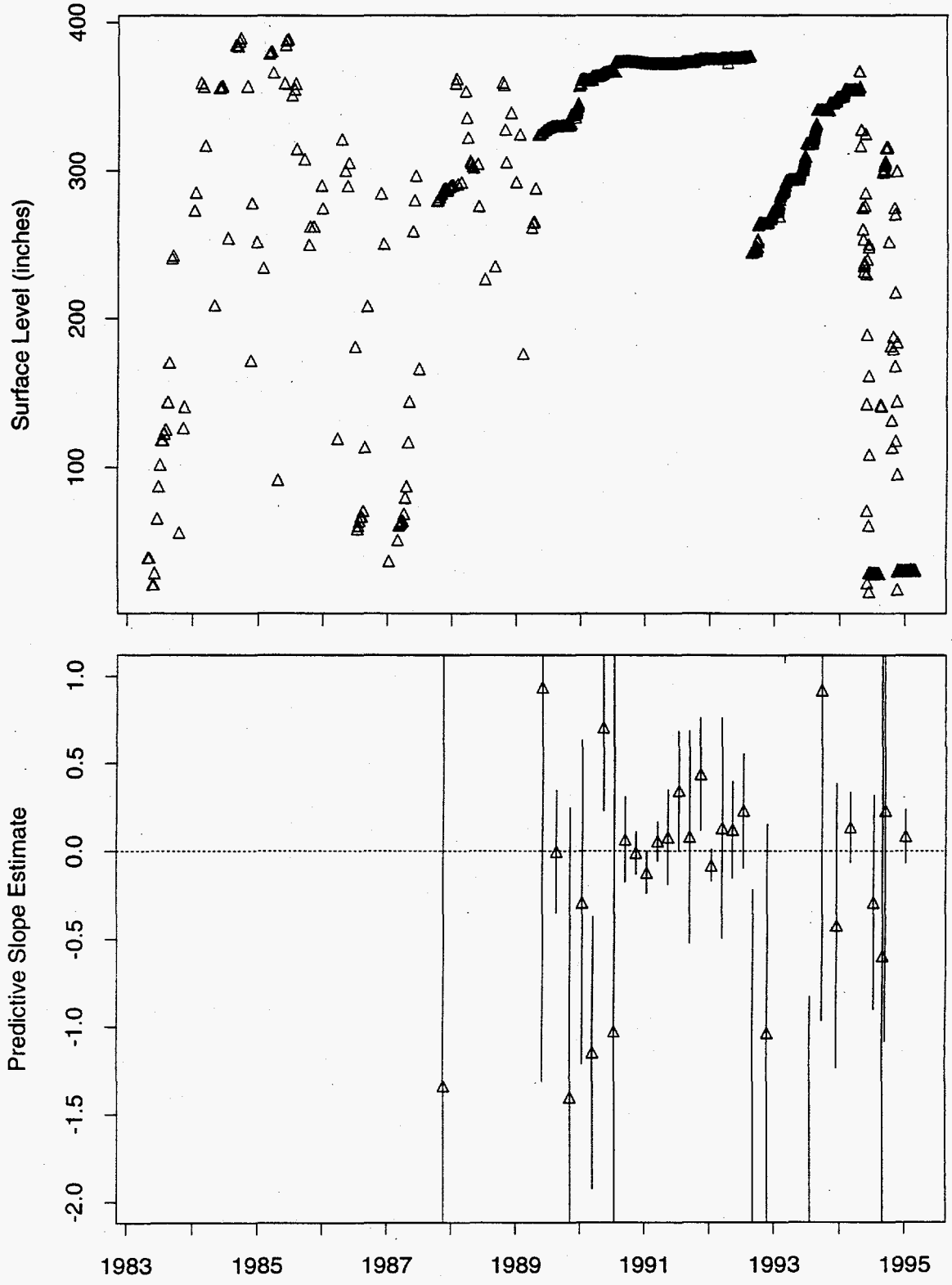

Figure 55: Tank AW–102 MT Data

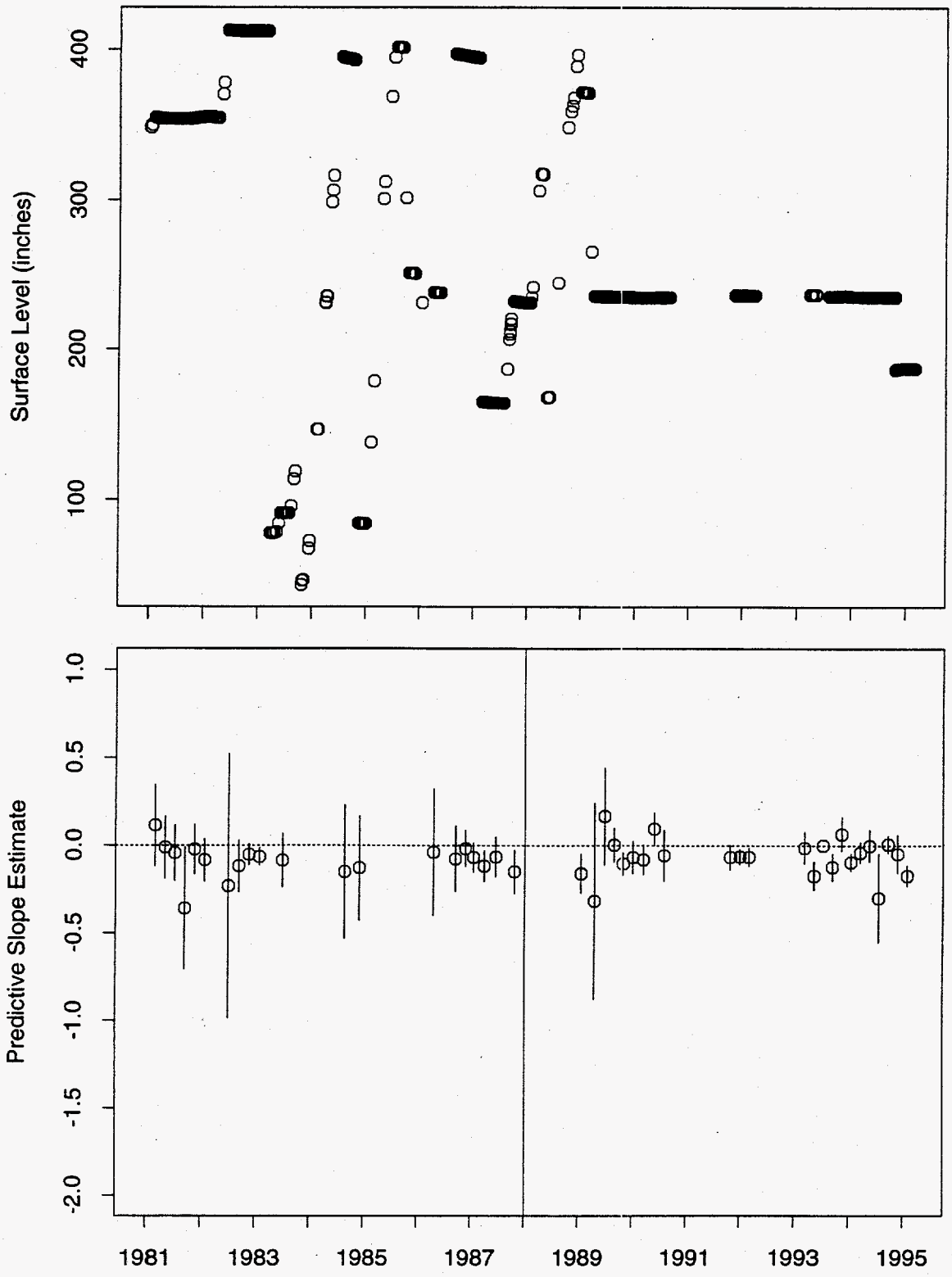

Figure 56: Tank AW–103 FIC Data

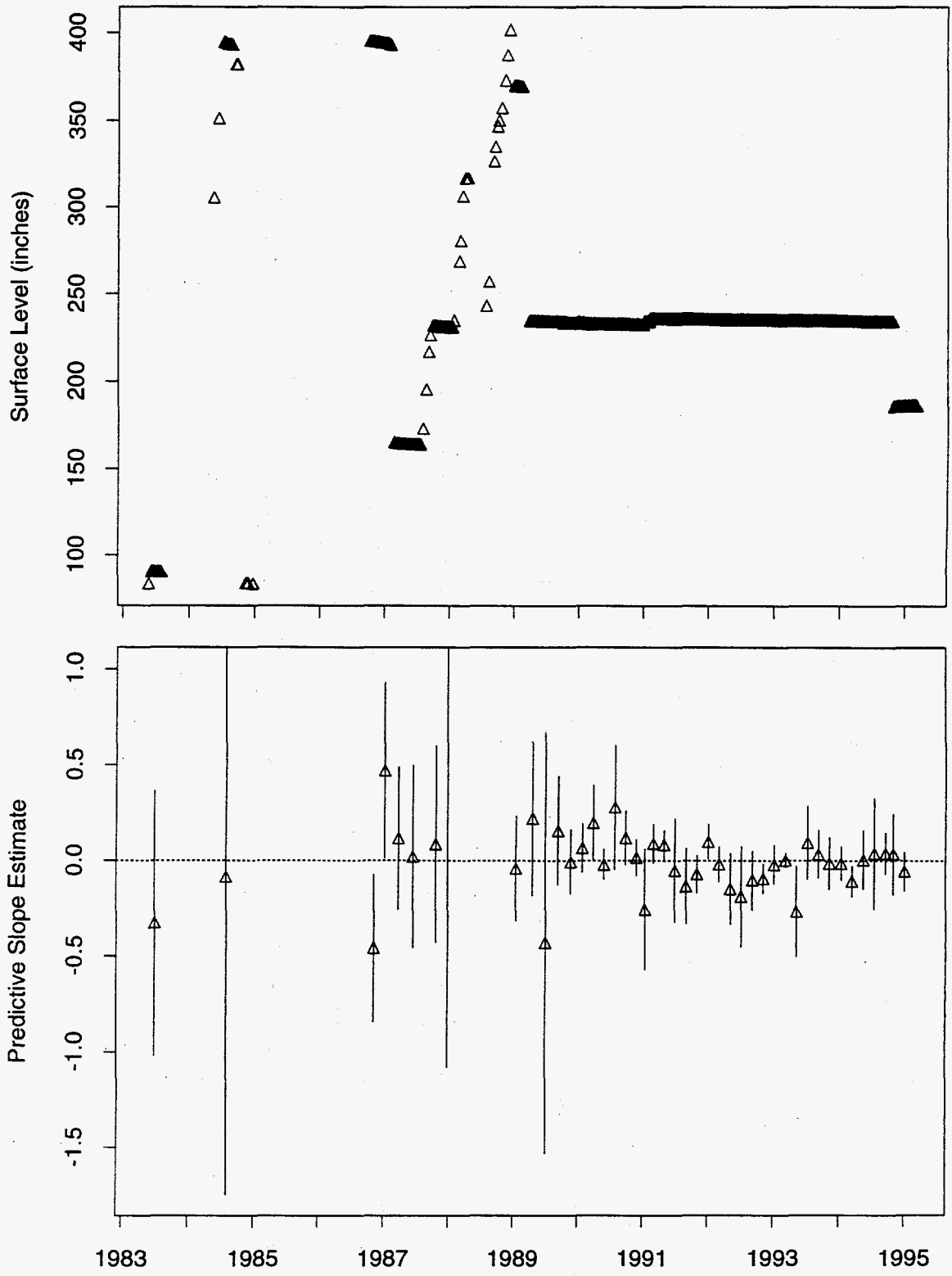

Figure 57: Tank AW–103 MT Data

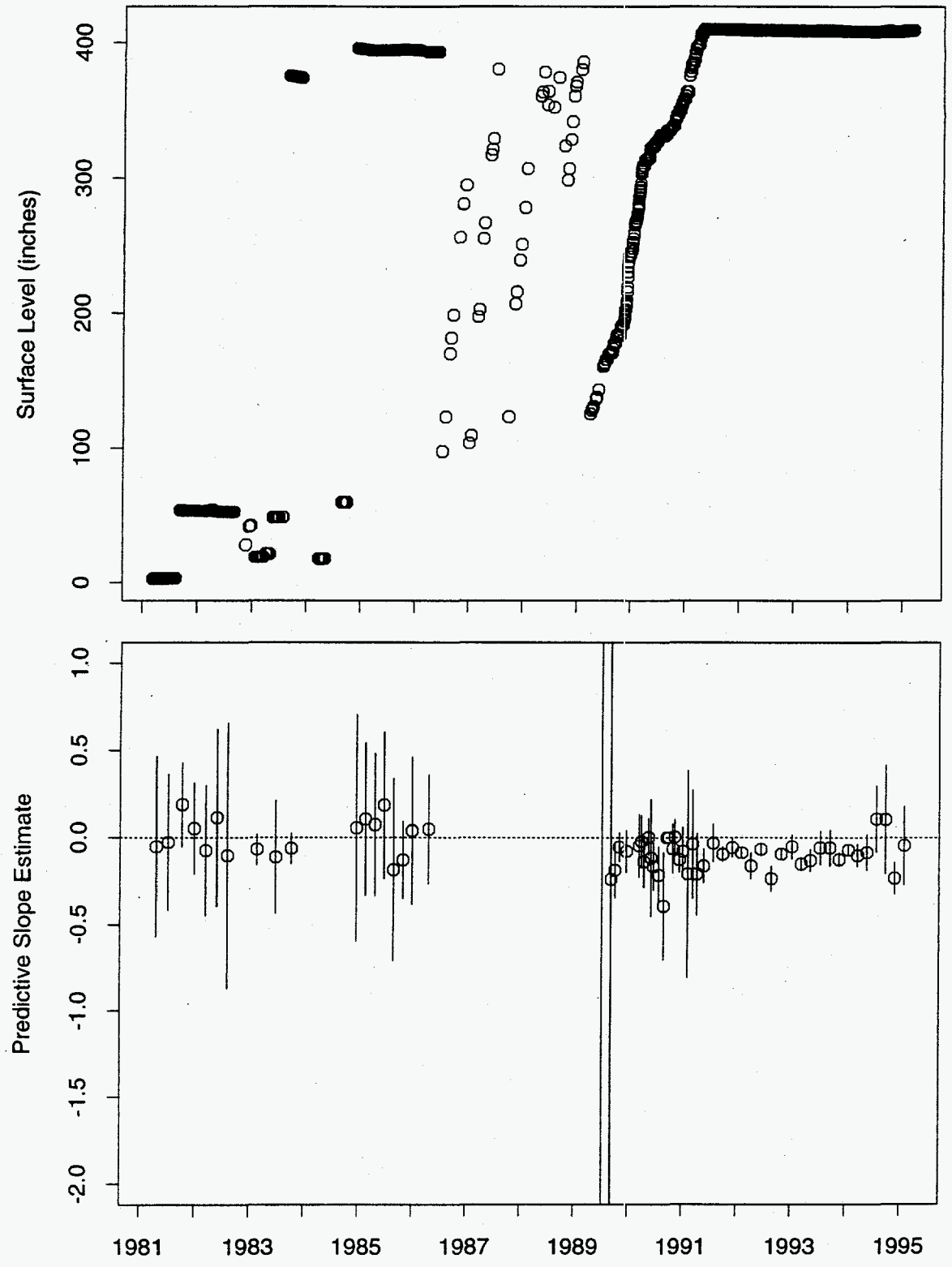

Figure 58: Tank AW-104 FIC Data

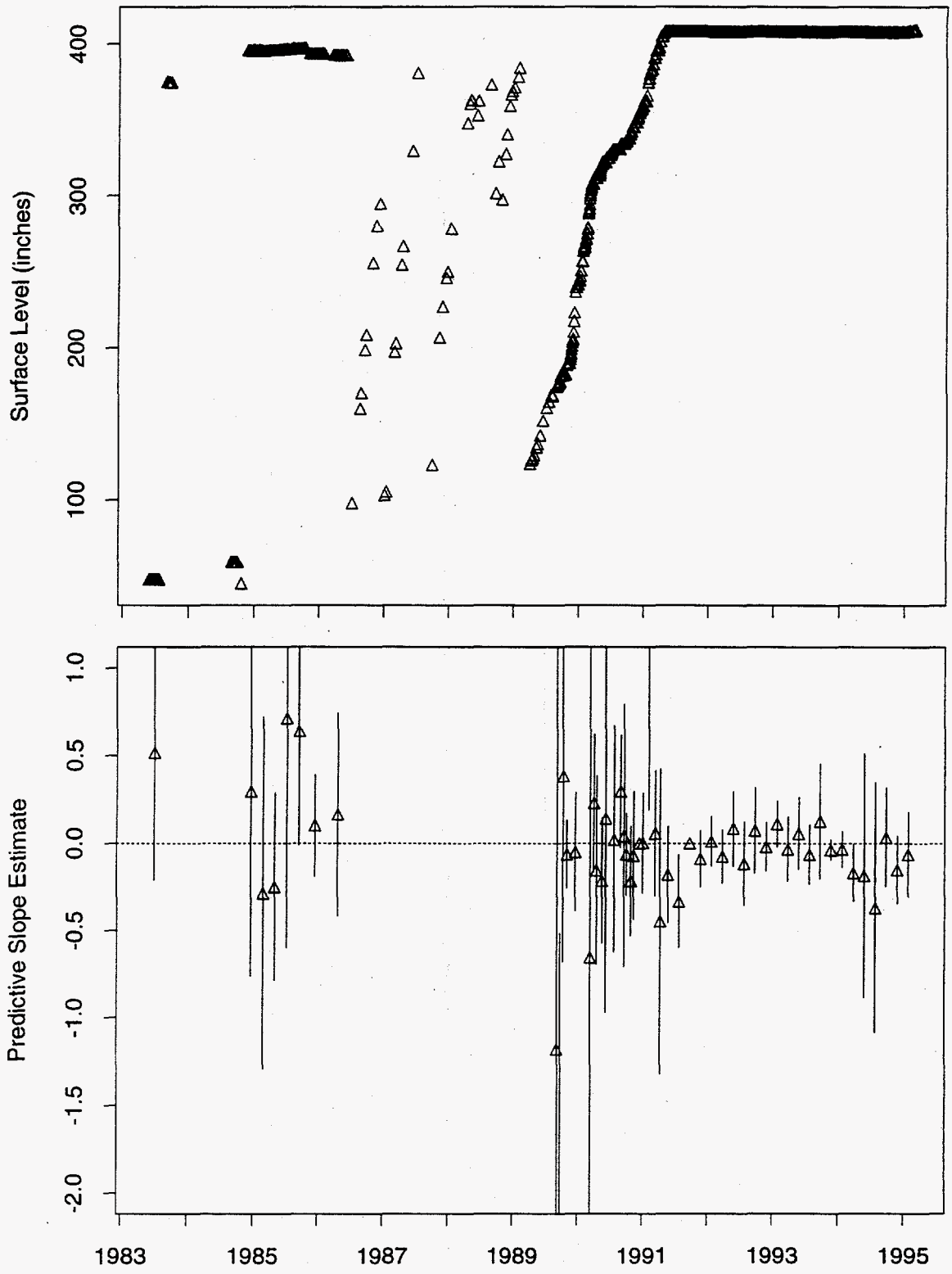

Figure 59: Tank AW–104 MT Data

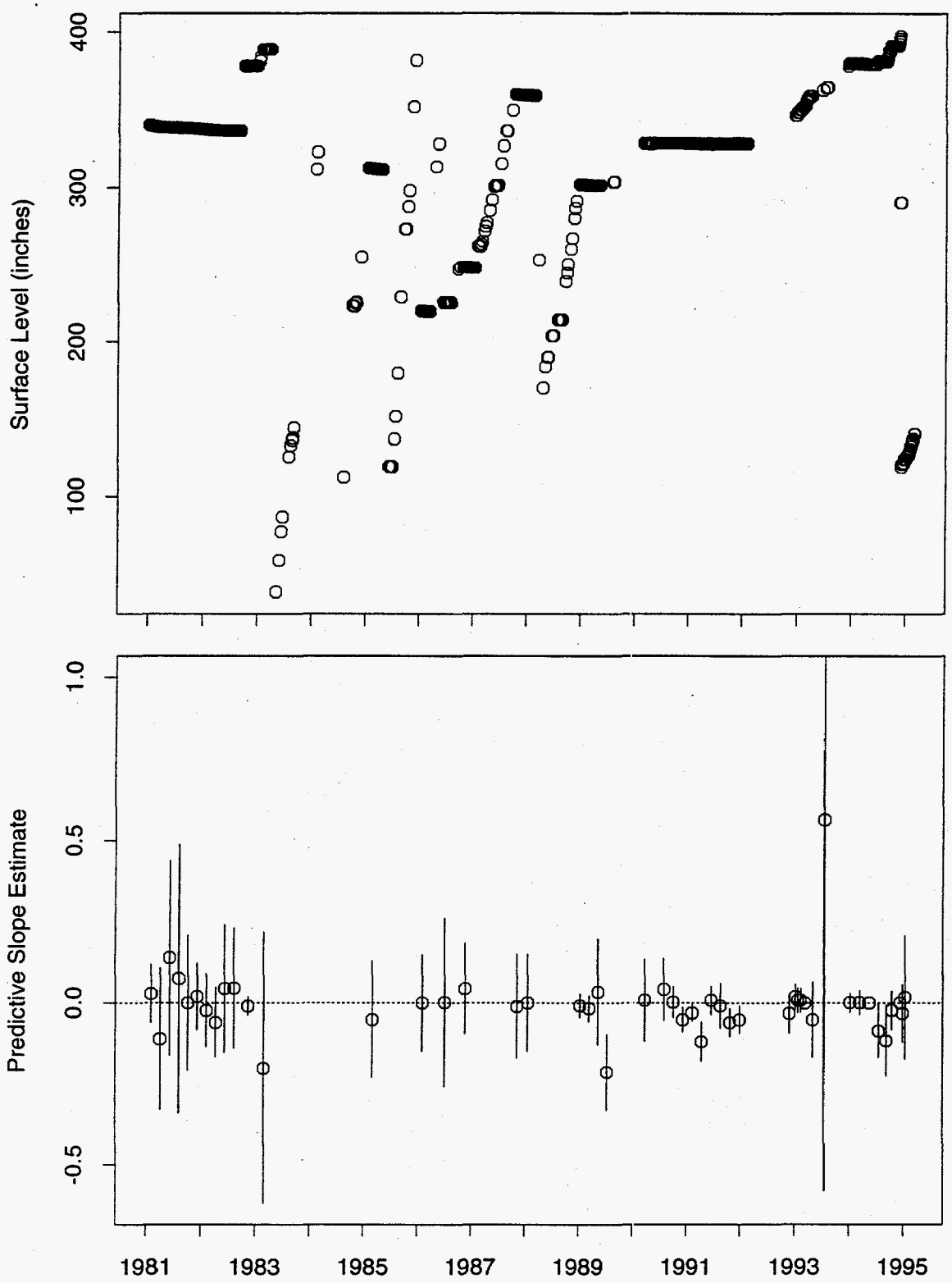

Figure 60: Tank AW–105 FIC Data

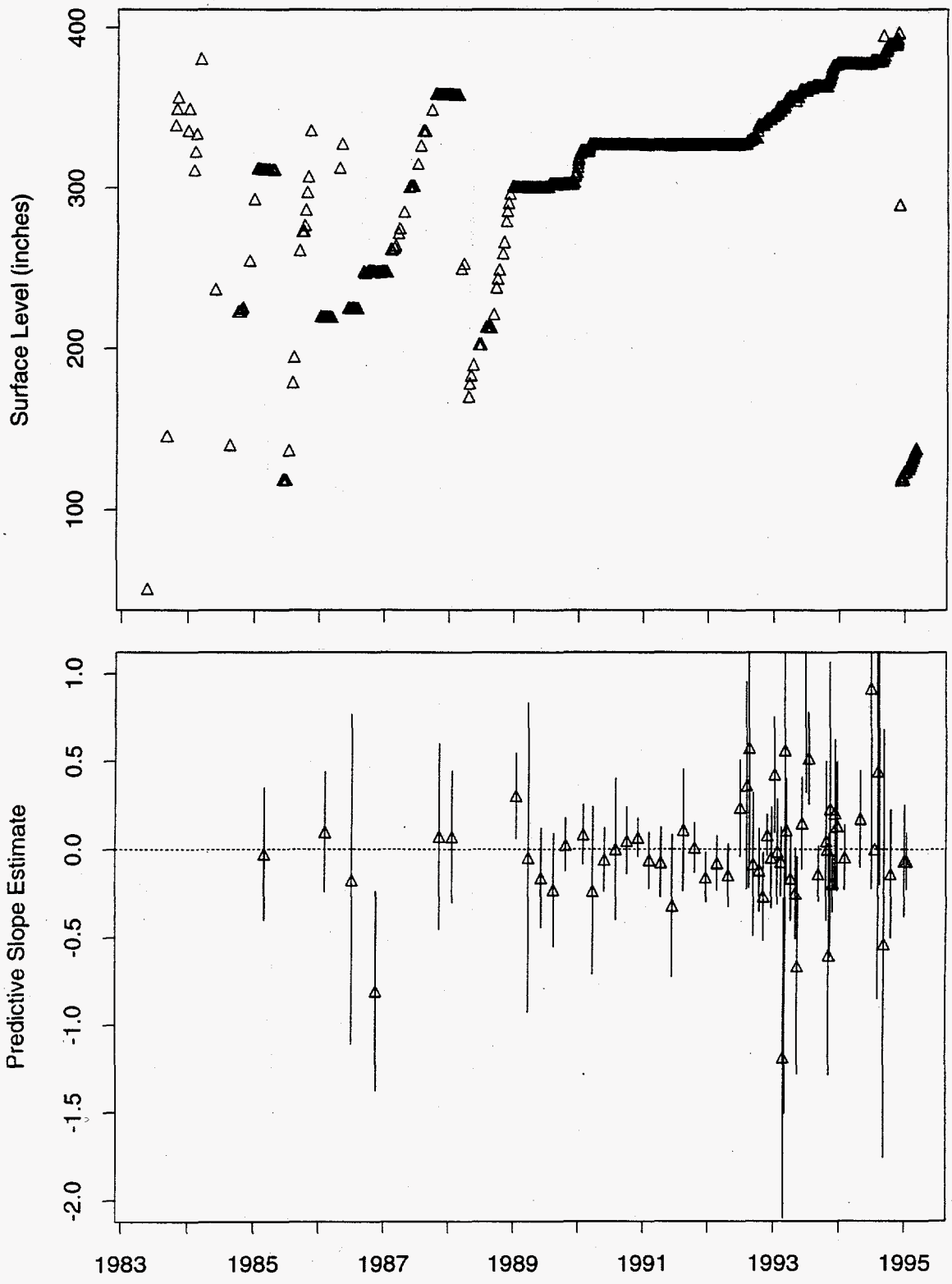

Figure 61: Tank AW–105 MT Data

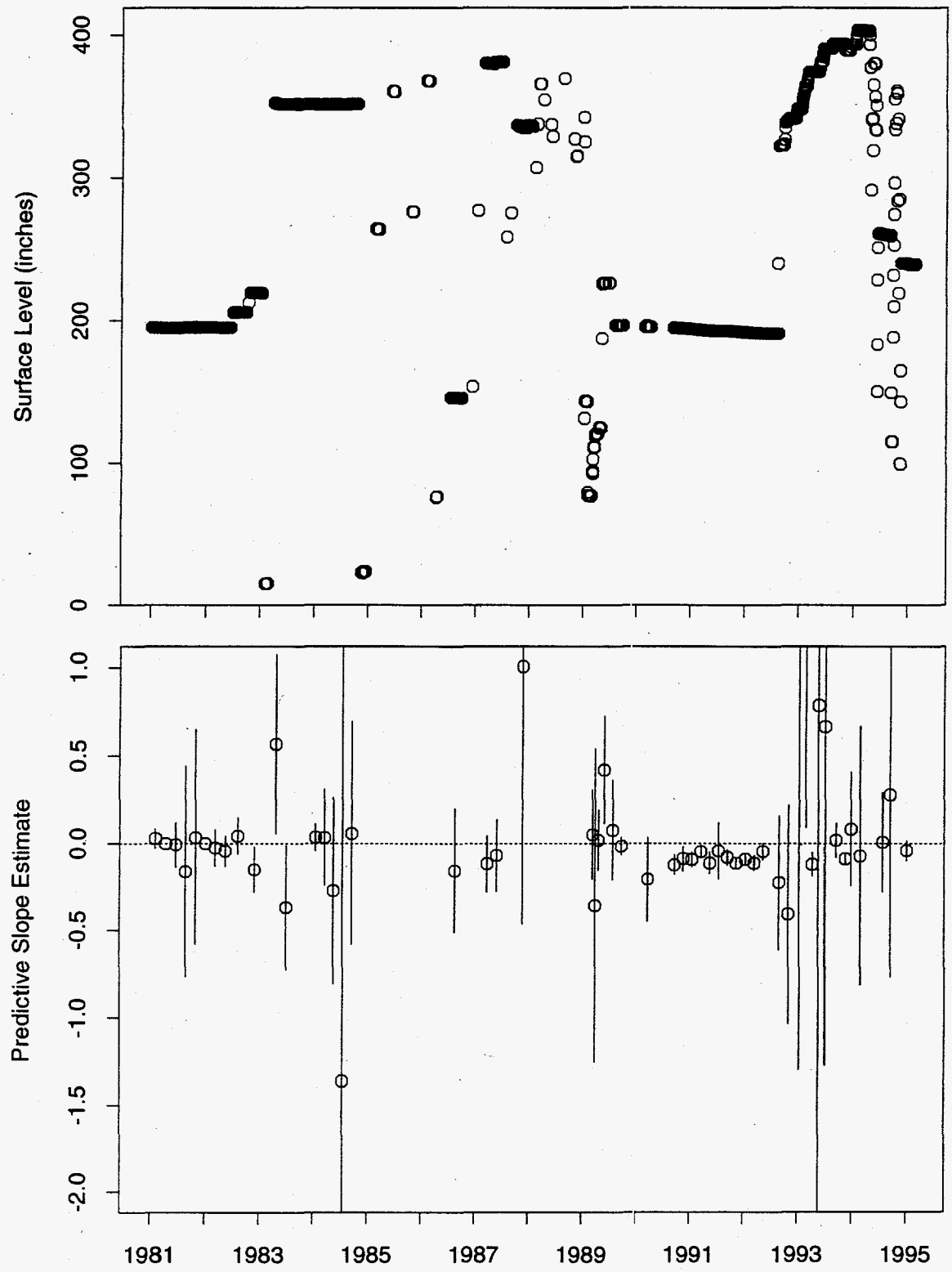

Figure 62: Tank AW–106 FIC Data

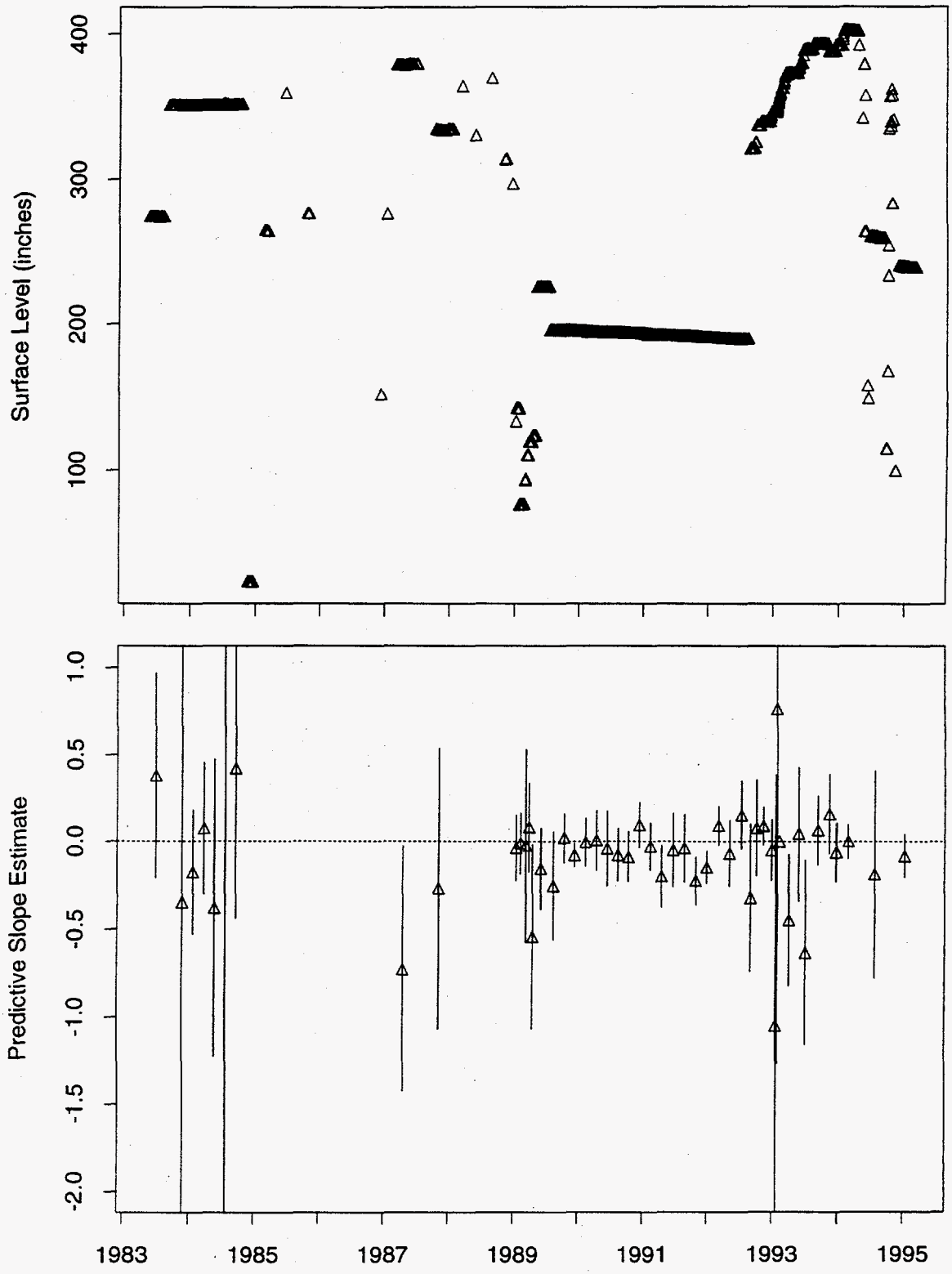

Figure 63: Tank AW-106 MT Data

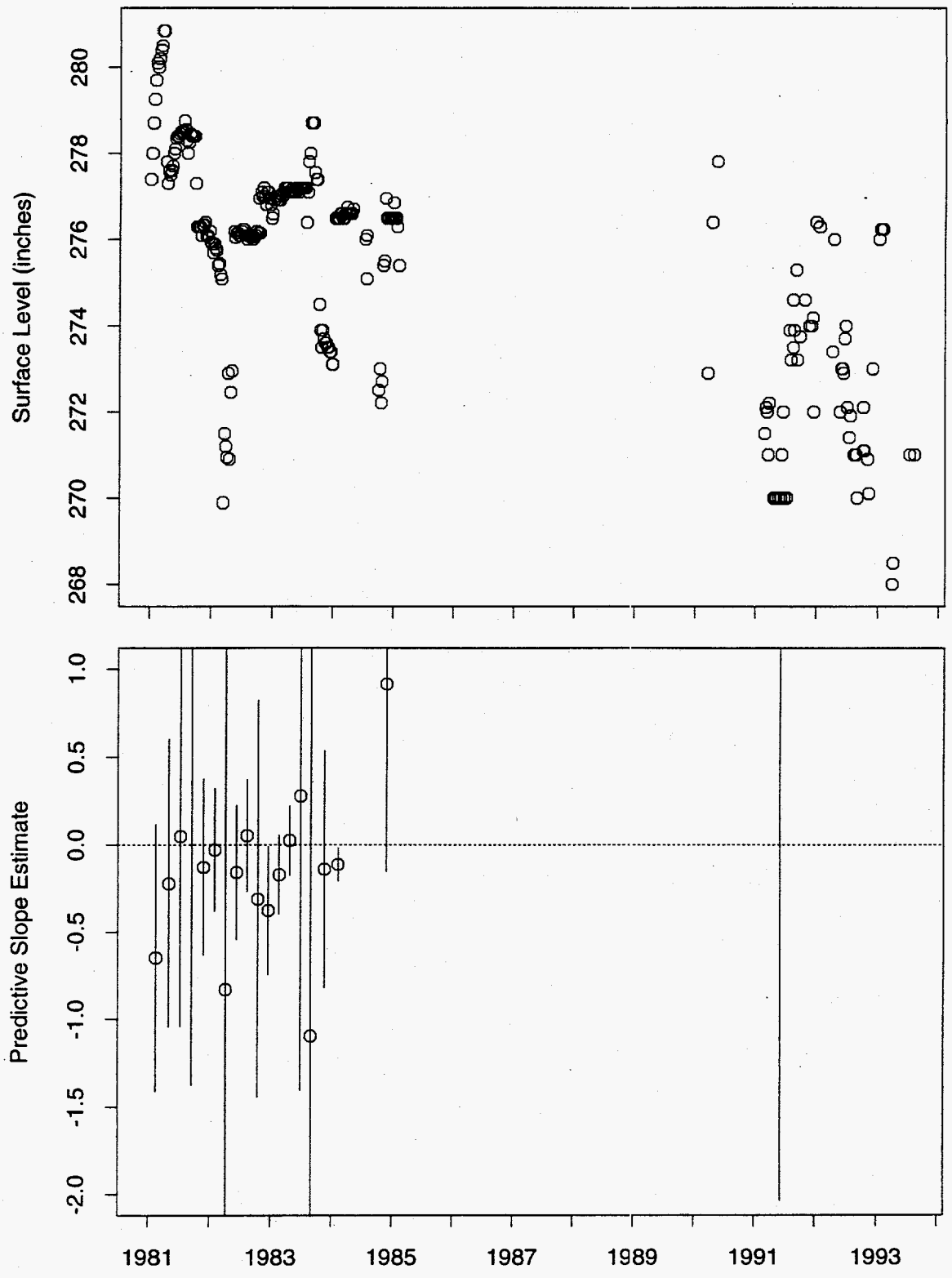

Figure 64: Tank AX-101 FIC Data

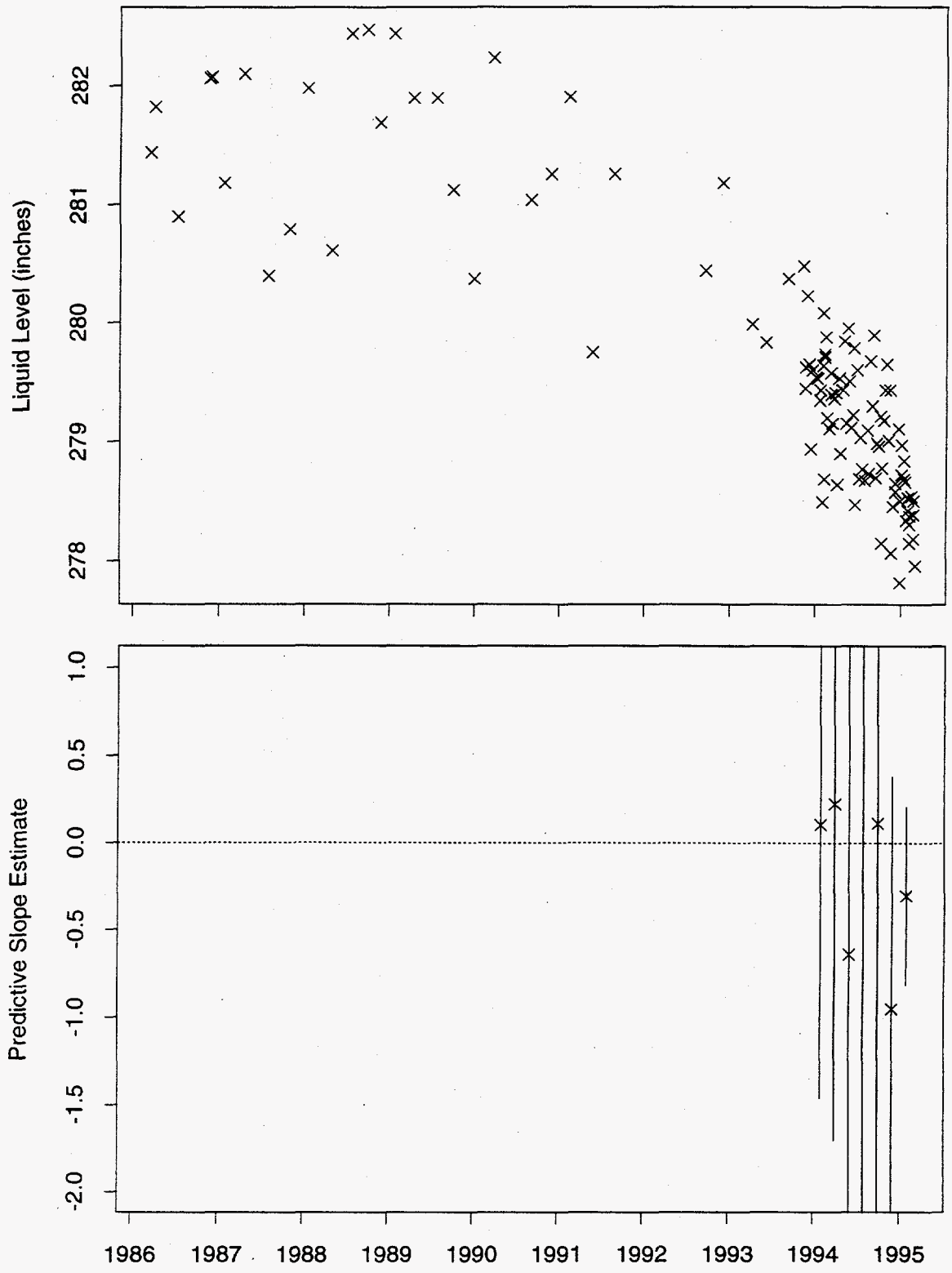

Figure 65: Tank AX–101 Neutron ILL Data

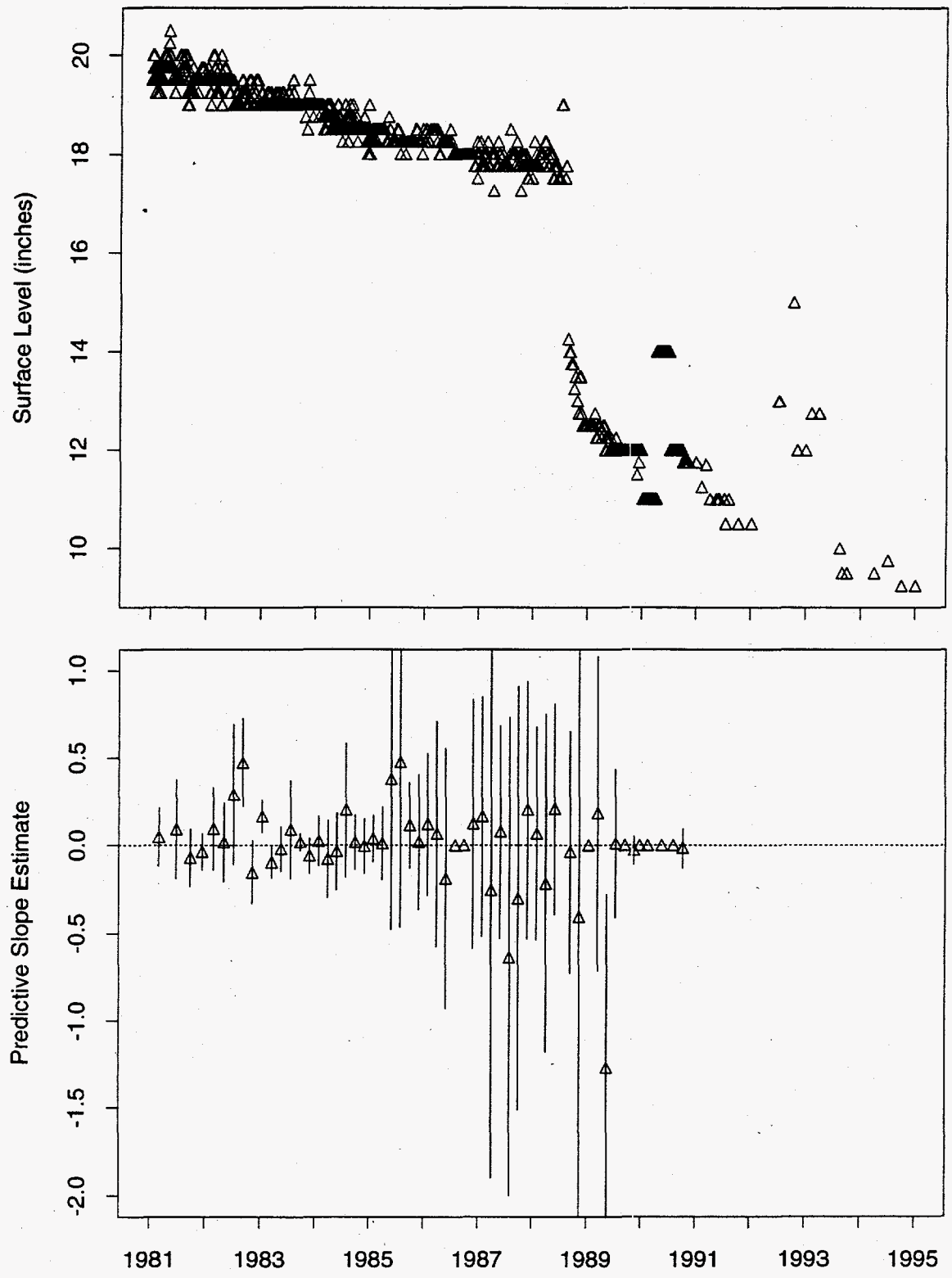

Figure 66: Tank AX-102 MT Data

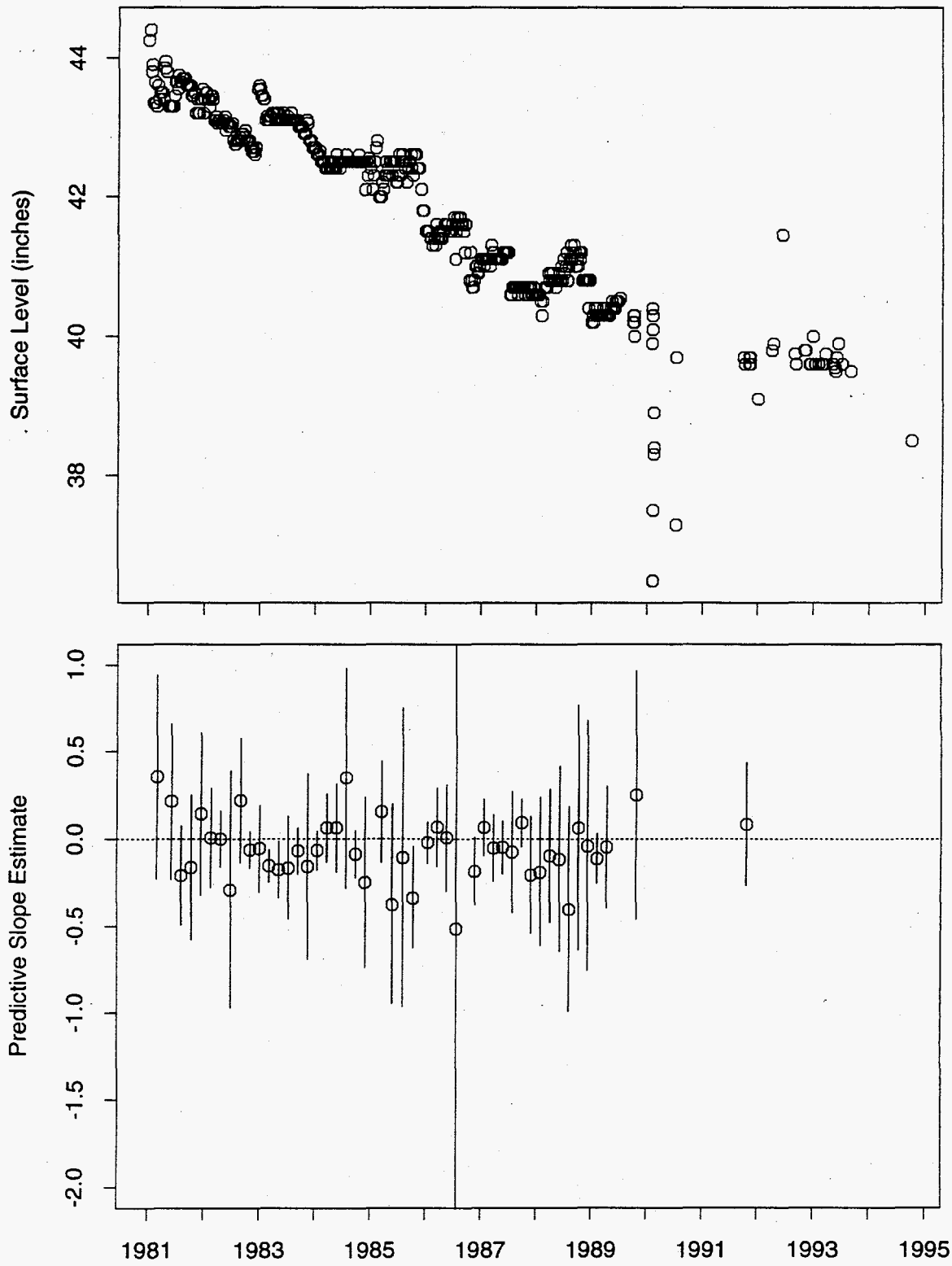

Figure 67: Tank AX–103 FIC Data

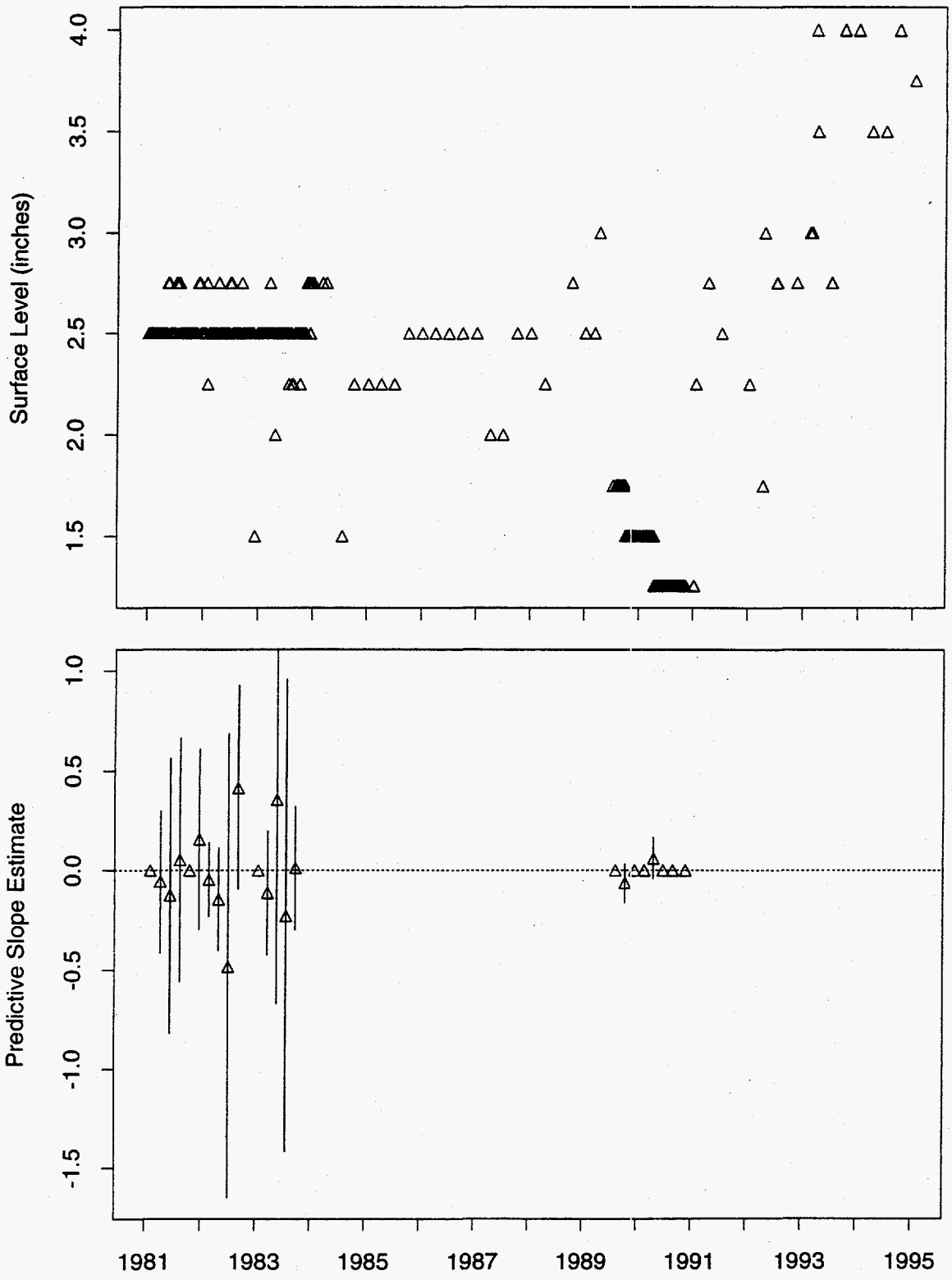

Figure 68: Tank AX–104 MT Data

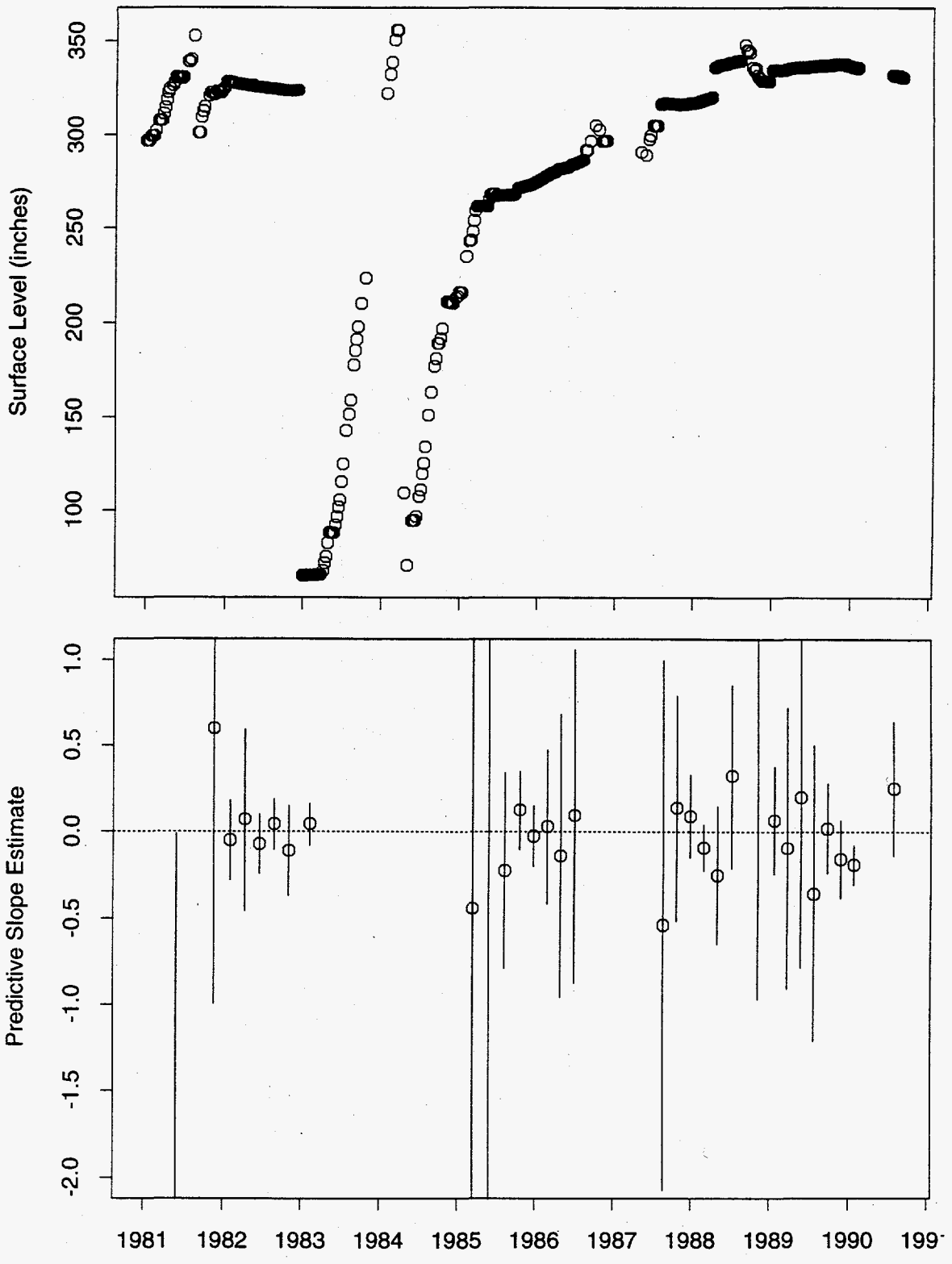

Figure 69: Tank AY-101 FIC Data

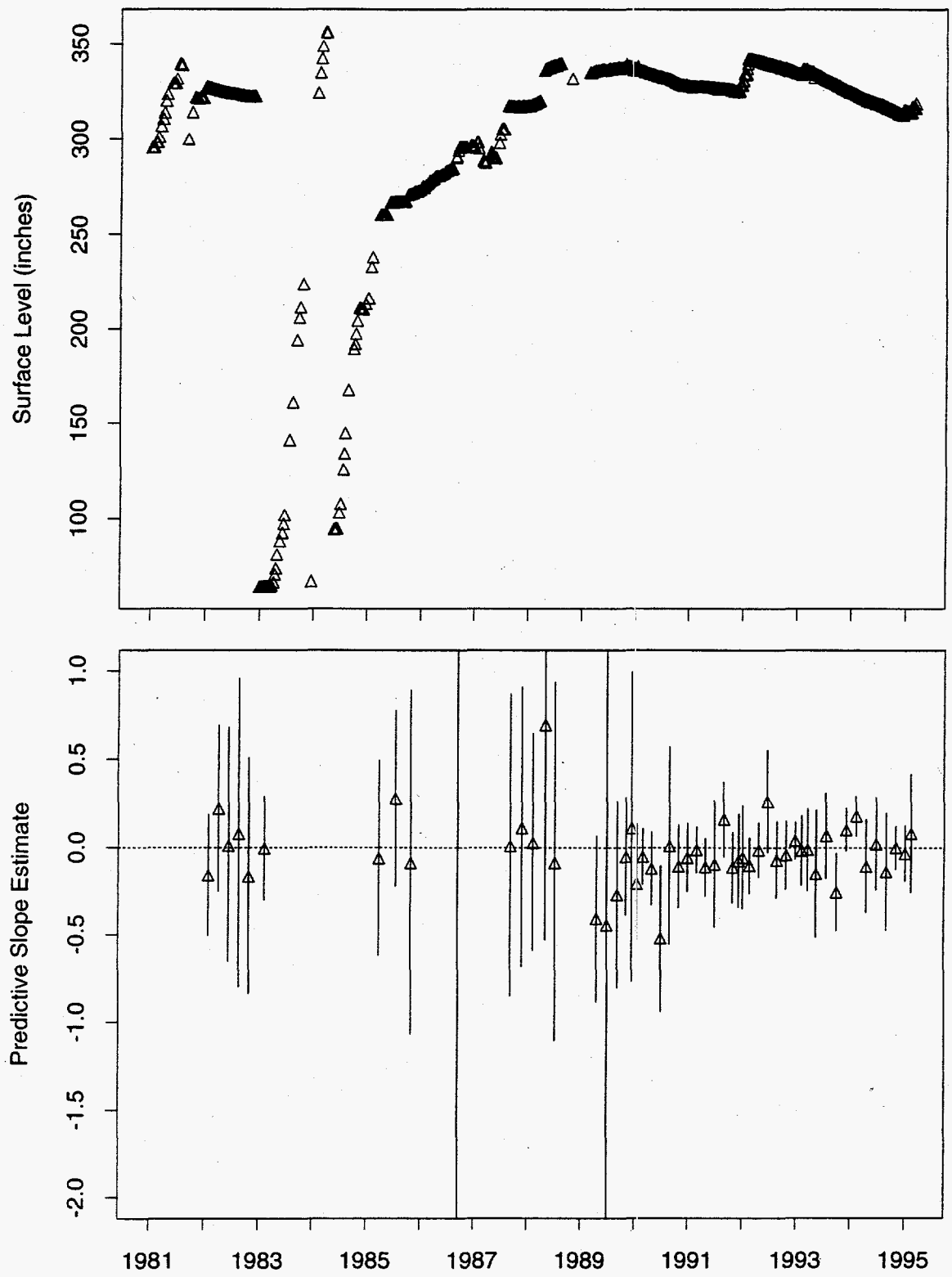

Figure 70: Tank AY–101 MT Data

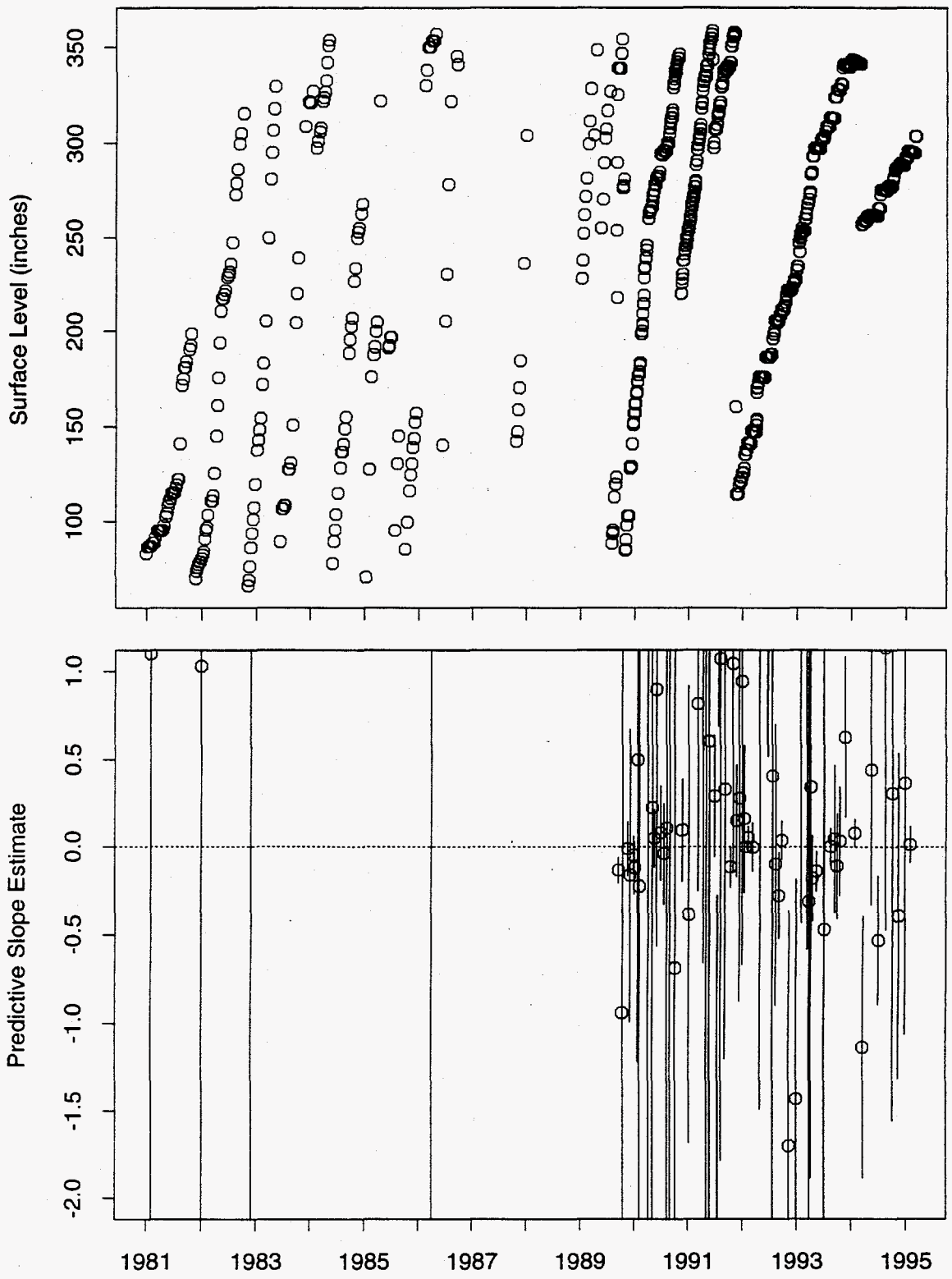

Figure 71: Tank AY–102 FIC Data

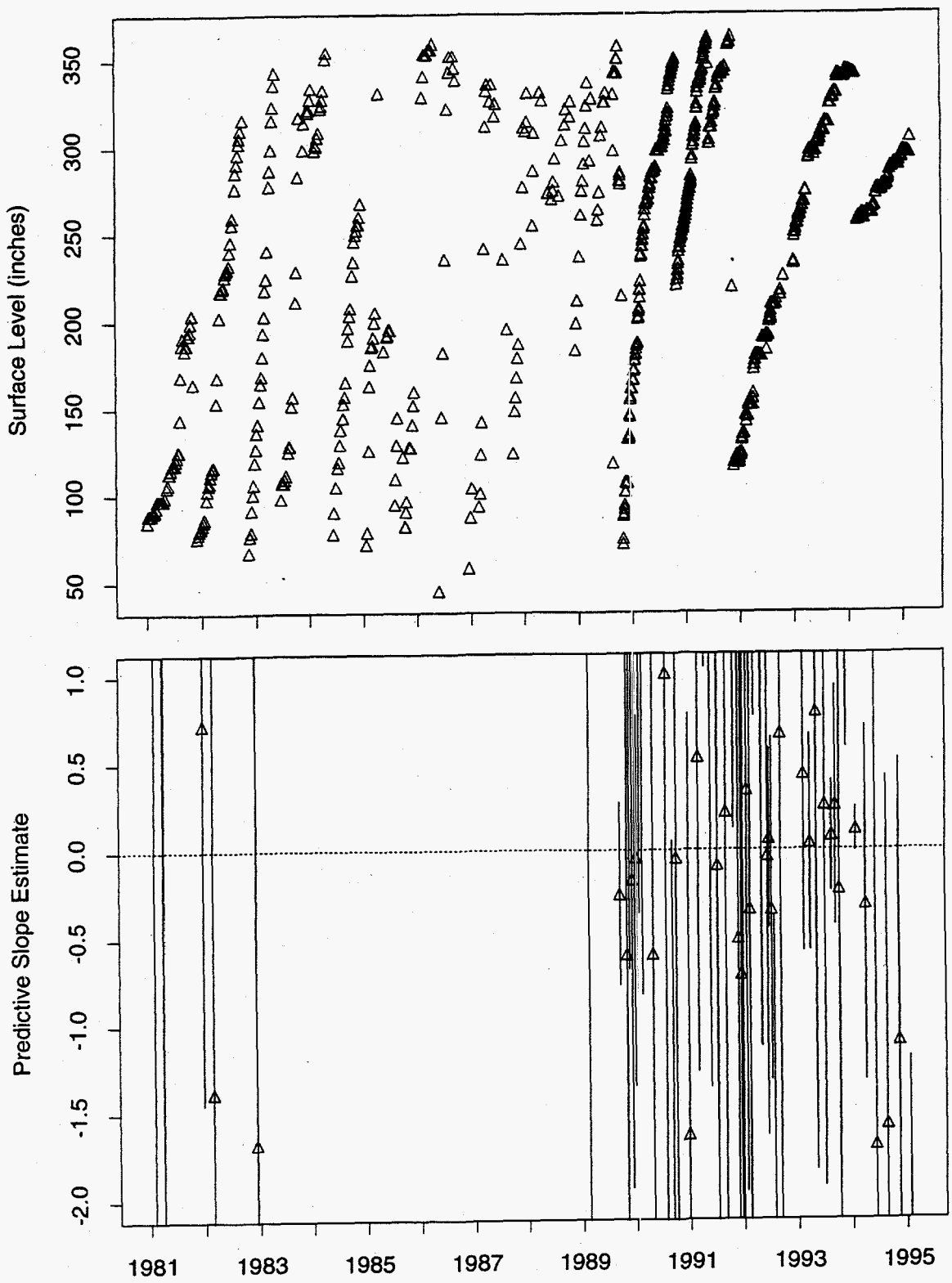

Figure 72: Tank AY-102 MT Data

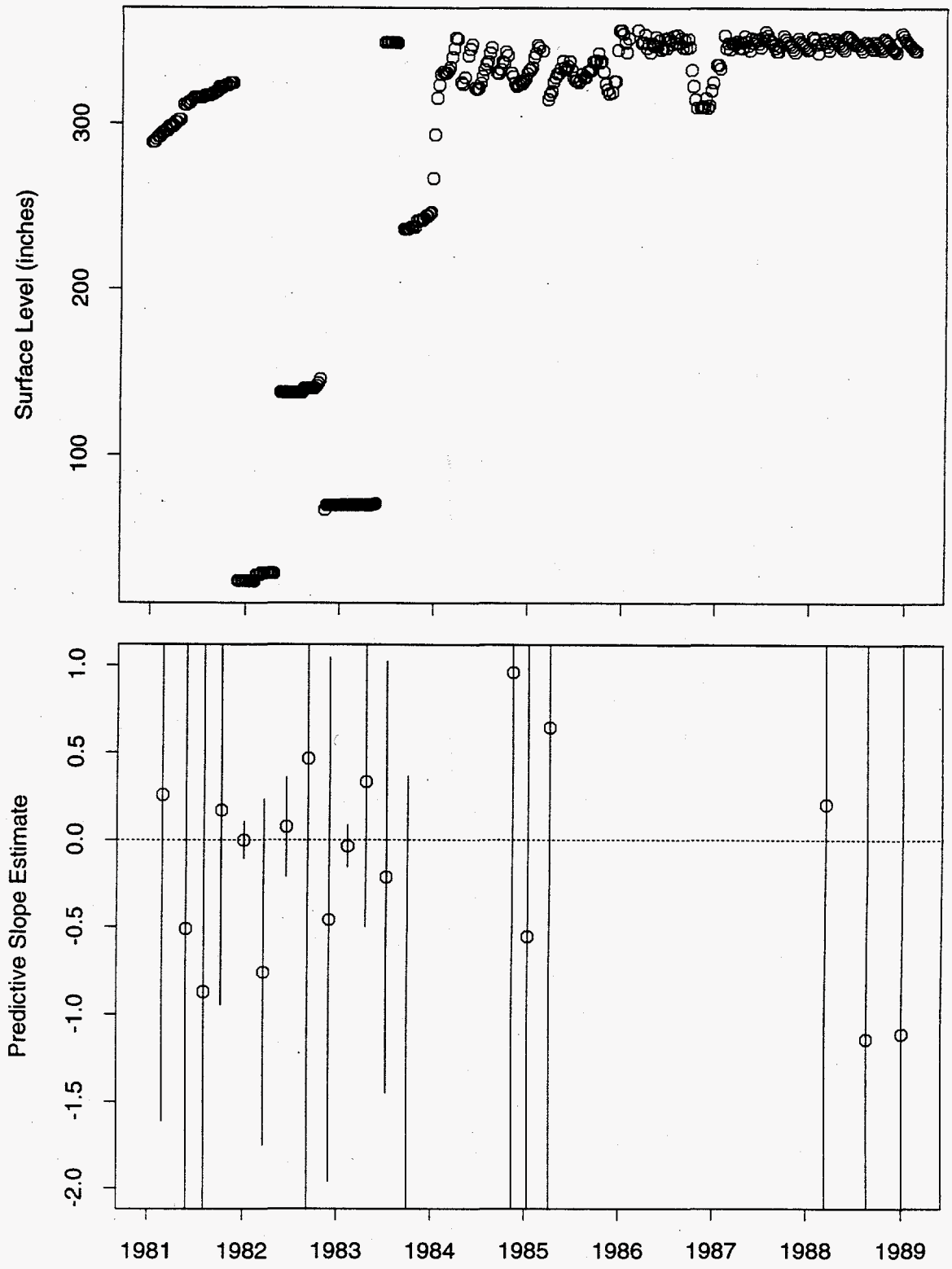

Figure 73: Tank AZ–101 FIC Data

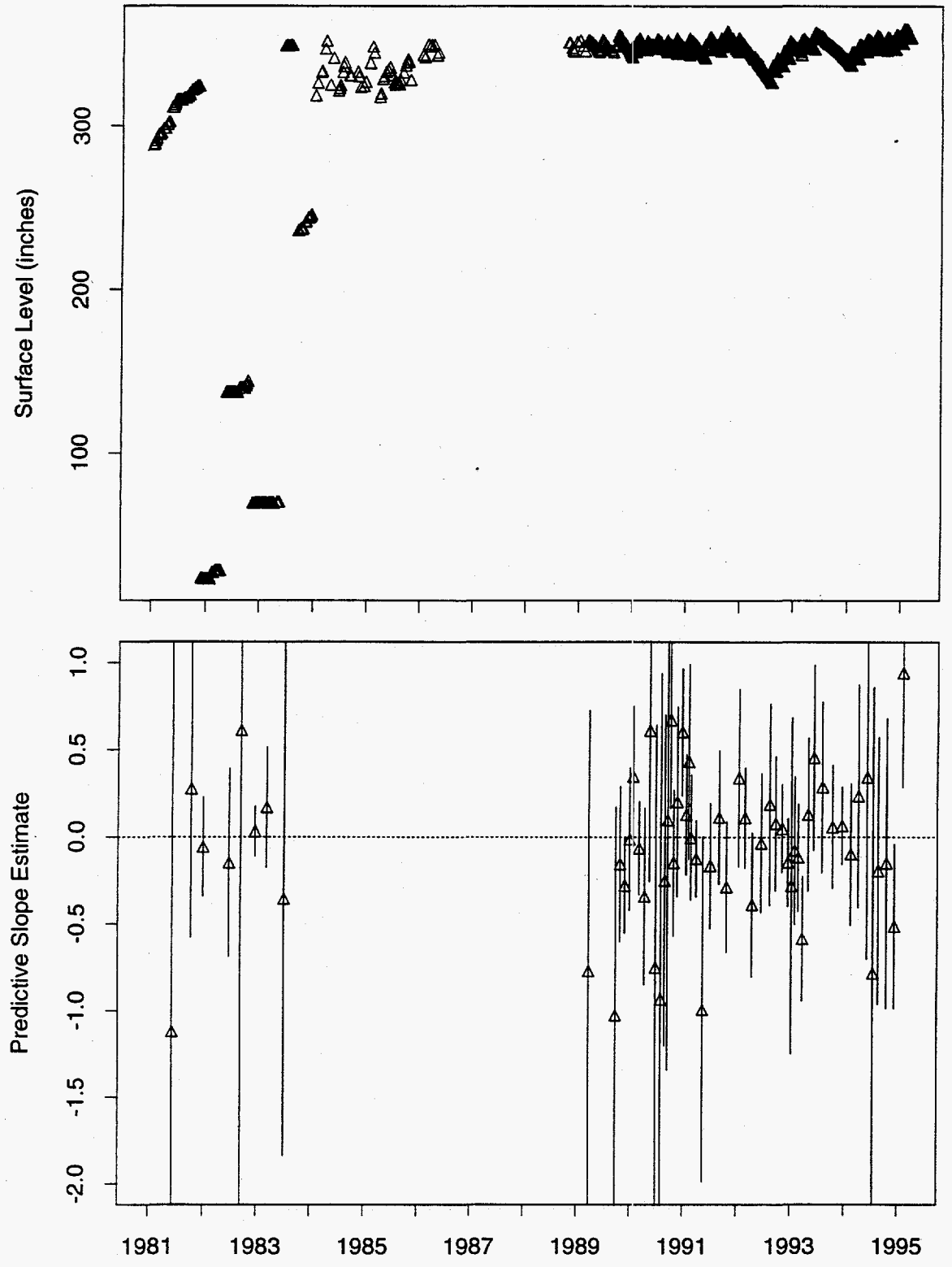

Figure 74: Tank AZ–101 MT Data

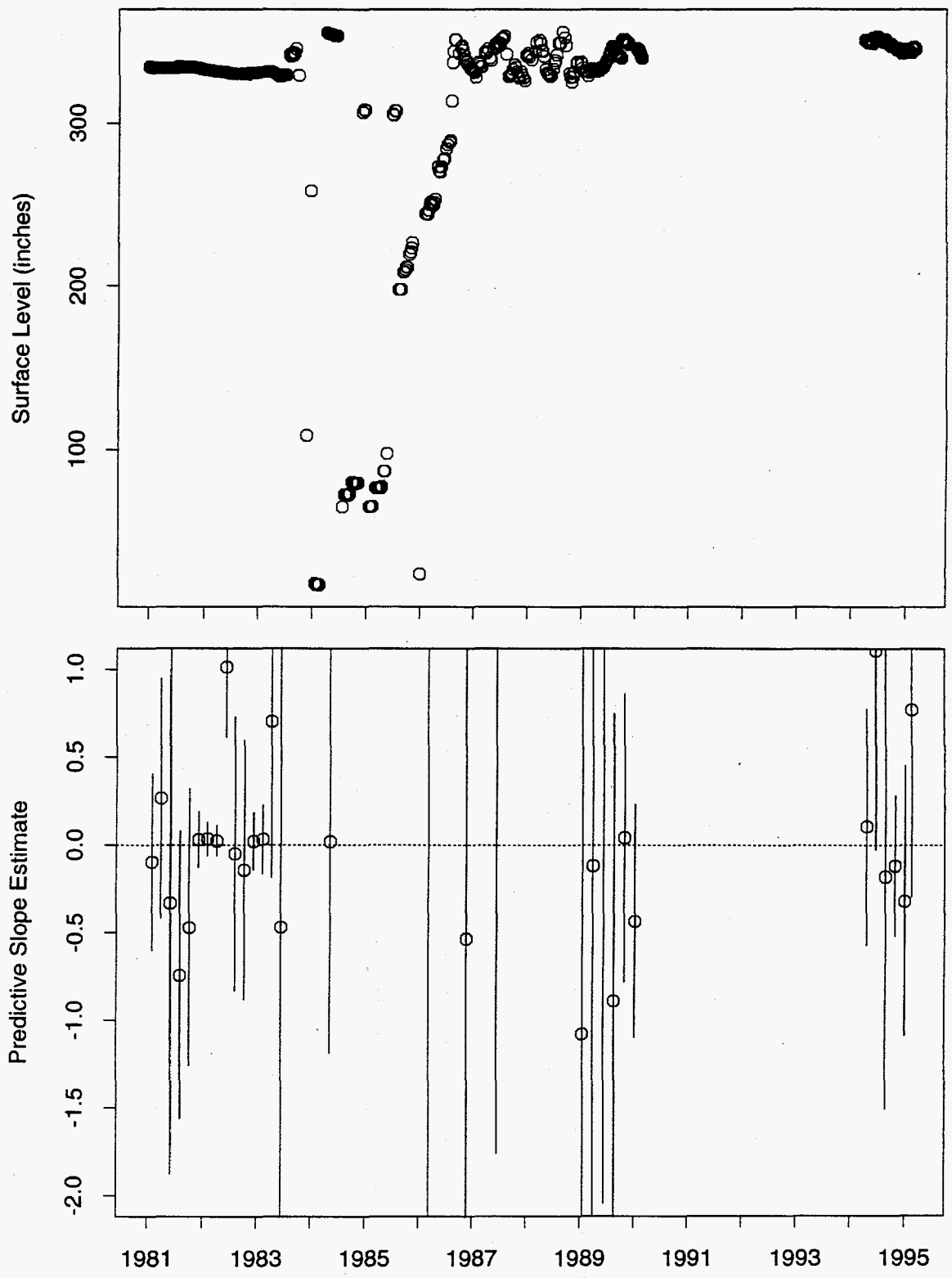

Figure 75: Tank AZ–102 FIC Data

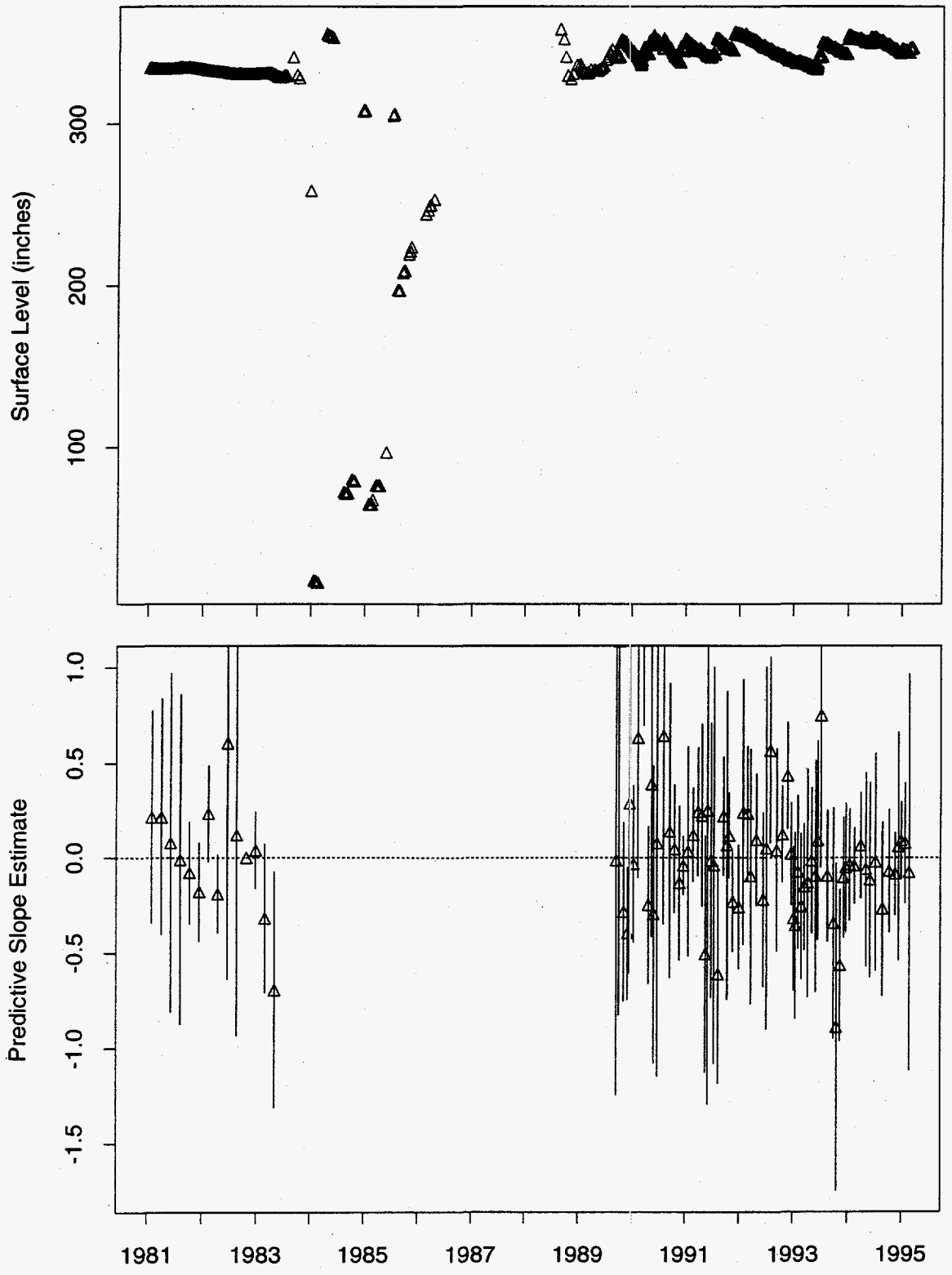

Figure 76: Tank AZ–102 MT Data

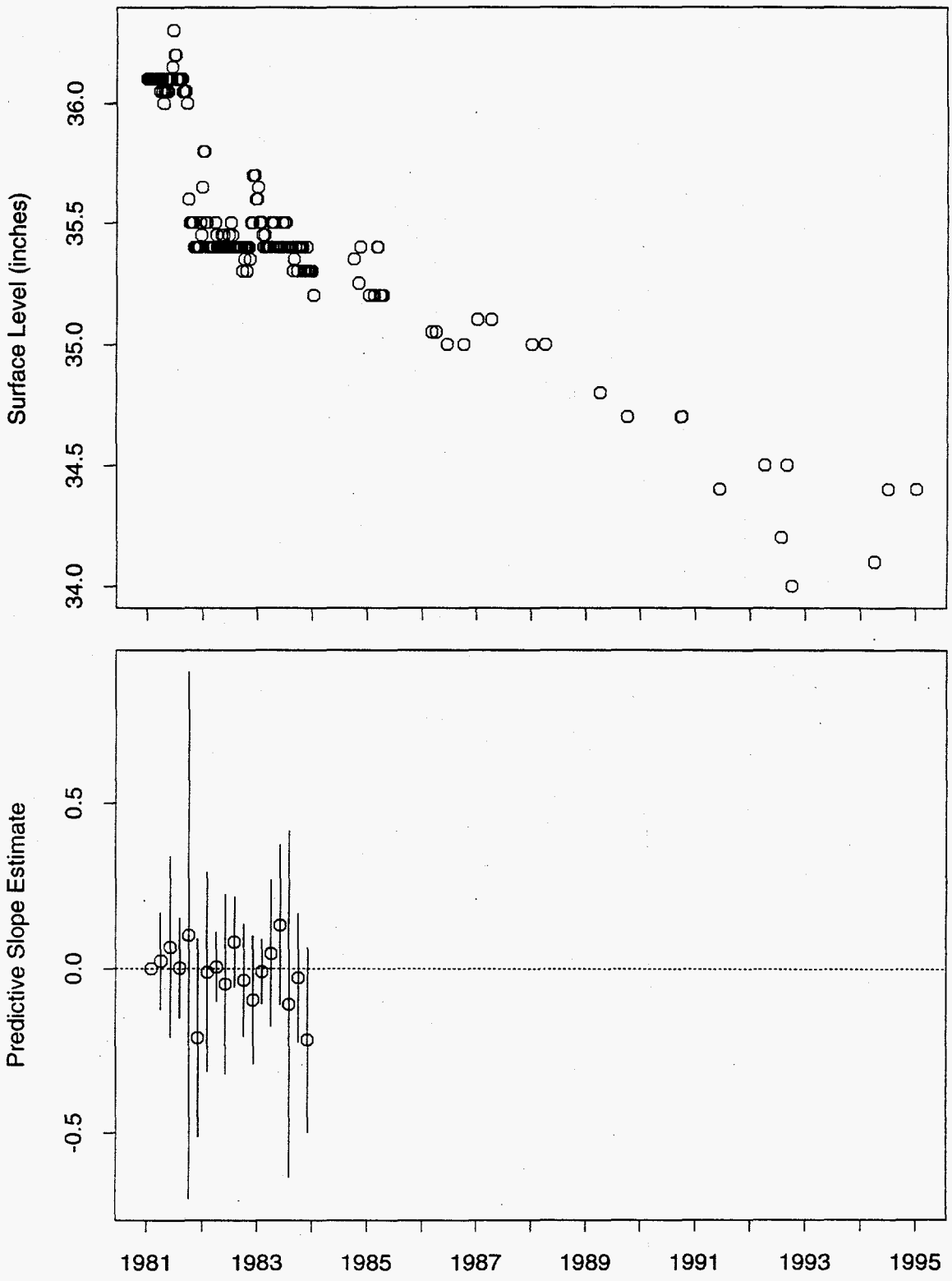

Figure 77: Tank B–101 FIC Data

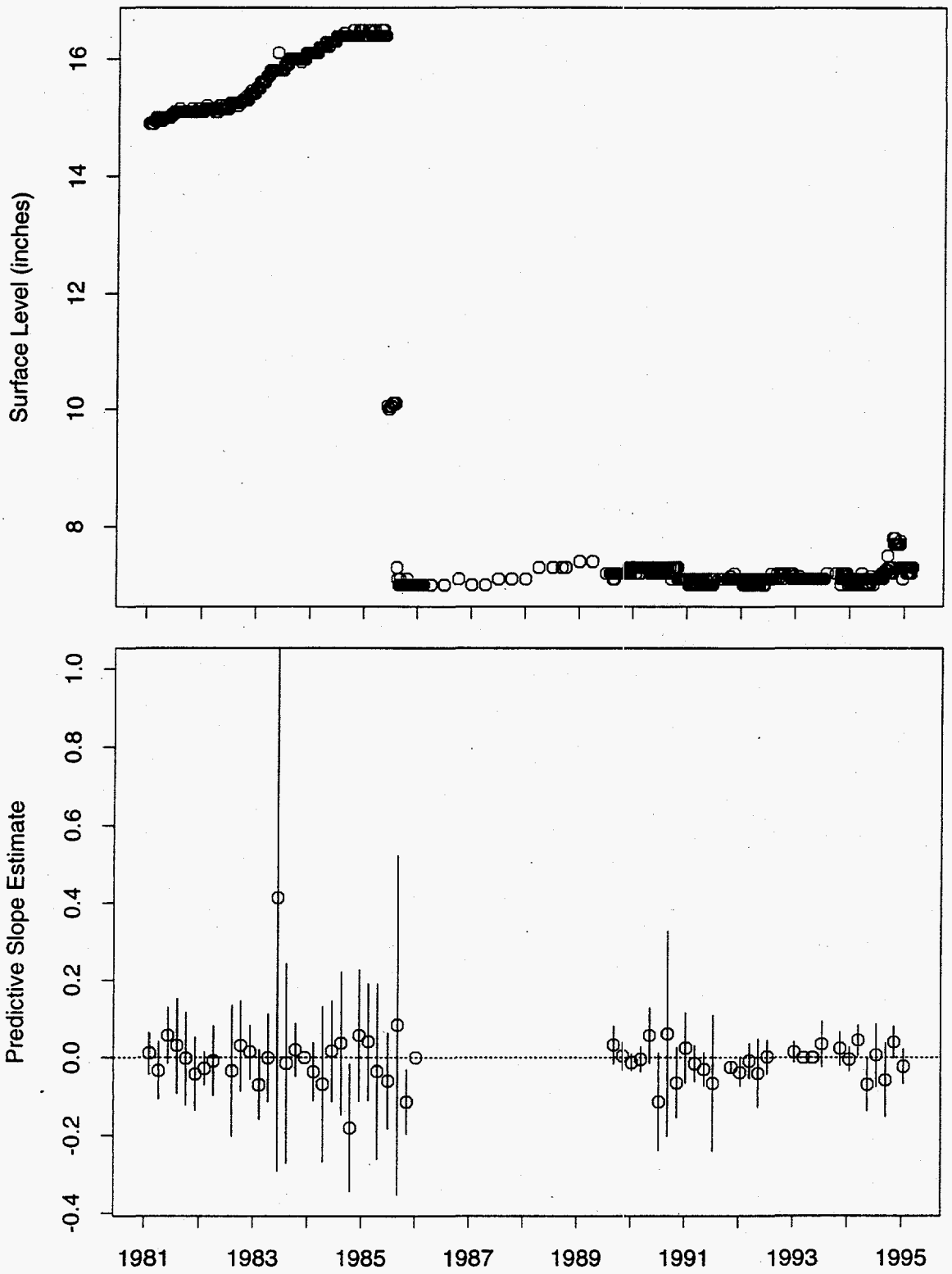

Figure 78: Tank B–102 FIC Data

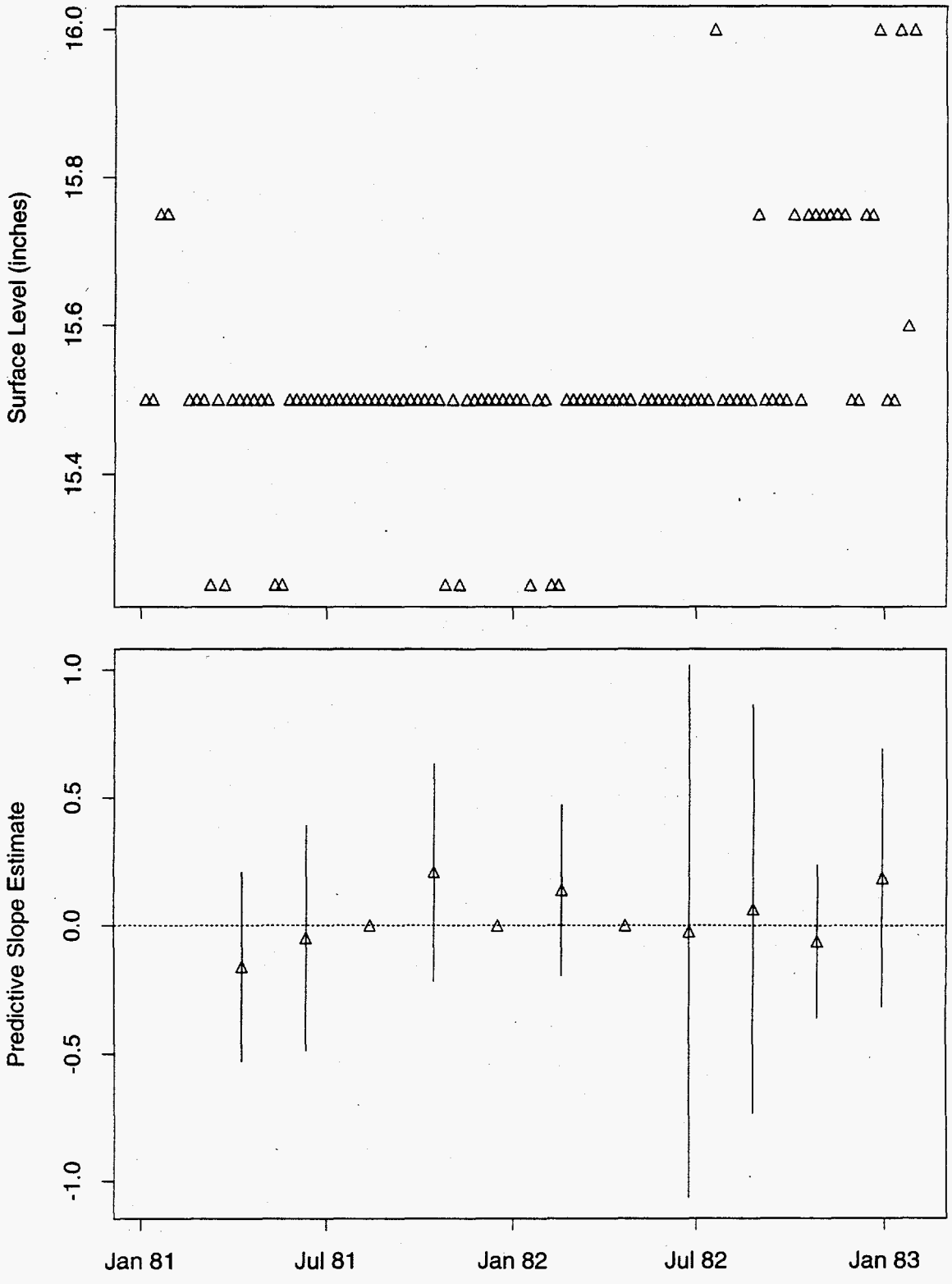

Figure 79: Tank B–102 MT Data

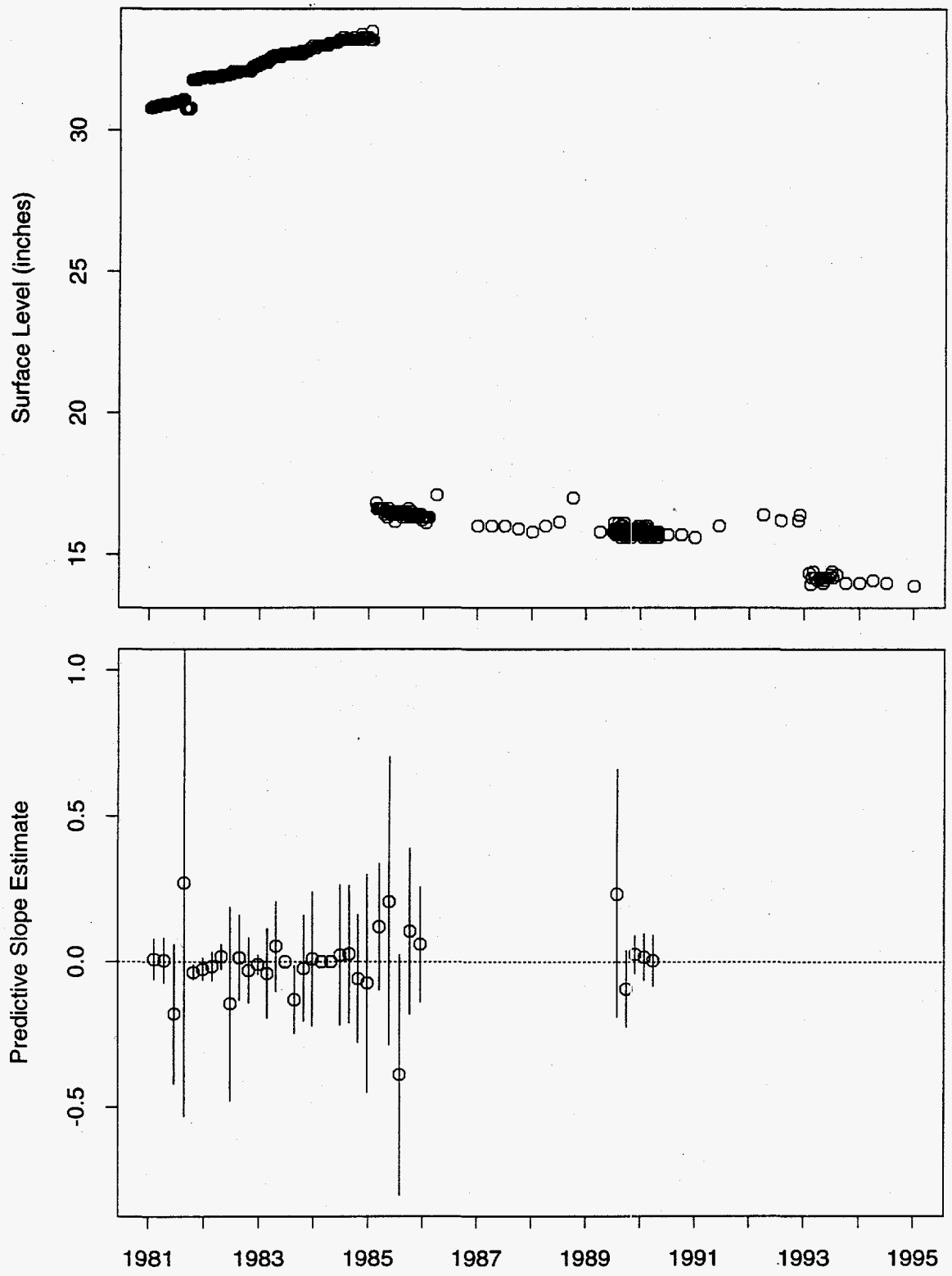

Figure 80: Tank B–103 FIC Data

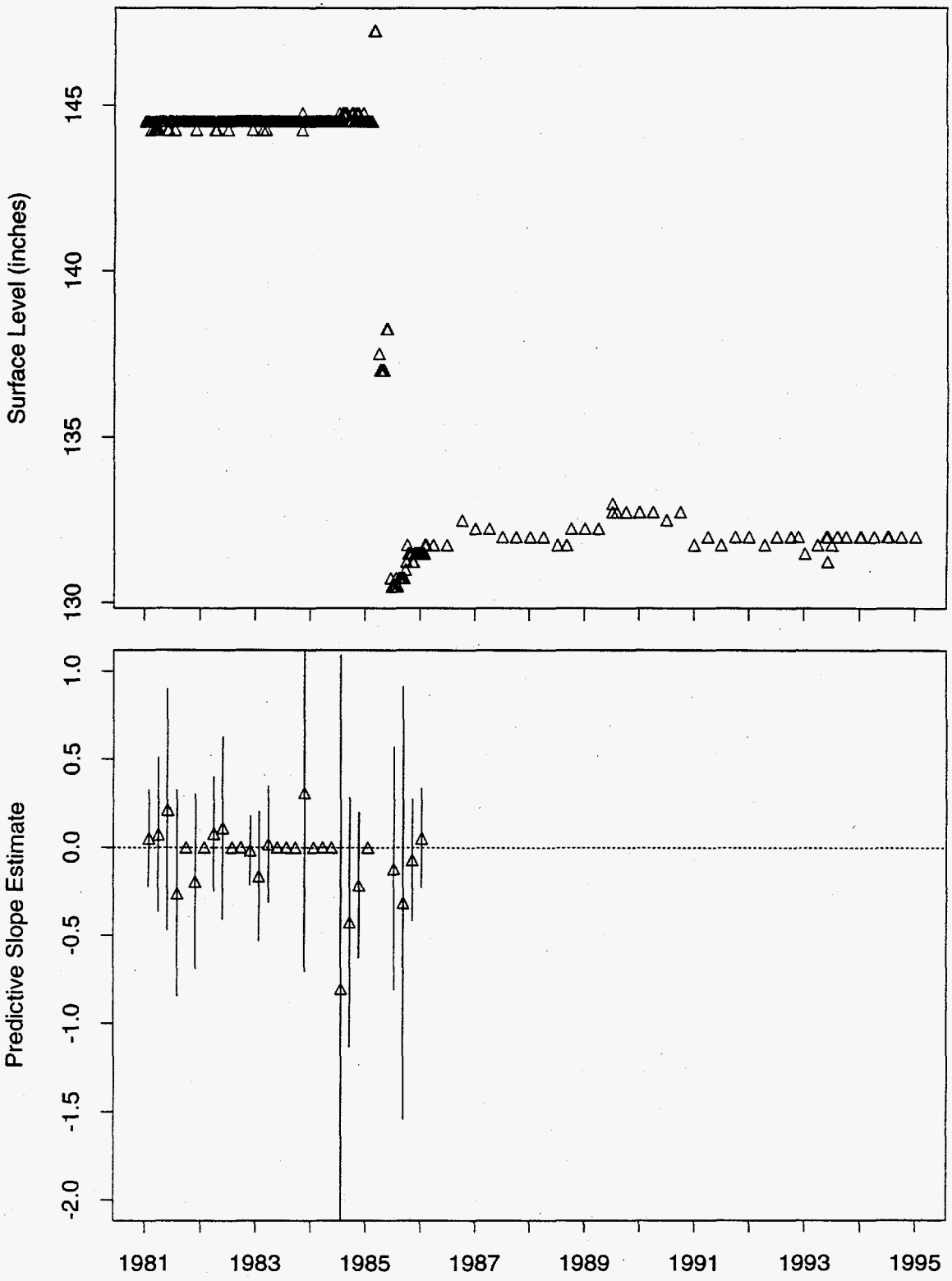

Figure 81: Tank B–104 MT Data

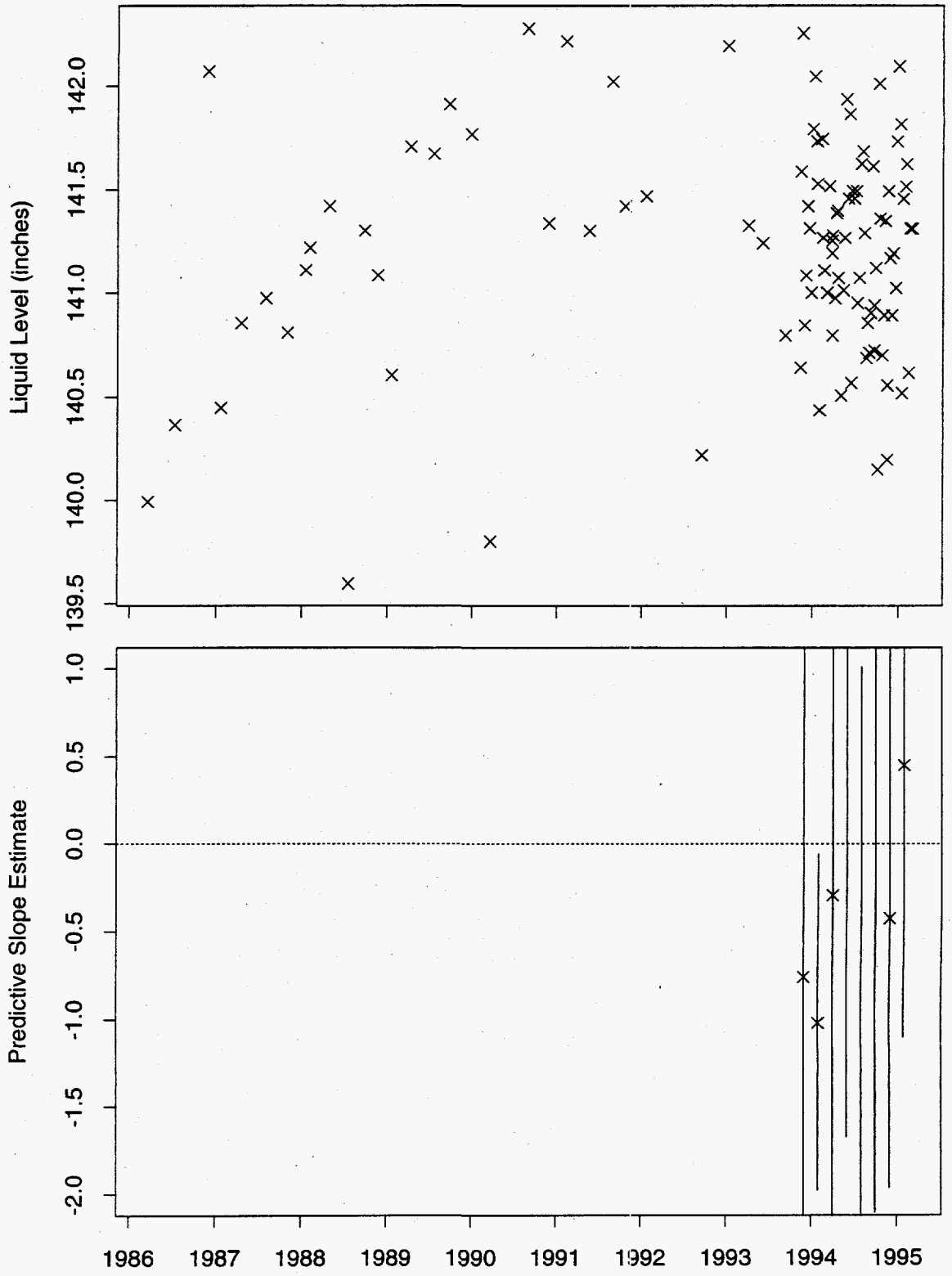

Figure 82: Tank B–104 Neutron ILL Data

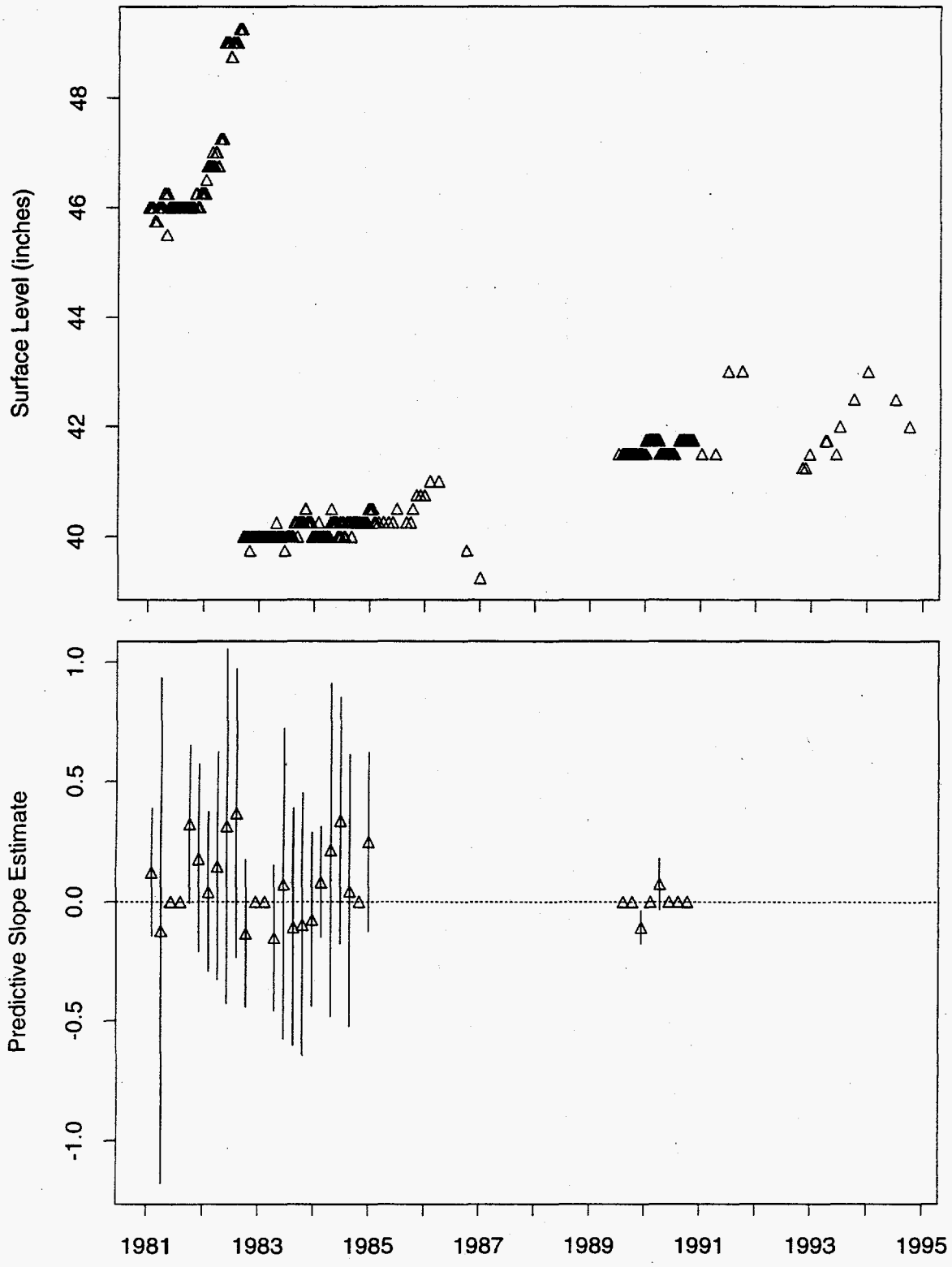

Figure 83: Tank B–105 MT Data

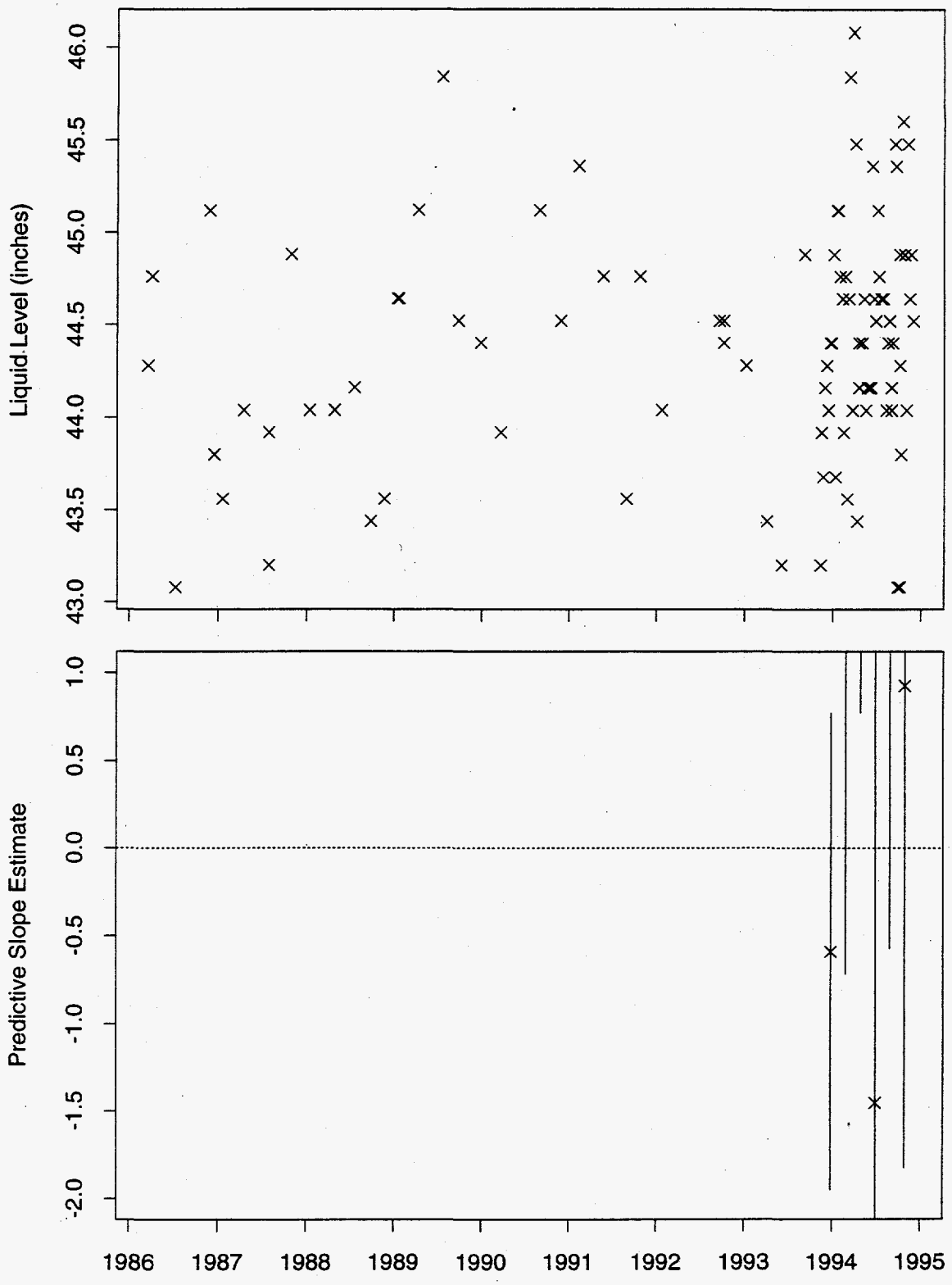

Figure 84: Tank B-105 Neutron ILL Data

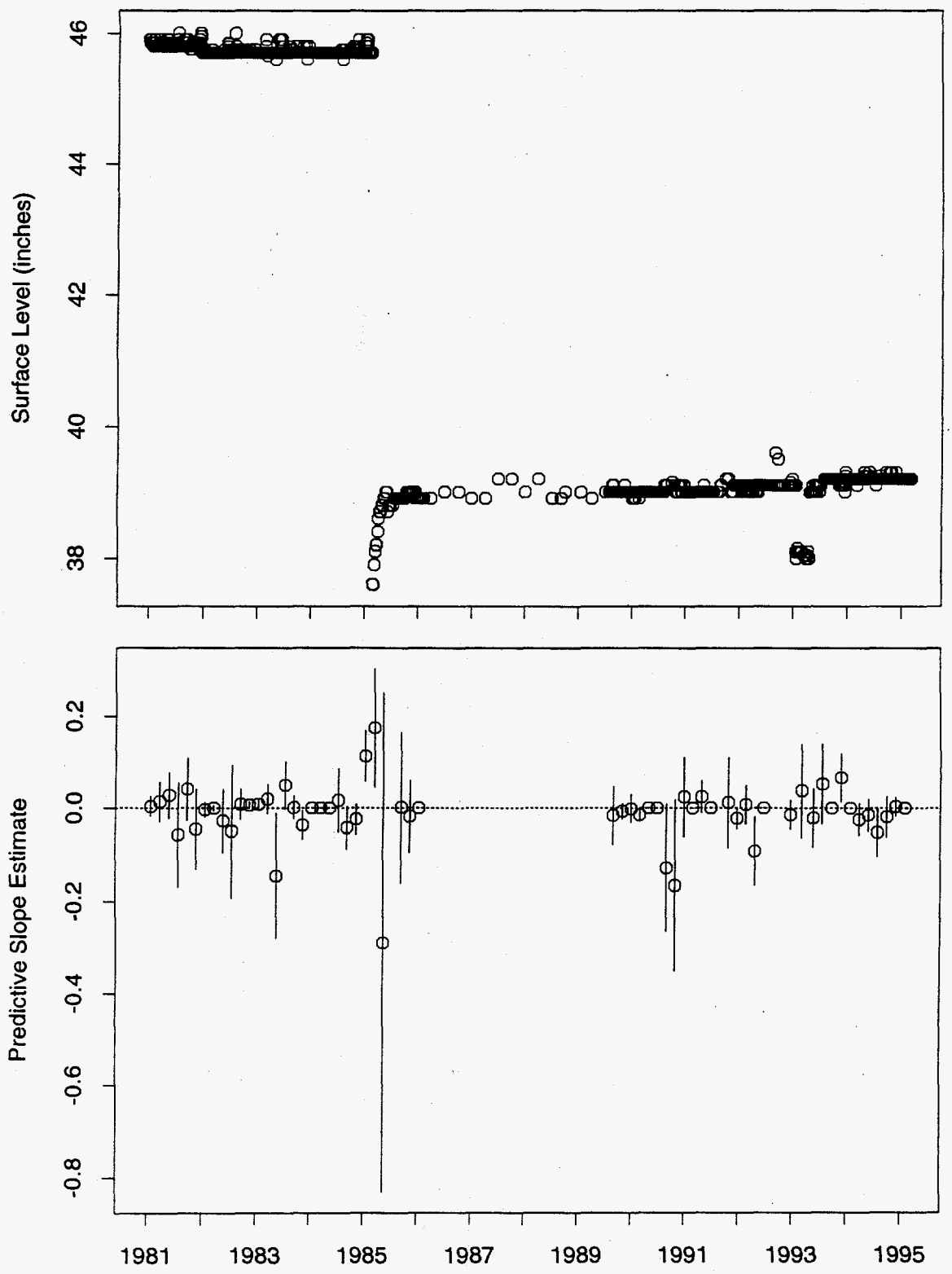

Figure 85: Tank B–106 FIC Data

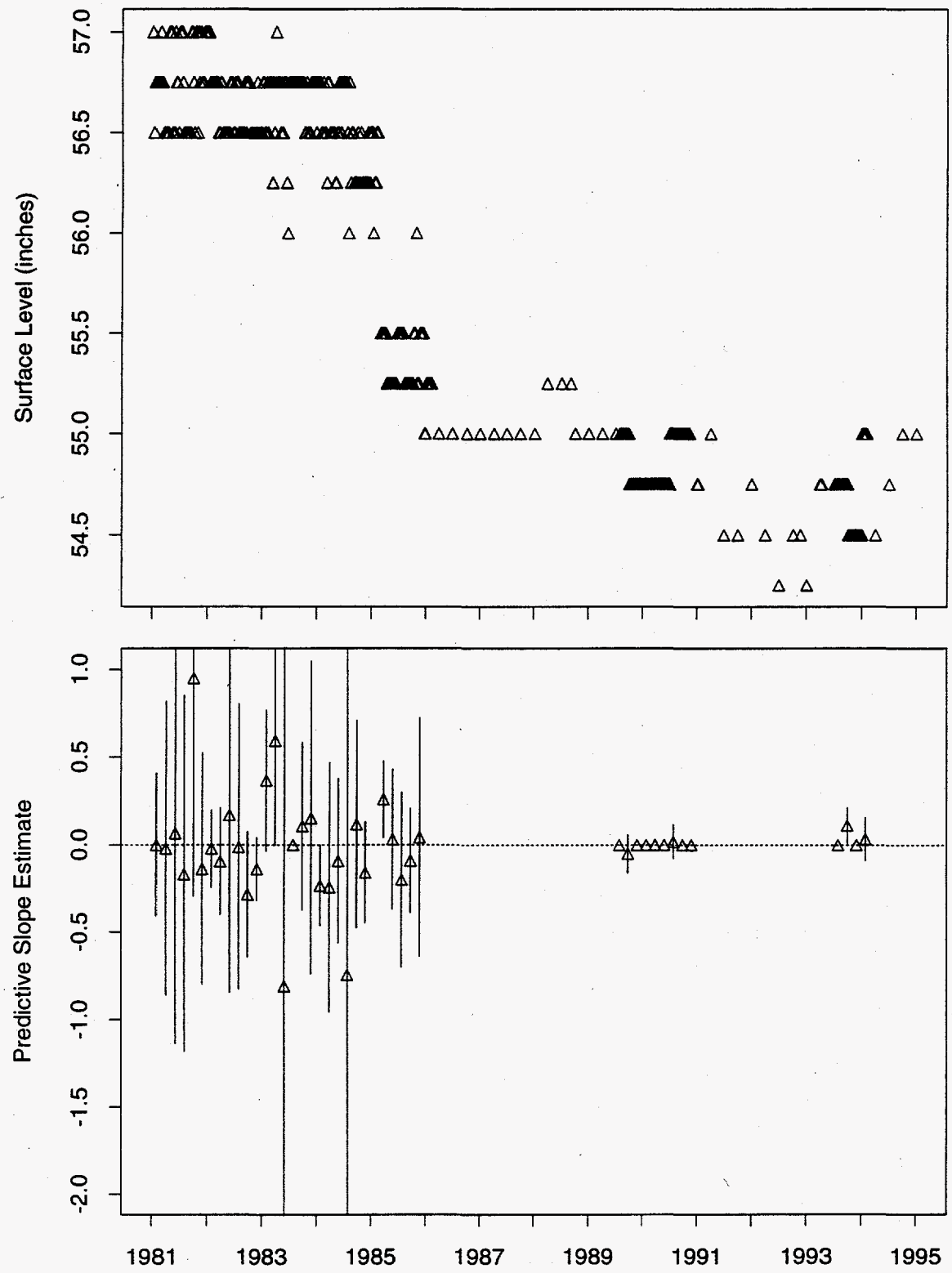

Figure 86: Tank B–107 MT Data

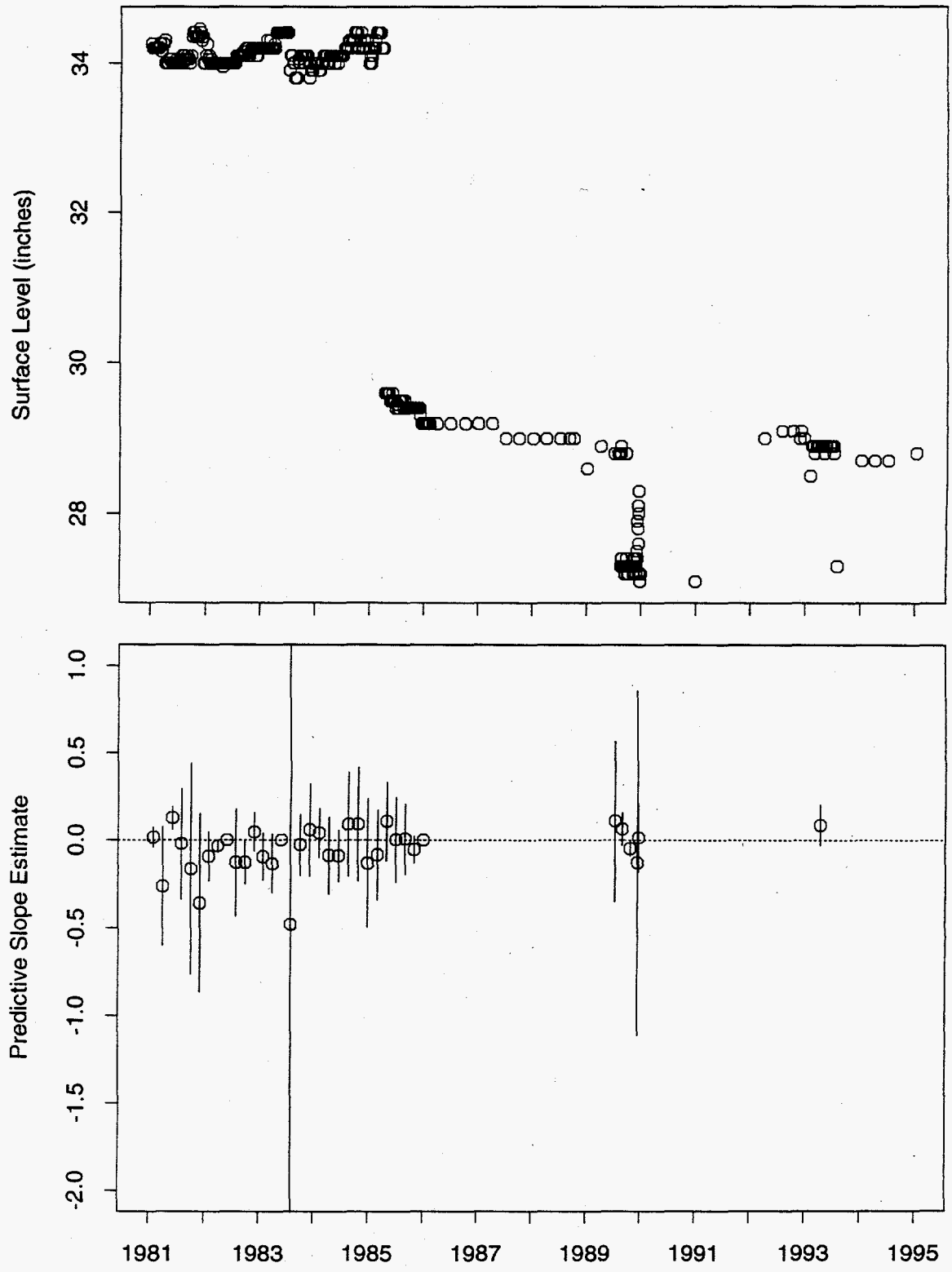

Figure 87: Tank B-108 FIC Data

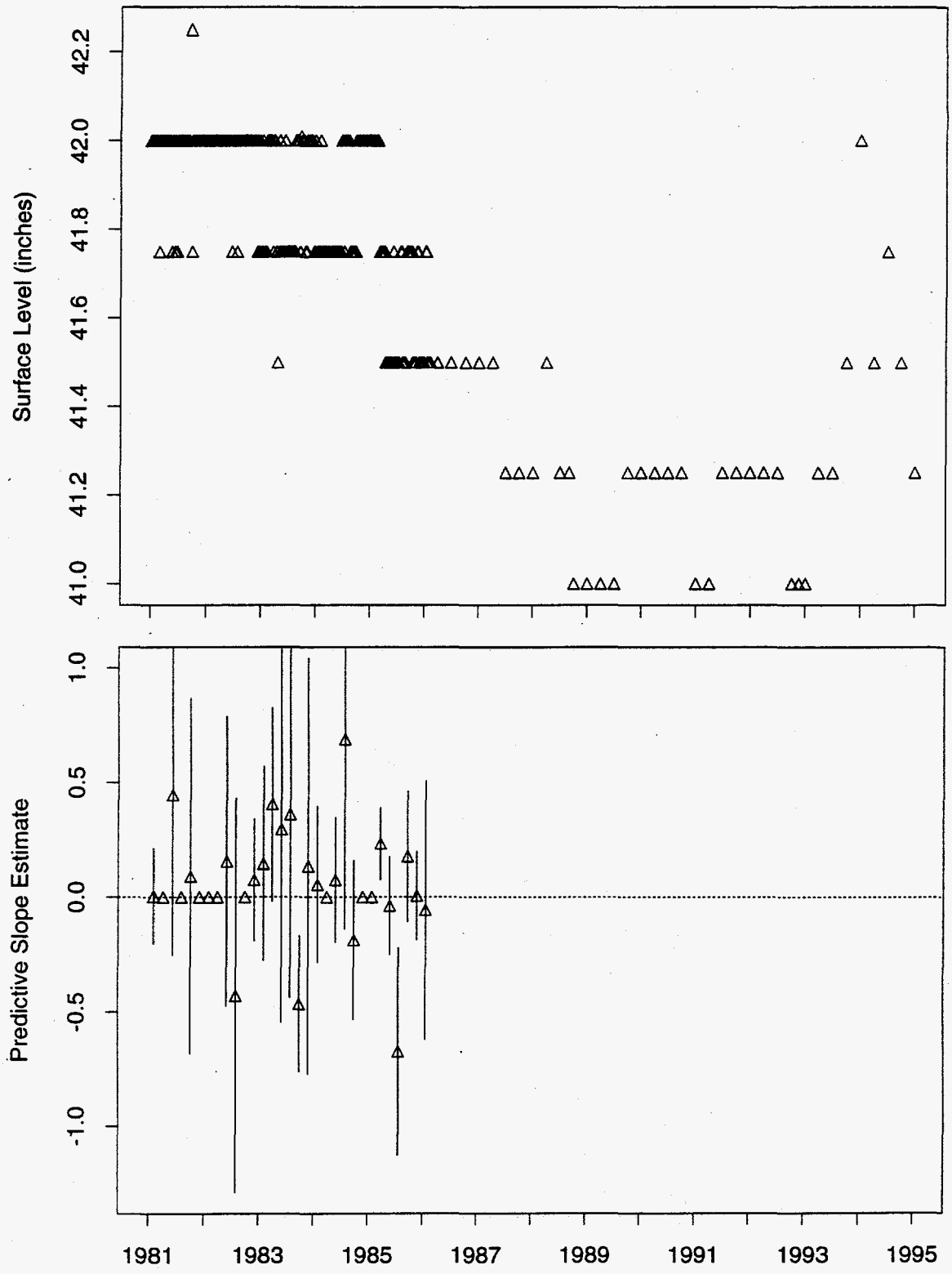

Figure 88: Tank B–109 MT Data

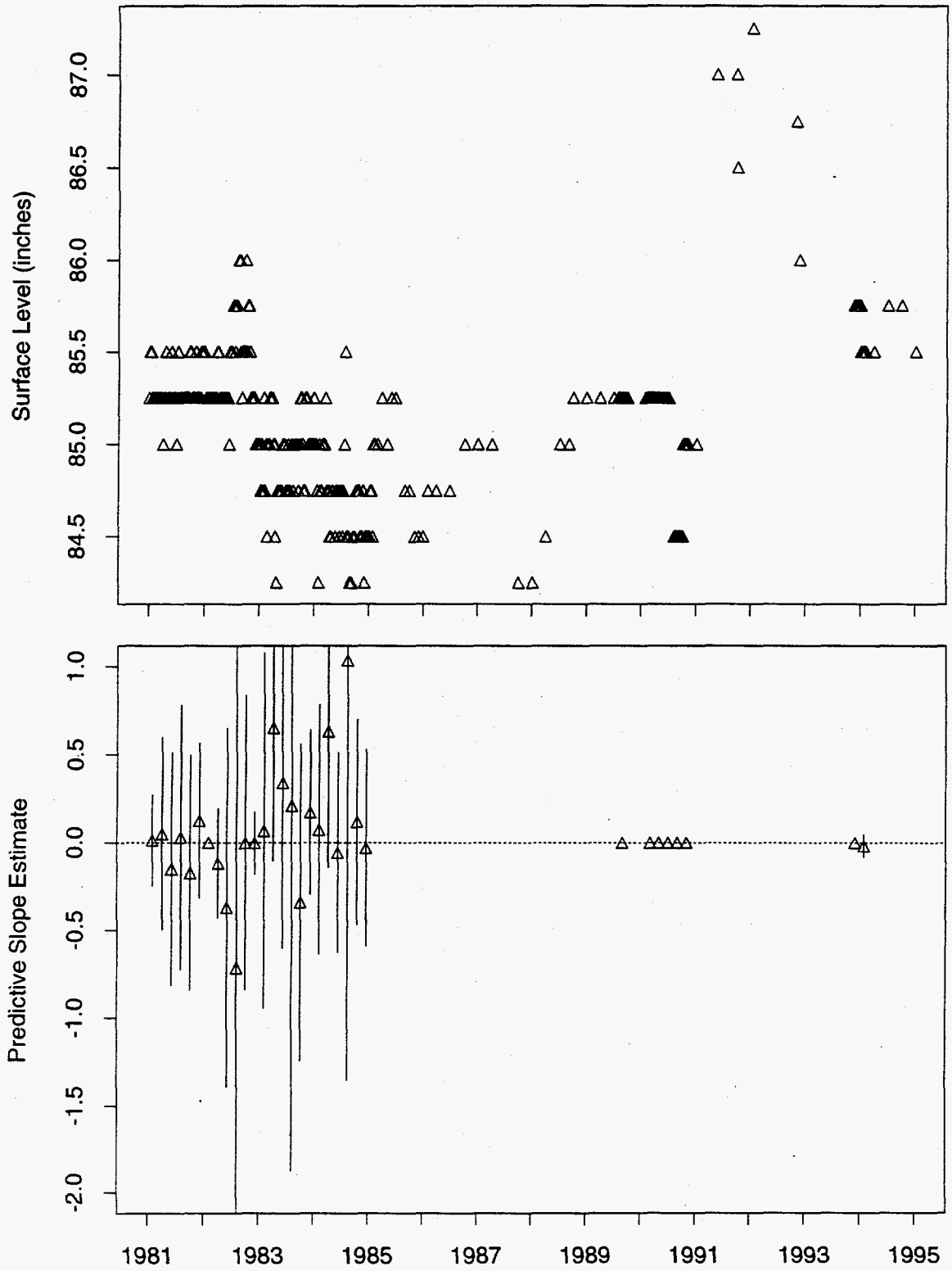

Figure 89: Tank B–110 MT Data

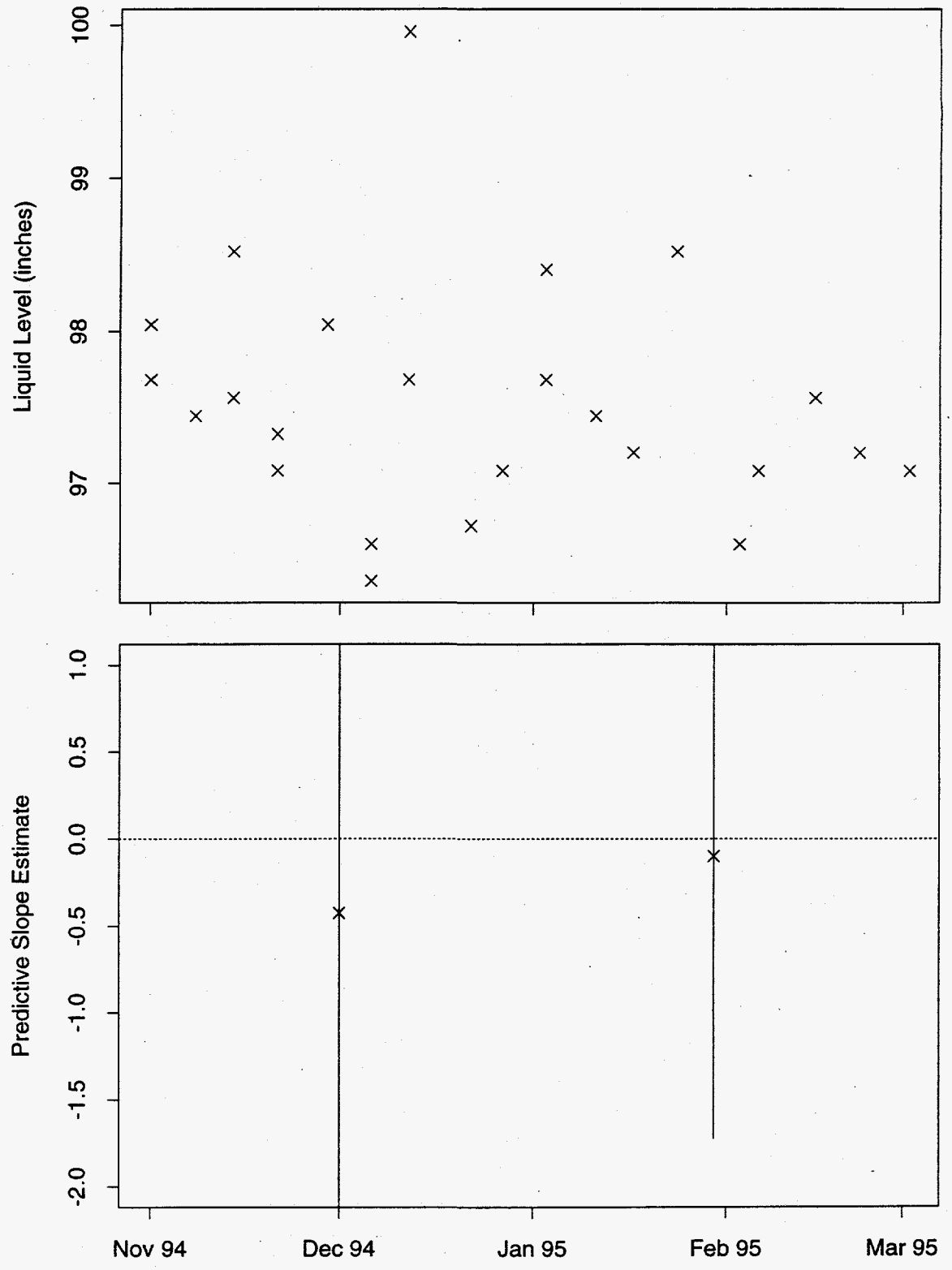

Figure 90: Tank B-110 Neutron ILL Data

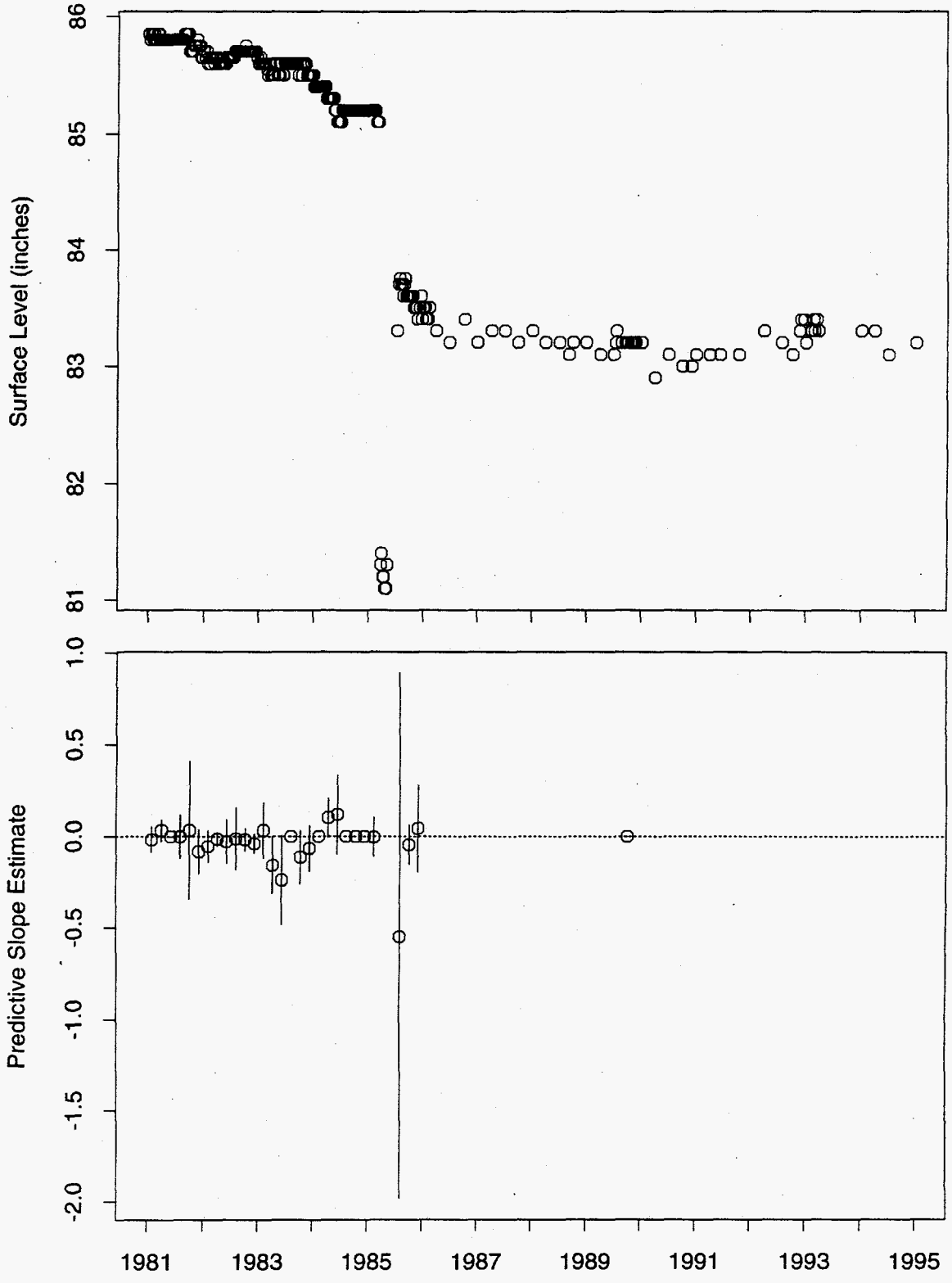

Figure 91: Tank B–111 FIC Data

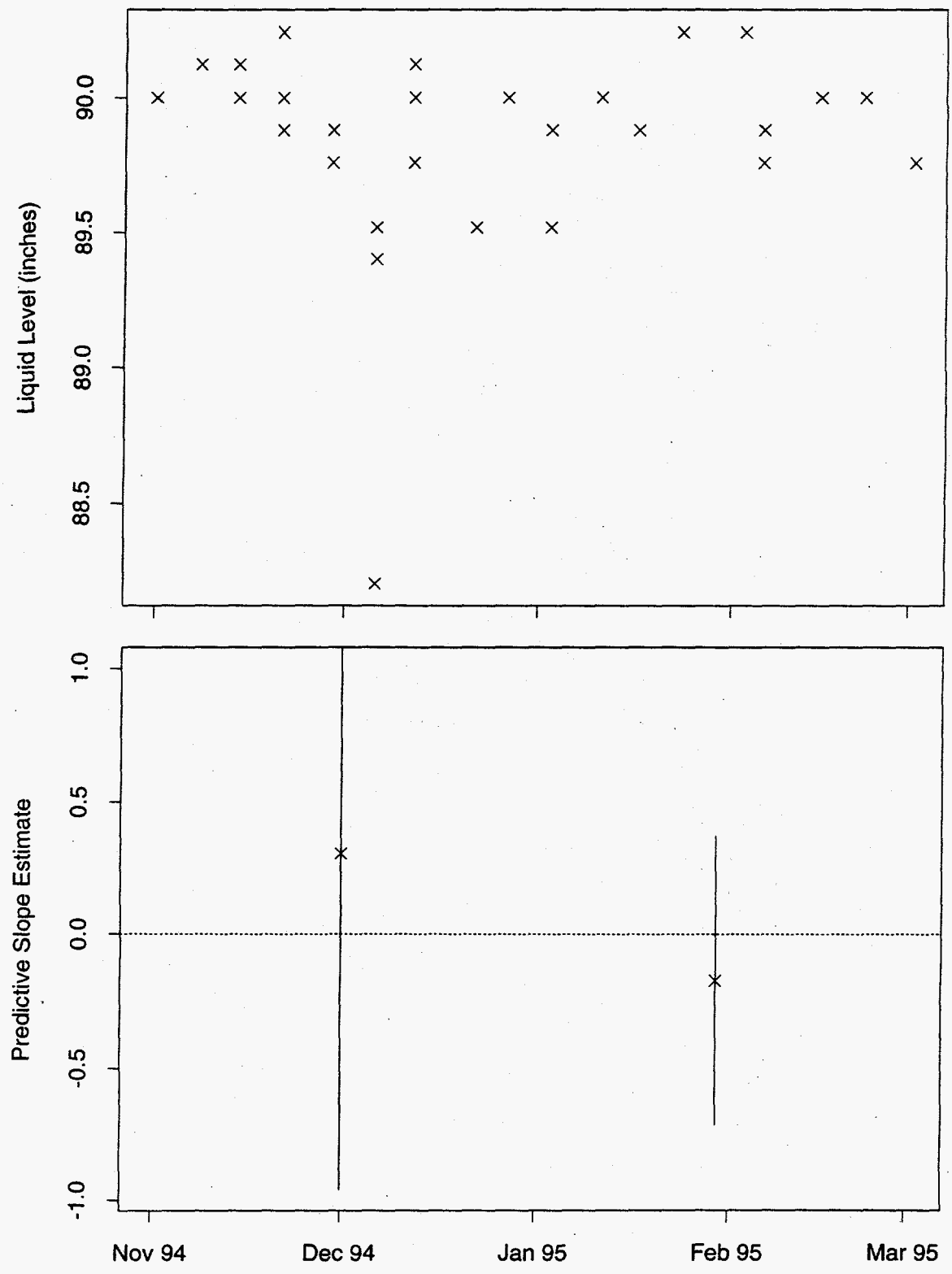

Figure 92: Tank B–111 Neutron ILL Data

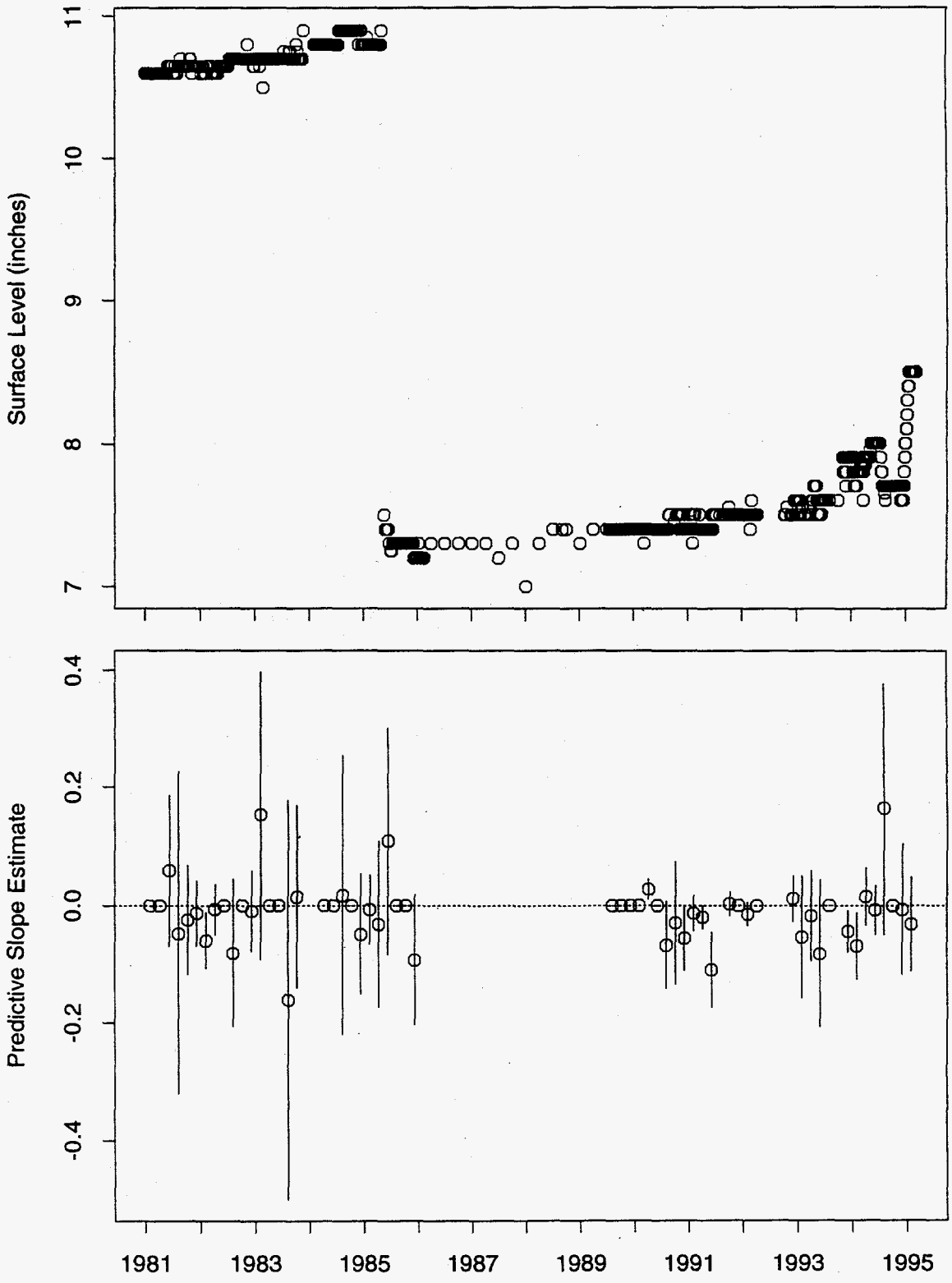

Figure 93: Tank B–112 FIC Data

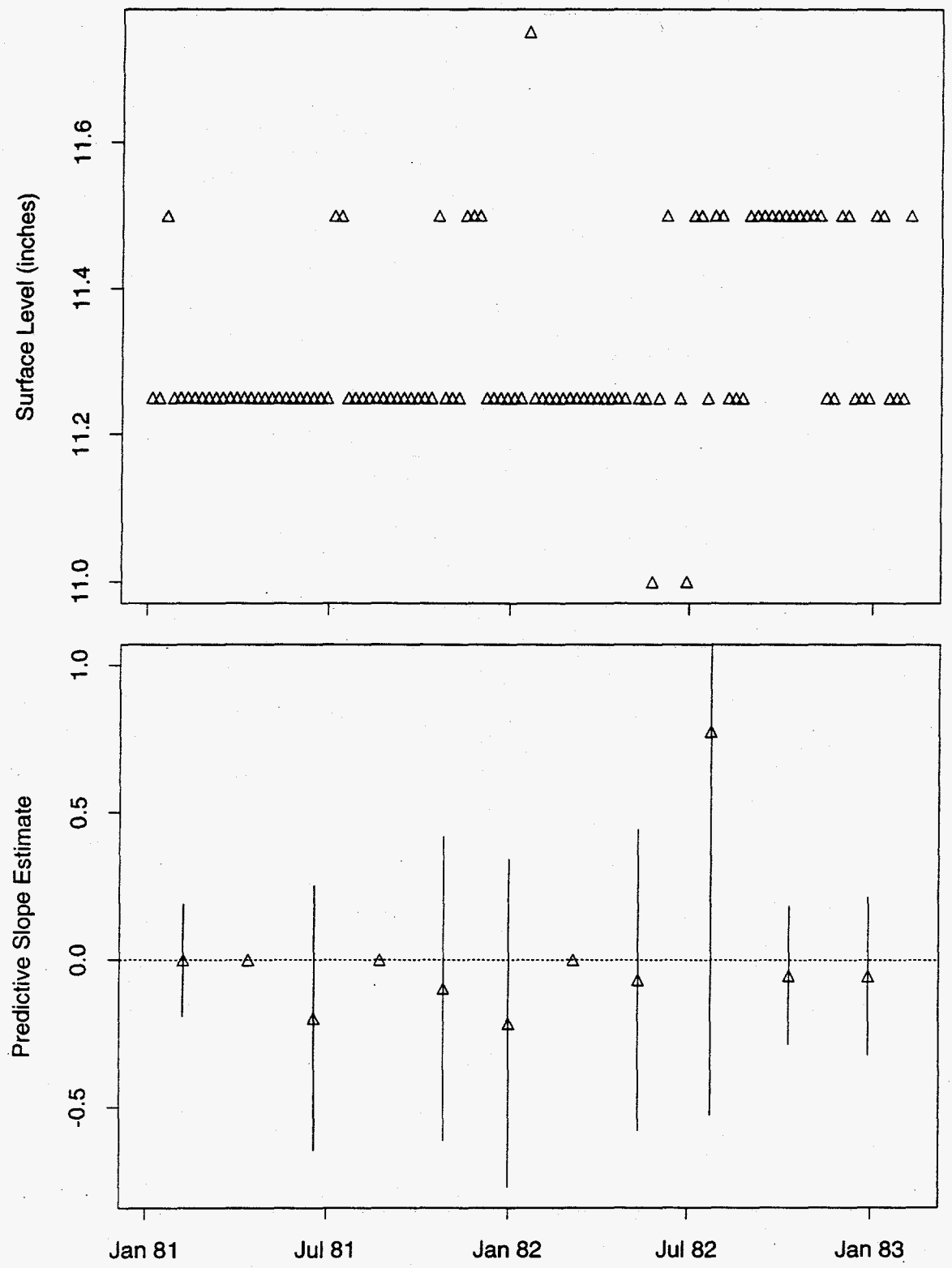

Figure 94: Tank B–112 MT Data

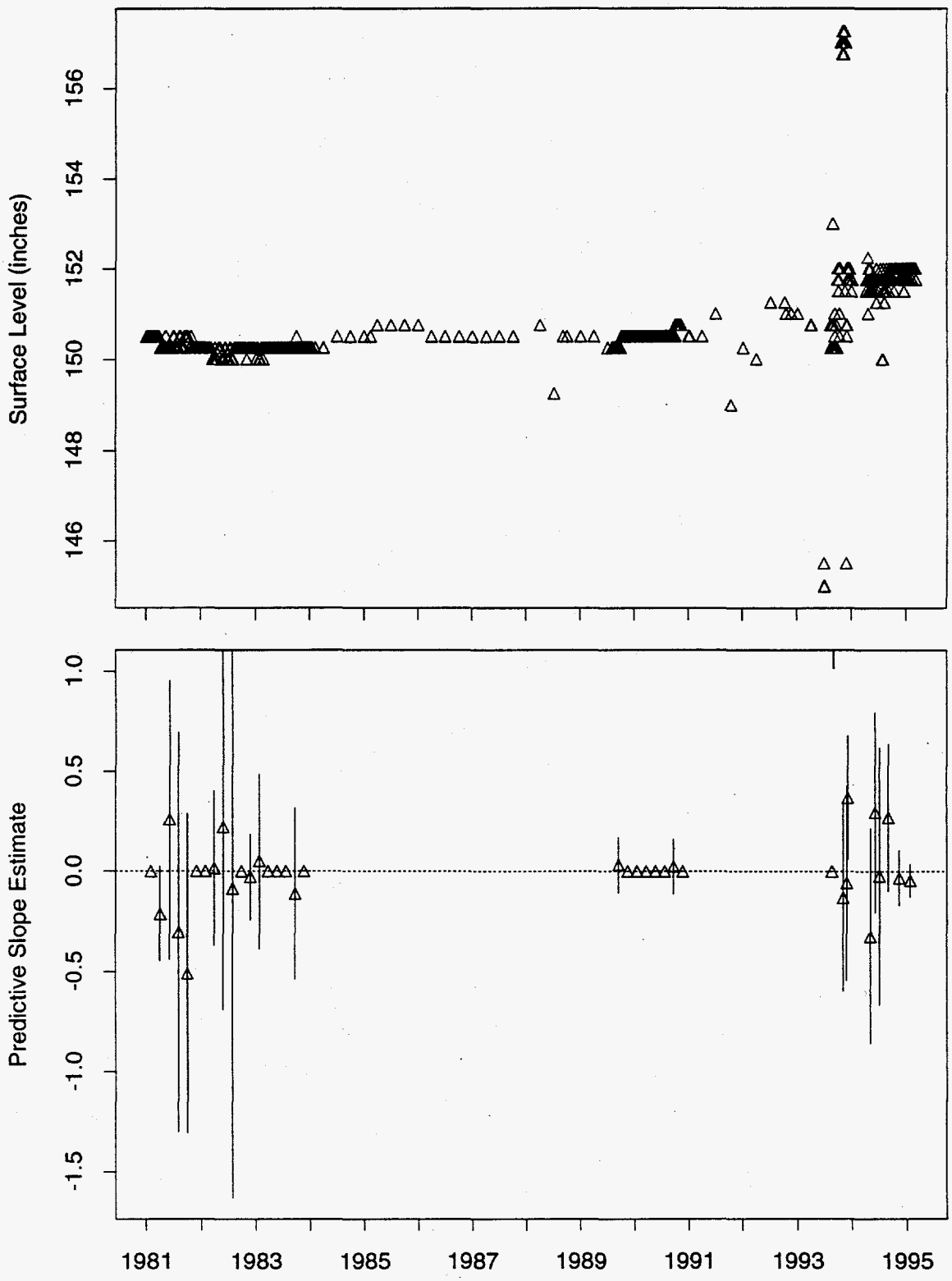

Figure 95: Tank B–201 MT Data

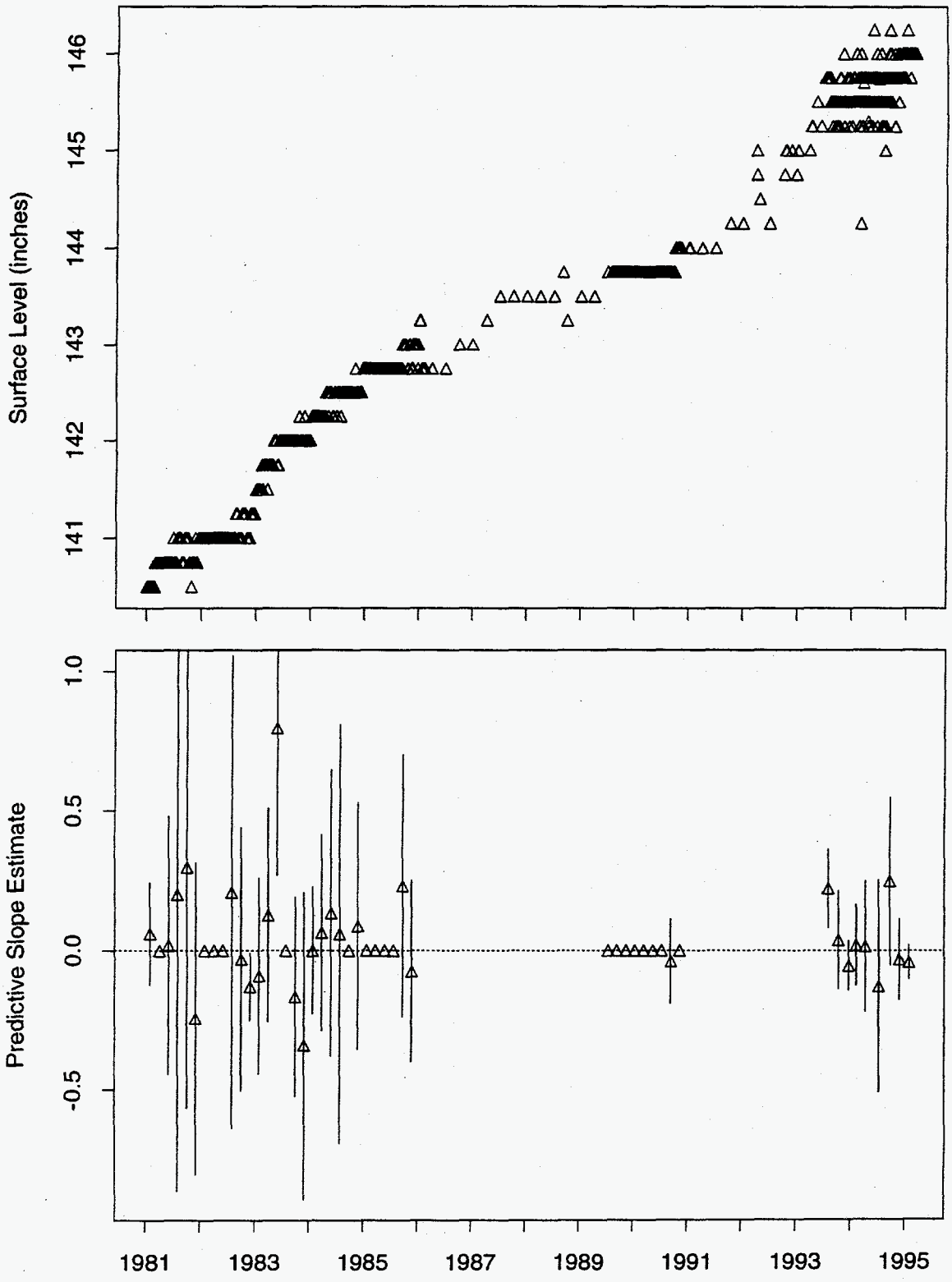

Figure 96: Tank B–202 MT Data

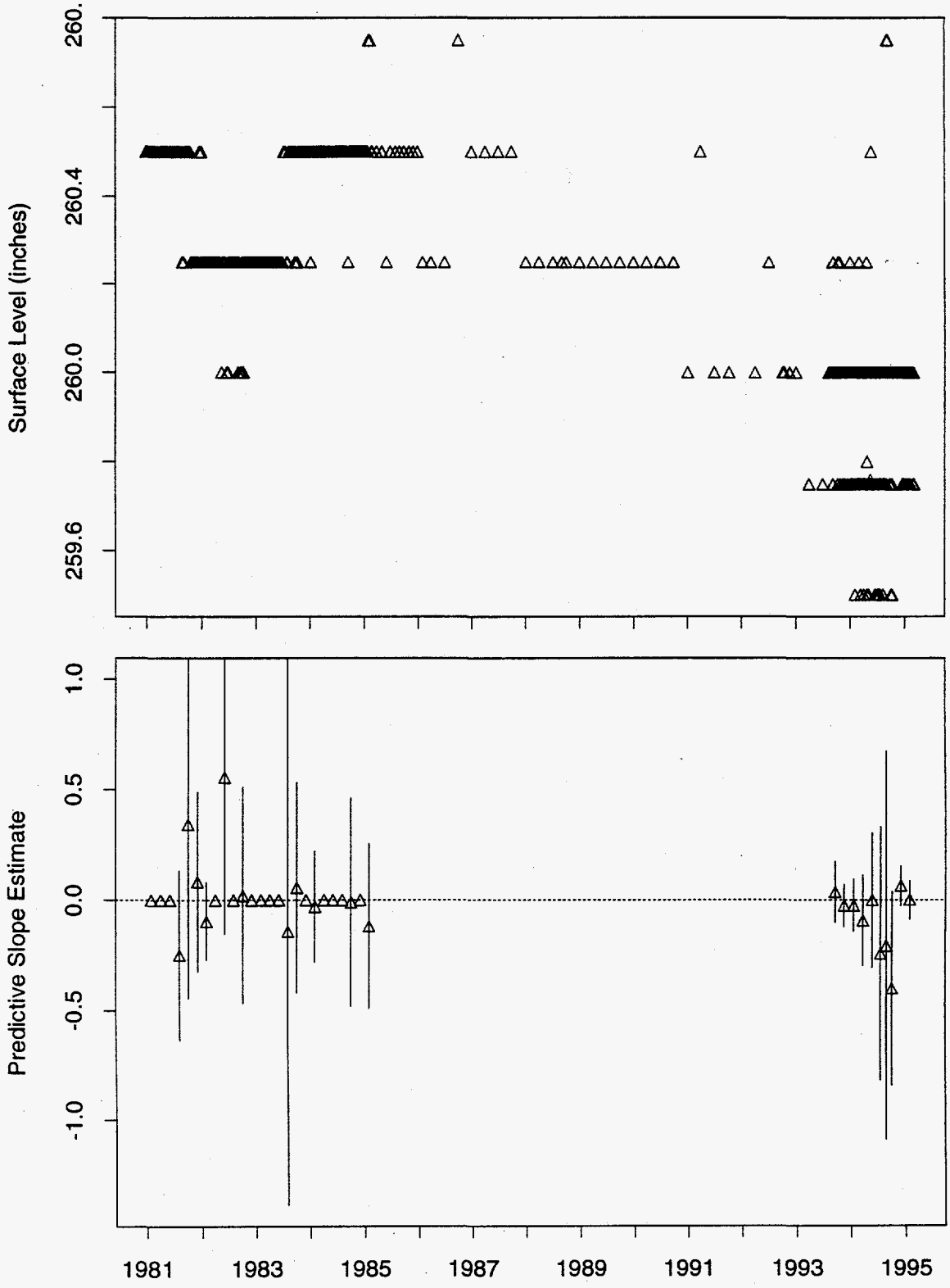

Figure 97: Tank B-203 MT Data

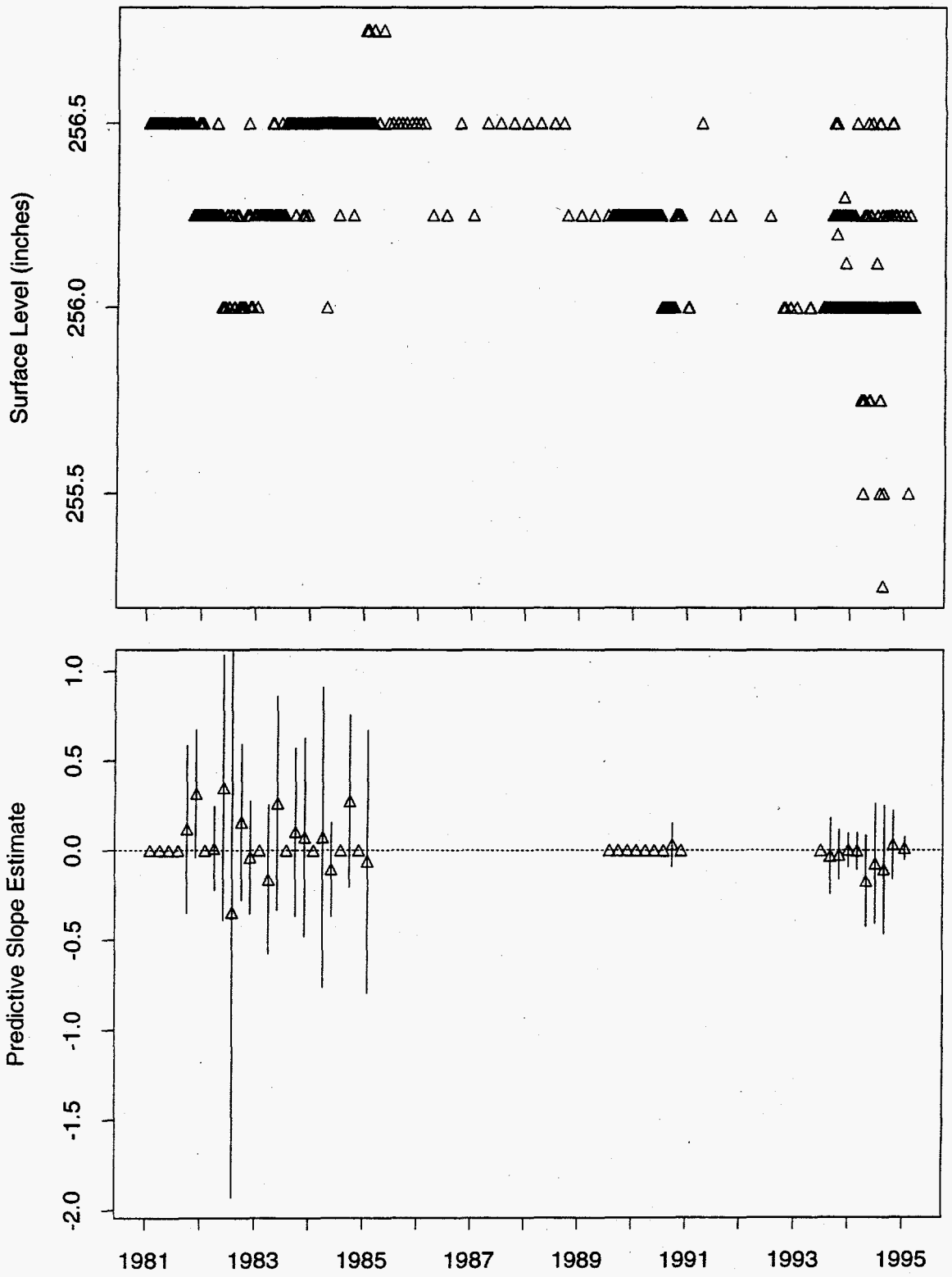

Figure 98: Tank B–204 MT Data

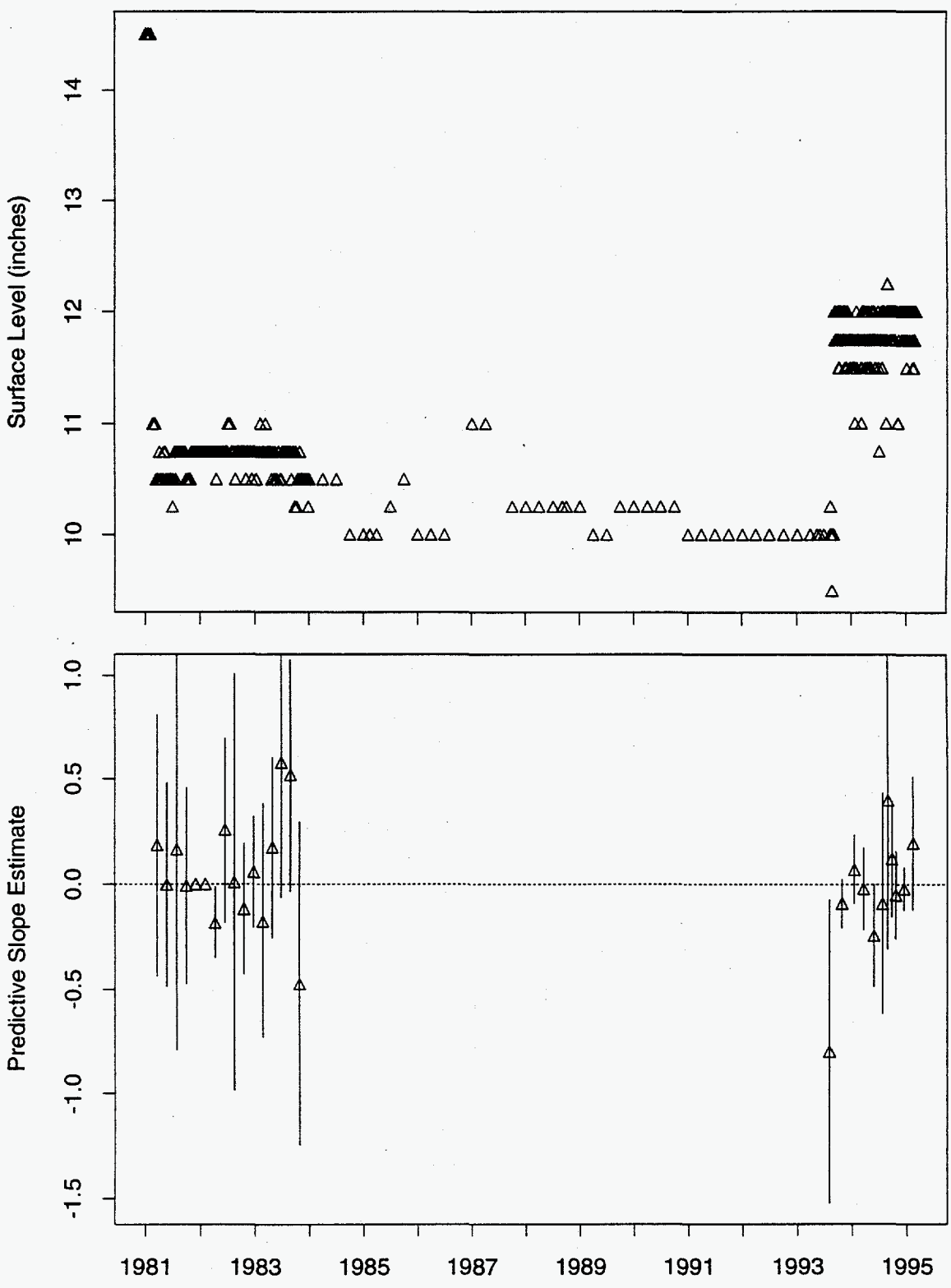

Figure 99: Tank BX–101 MT Data

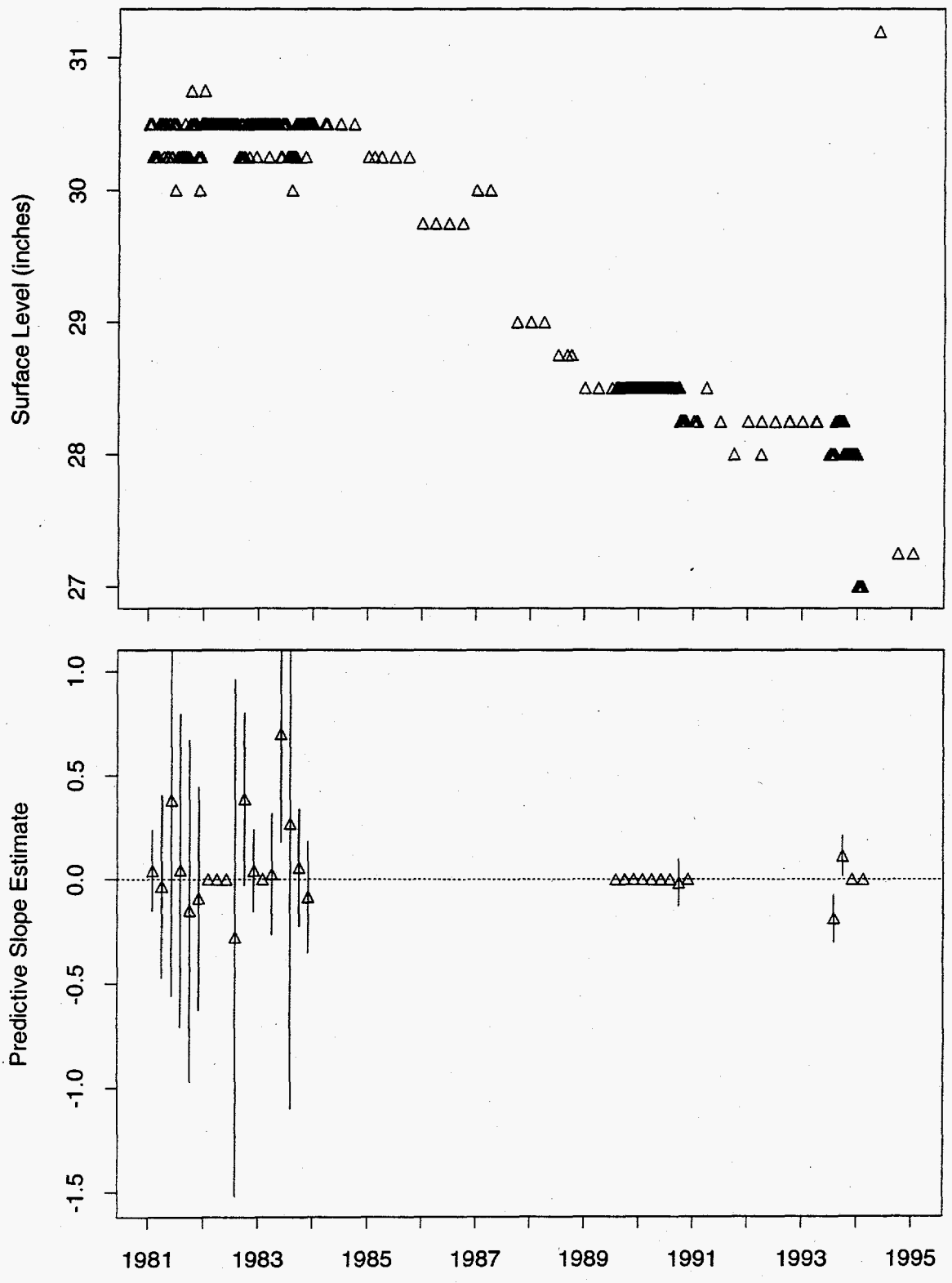

Figure 100: Tank BX–102 MT Data

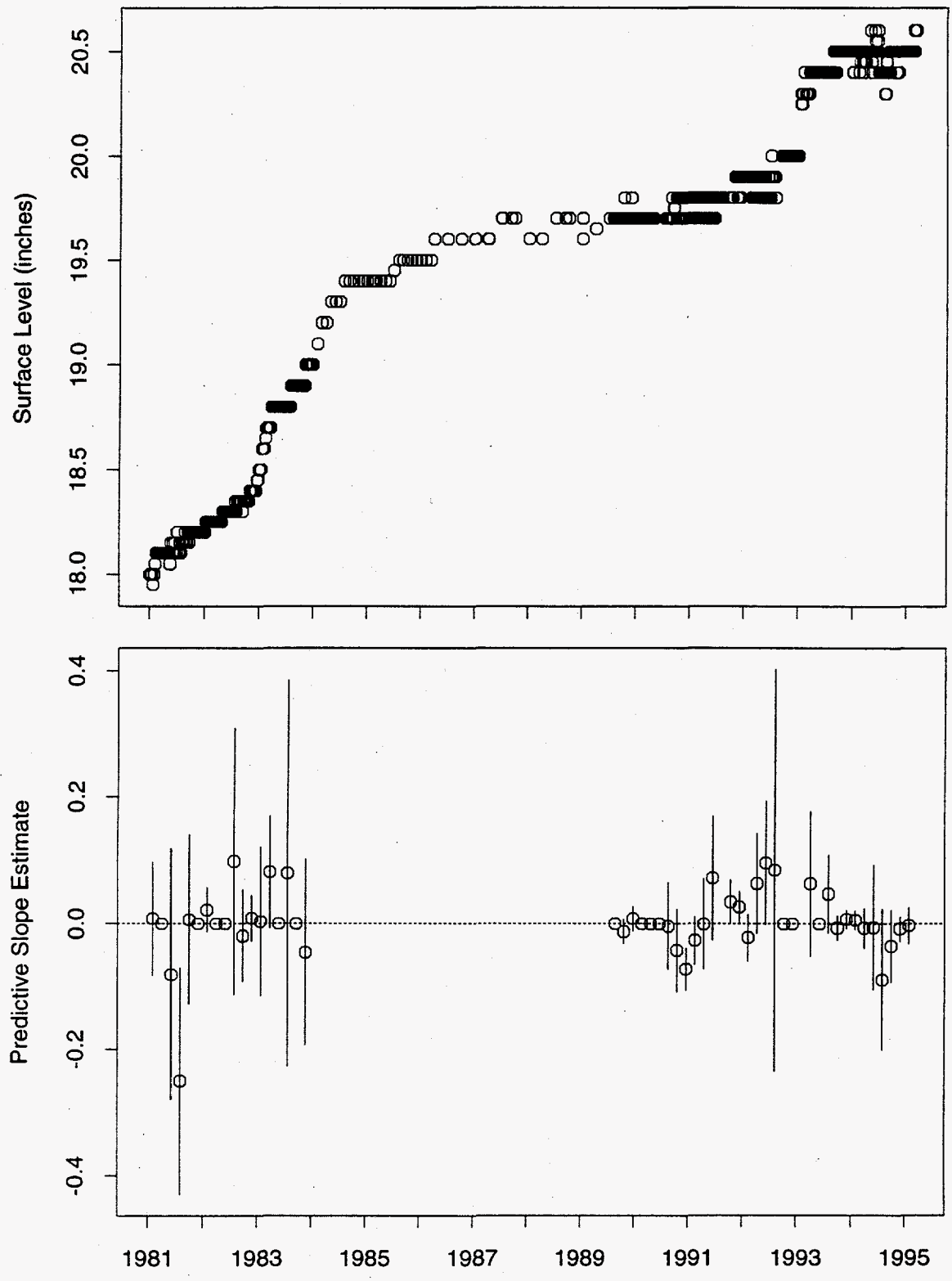

Figure 101: Tank BX–103 FIC Data

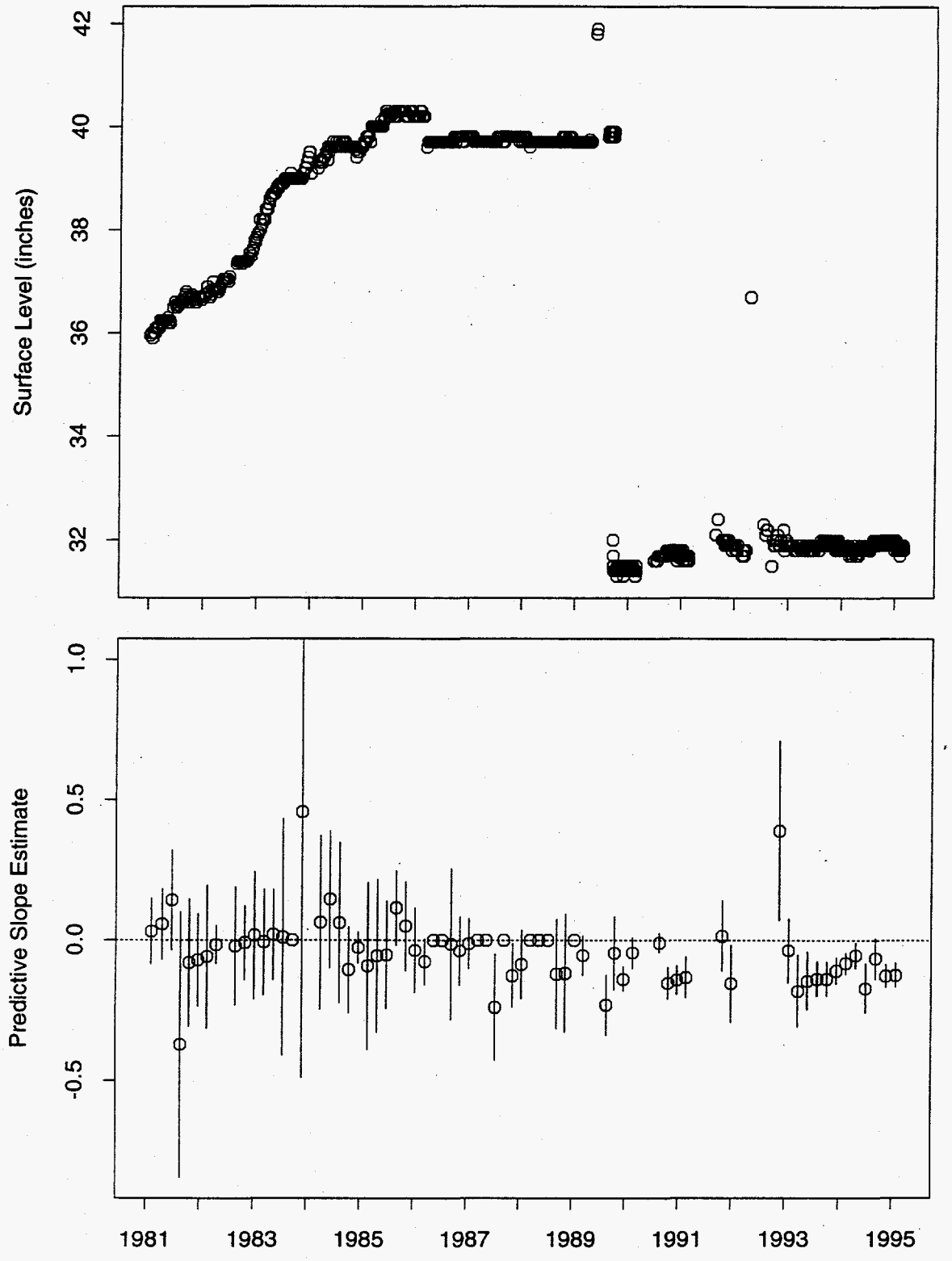

Figure 102: Tank BX–104 FIC Data

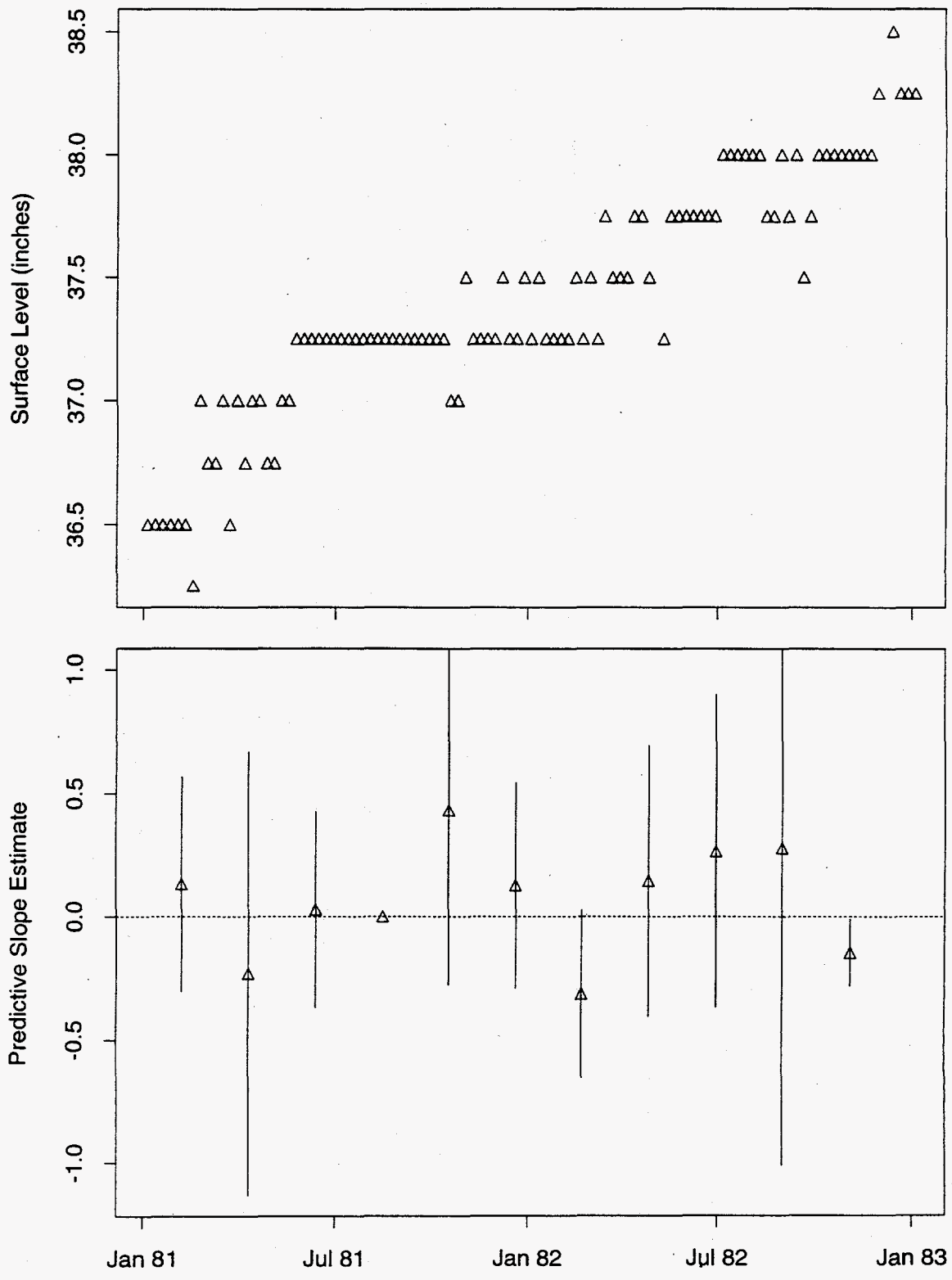

Figure 103: Tank BX–104 MT Data

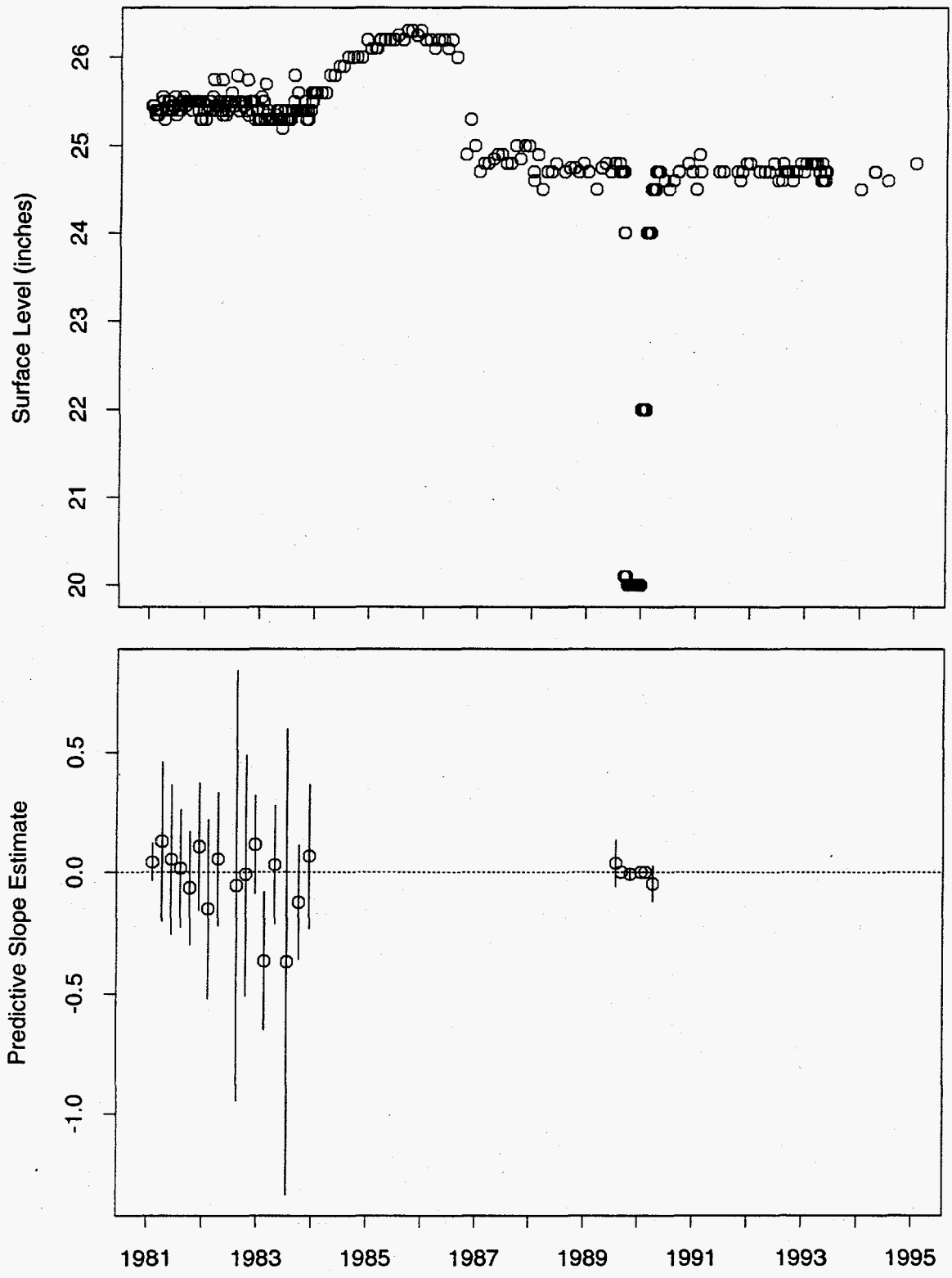

Figure 104: Tank BX–105 FIC Data

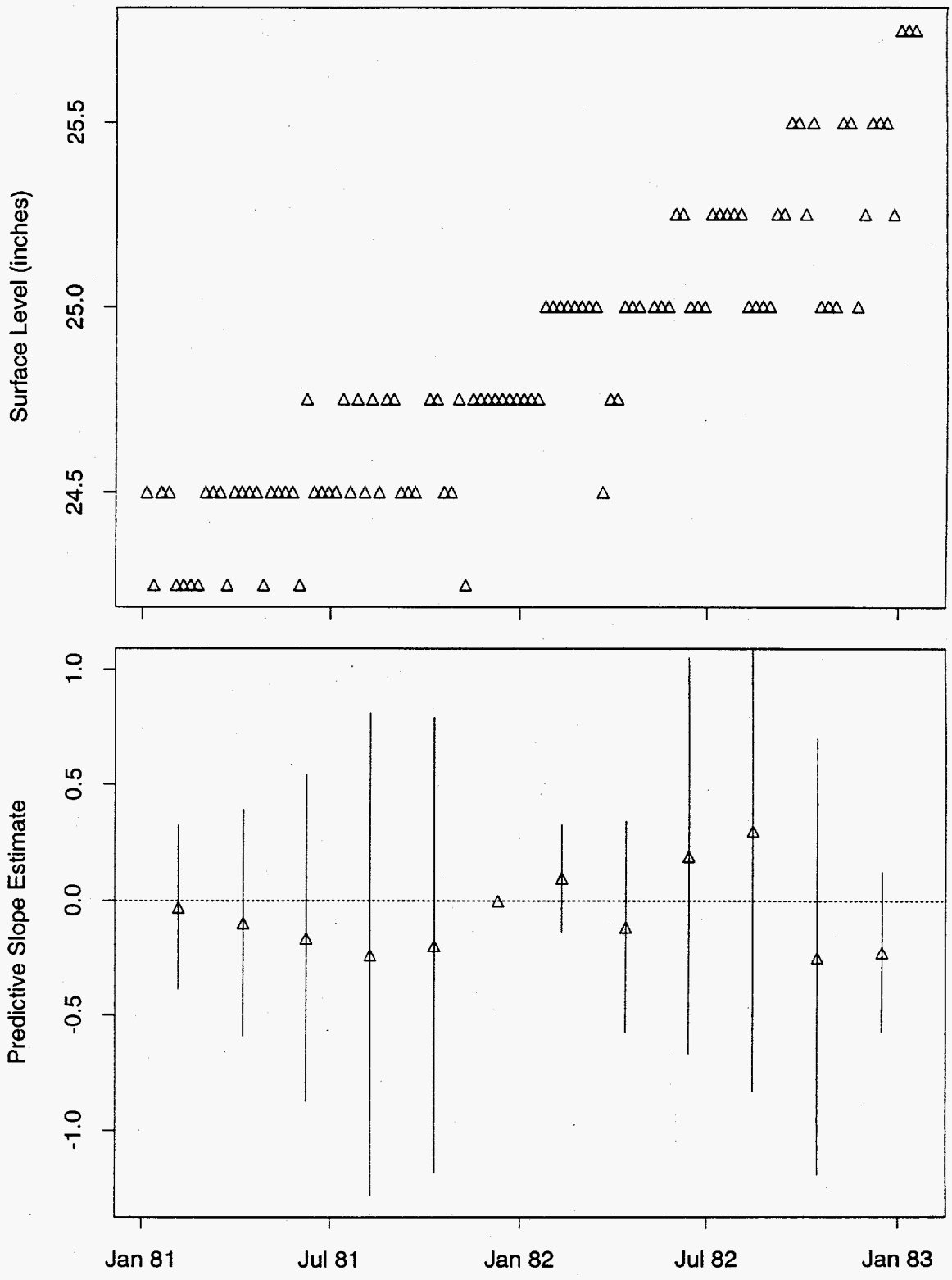

Figure 105: Tank BX–105 MT Data

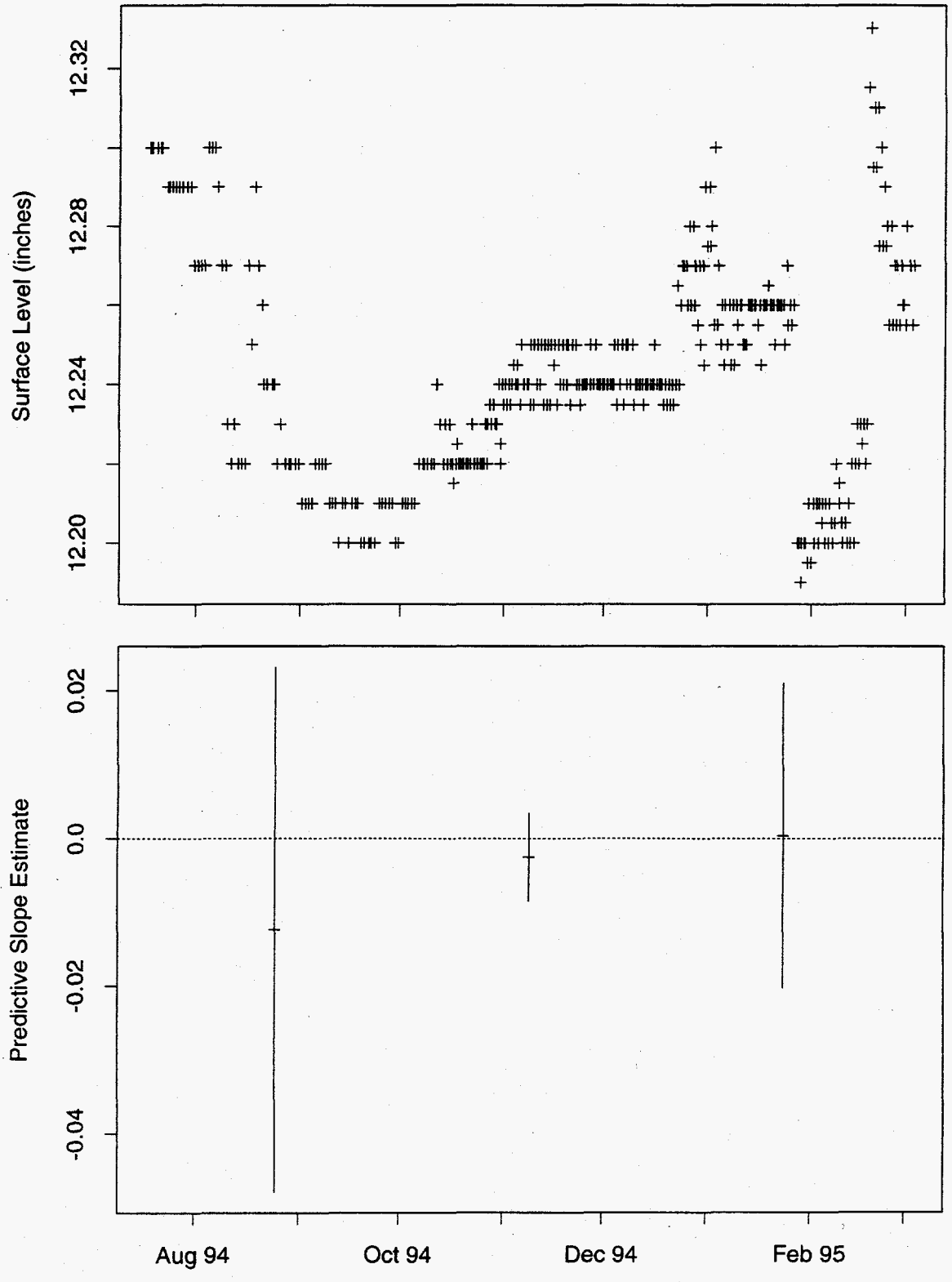

Figure 106: Tank BX–106 ENRAF Data

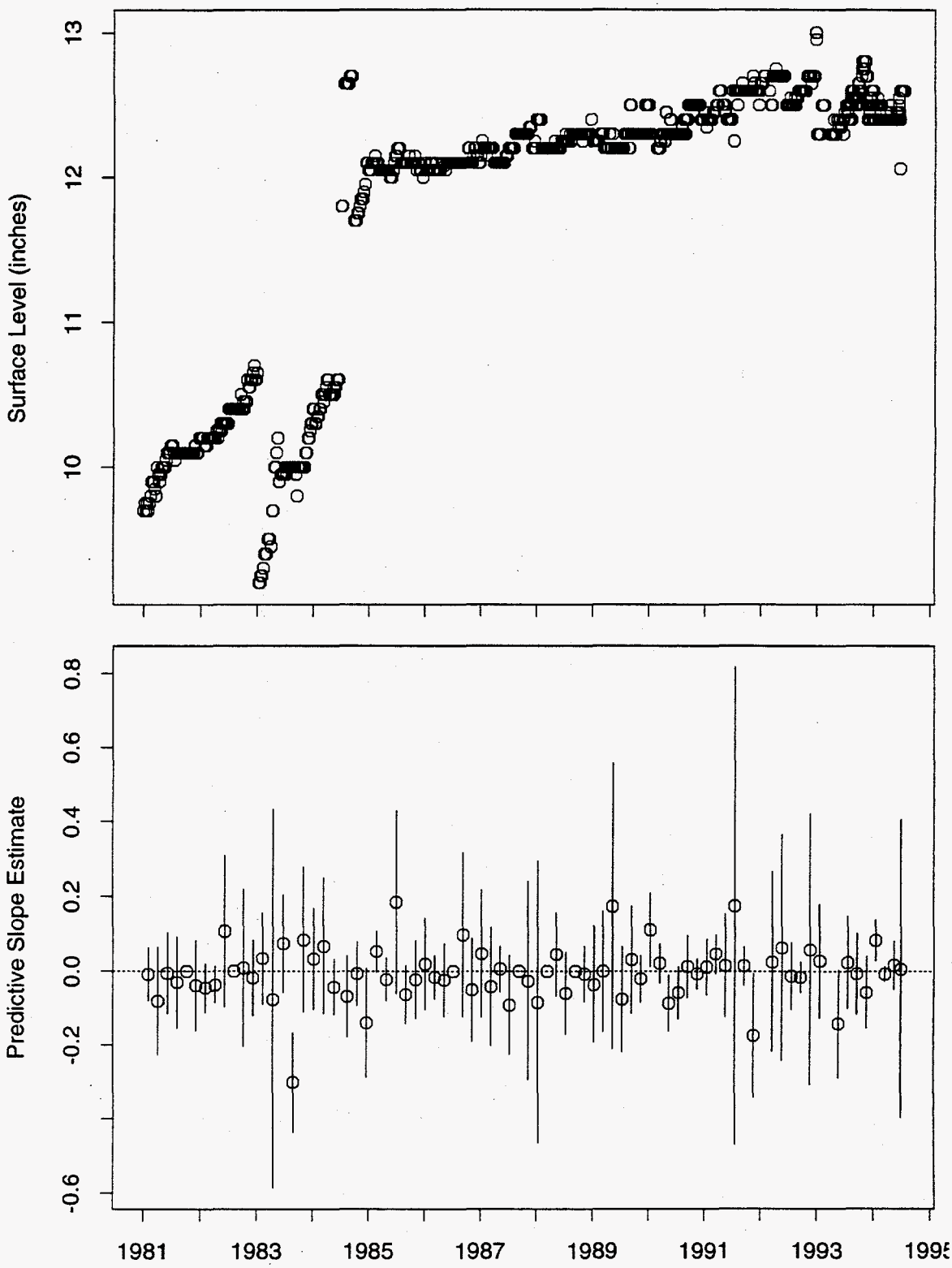

Figure 107: Tank BX–106 FIC Data

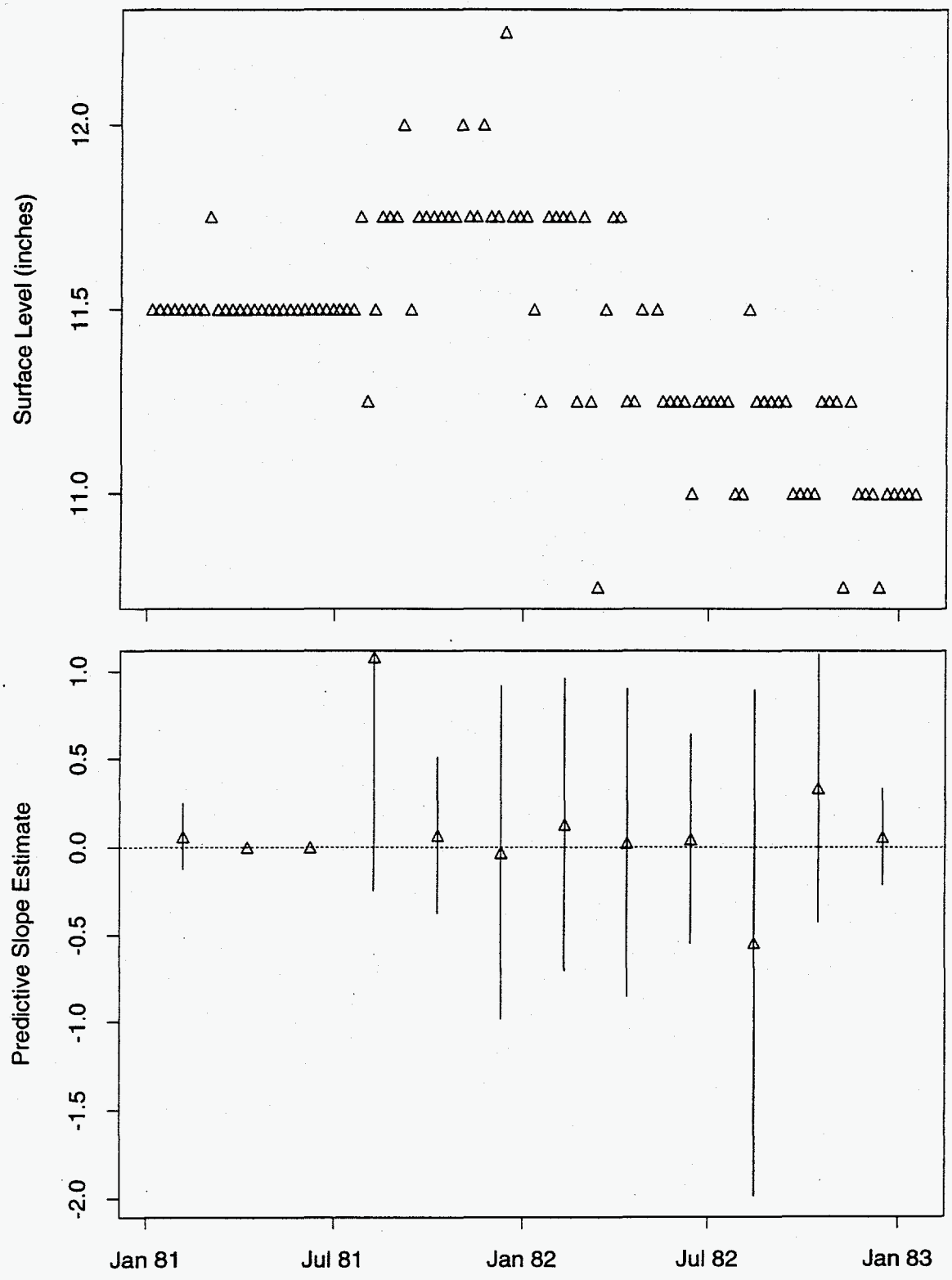

Figure 108: Tank BX–106 MT Data

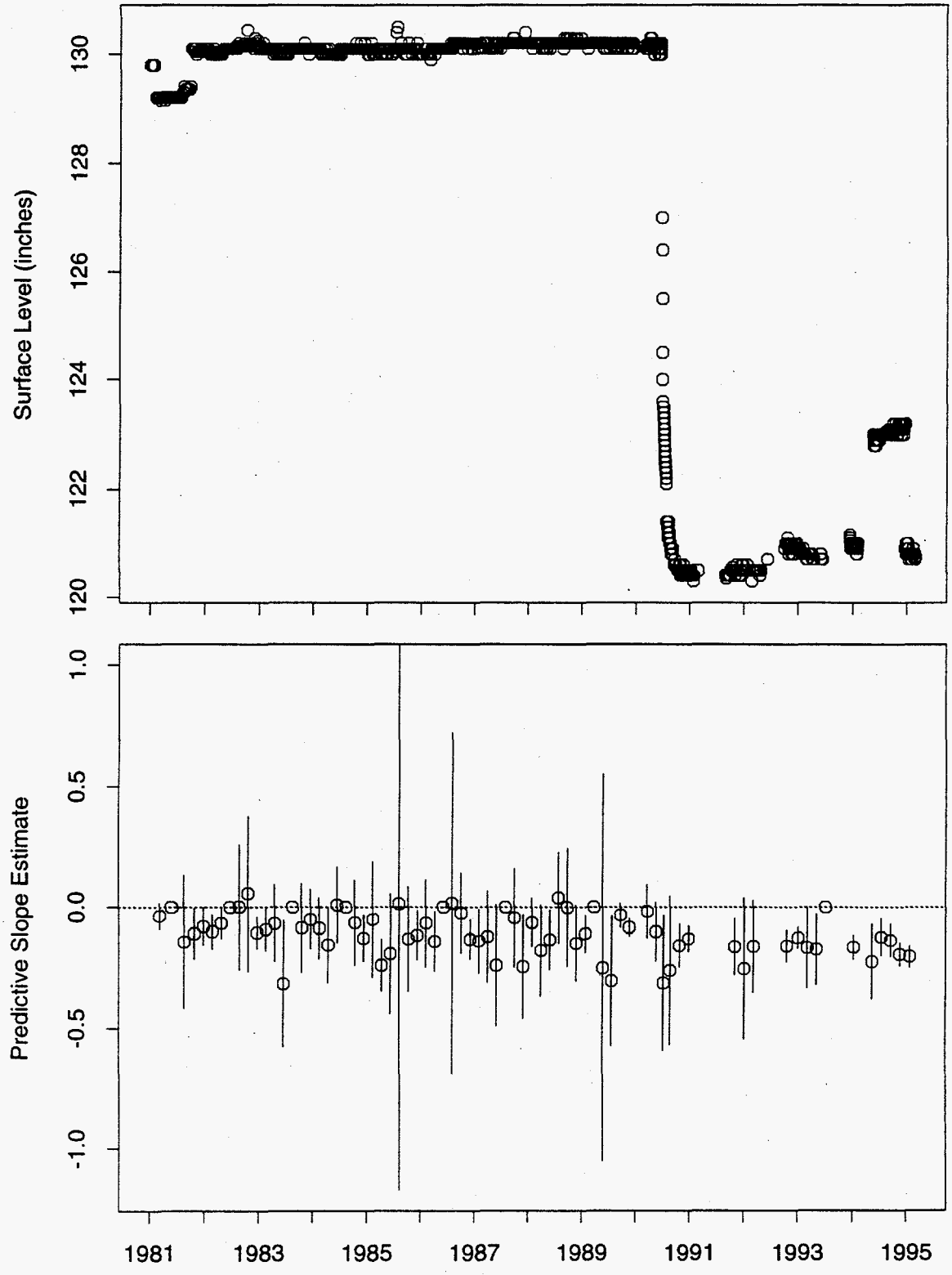

Figure 109: Tank BX–107 FIC Data

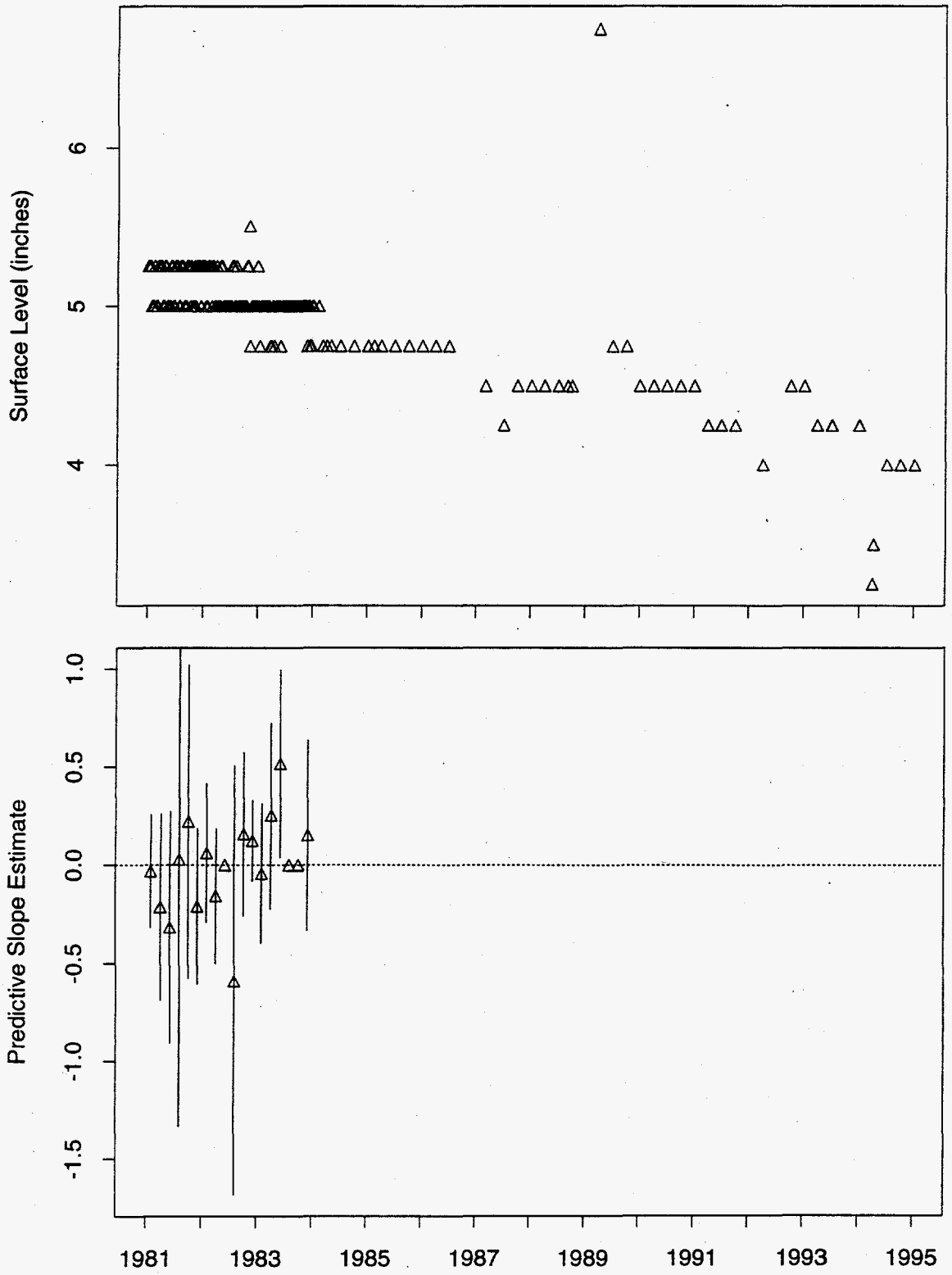

Figure 110: Tank BX–108 MT Data

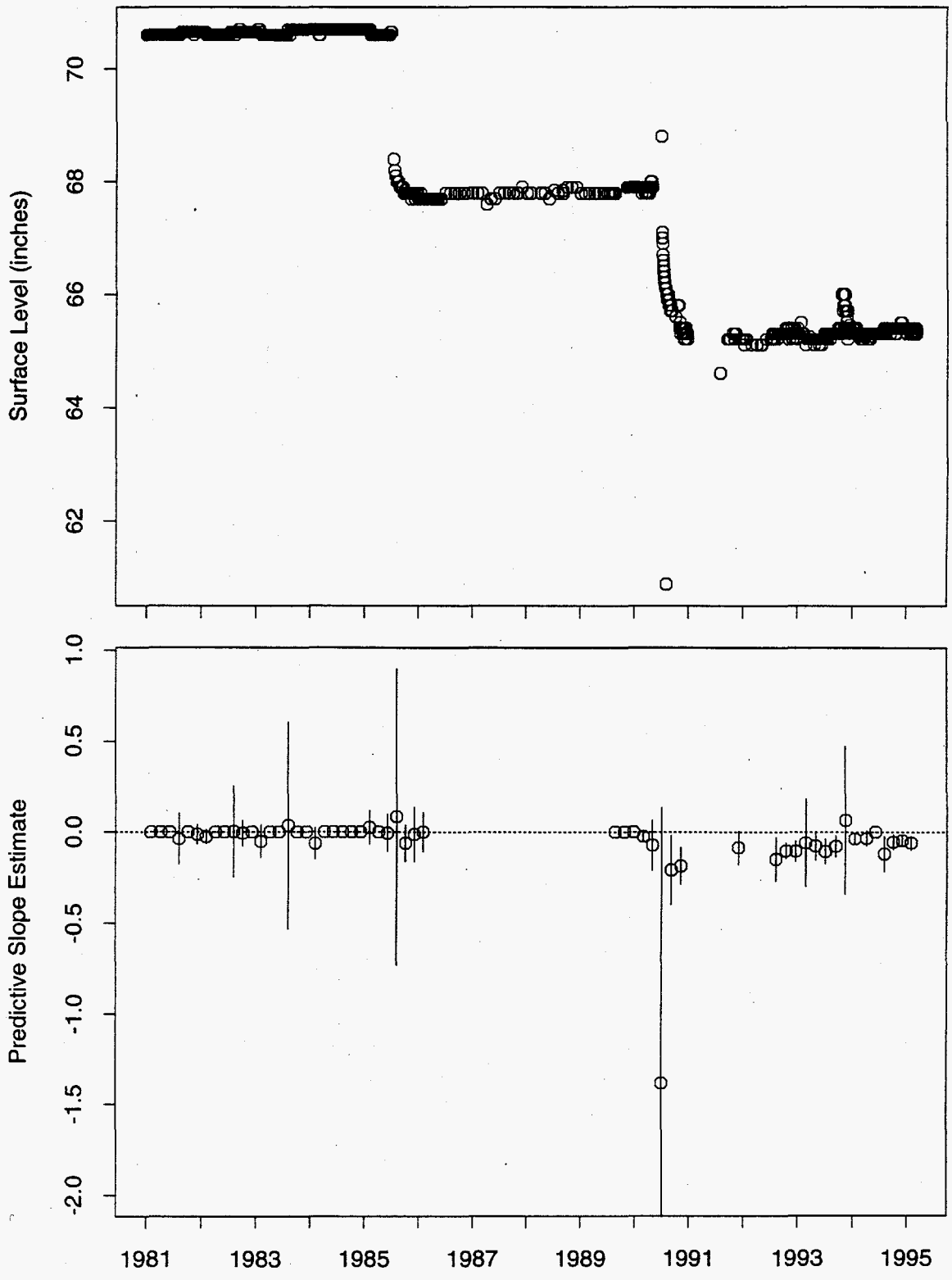

Figure 111: Tank BX-109 FIC Data

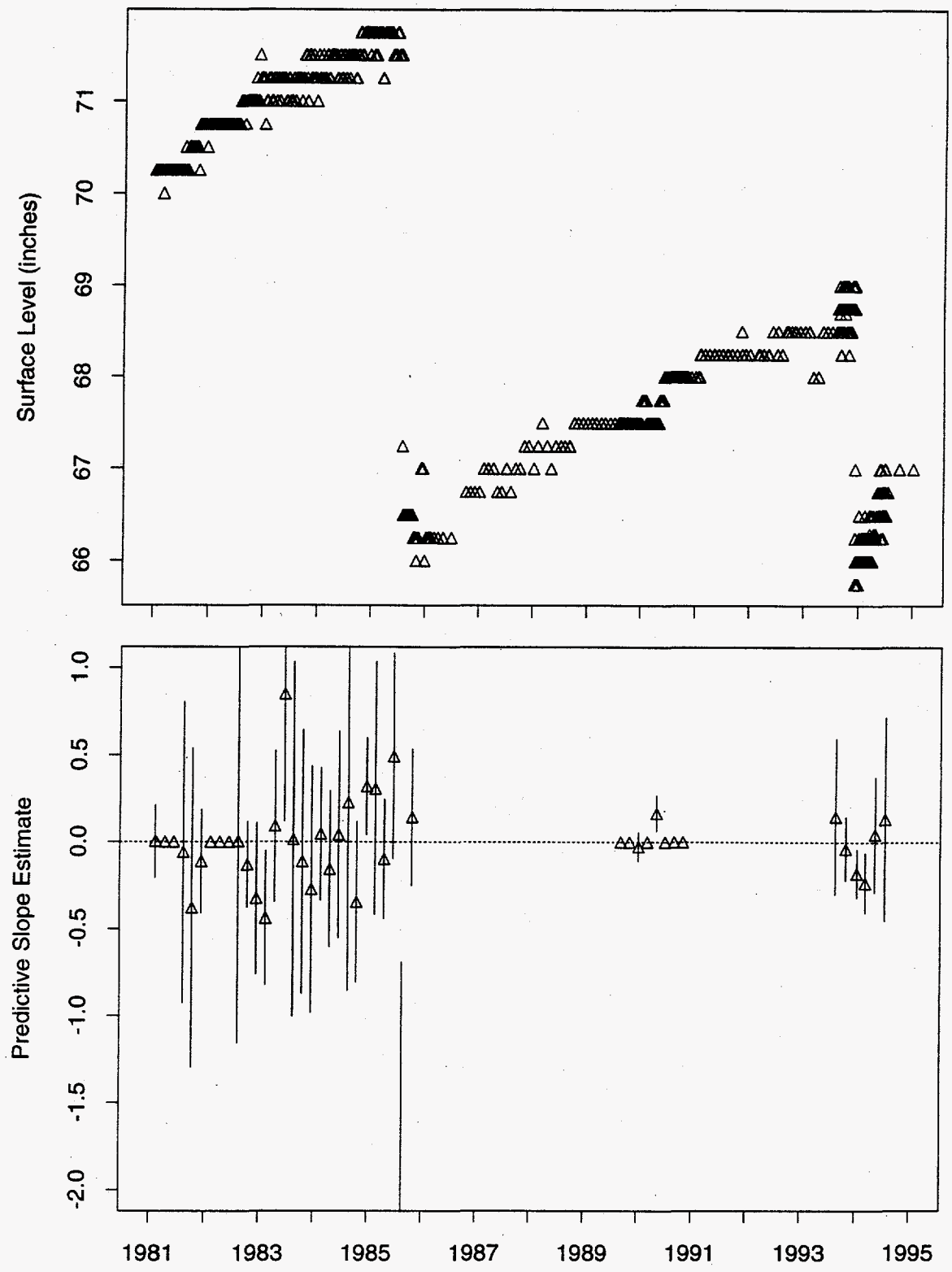

Figure 112: Tank BX–110 MT Data

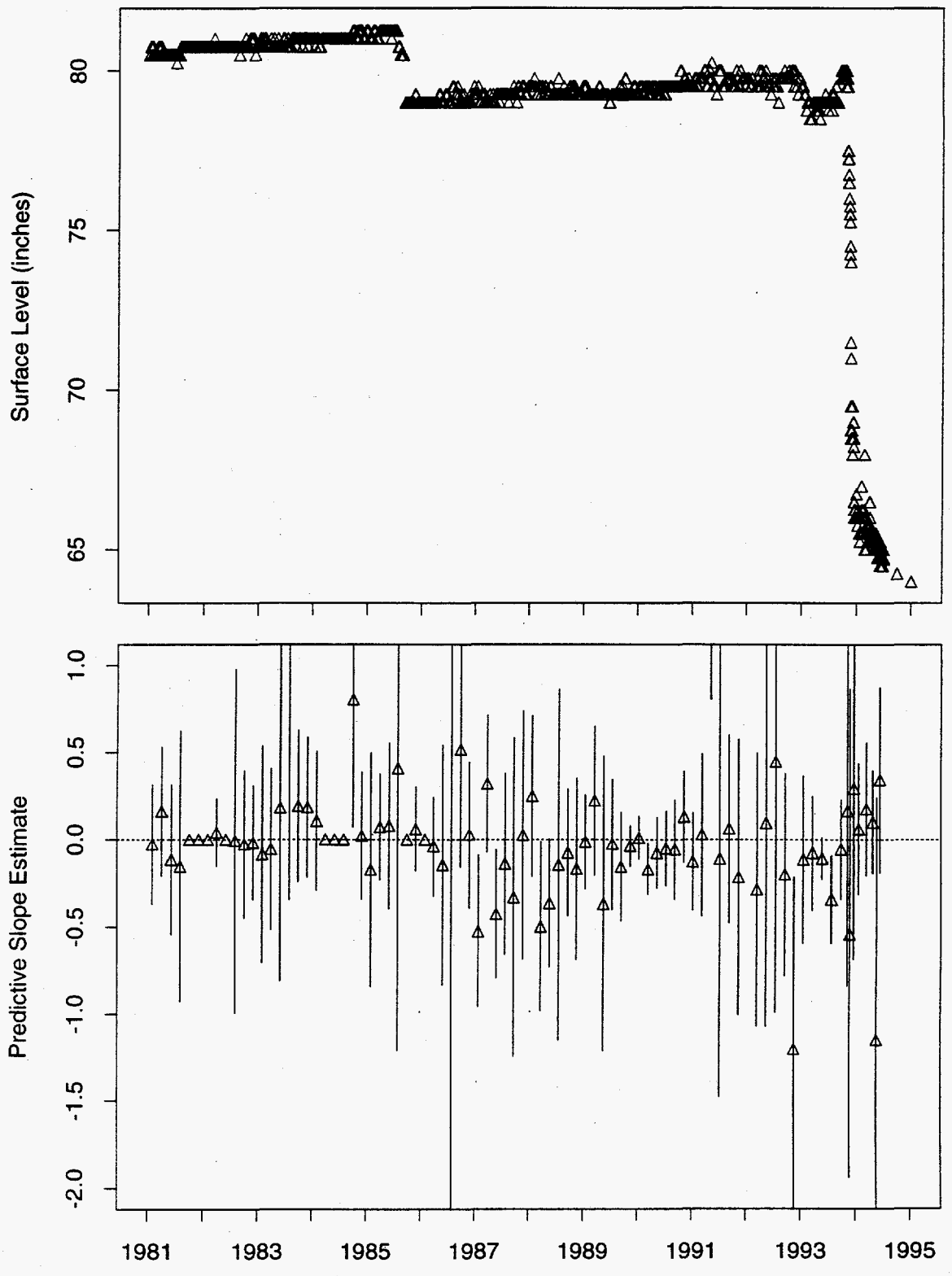

Figure 113: Tank BX-111 MT Data

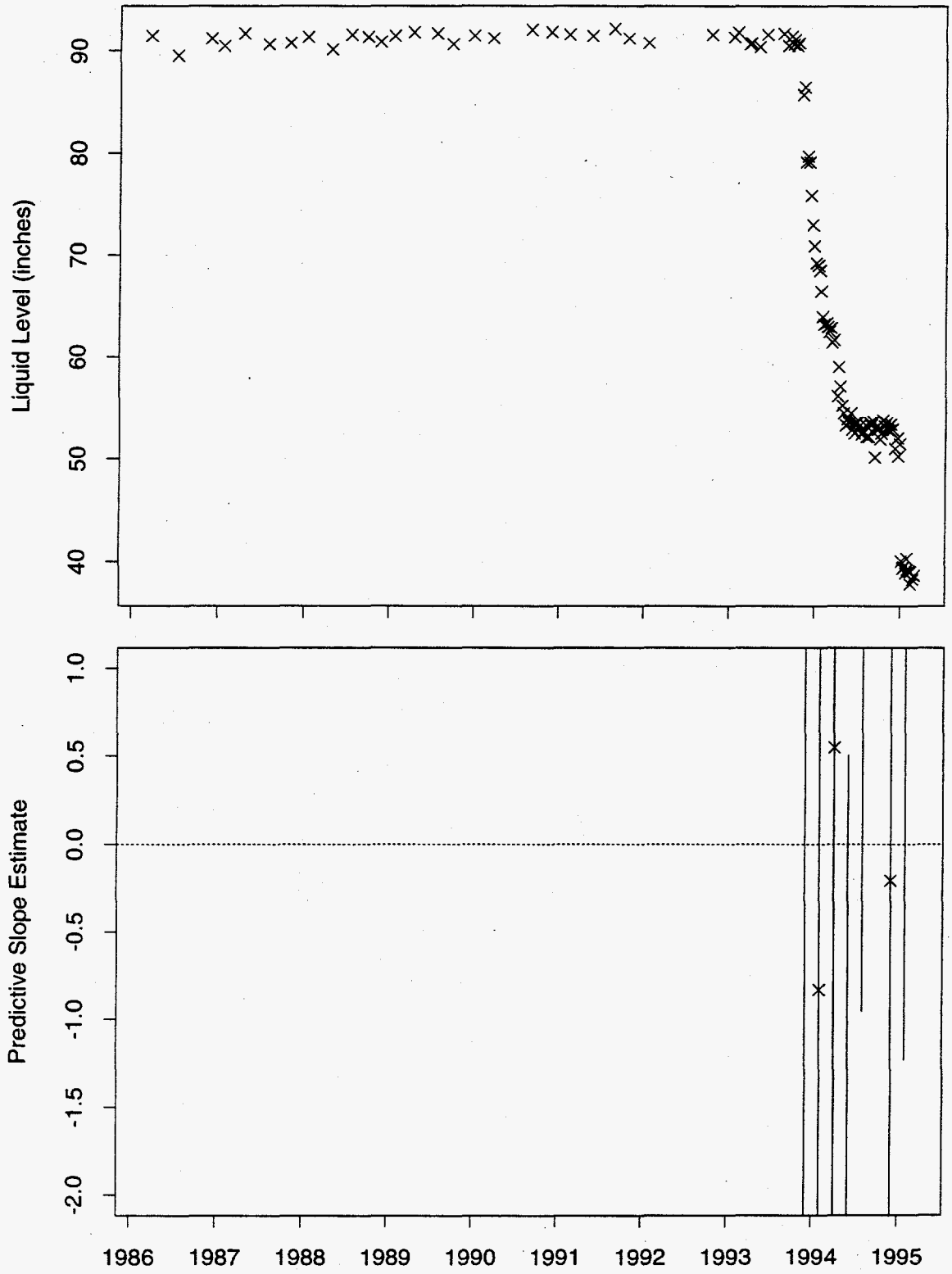

Figure 114: Tank BX–111 Neutron ILL Data

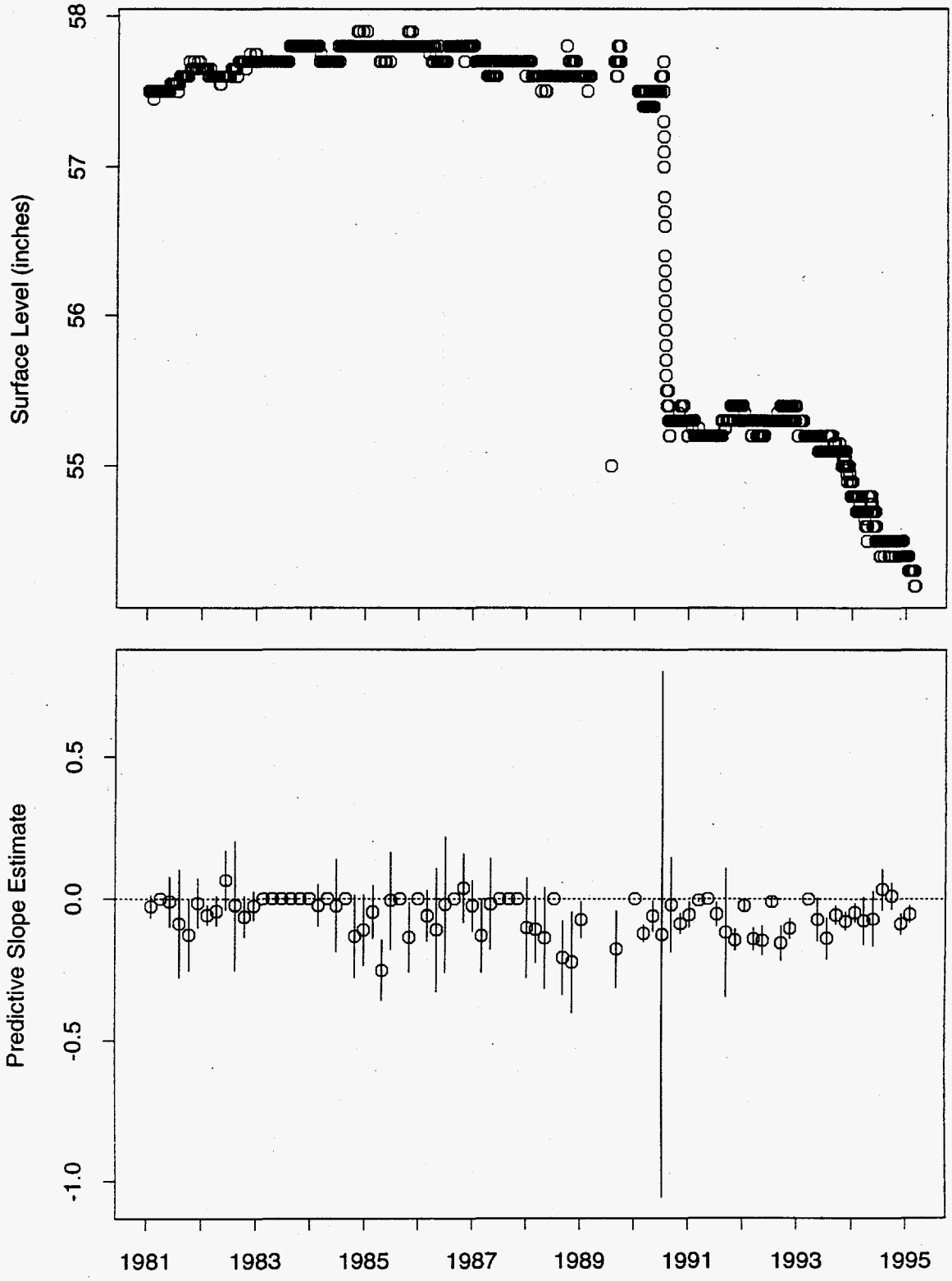

Figure 115: Tank BX–112 FIC Data

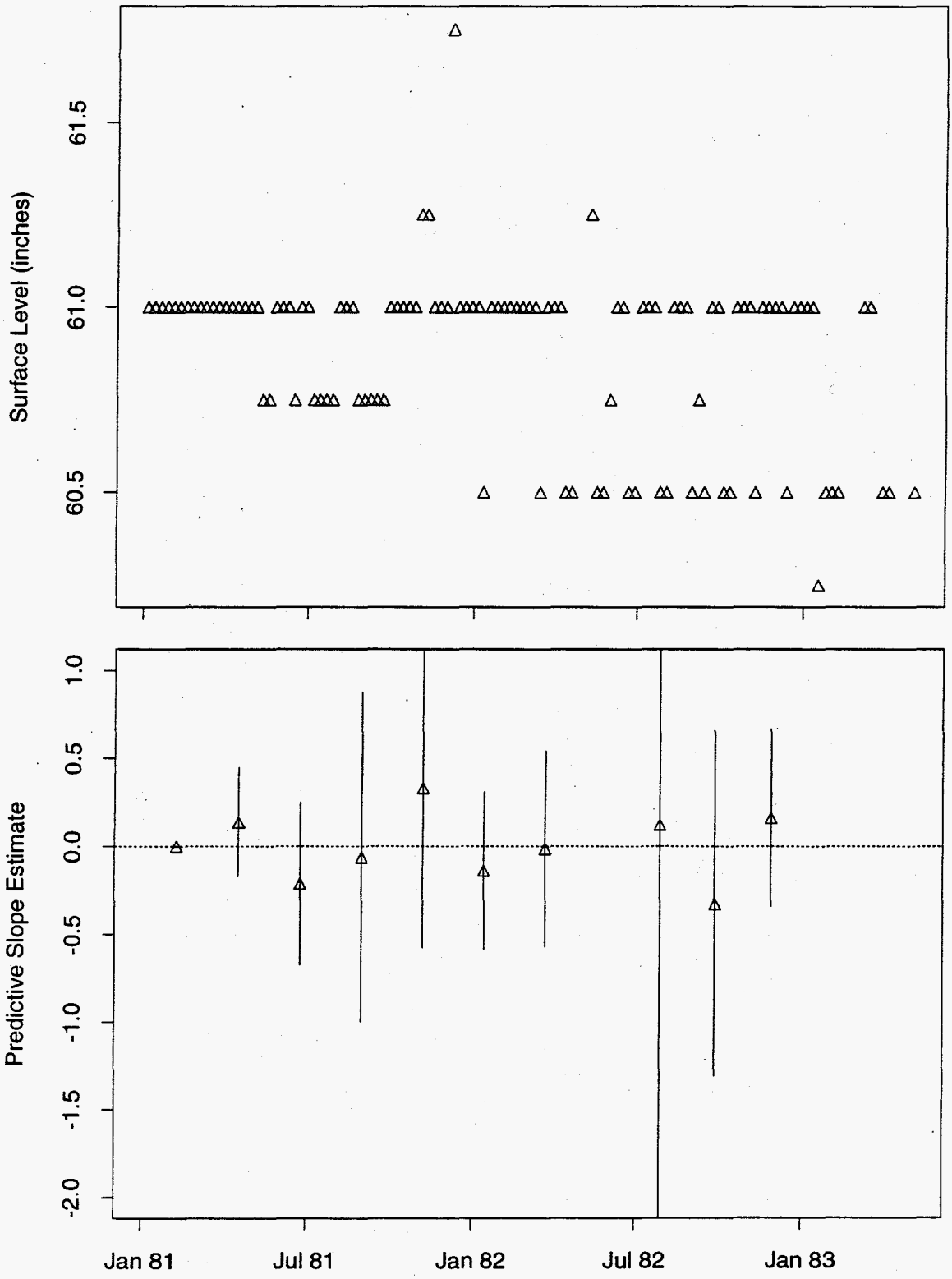

Figure 116: Tank BX–112 MT Data

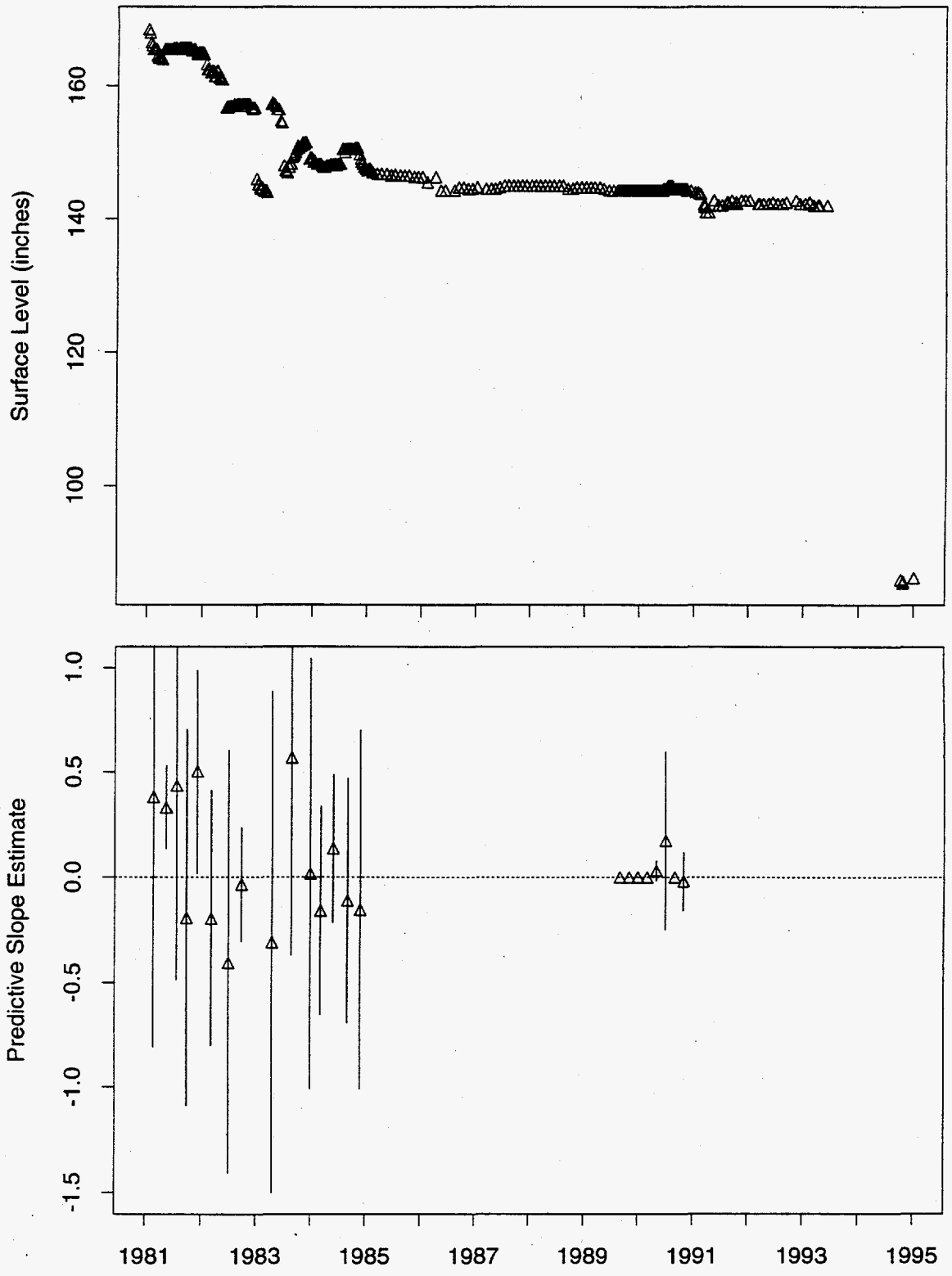

Figure 117: Tank BY–101 MT Data

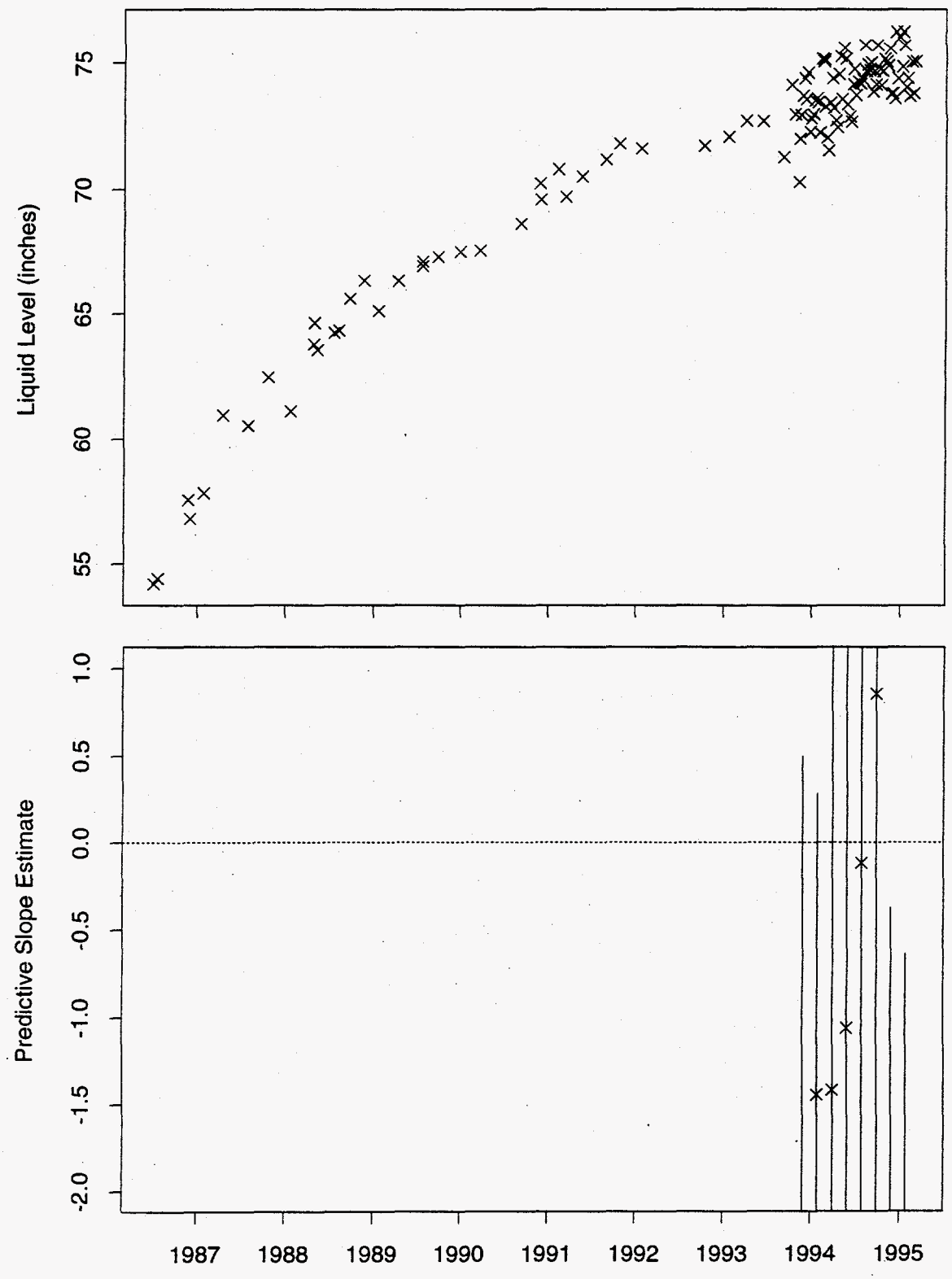

Figure 118: Tank BY-101 Neutron ILL Data

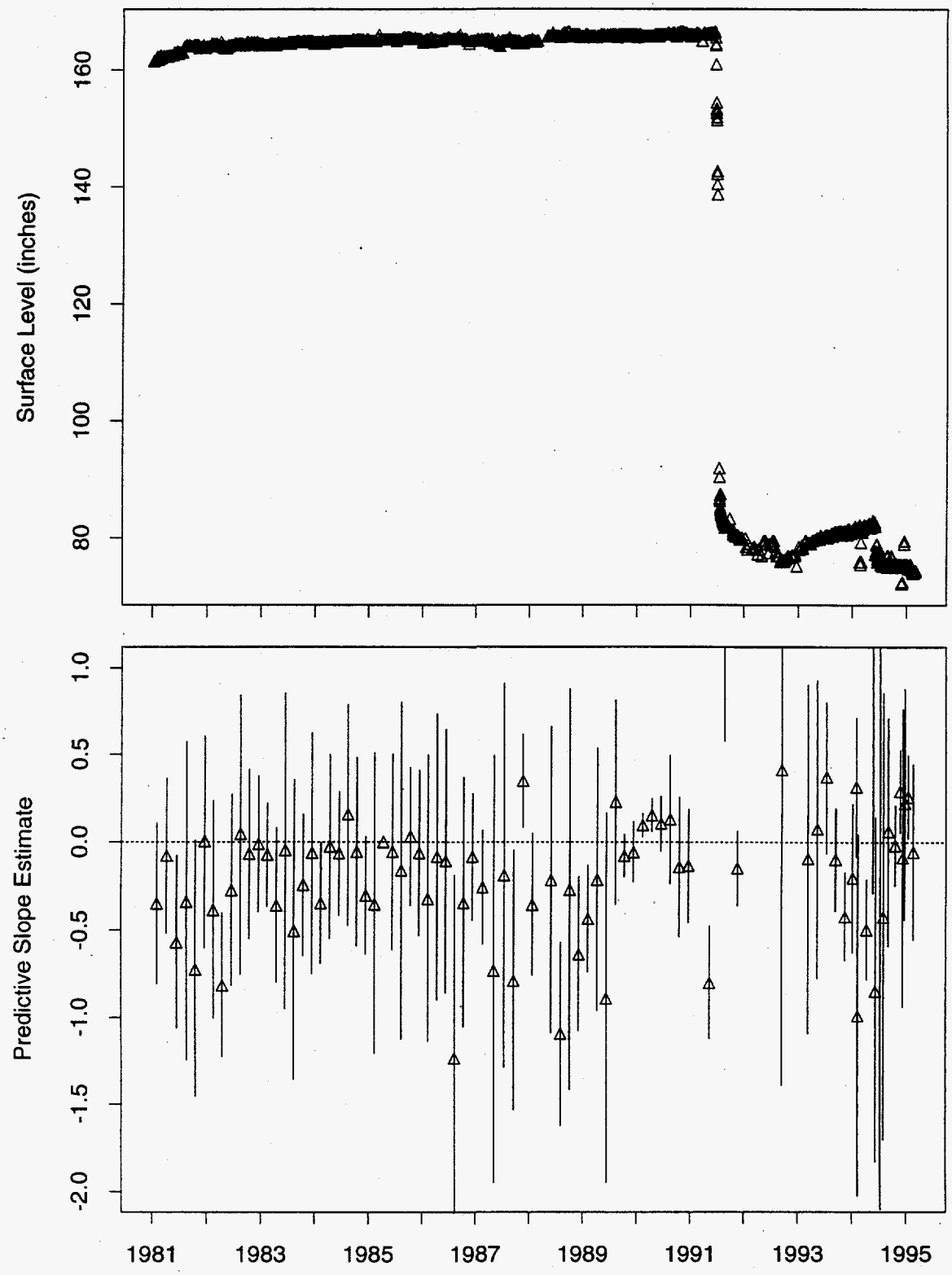

Figure 119: Tank BY–102 MT Data

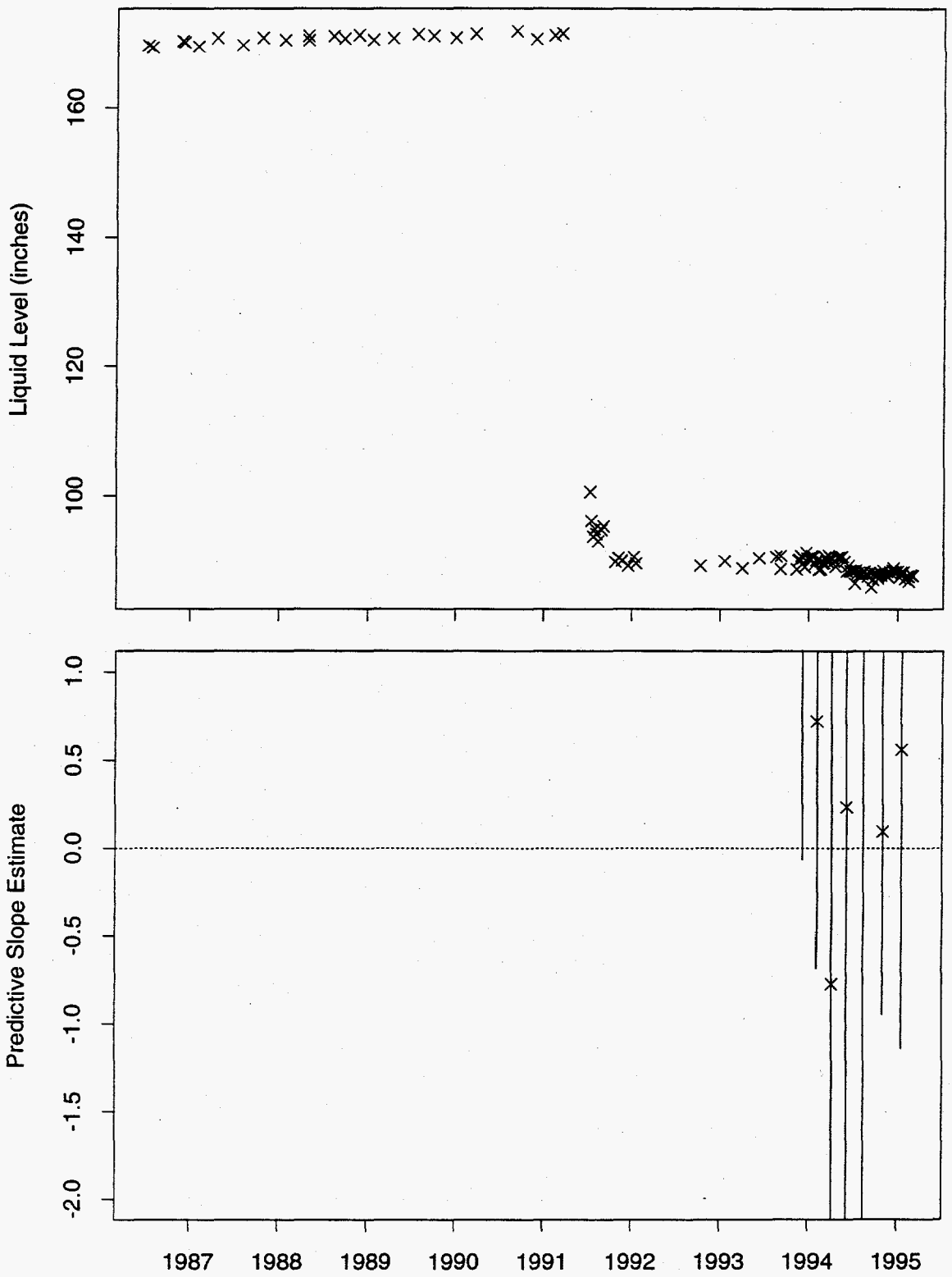

Figure 120: Tank BY–102 Neutron ILL Data

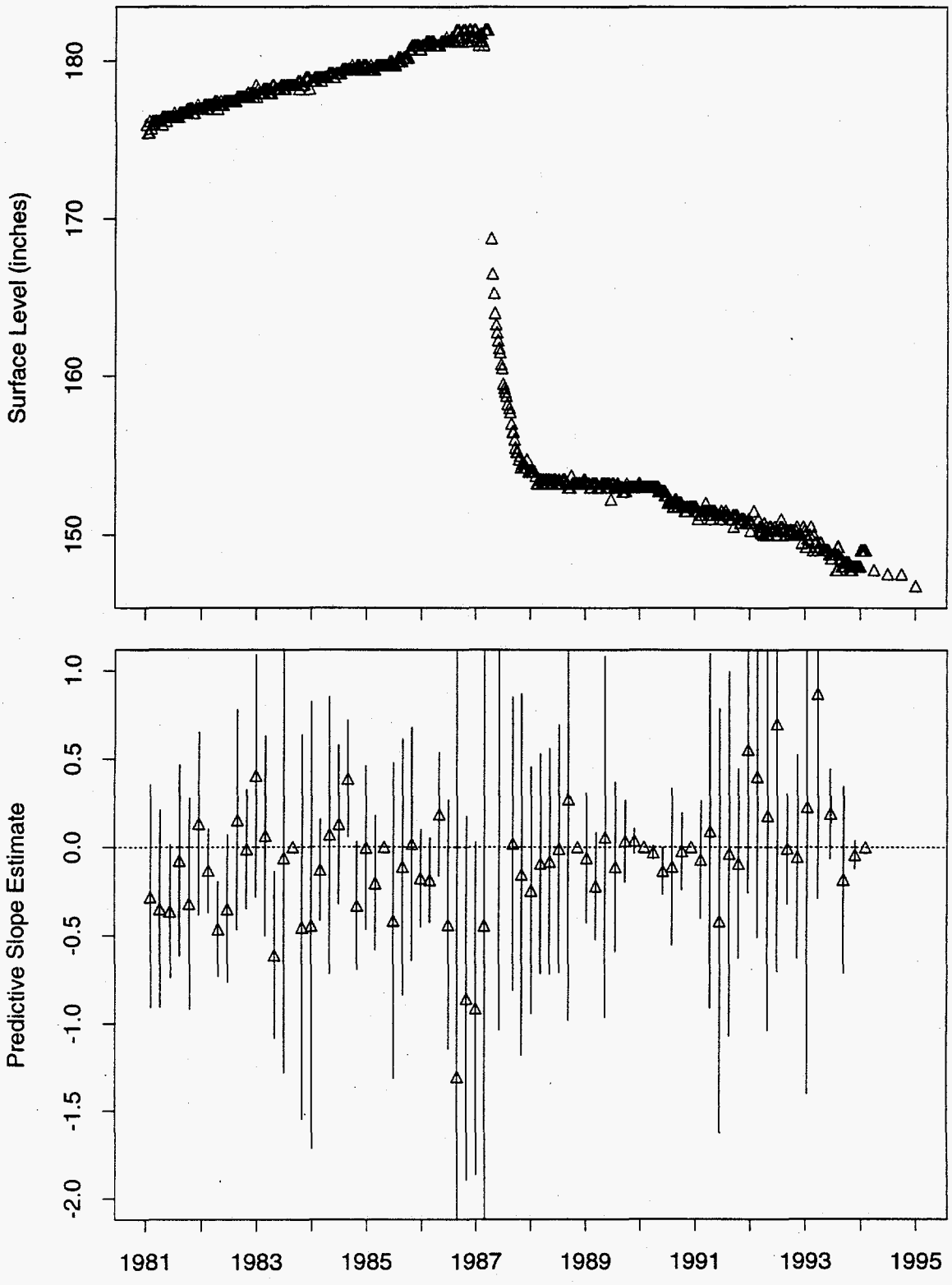

Figure 121: Tank BY–103 MT Data

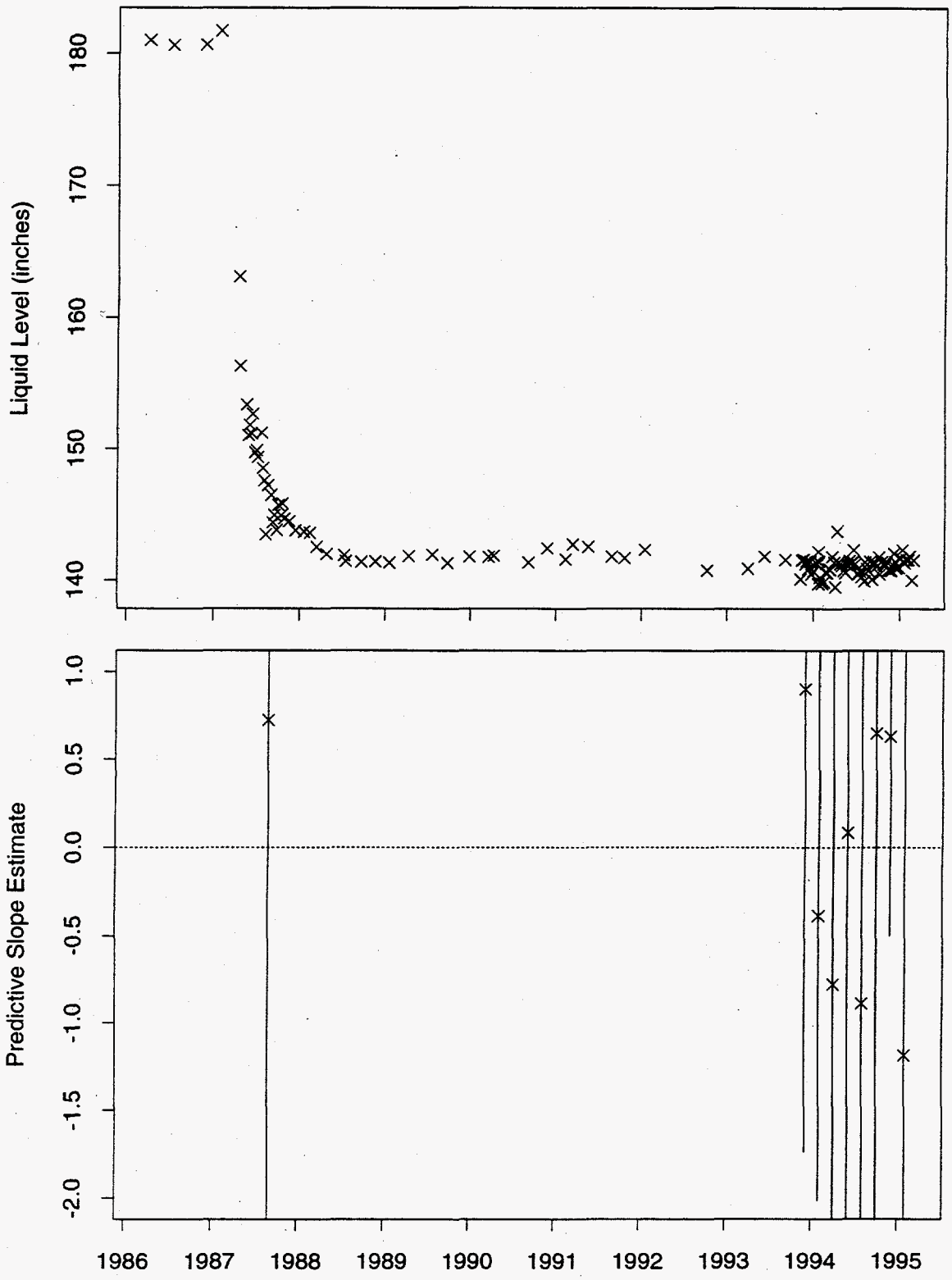

Figure 122: Tank BY-103 Neutron ILL Data

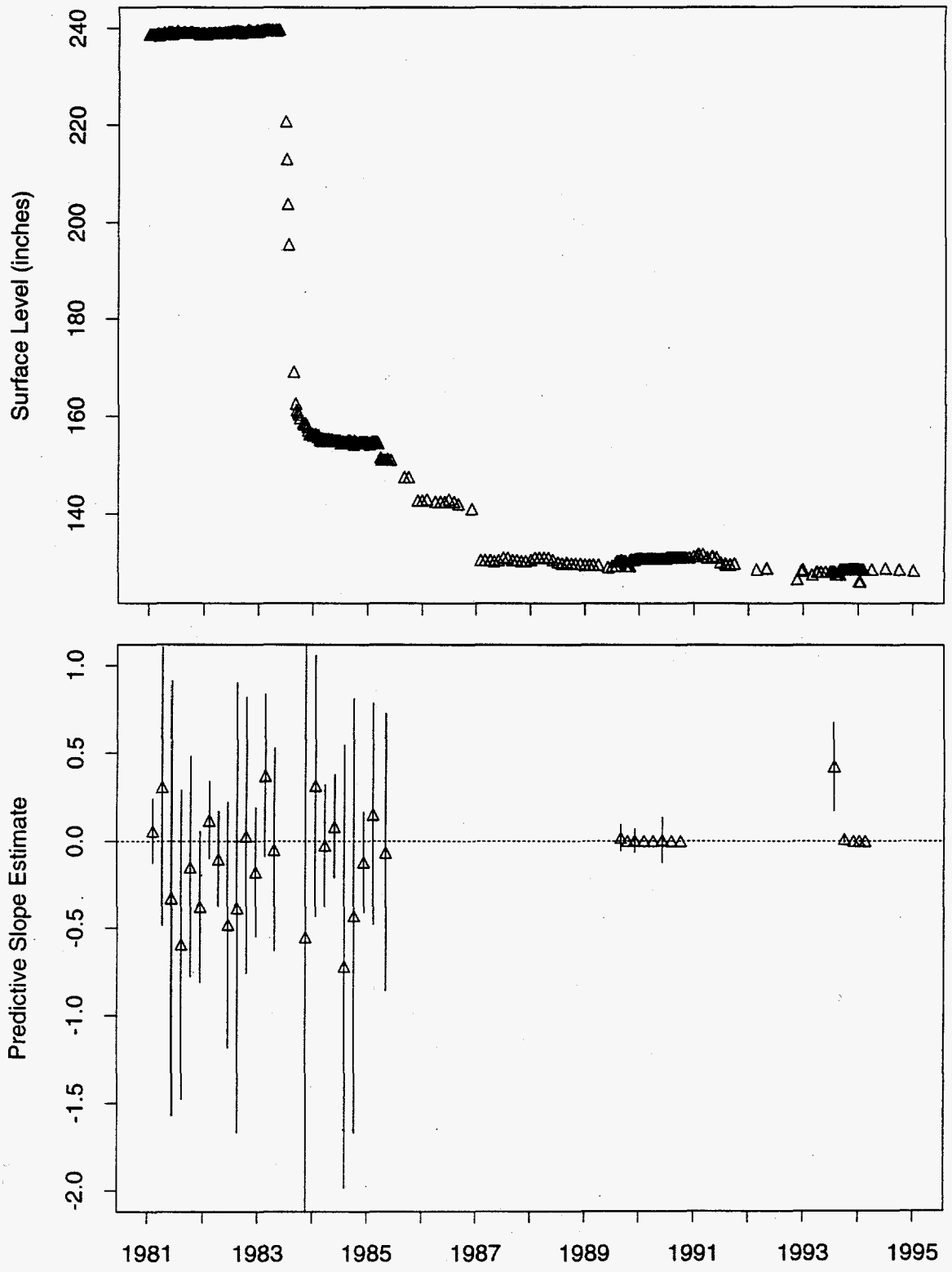

Figure 123: Tank BY–104 MT Data

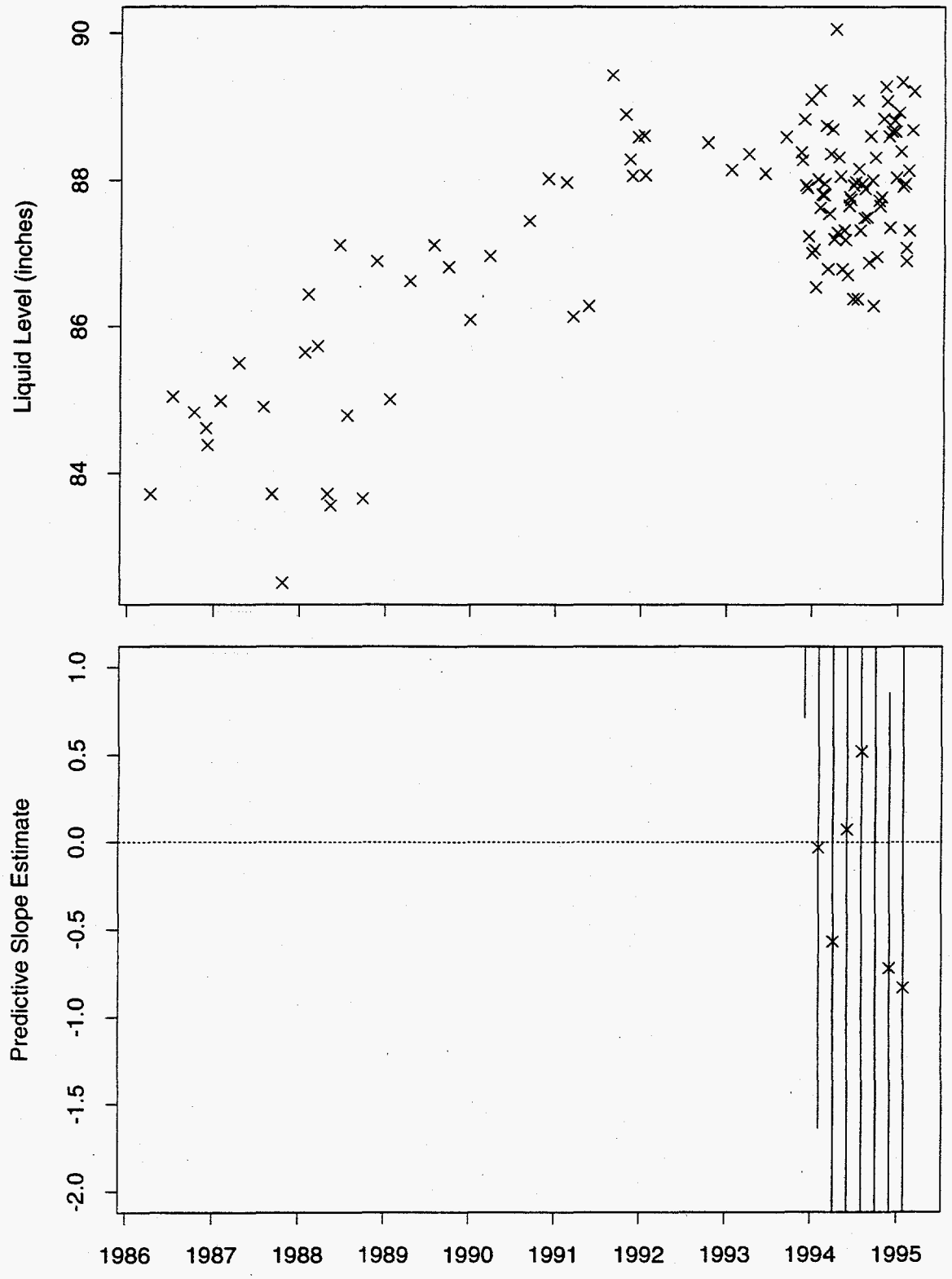

Figure 124: Tank BY–104 Neutron ILL Data

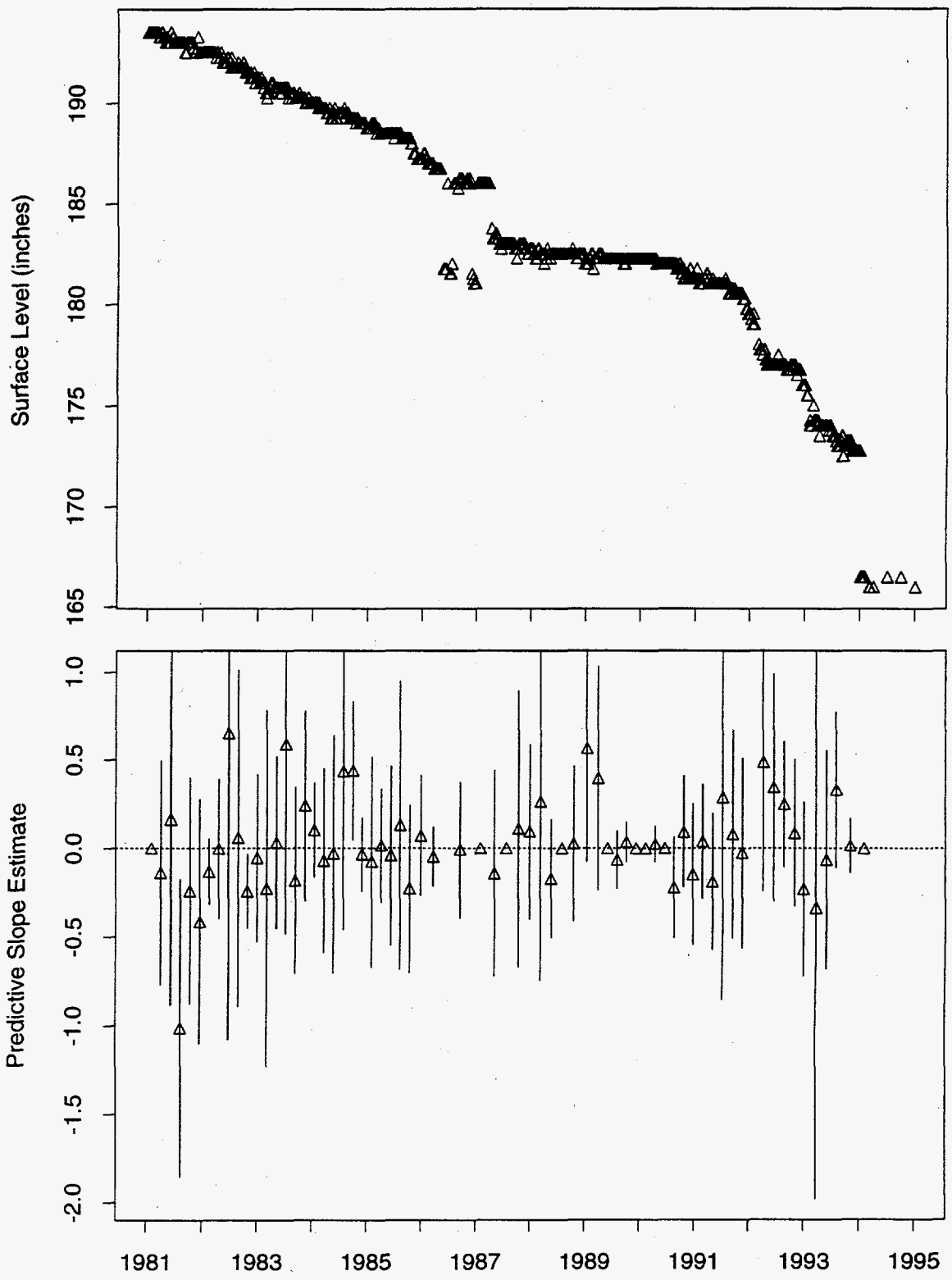

Figure 125: Tank BY–105 MT Data

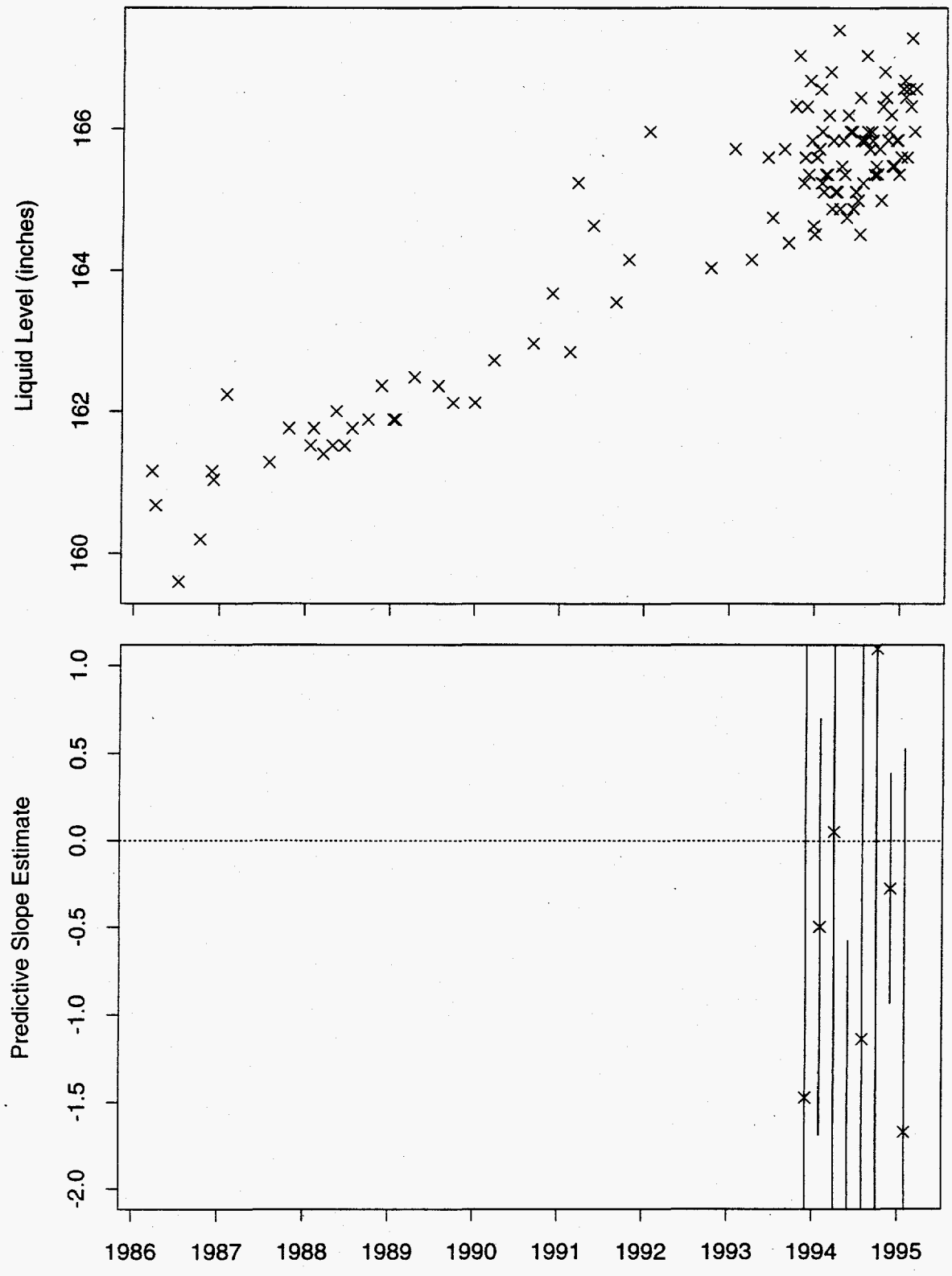

Figure 126: Tank BY–105 Neutron ILL Data

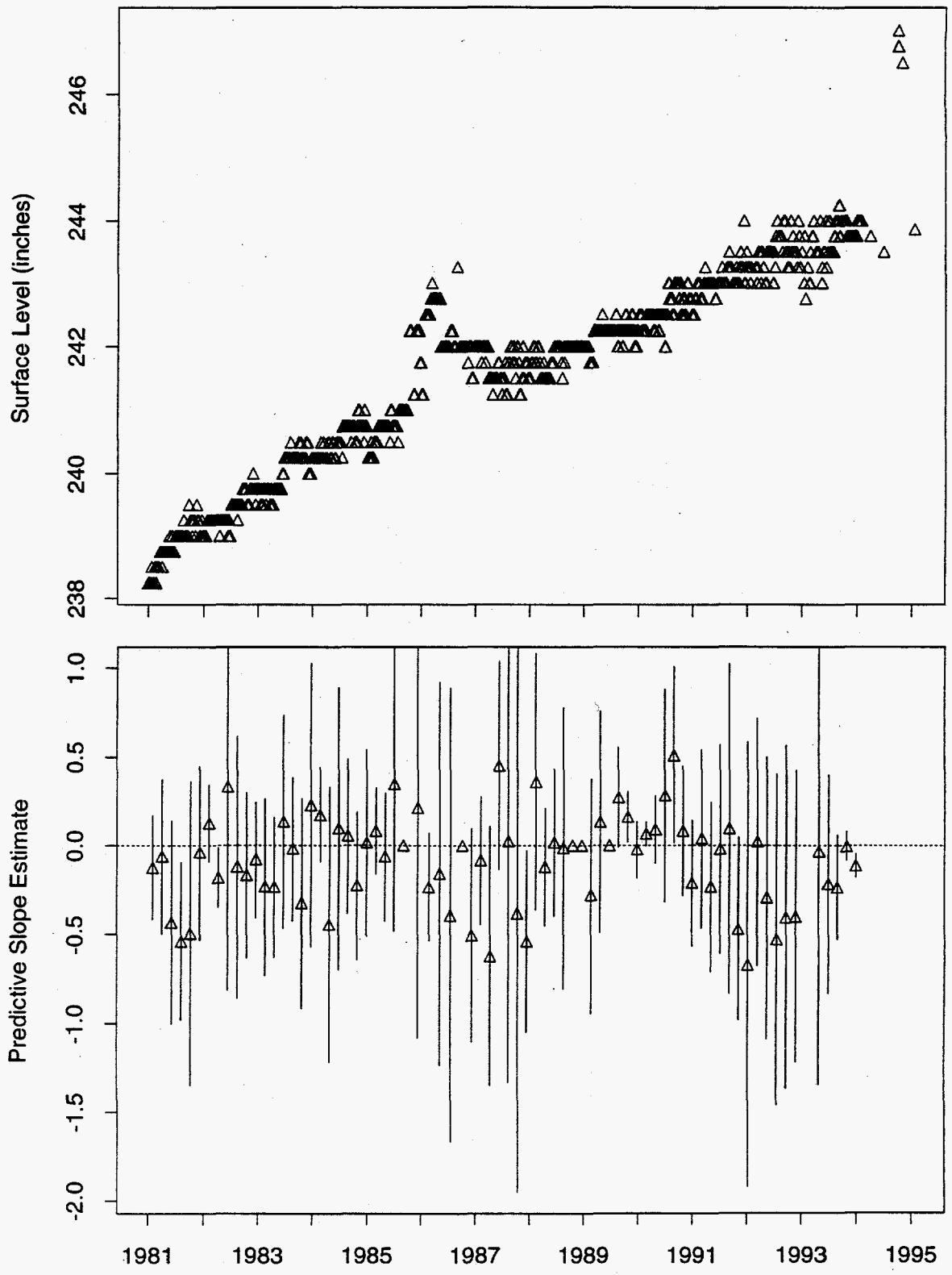

Figure 127: Tank BY–106 MT Data

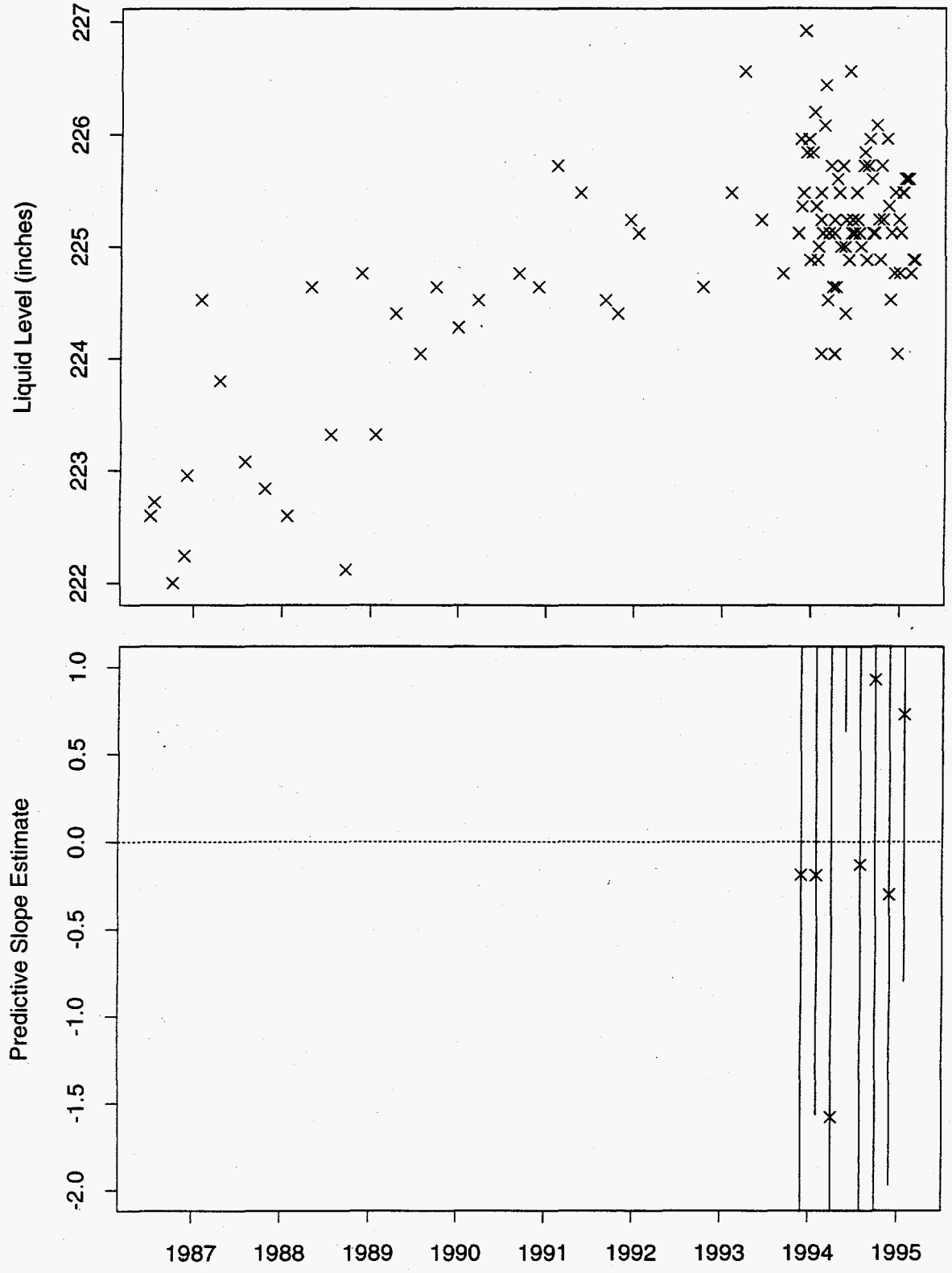

Figure 128: Tank BY–106 Neutron ILL Data

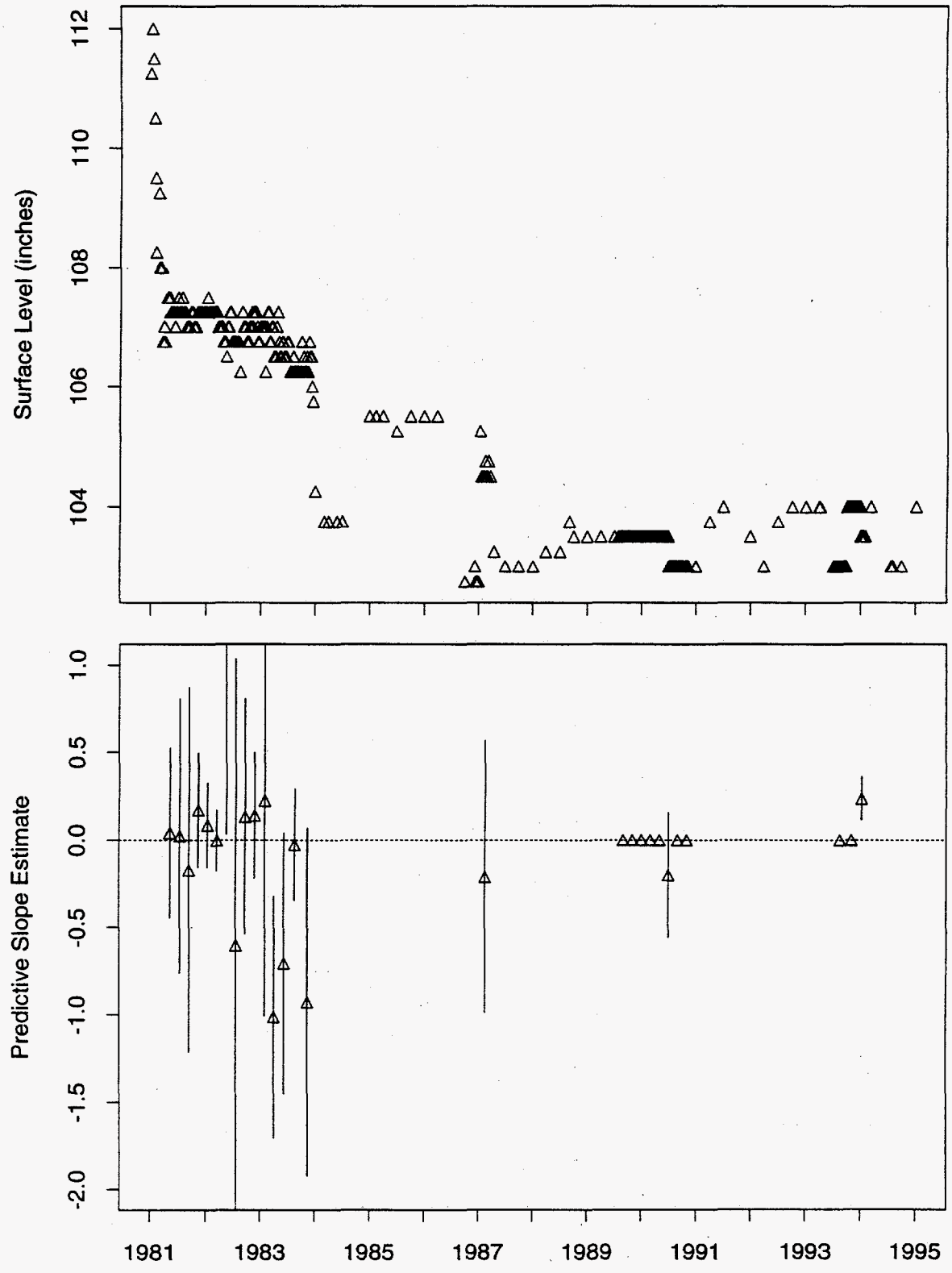

Figure 129: Tank BY–107 MT Data

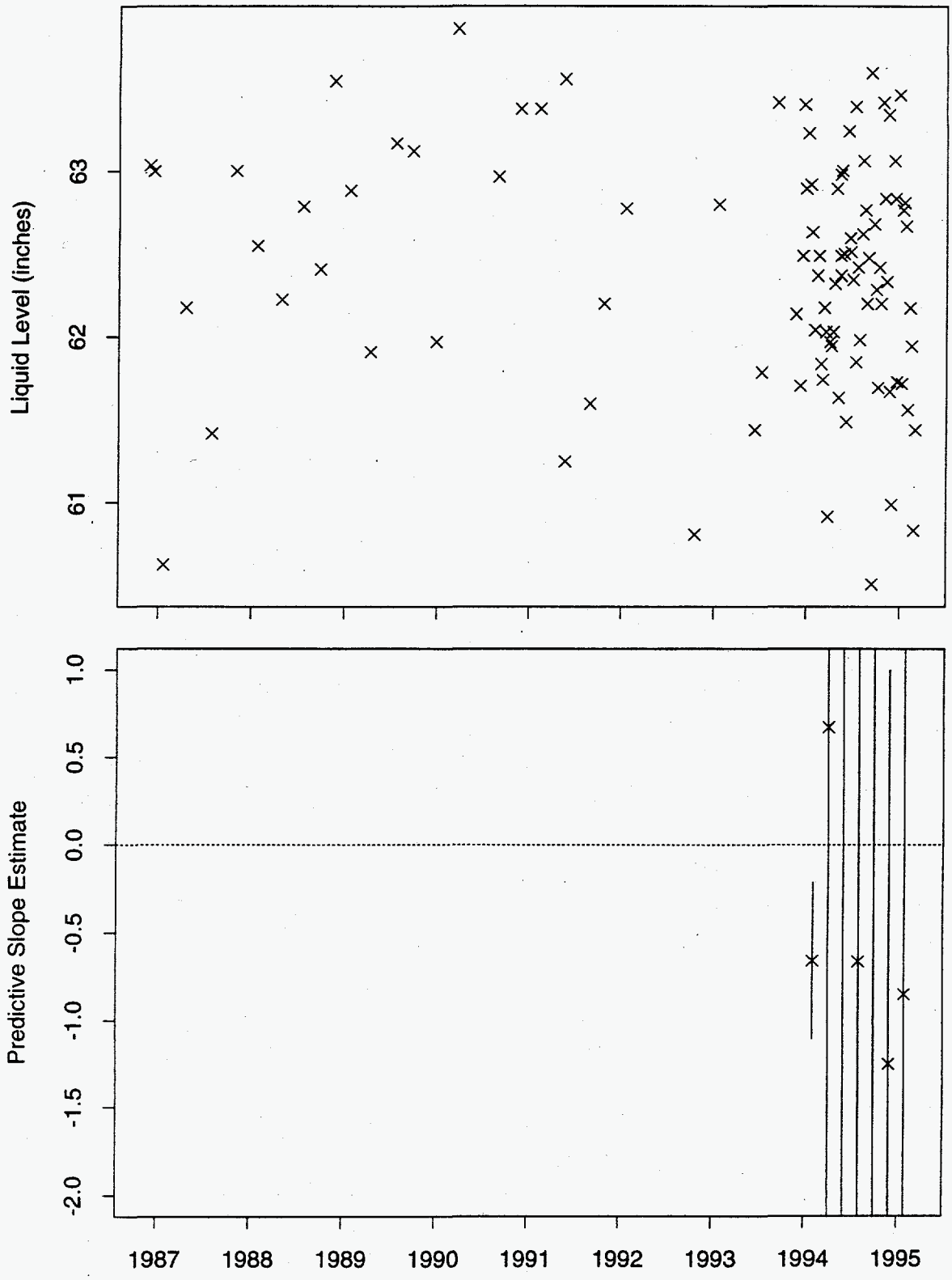

Figure 130: Tank BY–107 Neutron ILL Data

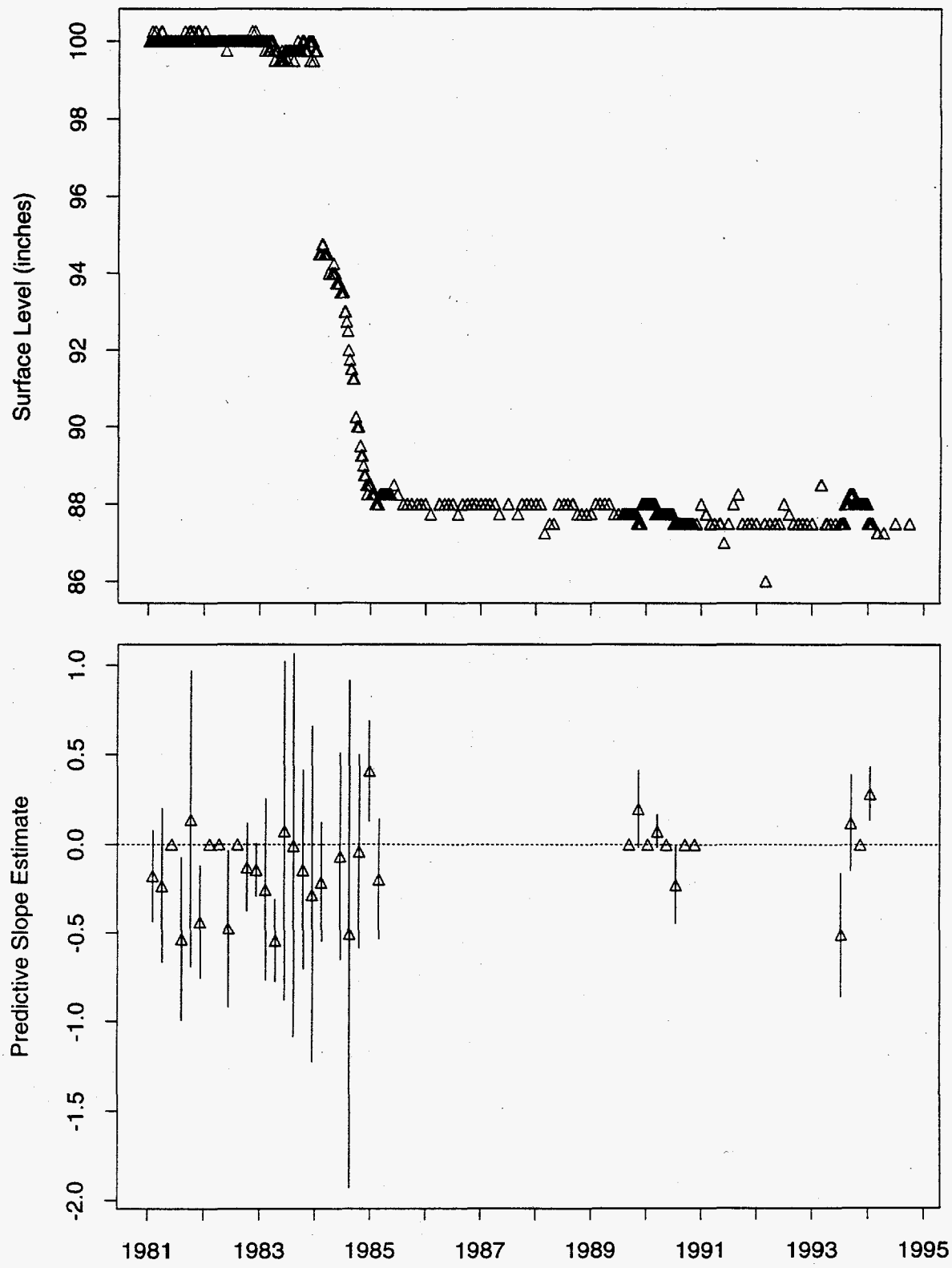

Figure 131: Tank BY-108 MT Data

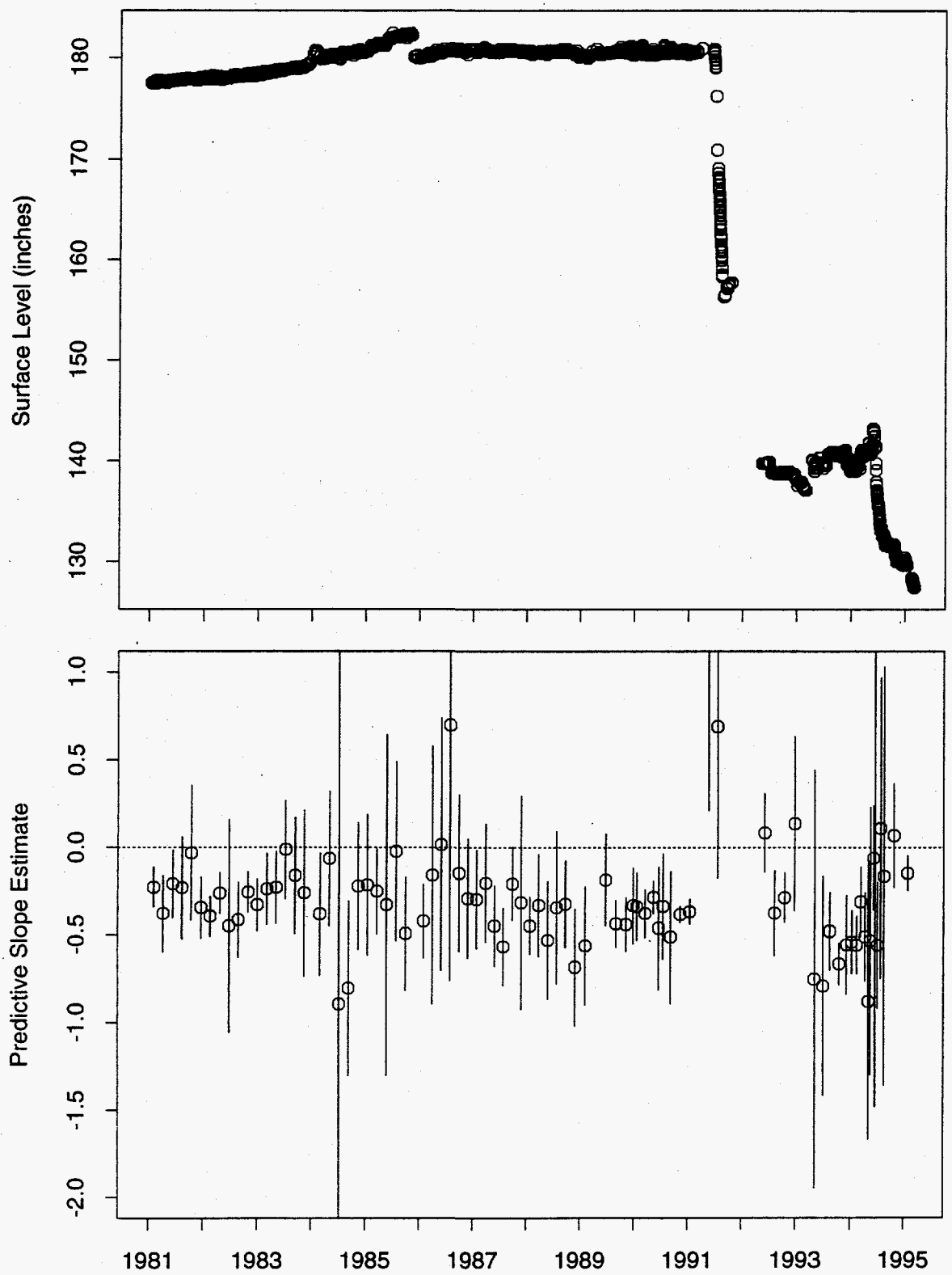

Figure 132: Tank BY–109 FIC Data

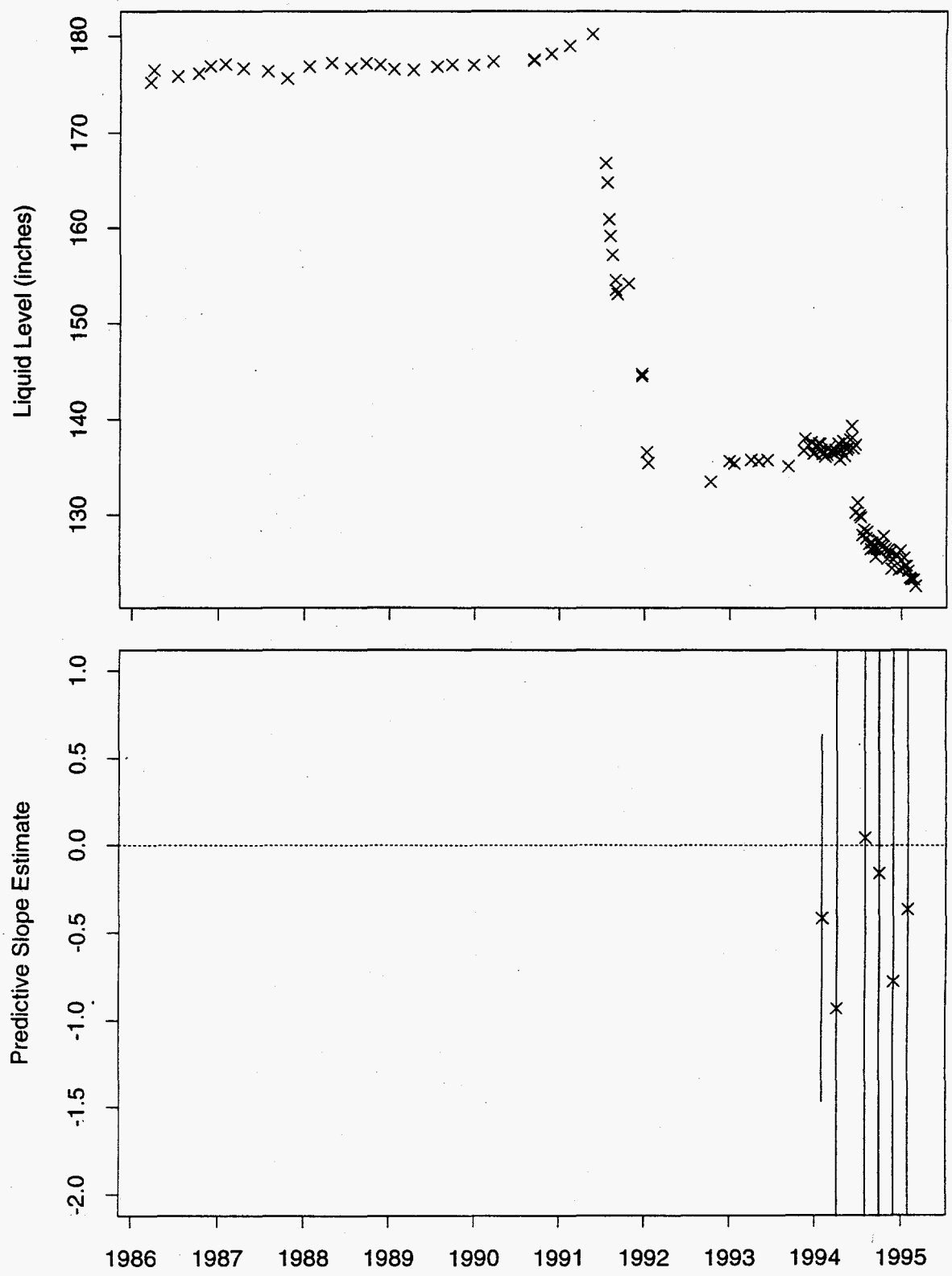

Figure 133: Tank BY–109 Neutron ILL Data

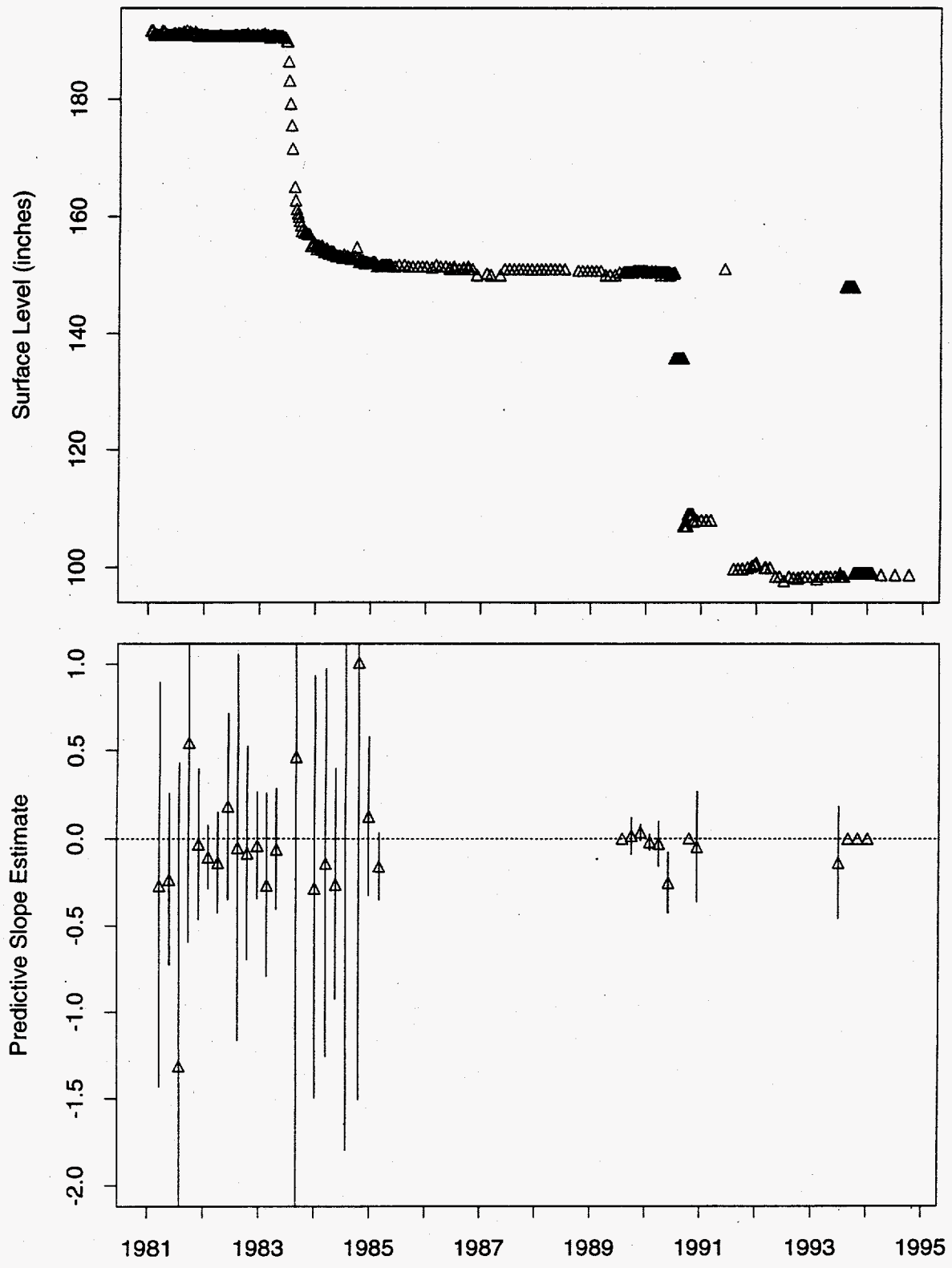

Figure 134: Tank BY–110 MT Data

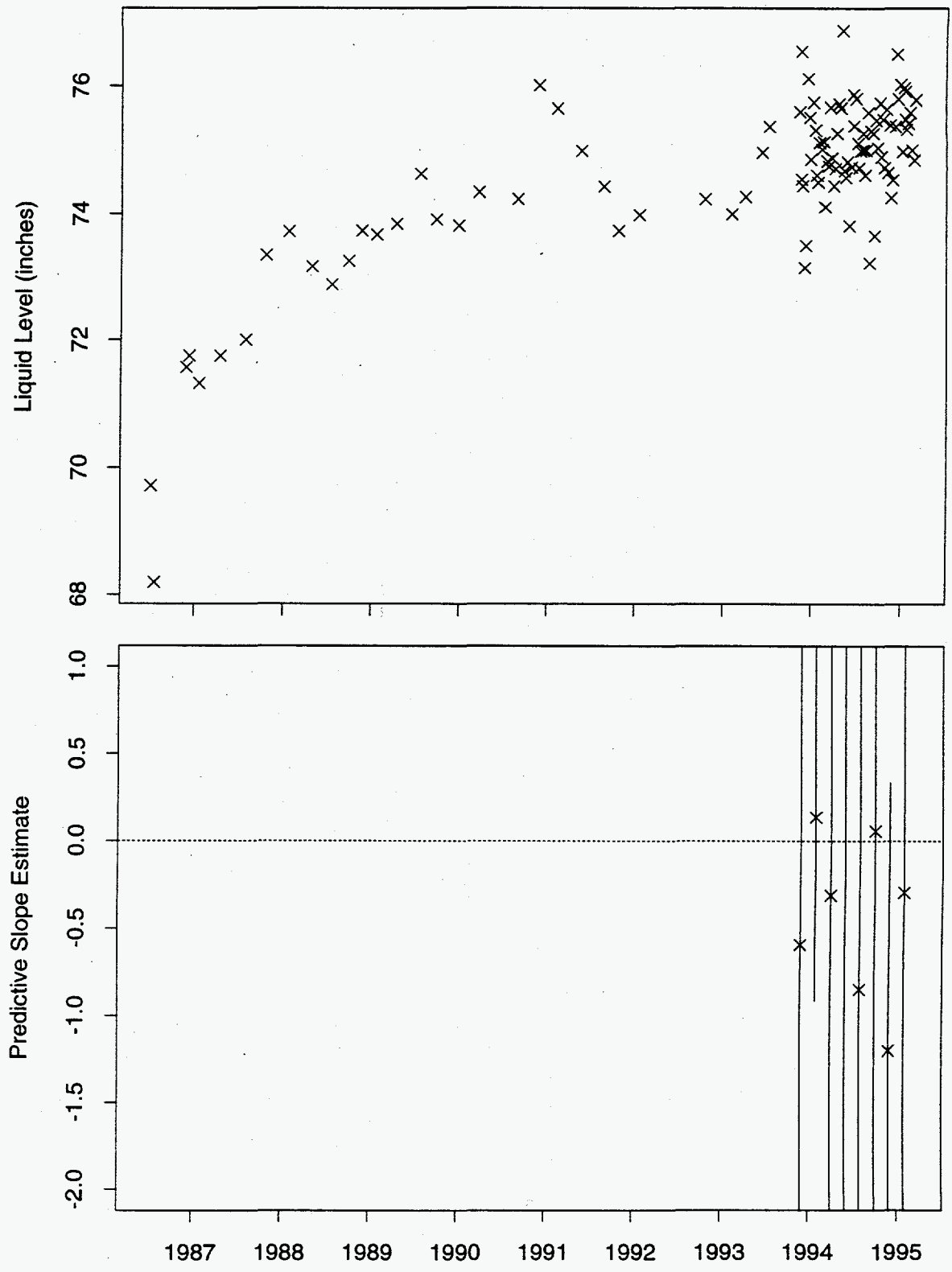

Figure 135: Tank BY–110 Neutron ILL Data

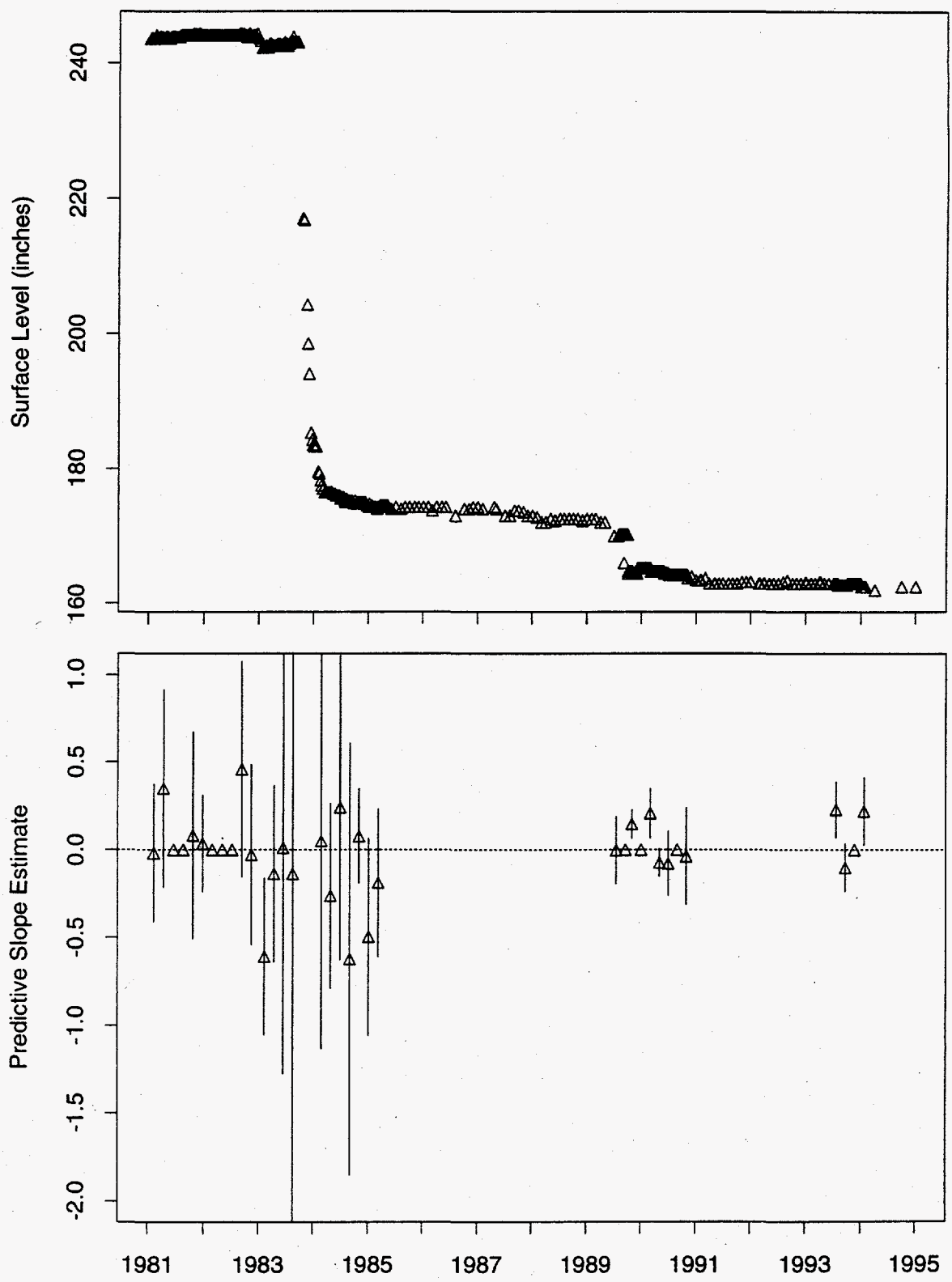

Figure 136: Tank BY–111 MT Data

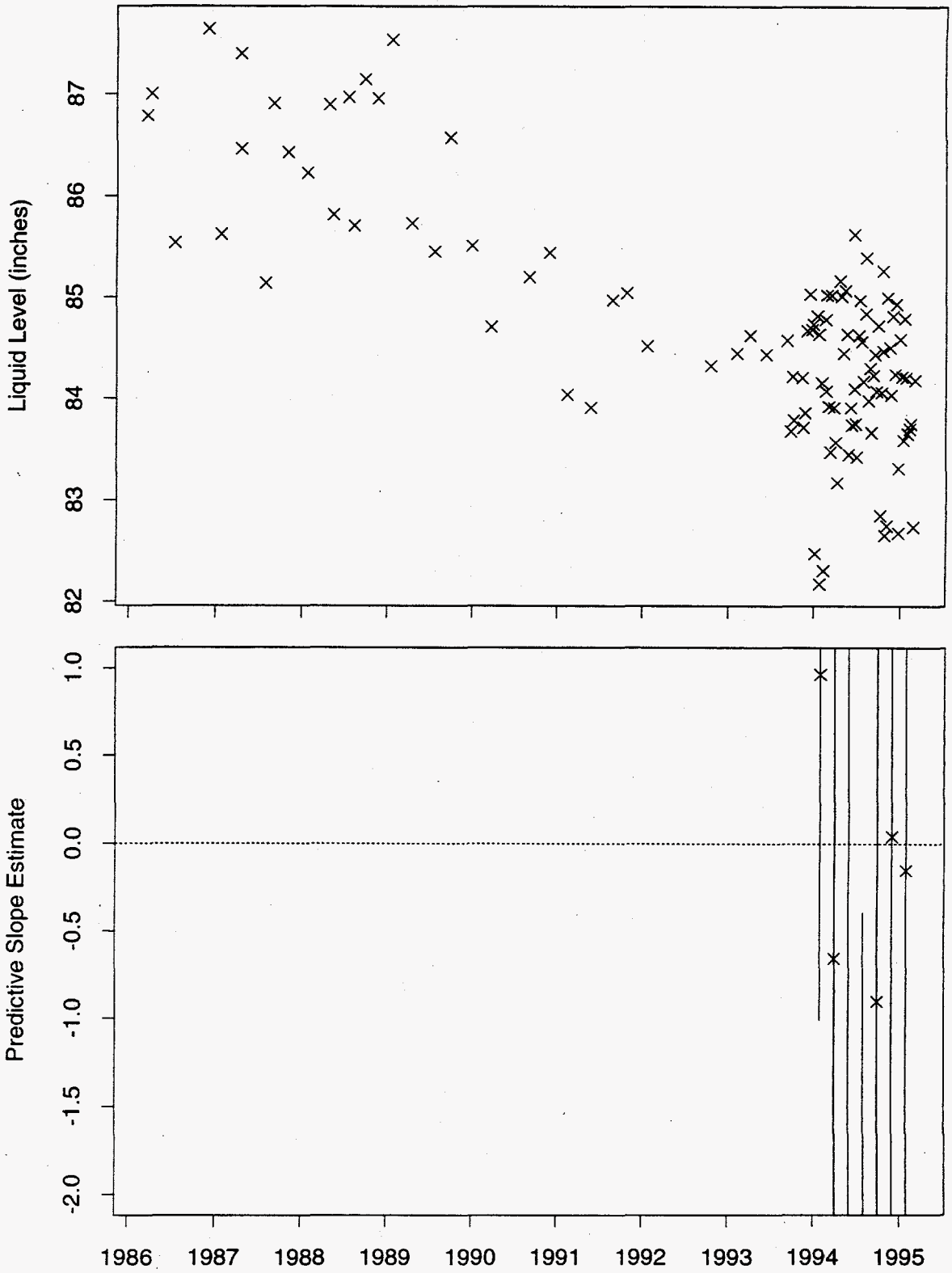

Figure 137: Tank BY-111 Neutron ILL Data

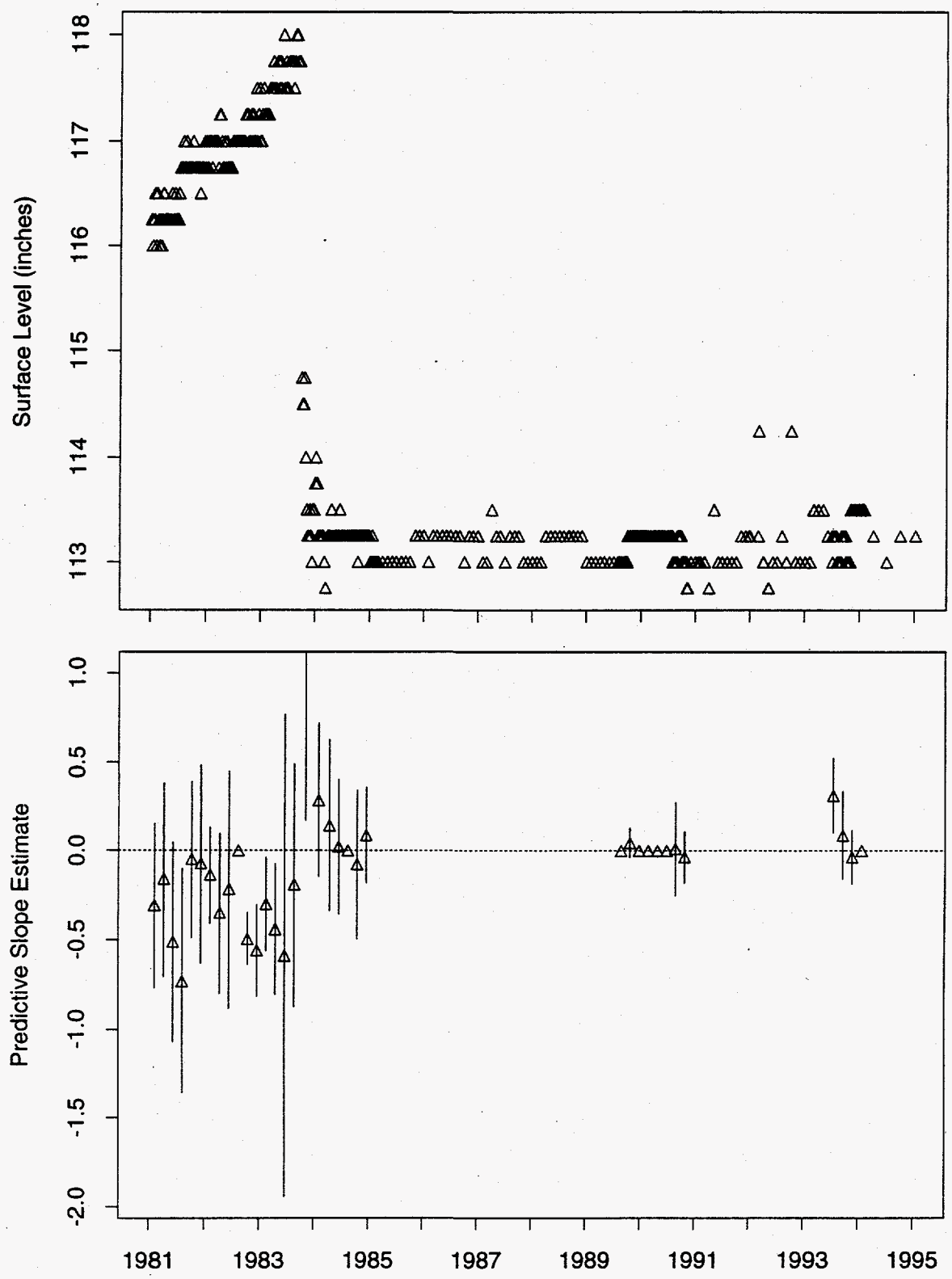

Figure 138: Tank BY–112 MT Data

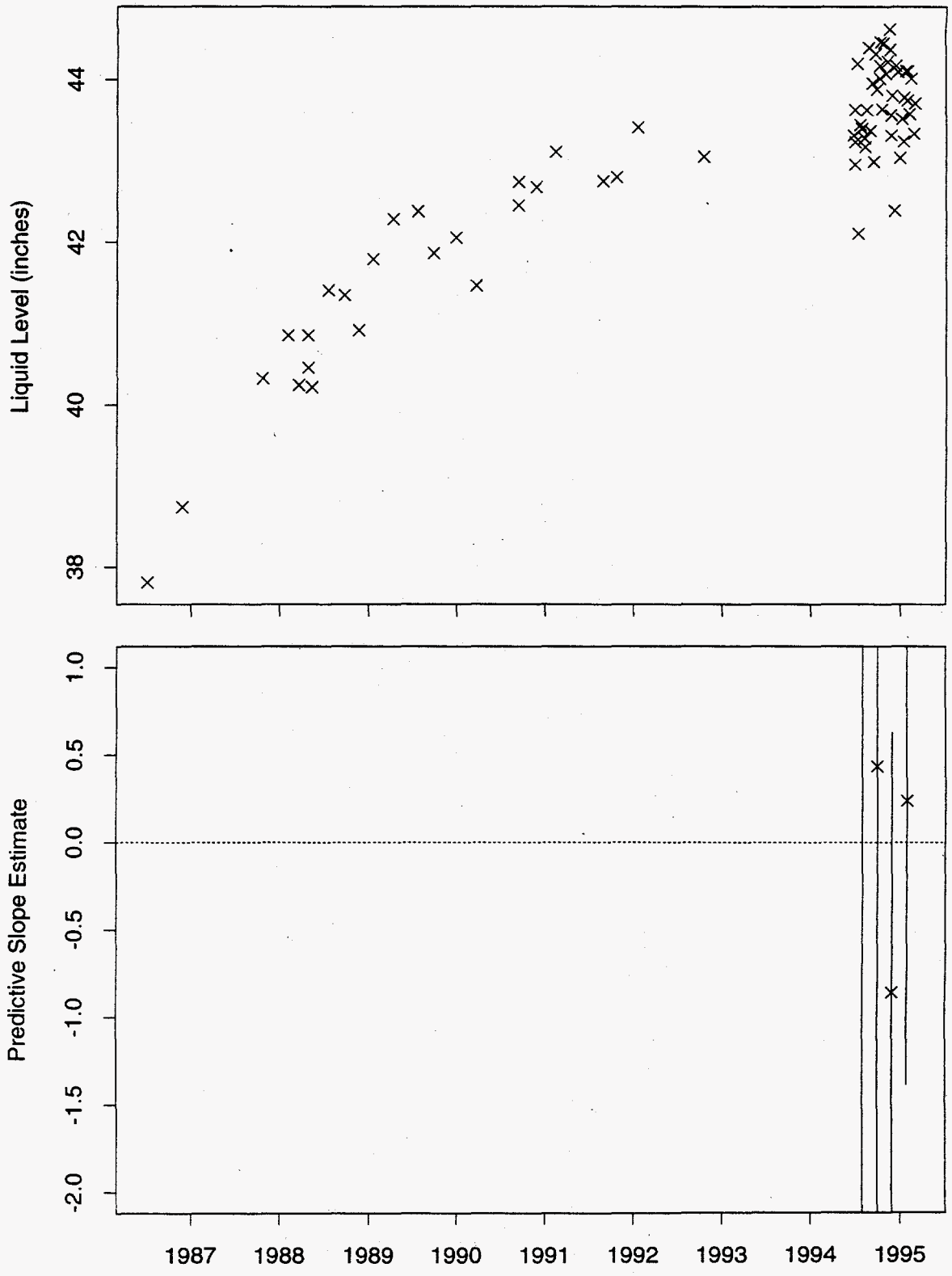

Figure 139: Tank BY–112 Neutron ILL Data

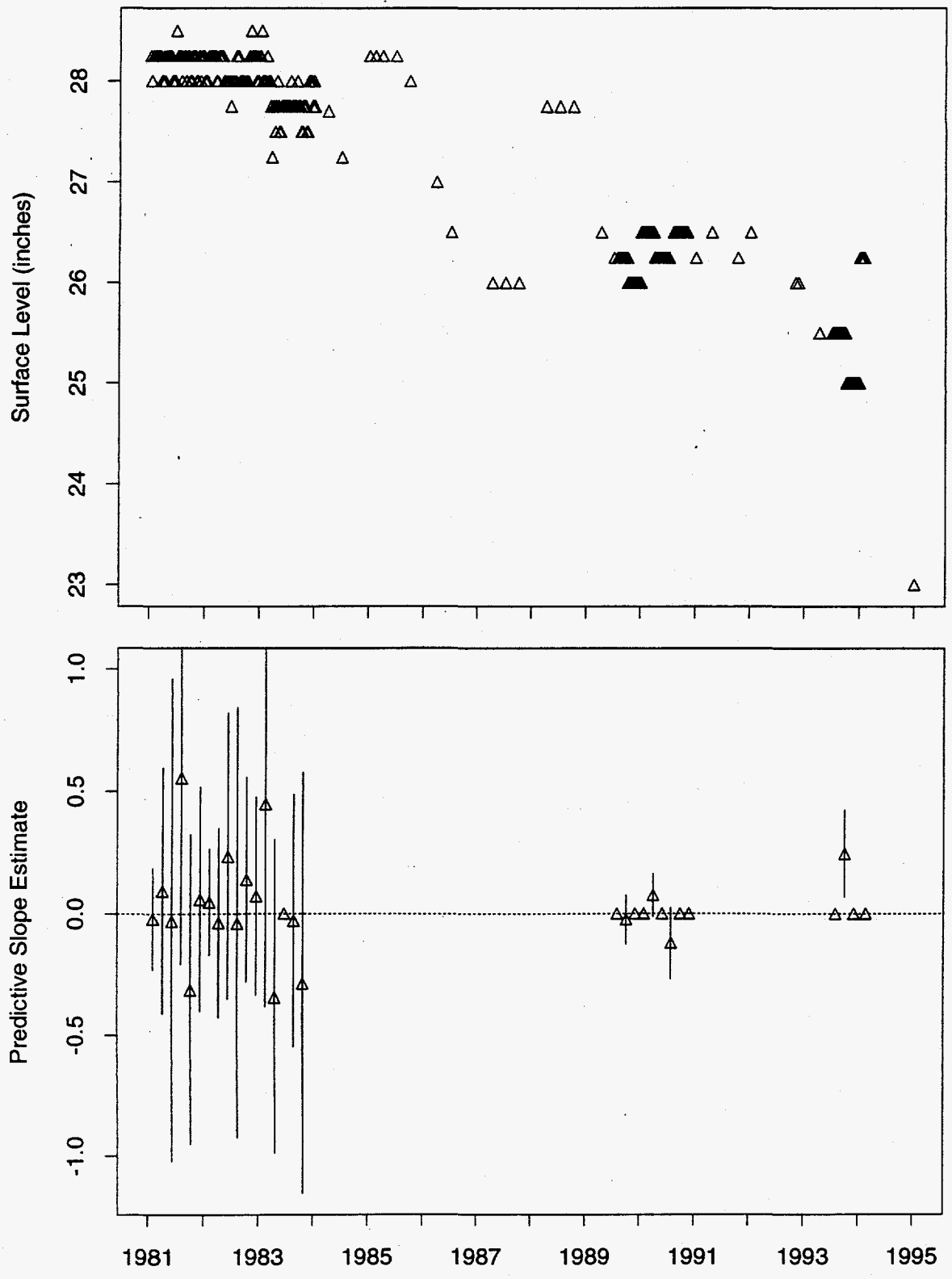

Figure 140: Tank C–101 MT Data

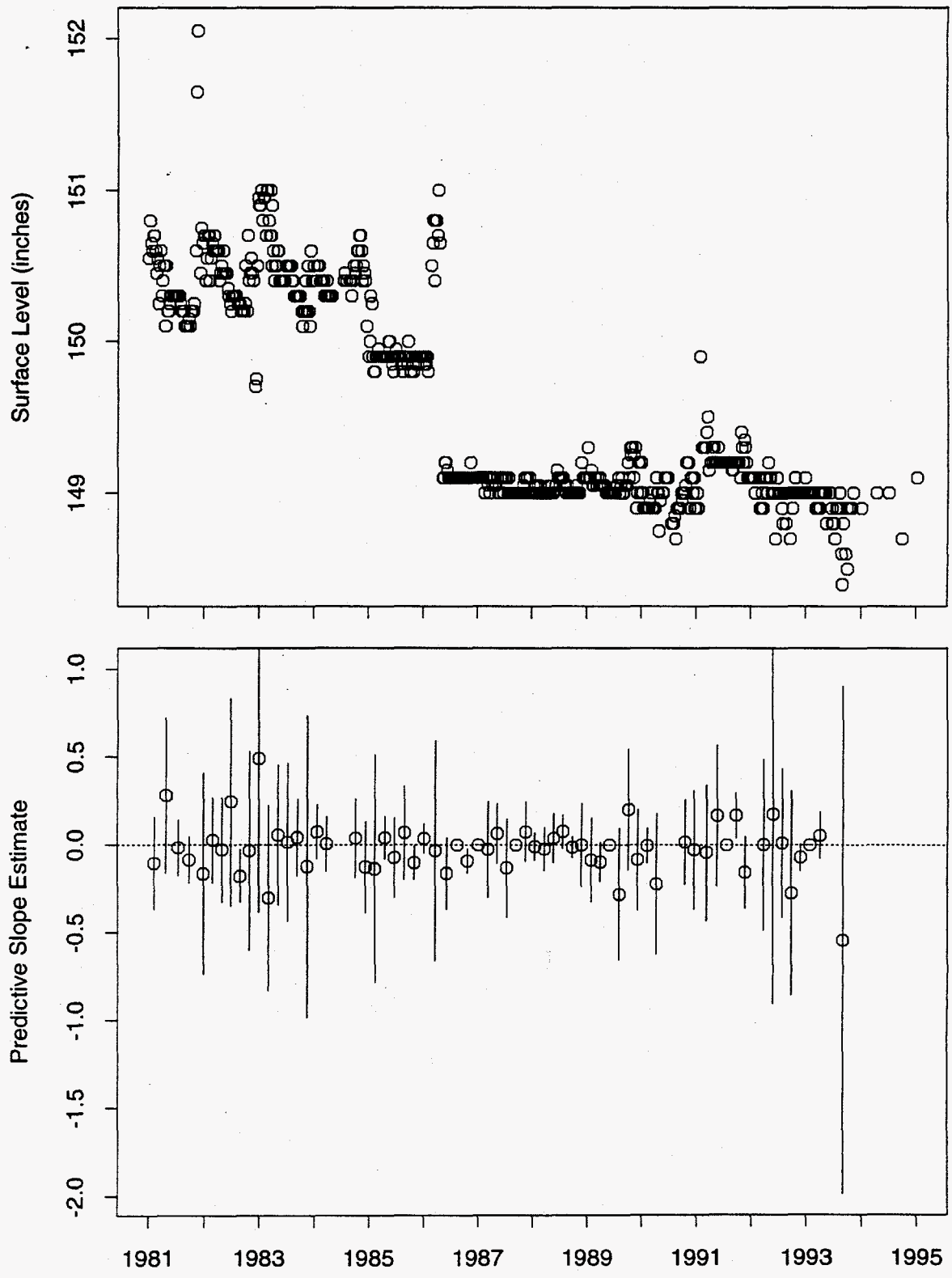

Figure 141: Tank C-102 FIC Data

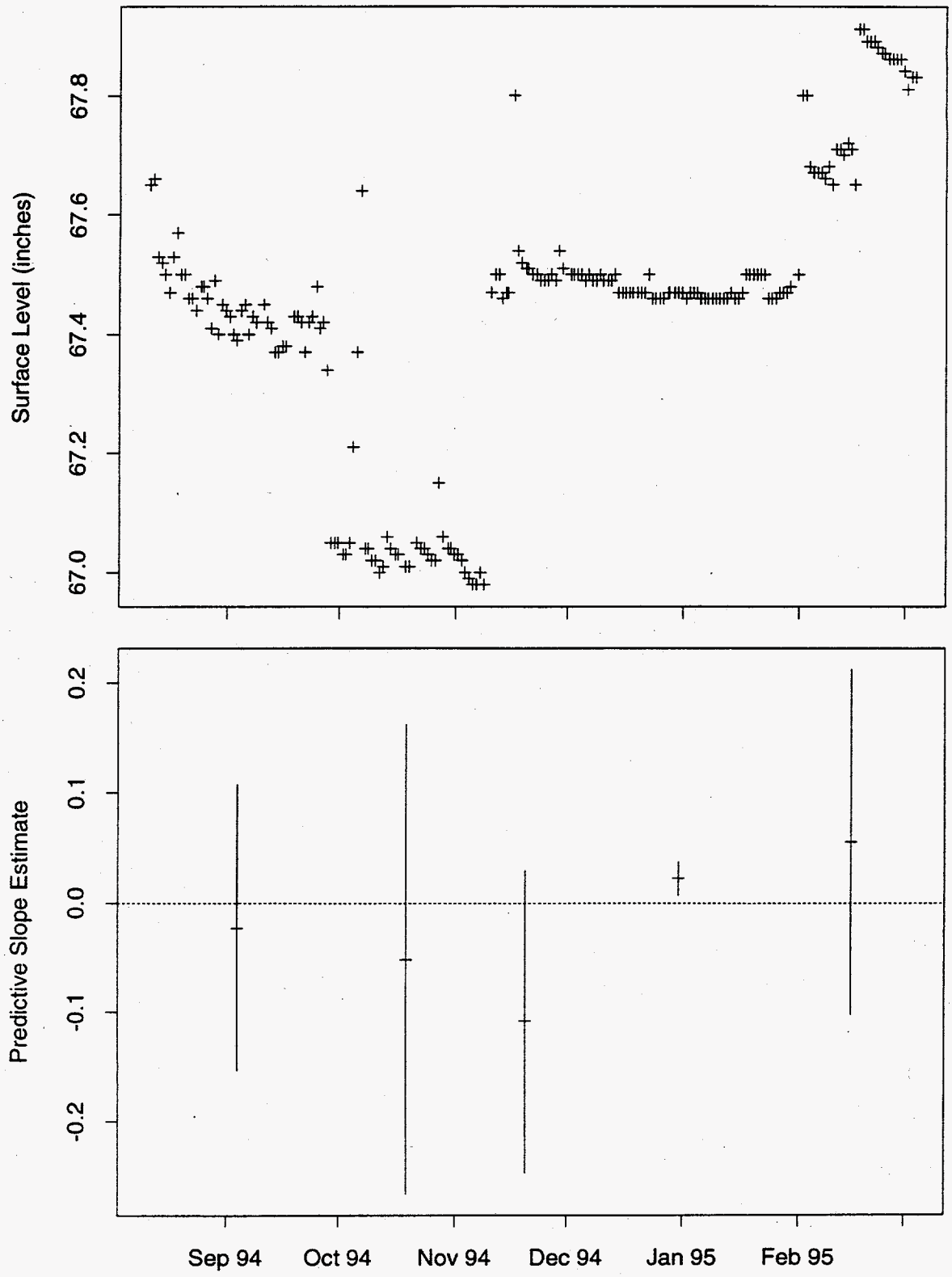

Figure 142: Tank C-103 ENRAF Data

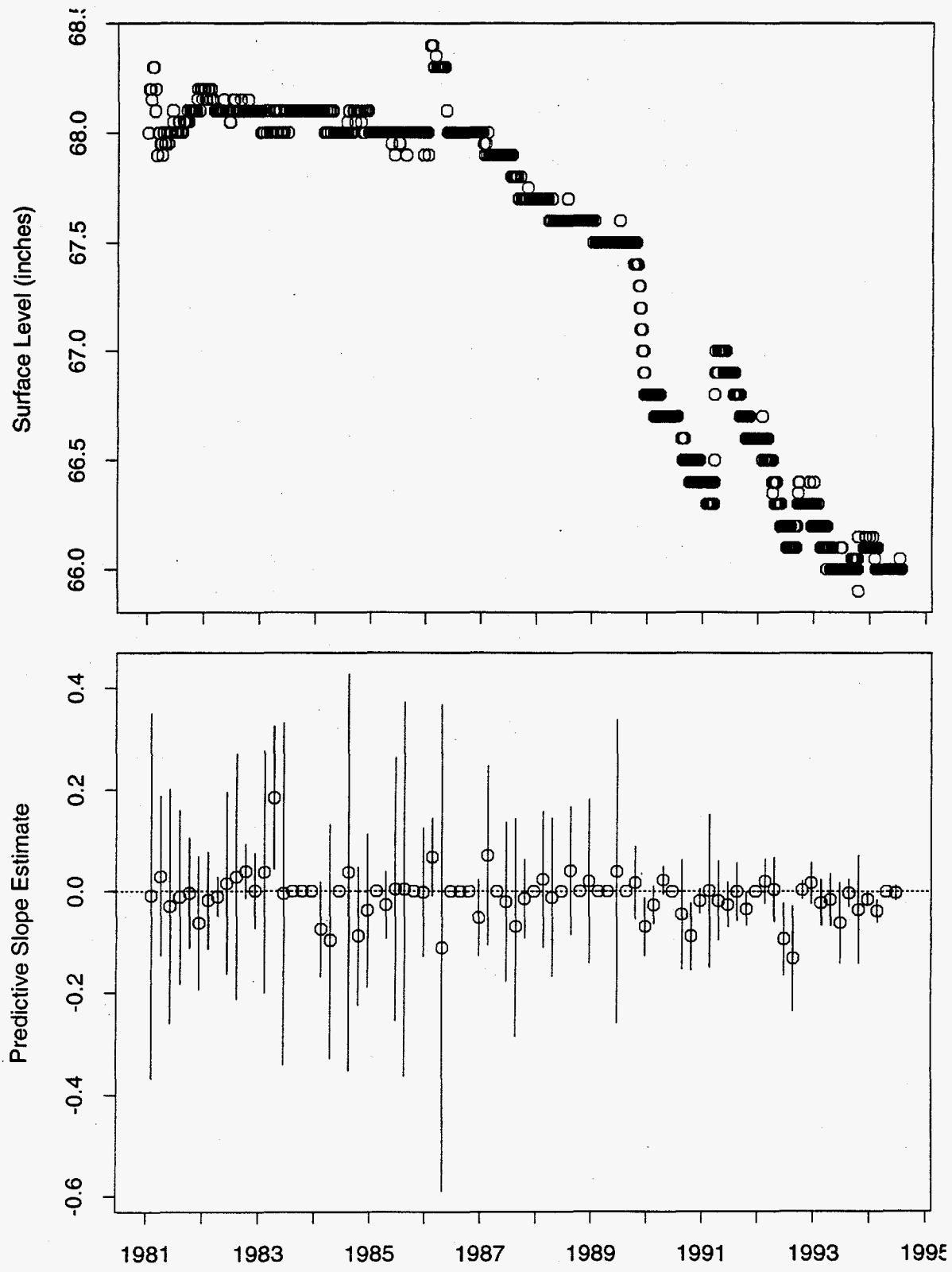

Figure 143: Tank C–103 FIC Data

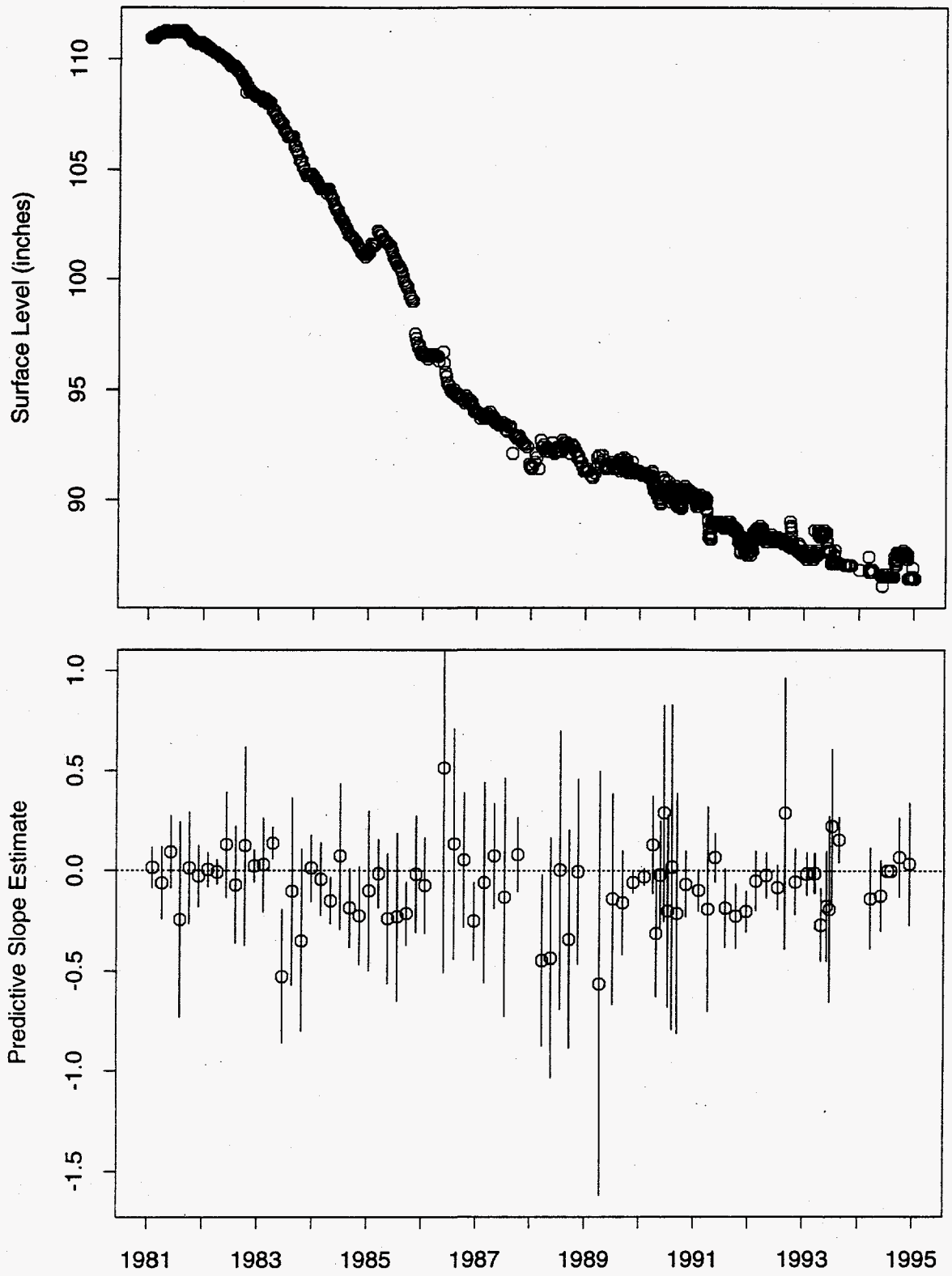

Figure 144: Tank C–104 FIC Data

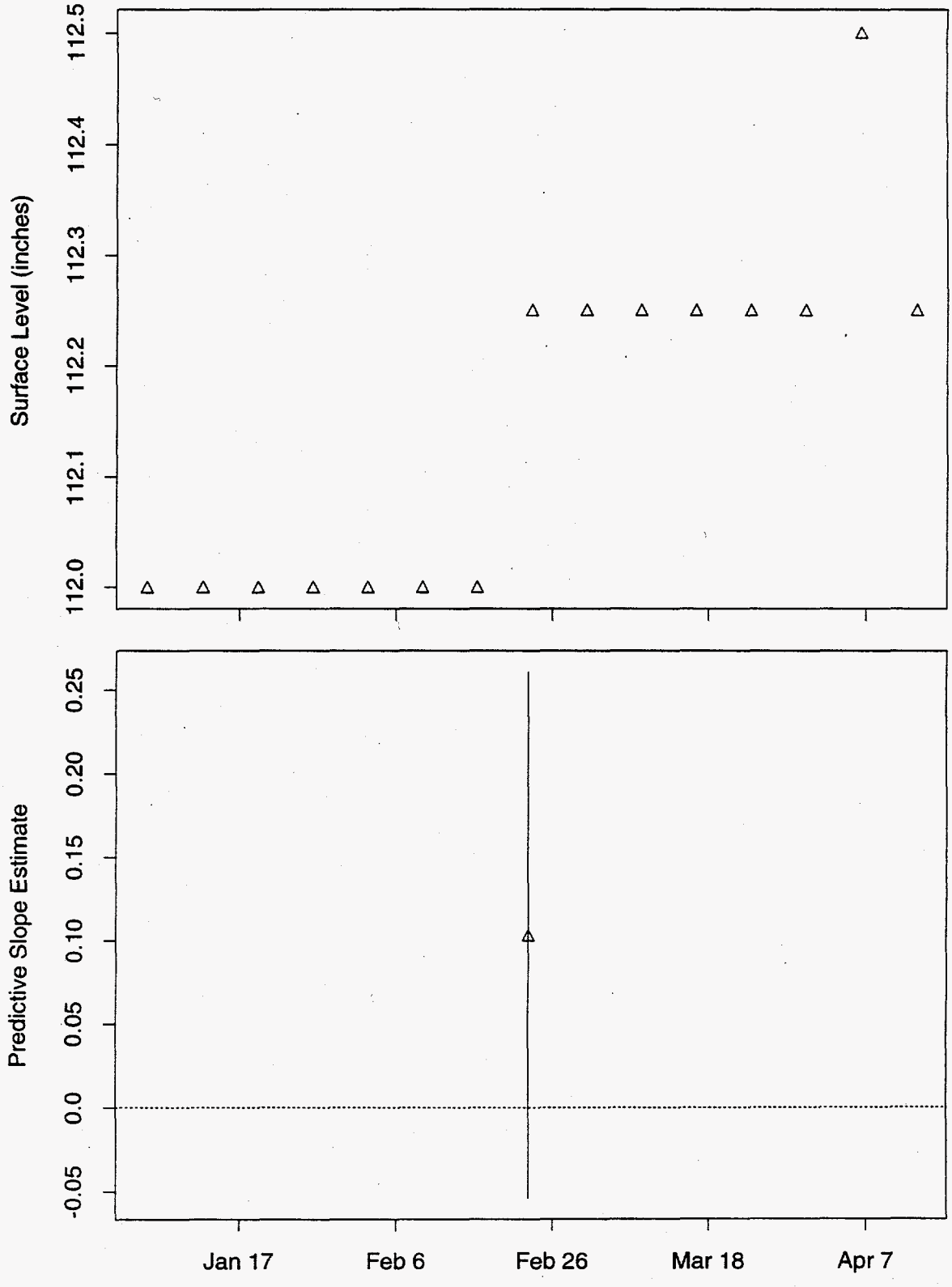

Figure 145: Tank C–104 MT Data

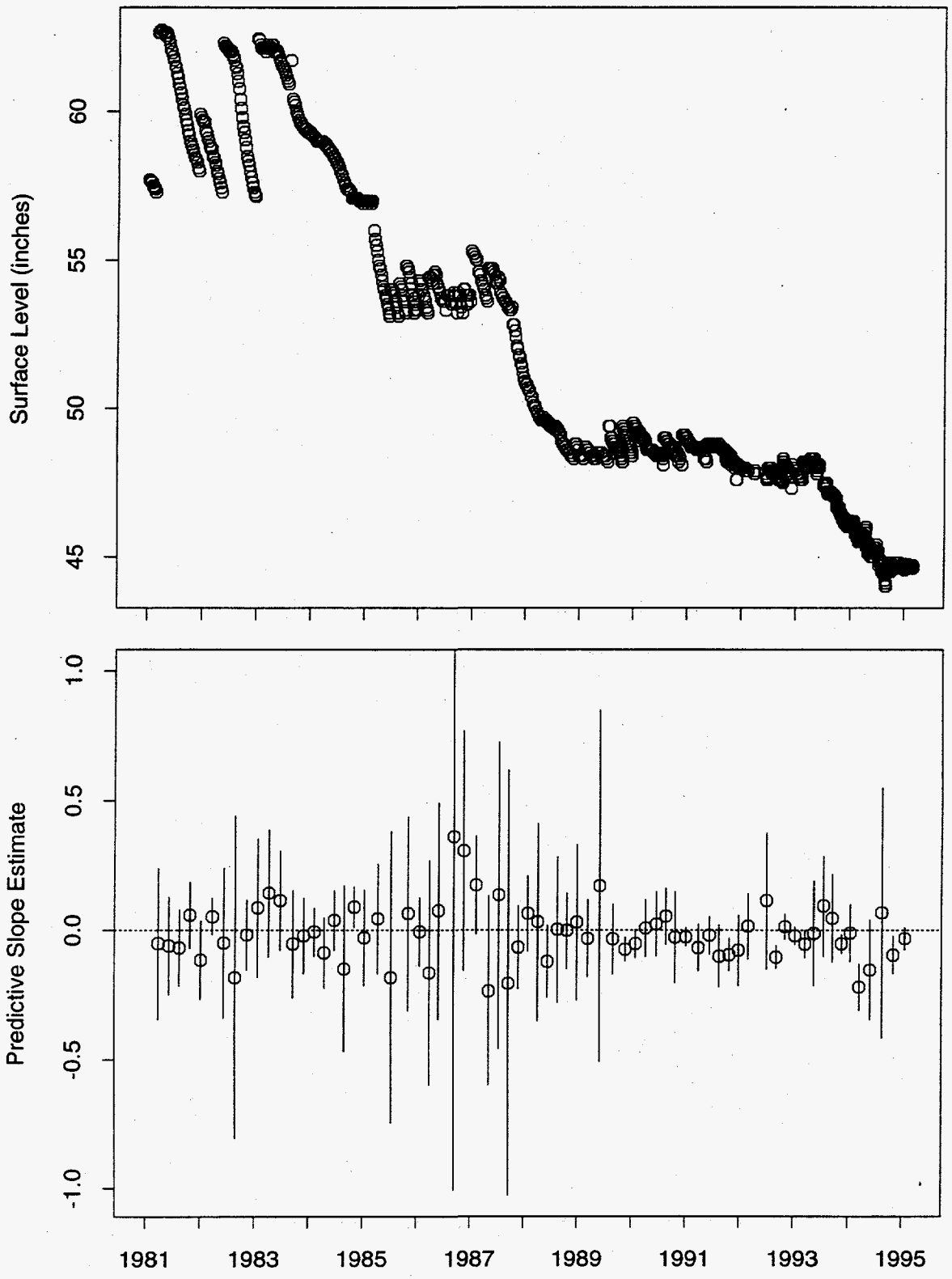

Figure 146: Tank C–105 FIC Data

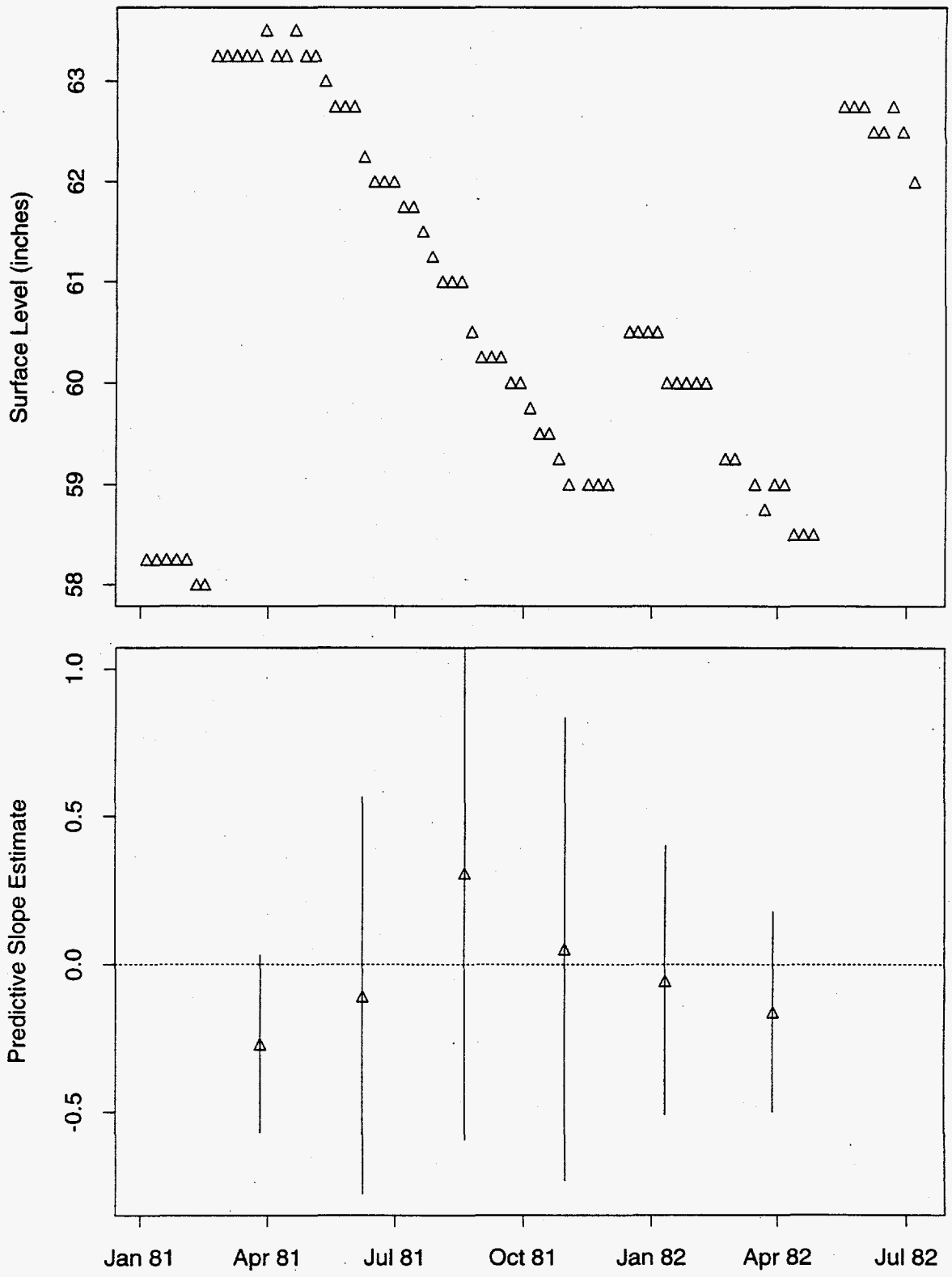

Figure 147: Tank C–105 MT Data

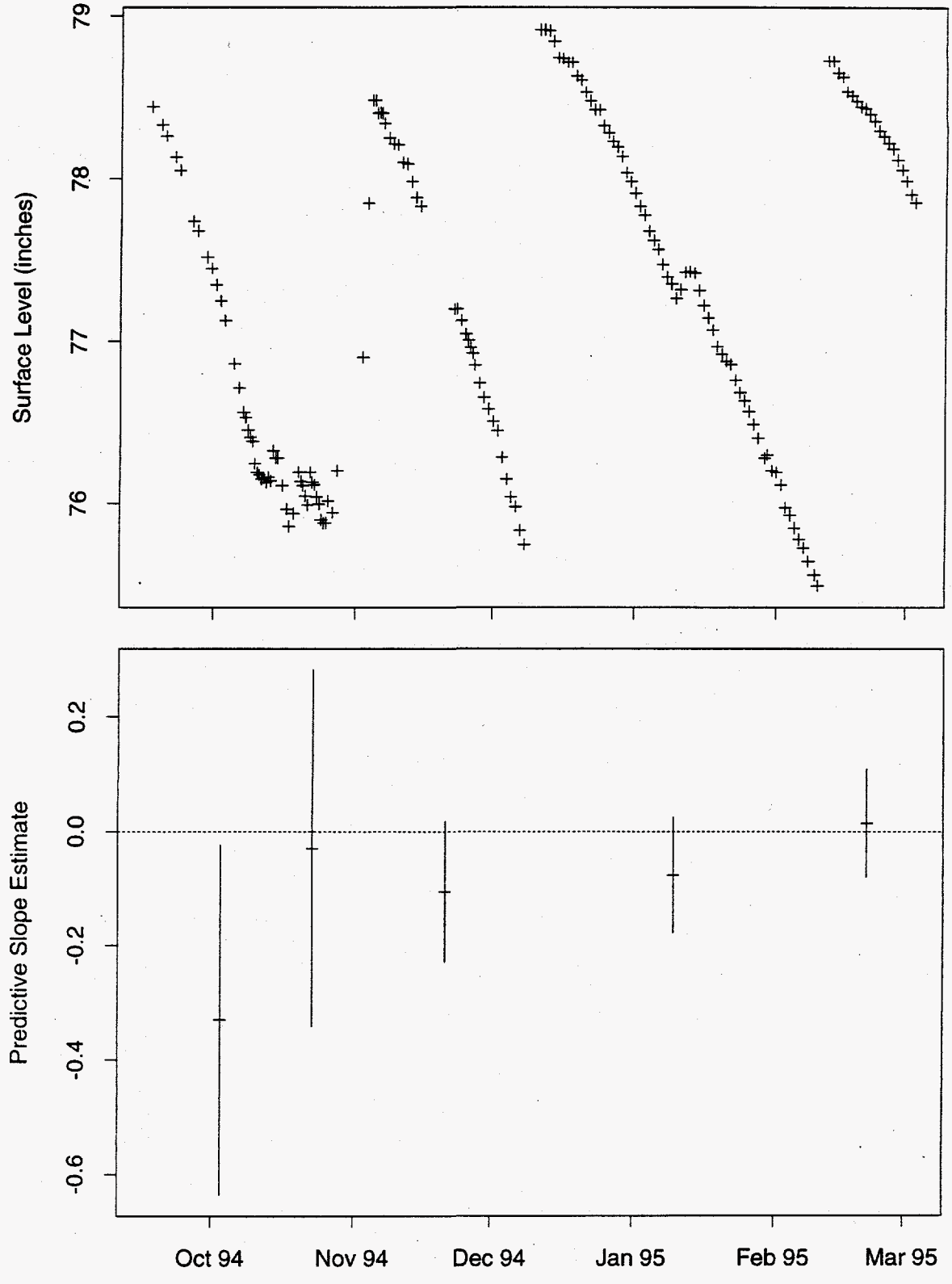

Figure 148: Tank C–106 ENRAF Data

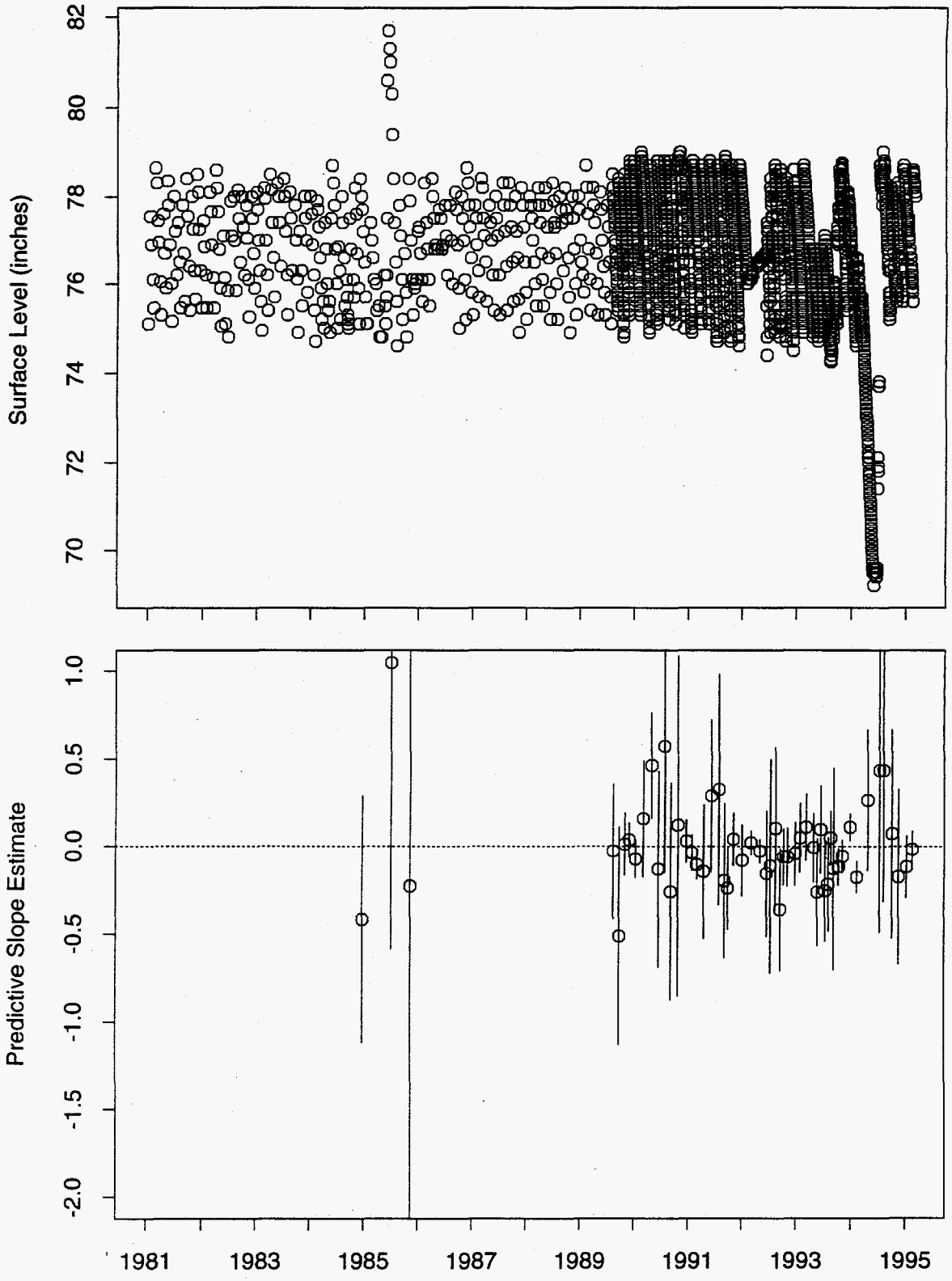

Figure 149: Tank C–106 FIC Data

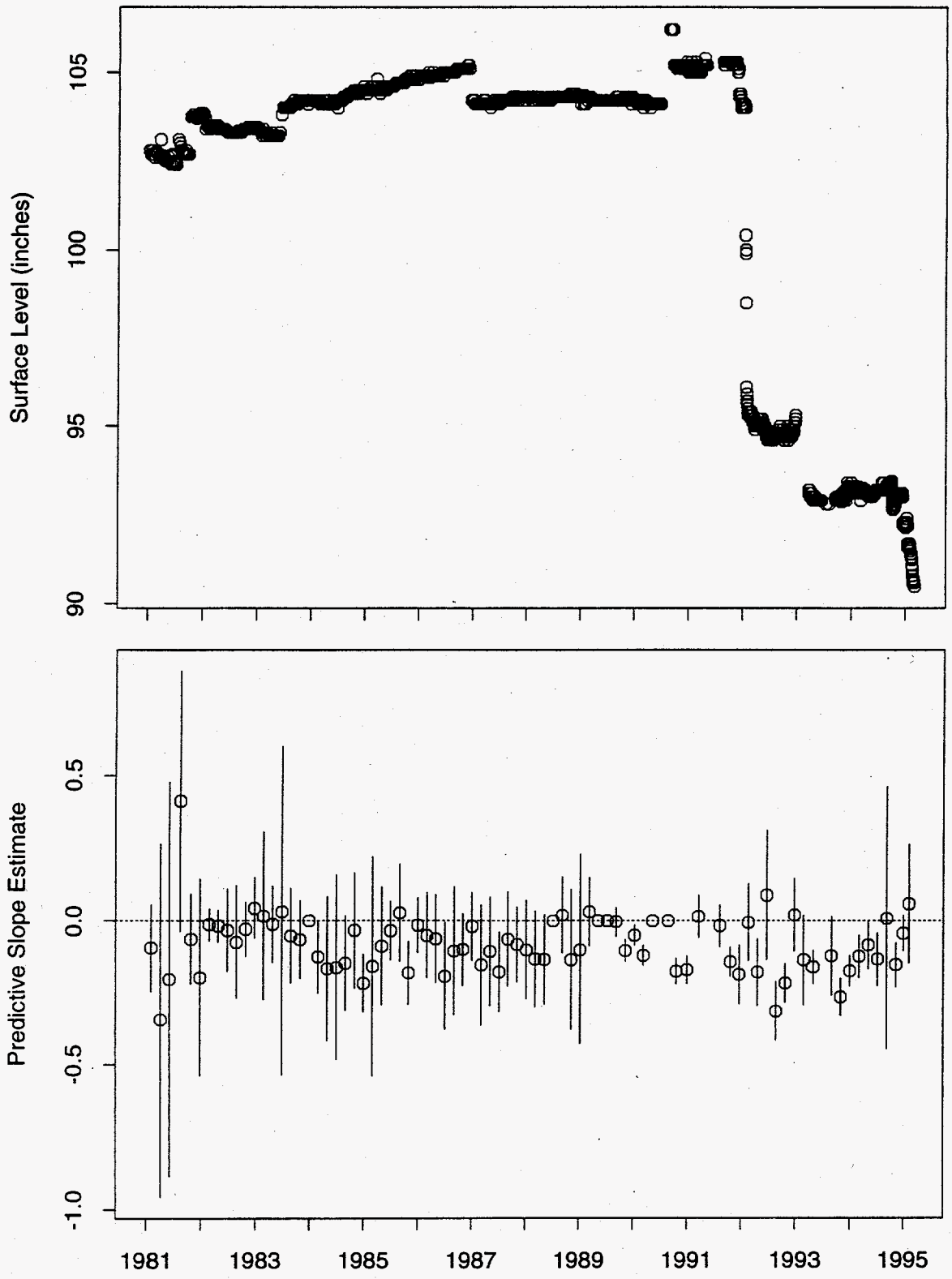

Figure 150: Tank C-107 FIC Data

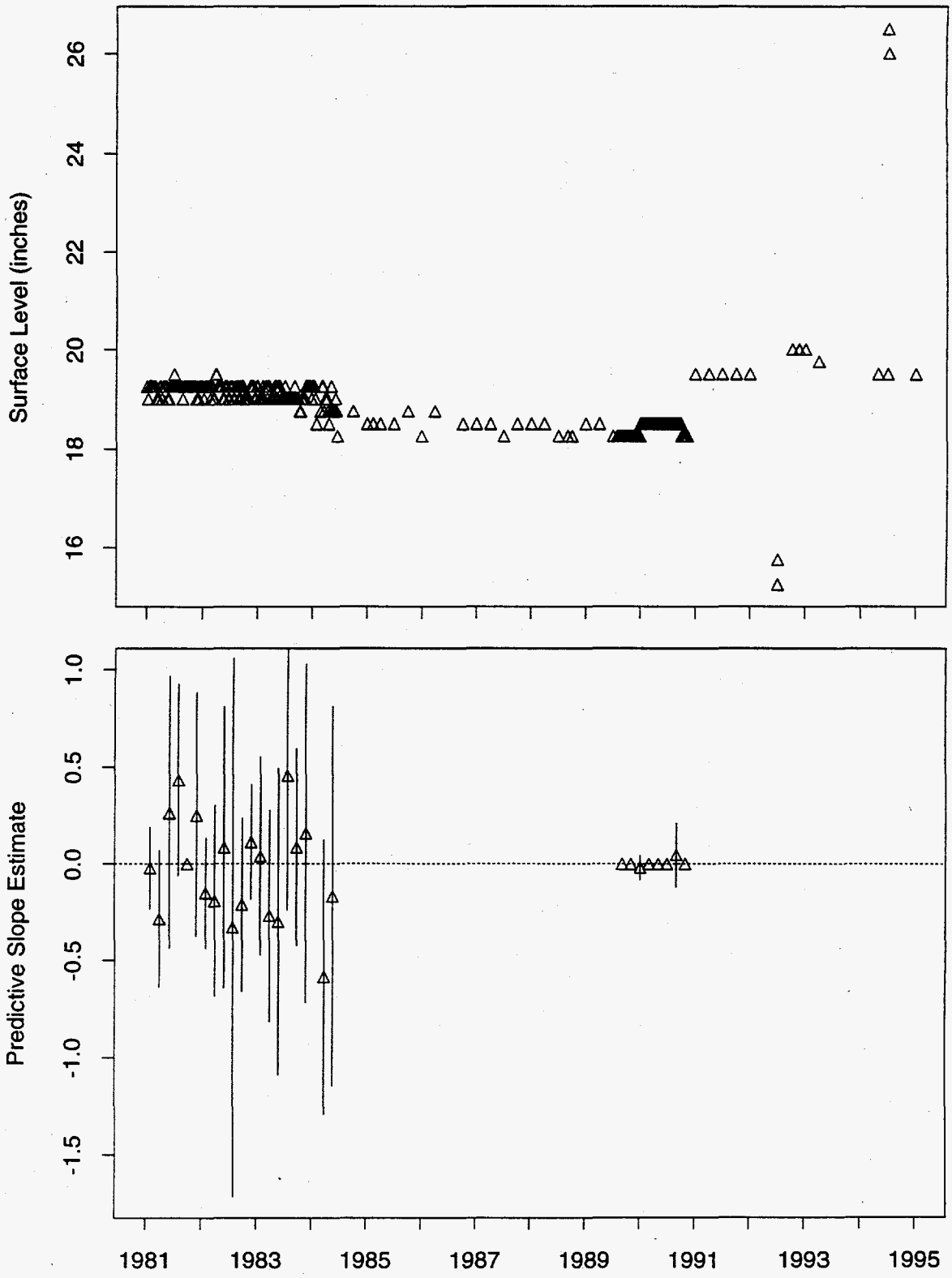

Figure 151: Tank C-108 MT Data

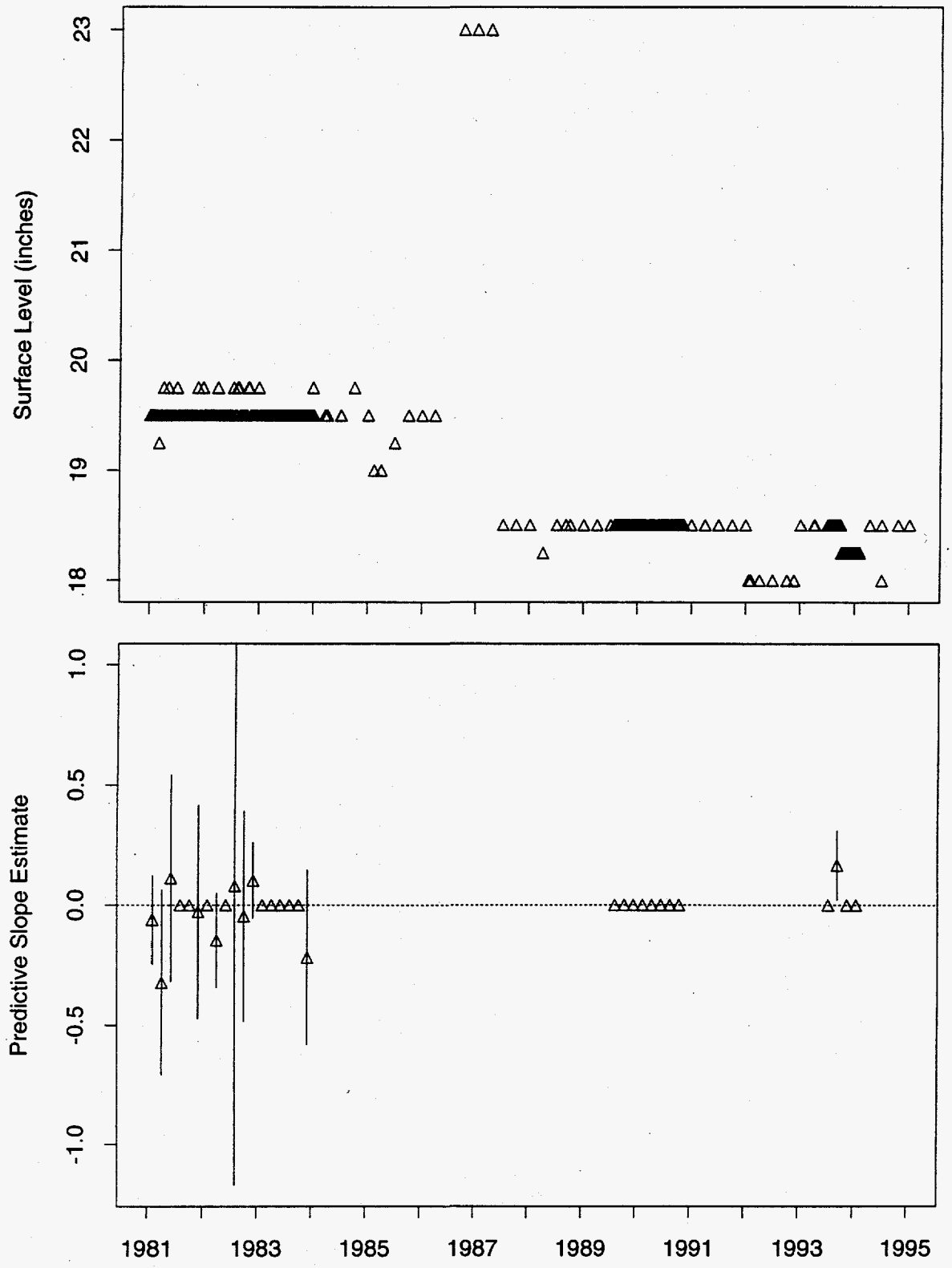

Figure 152: Tank C-109 MT Data

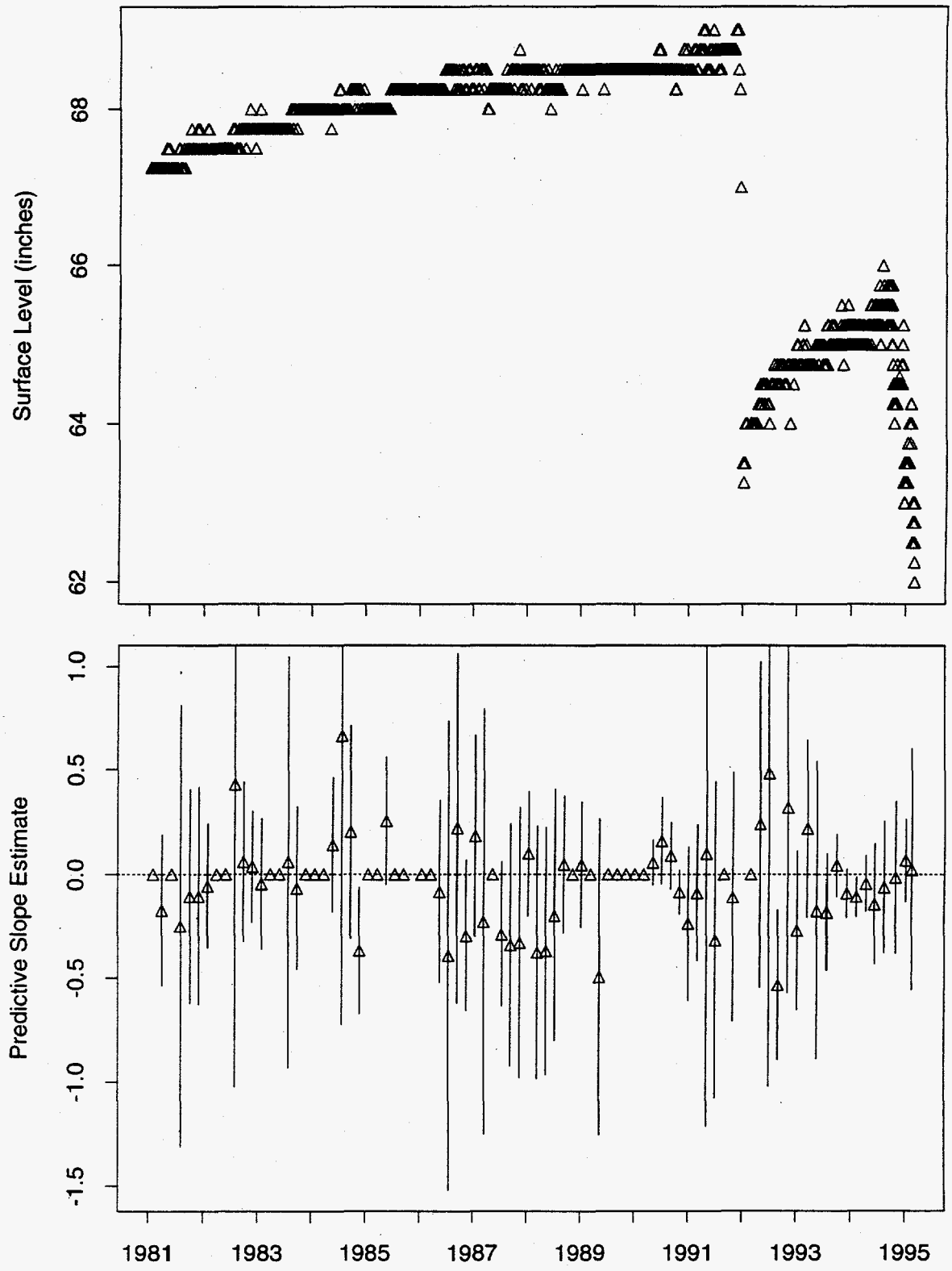

Figure 153: Tank C–110 MT Data

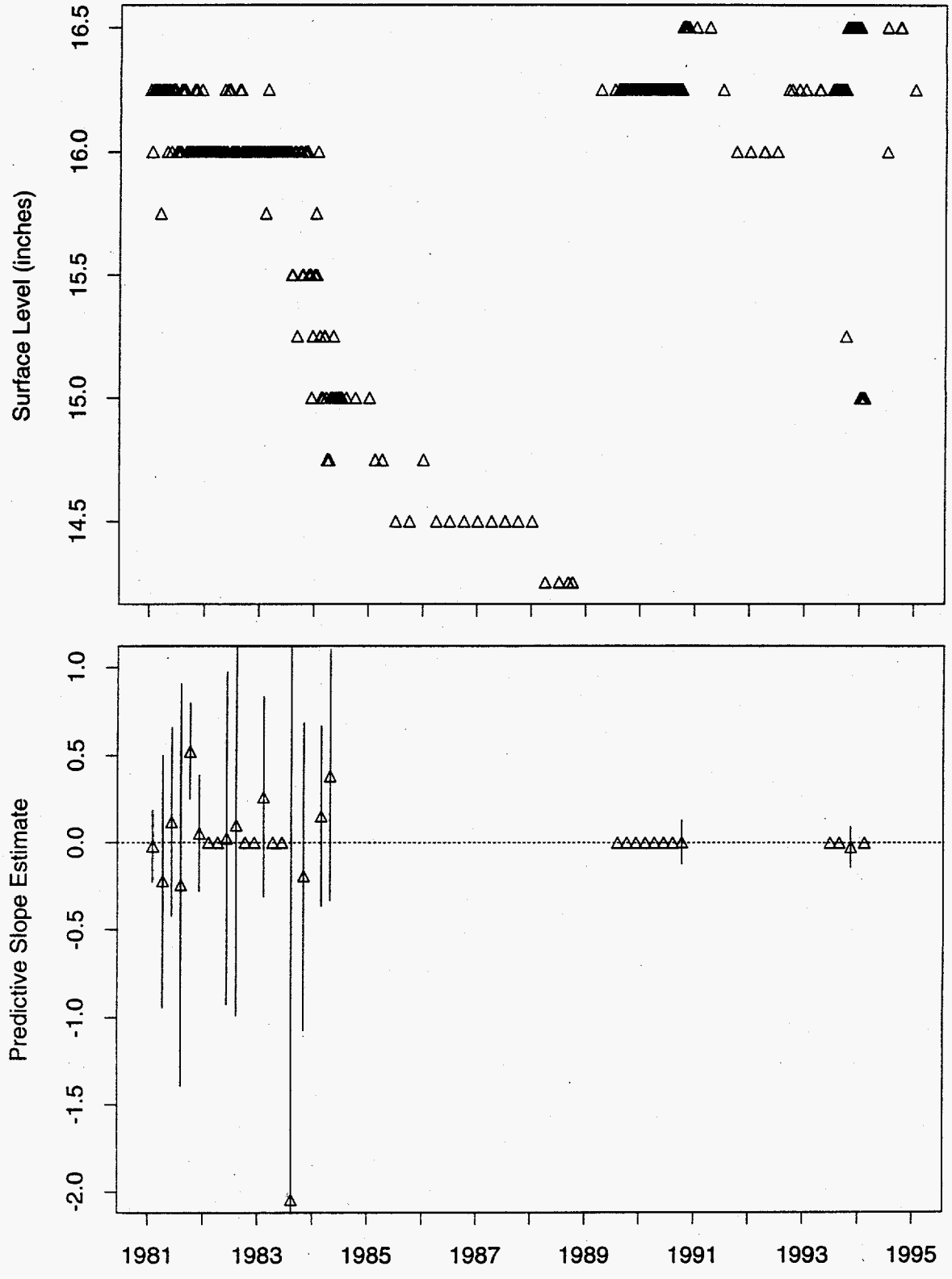

Figure 154: Tank C–111 MT Data

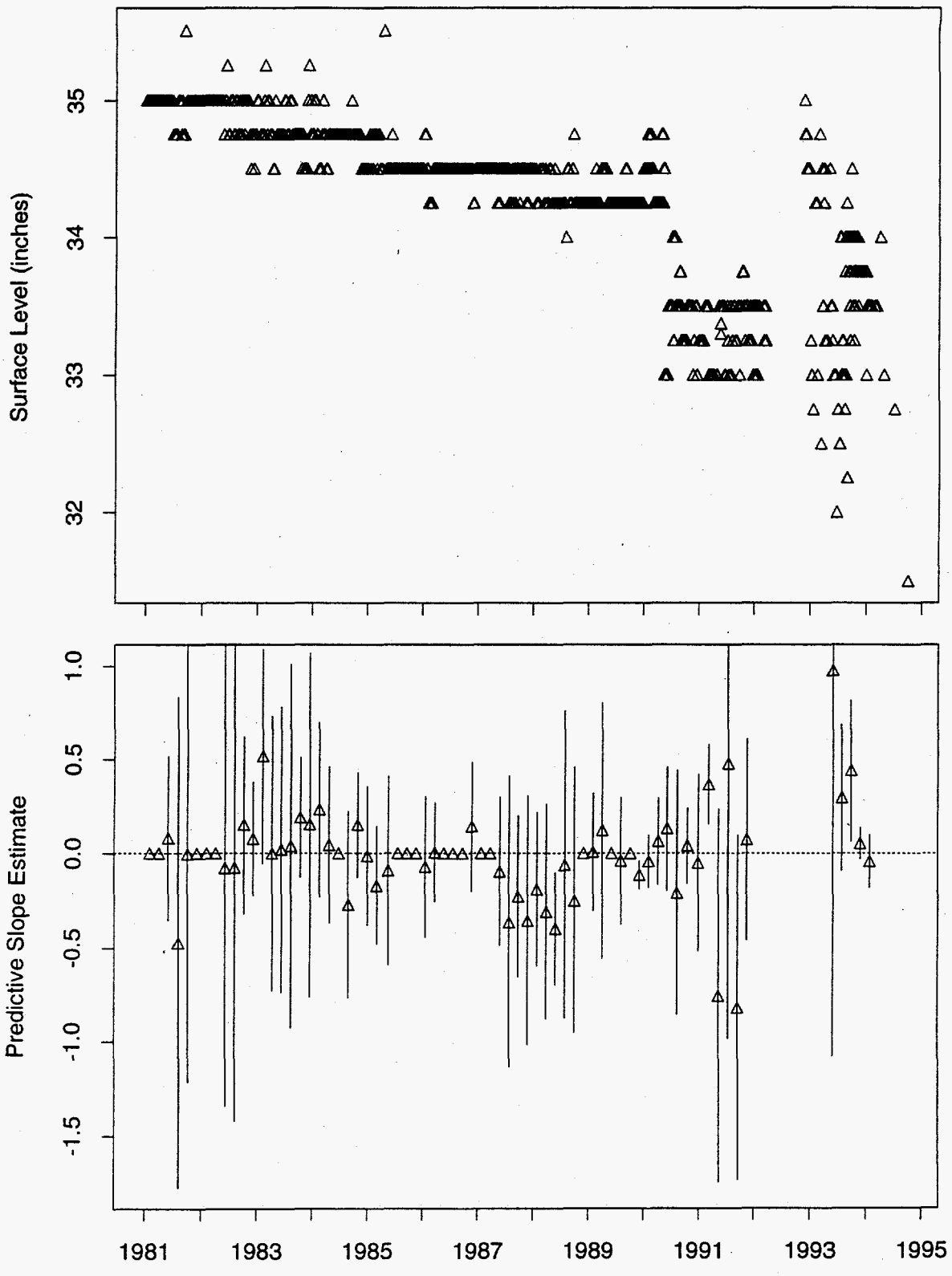

Figure 155: Tank C-112 MT Data

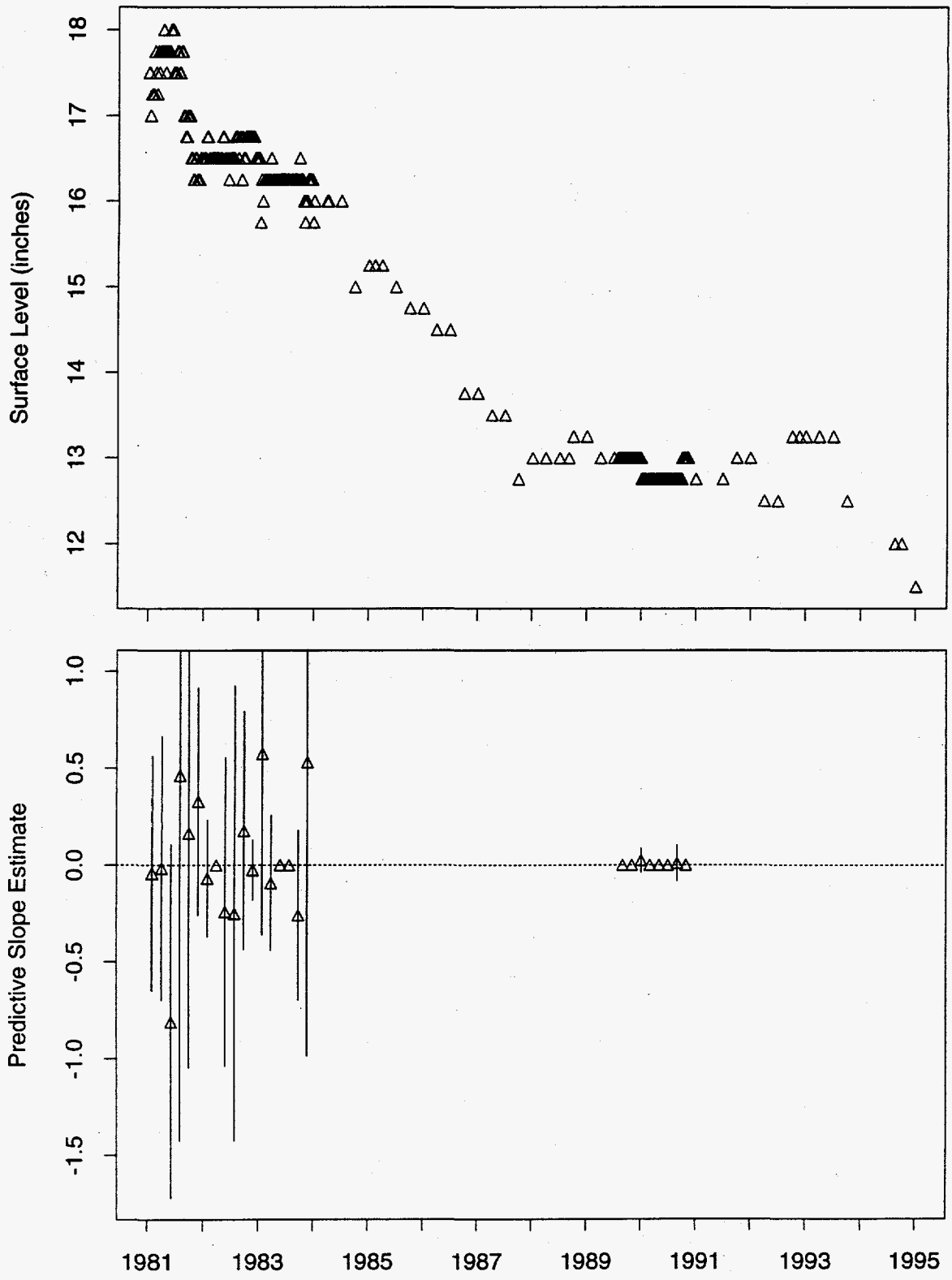

Figure 156: Tank C-201 MT Data

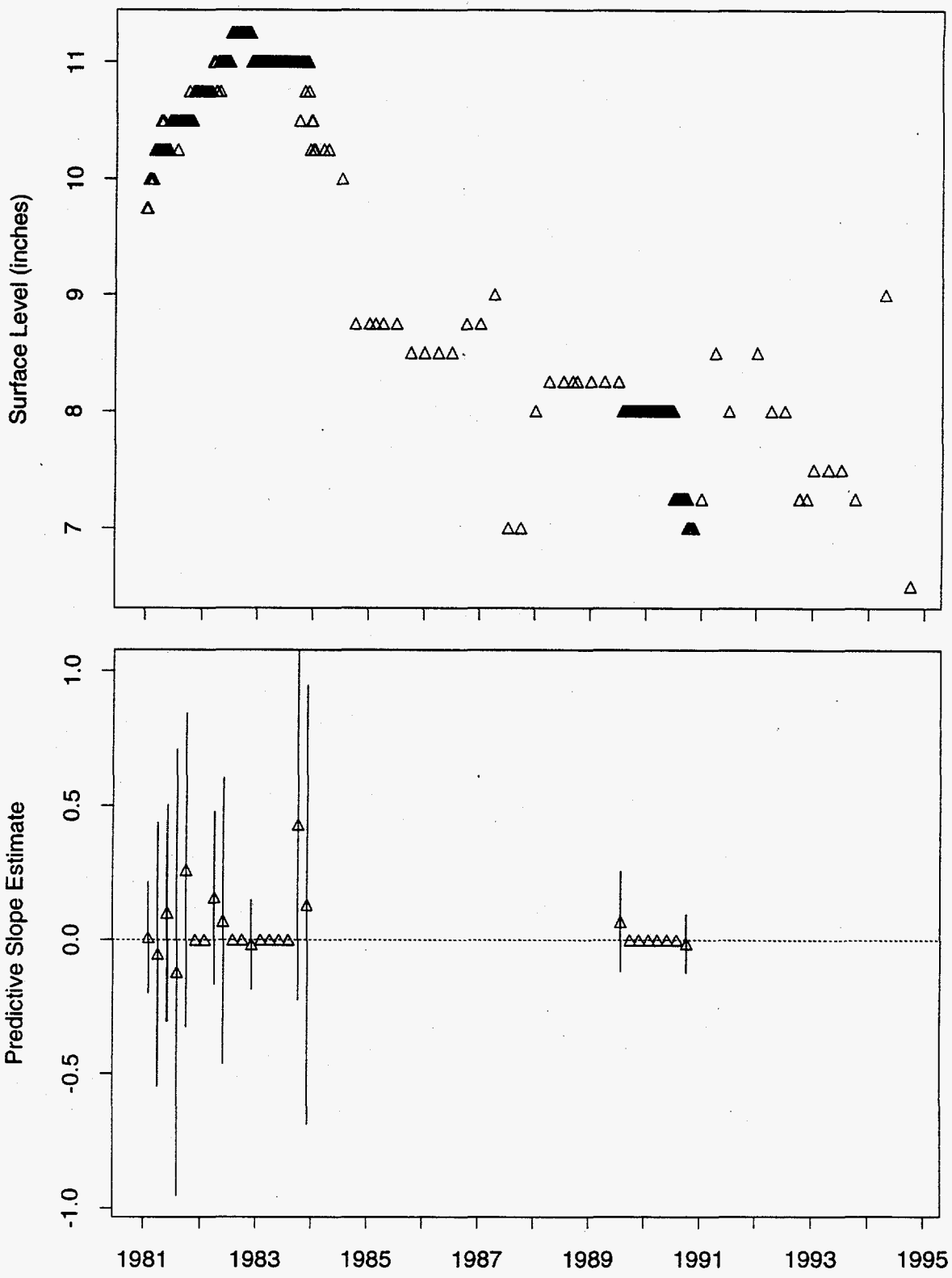

Figure 157: Tank C–202 MT Data

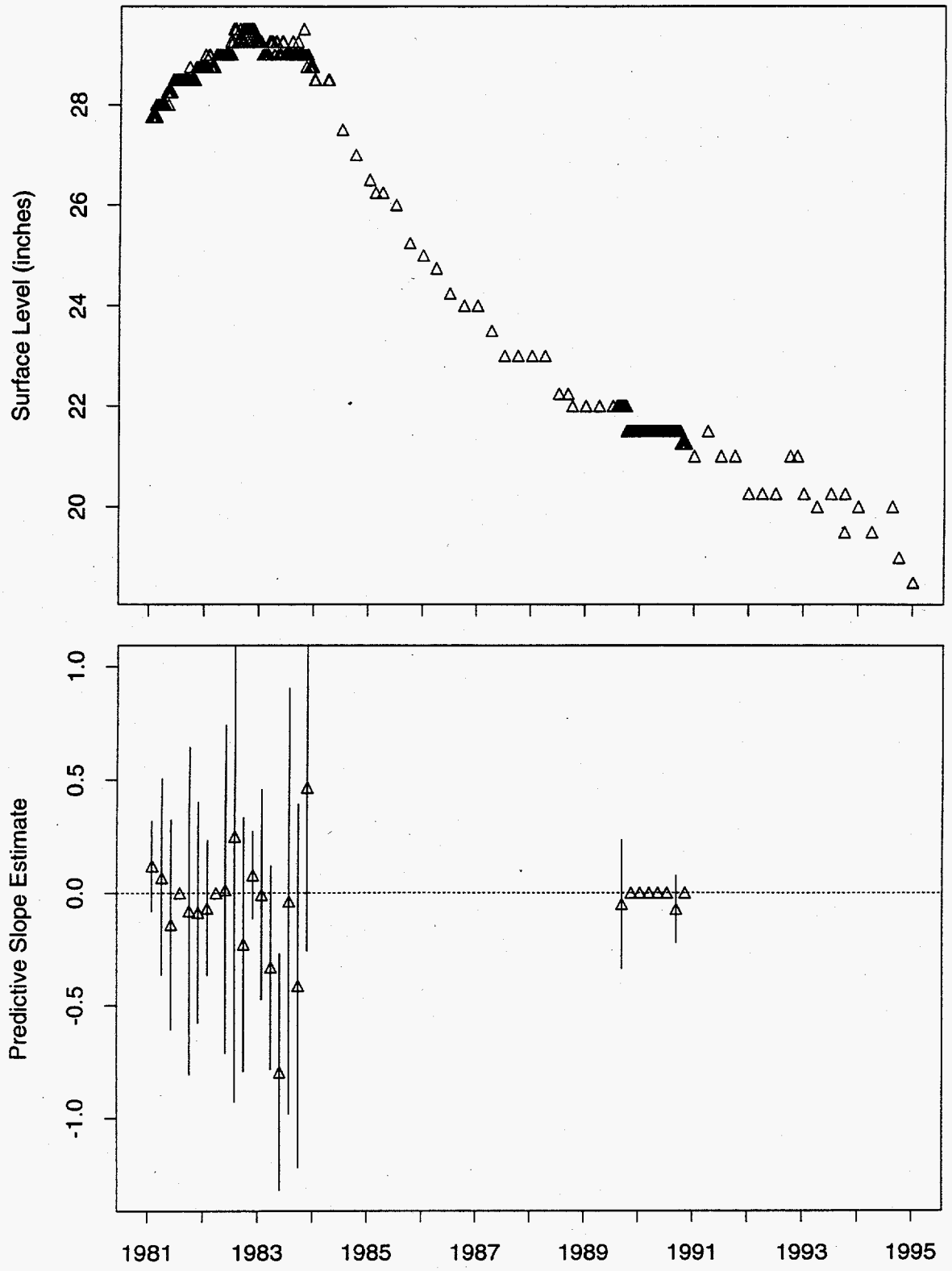

Figure 158: Tank C-203 MT Data

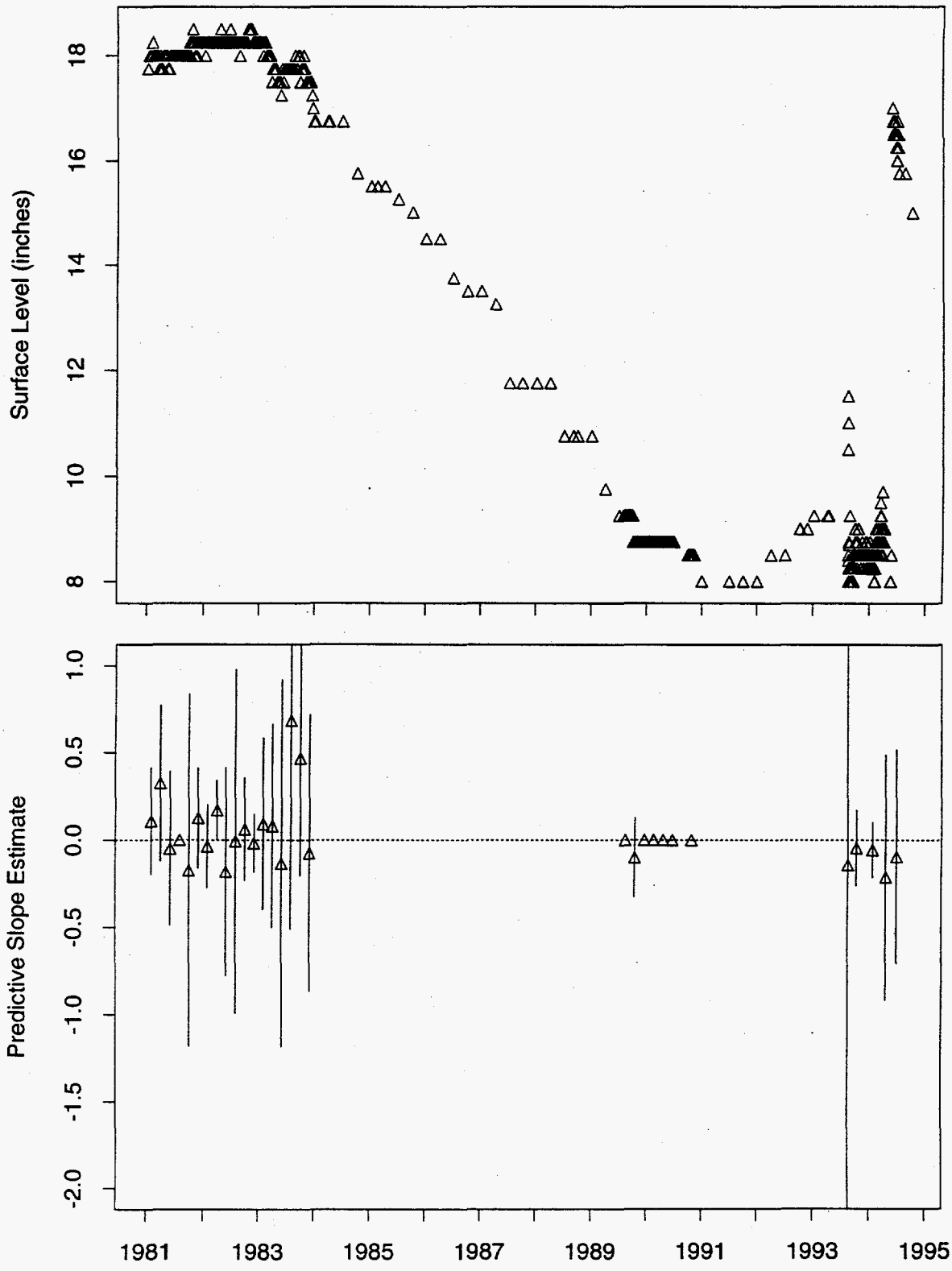

Figure 159: Tank C–204 MT Data

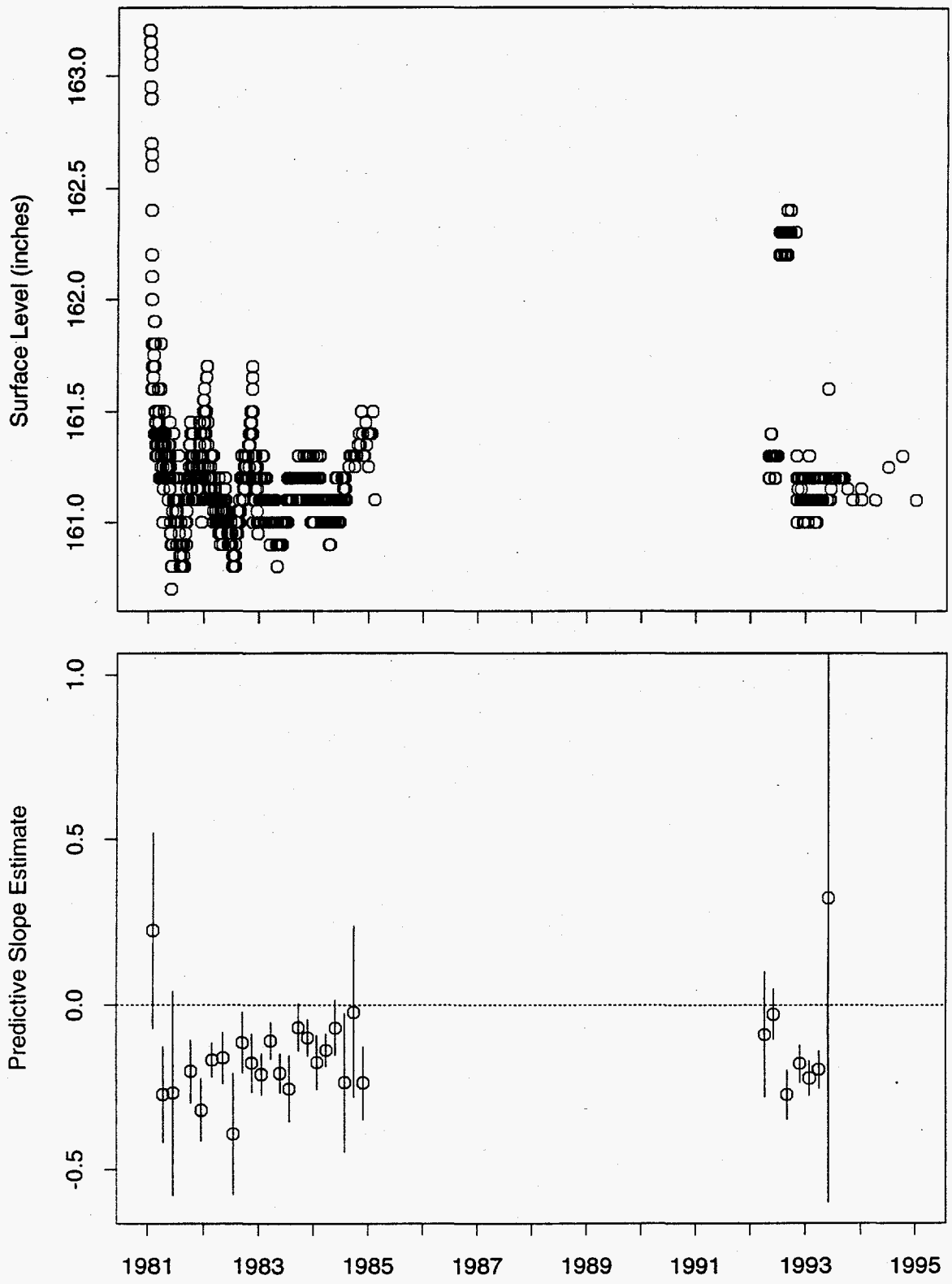

Figure 160: Tank S–101 FIC Data

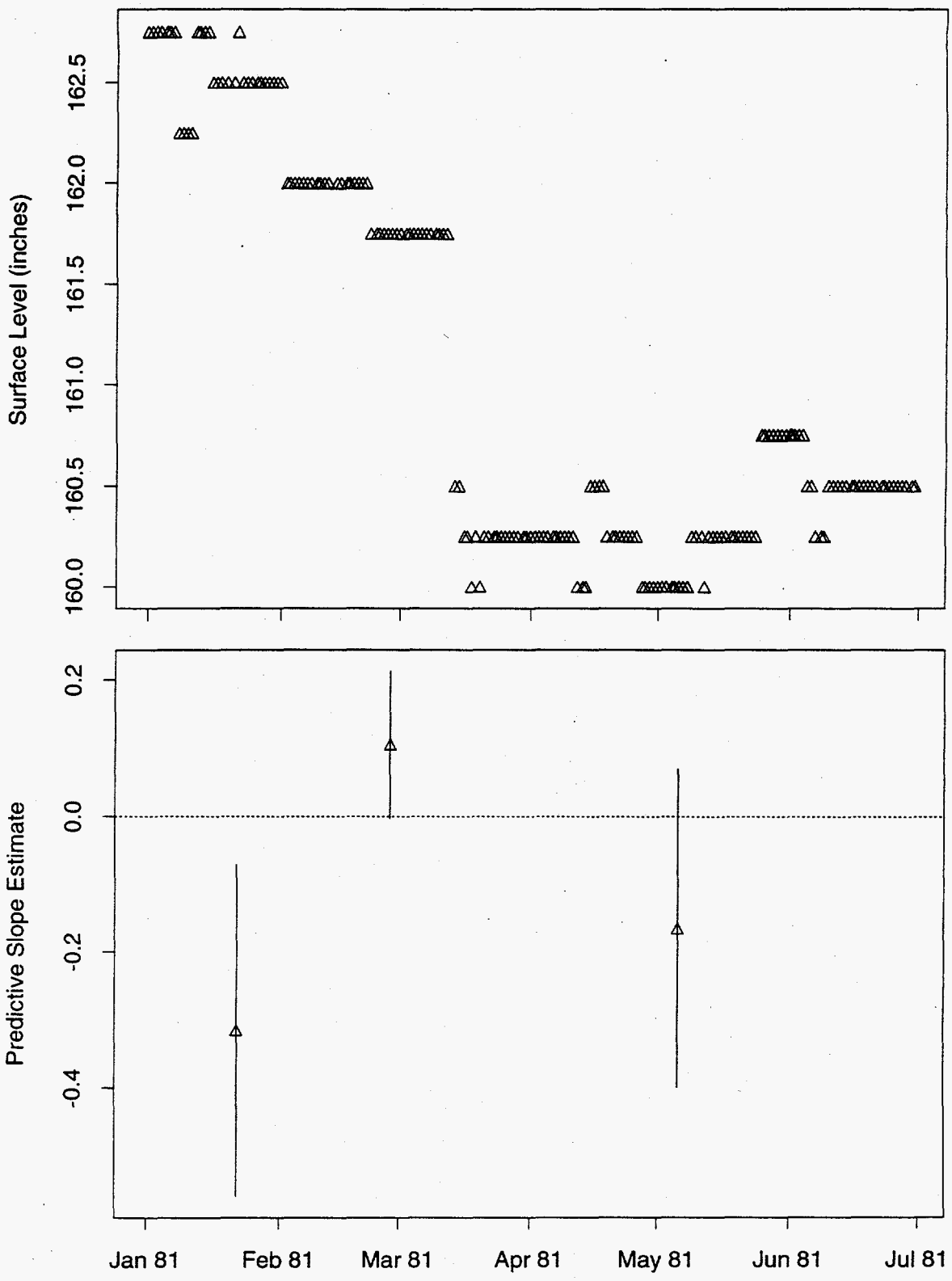

Figure 161: Tank S–101 MT Data

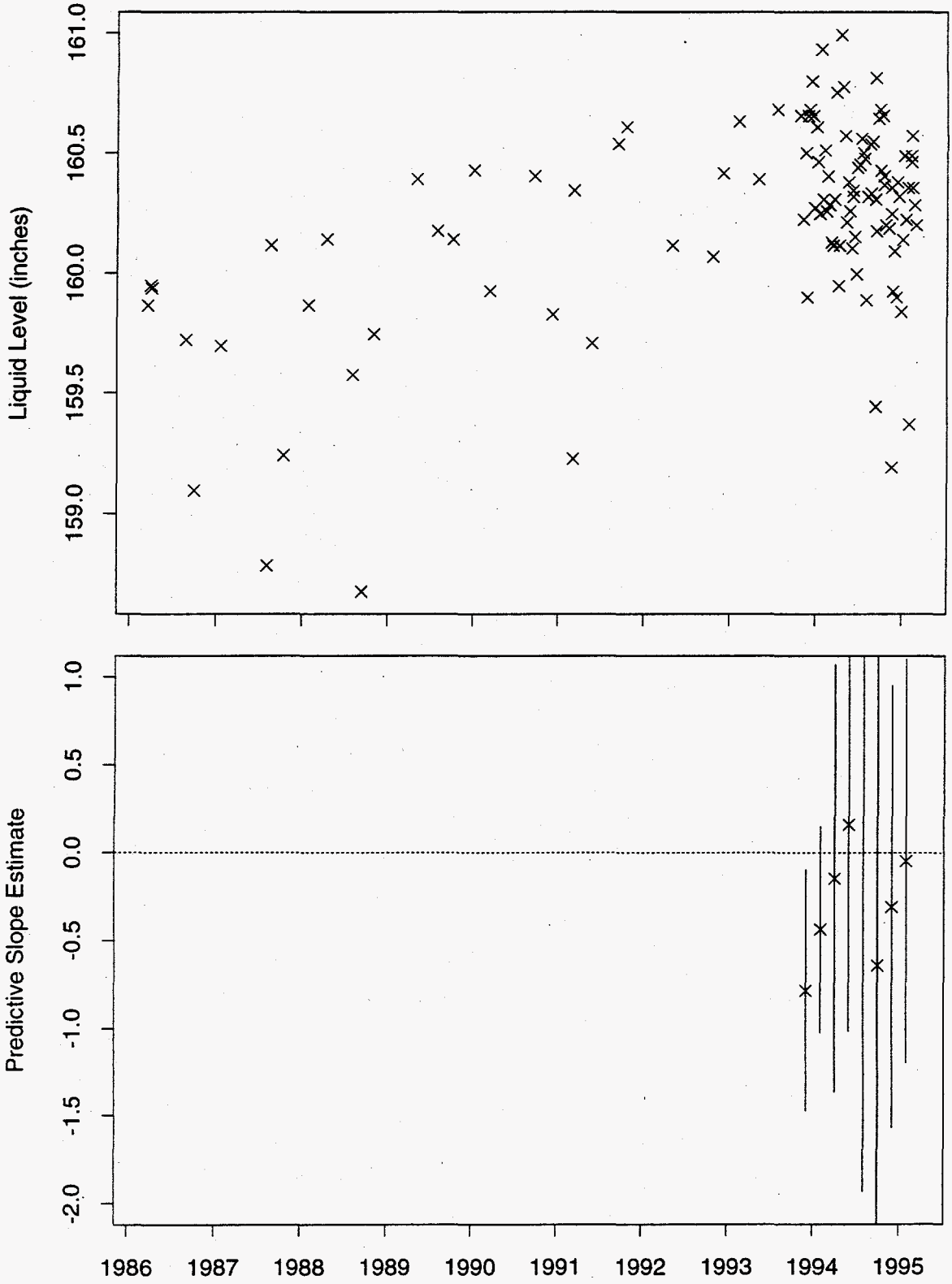

Figure 162: Tank S–101 Neutron ILL Data

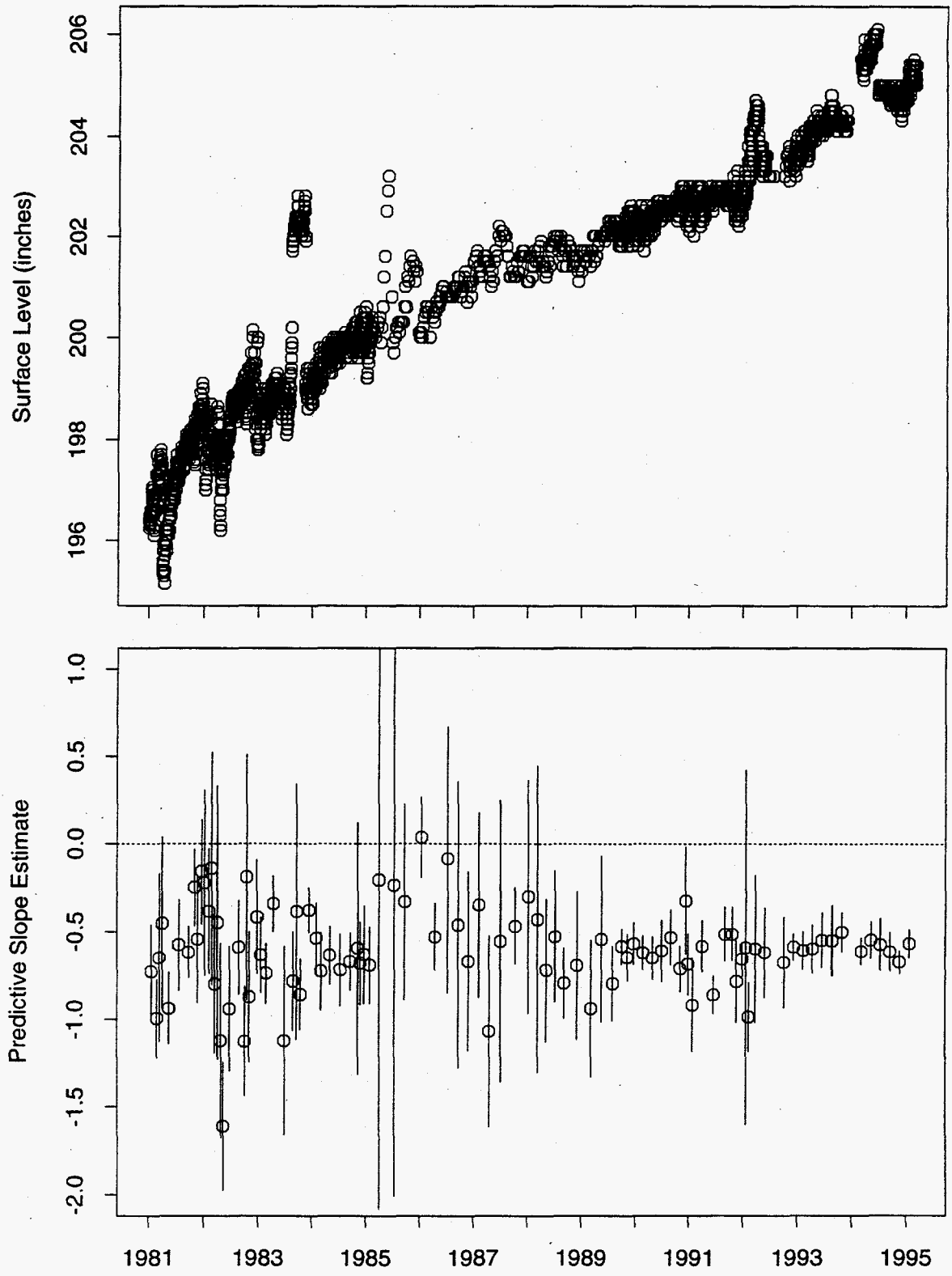

Figure 163: Tank S–102 FIC Data

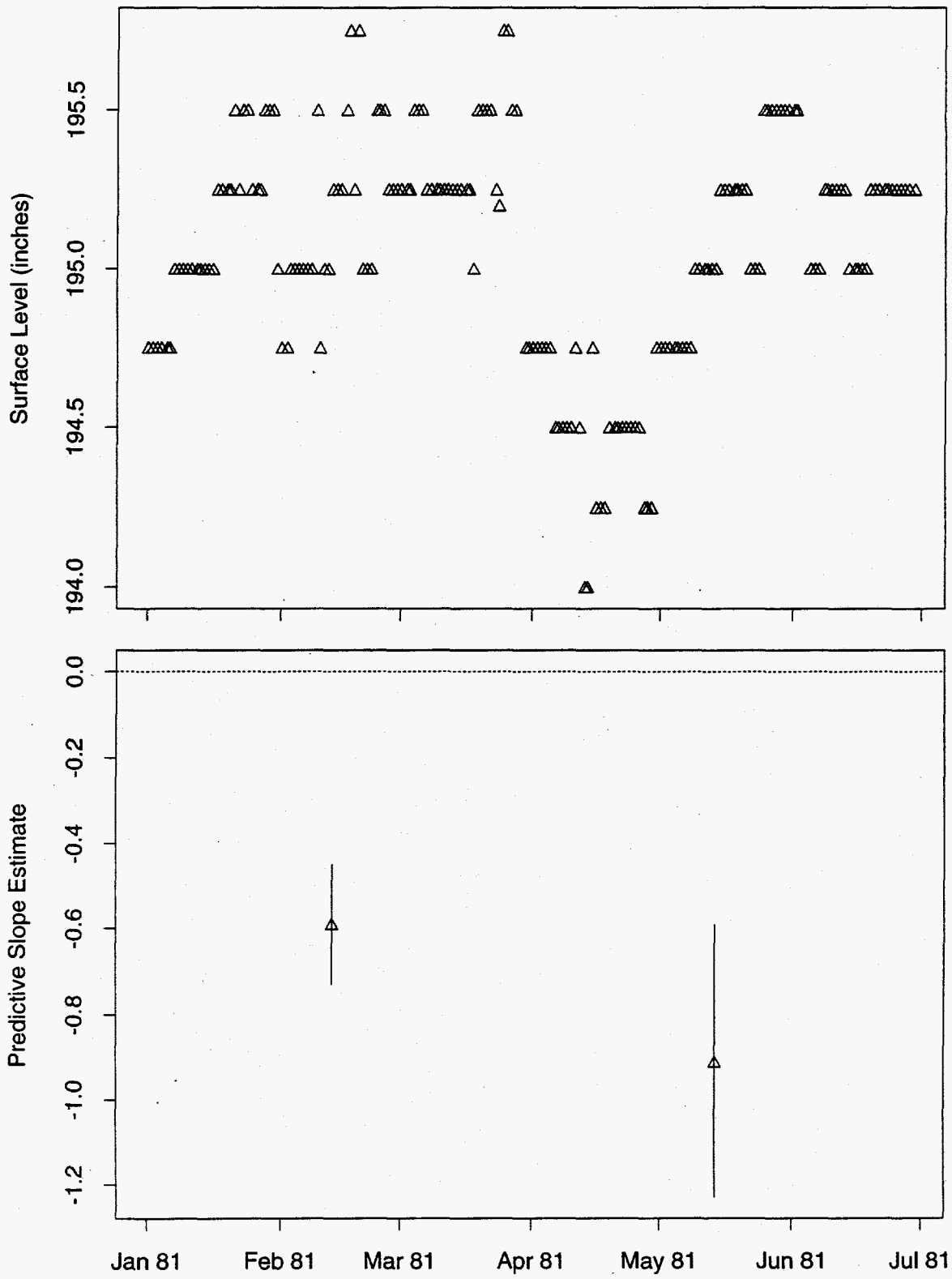

Figure 164: Tank S–102 MT Data

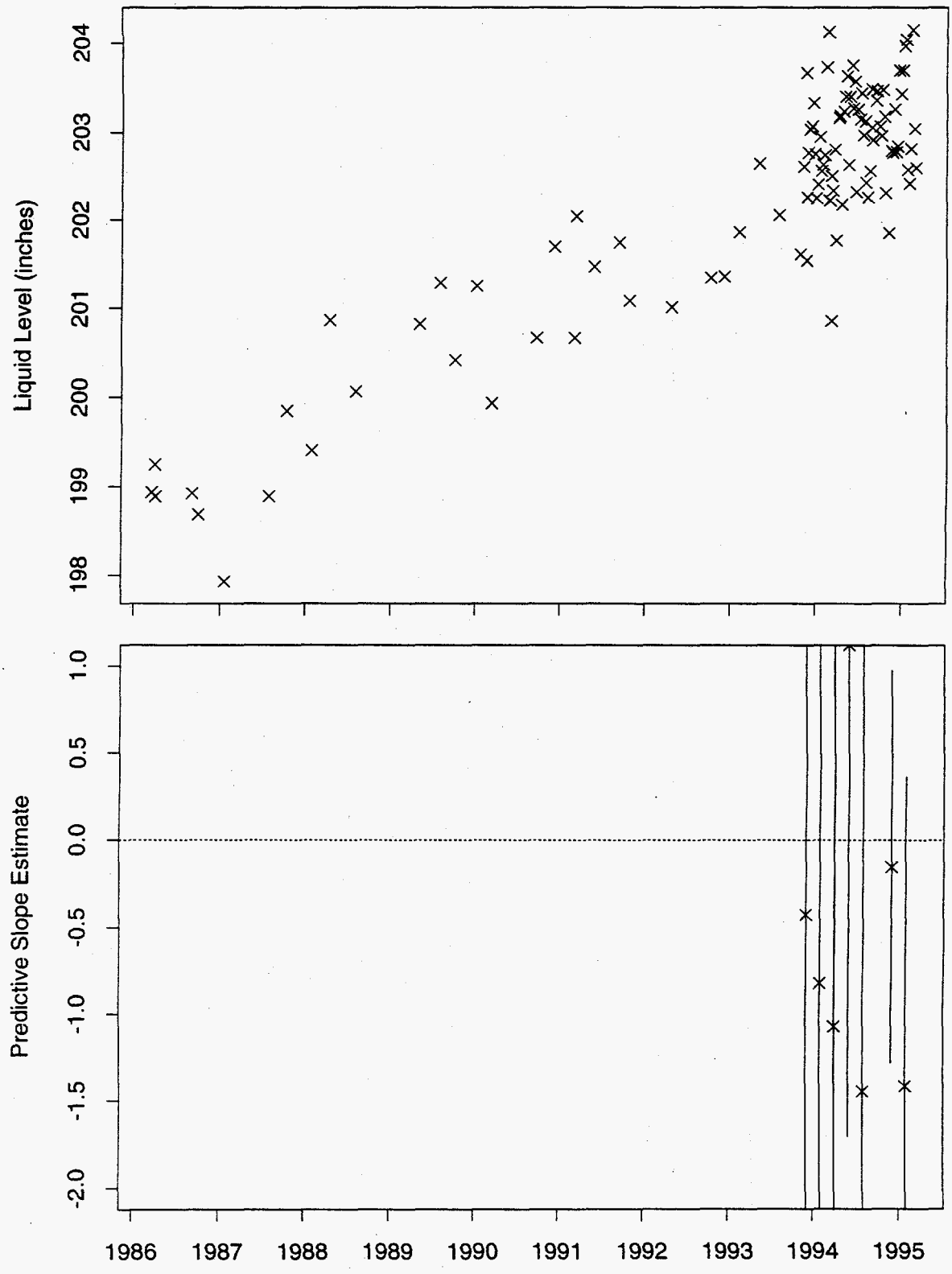

Figure 165: Tank S-102 Neutron ILL Data

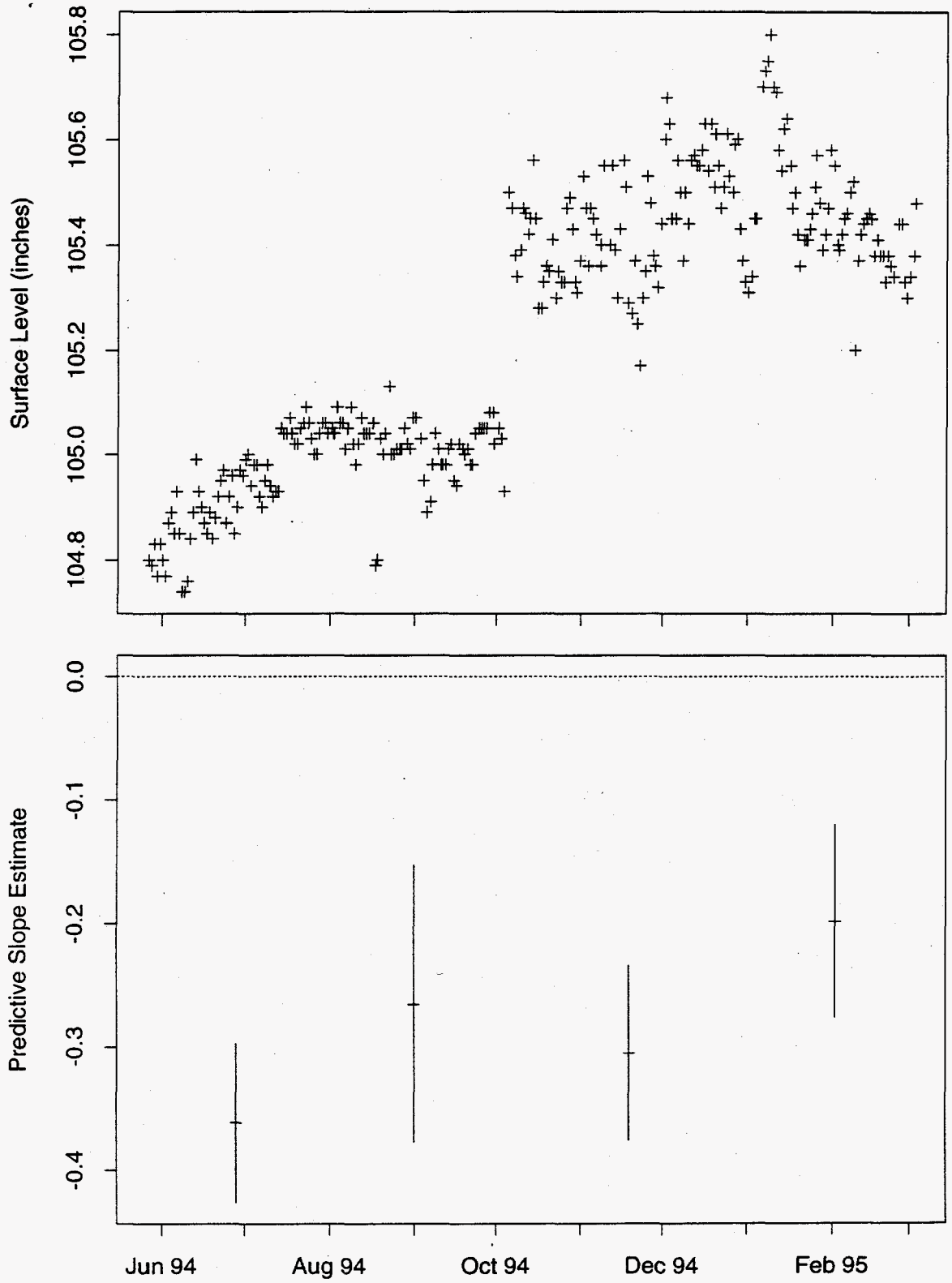

Figure 166: Tank S-103 ENRAF Data

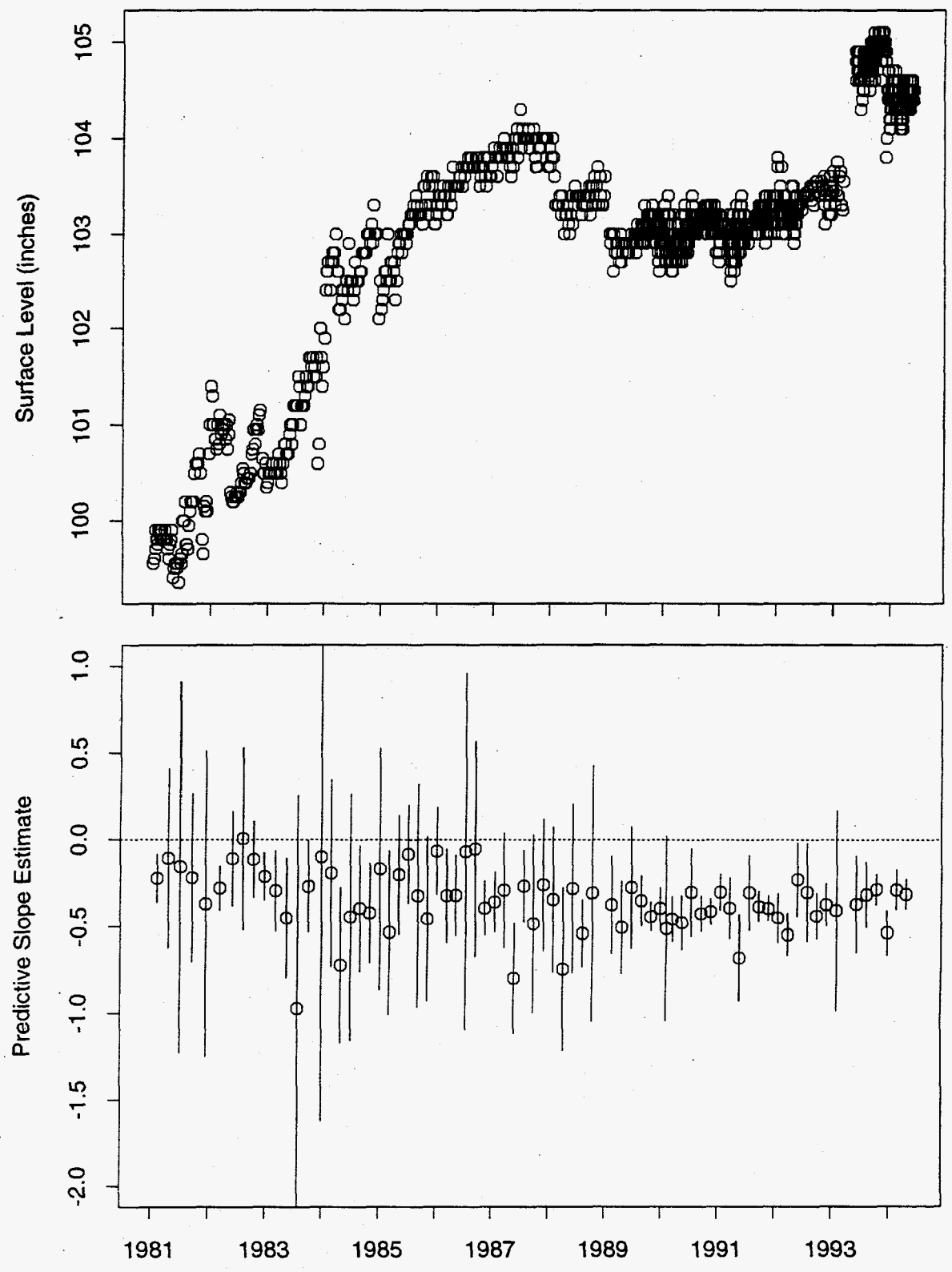

Figure 167: Tank S-103 FIC Data

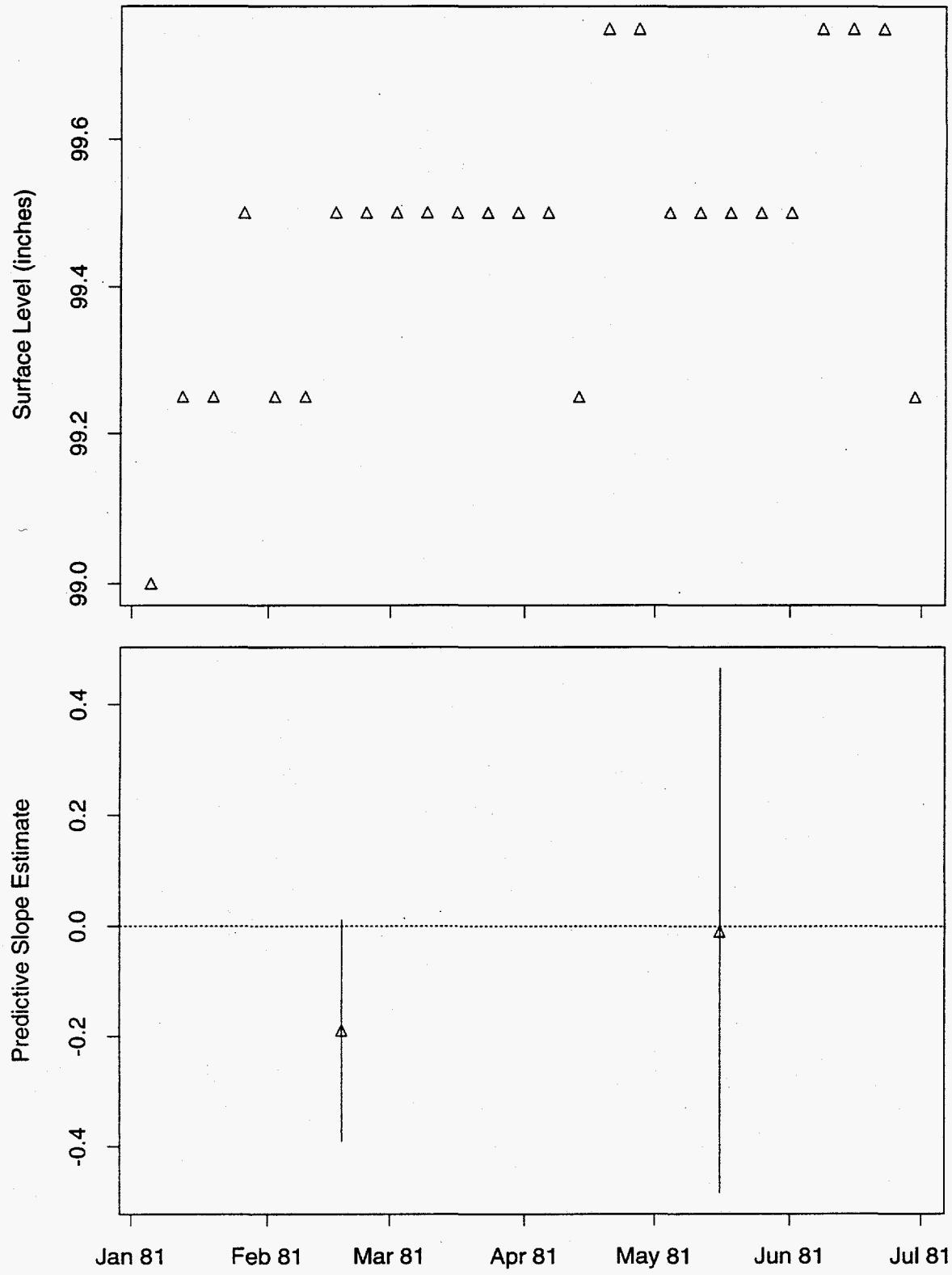

Figure 168: Tank S-103 MT Data

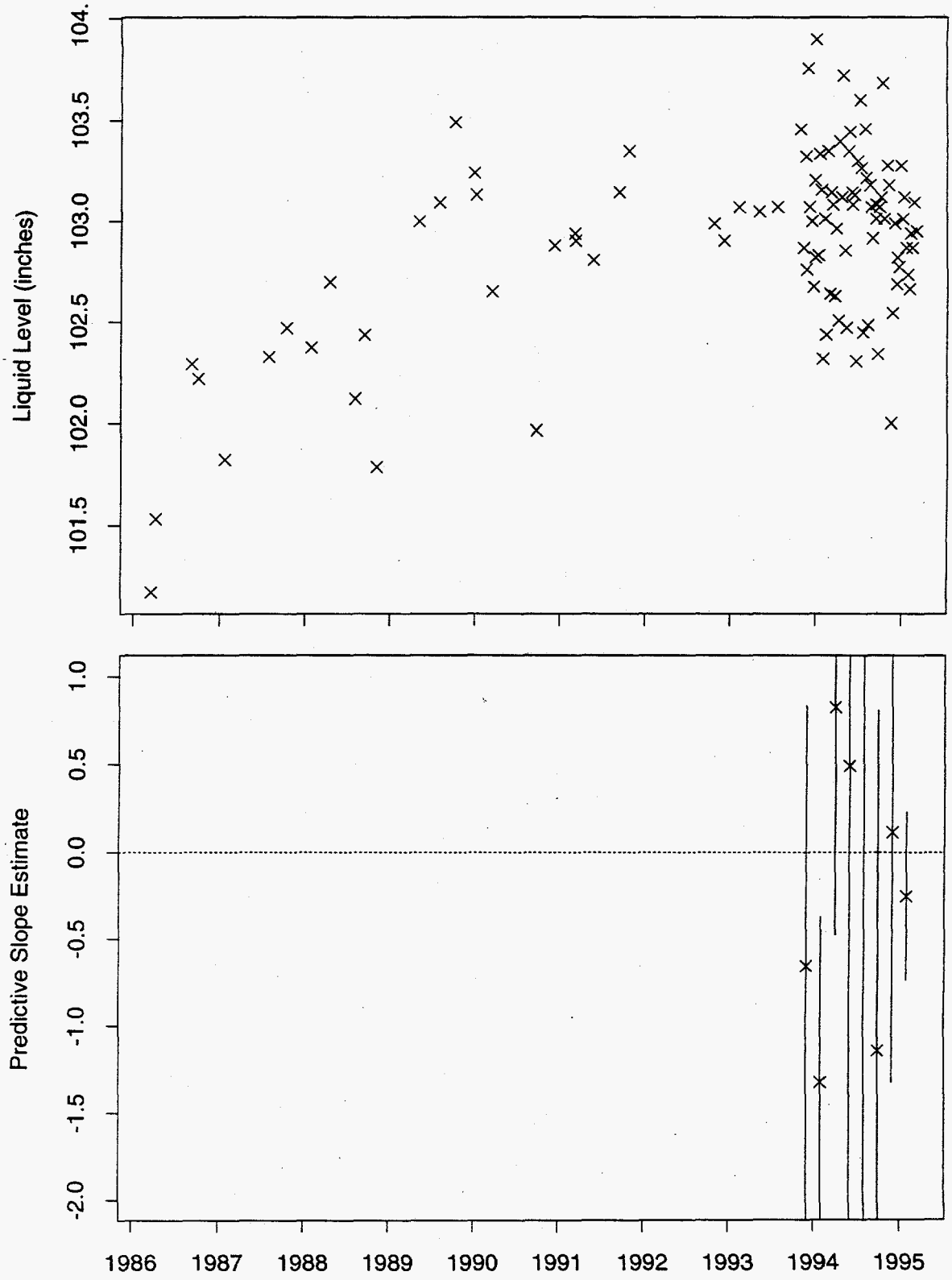

Figure 169: Tank S–103 Neutron ILL Data

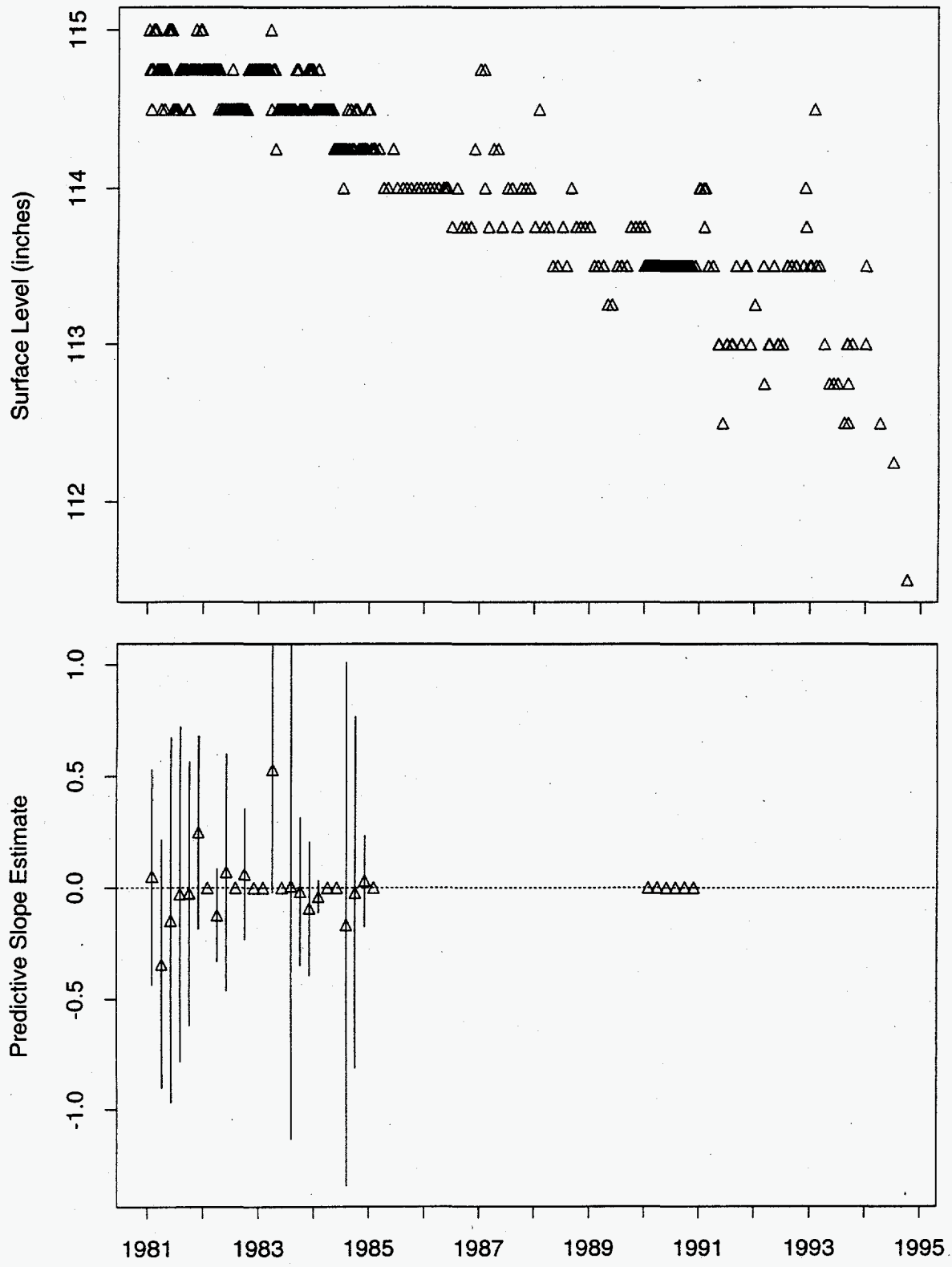

Figure 170: Tank S–104 MT Data

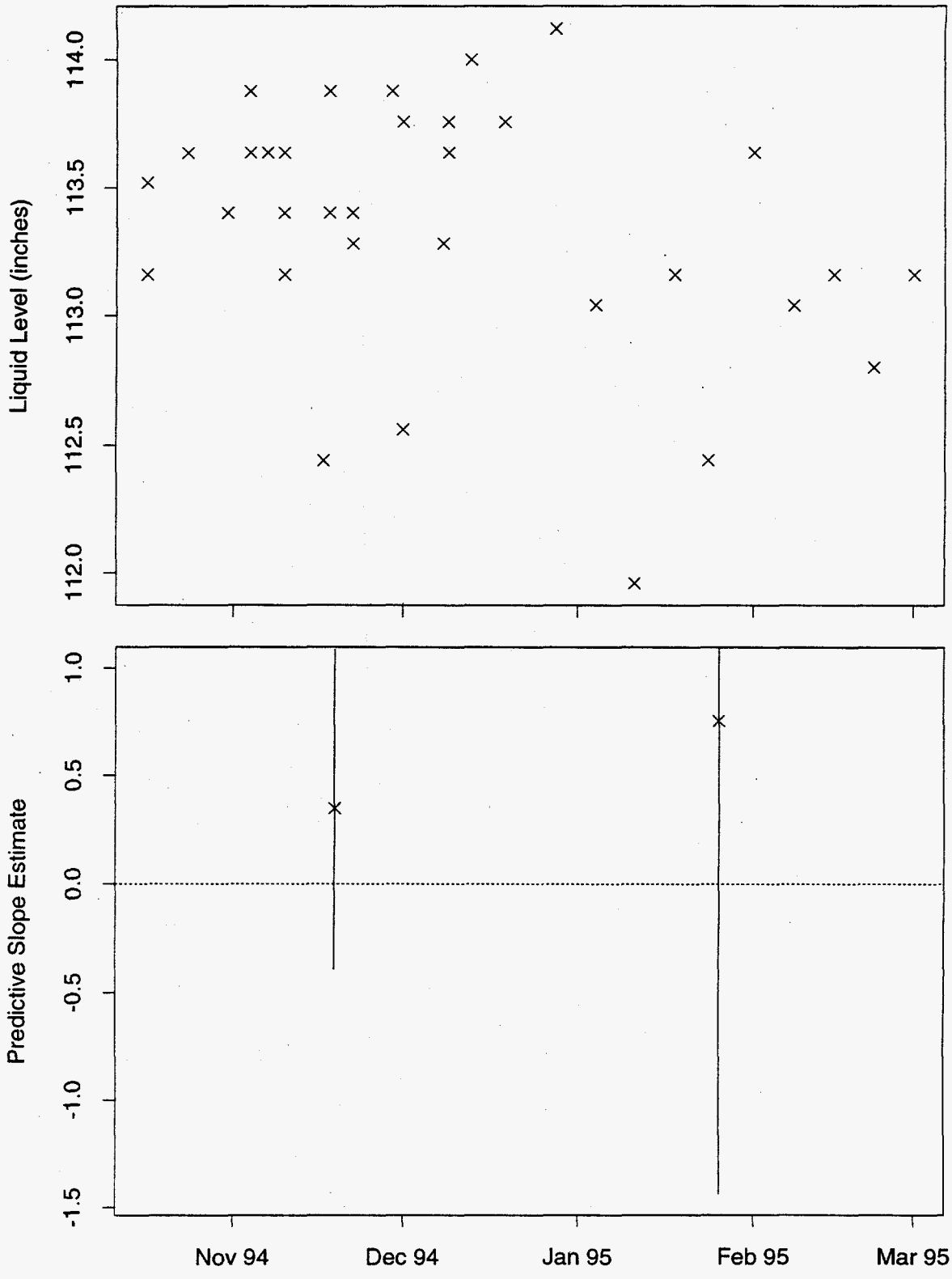

Figure 171: Tank S–104 Neutron ILL Data

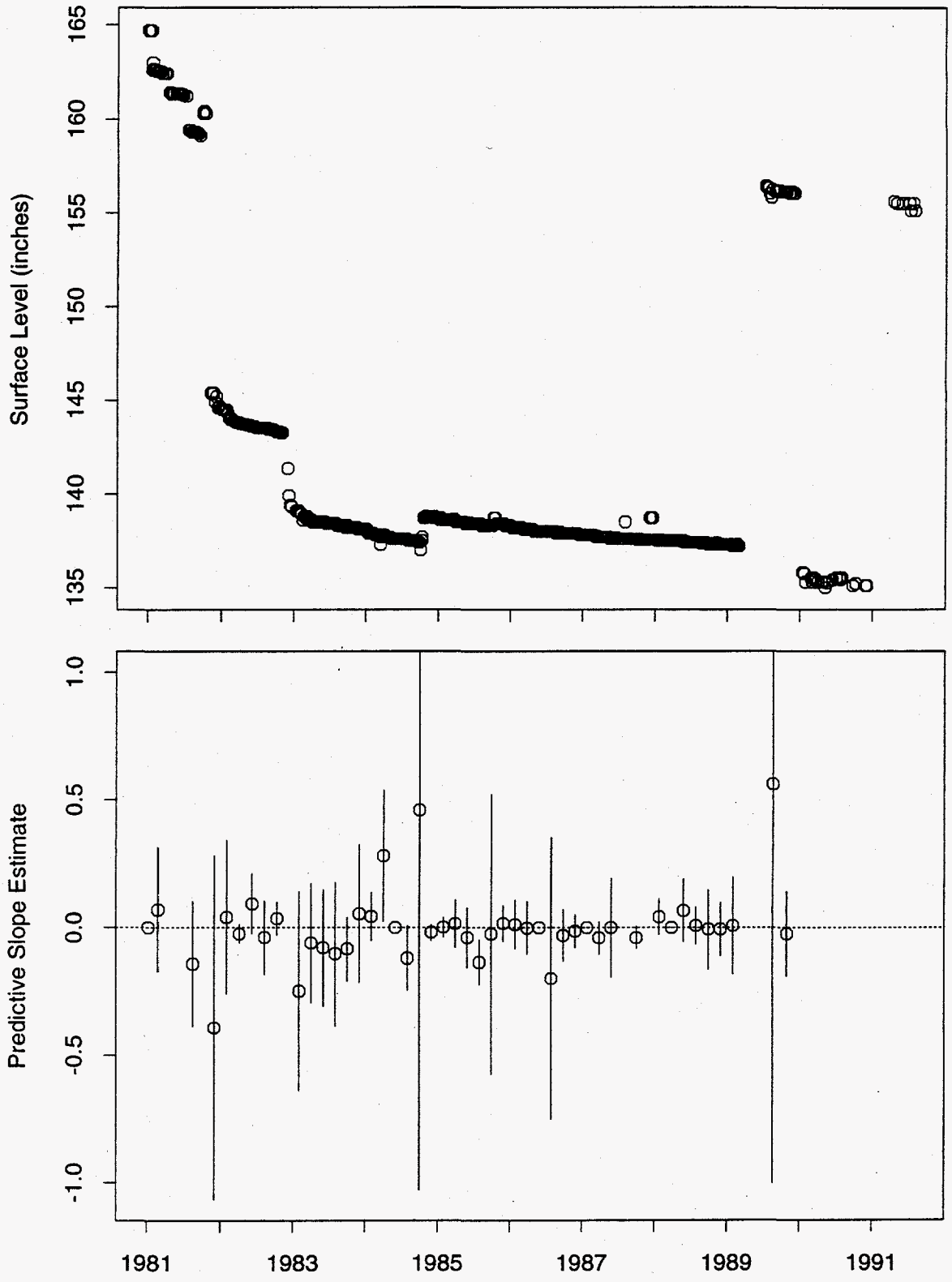

Figure 172: Tank S-105 FIC Data

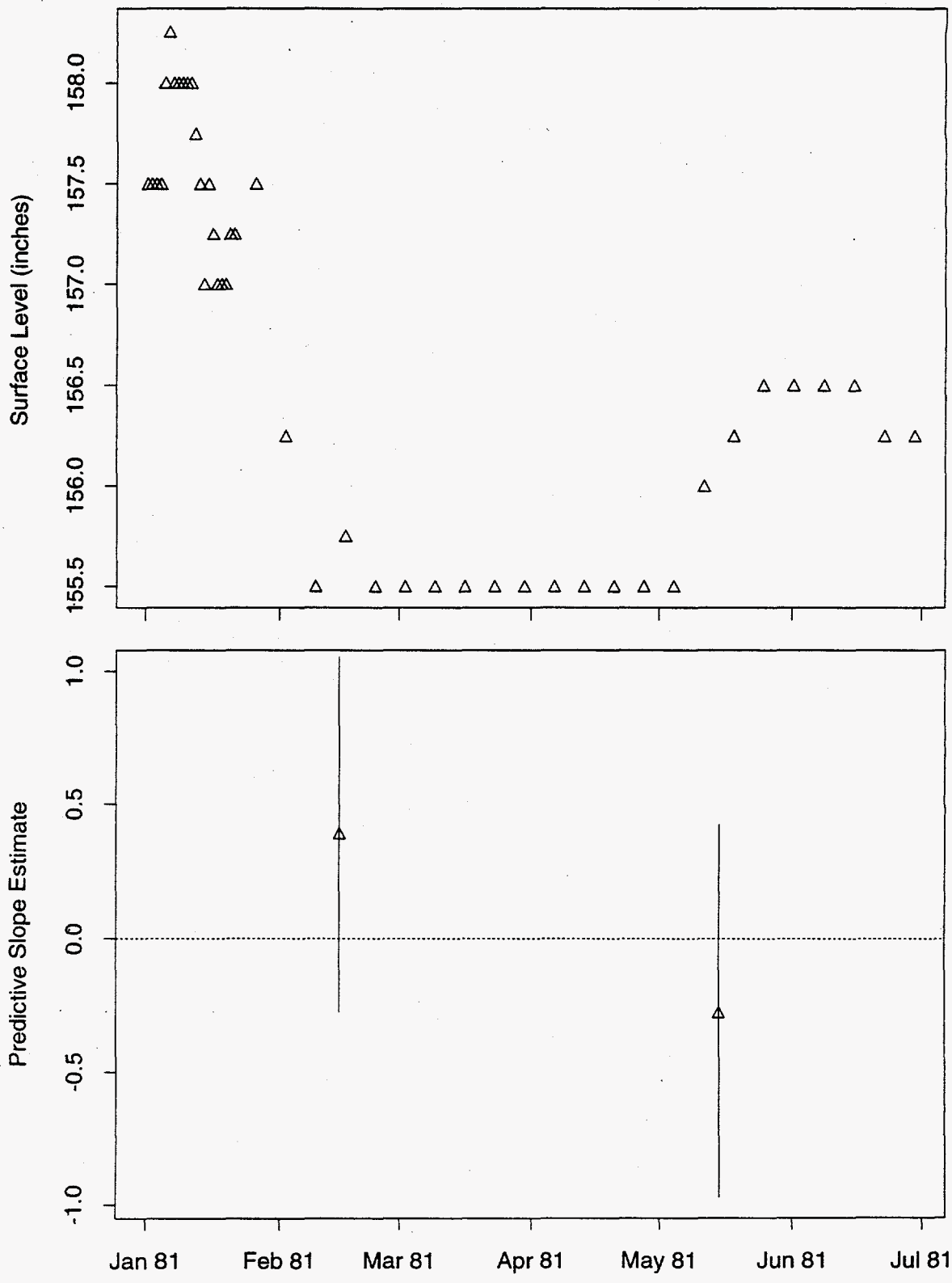

Figure 173: Tank S–105 MT Data

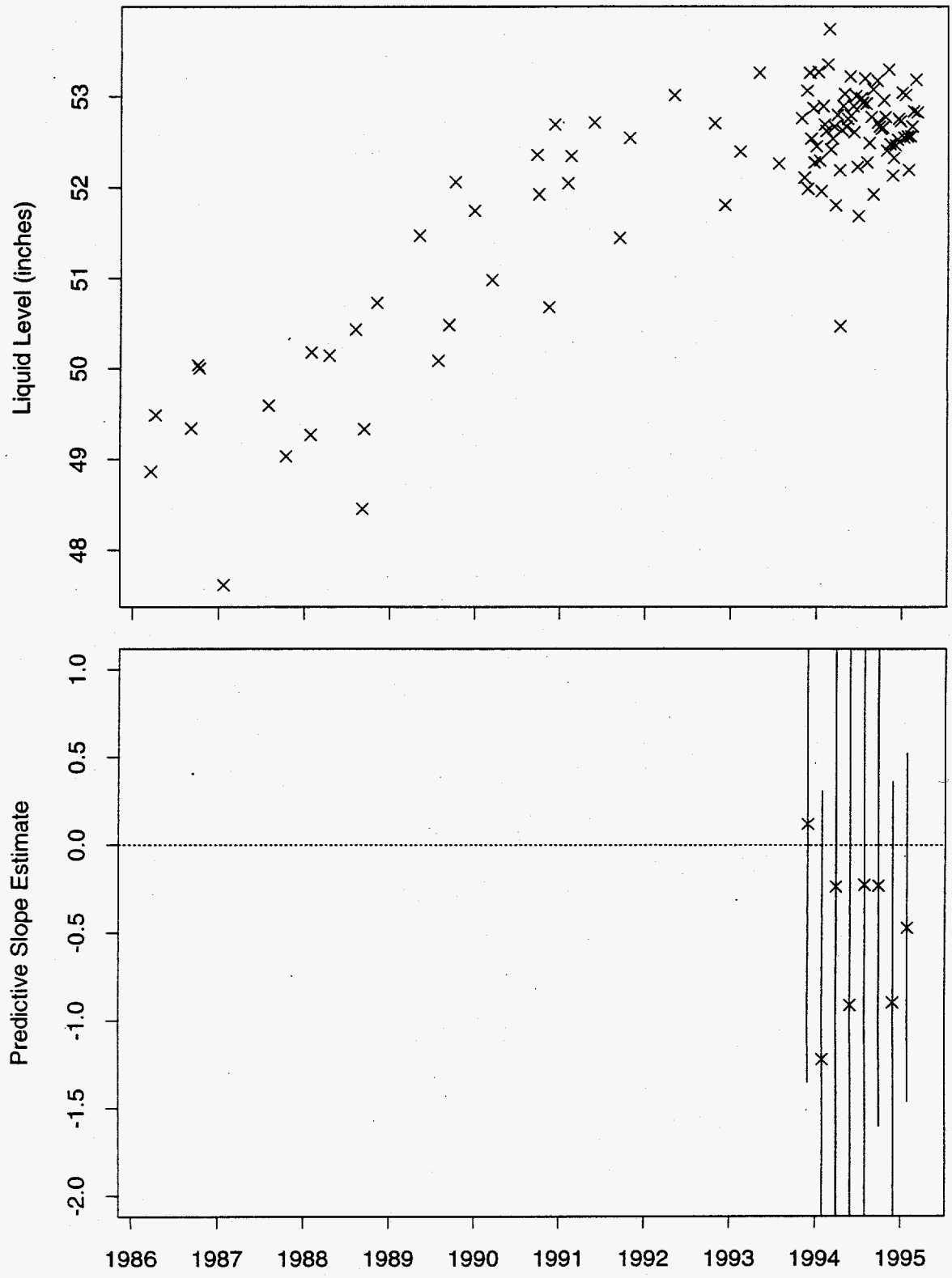

Figure 174: Tank S–105 Neutron ILL Data

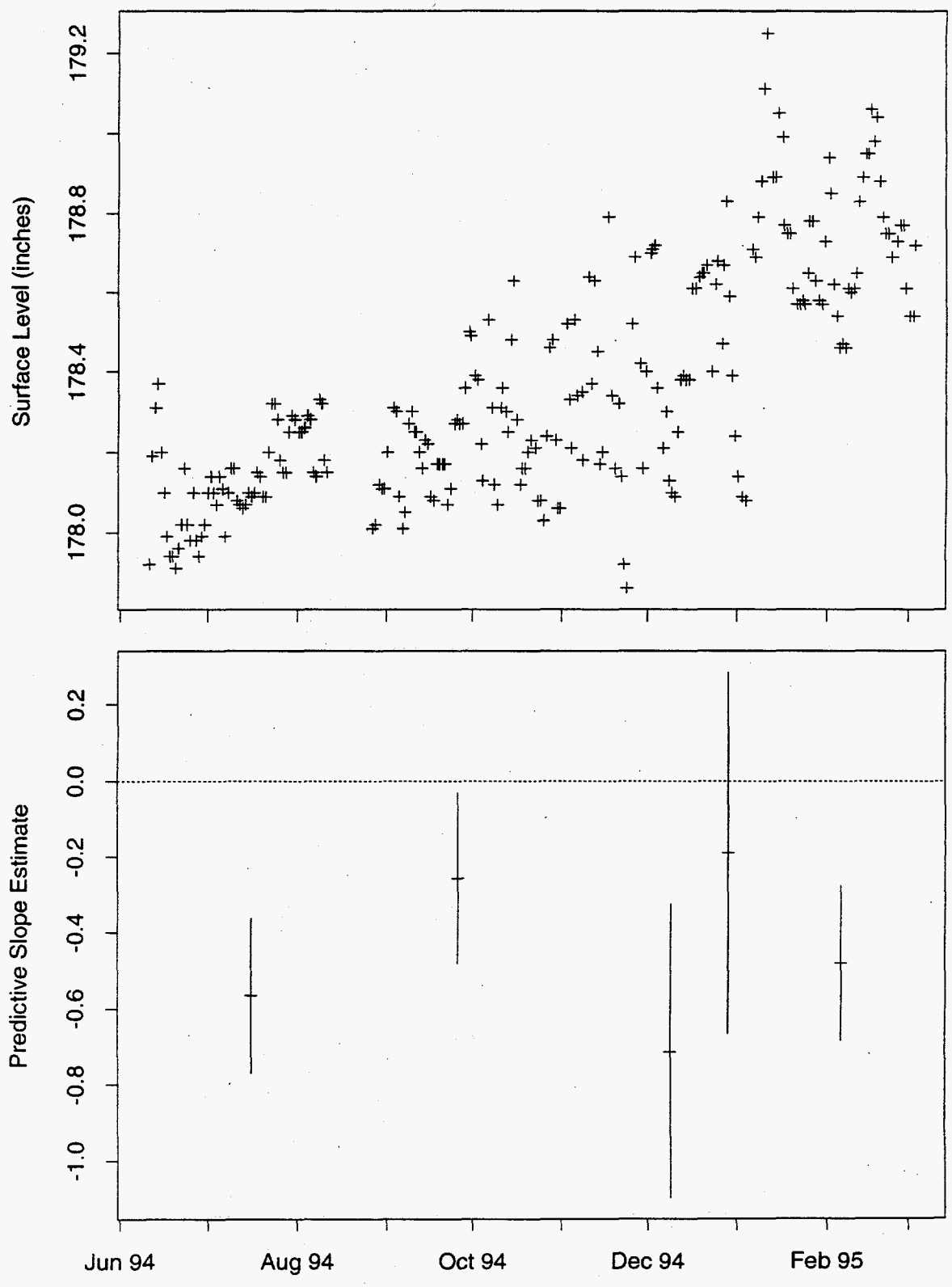

Figure 175: Tank S-106 ENRAF Data

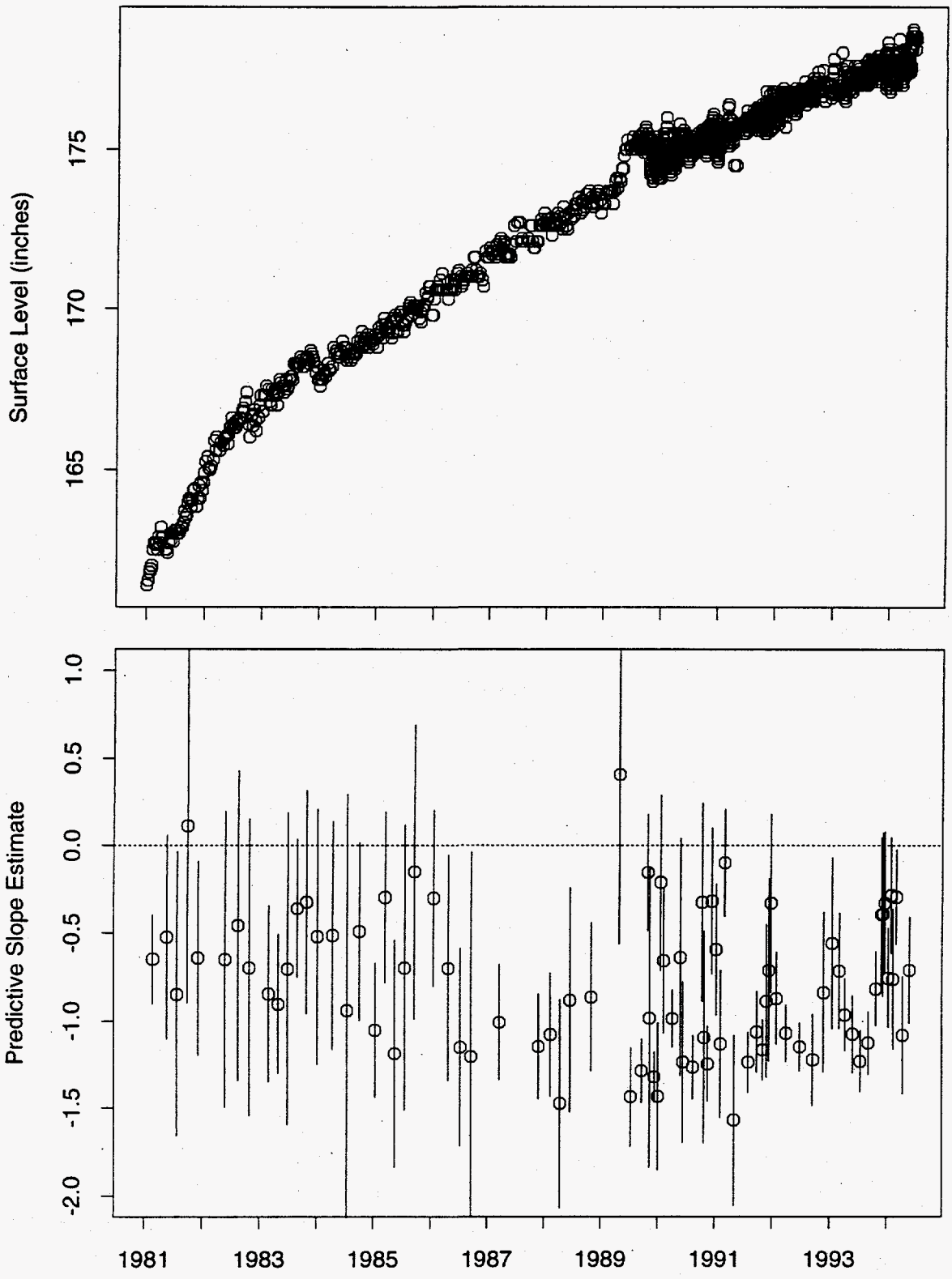

Figure 176: Tank S–106 FIC Data

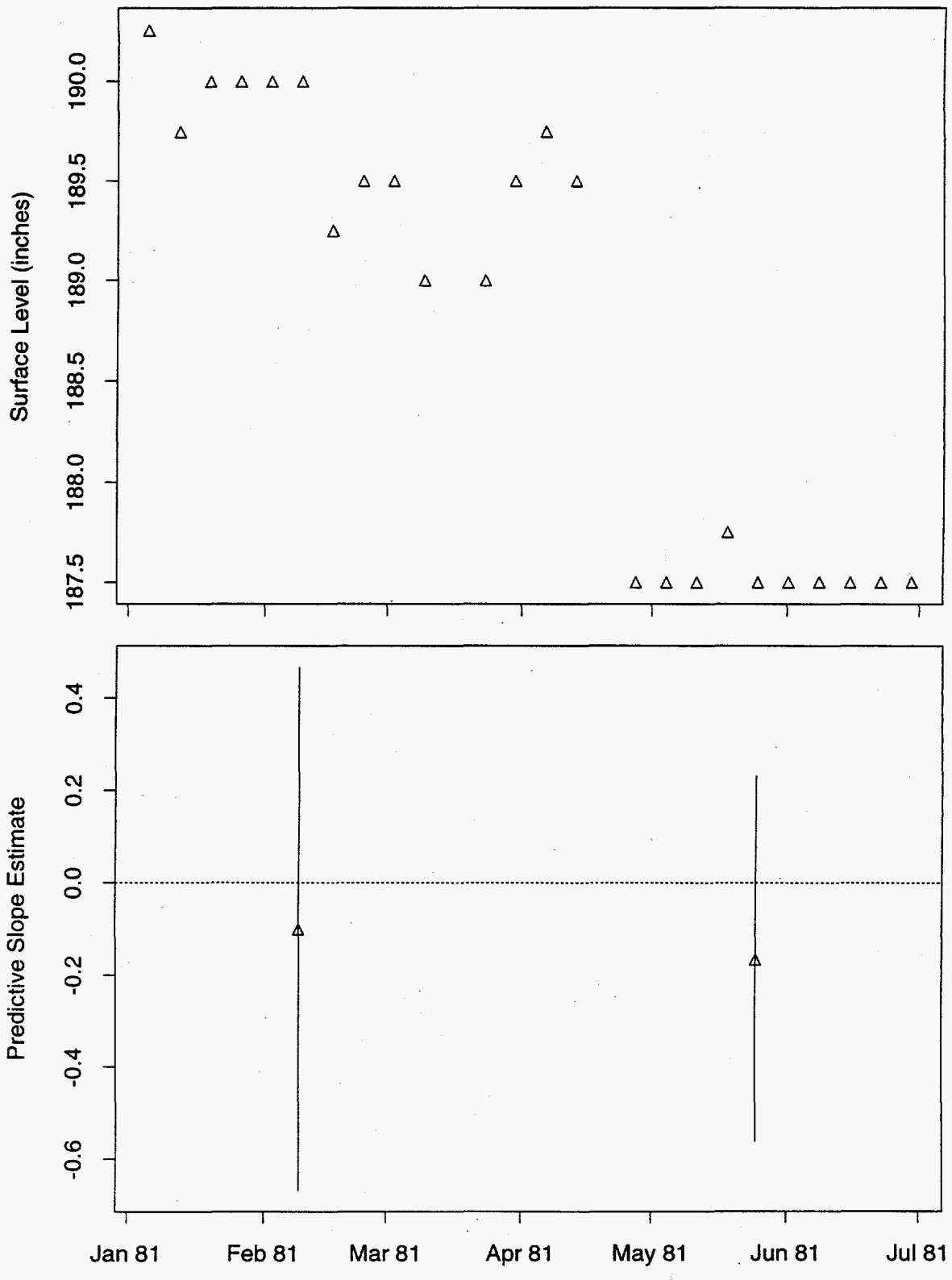

Figure 177: Tank S–106 MT Data

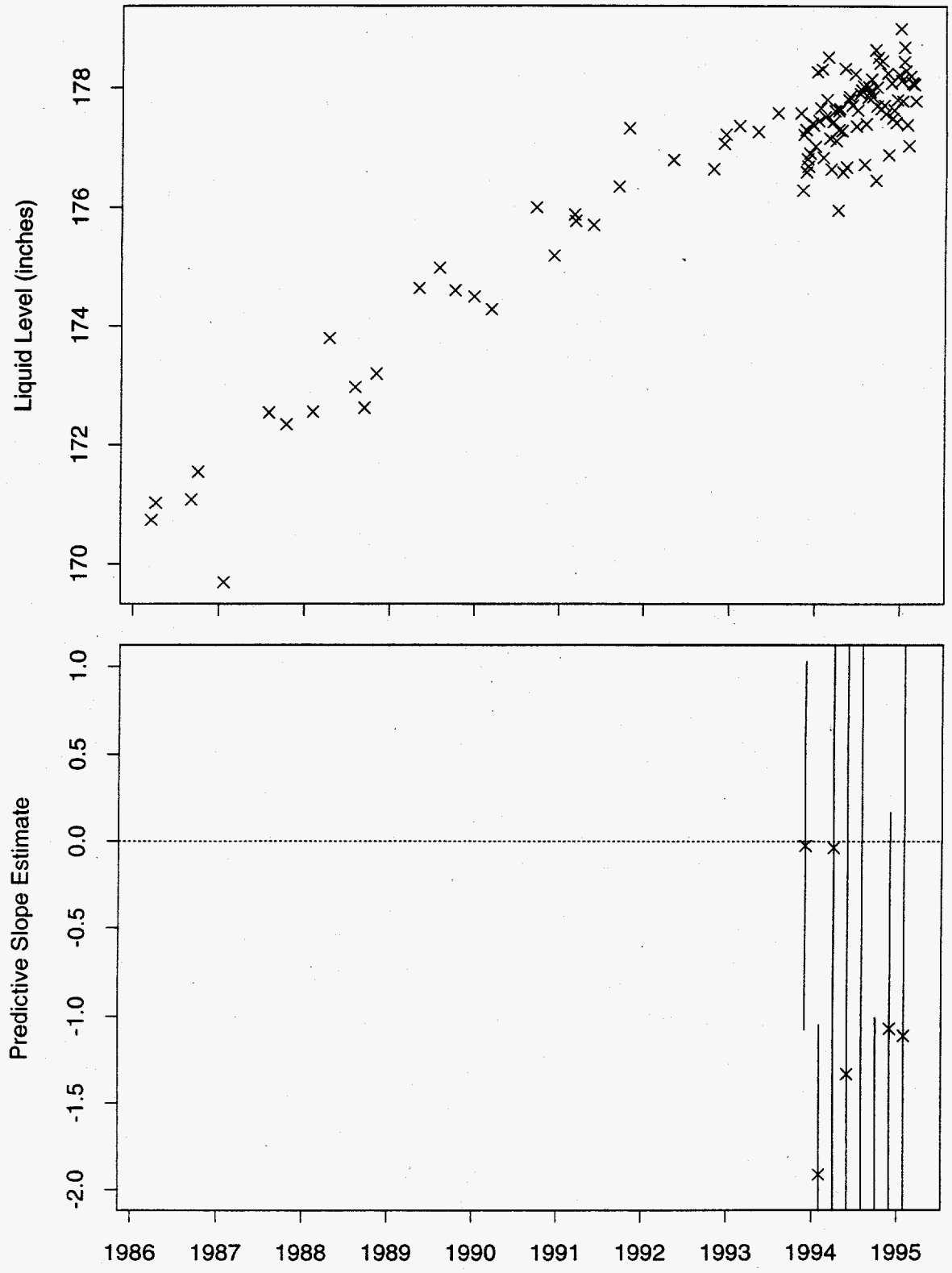

Figure 178: Tank S–106 Neutron ILL Data

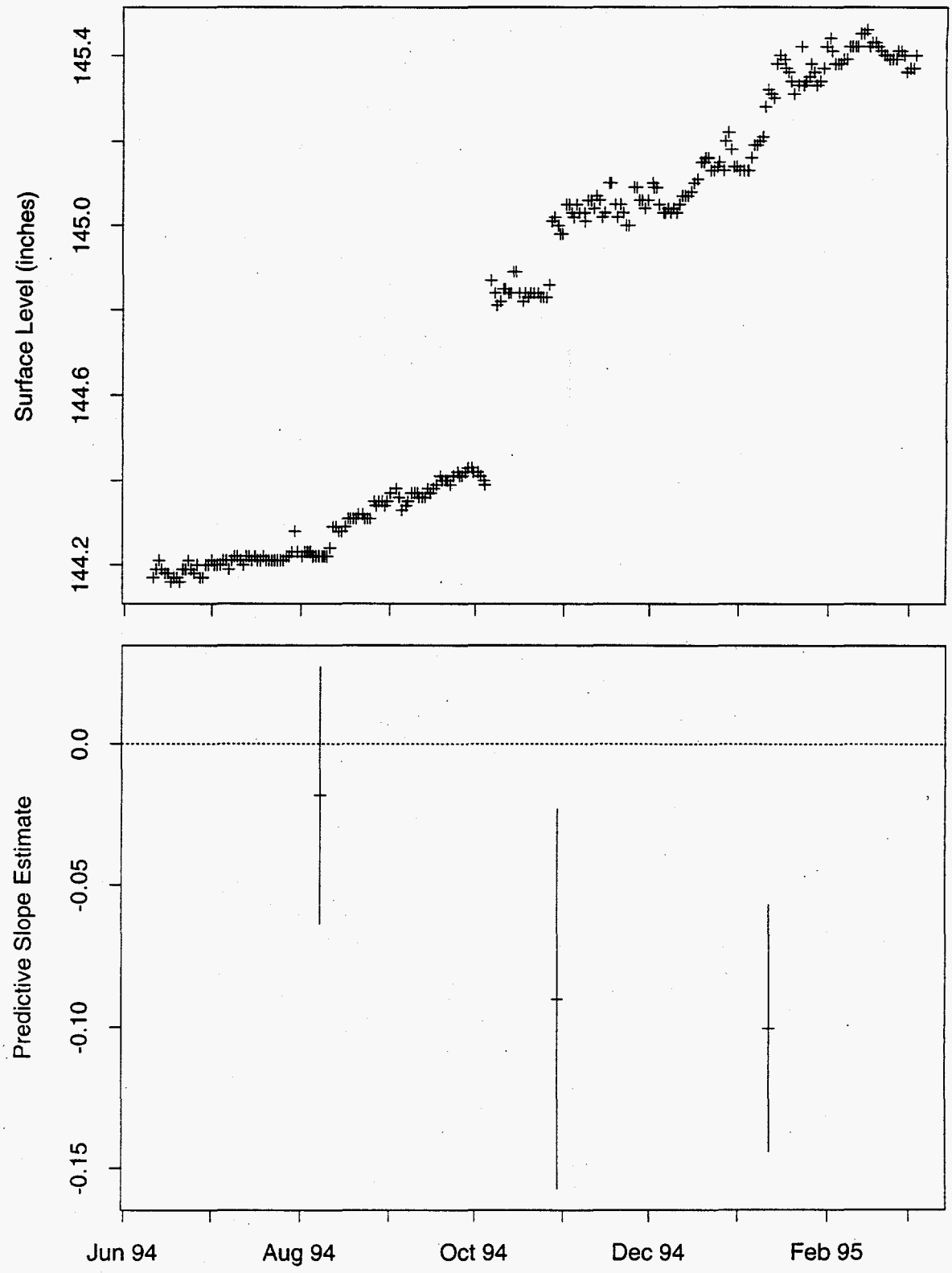

Figure 179: Tank S–107 ENRAF Data

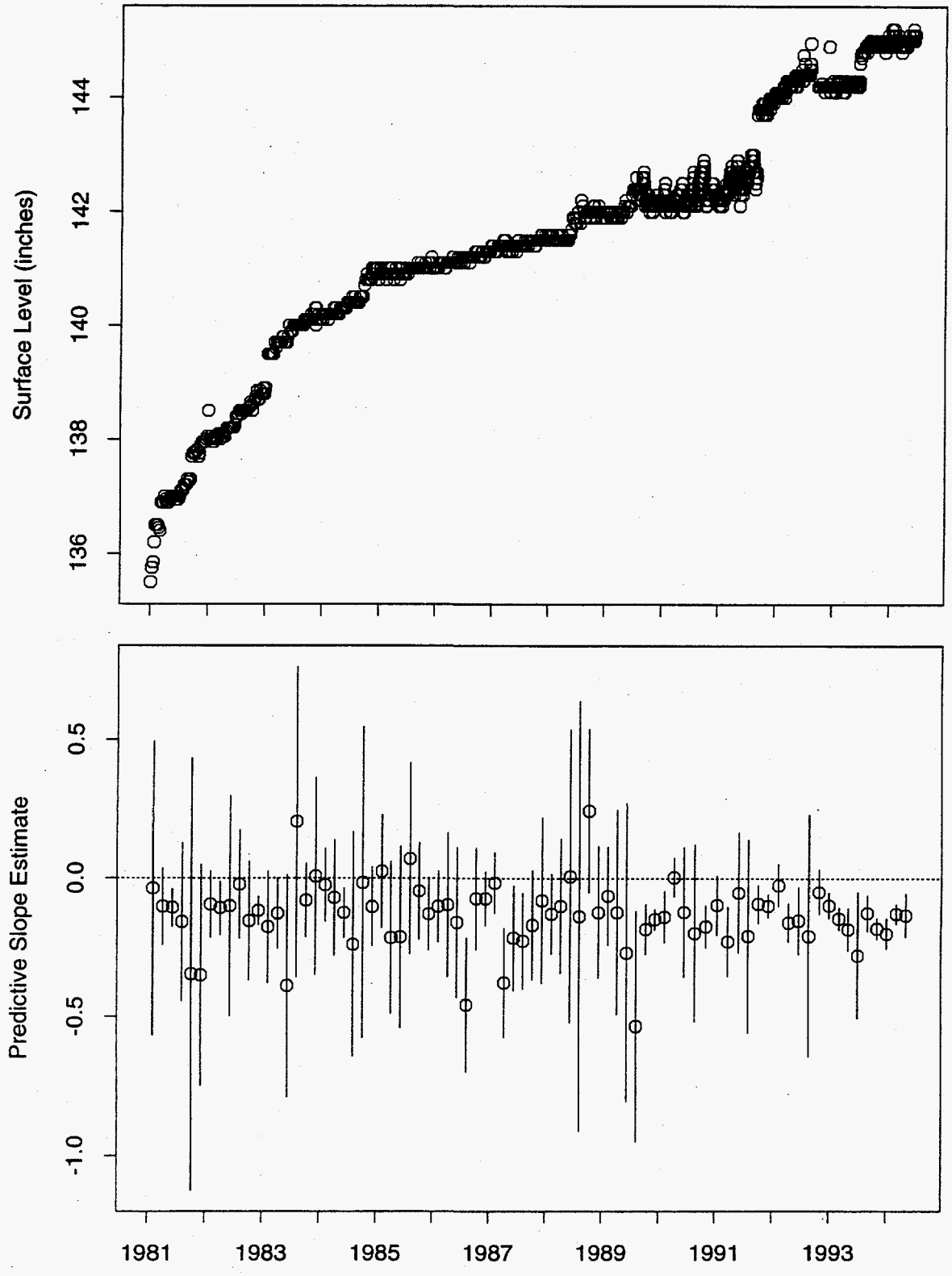

Figure 180: Tank S–107 FIC Data

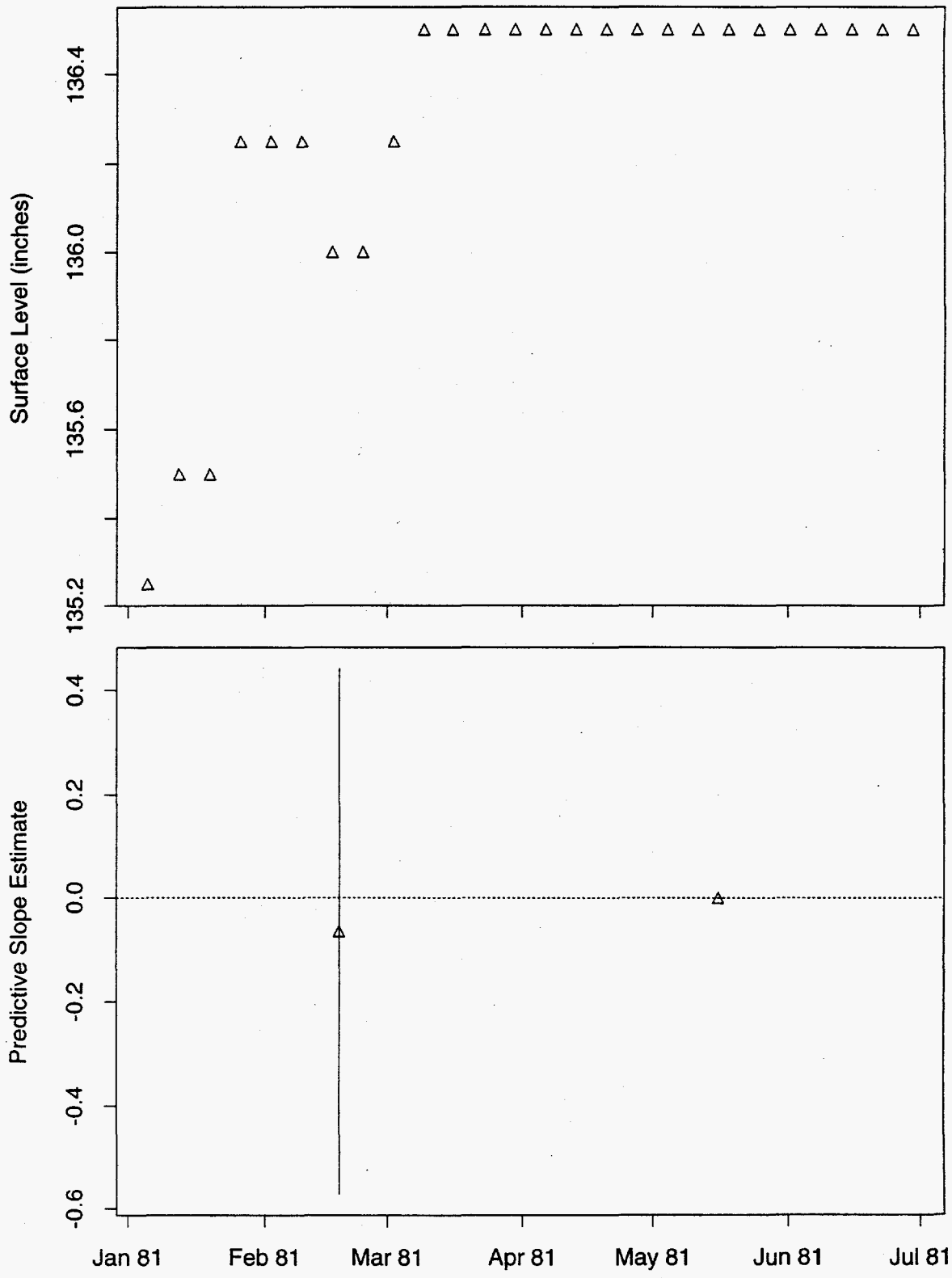

Figure 181: Tank S-107 MT Data

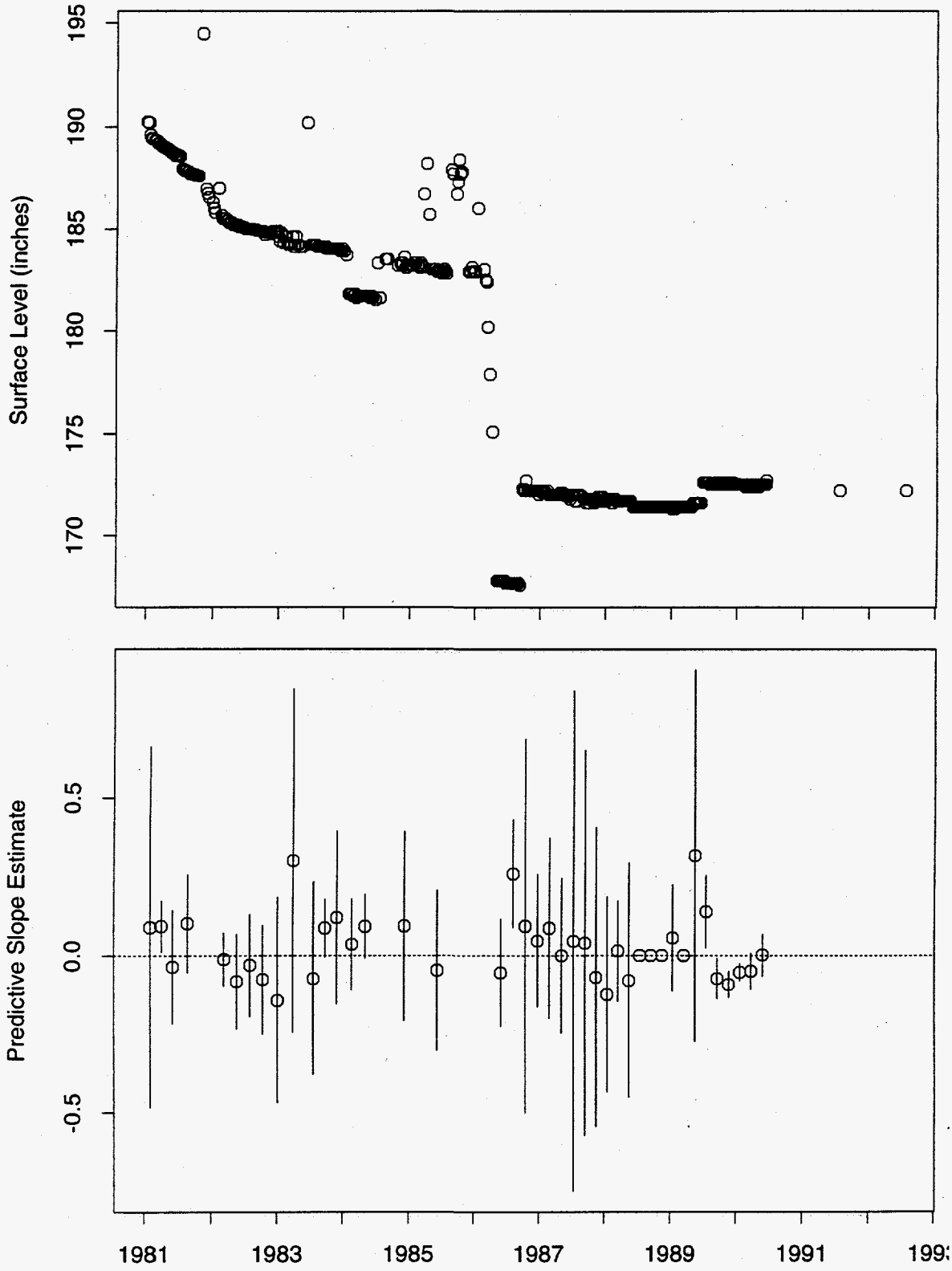

Figure 182: Tank S-108 FIC Data

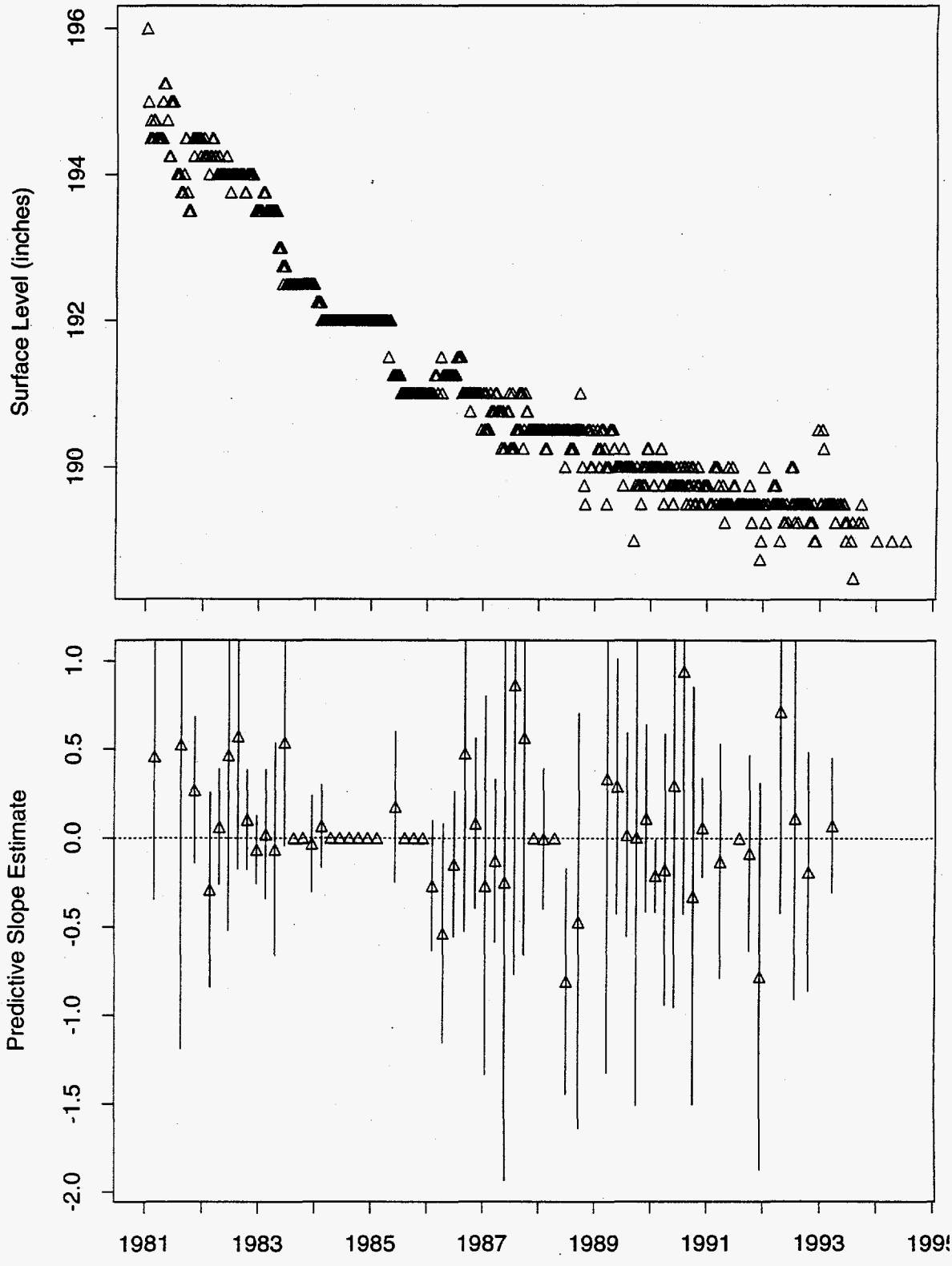

Figure 183: Tank S–108 MT Data

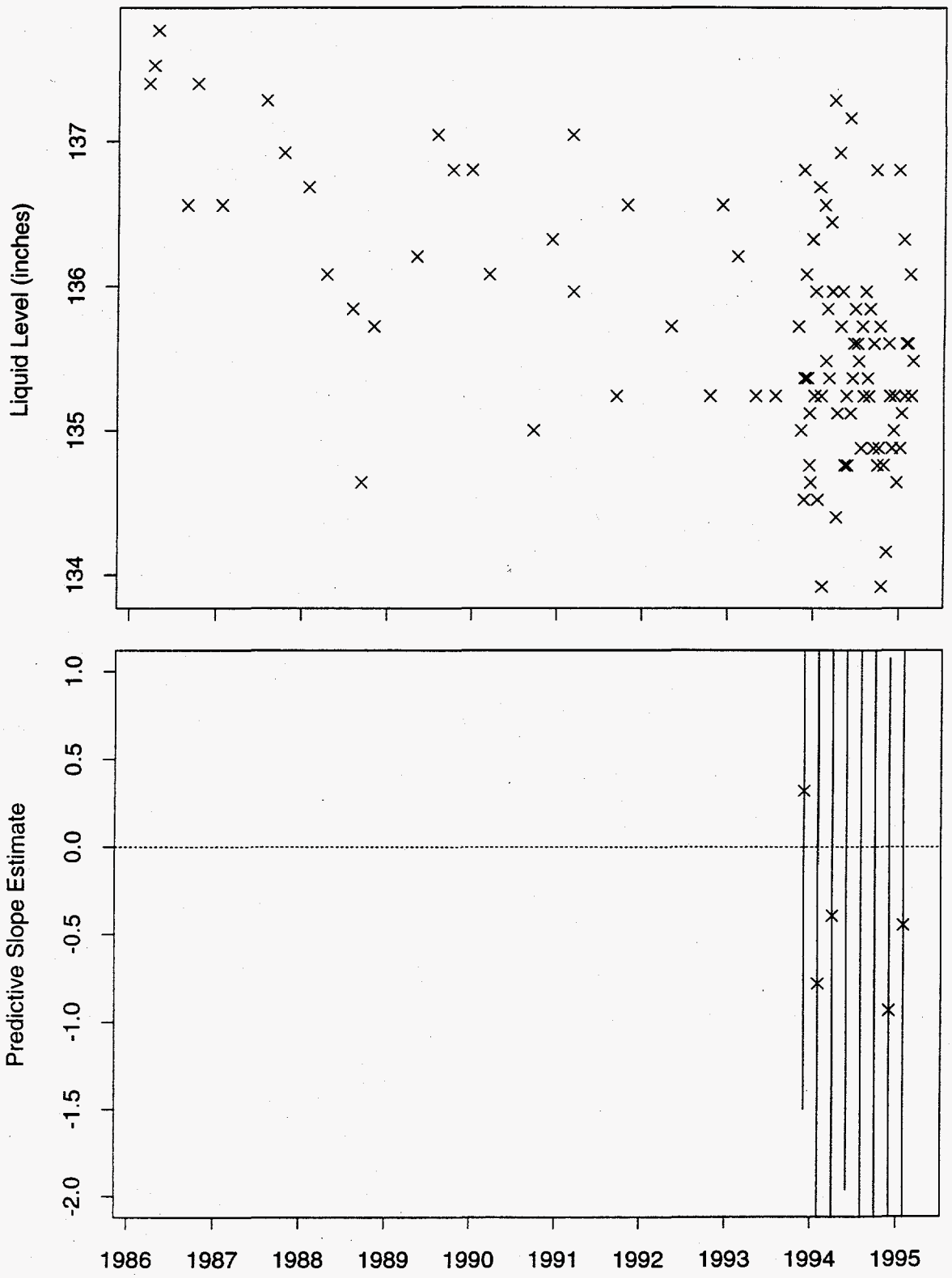

Figure 184: Tank S–108 Neutron ILL Data

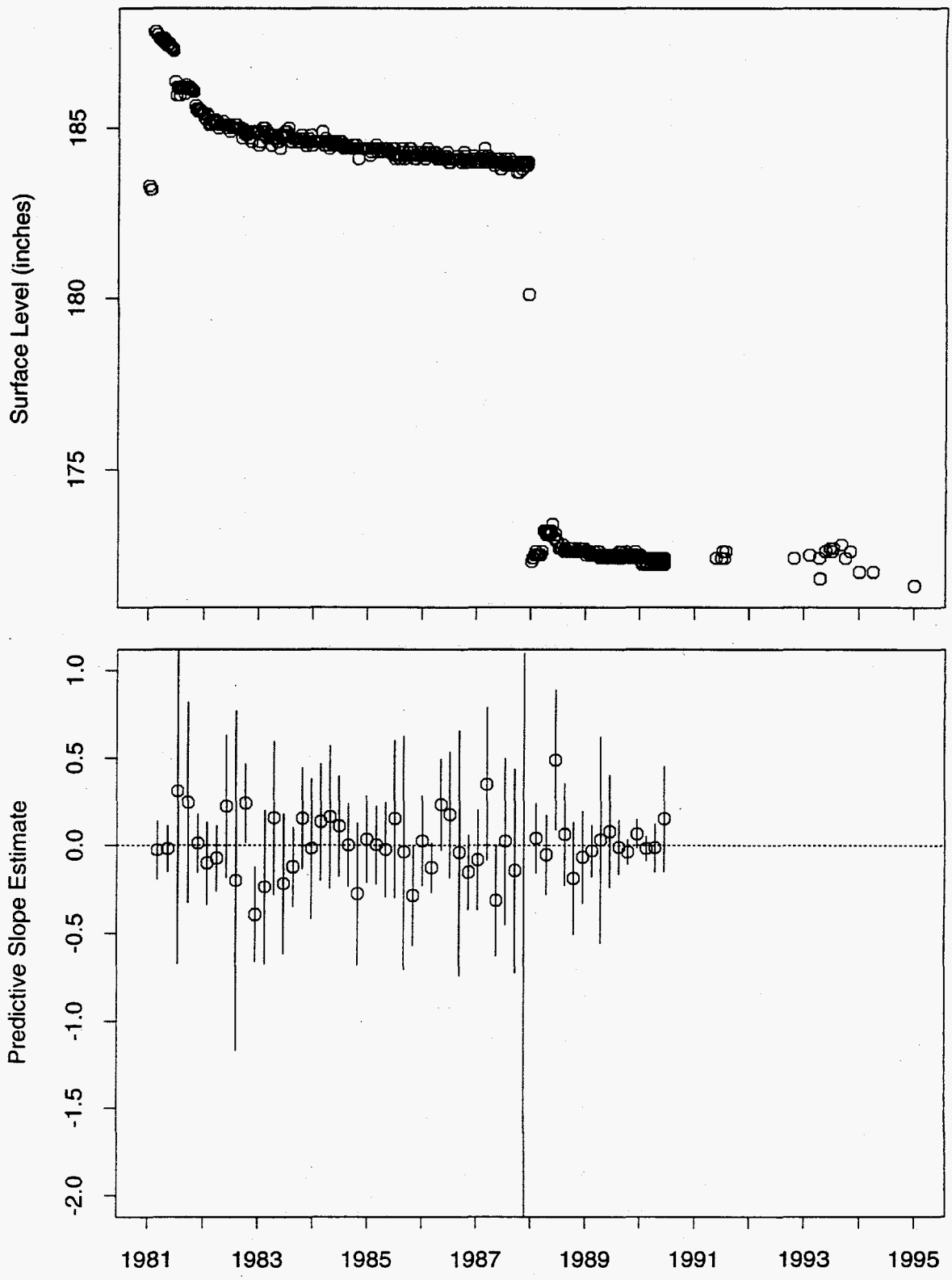

Figure 185: Tank S–109 FIC Data

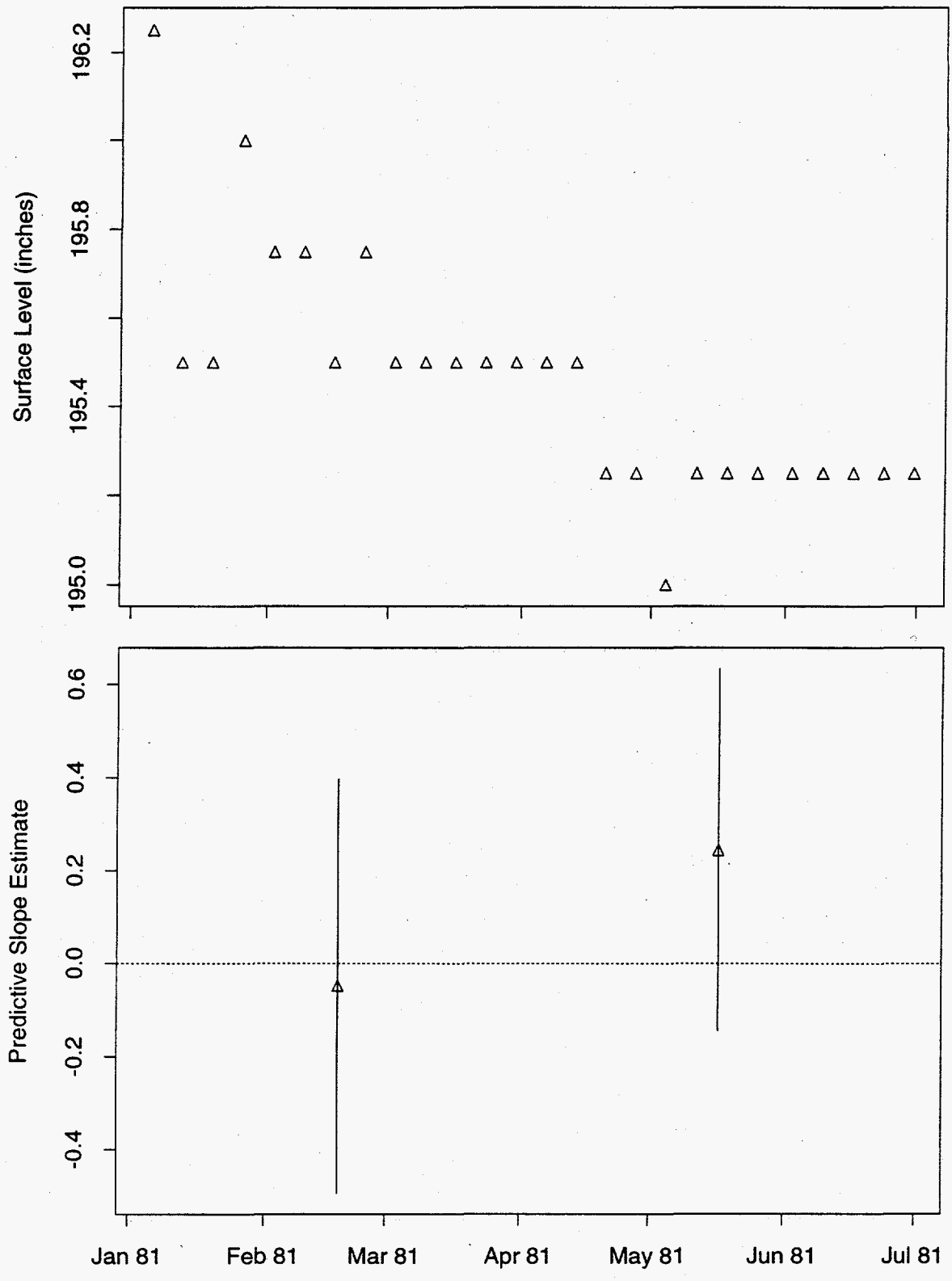

Figure 186: Tank S–109 MT Data

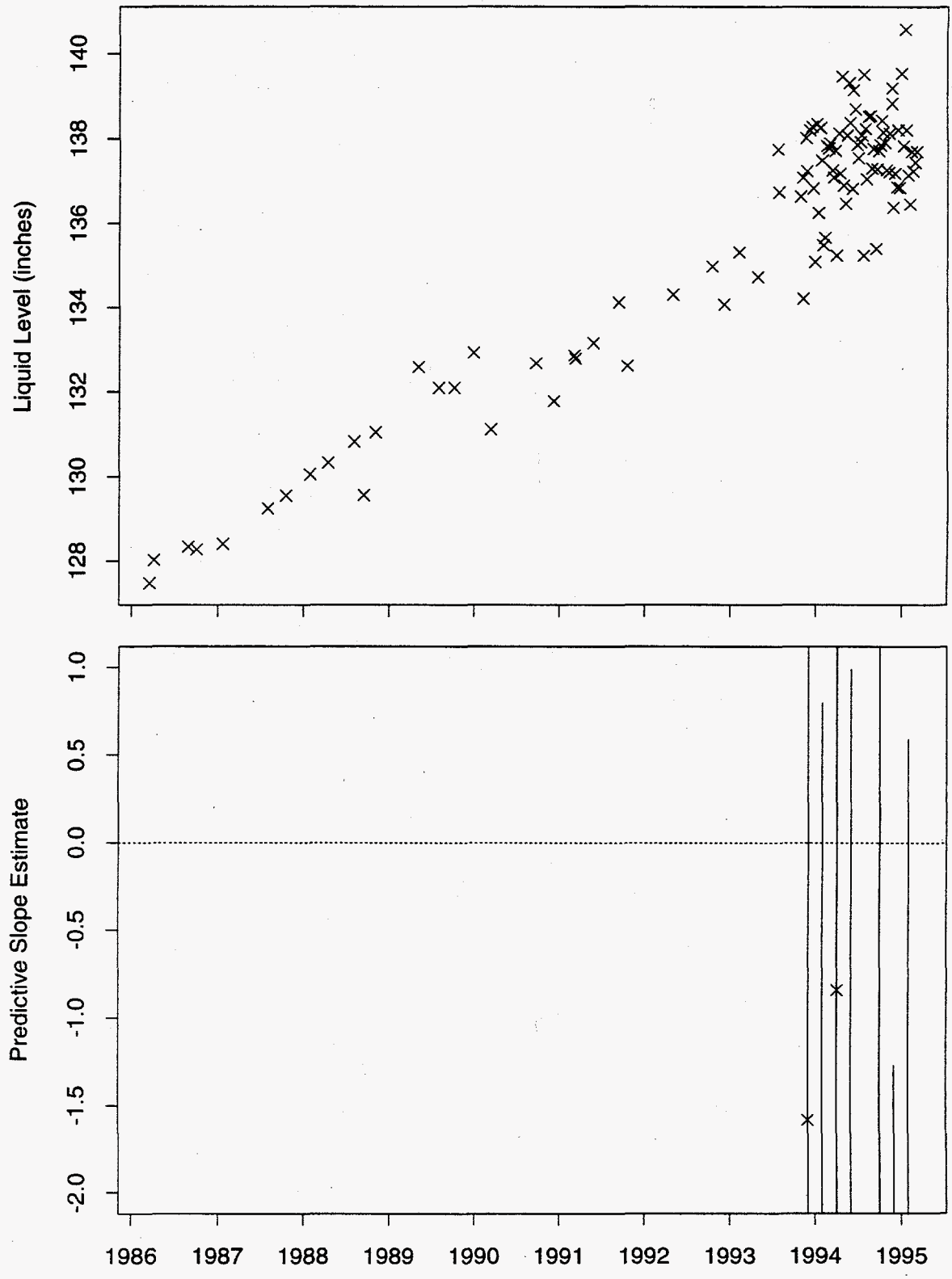

Figure 187: Tank S–109 Neutron ILL Data

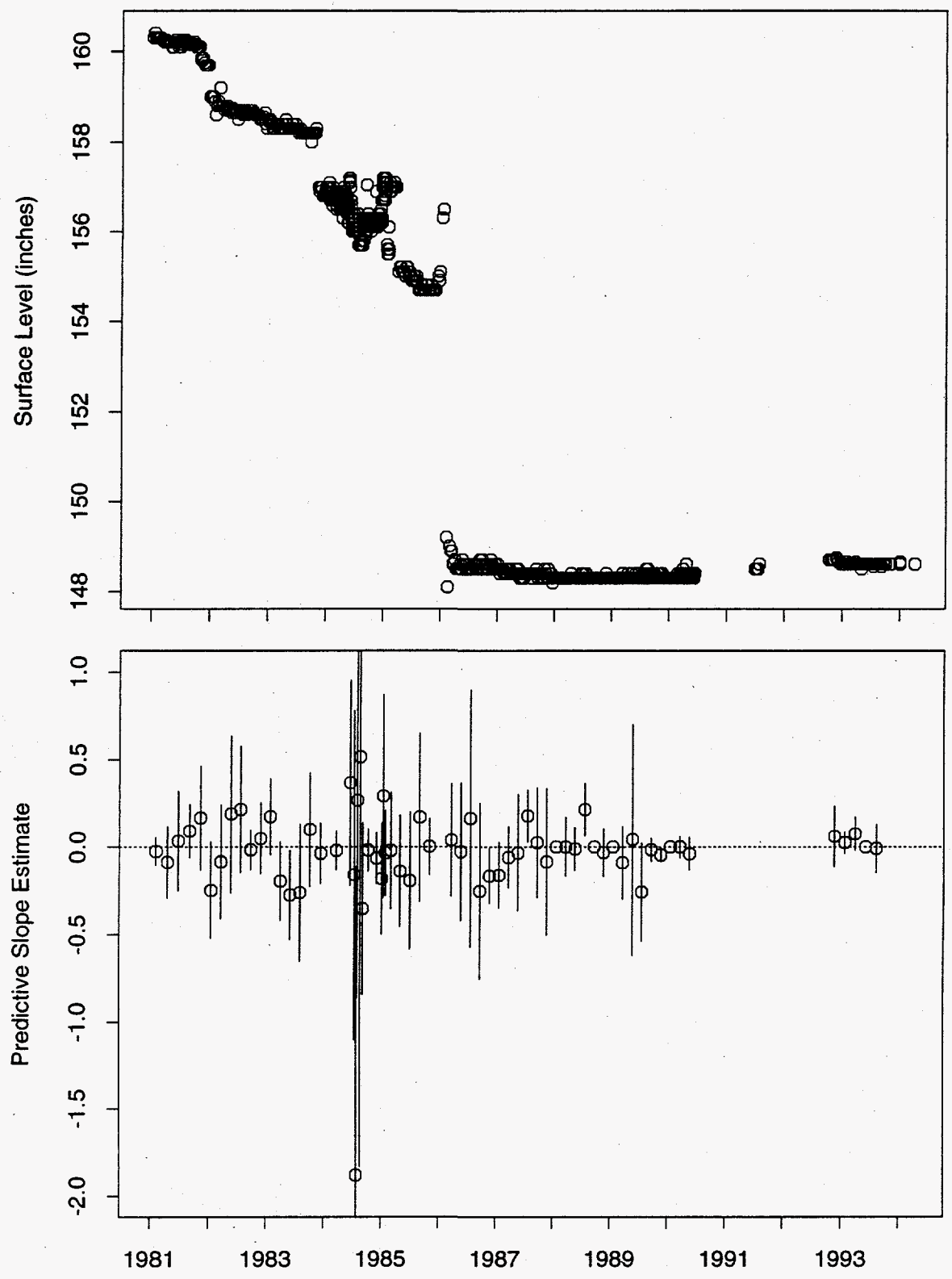

Figure 188: Tank S-110 FIC Data

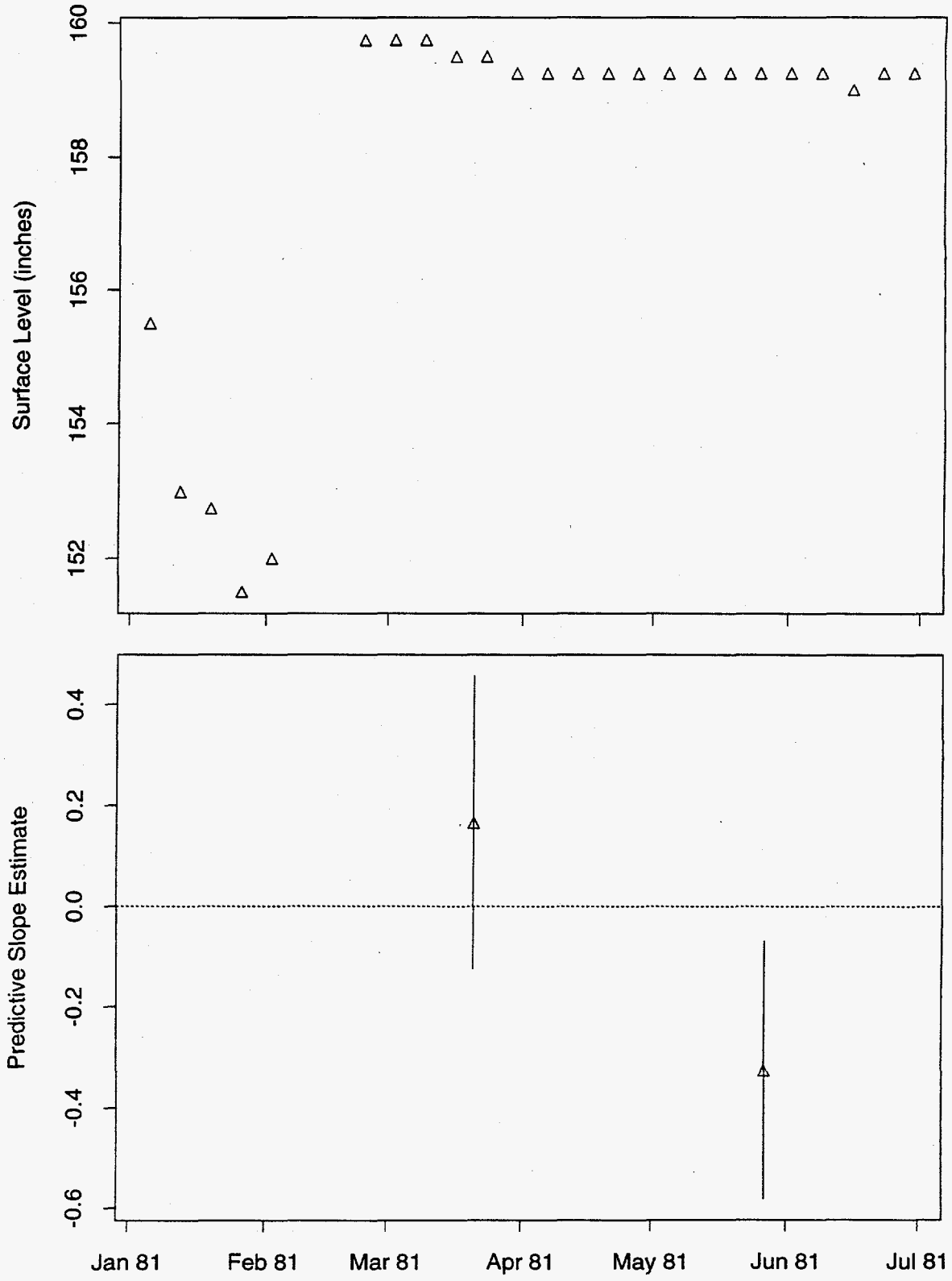

Figure 189: Tank S–110 MT Data

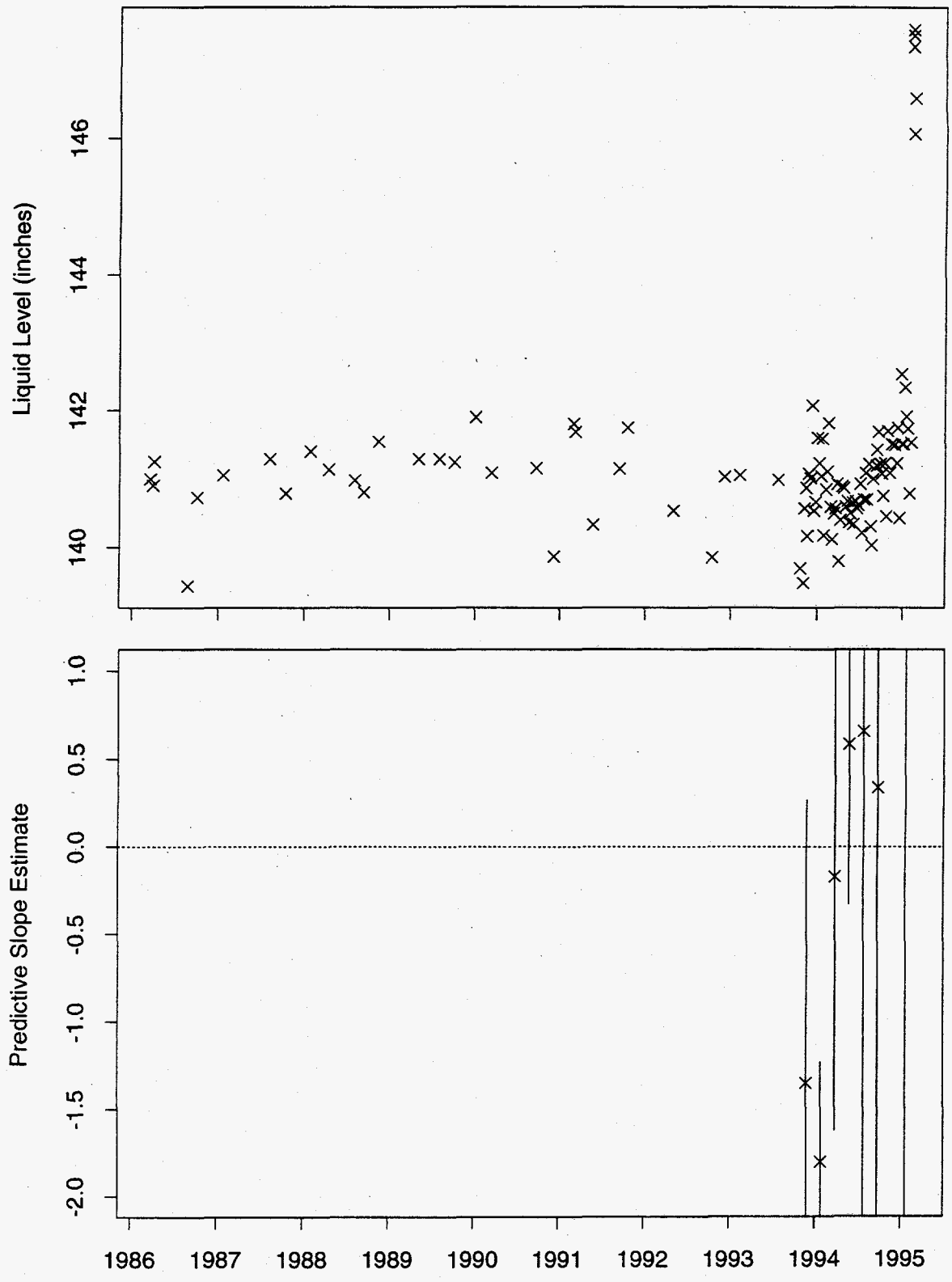

Figure 190: Tank S-110 Neutron ILL Data

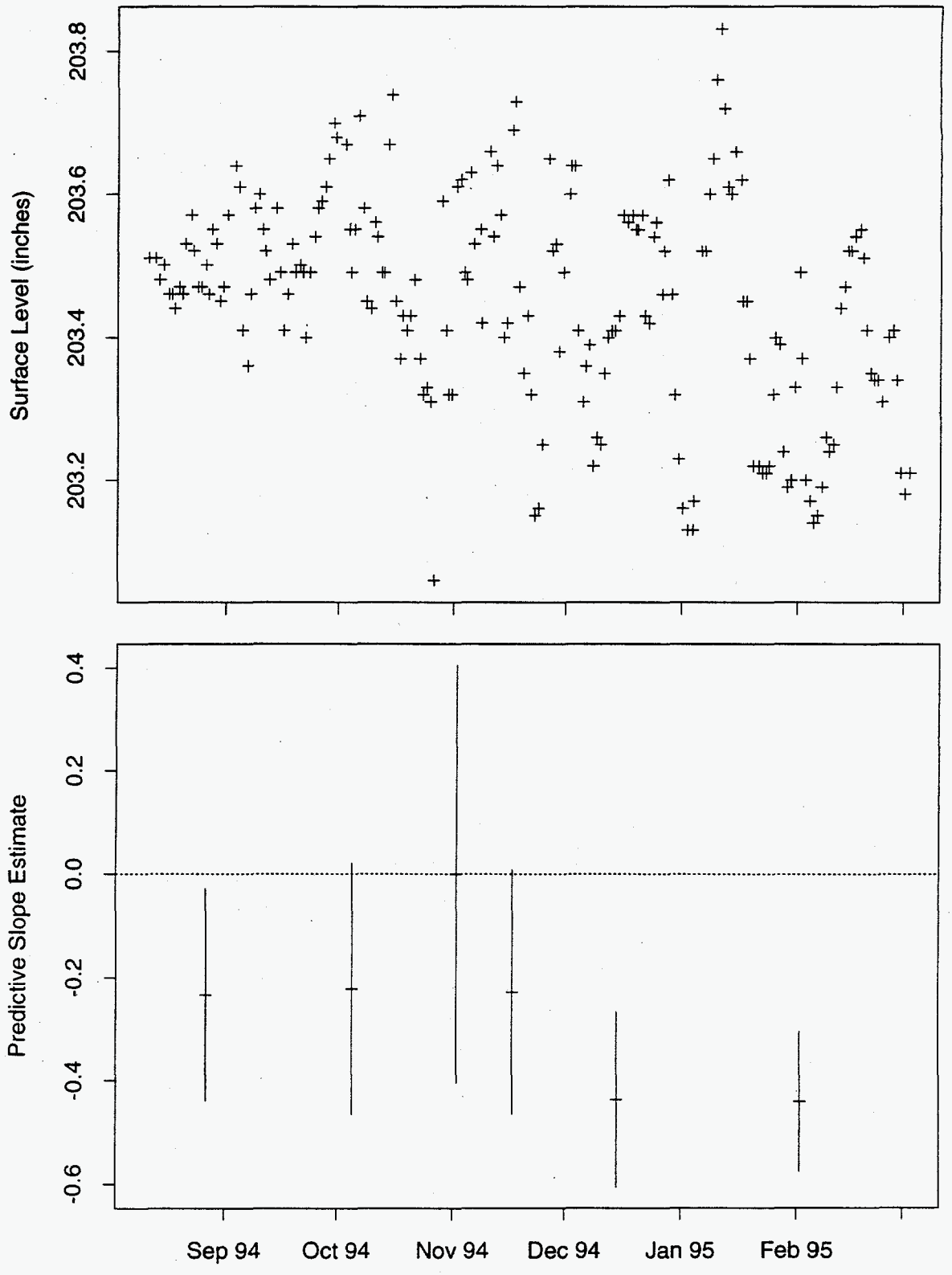

Figure 191: Tank S-111 ENRAF Data

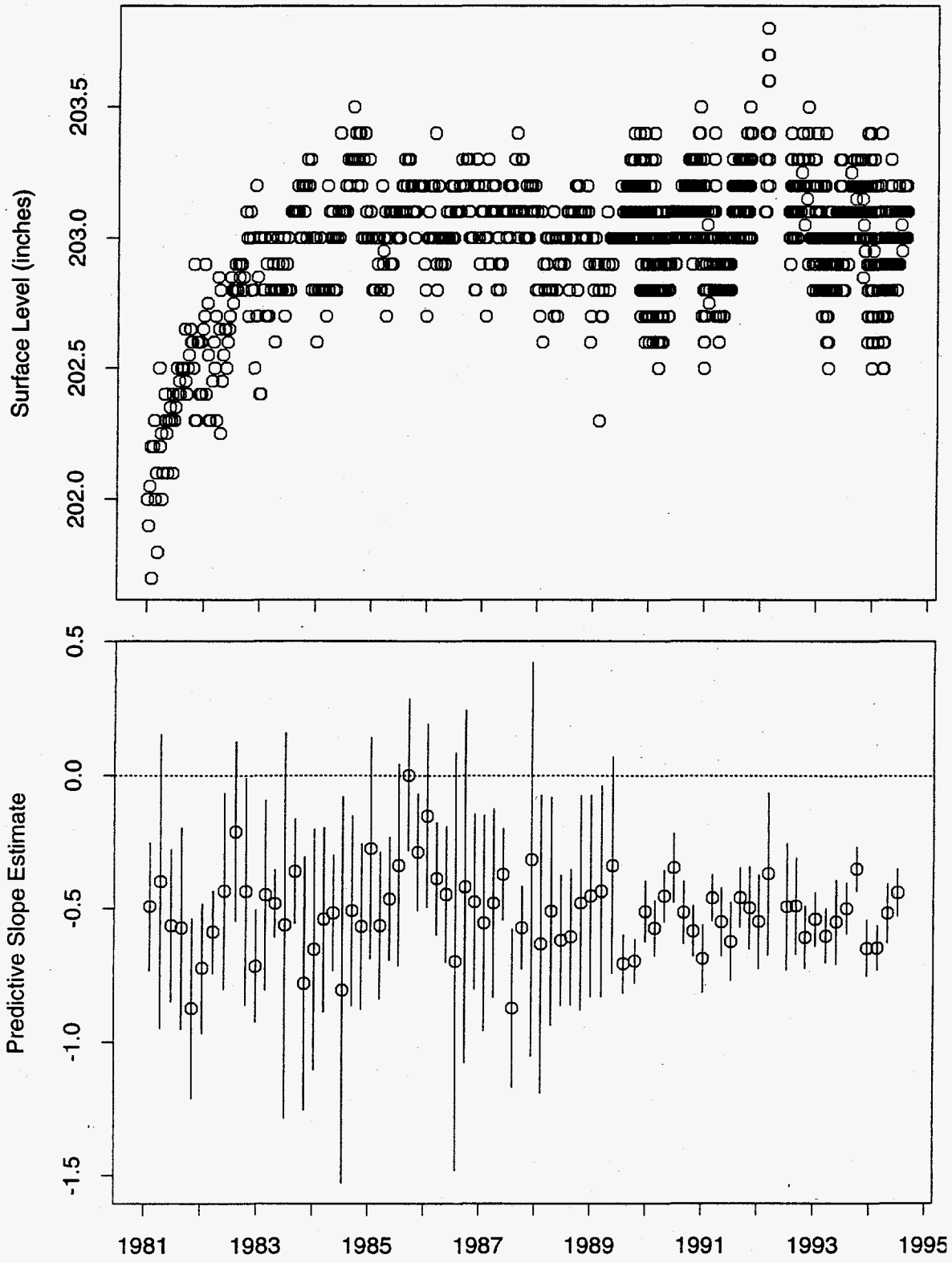

Figure 192: Tank S–111 FIC Data

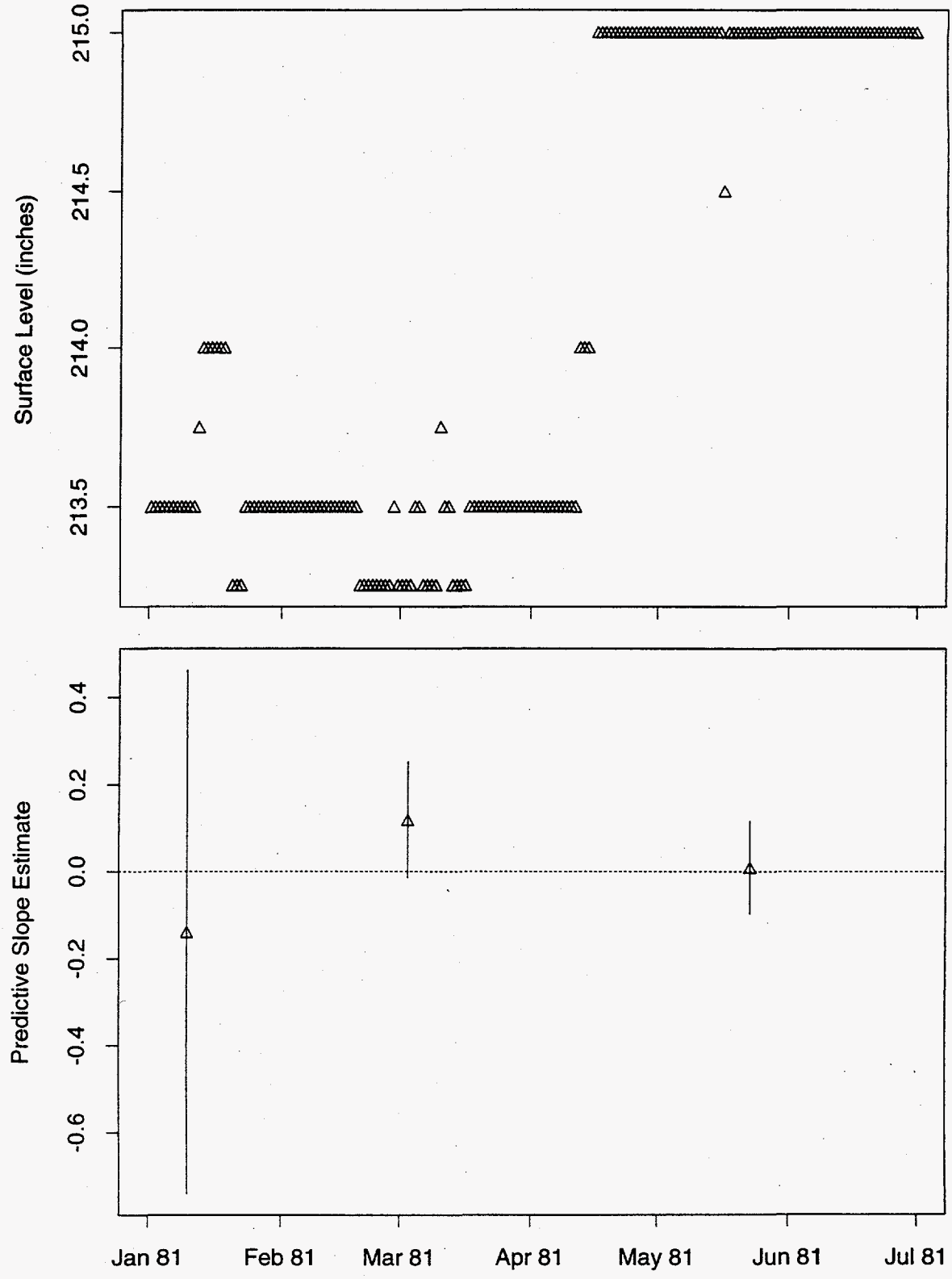

Figure 193: Tank S-111 MT Data

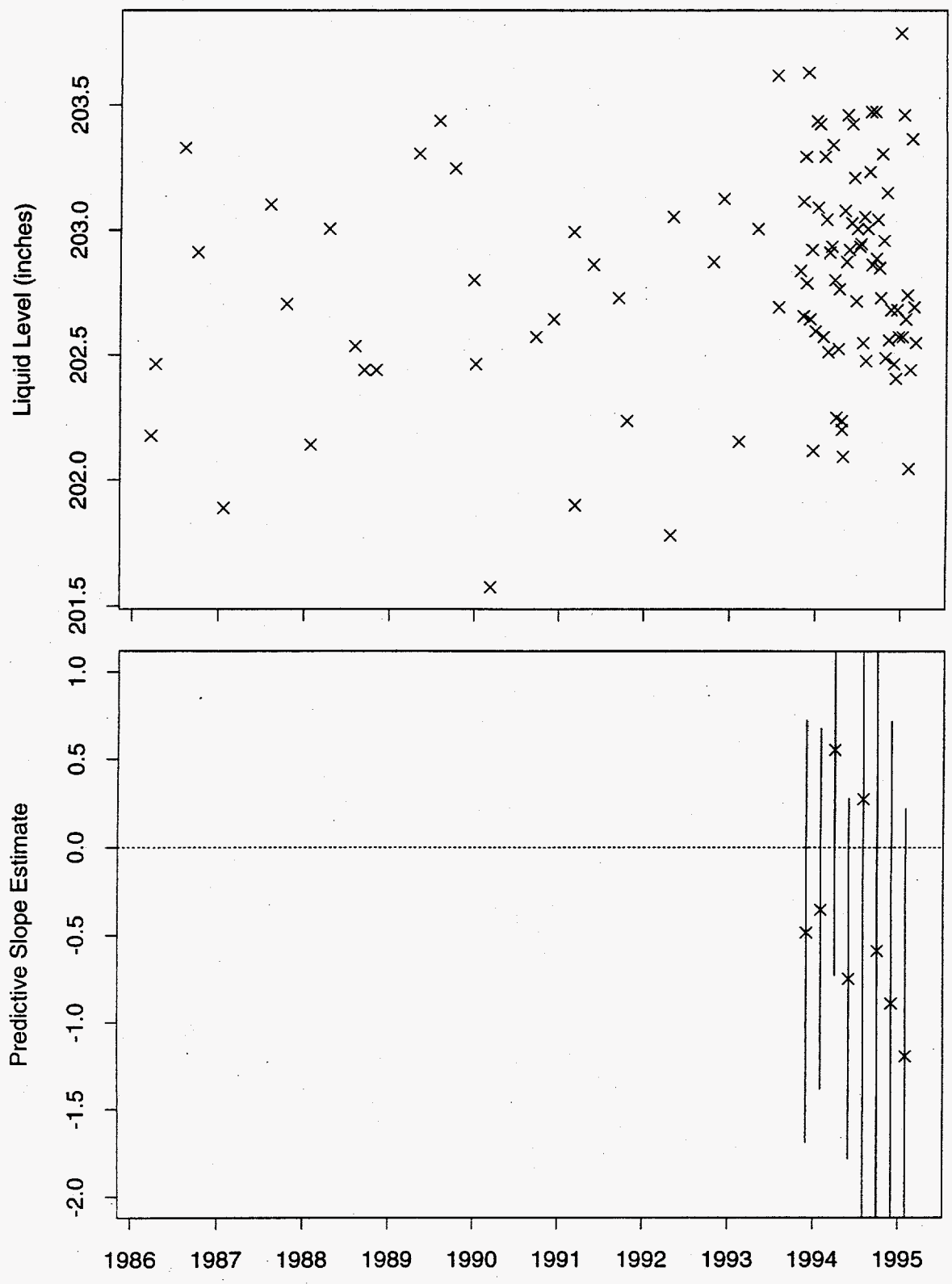

Figure 194: Tank S–111 Neutron ILL Data

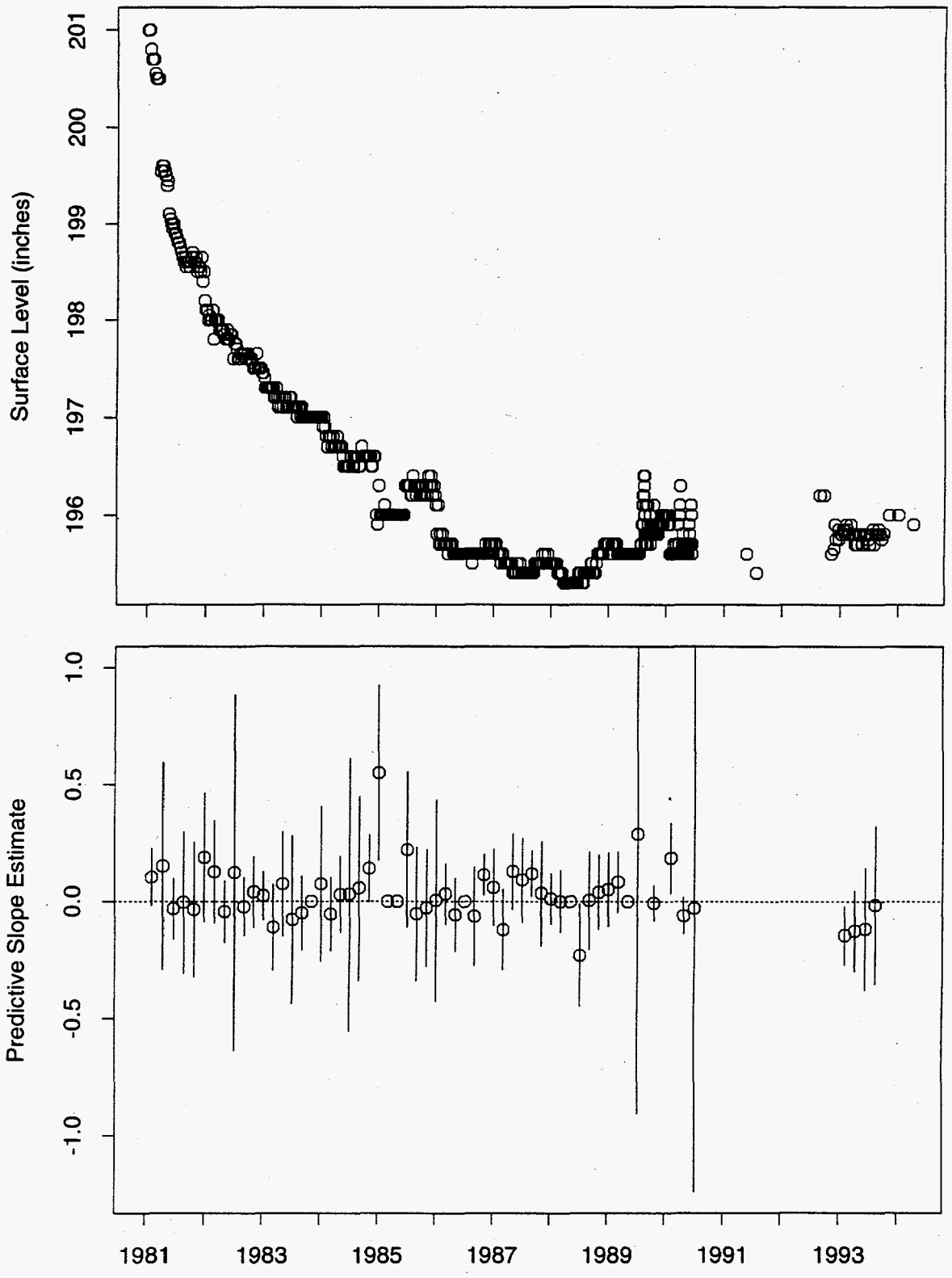

Figure 195: Tank S–112 FIC Data

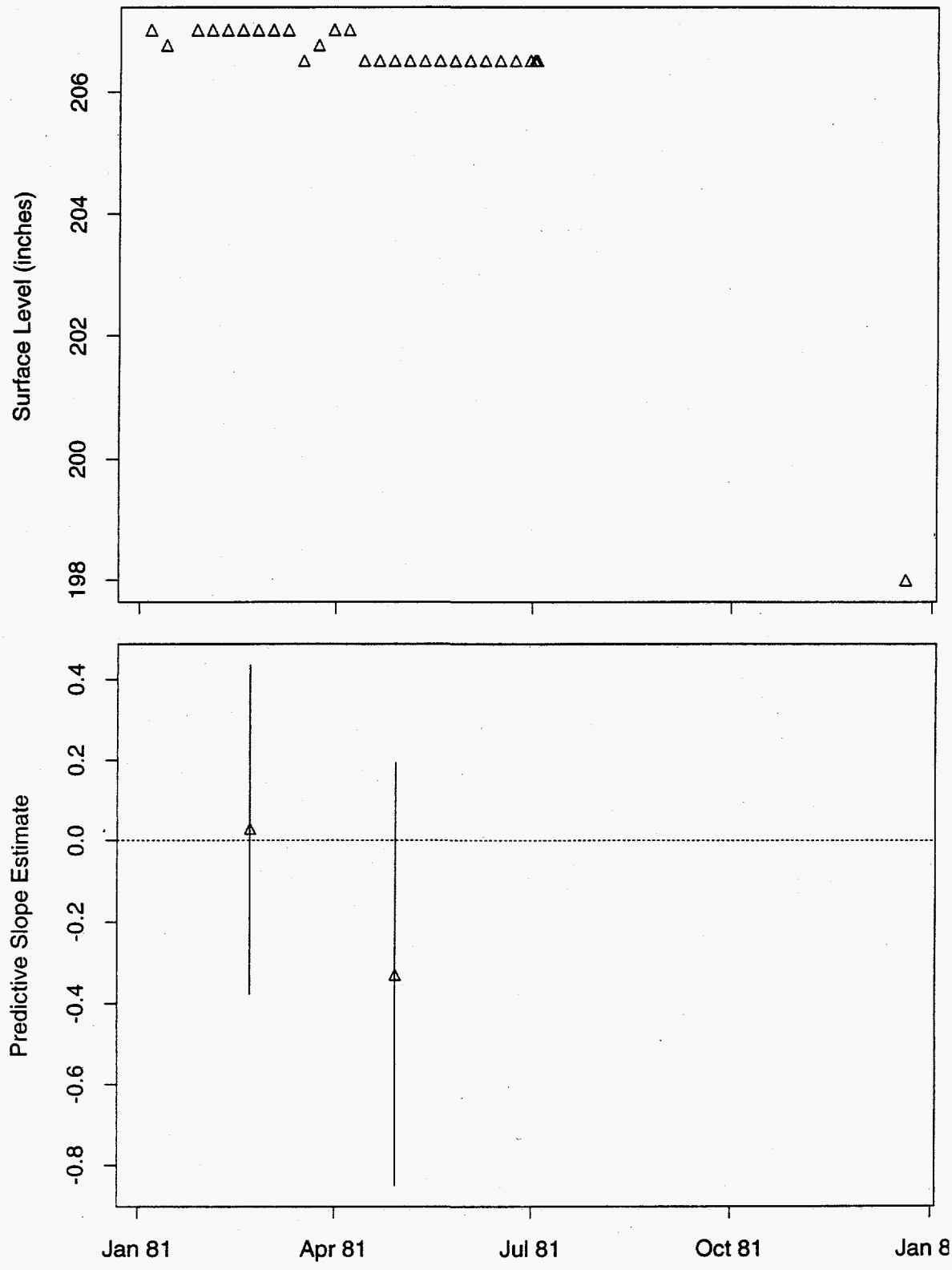

Figure 196: Tank S–112 MT Data

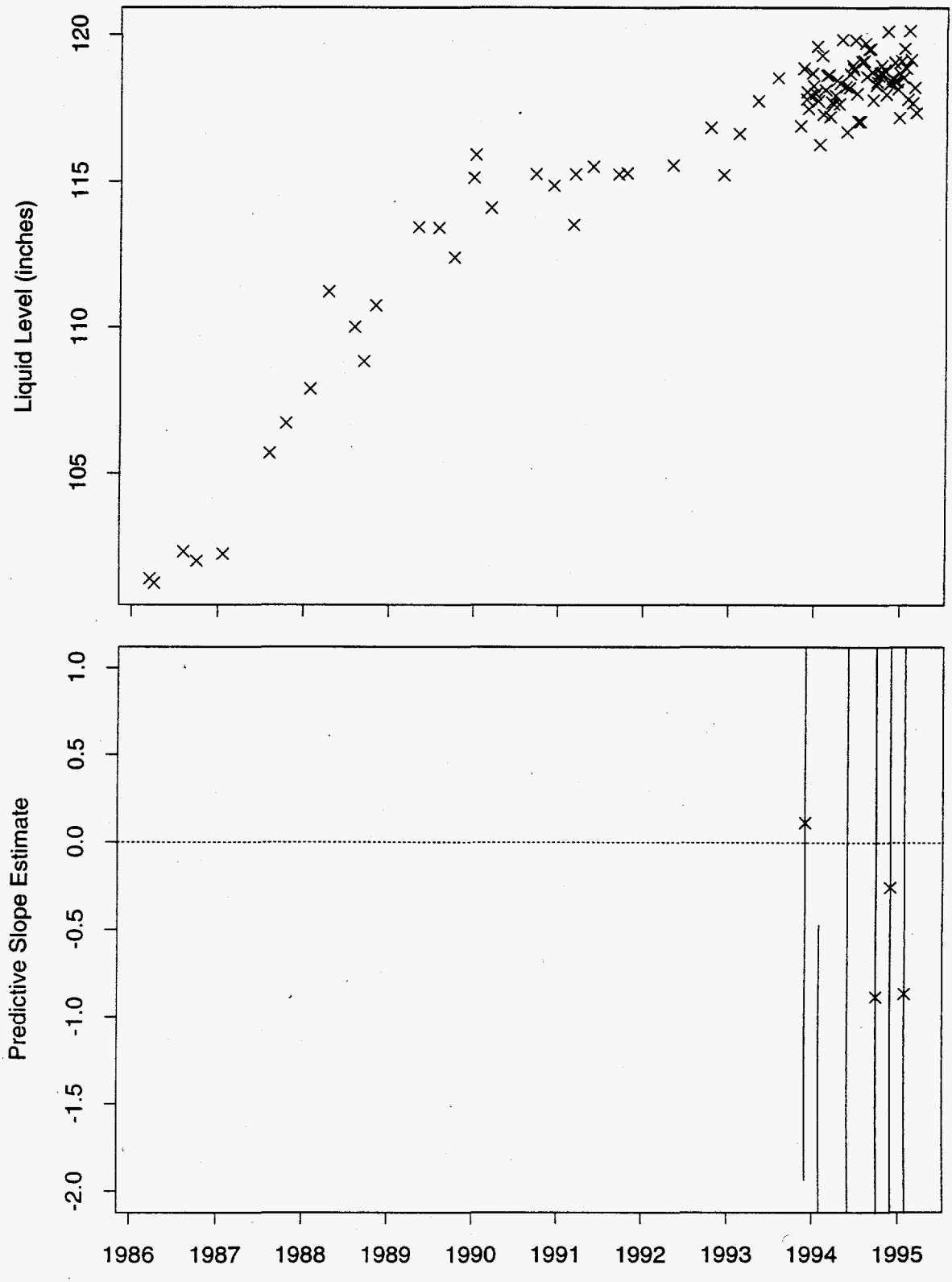

Figure 197: Tank S–112 Neutron ILL Data

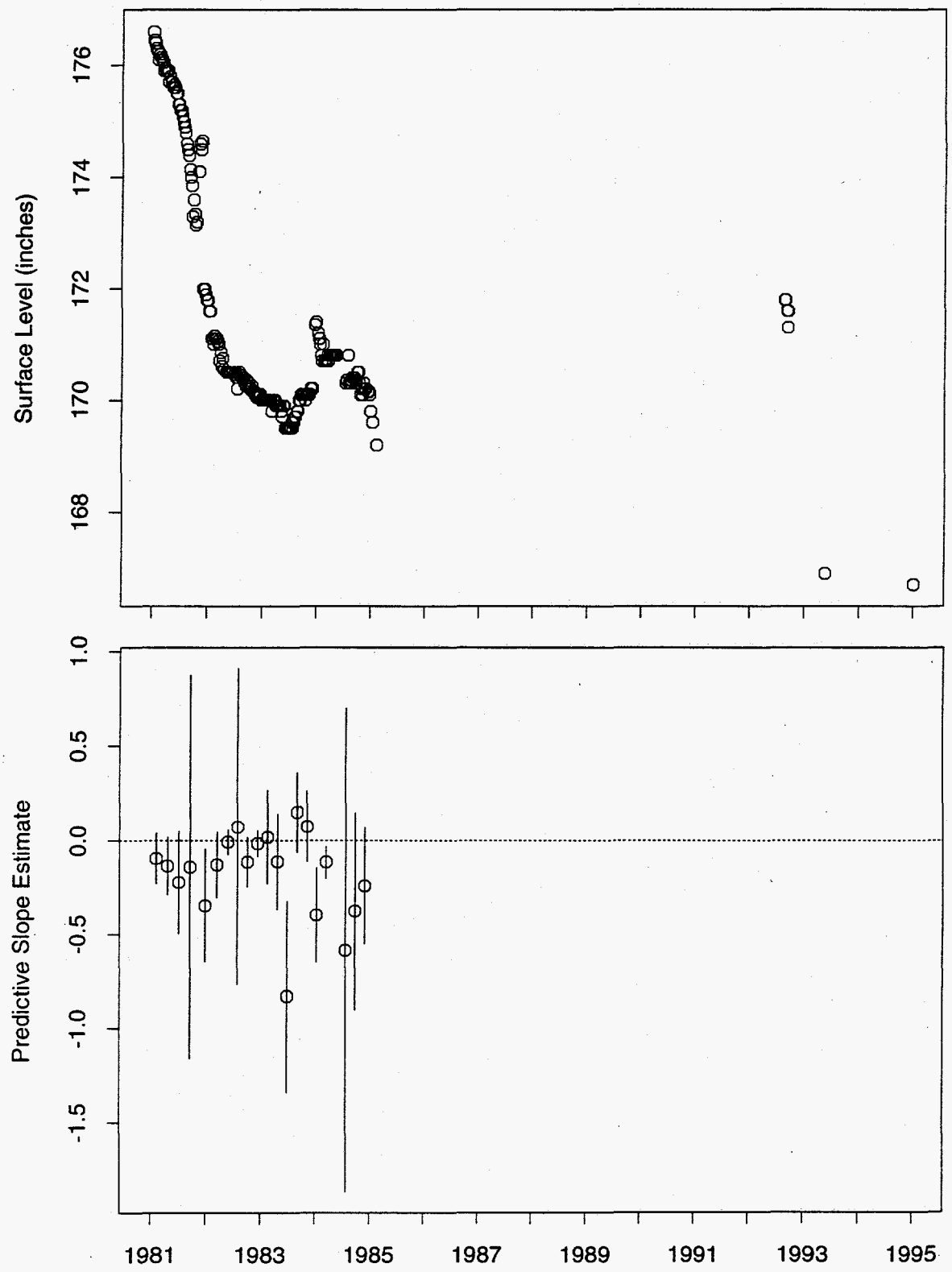

Figure 198: Tank SX–101 FIC Data

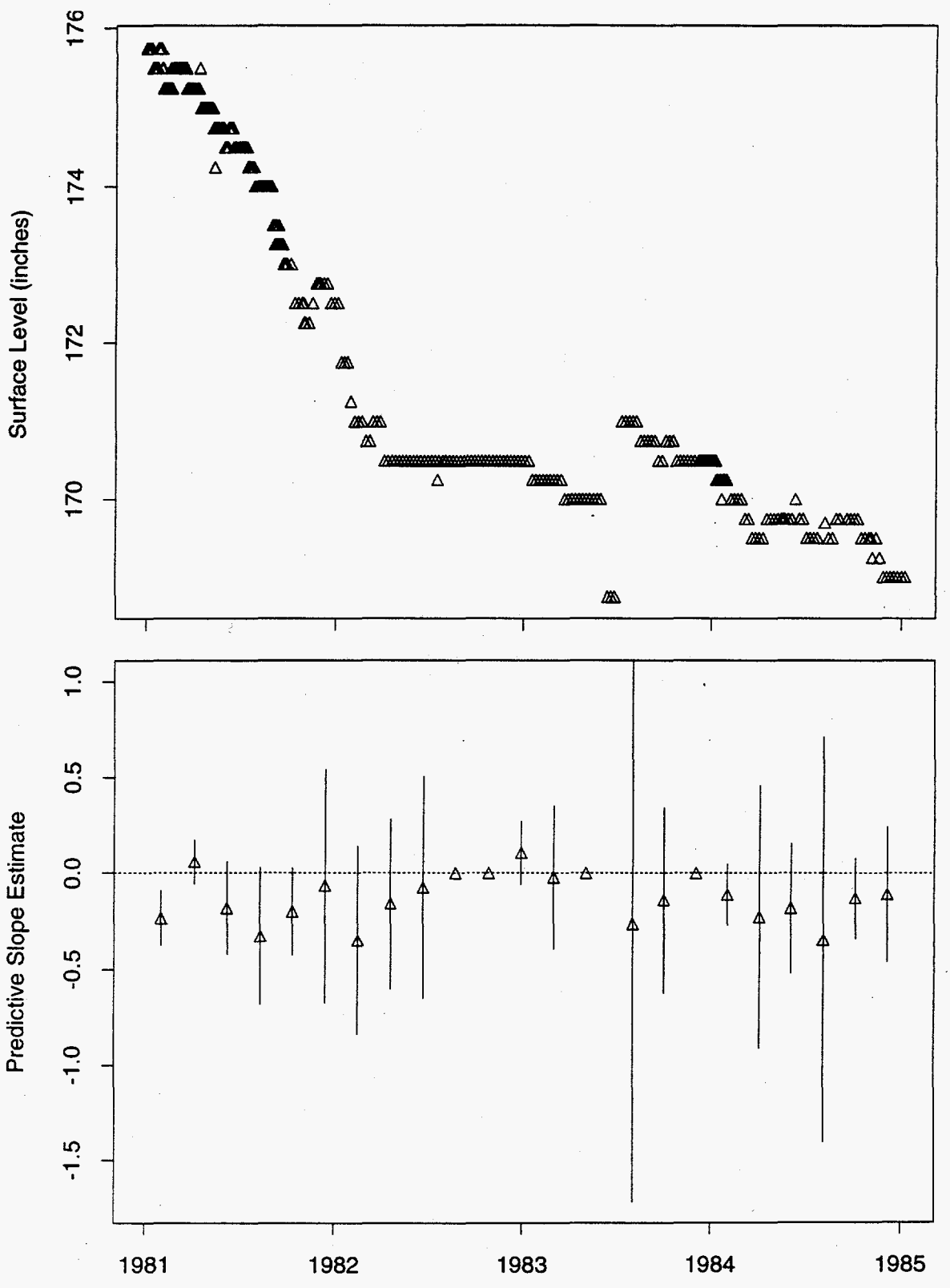

Figure 199: Tank SX–101 MT Data

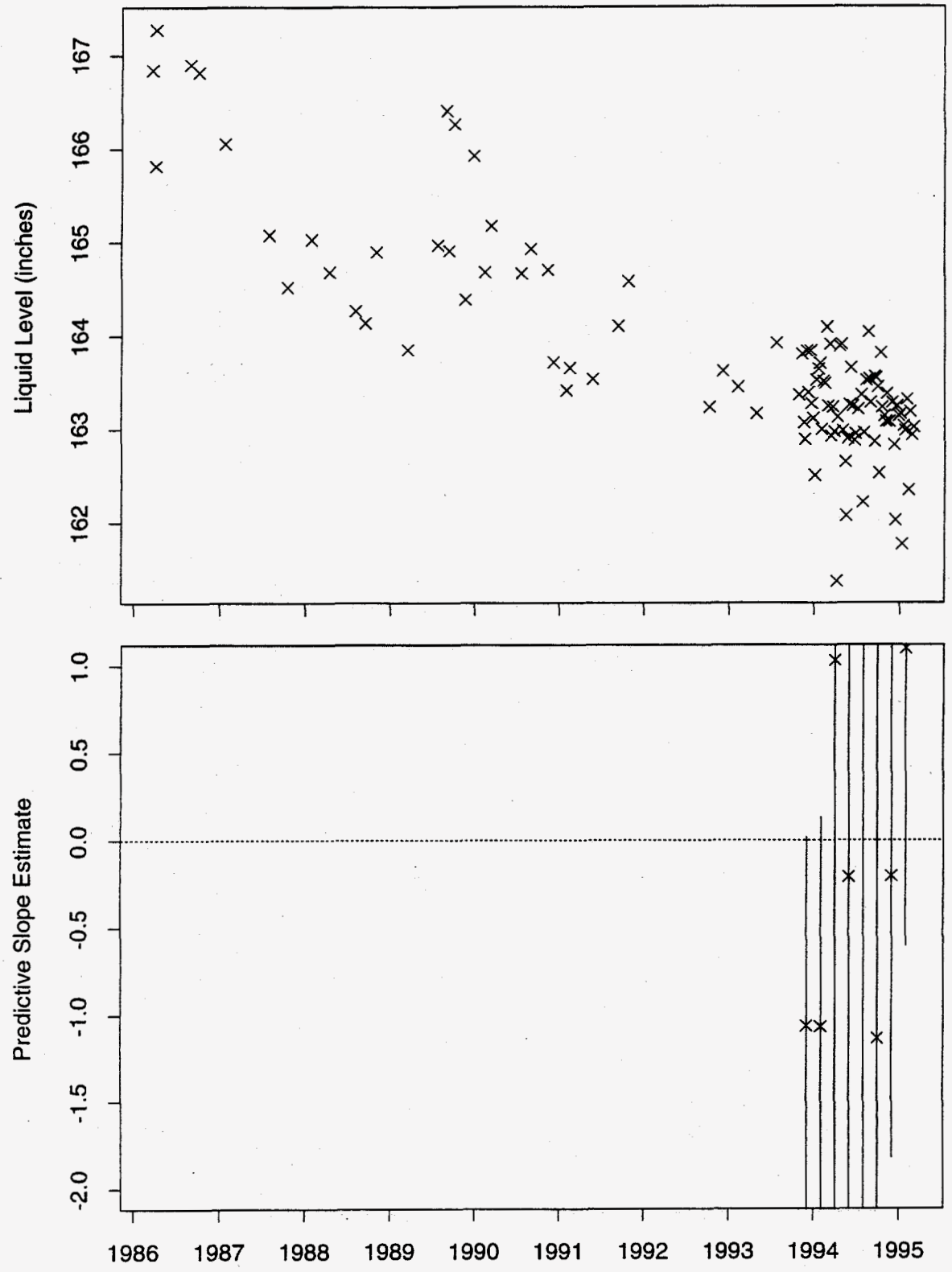

Figure 200: Tank SX–101 Neutron ILL Data

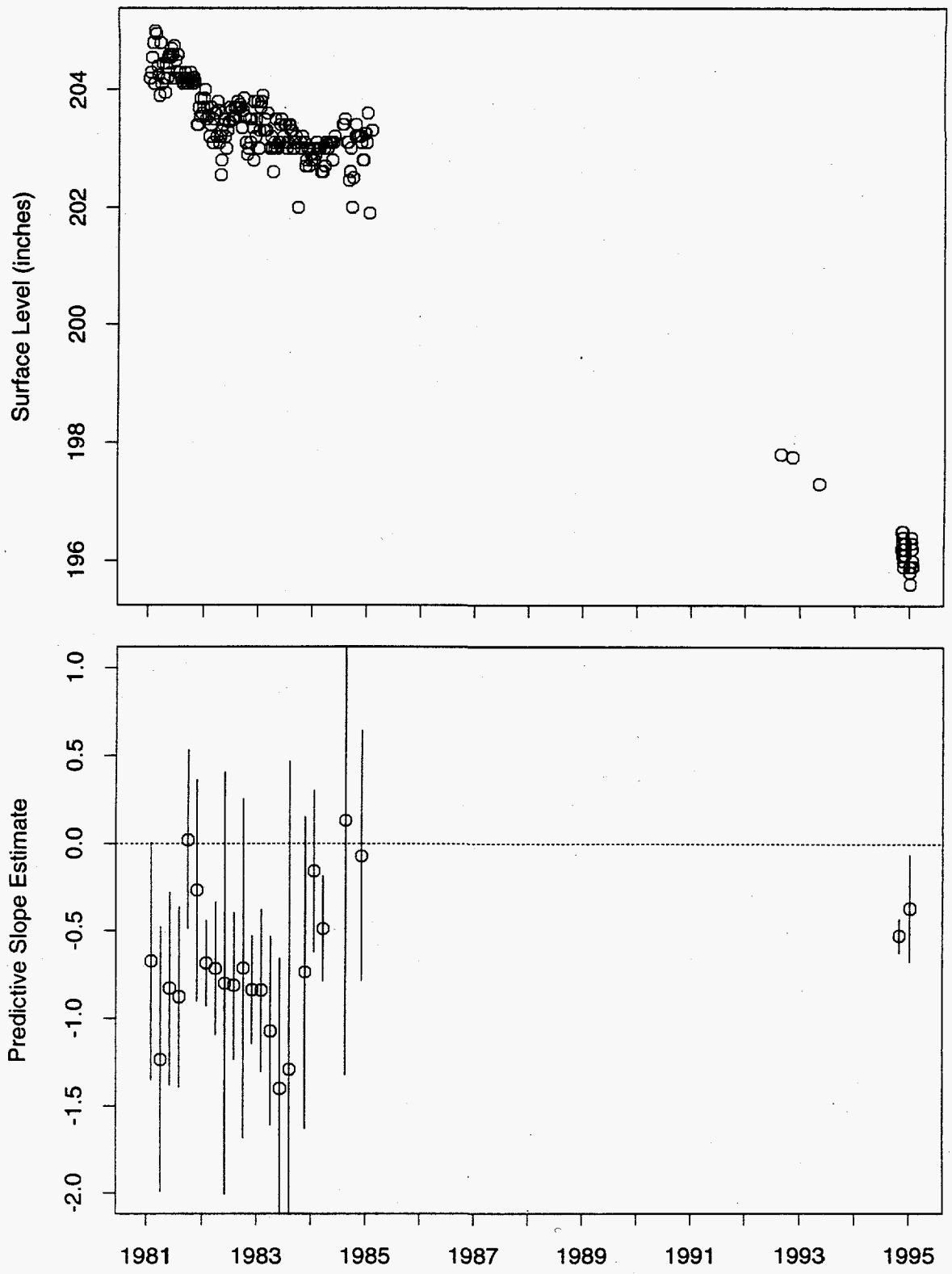

Figure 201: Tank SX–102 FIC Data

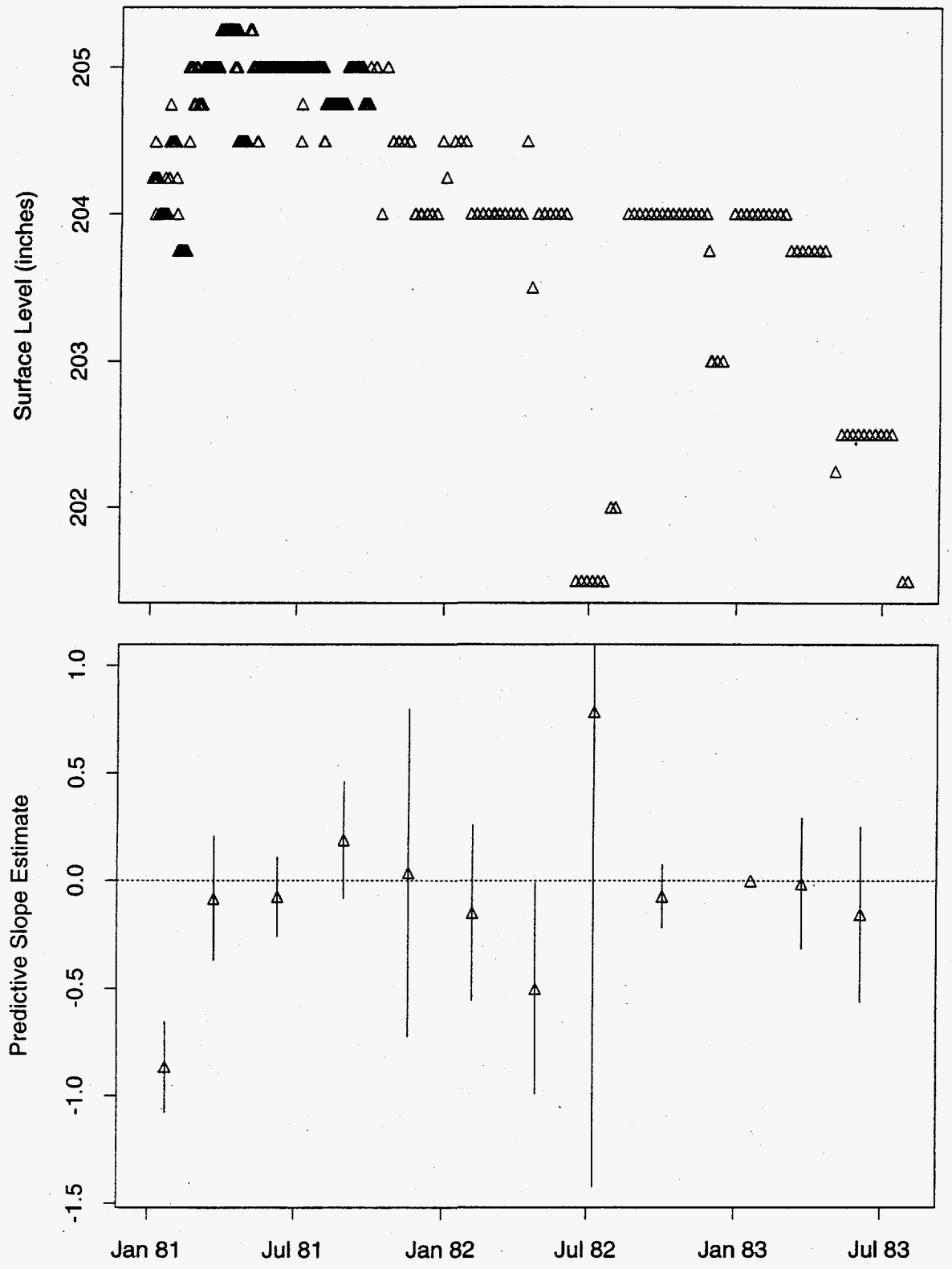

Figure 202: Tank SX–102 MT Data

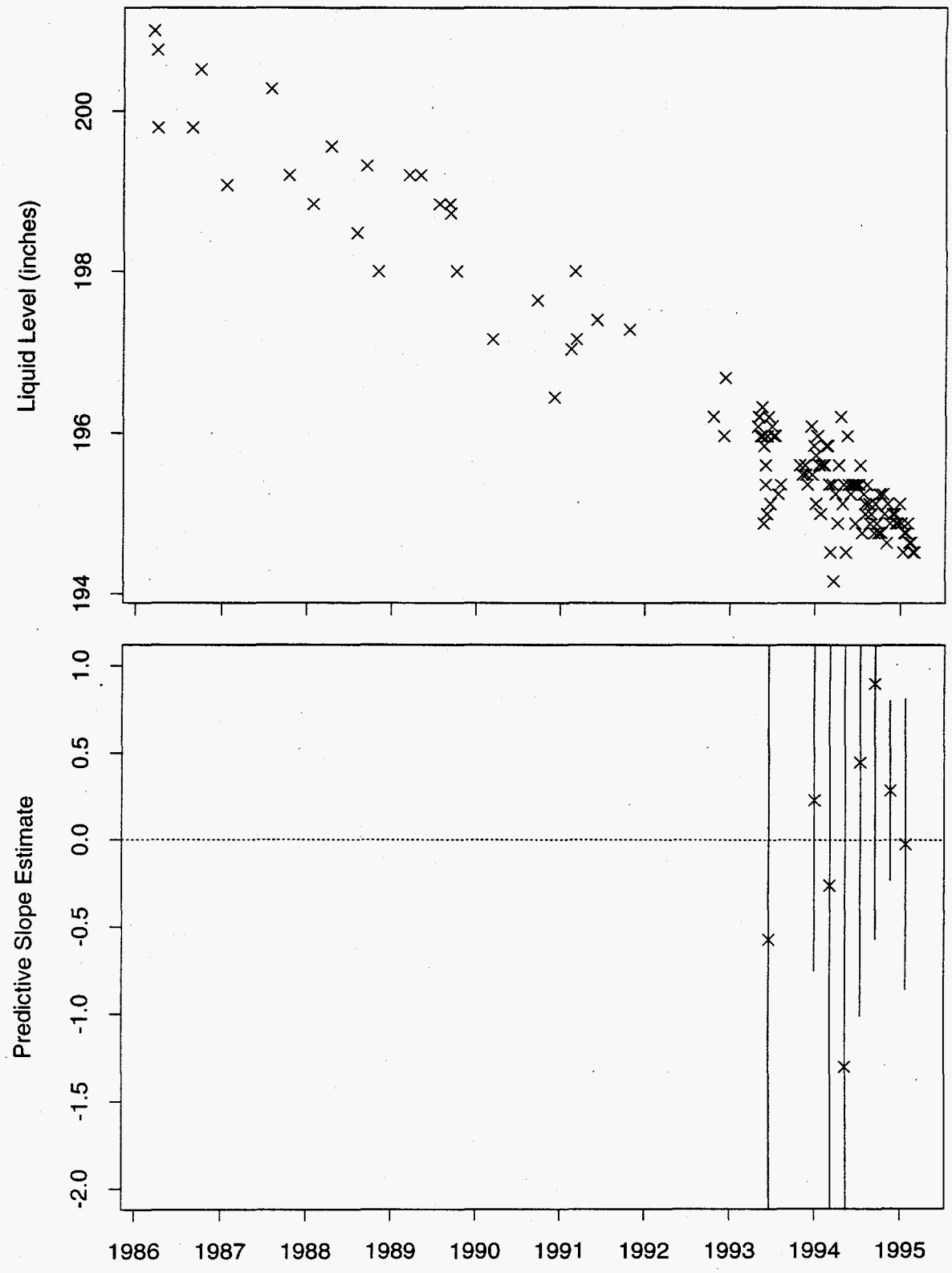

Figure 203: Tank SX–102 Neutron ILL Data

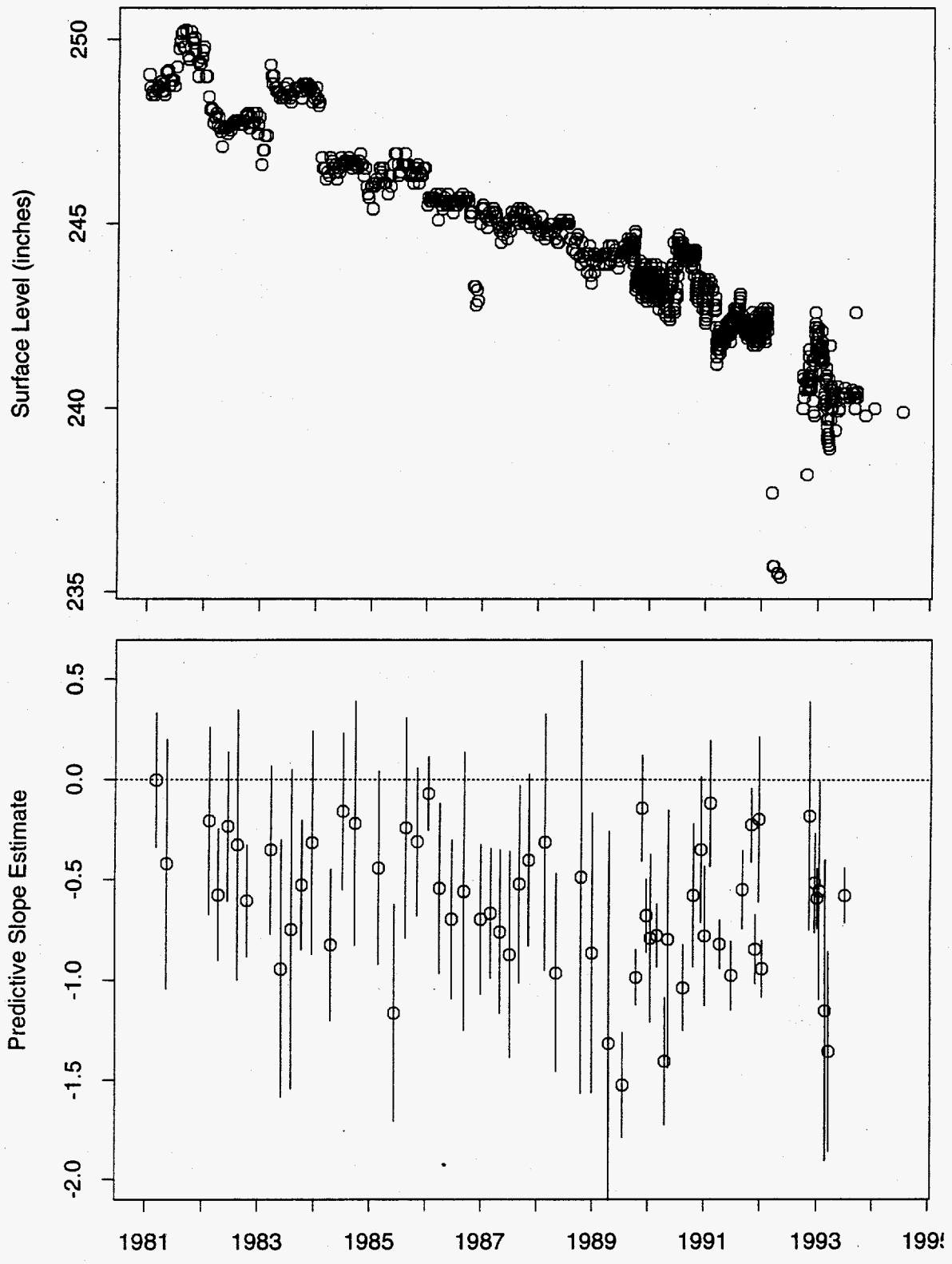

Figure 204: Tank SX–103 FIC Data

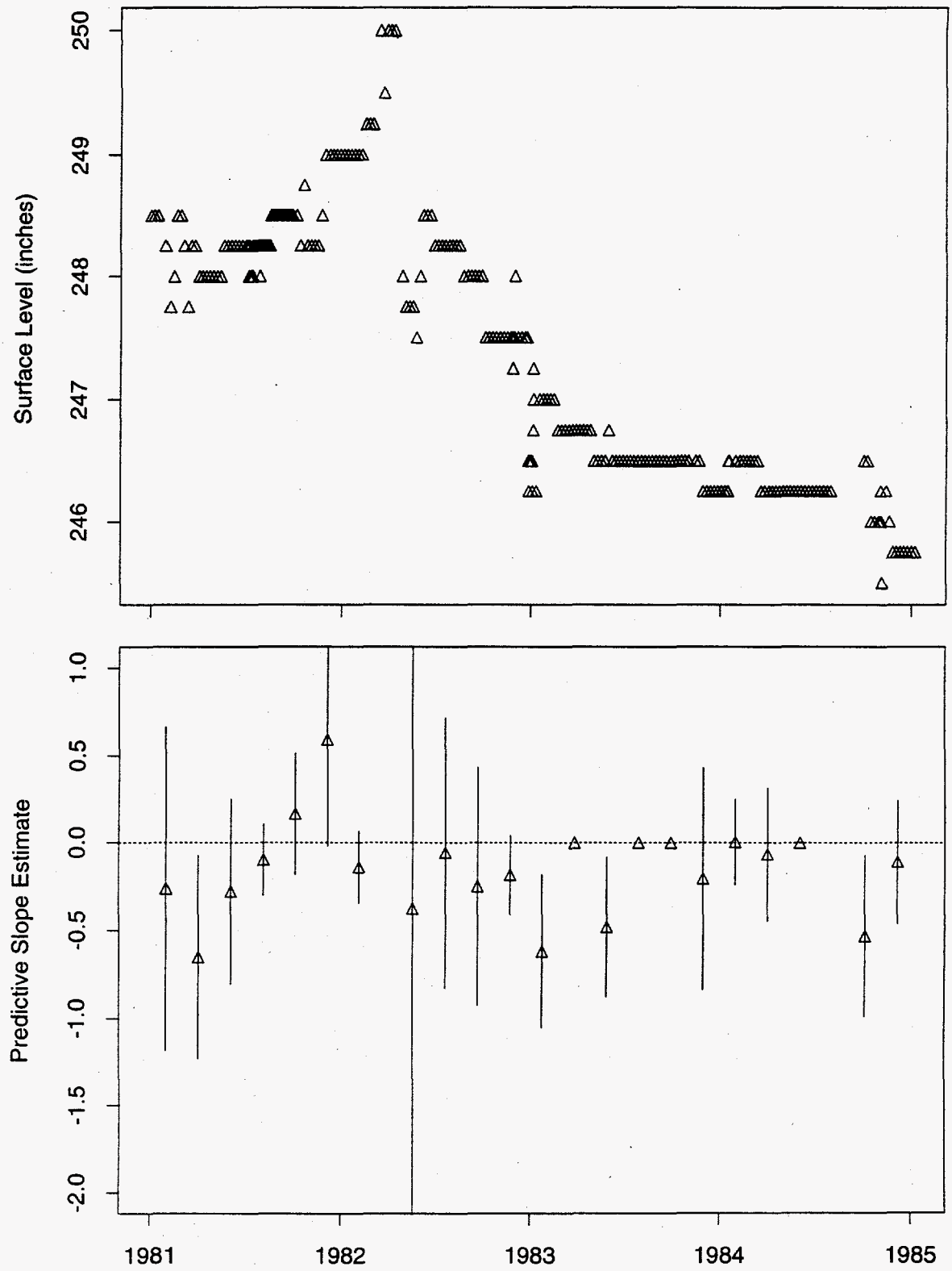

Figure 205: Tank SX–103 MT Data

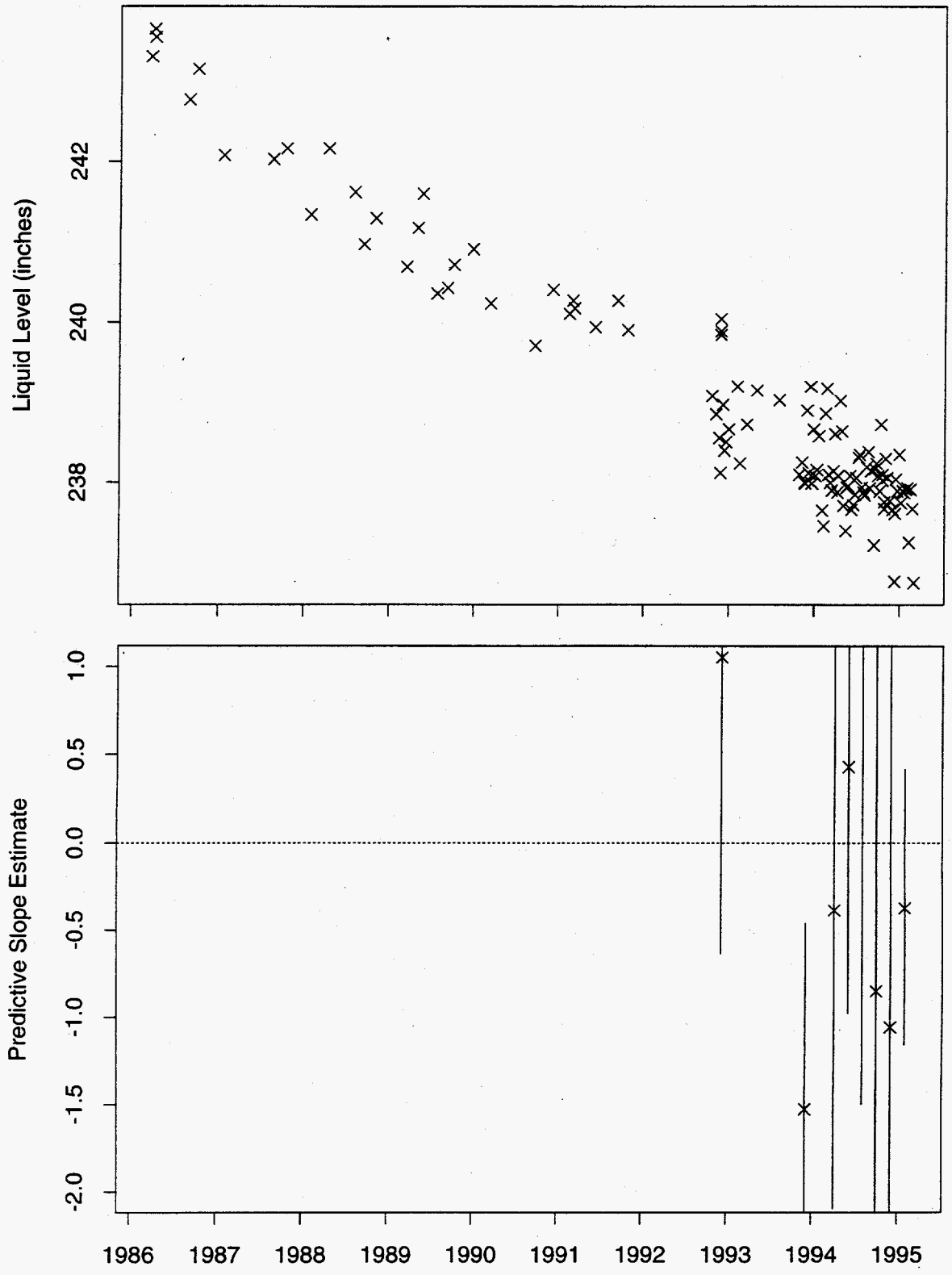

Figure 206: Tank SX–103 Neutron ILL Data

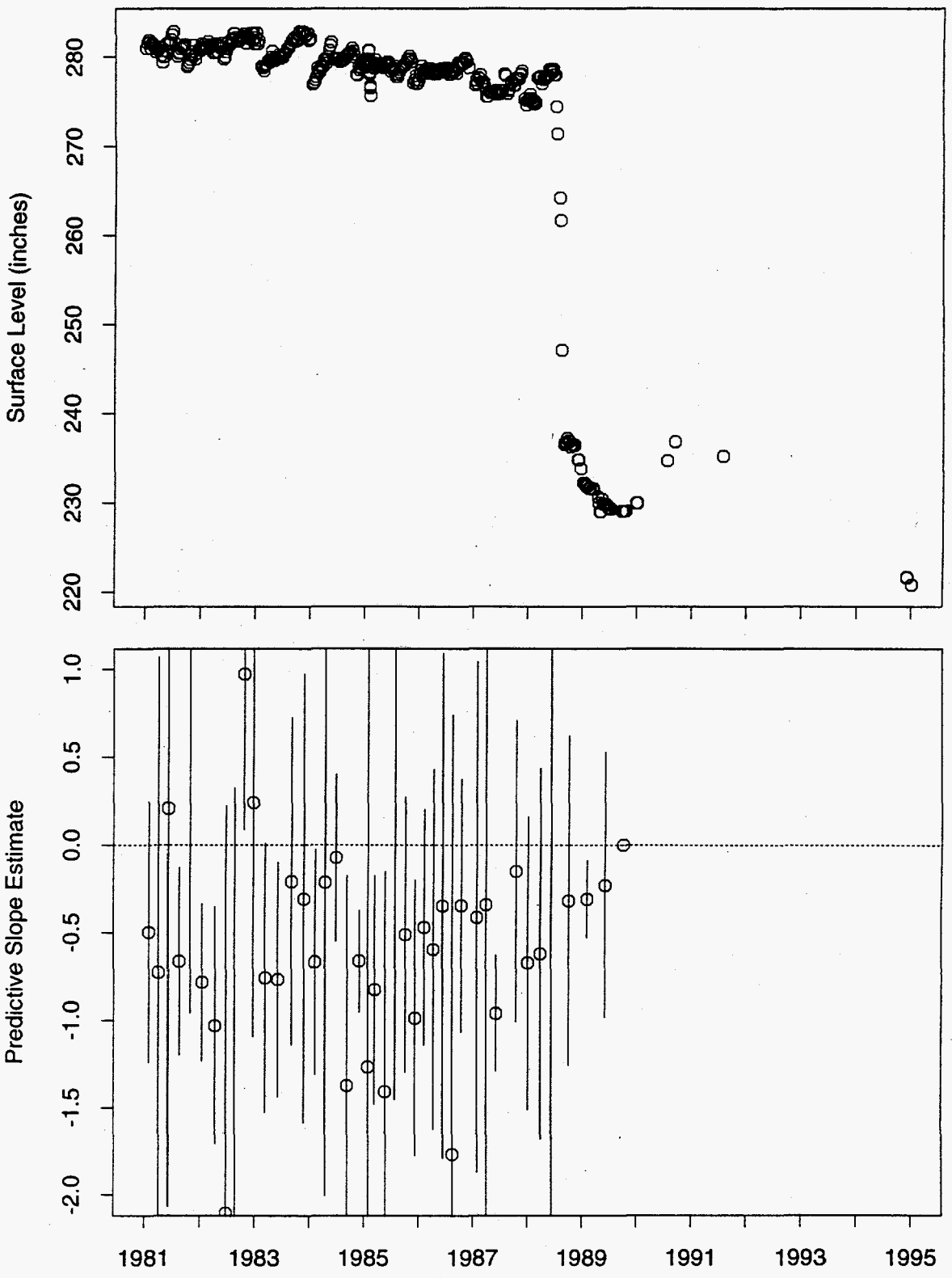

Figure 207: Tank SX–104 FIC Data

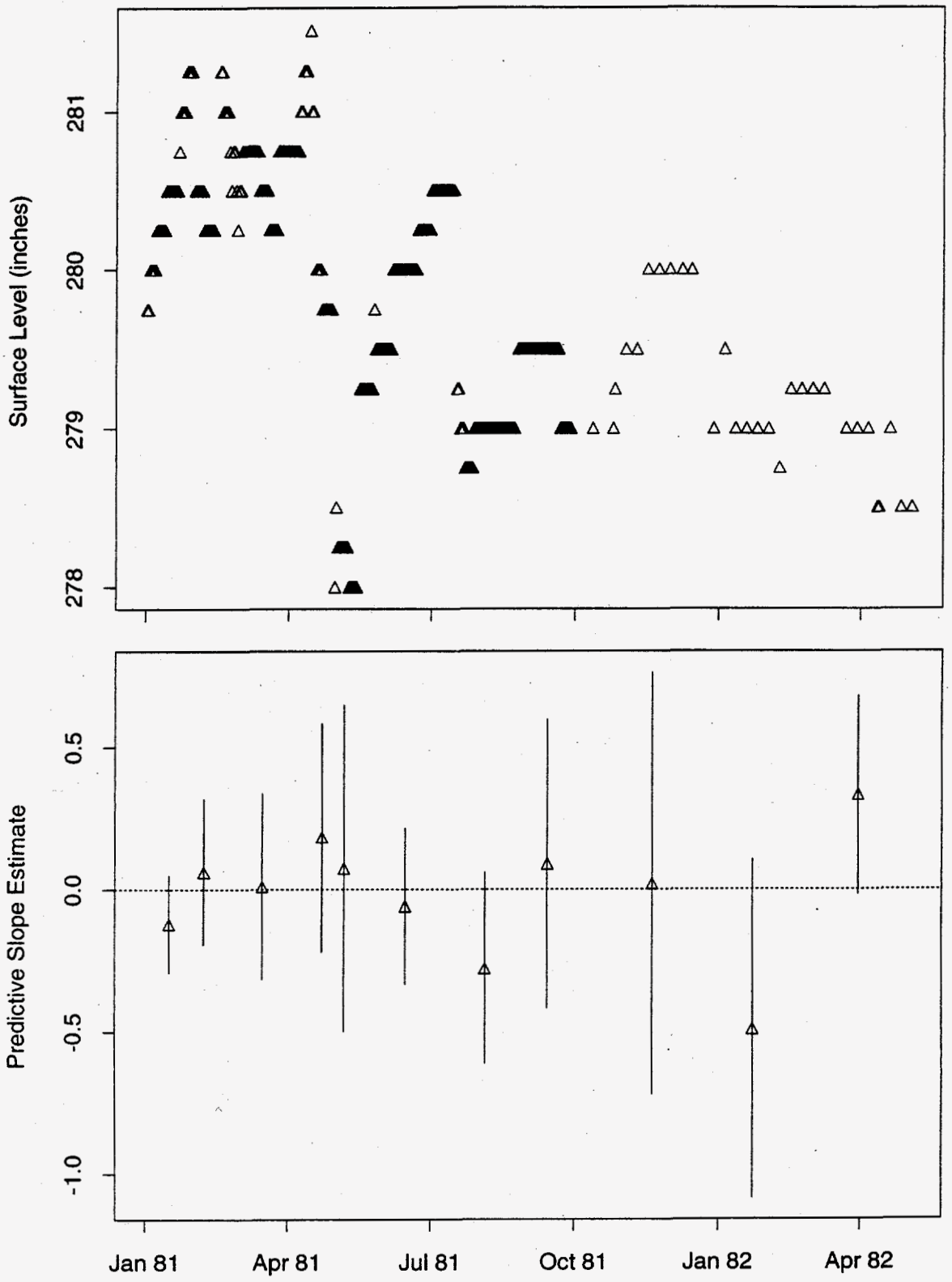

Figure 208: Tank SX–104 MT Data

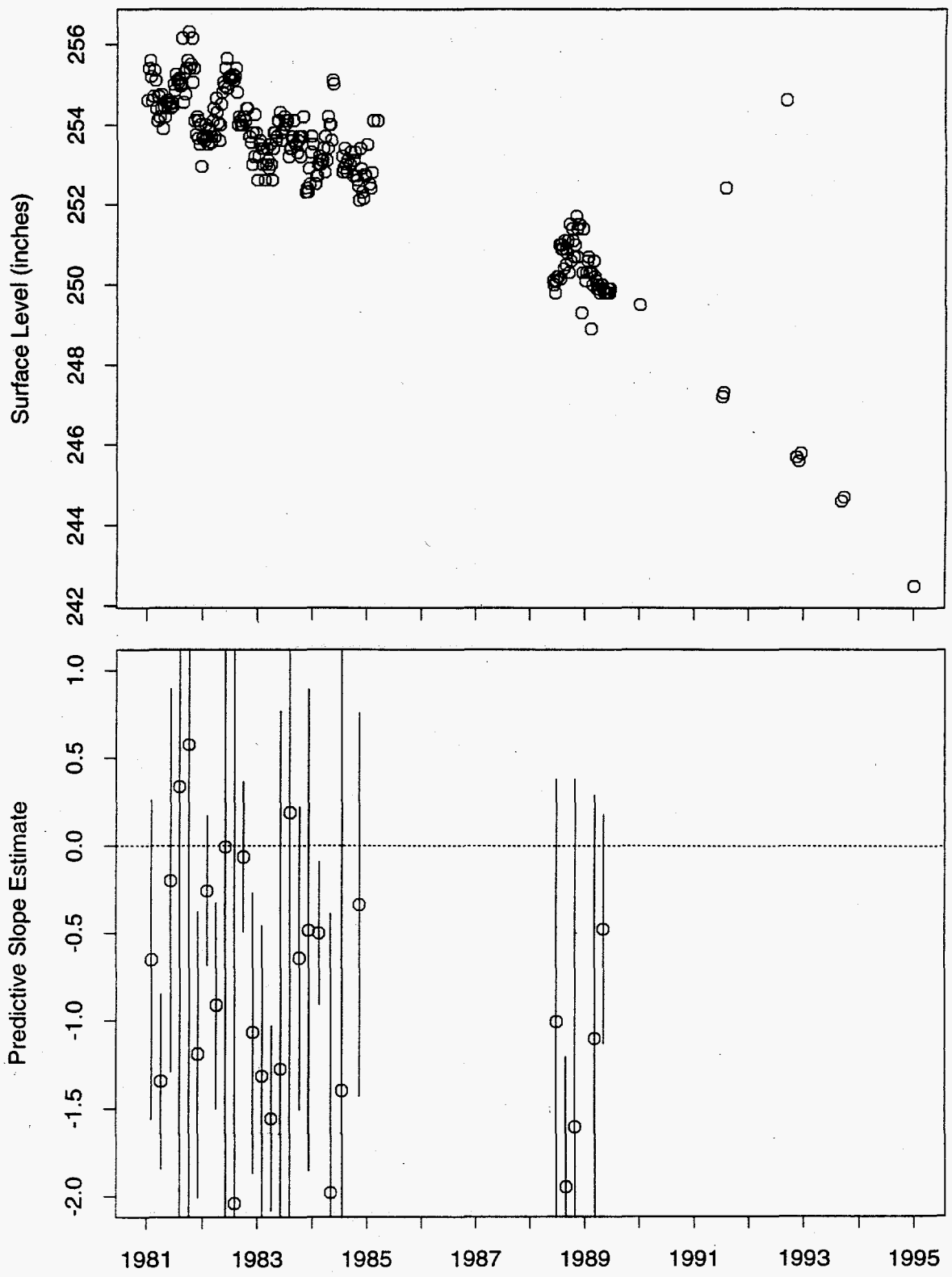

Figure 209: Tank SX–105 FIC Data

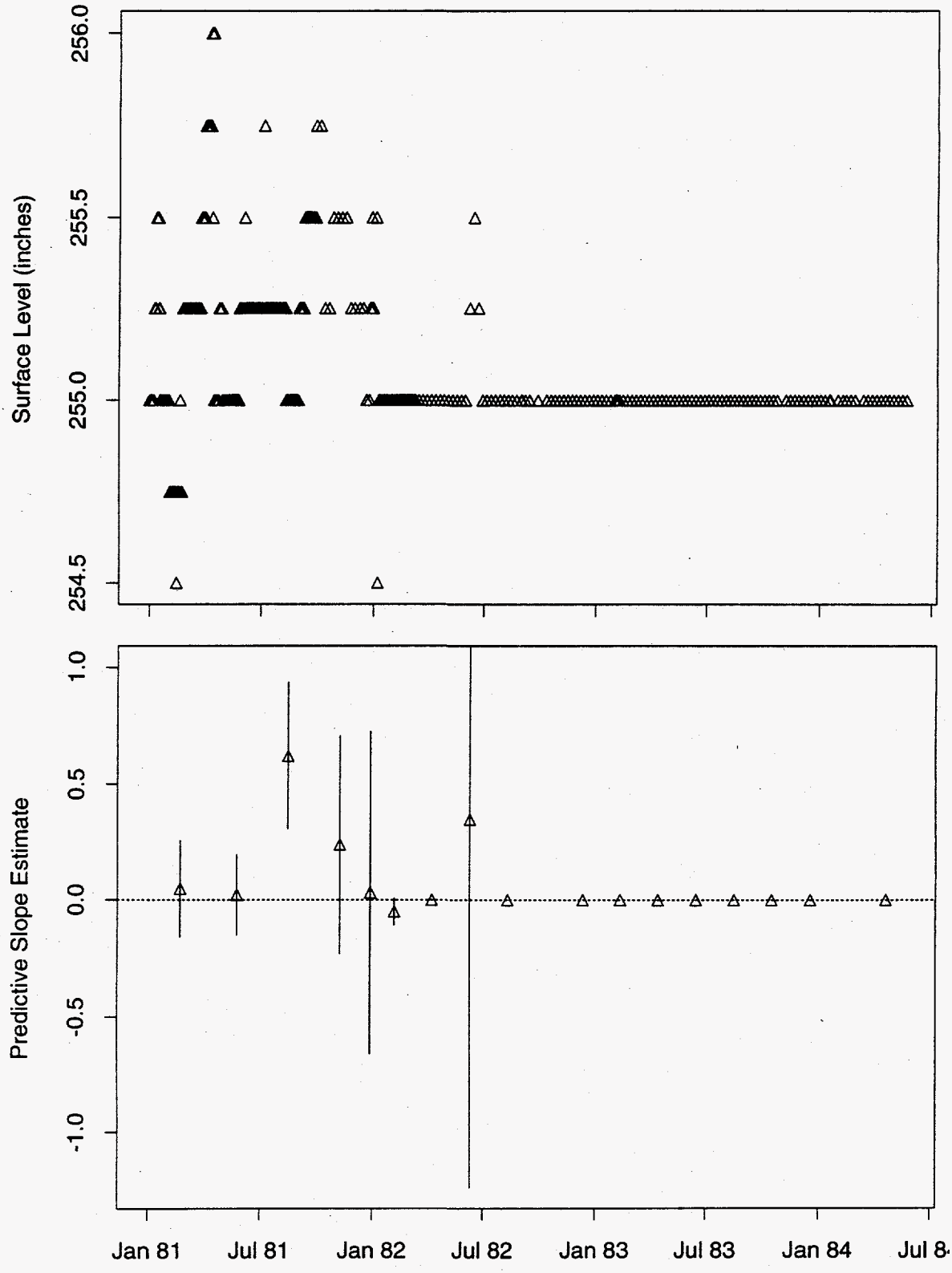

Figure 210: Tank SX–105 MT Data

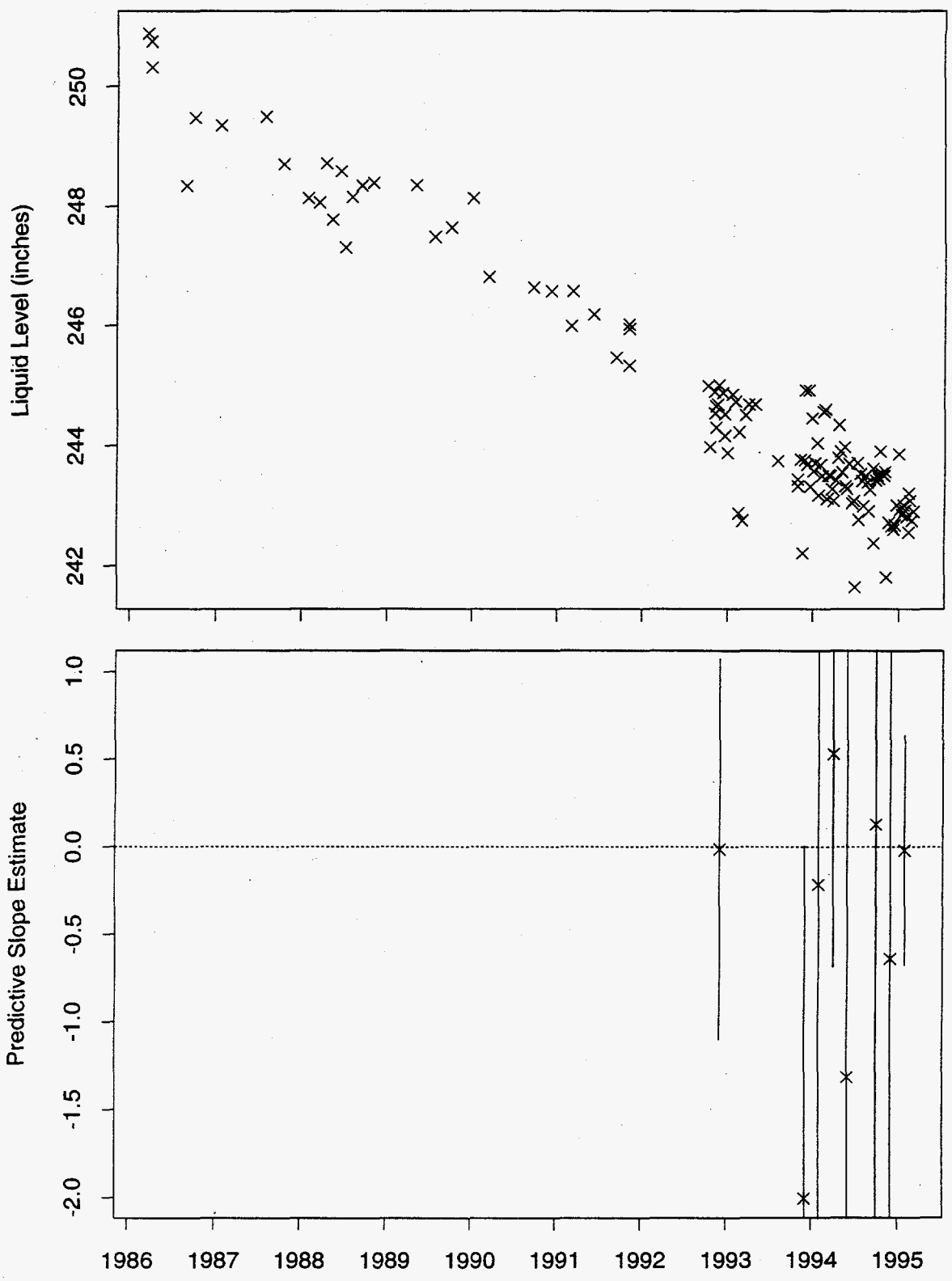

Figure 211: Tank SX–105 Neutron ILL Data

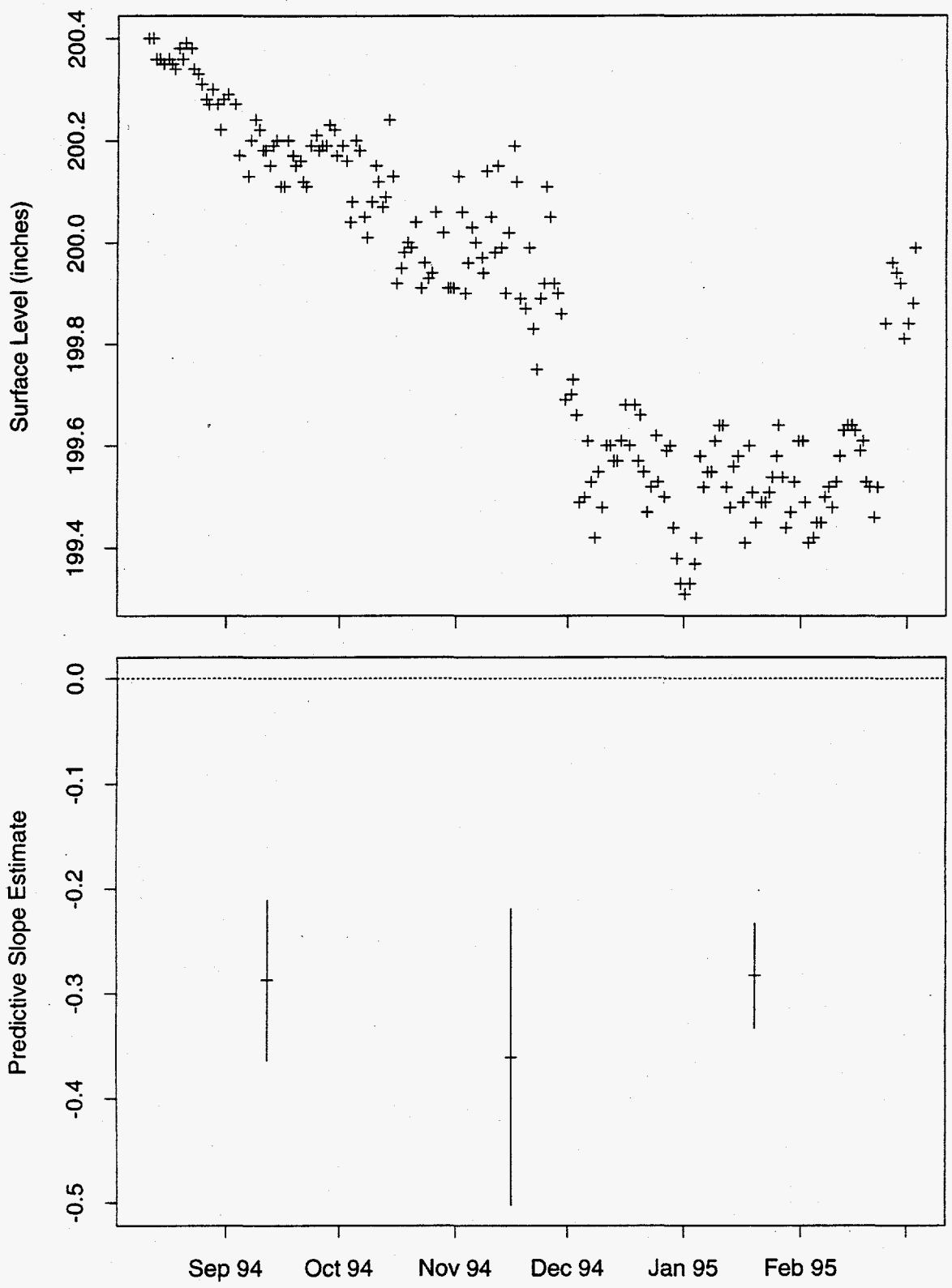

Figure 212: Tank SX–106 ENRAF Data

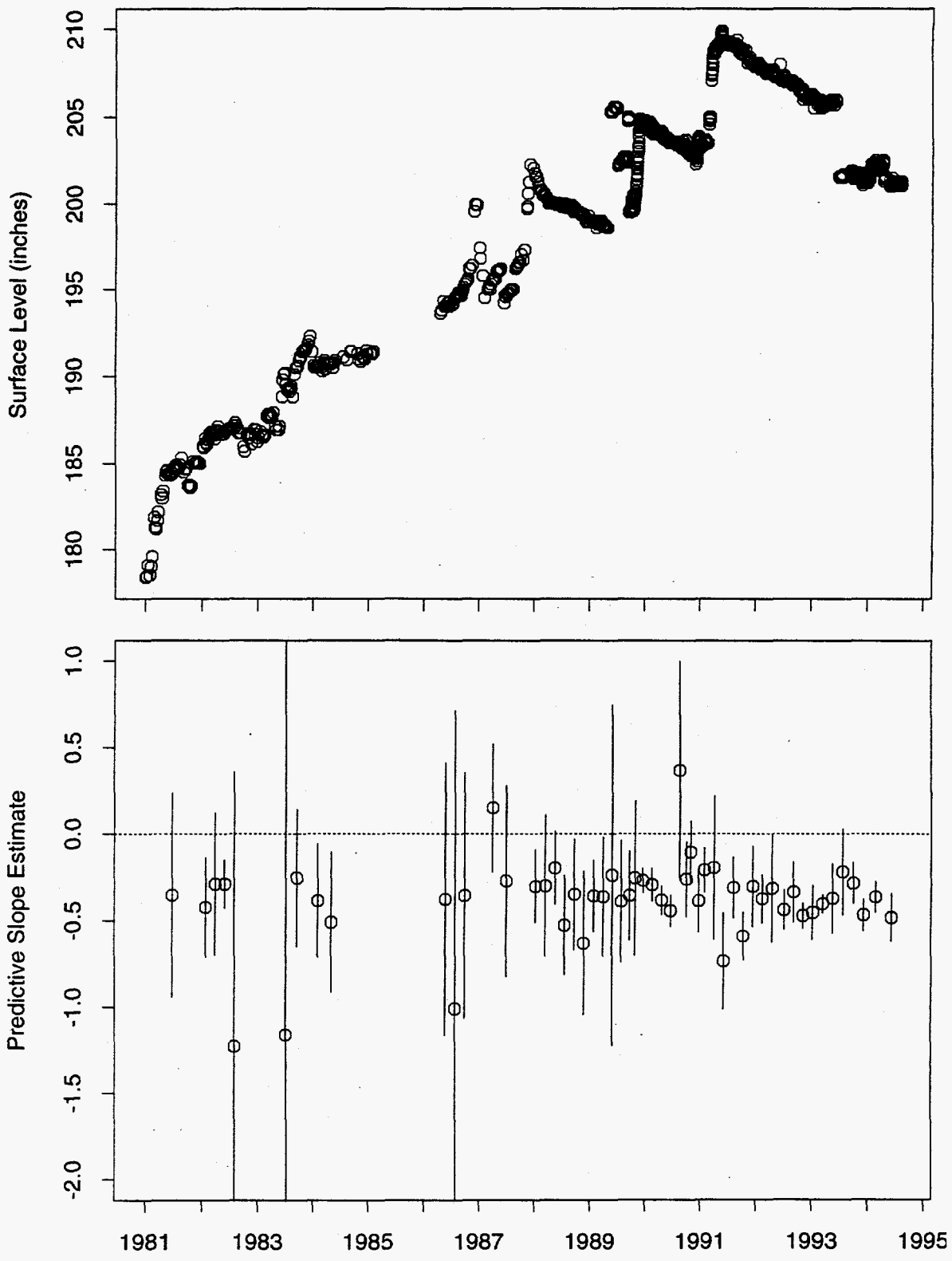

Figure 213: Tank SX–106 FIC Data

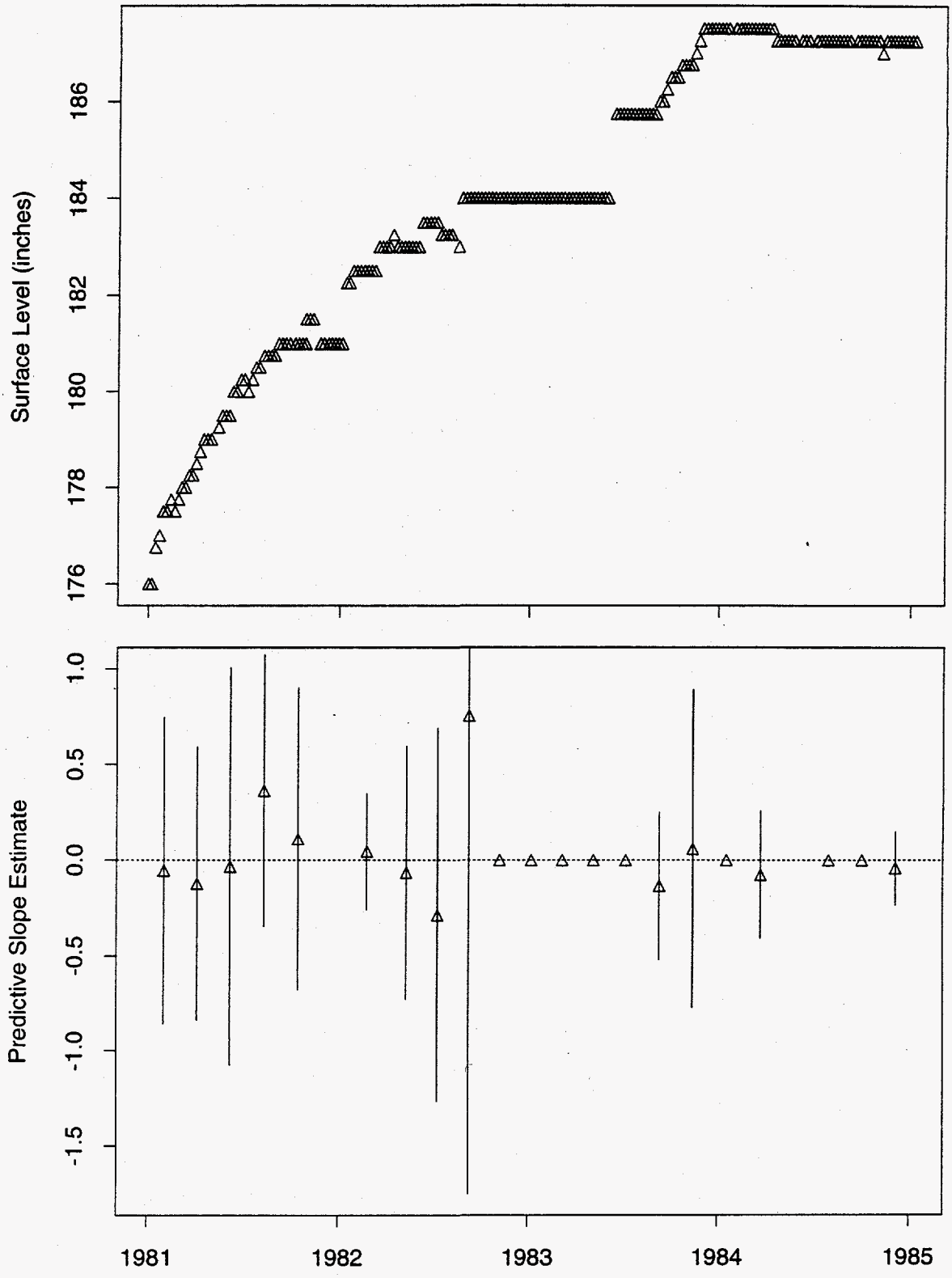

Figure 214: Tank SX-106 MT Data

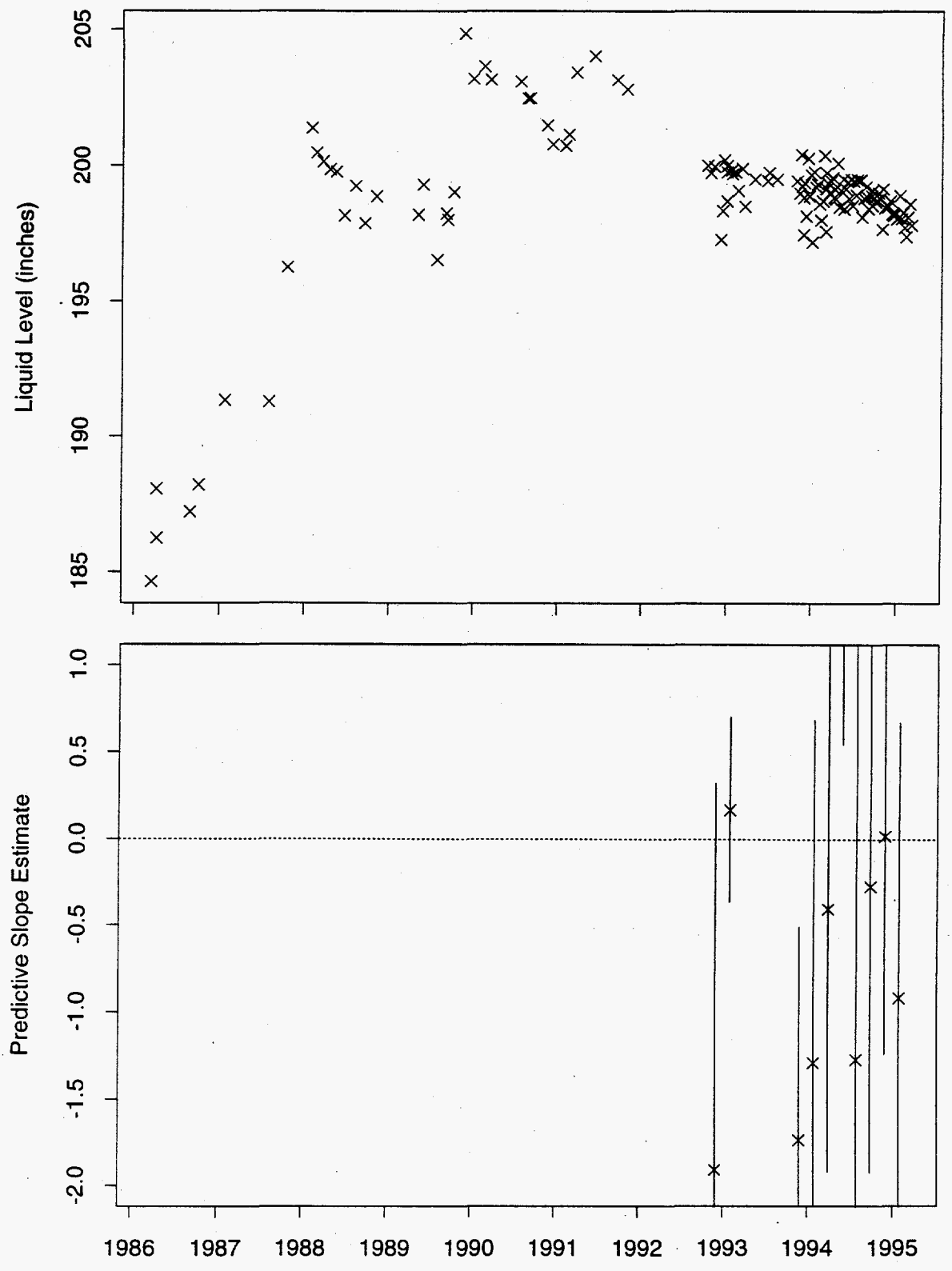

Figure 215: Tank SX–106 Neutron ILL Data

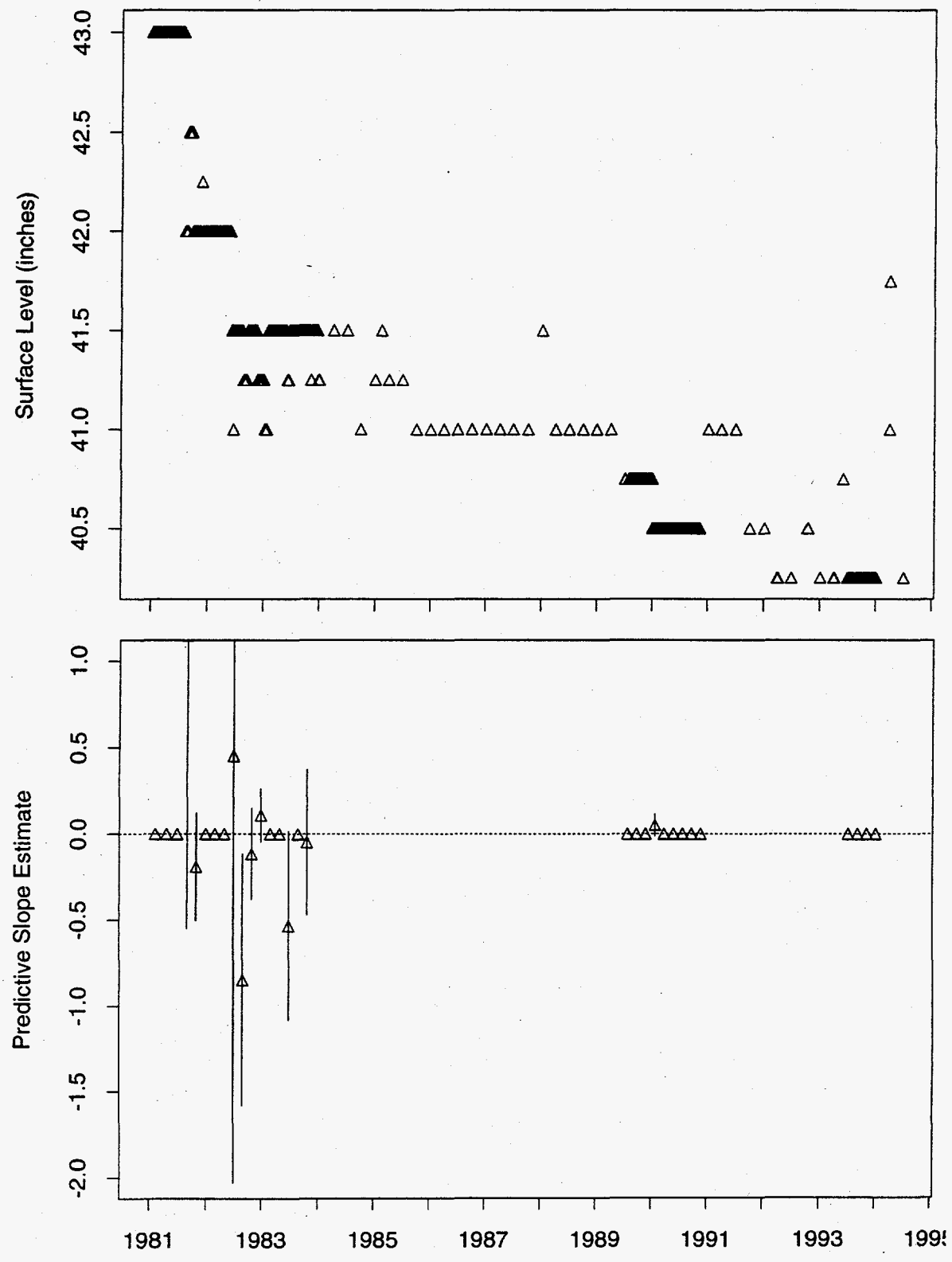

Figure 216: Tank SX–107 MT Data

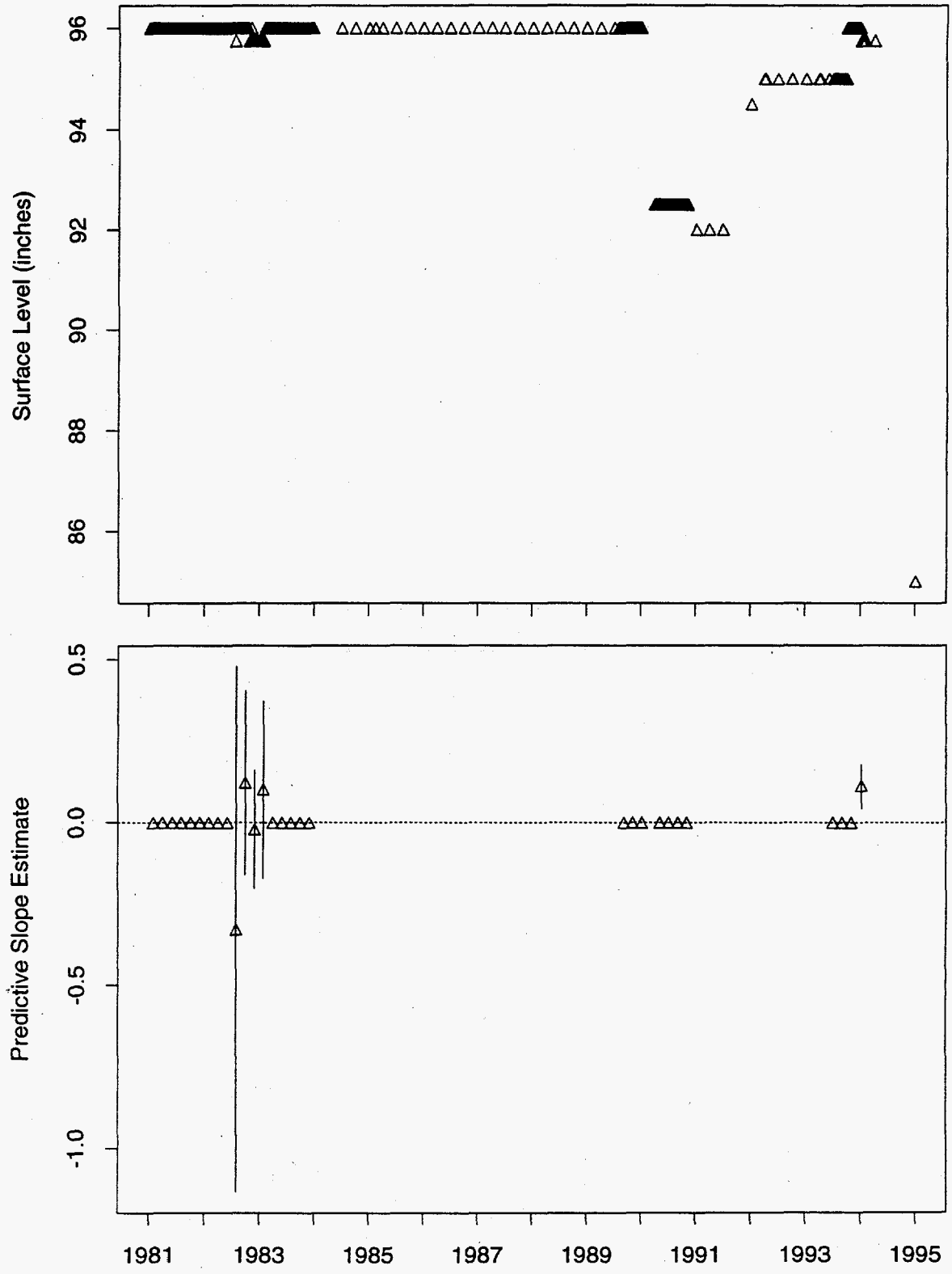

Figure 217: Tank SX-109 MT Data

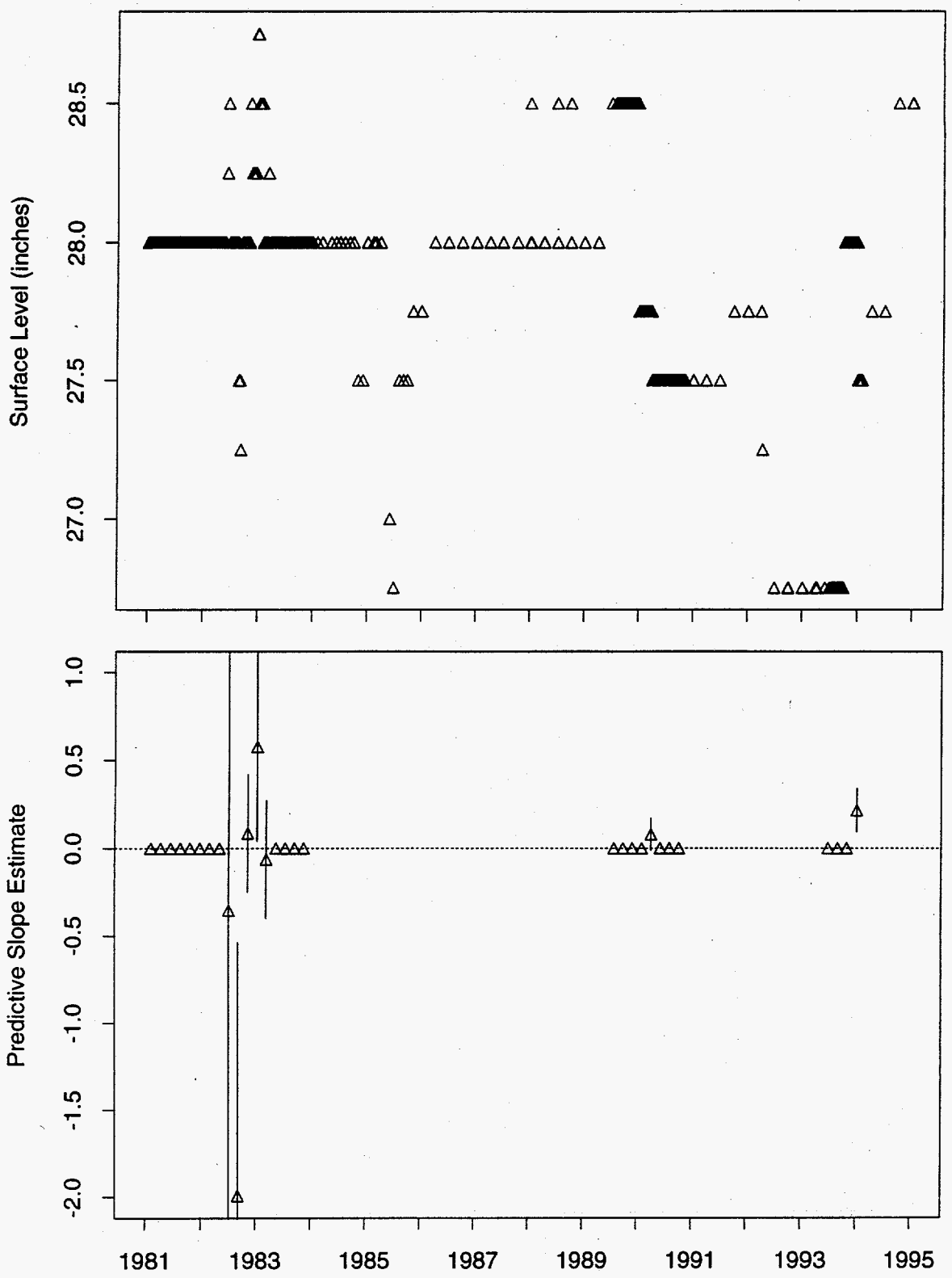

Figure 218: Tank SX–110 MT Data

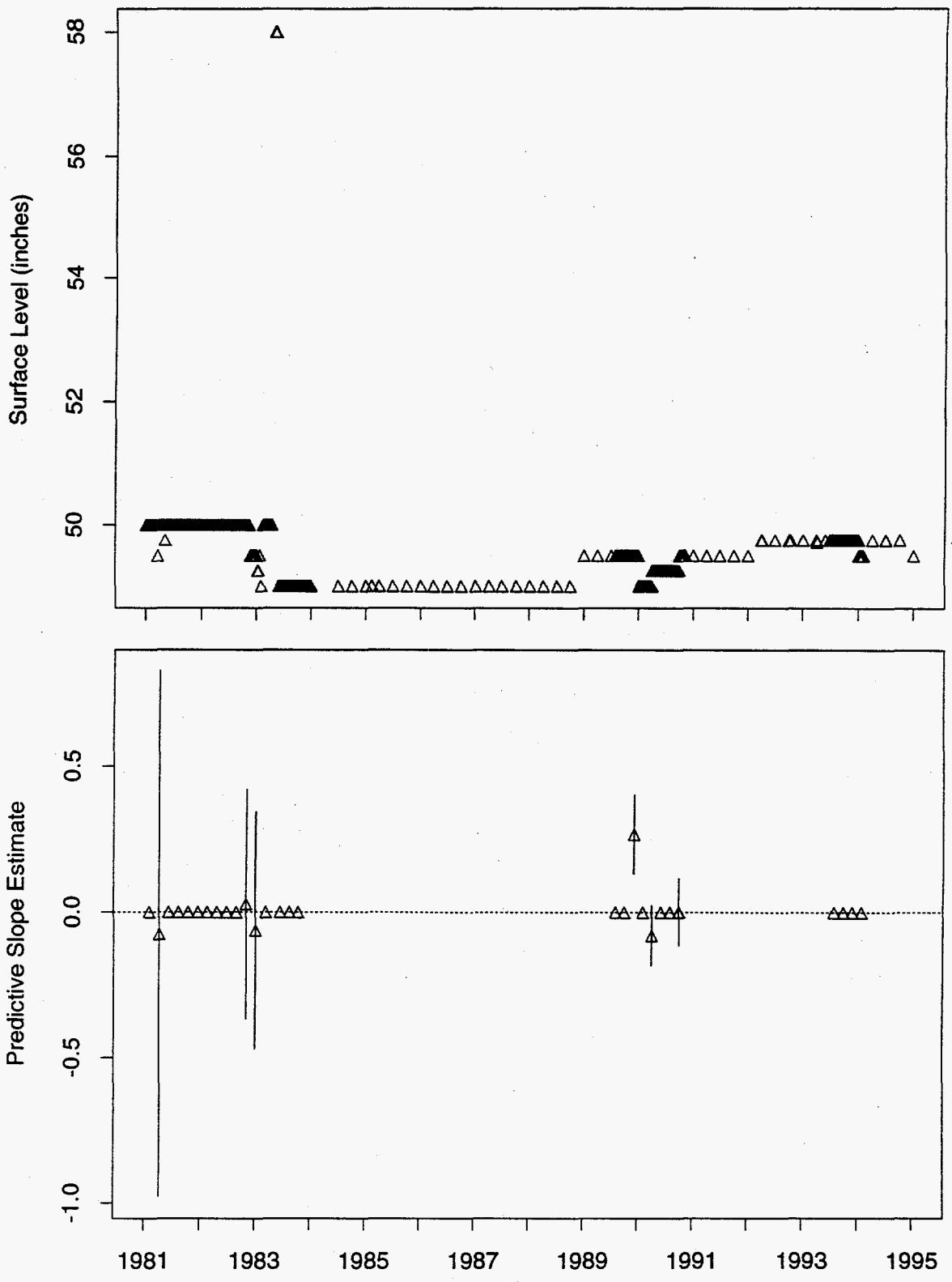

Figure 219: Tank SX-111 MT Data

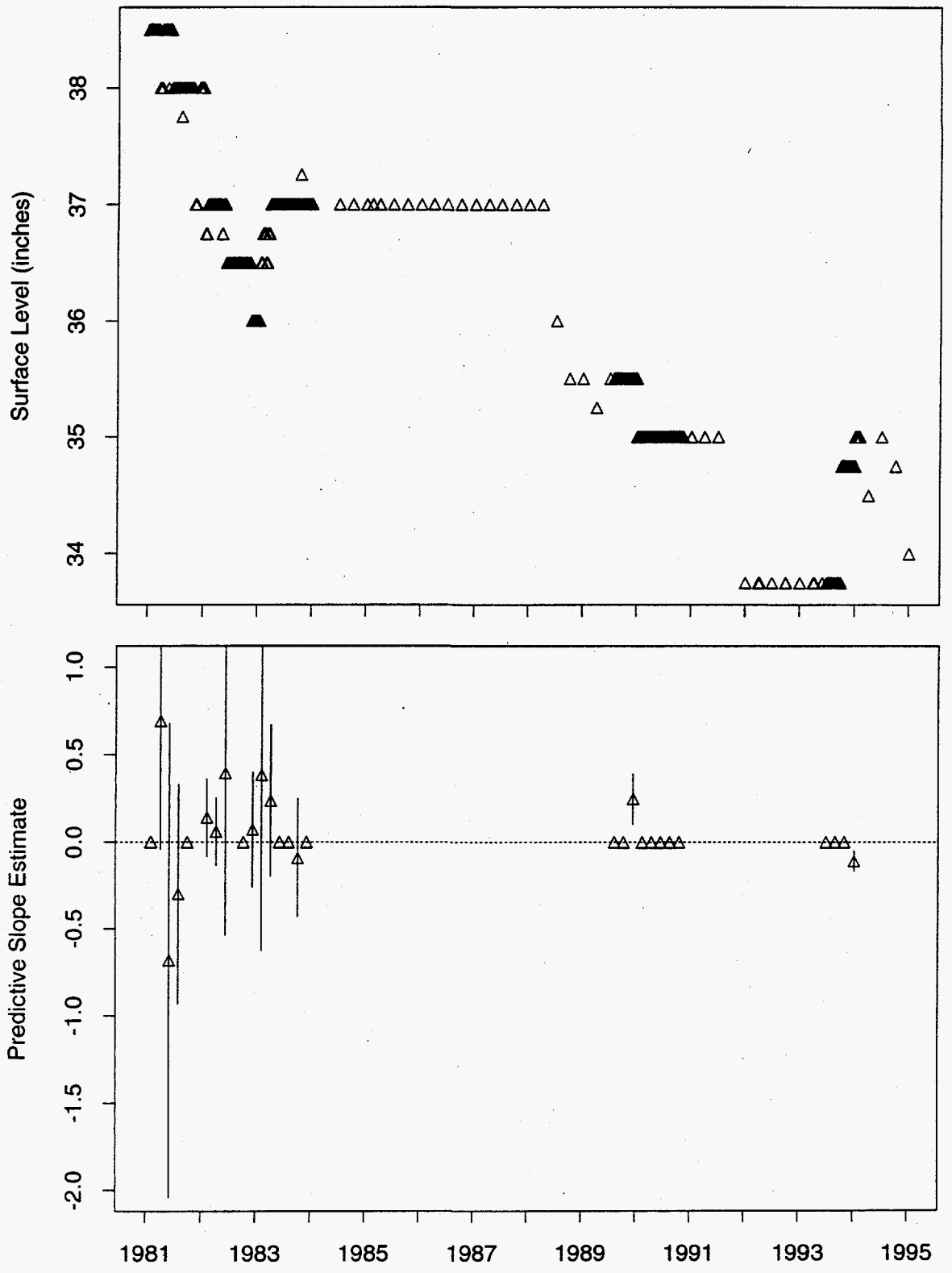

Figure 220: Tank SX–112 MT Data

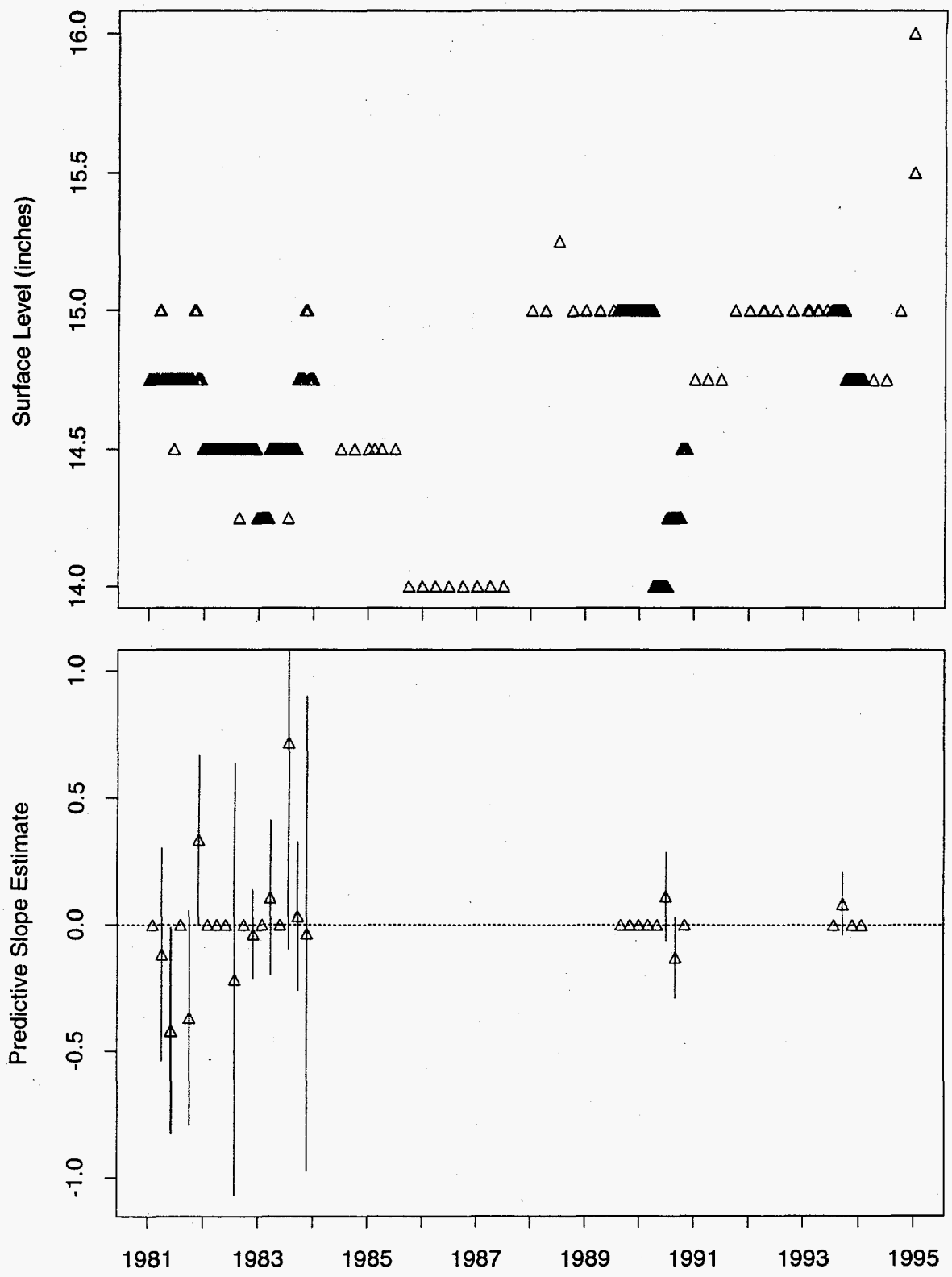

Figure 221: Tank SX–113 MT Data

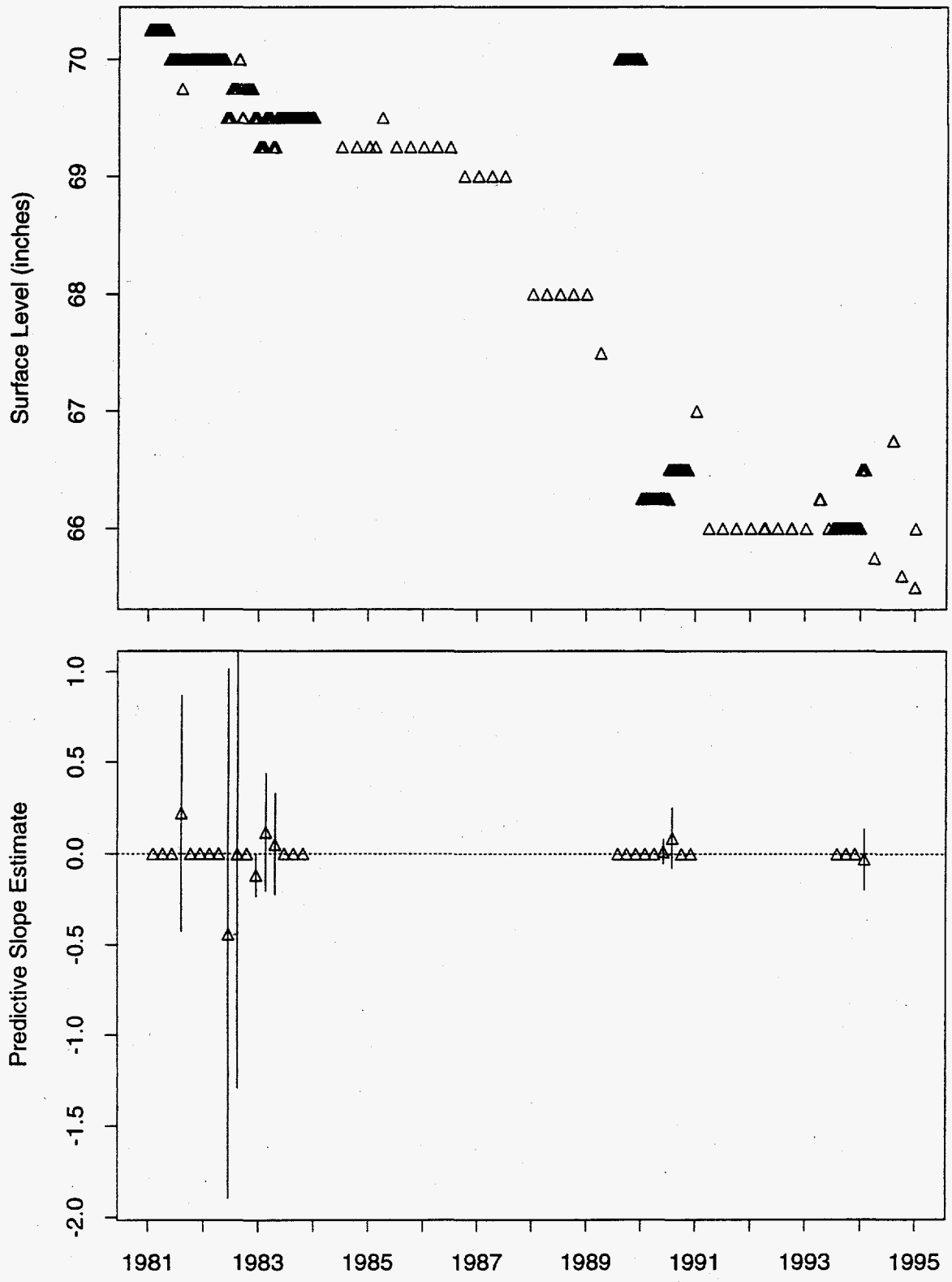

Figure 222: Tank SX–114 MT Data

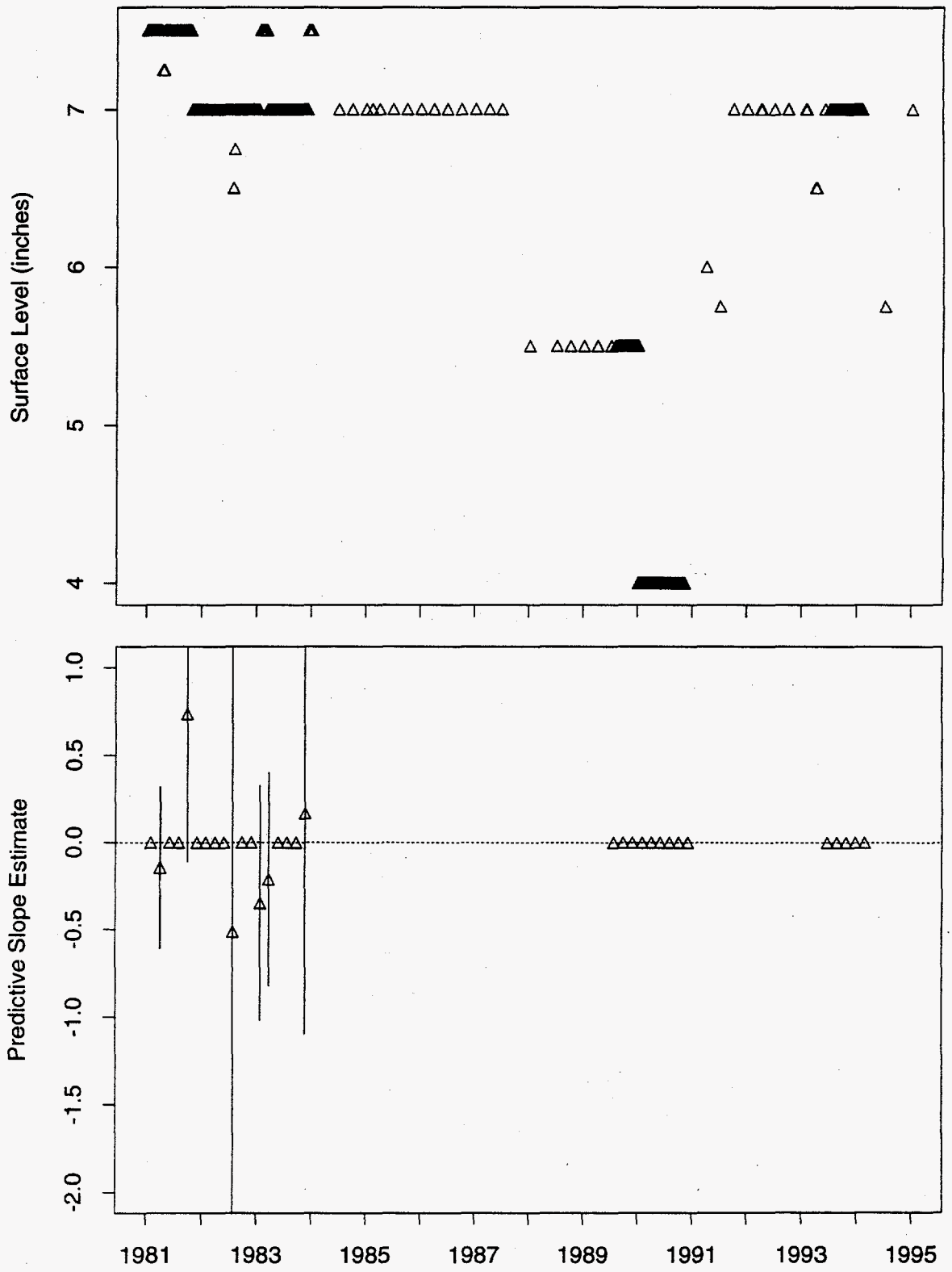

Figure 223: Tank SX–115 MT Data

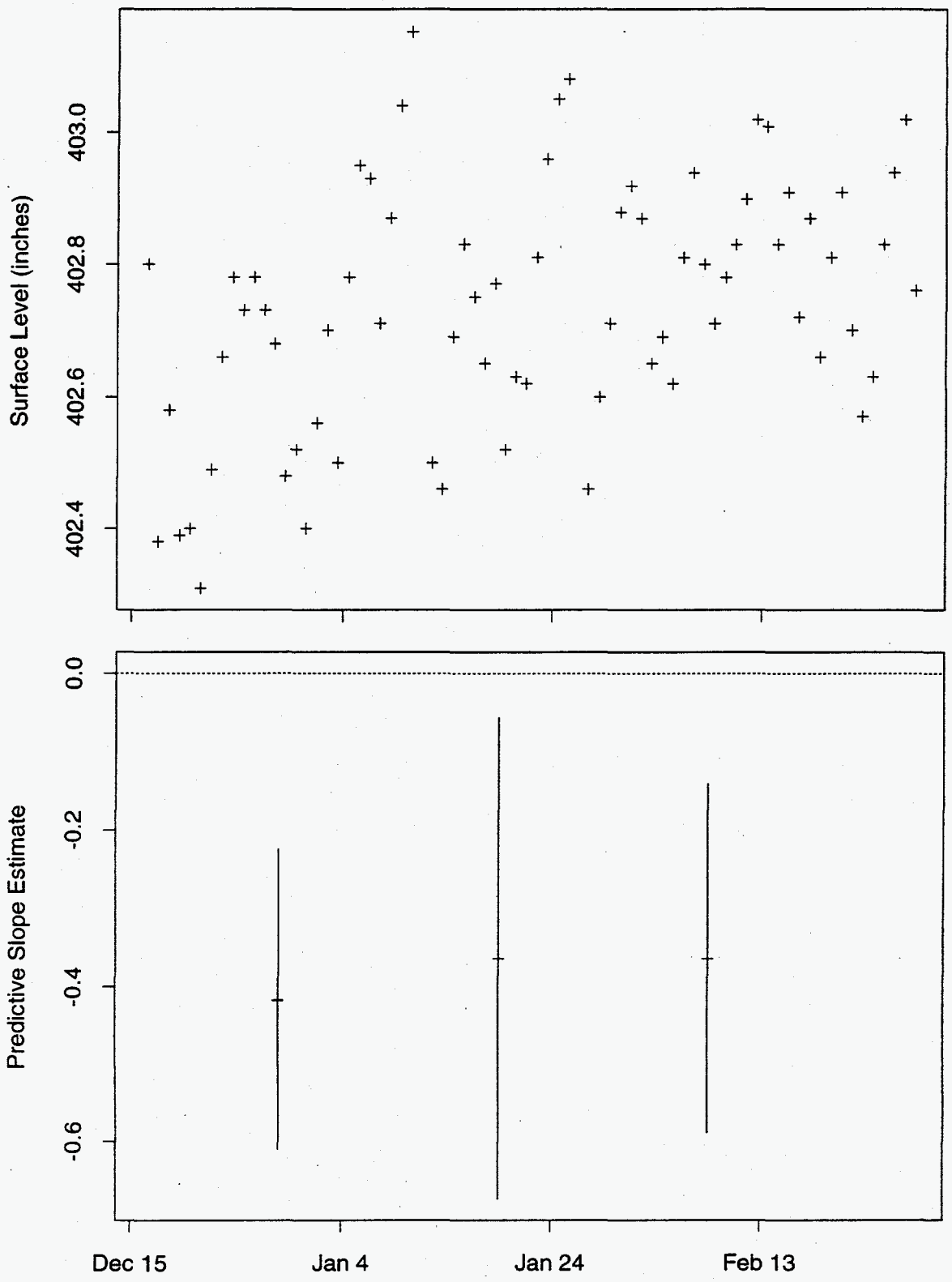

Figure 224: Tank SY–101 ENRAF Data

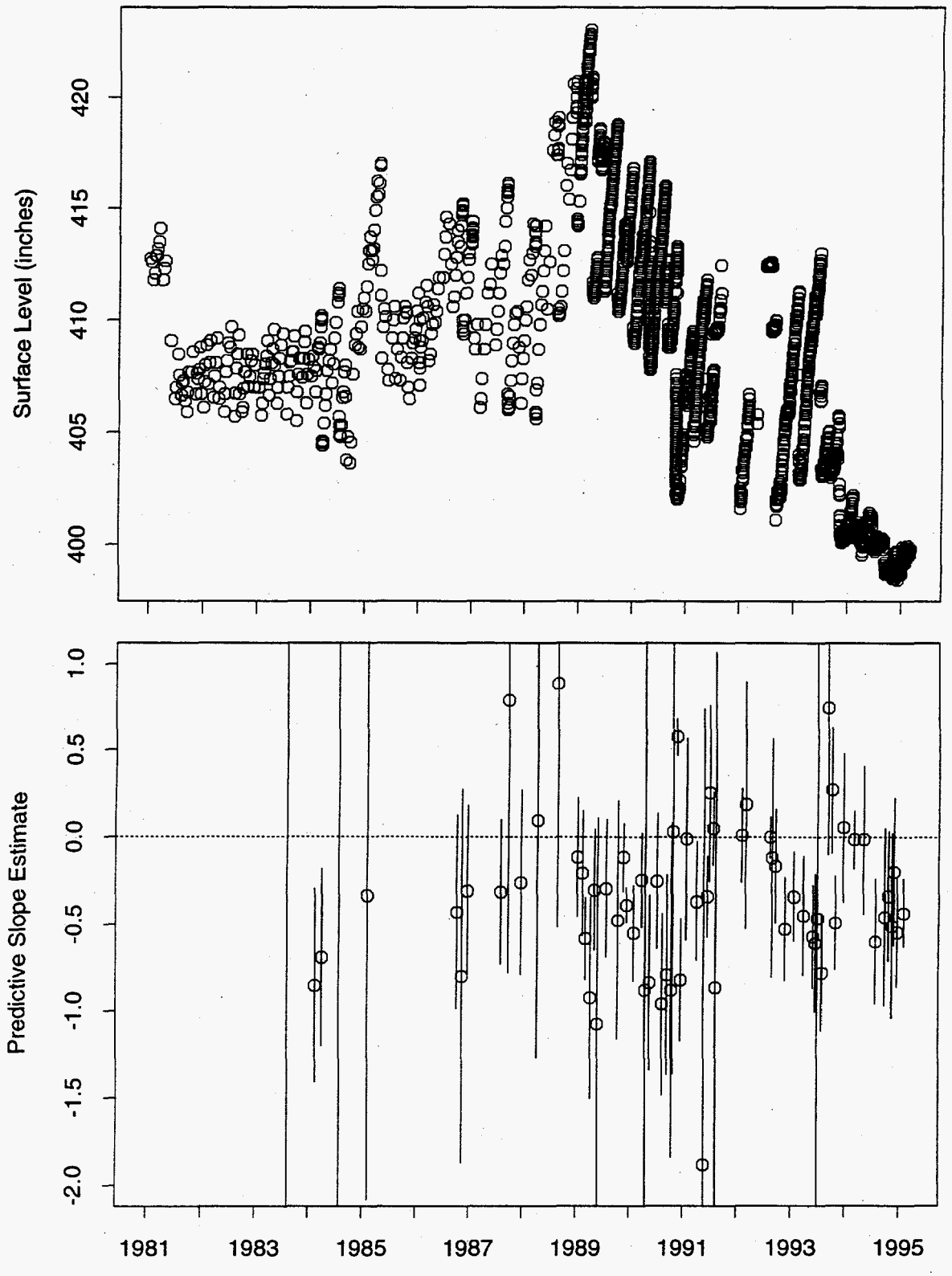

Figure 225: Tank SY–101 FIC Data

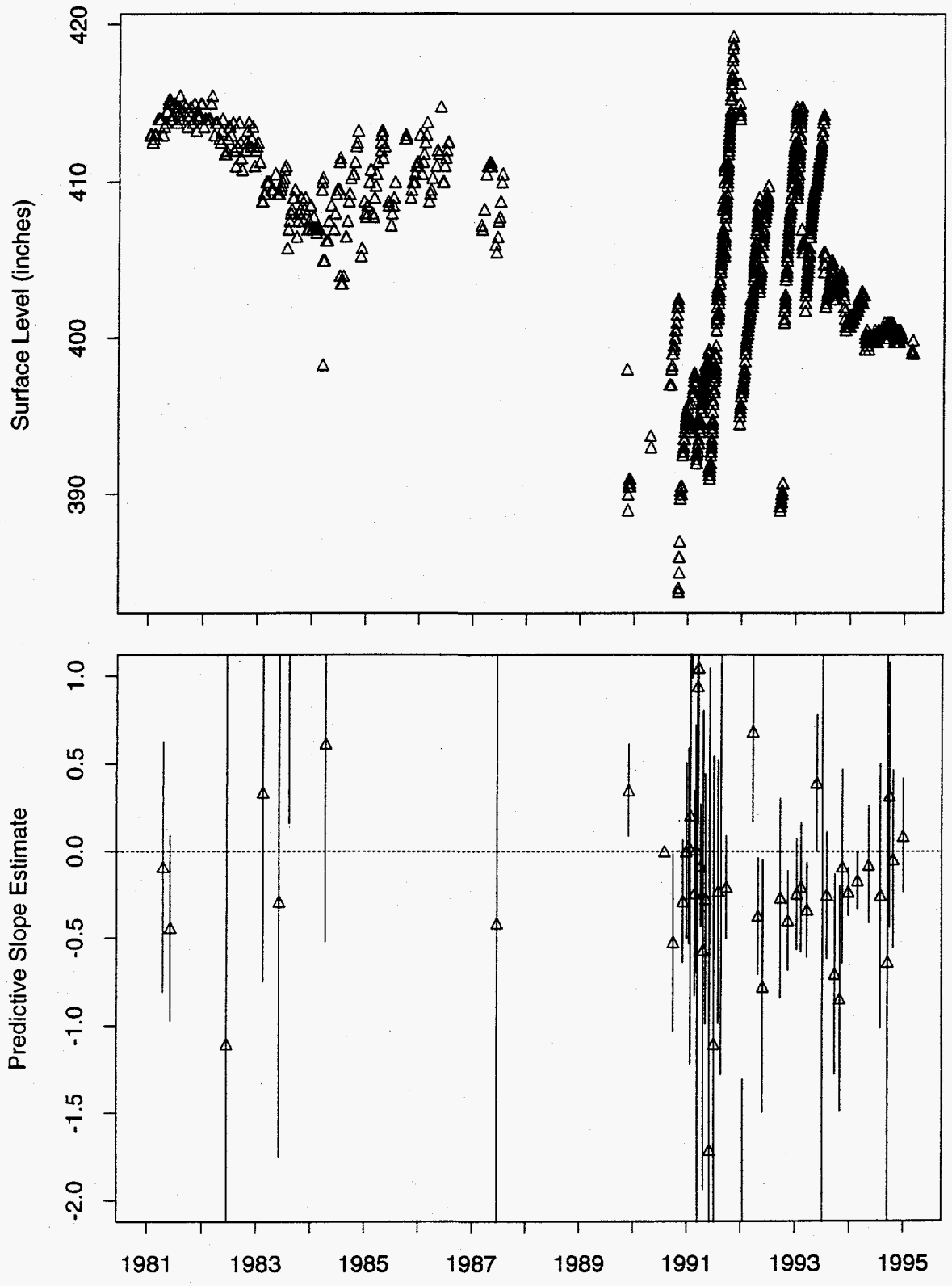

Figure 226: Tank SY–101 MT Data

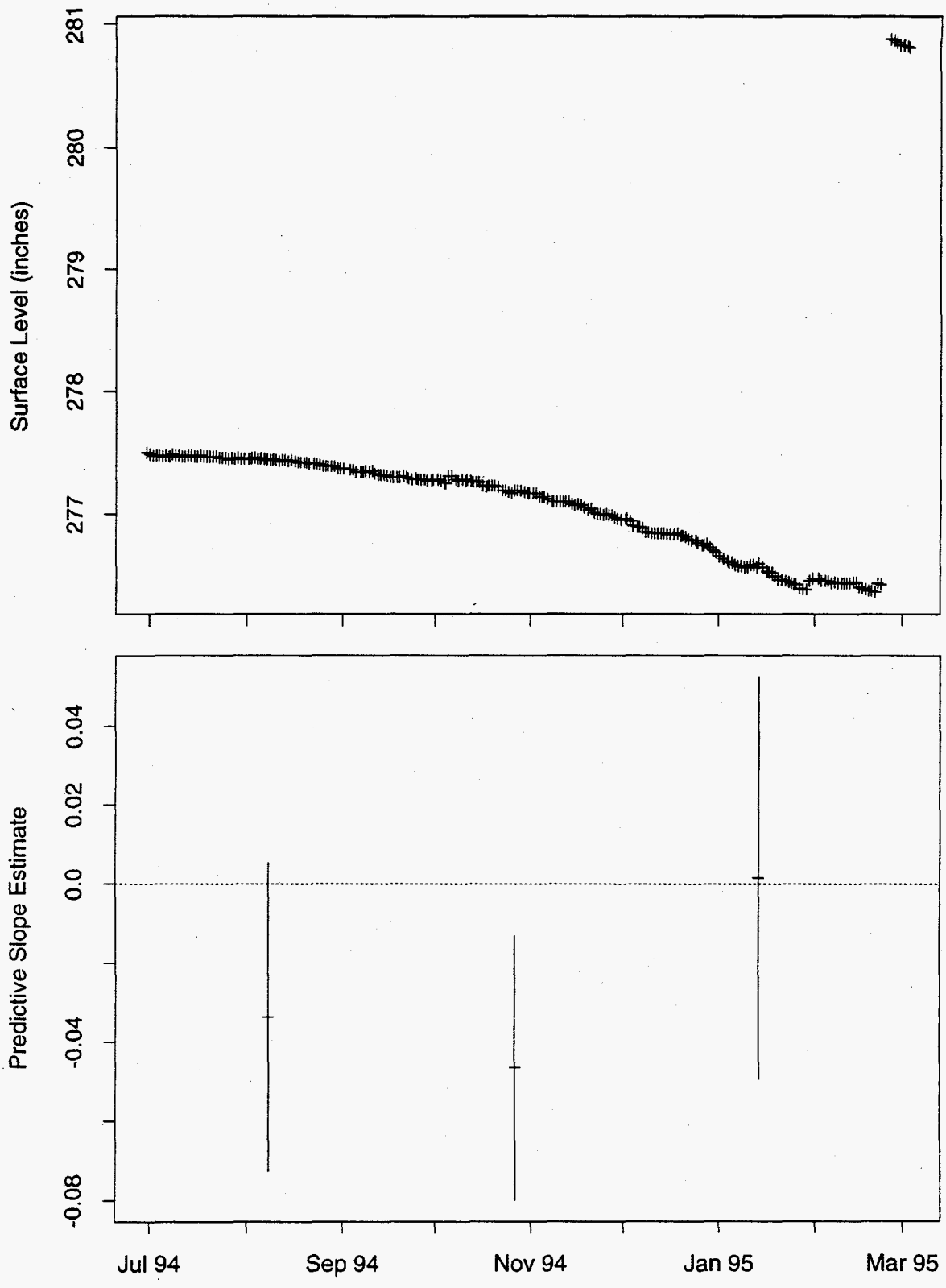

Figure 227: Tank SY–102 ENRAF Data

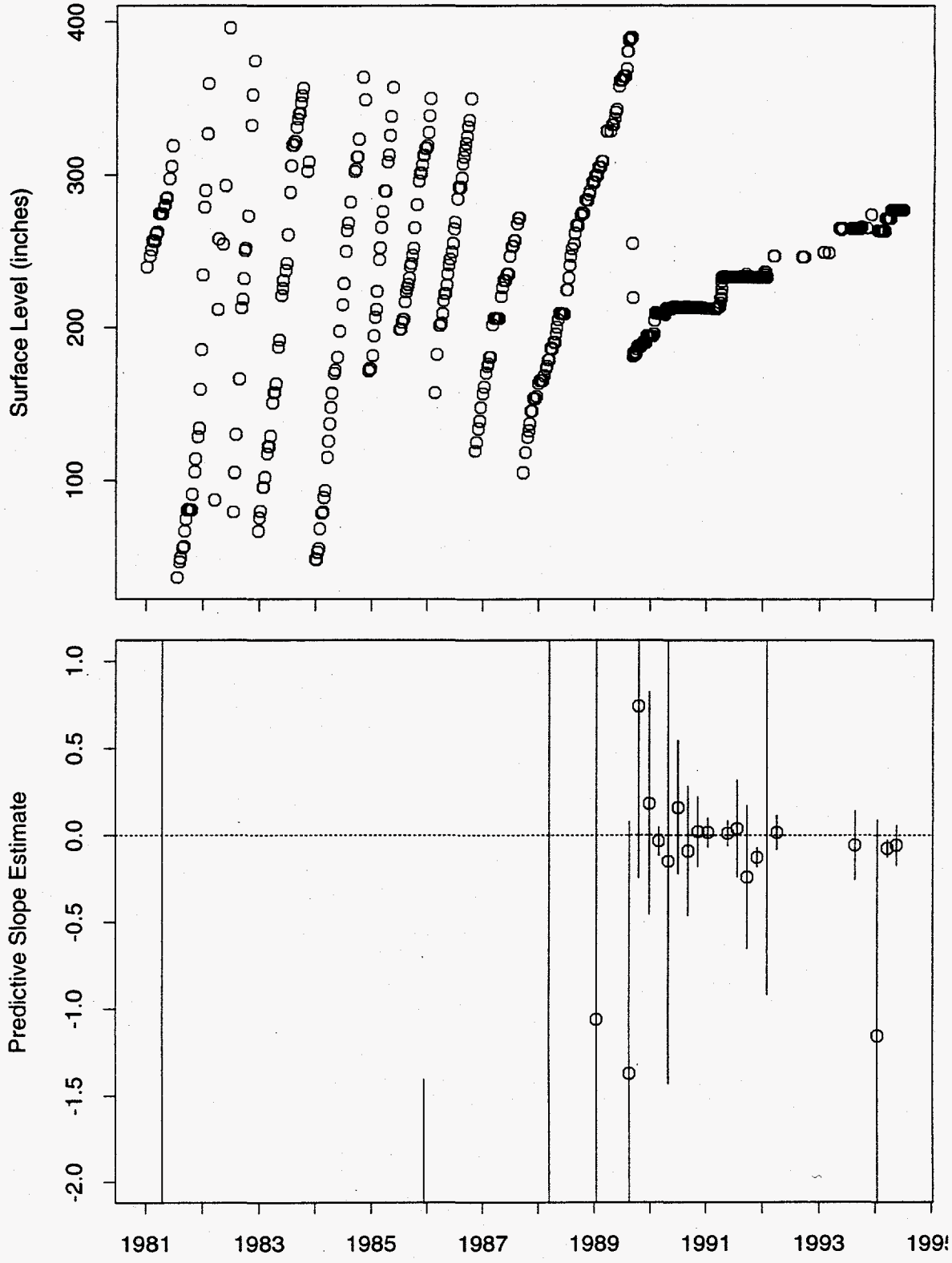

Figure 228: Tank SY–102 FIC Data

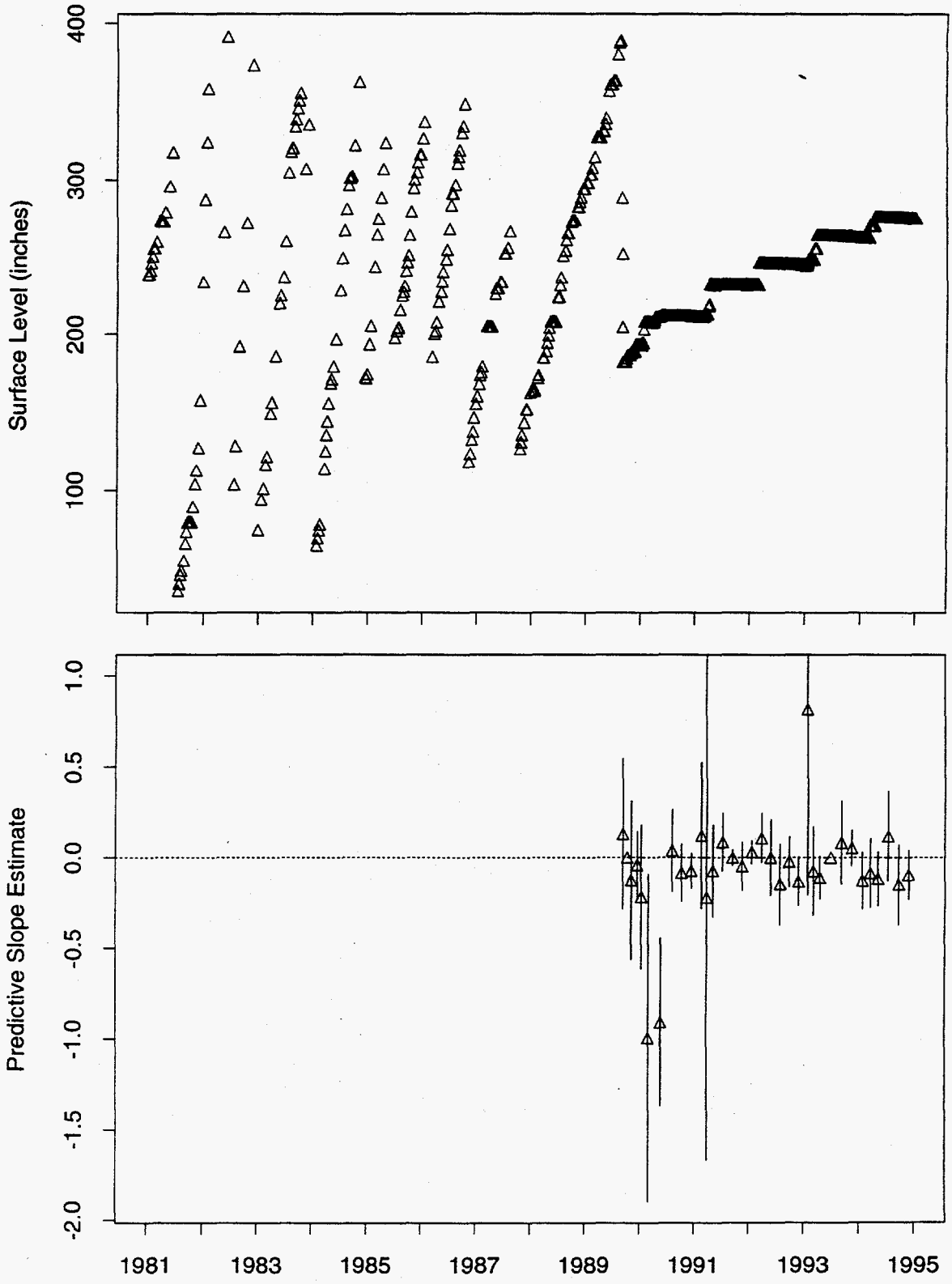

Figure 229: Tank SY–102 MT Data

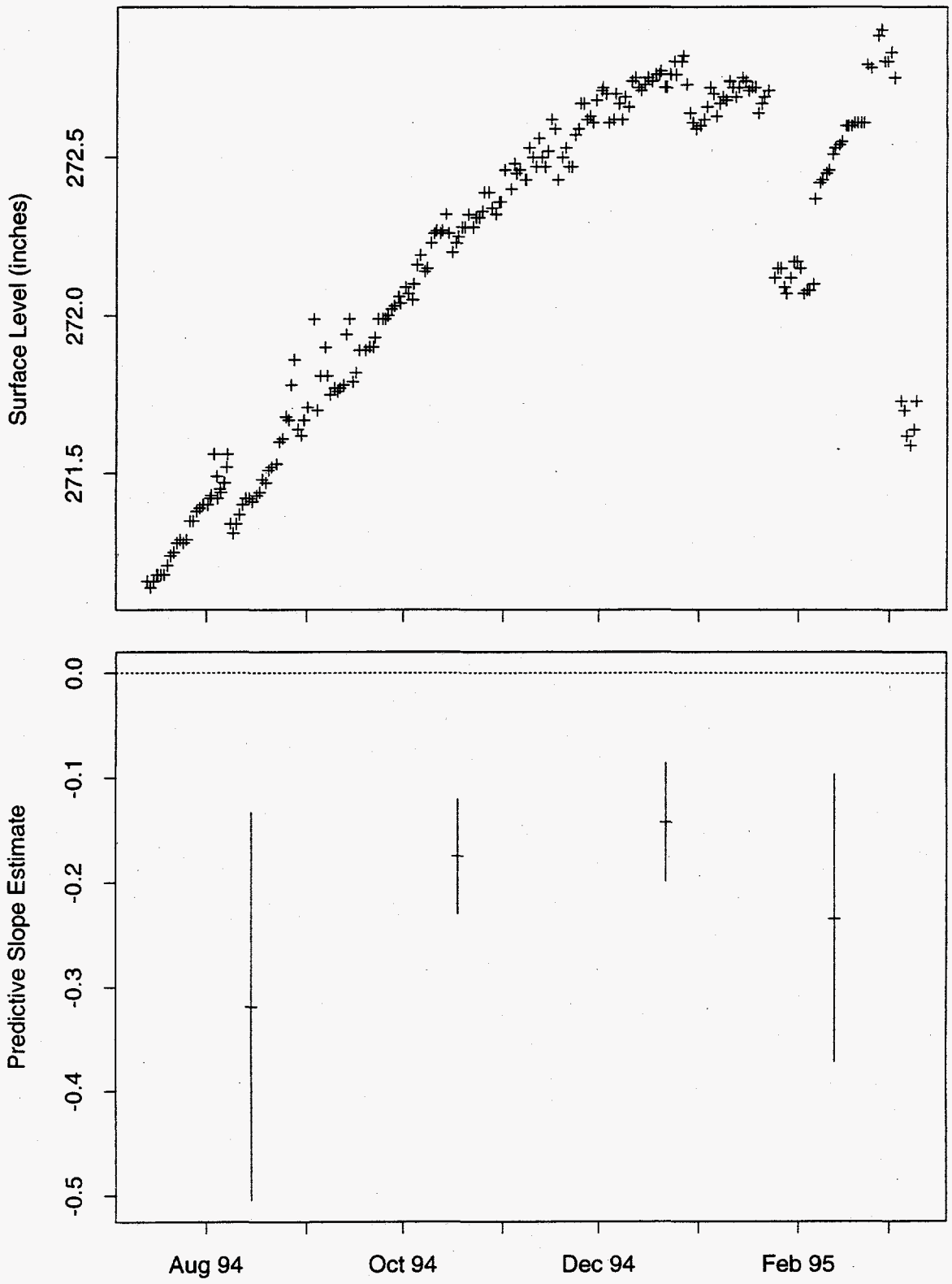

Figure 230: Tank SY–103 ENRAF Data

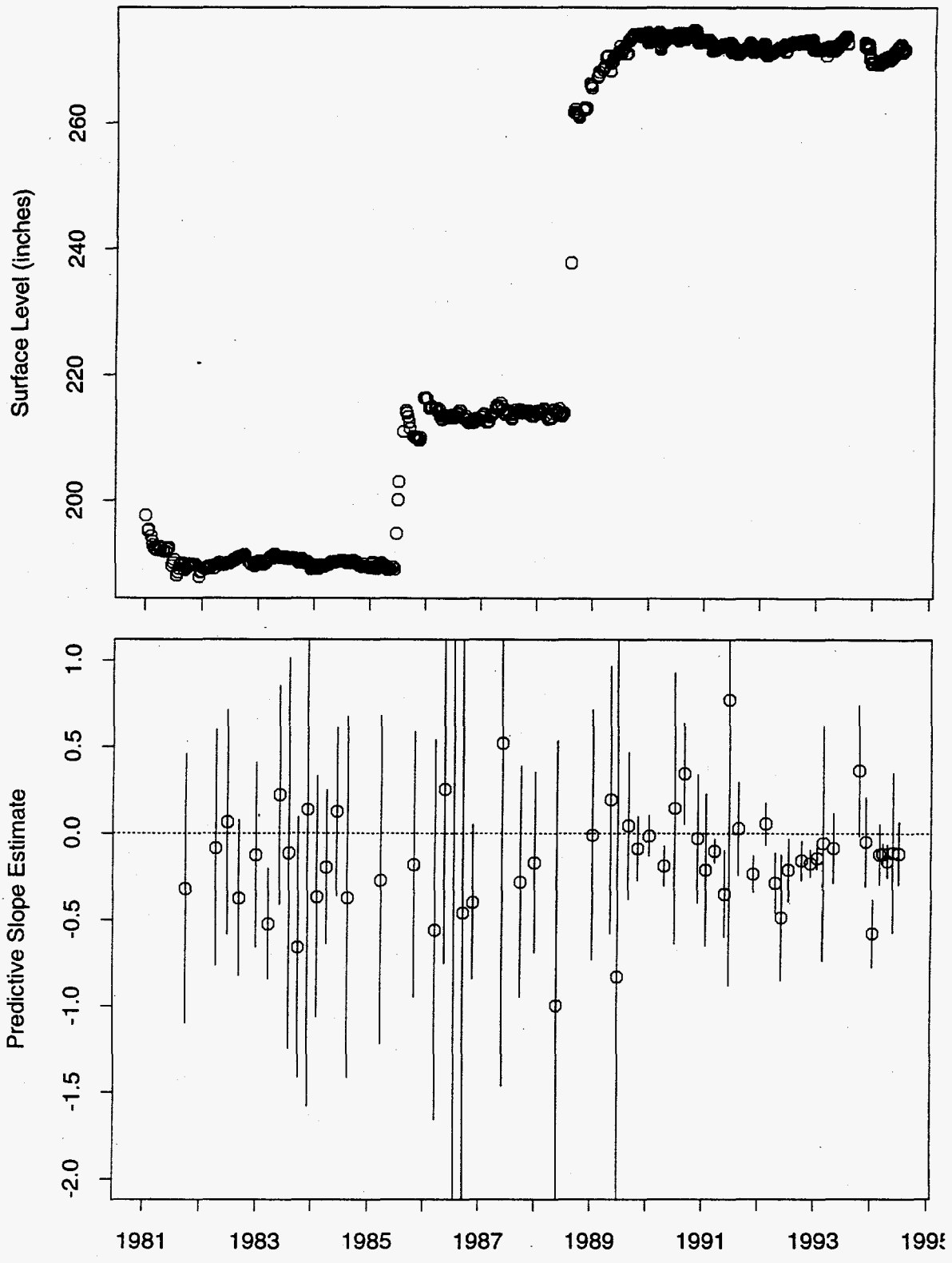

Figure 231: Tank SY–103 FIC Data

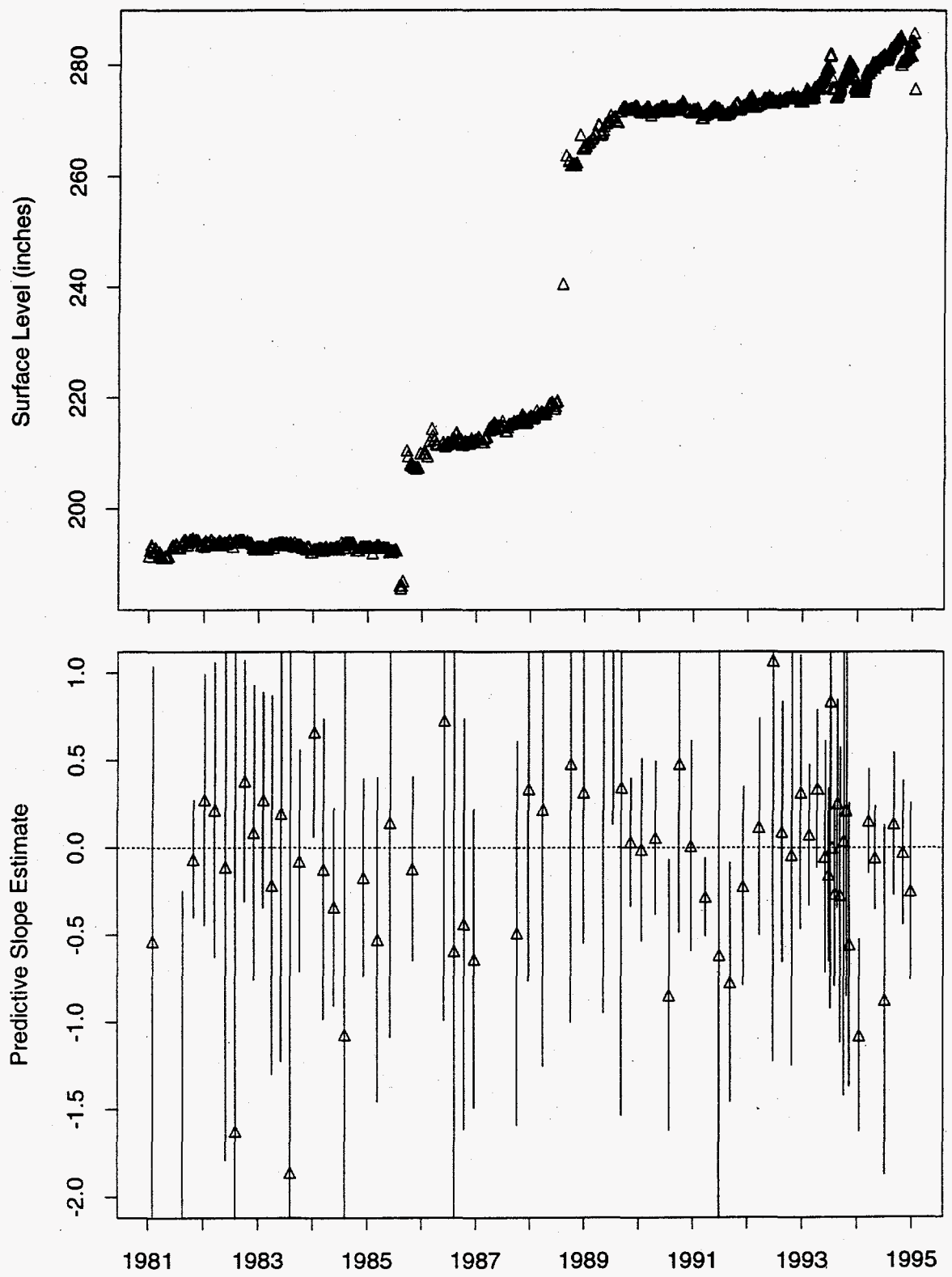

Figure 232: Tank SY–103 MT Data

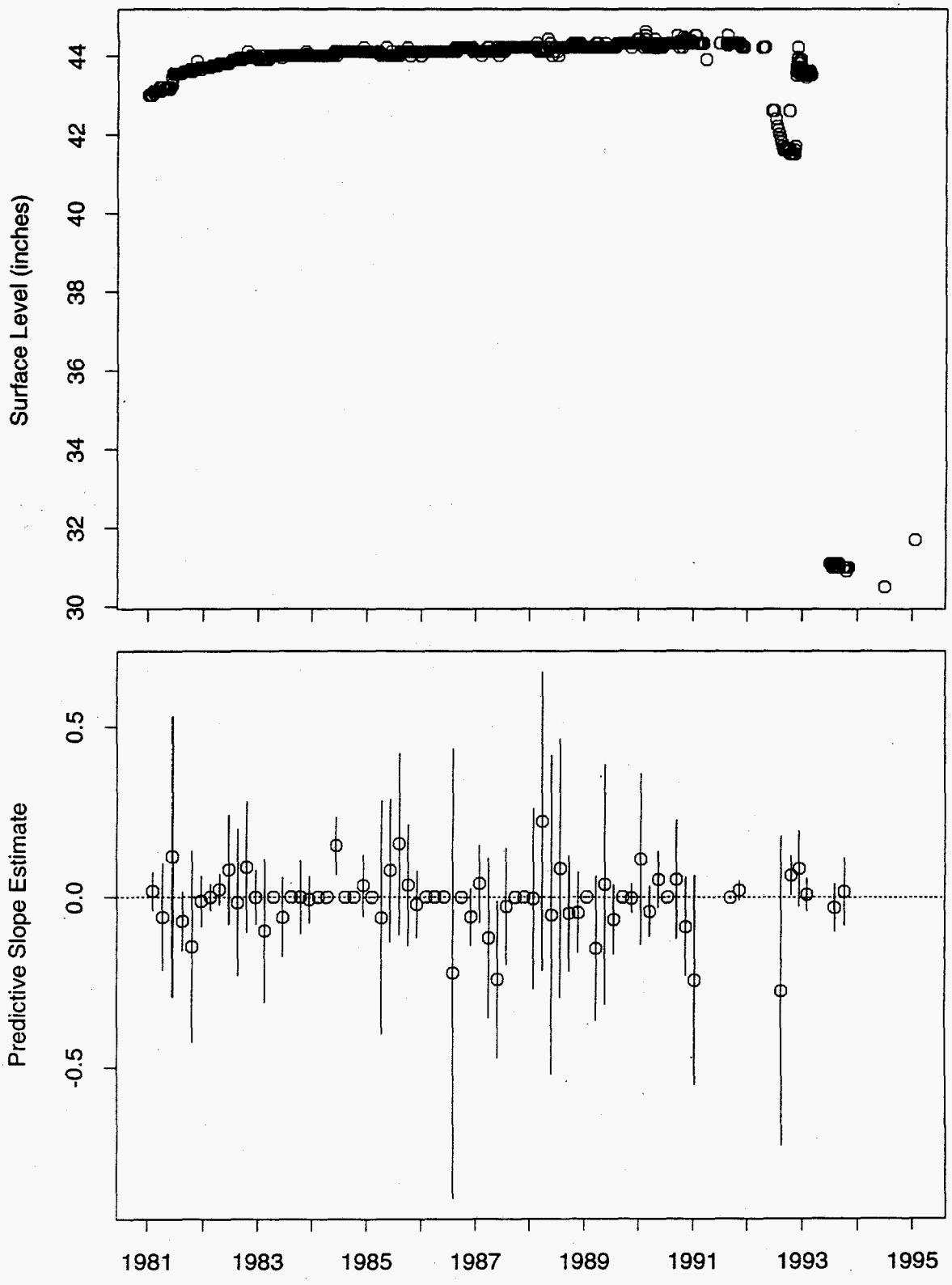

Figure 233: Tank T–101 FIC Data

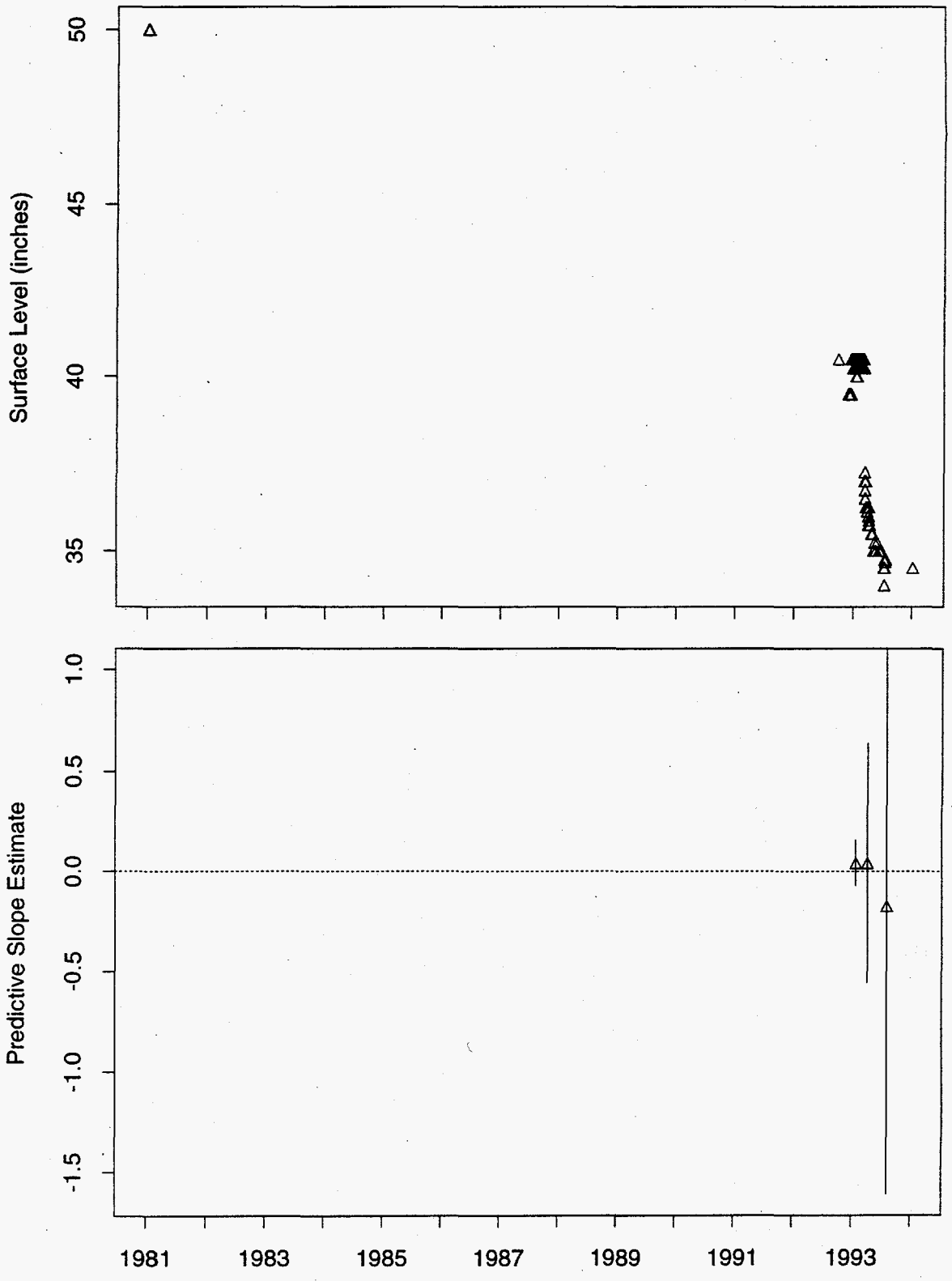

Figure 234: Tank T-101 MT Data

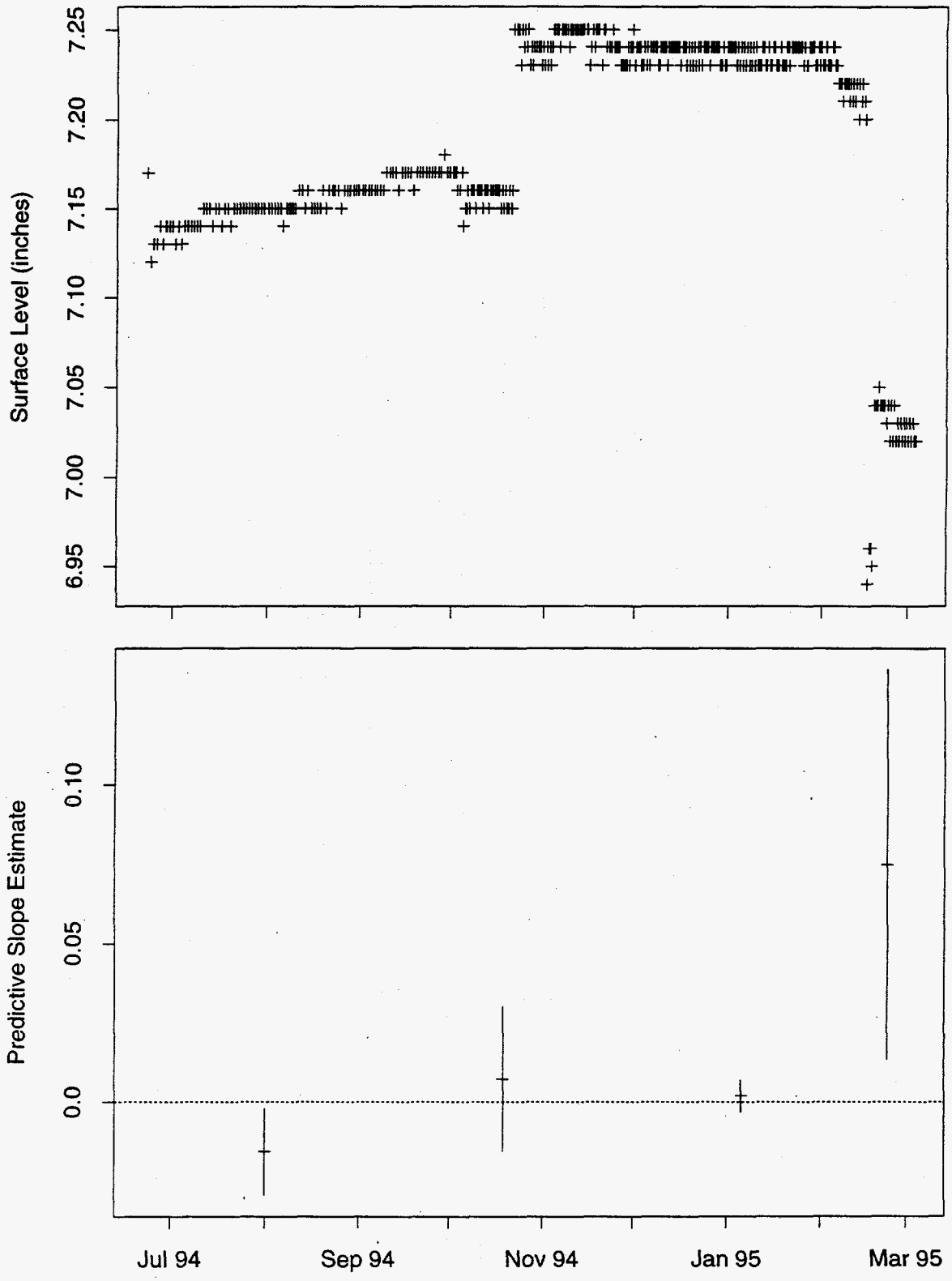

Figure 235: Tank T-102 ENRAF Data

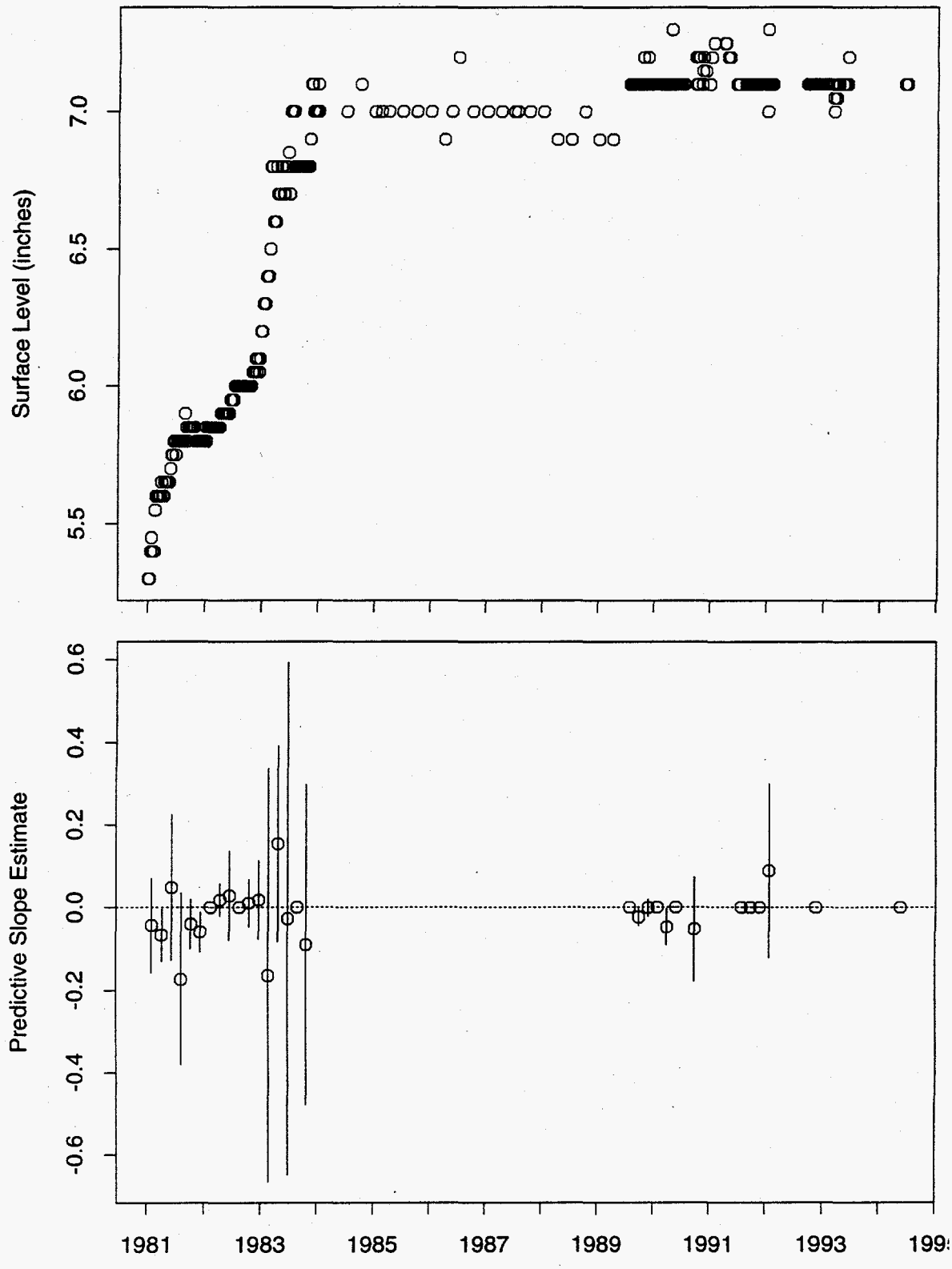

Figure 236: Tank T-102 FIC Data

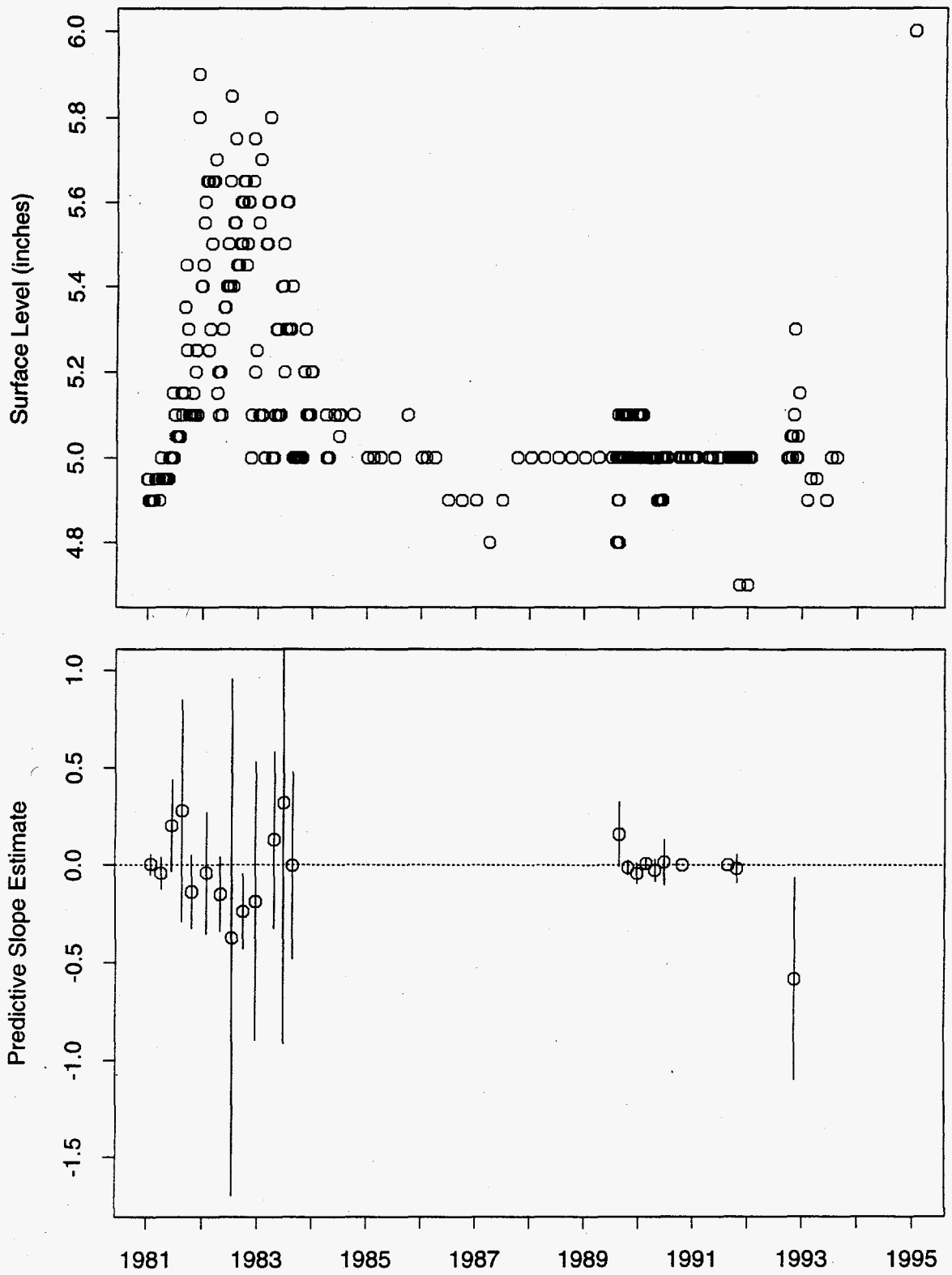

Figure 237: Tank T-103 FIC Data

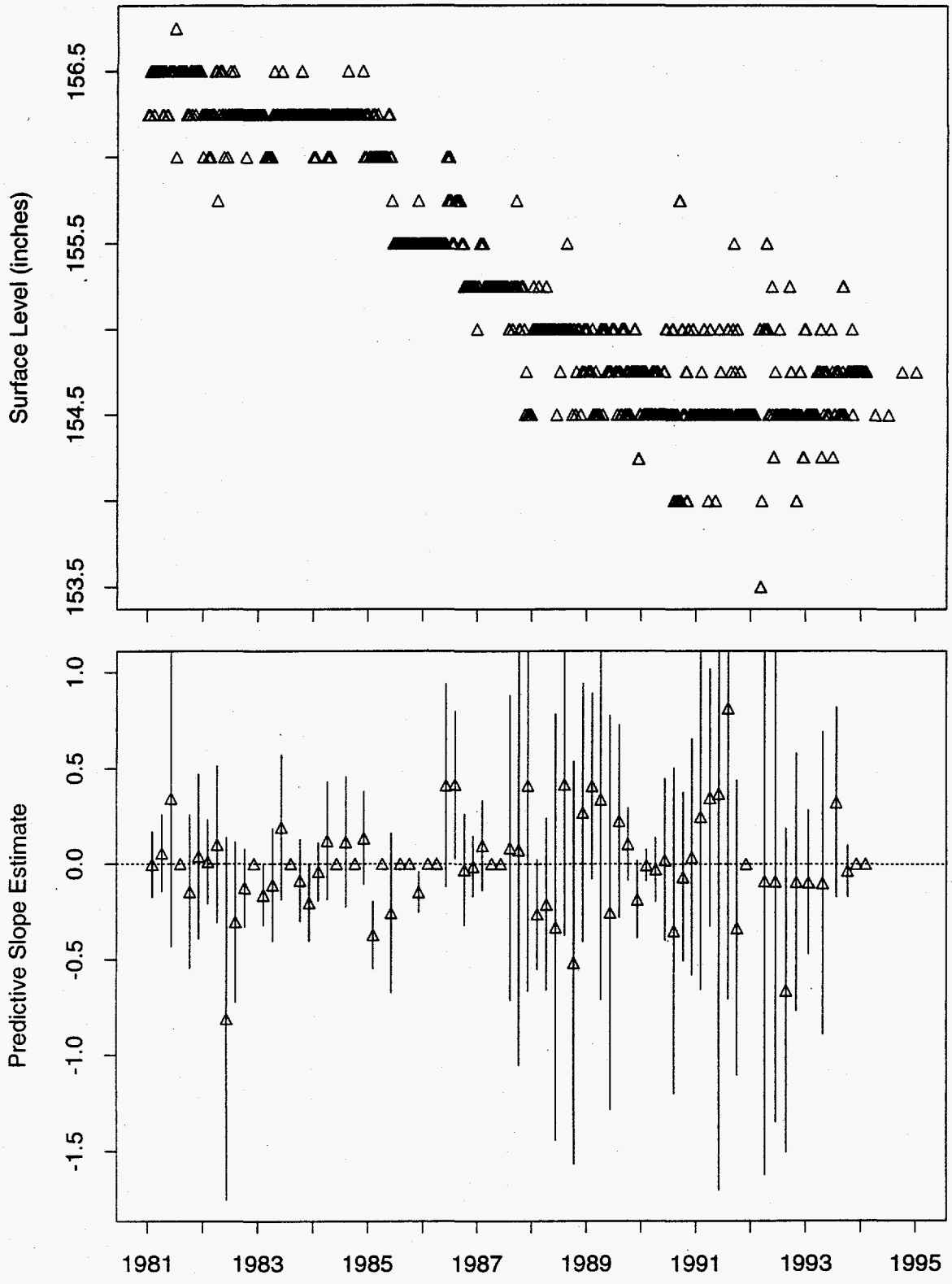

Figure 238: Tank T–104 MT Data

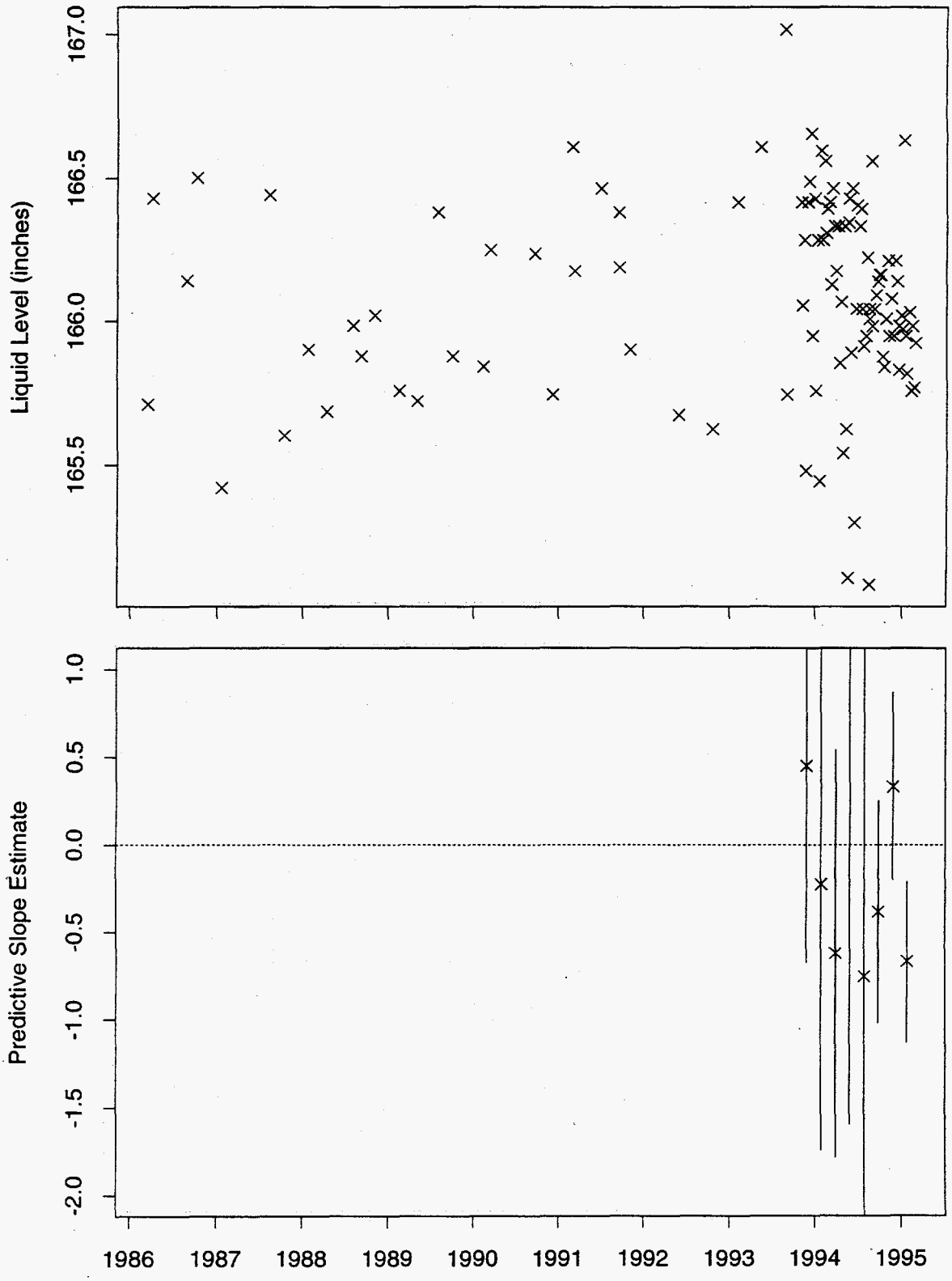

Figure 239: Tank T–104 Neutron ILL Data

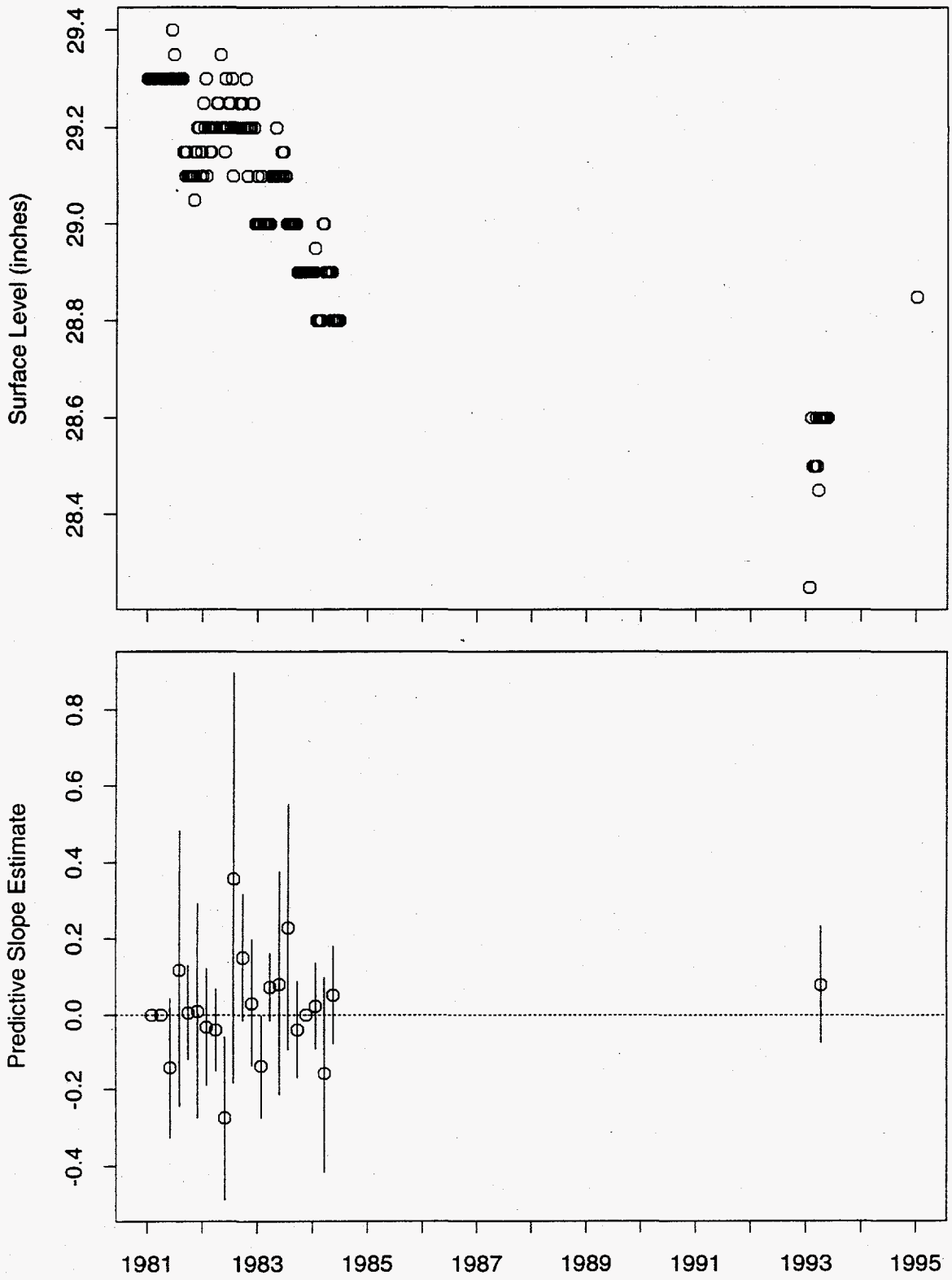

Figure 240: Tank T-105 FIC Data

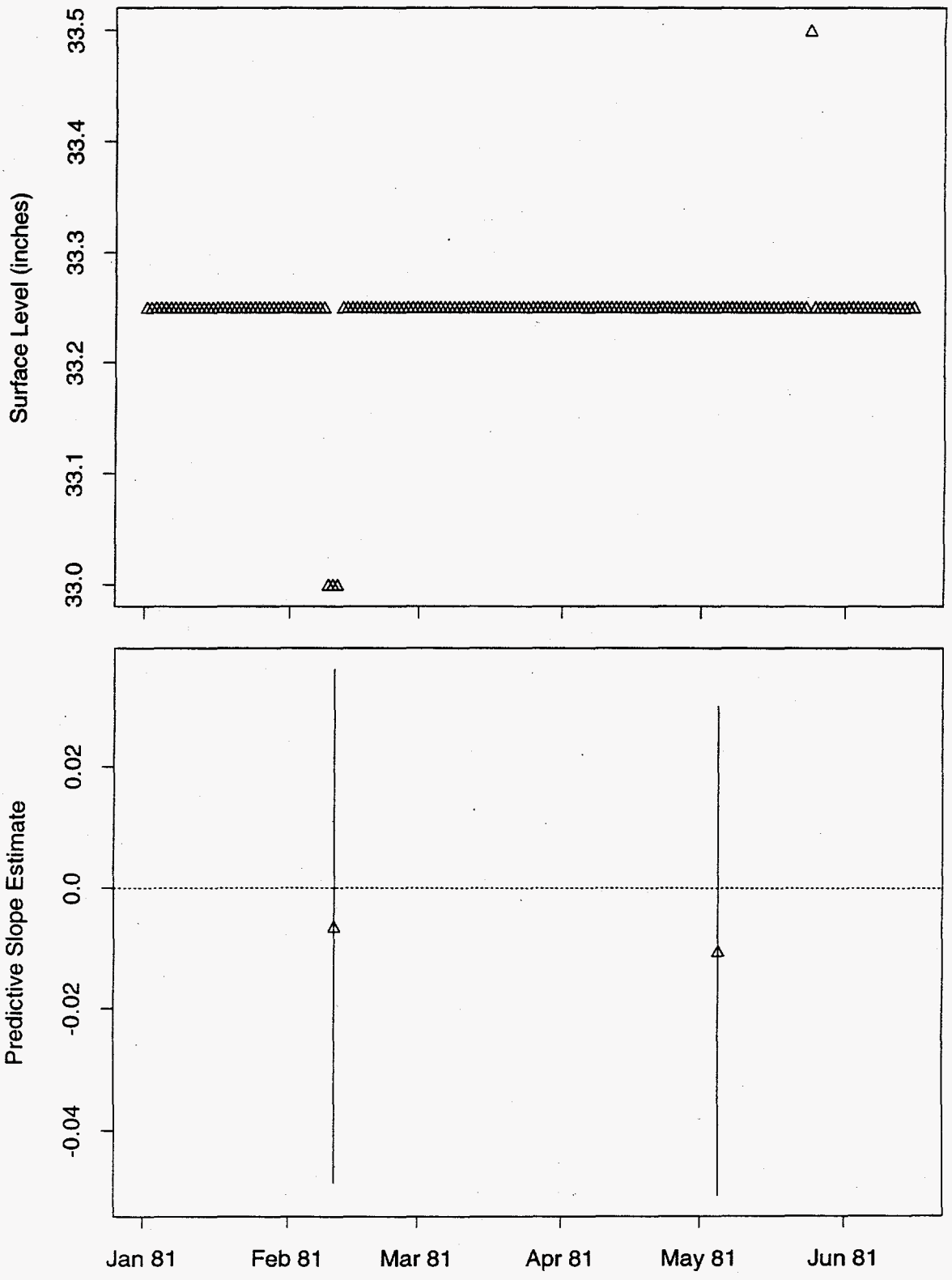

Figure 241: Tank T-105 MT Data

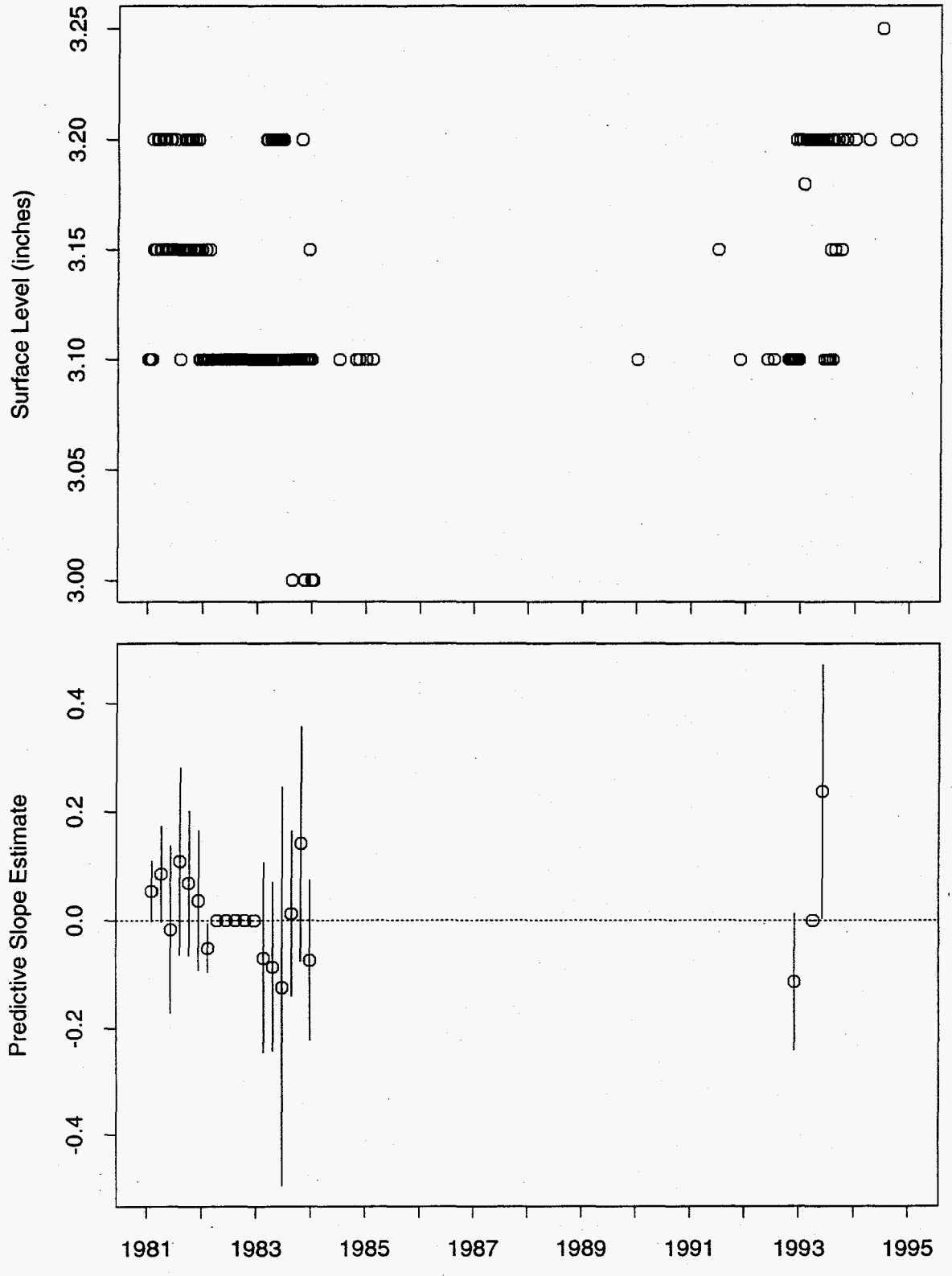

Figure 242: Tank T-106 FIC Data

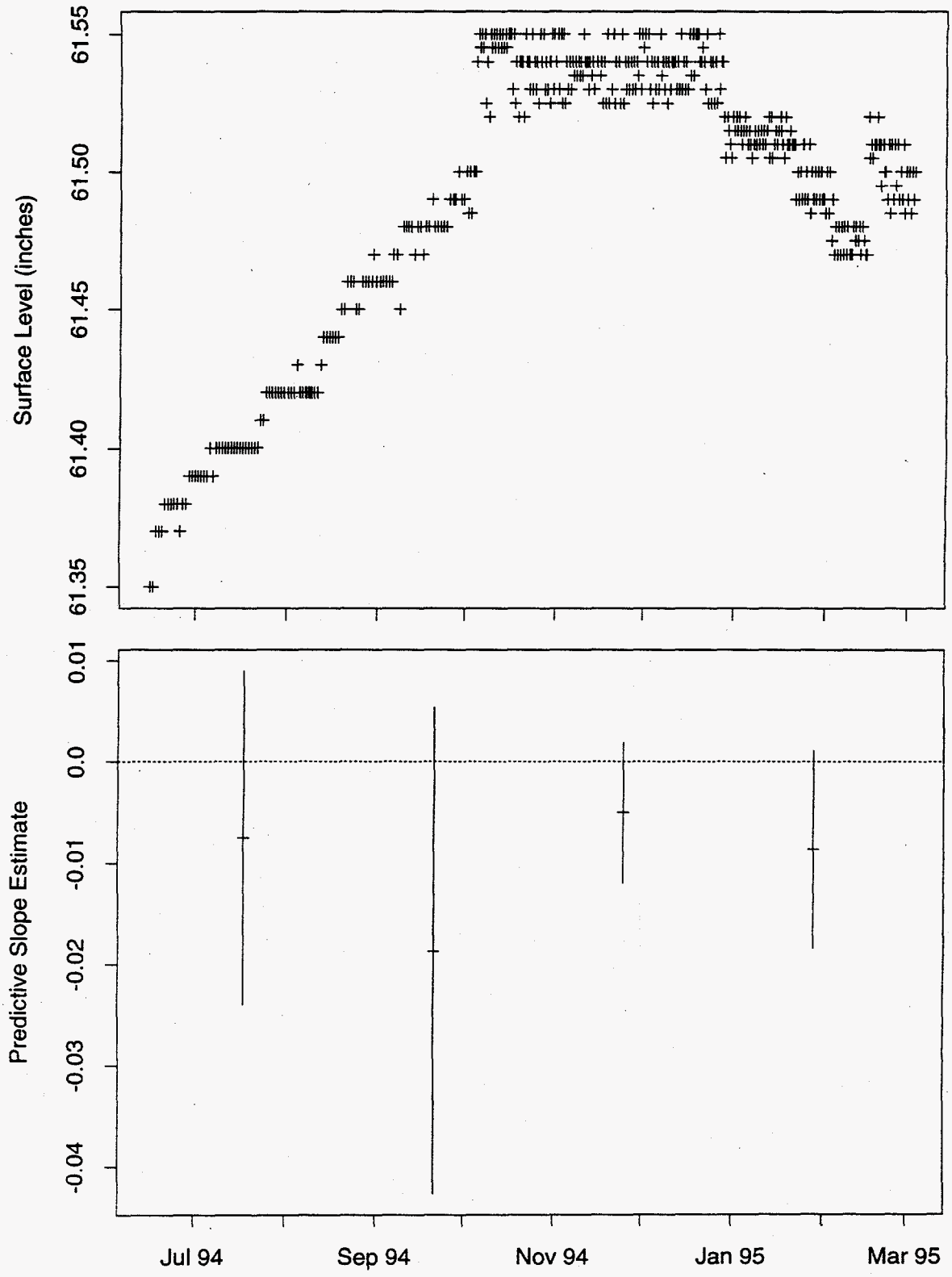

Figure 243: Tank T–107 ENRAF Data

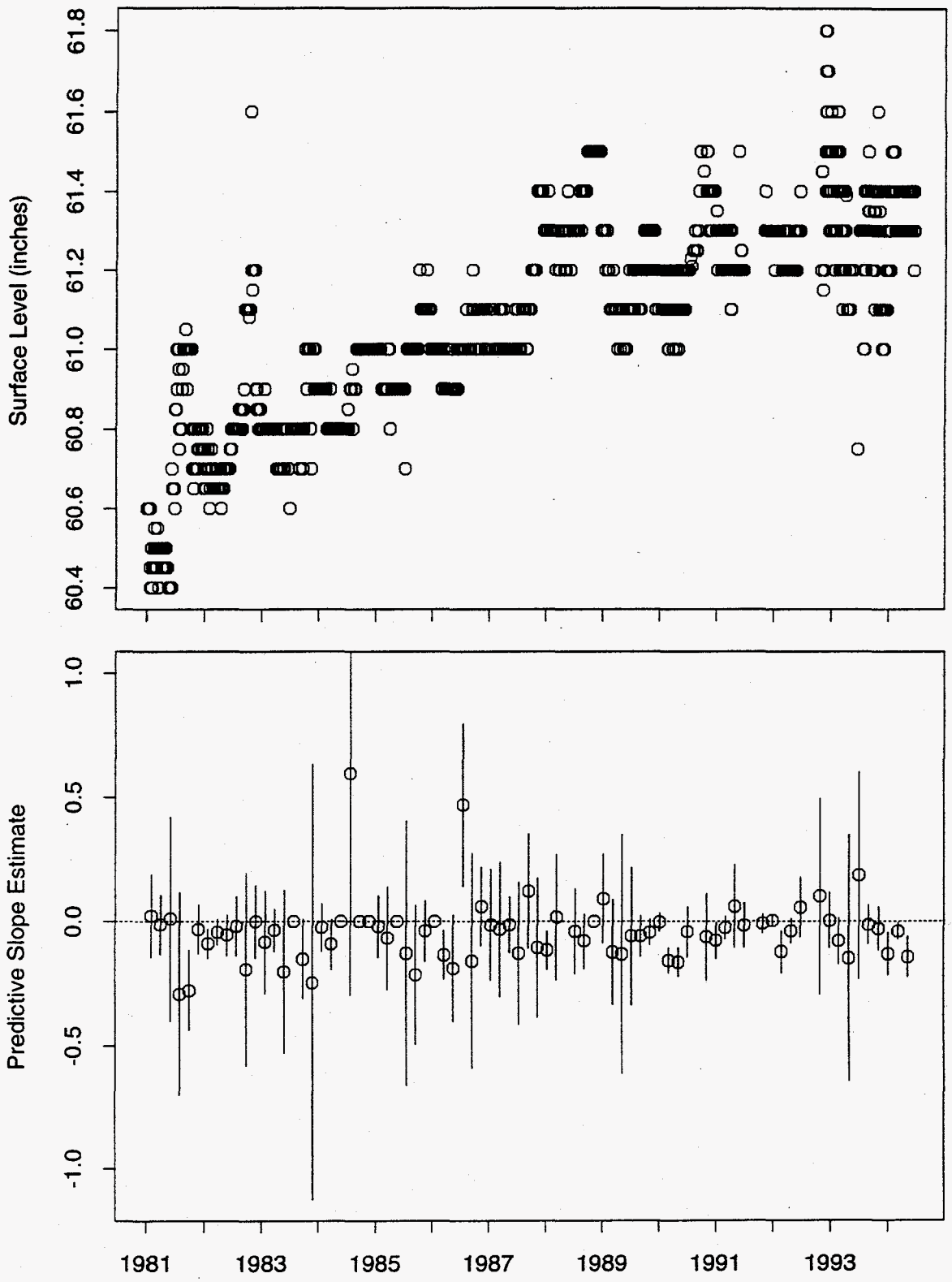

Figure 244: Tank T–107 FIC Data

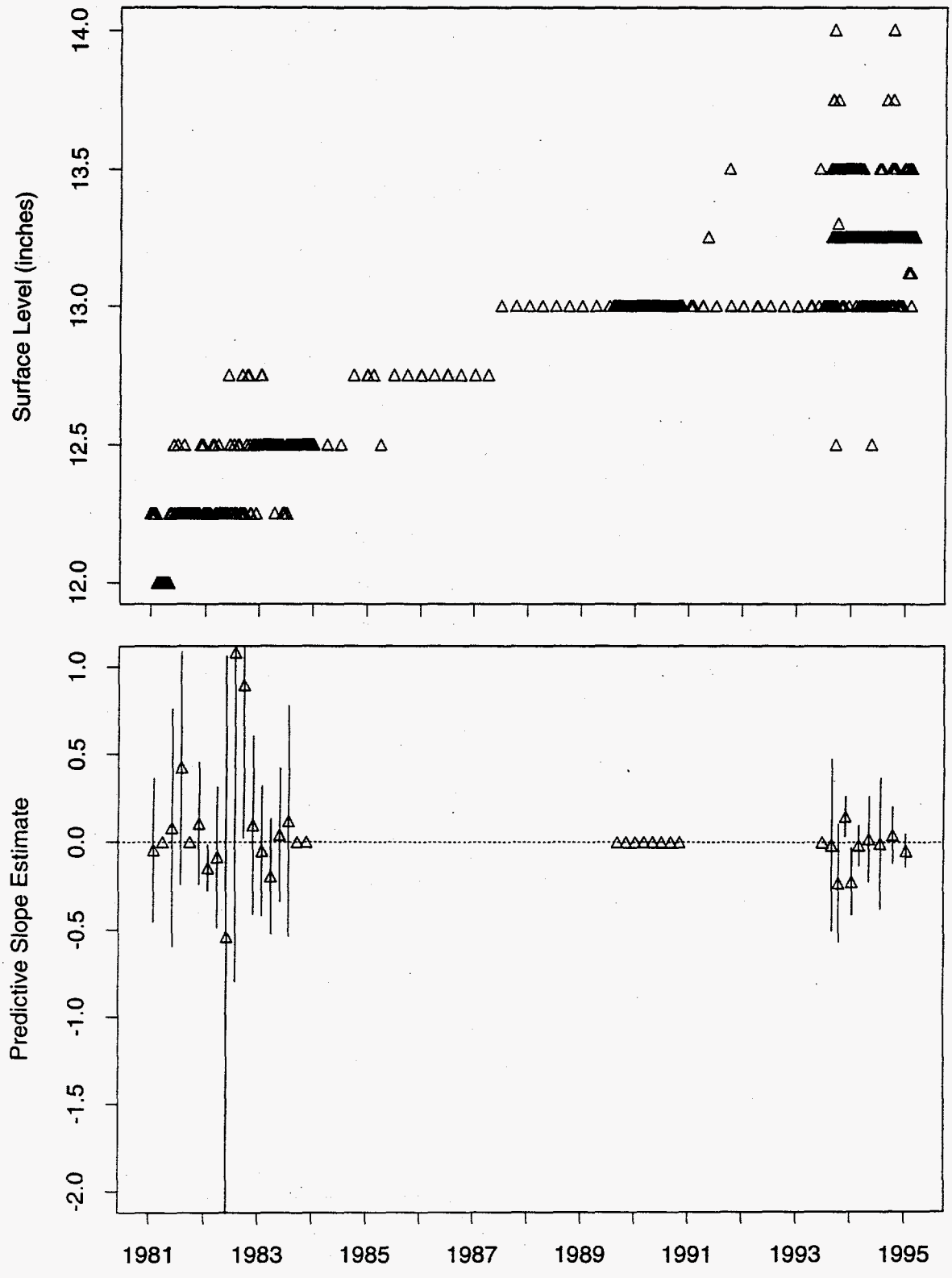

Figure 245: Tank T–108 MT Data

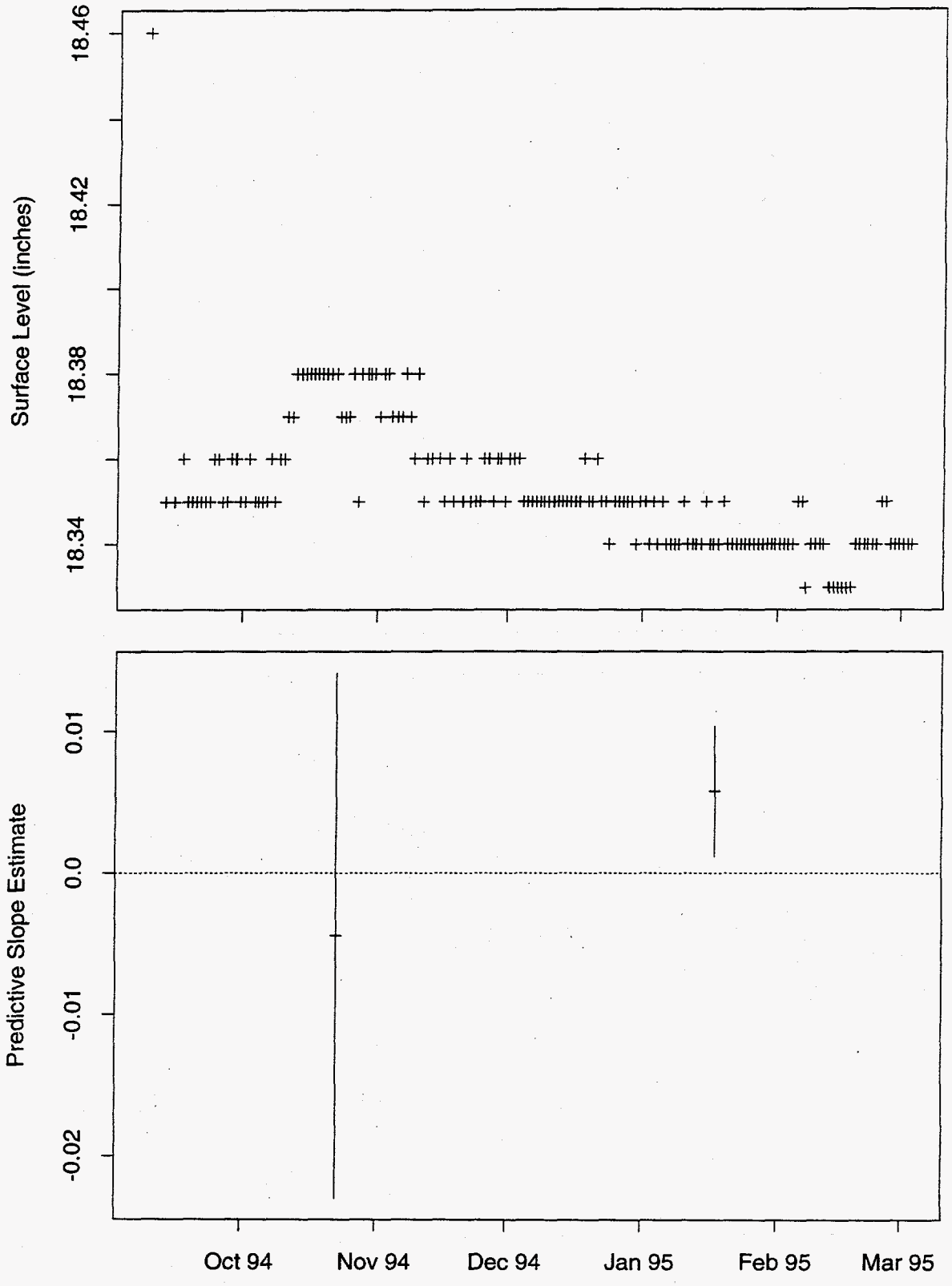

Figure 246: Tank T-109 ENRAF Data

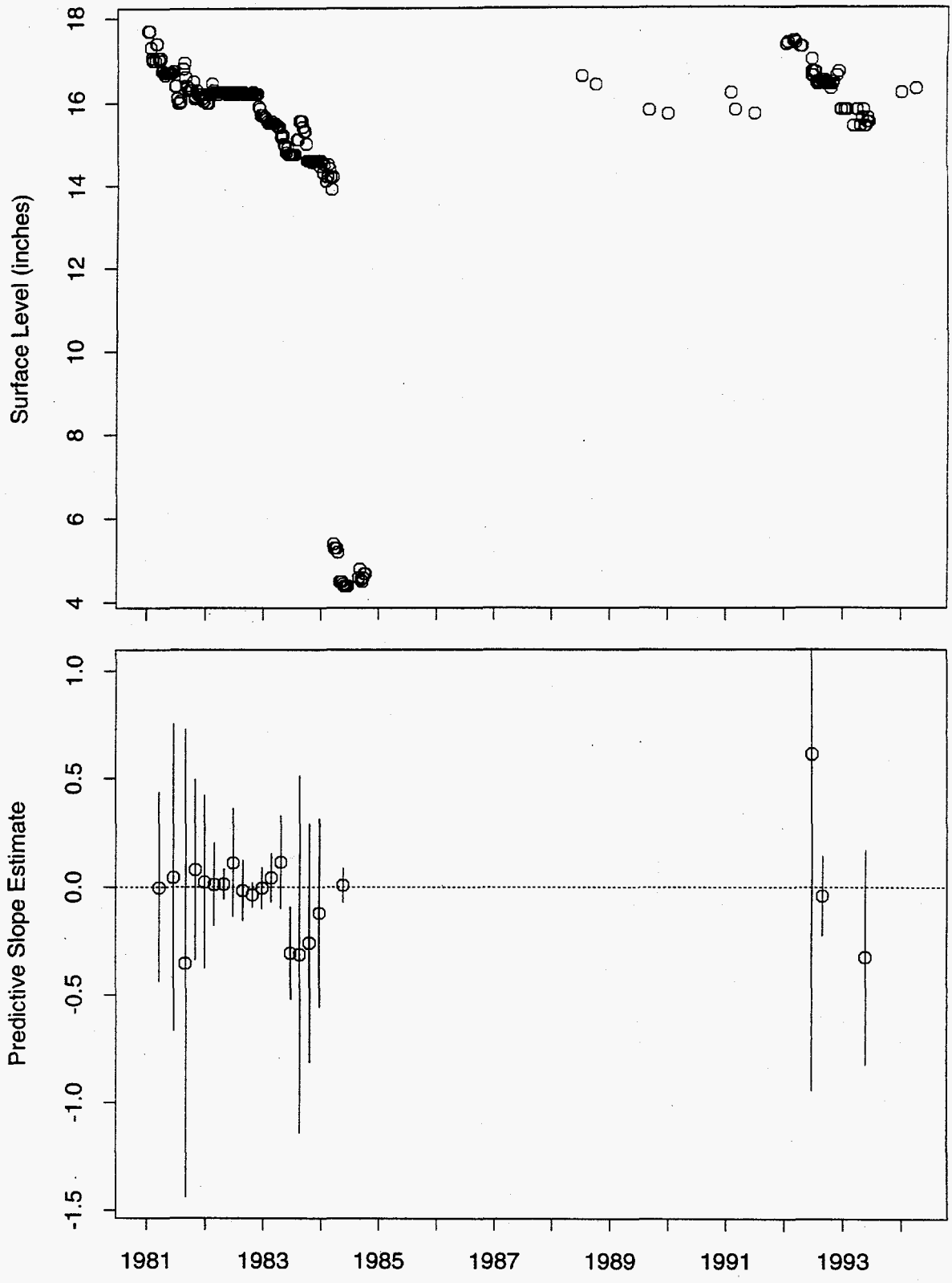

Figure 247: Tank T–109 FIC Data

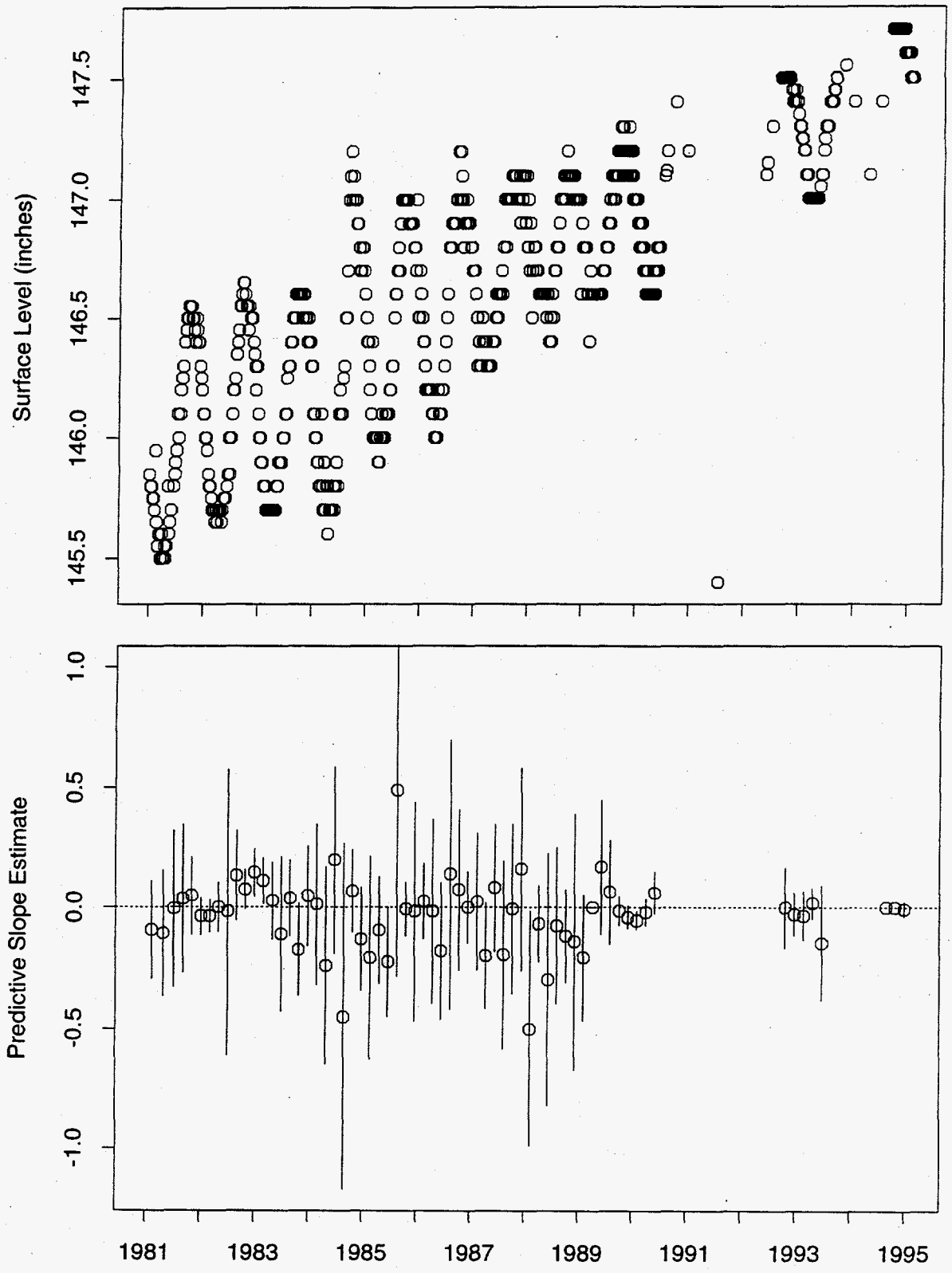

Figure 248: Tank T–110 FIC Data

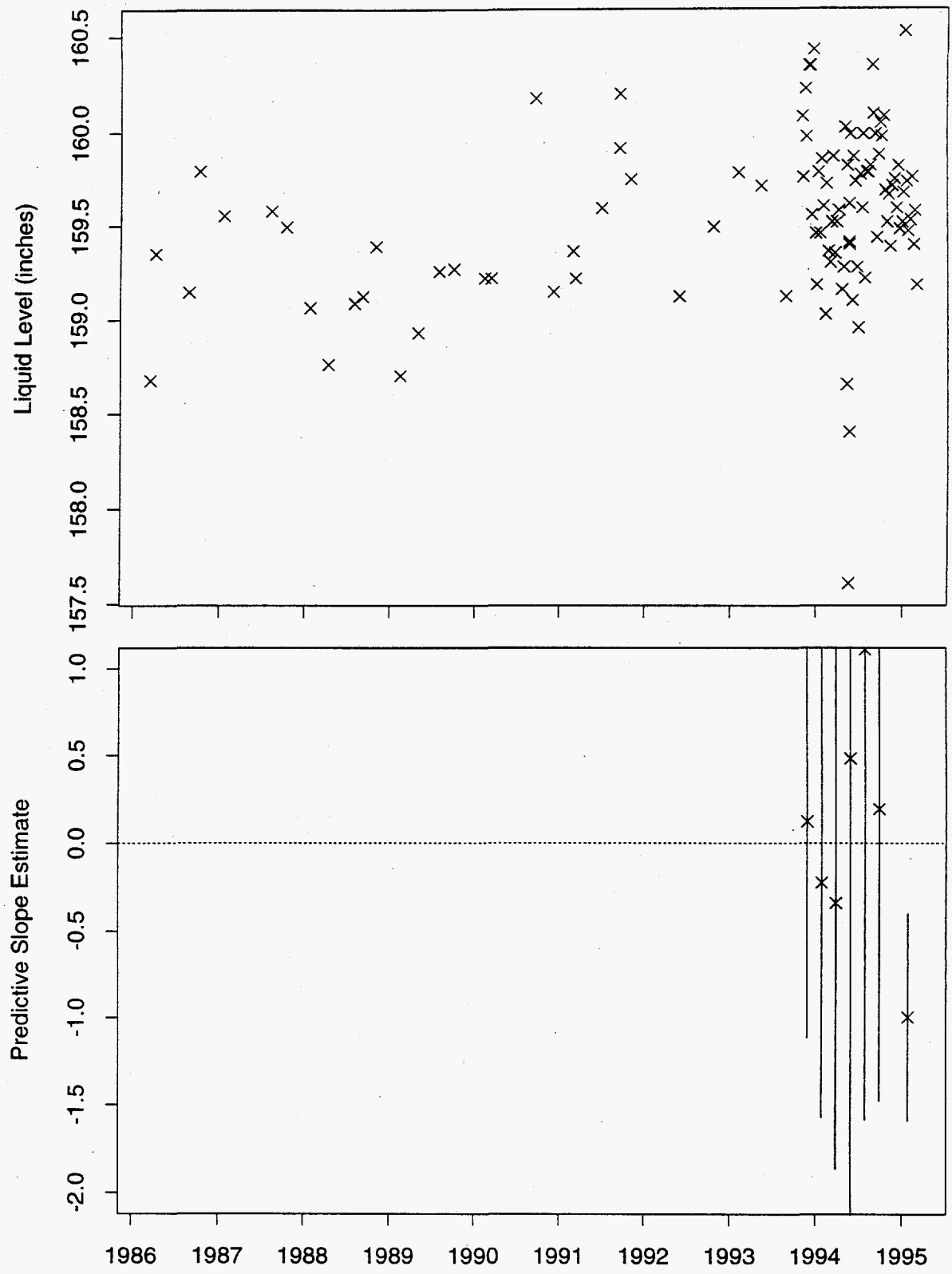

Figure 249: Tank T-110 Neutron ILL Data

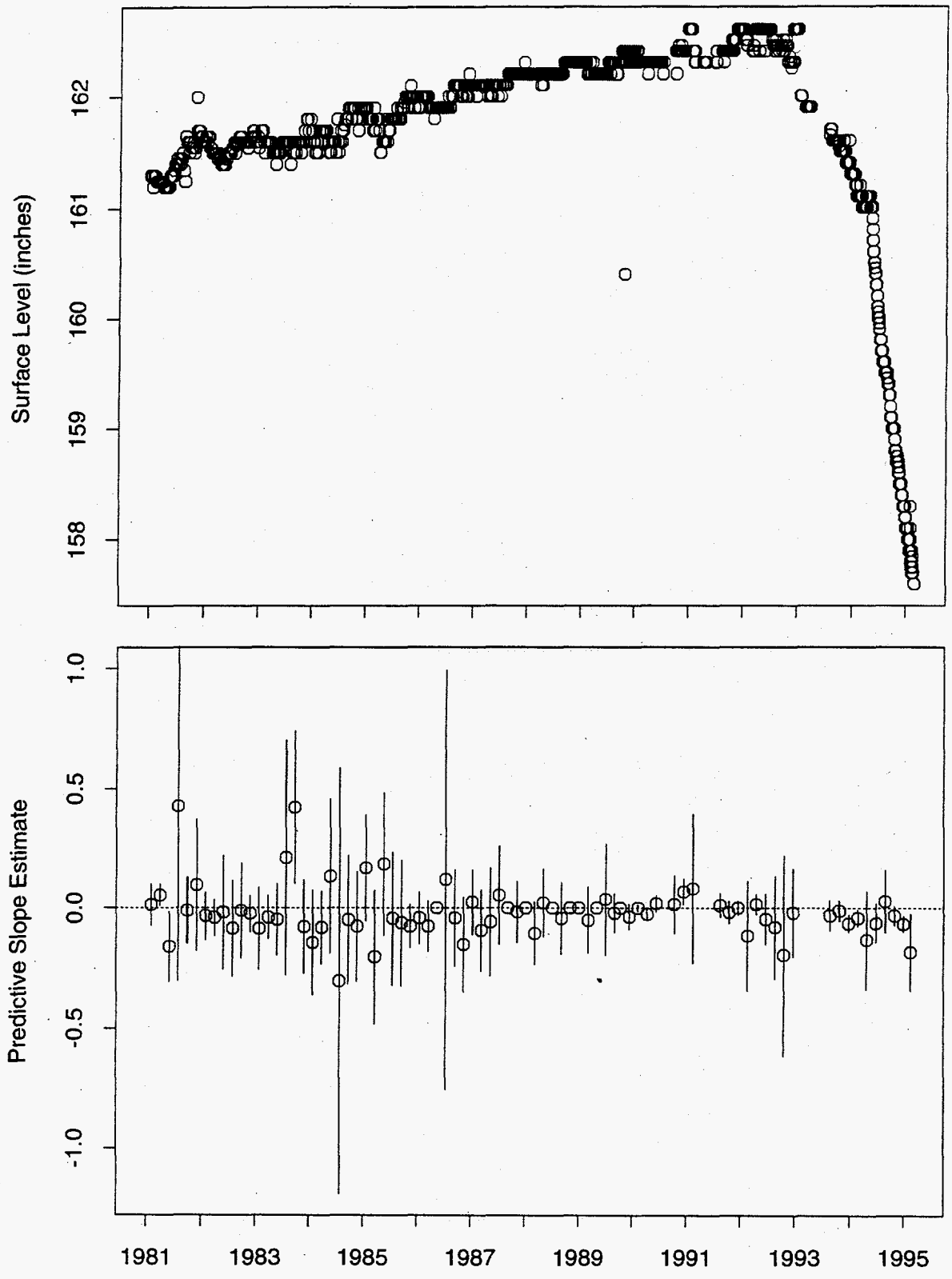

Figure 250: Tank T–111 FIC Data

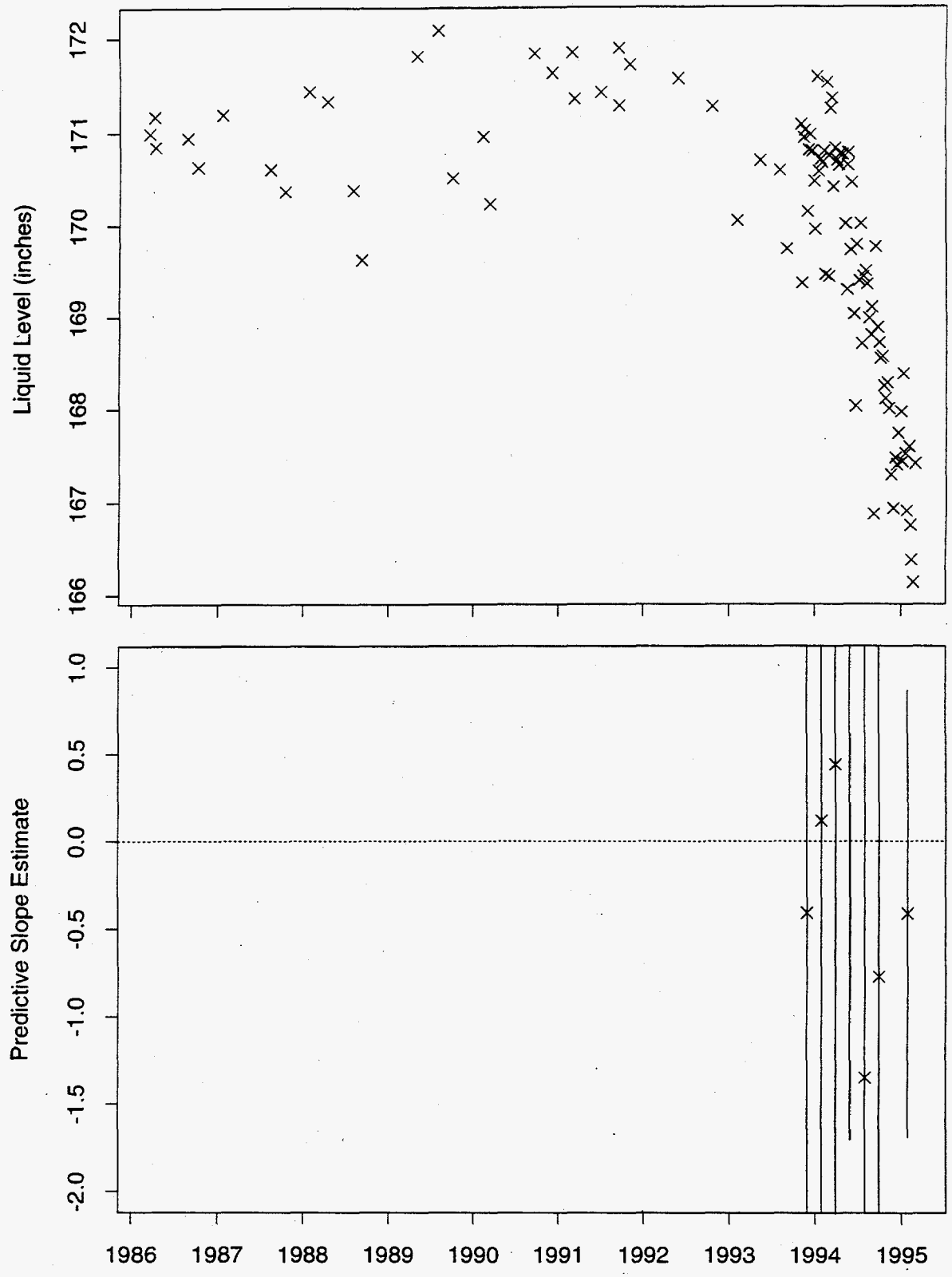

Figure 251: Tank T-111 Neutron ILL Data

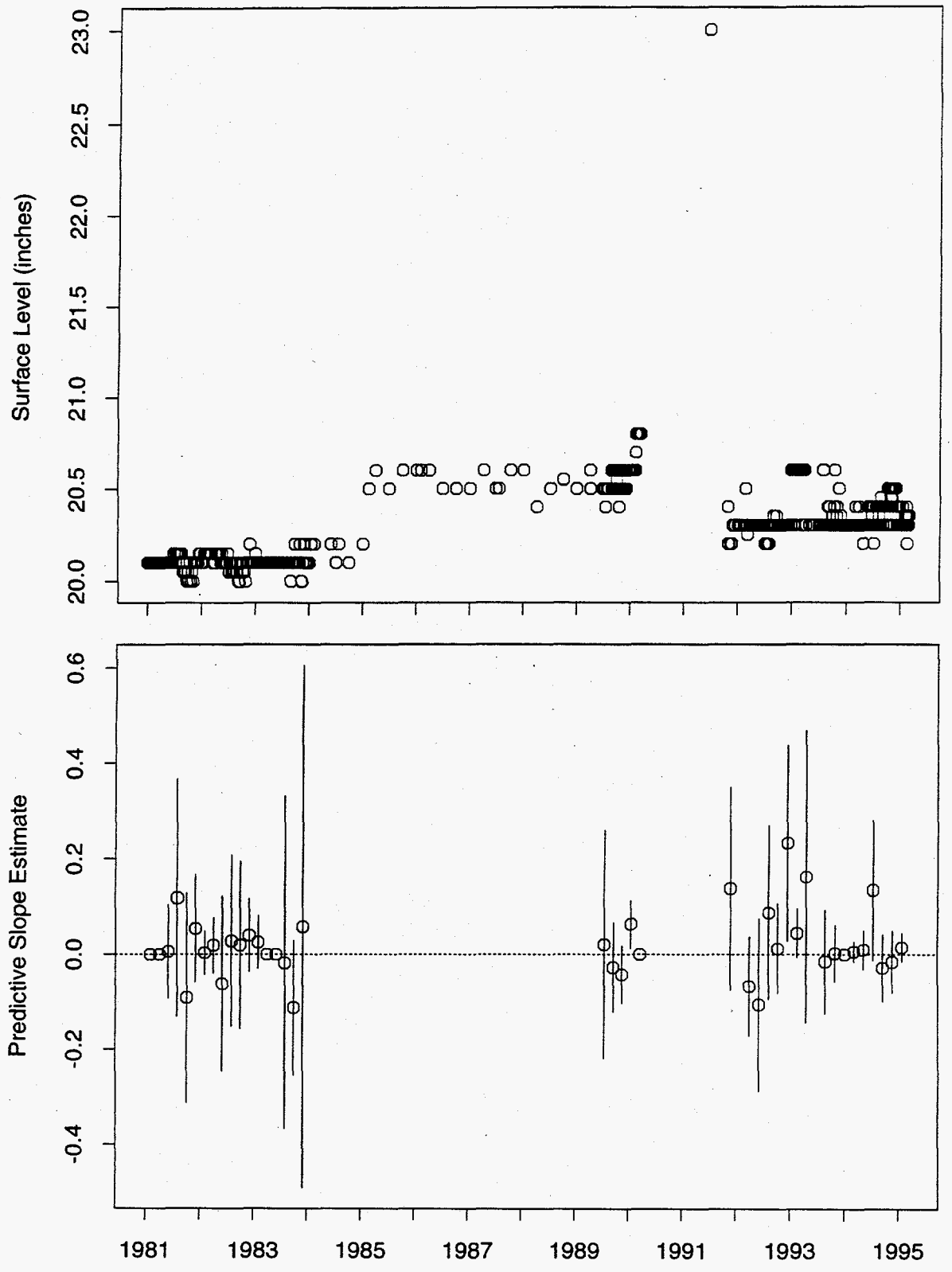

Figure 252: Tank T–112 FIC Data

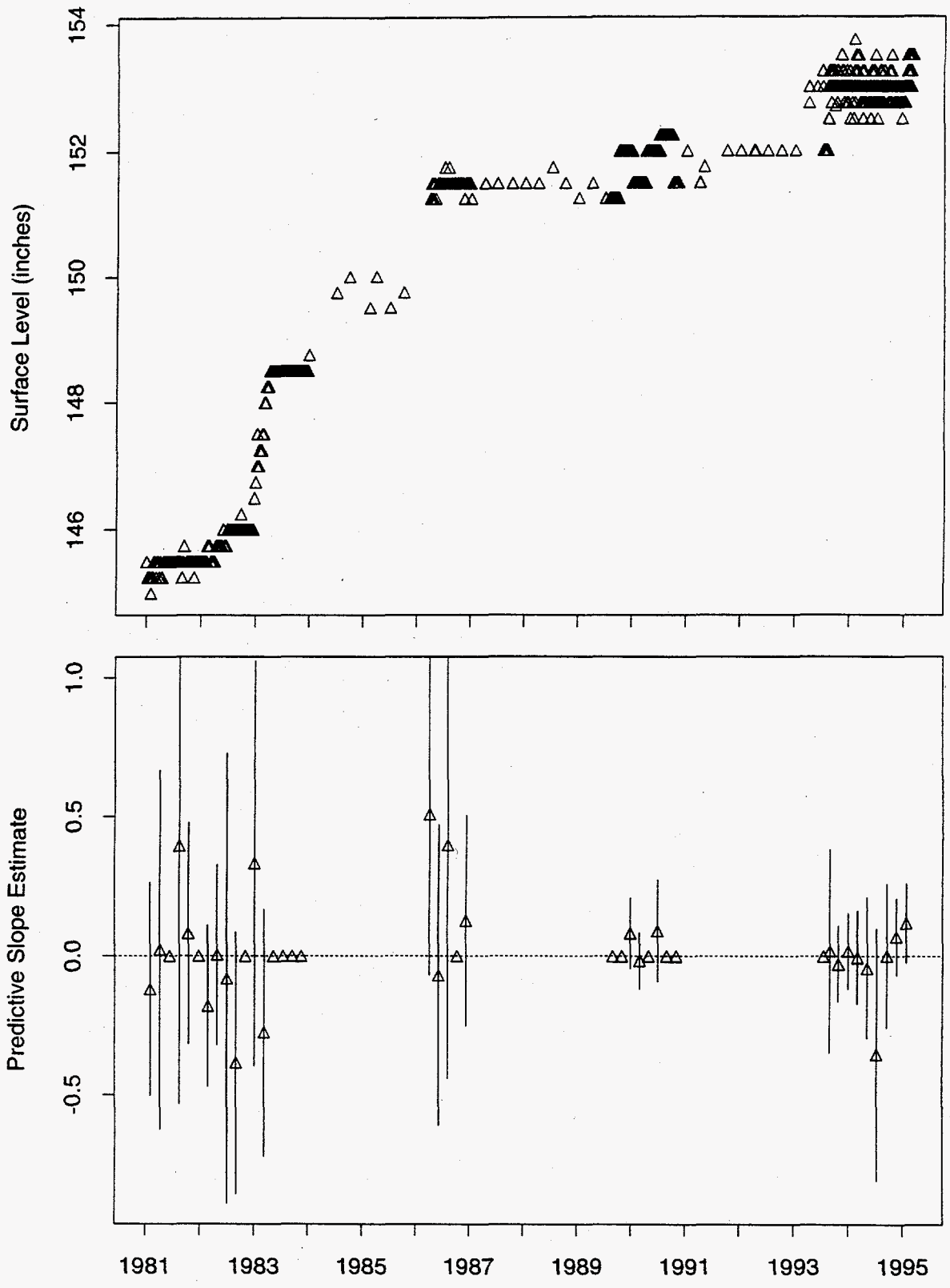

Figure 253: Tank T–201 MT Data

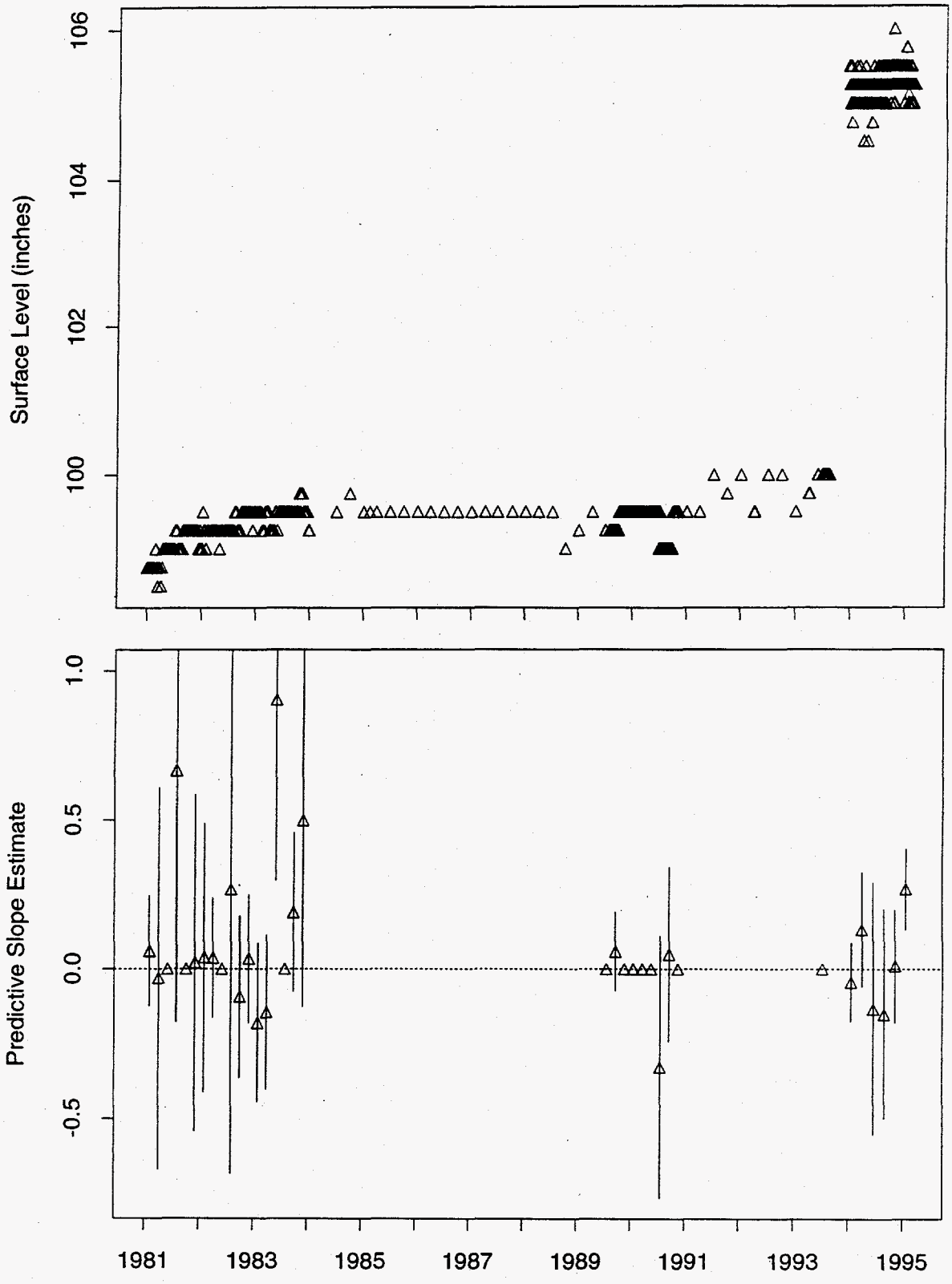

Figure 254: Tank T–202 MT Data

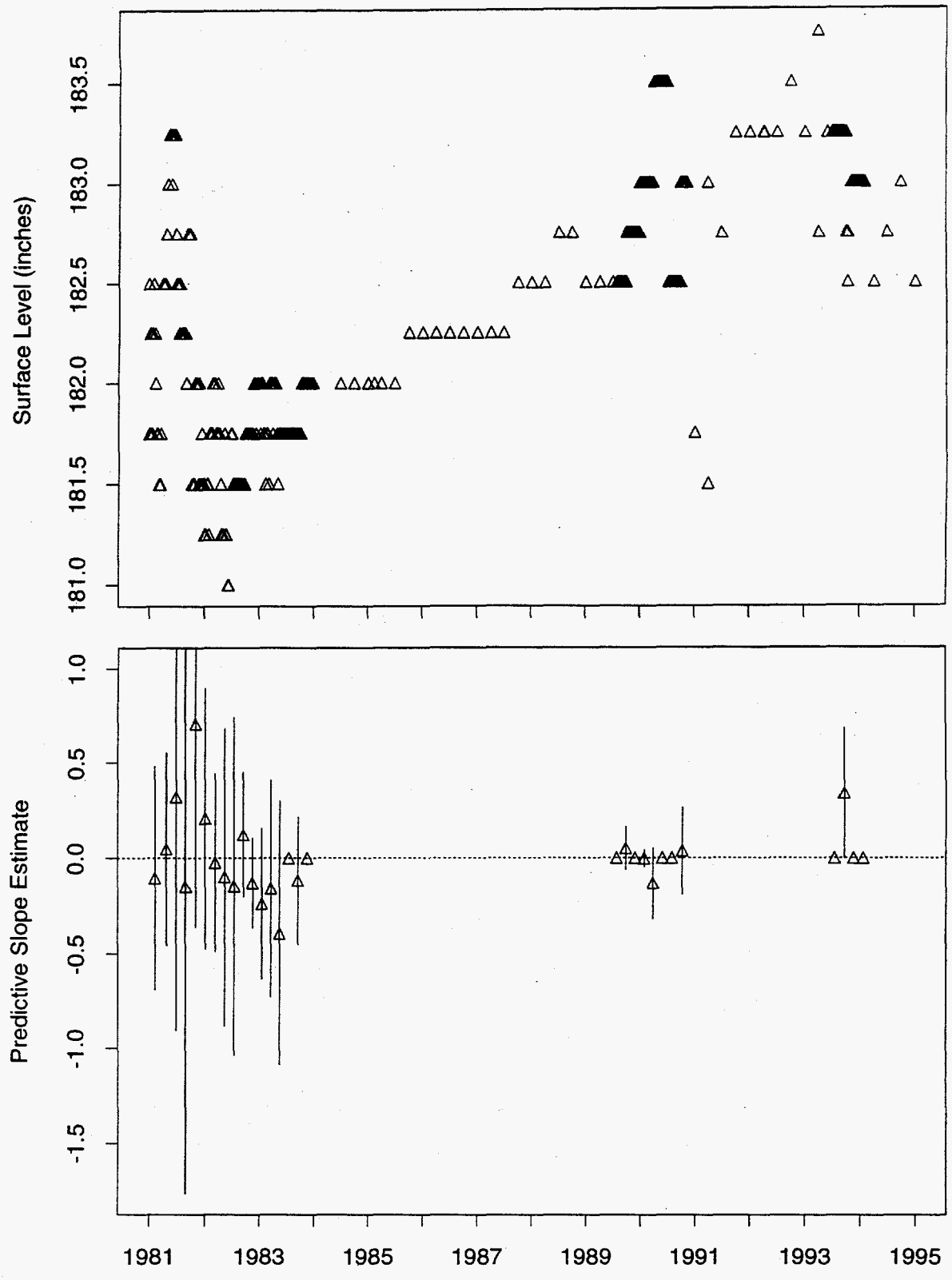

Figure 255: Tank T–203 MT Data

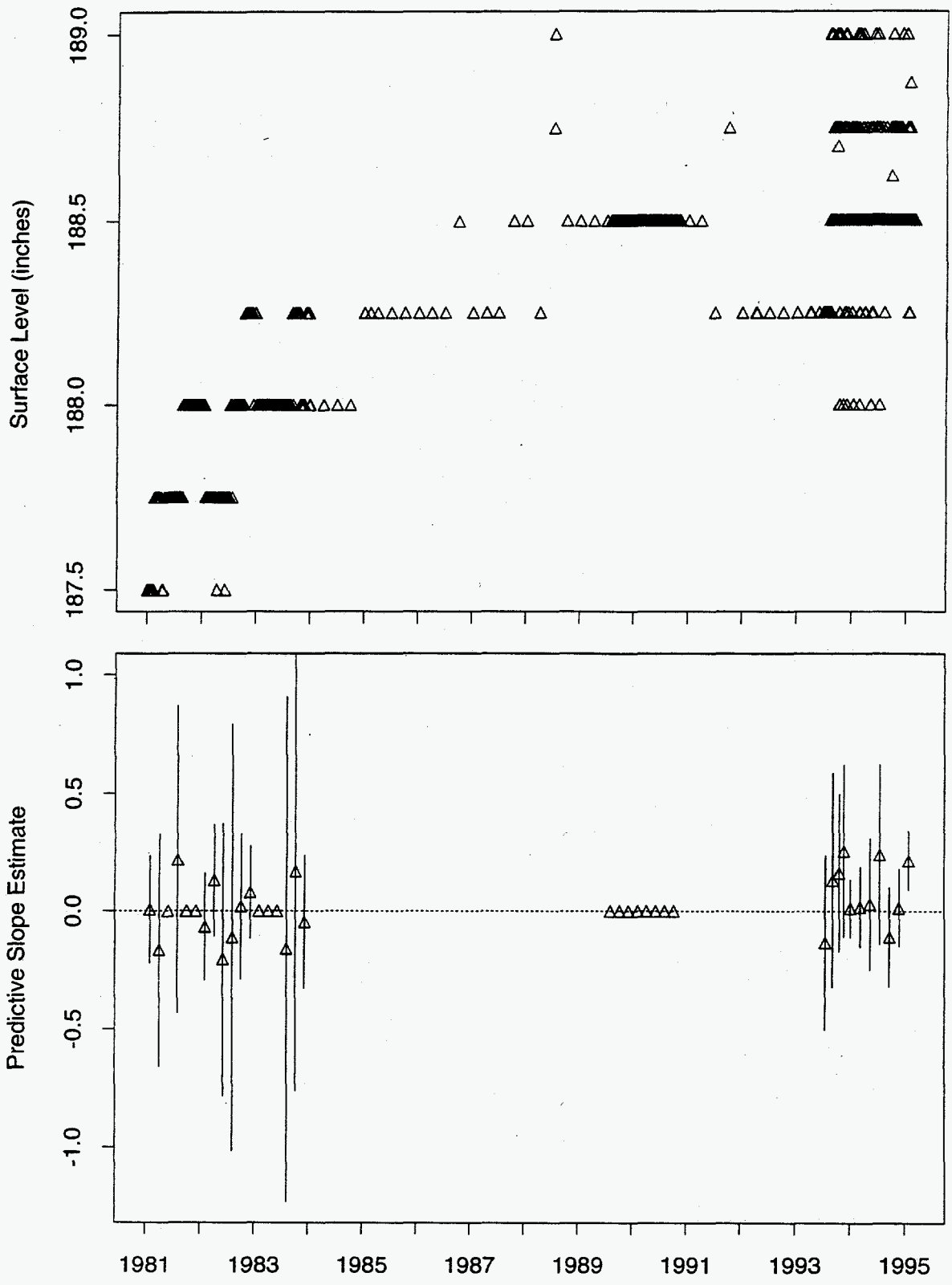

Figure 256: Tank T-204 MT Data

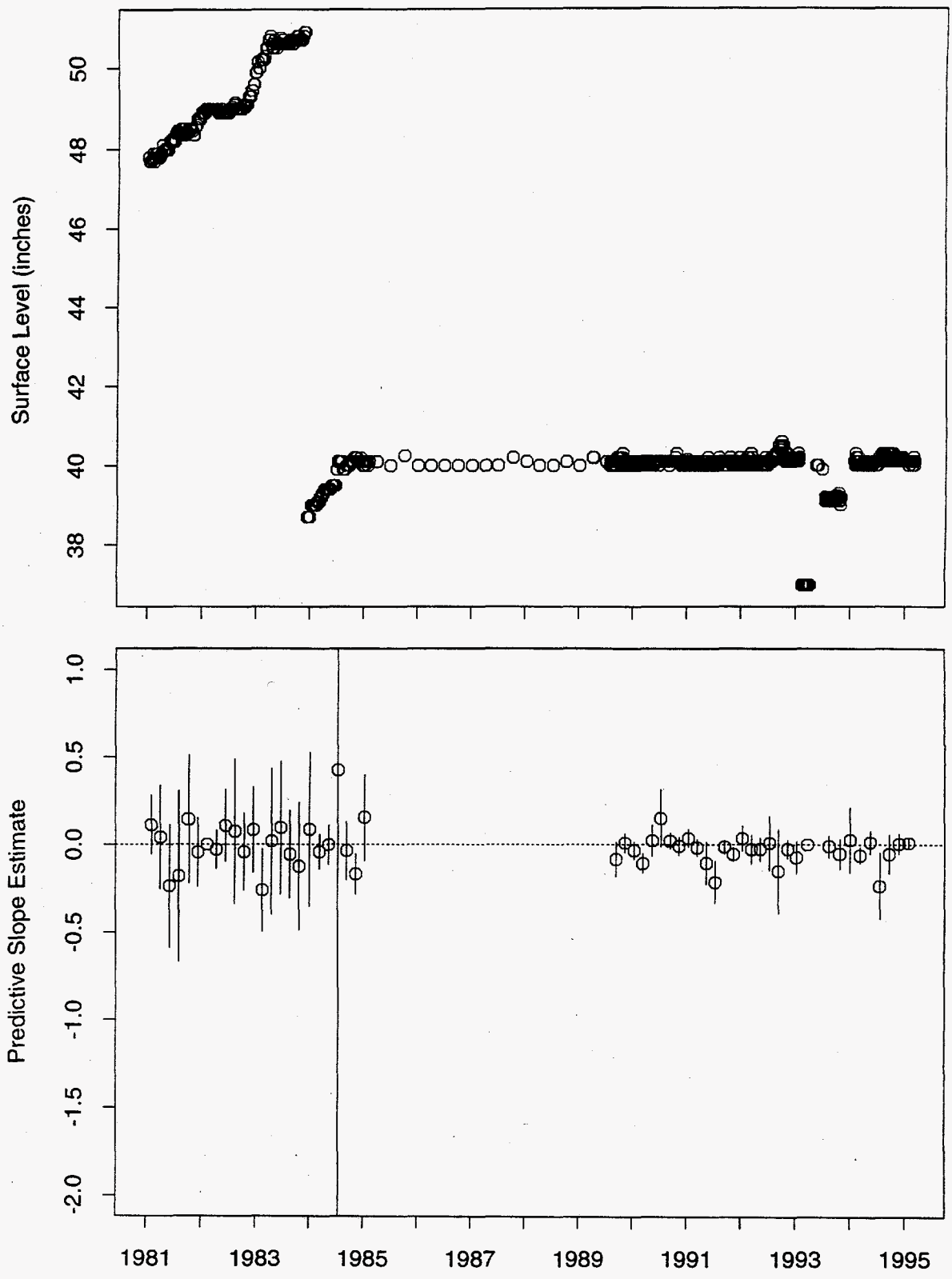

Figure 257: Tank TX–101 FIC Data

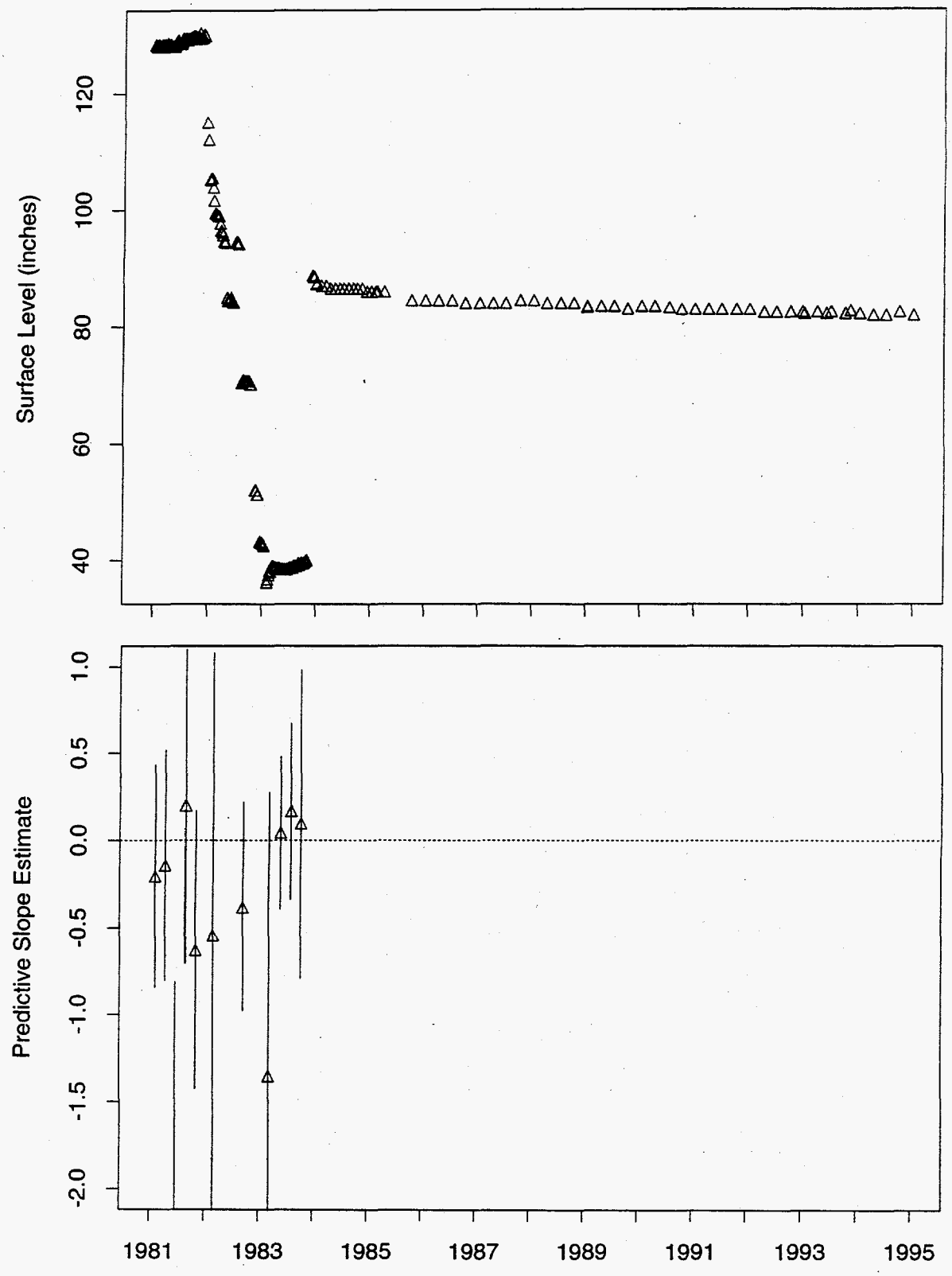

Figure 258: Tank TX–102 MT Data

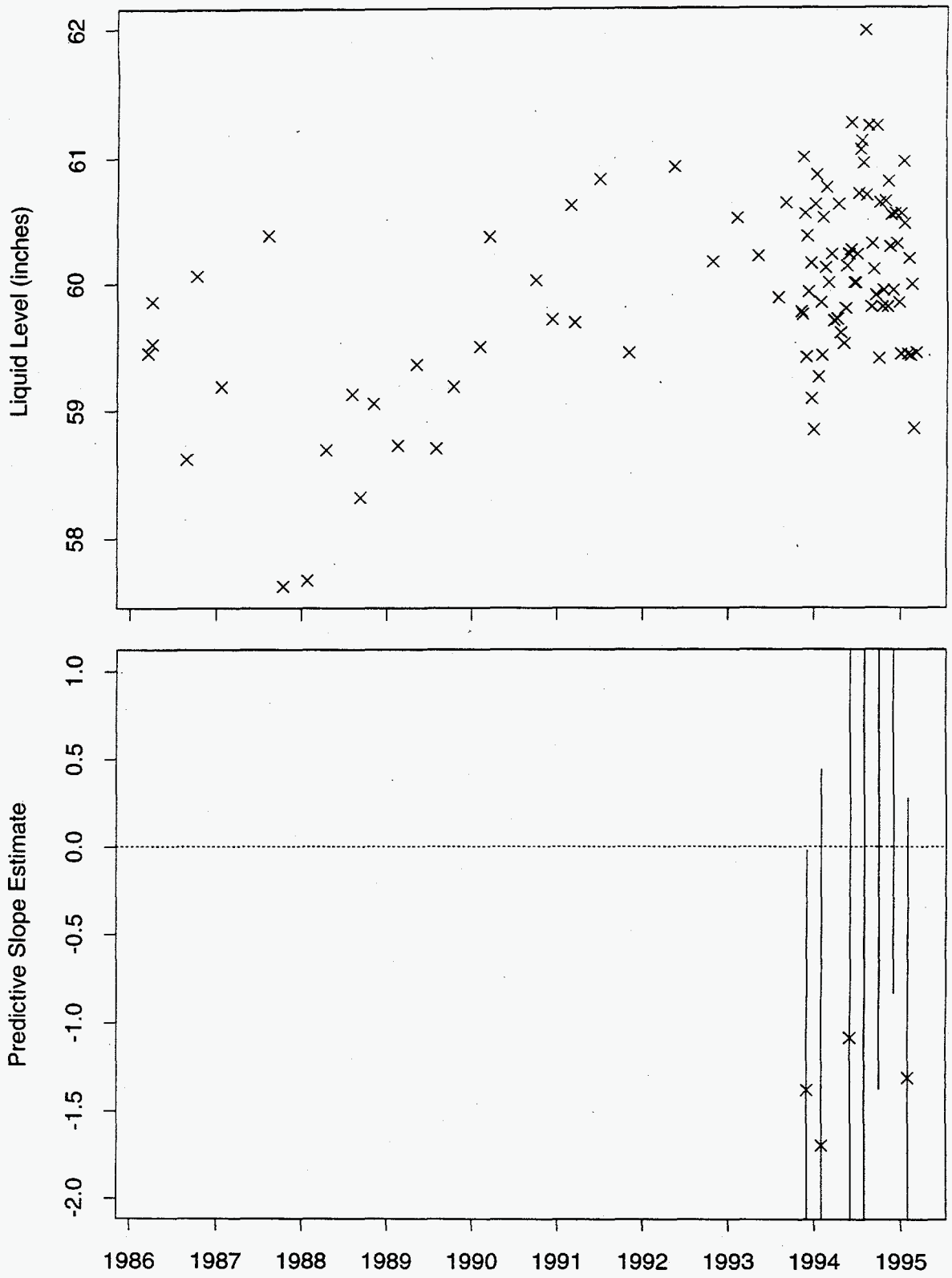

Figure 259: Tank TX–102 Neutron ILL Data

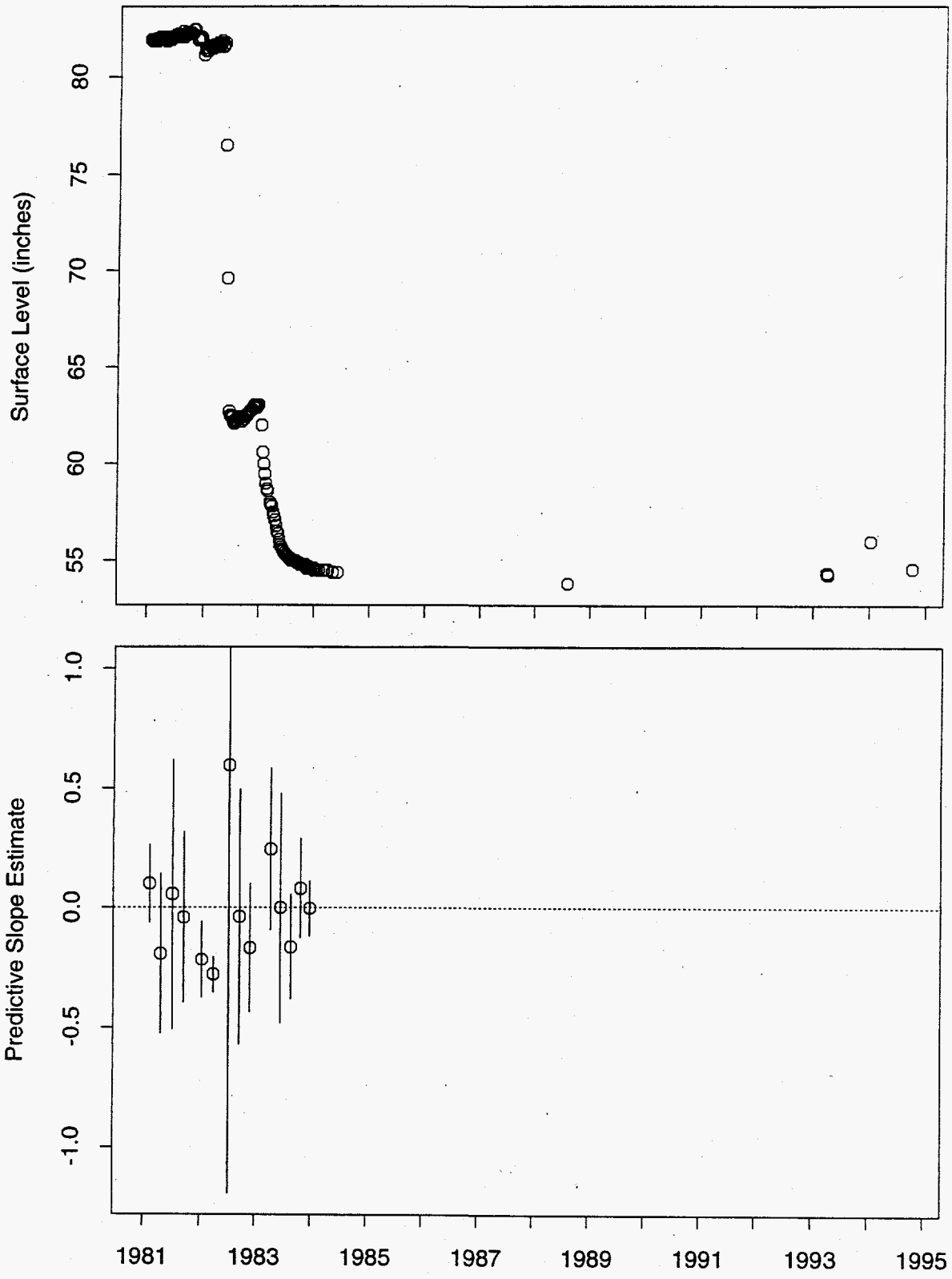

Figure 260: Tank TX–103 FIC Data

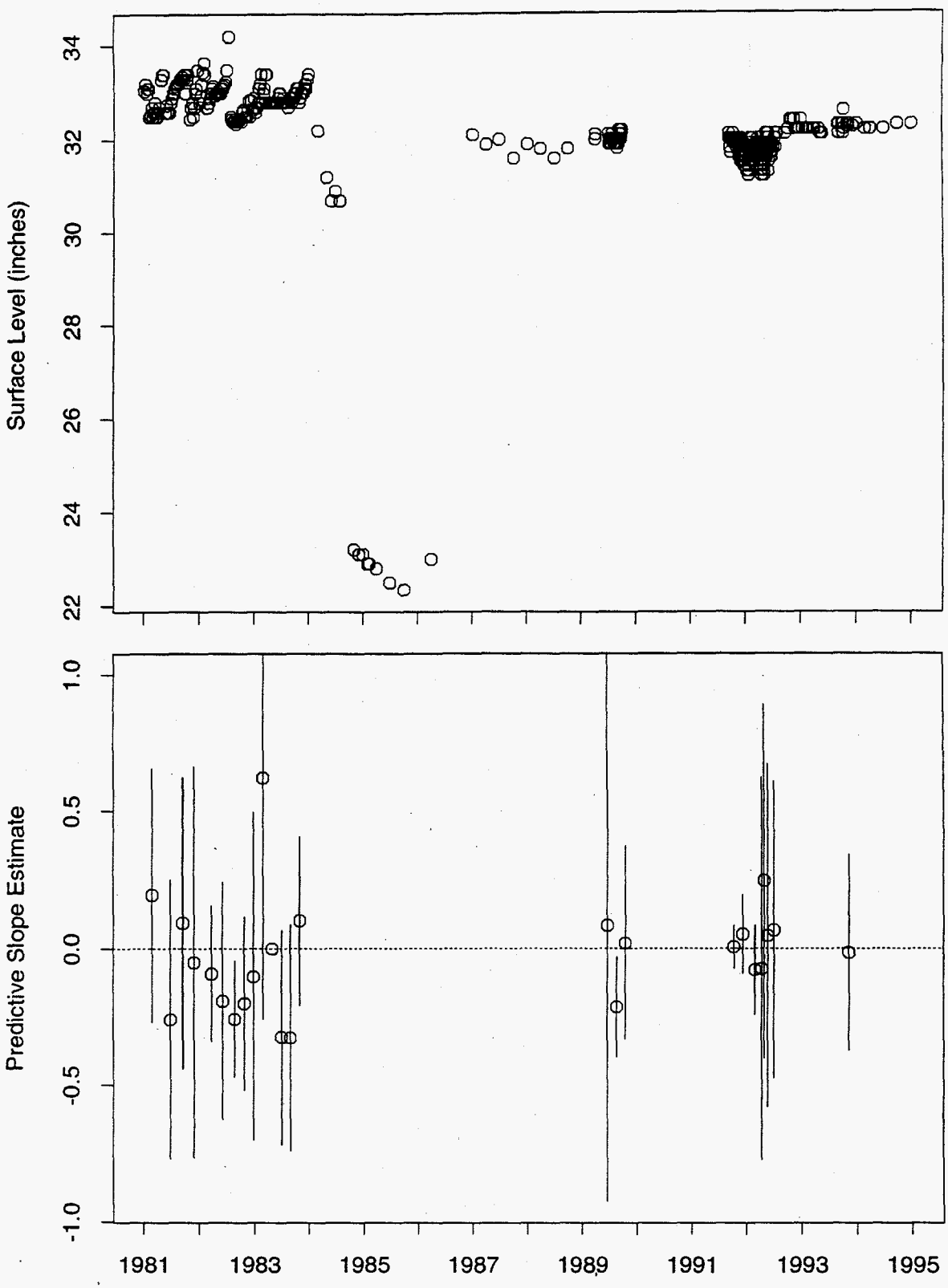

Figure 261: Tank TX–104 FIC Data

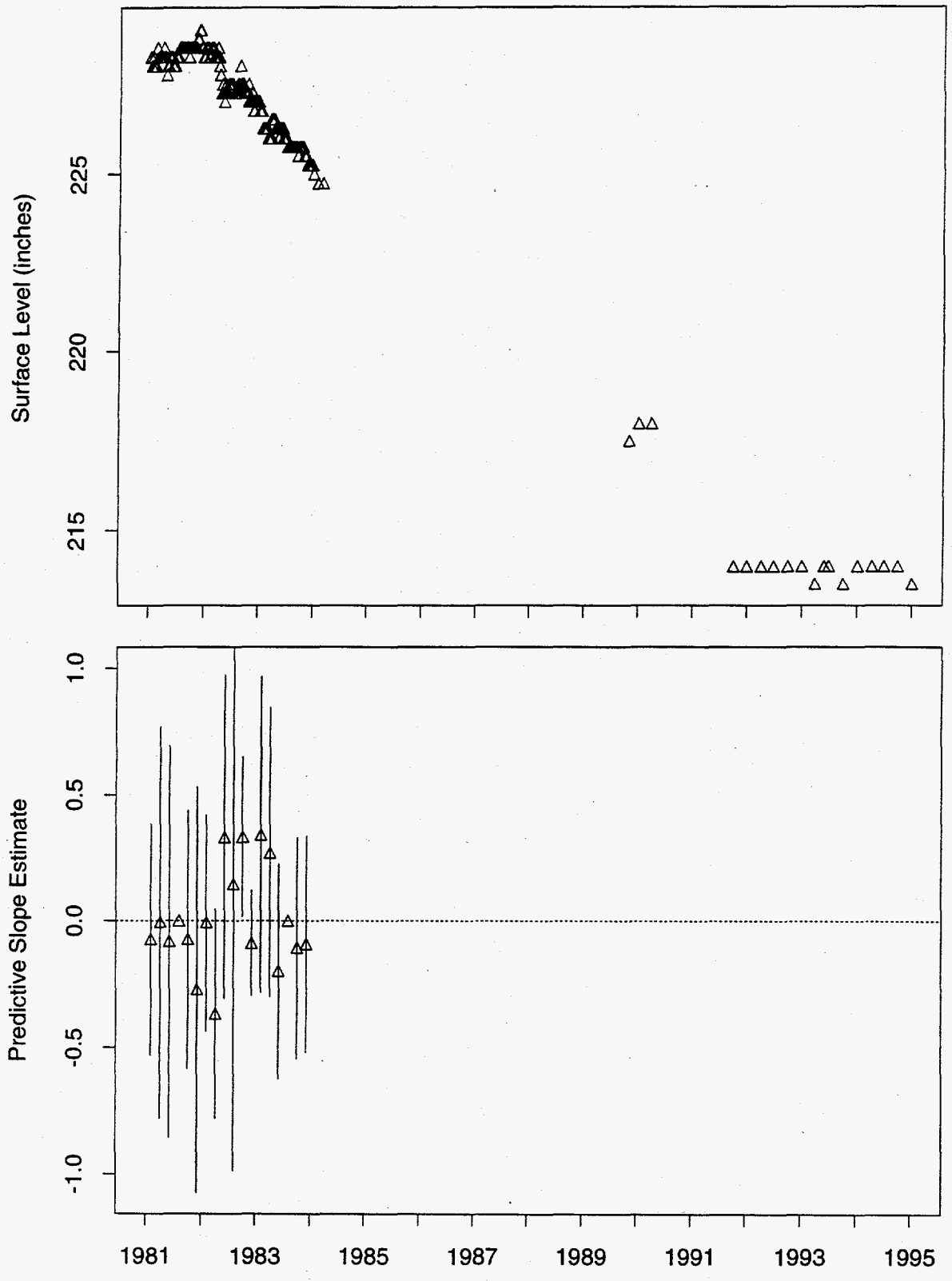

Figure 262: Tank TX-105 MT Data

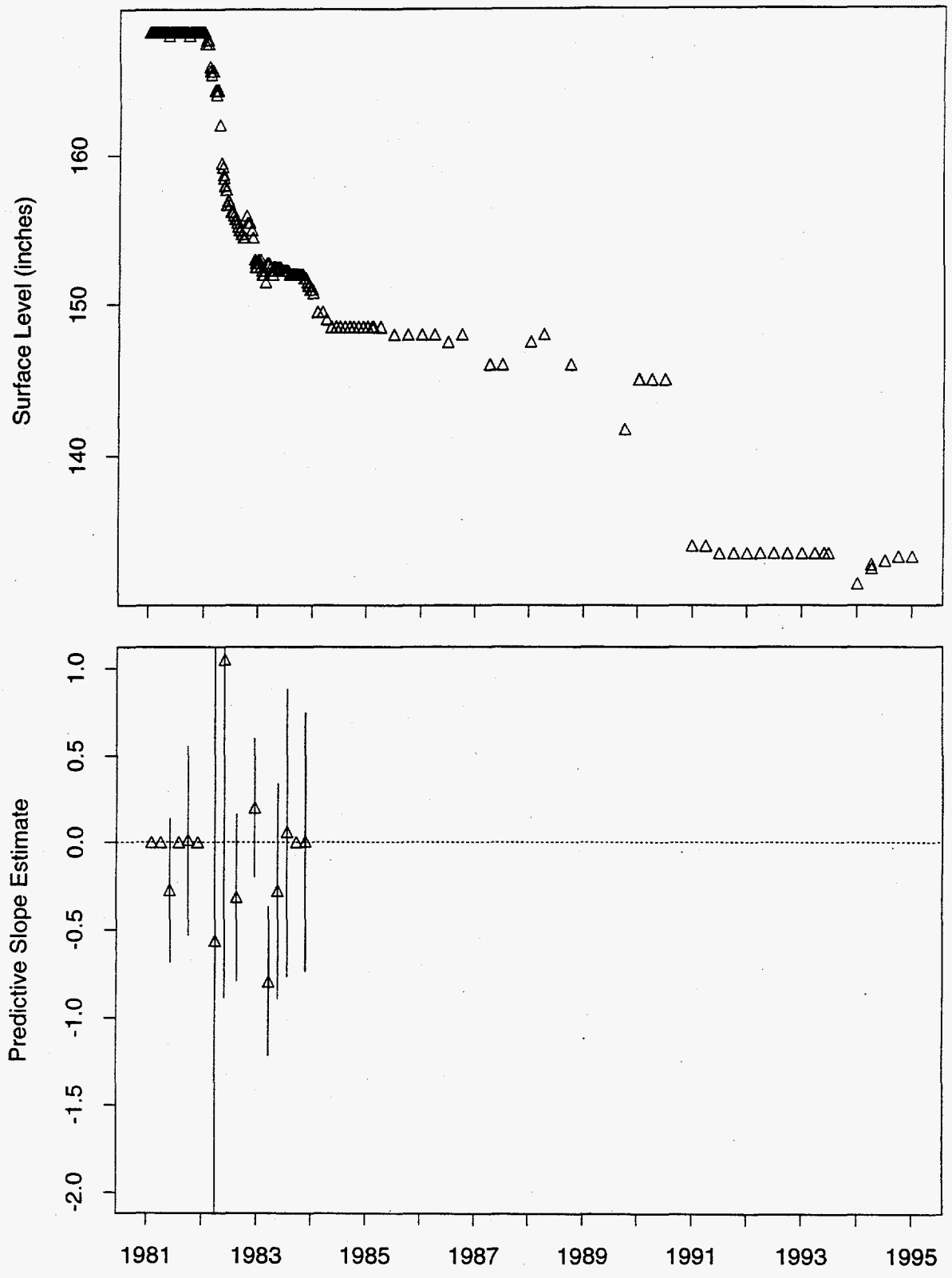

Figure 263: Tank TX–106 MT Data

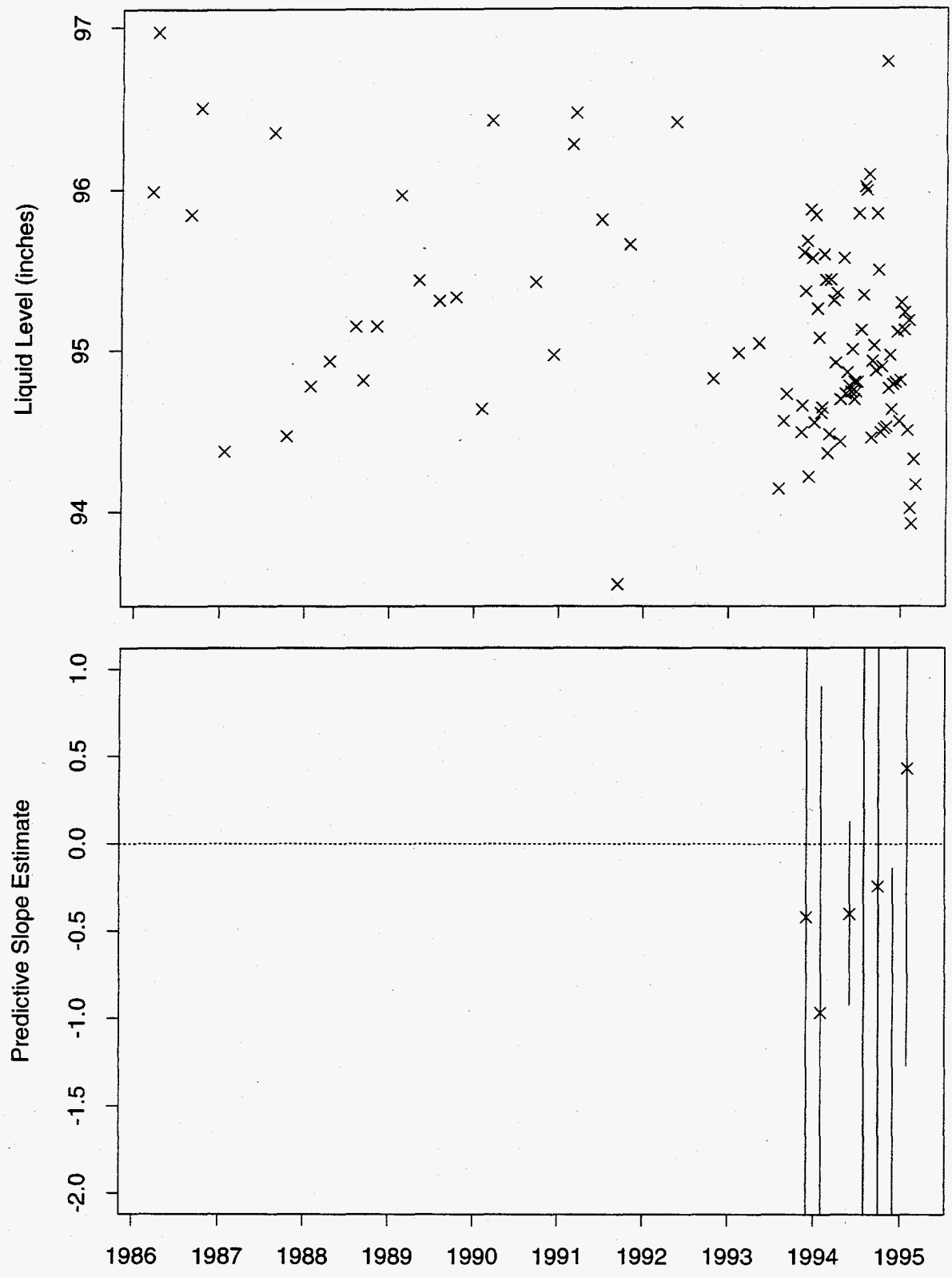

Figure 264: Tank TX–106 Neutron ILL Data

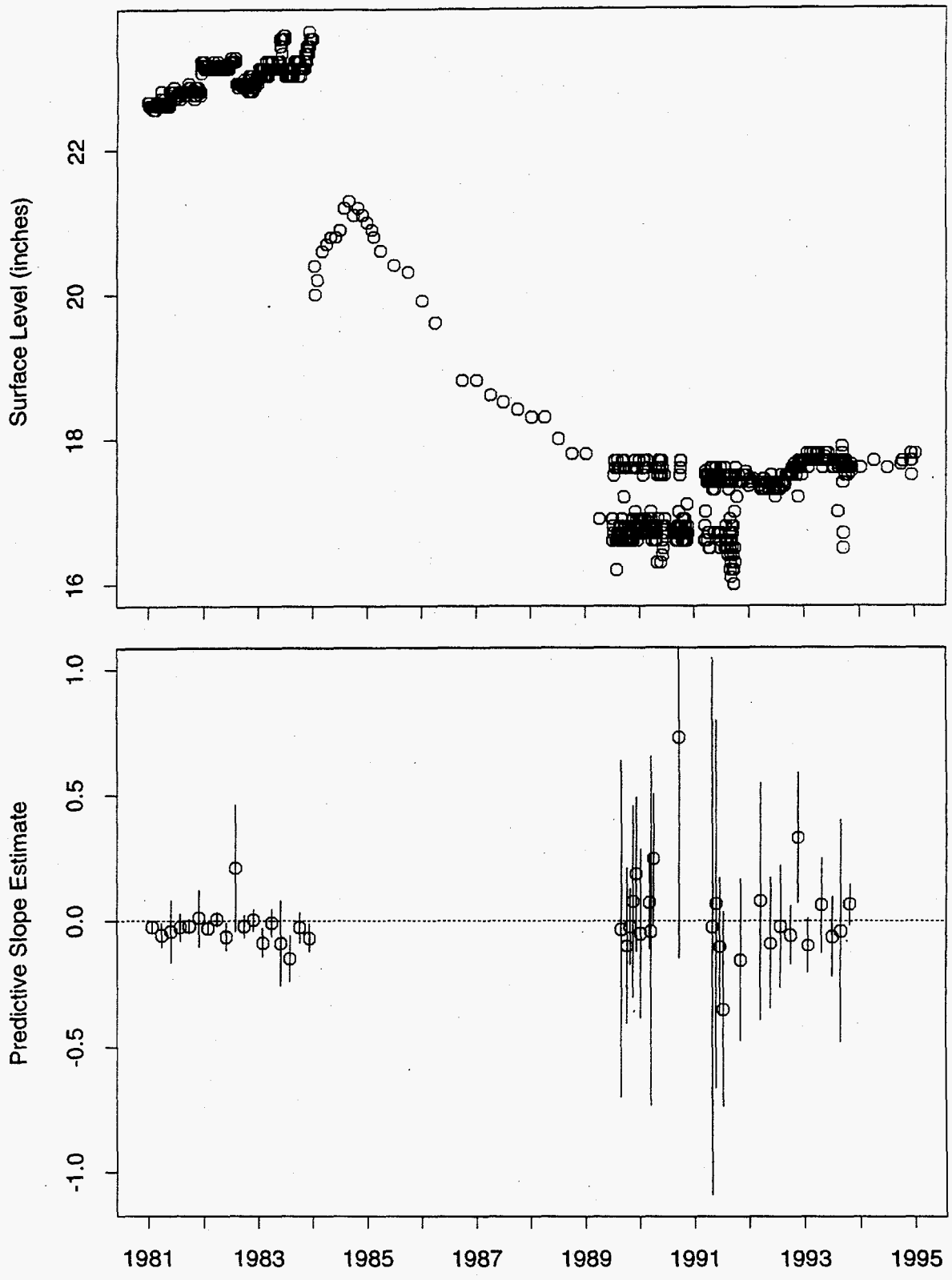

Figure 265: Tank TX–107 FIC Data

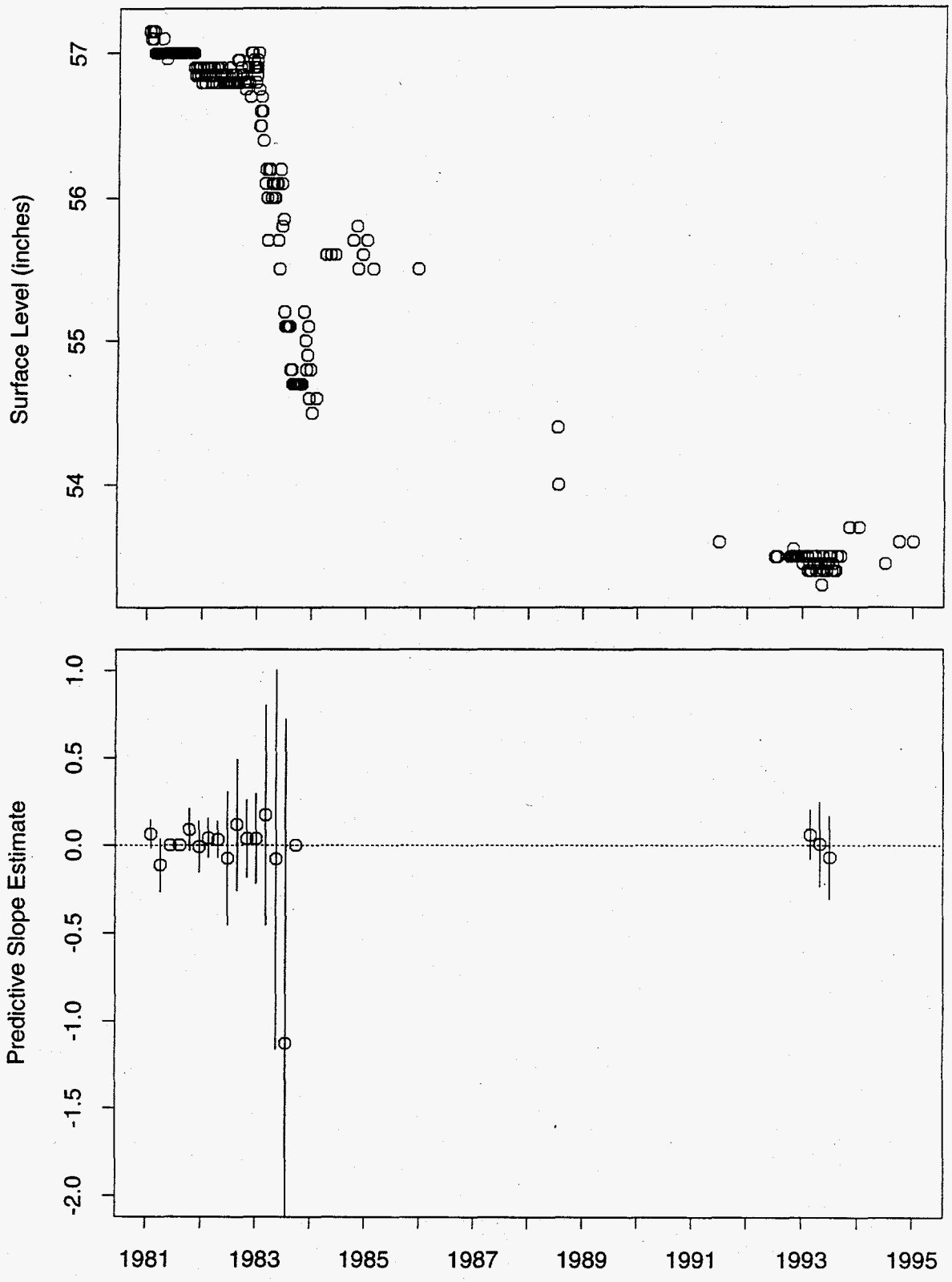

Figure 266: Tank TX–108 FIC Data

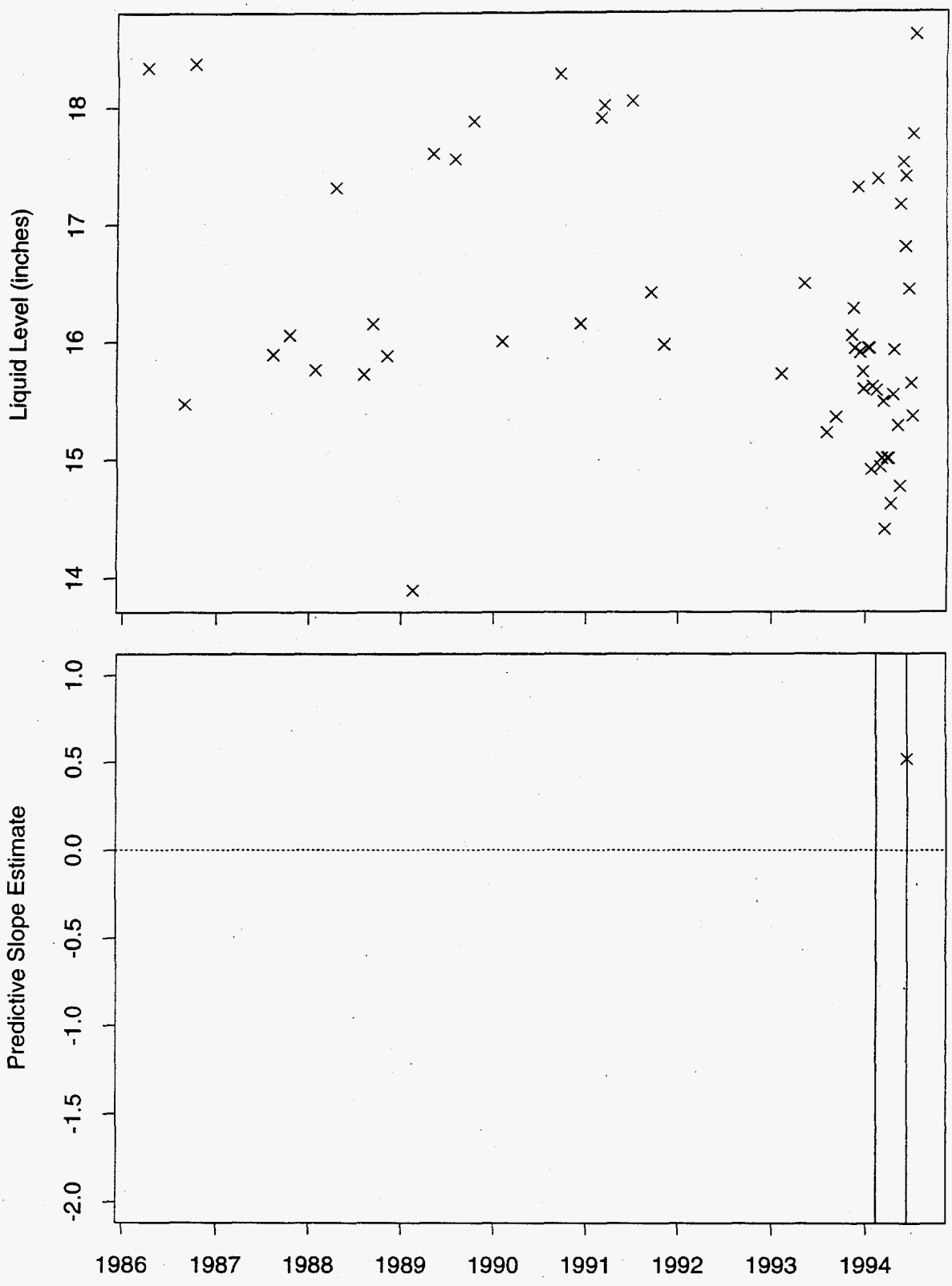

Figure 267: Tank TX-108 Neutron ILL Data

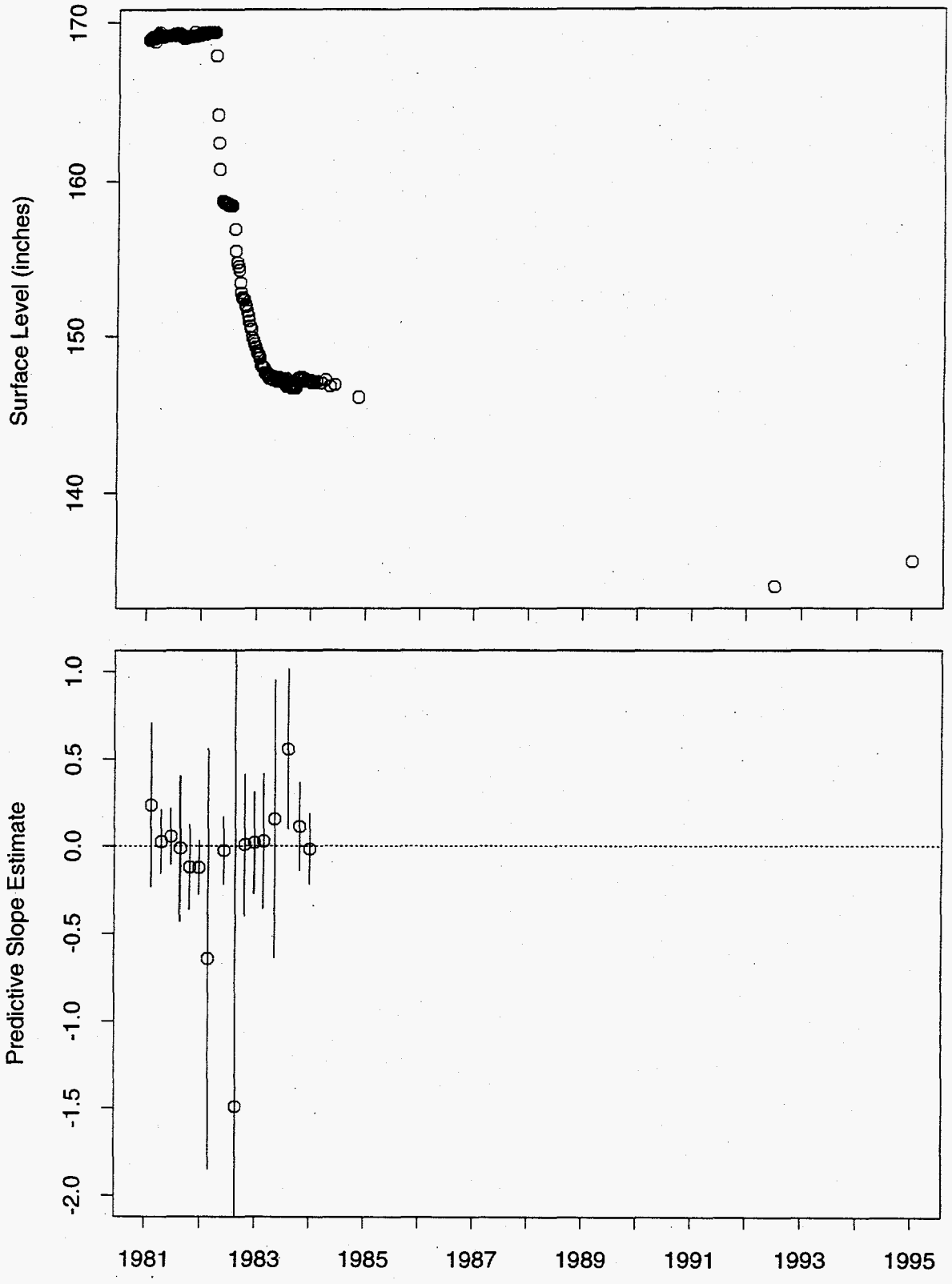

Figure 268: Tank TX-109 FIC Data

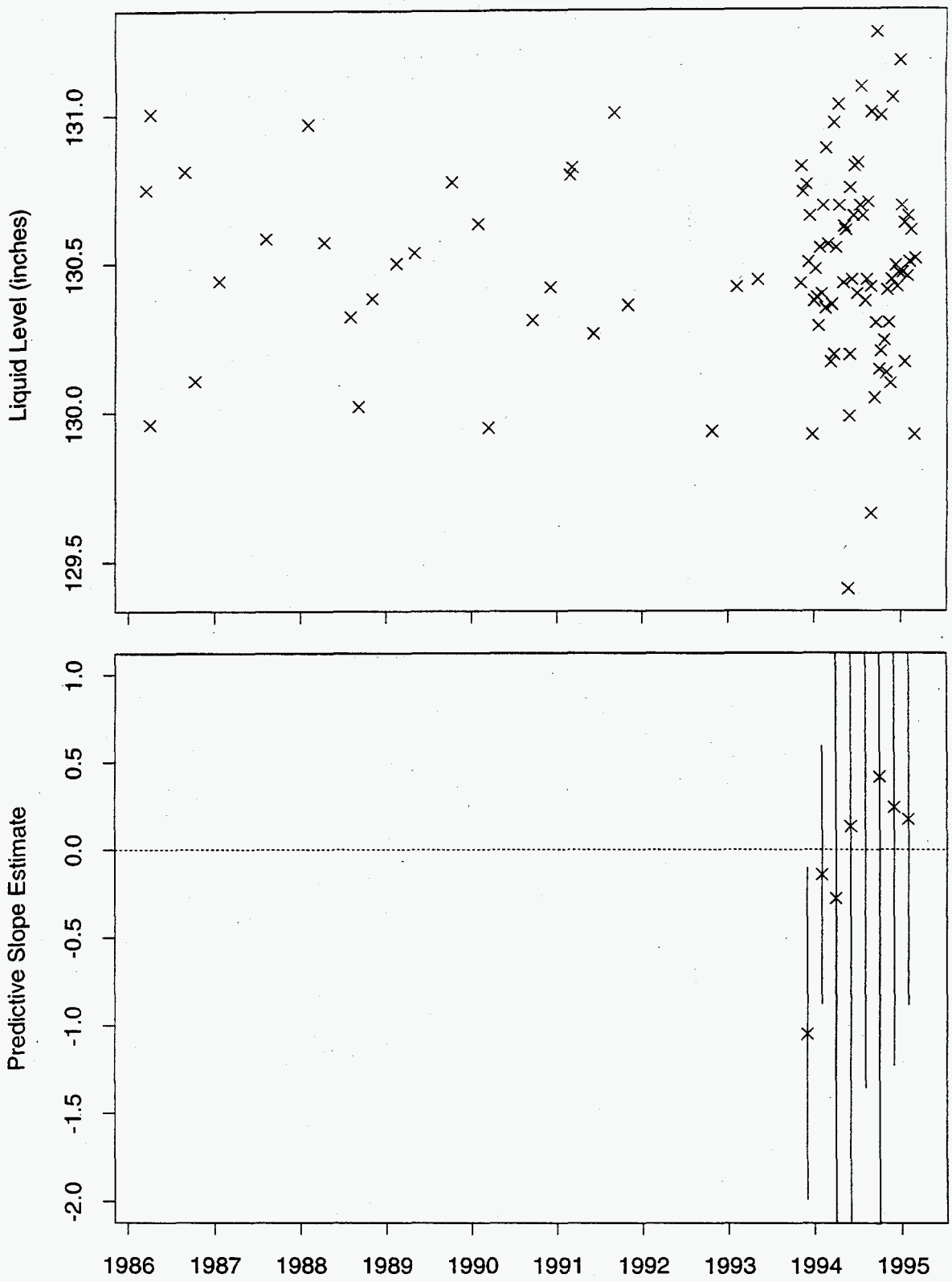

Figure 269: Tank TX–109 Neutron ILL Data

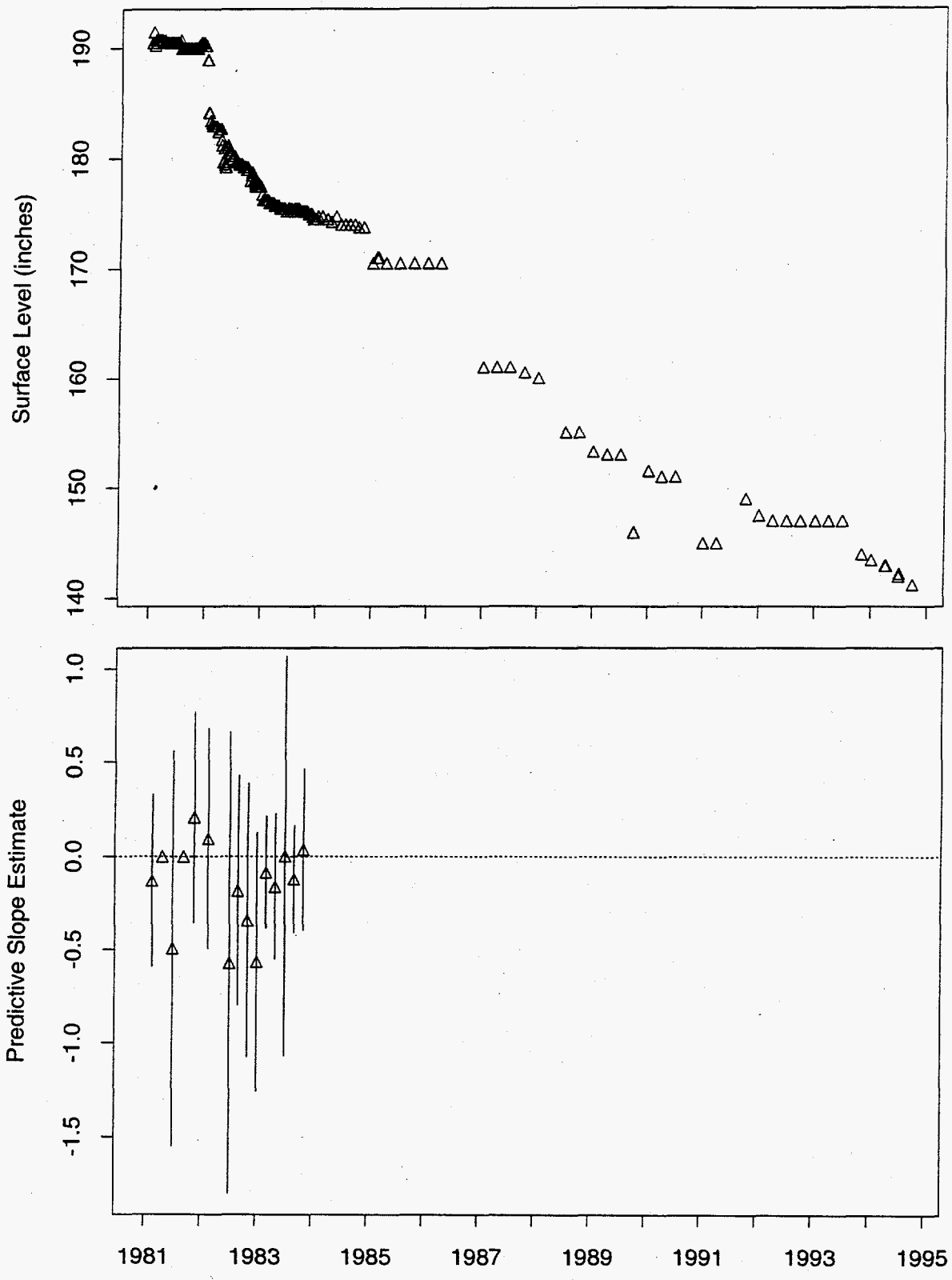

Figure 270: Tank TX–110 MT Data

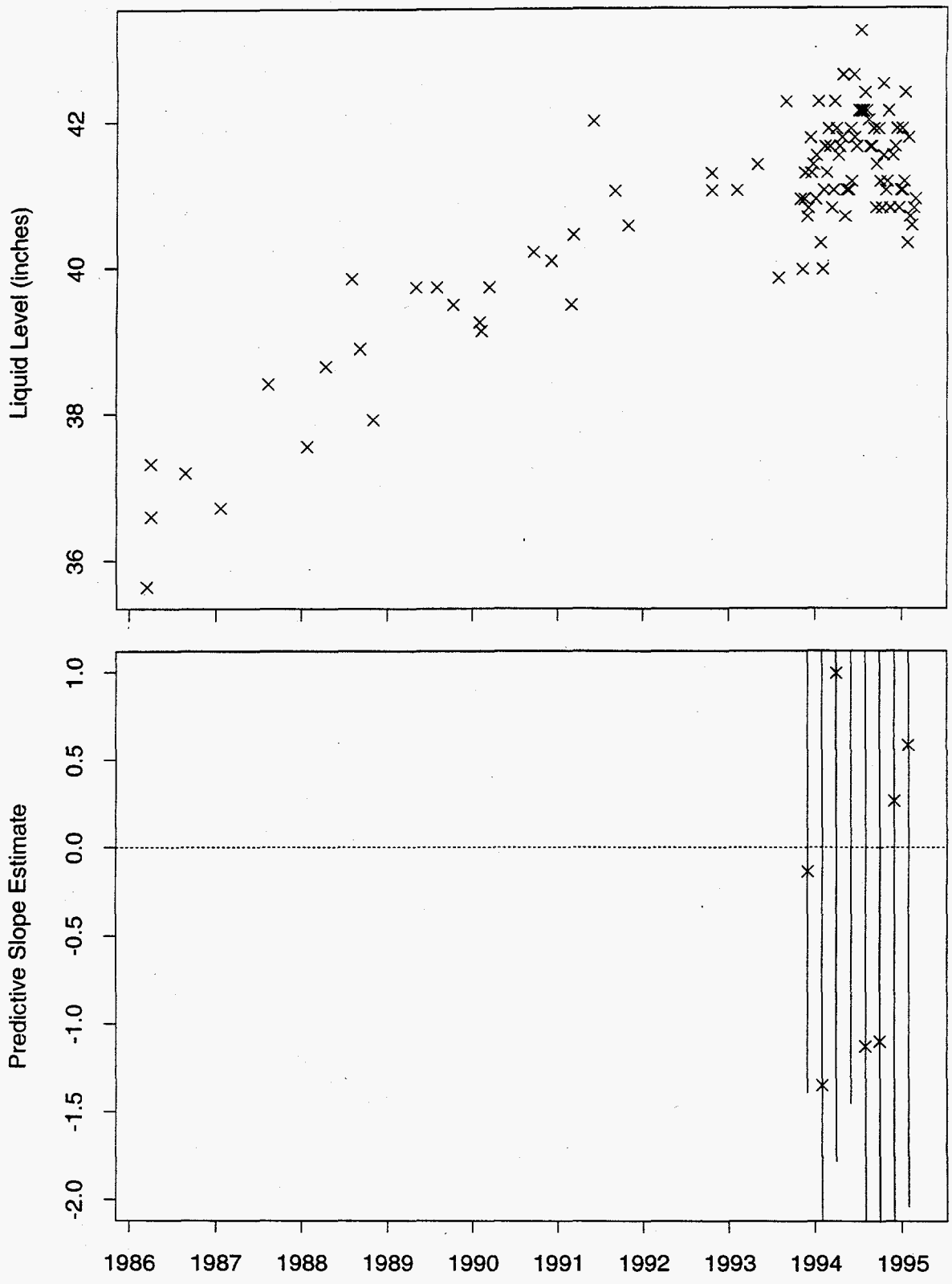

Figure 271: Tank TX–110 Neutron ILL Data

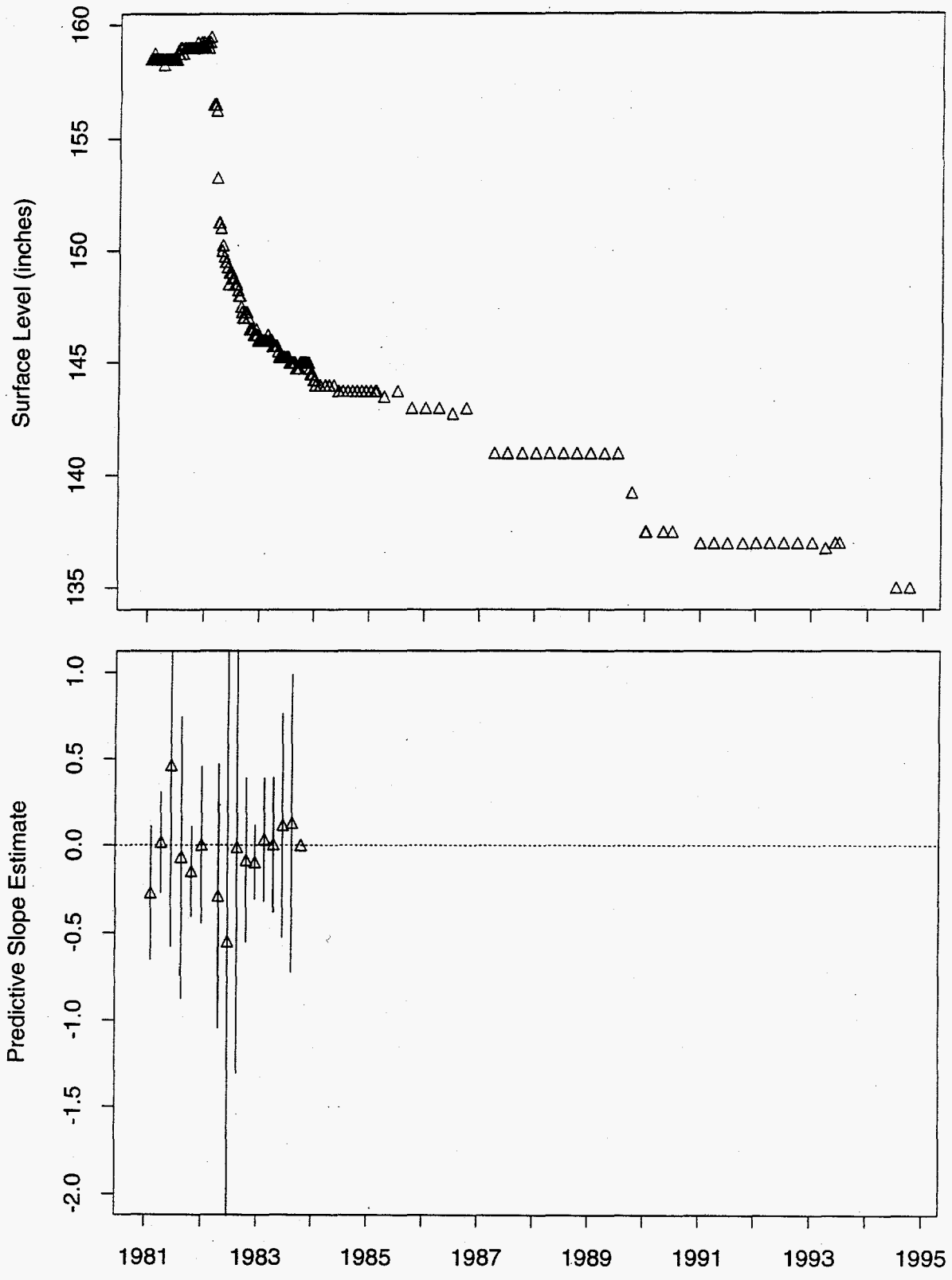

Figure 272: Tank TX–111 MT Data

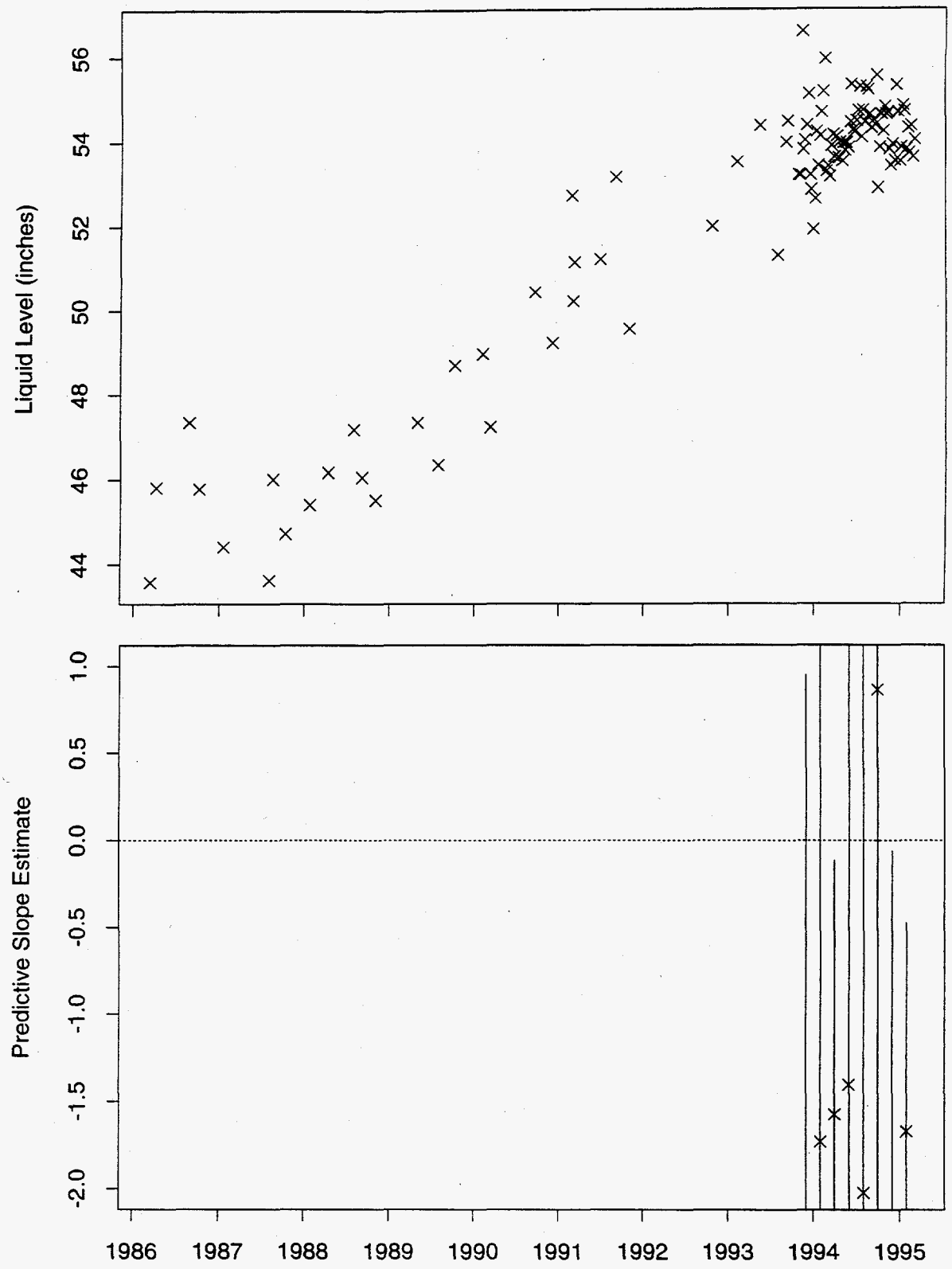

Figure 273: Tank TX–111 Neutron ILL Data

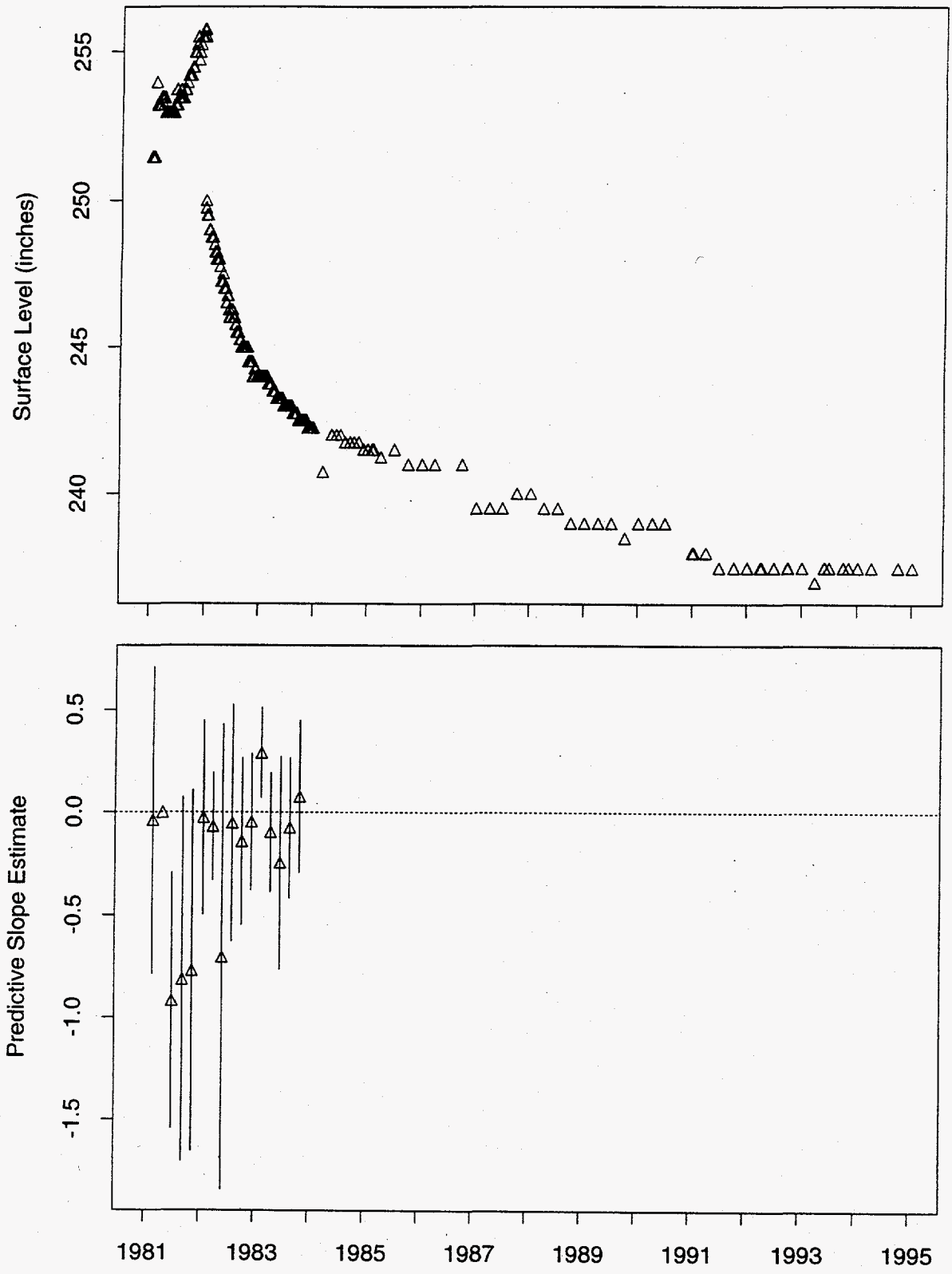

Figure 274: Tank TX-112 MT Data

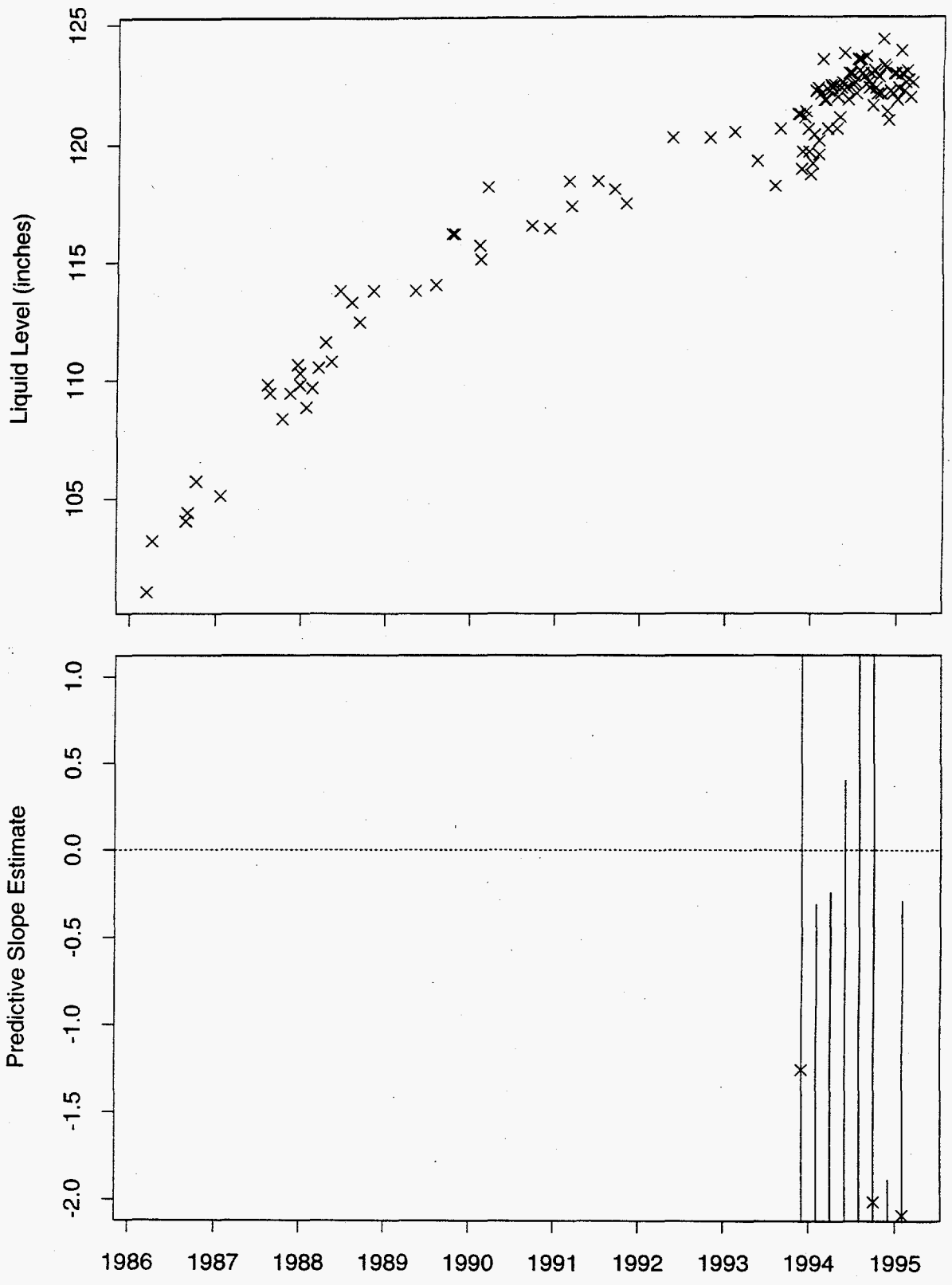

Figure 275: Tank TX–112 Neutron ILL Data

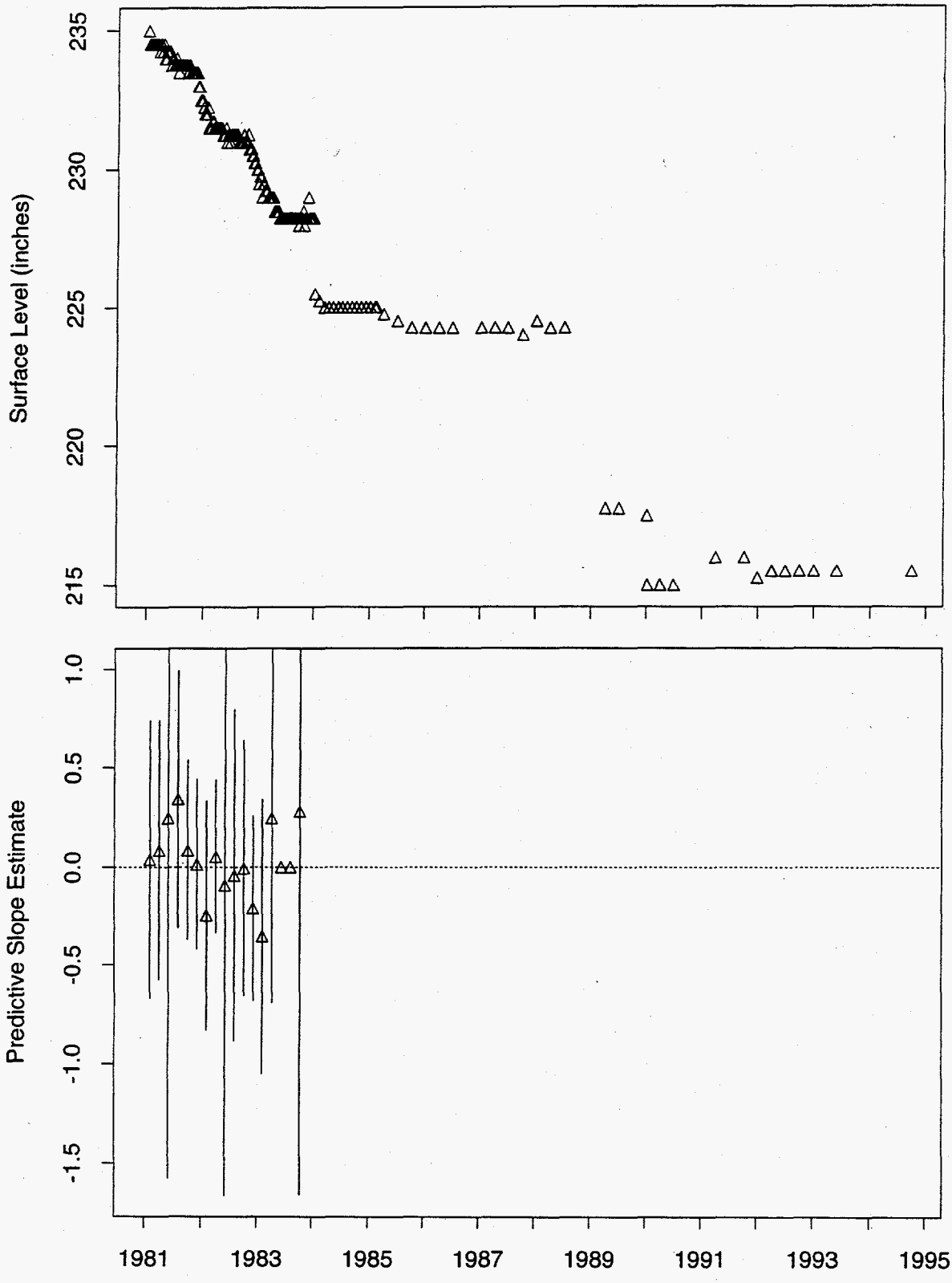

Figure 276: Tank TX–113 MT Data

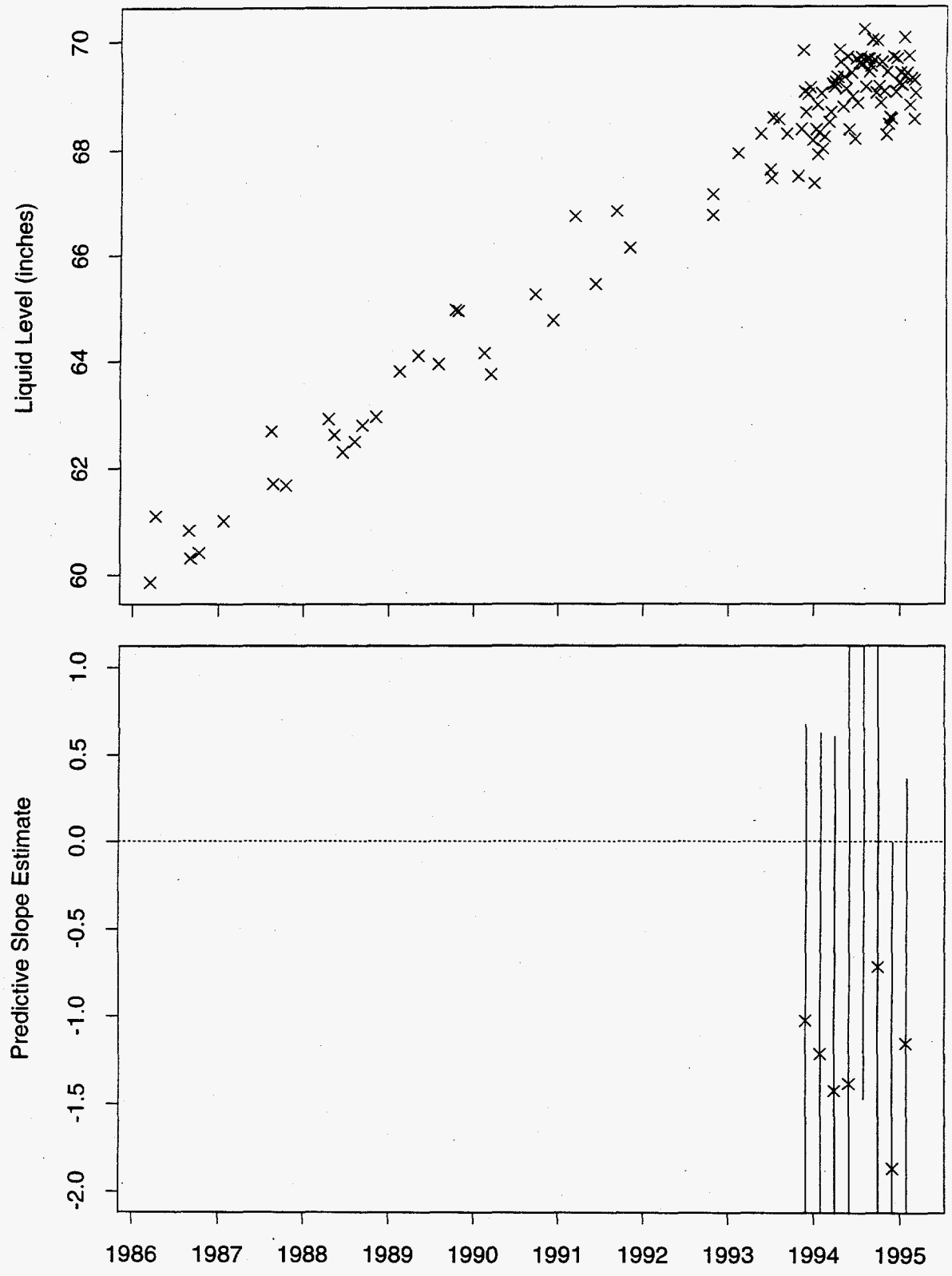

Figure 277: Tank TX–113 Neutron ILL Data

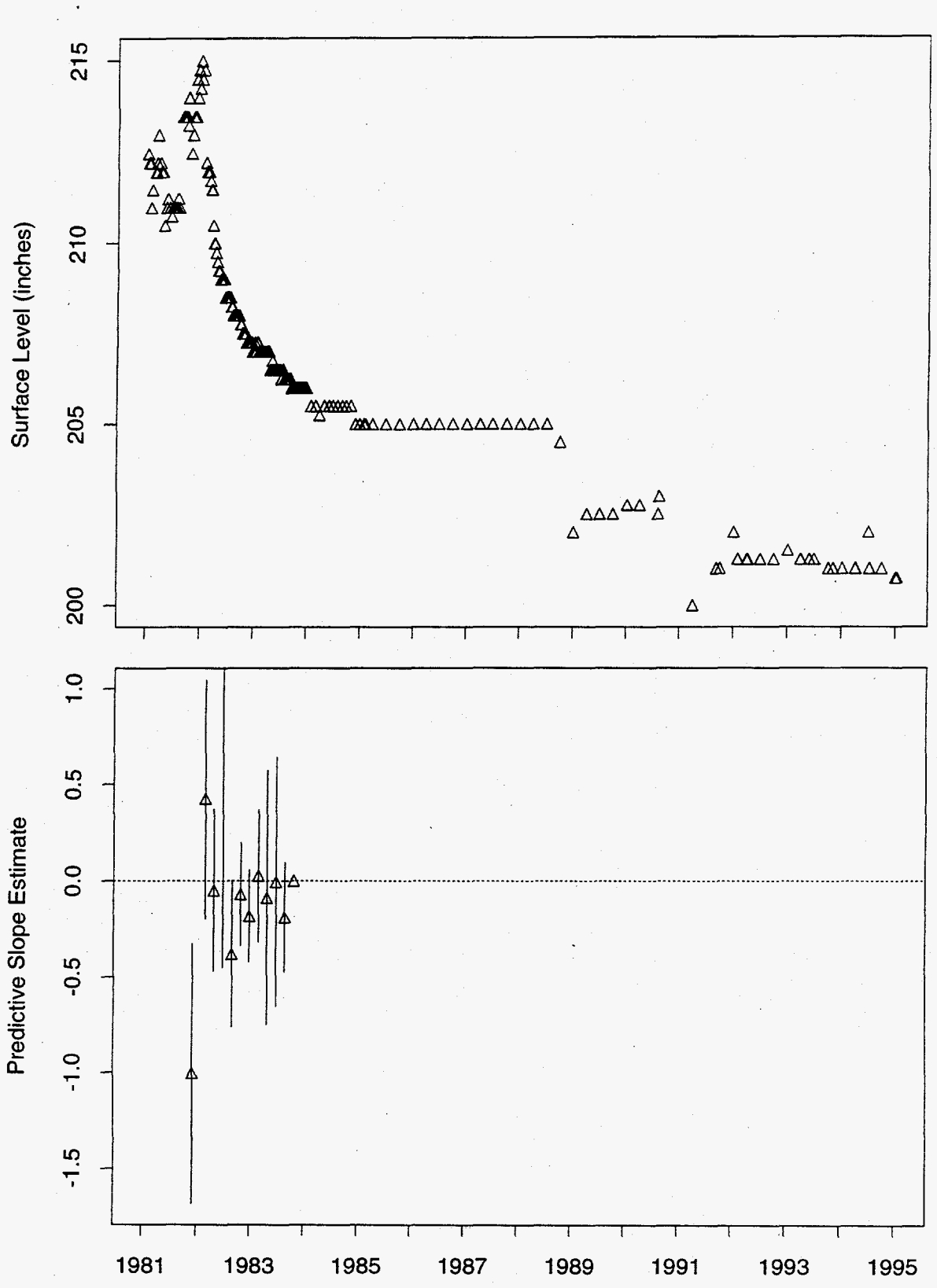

Figure 278: Tank TX–114 MT Data

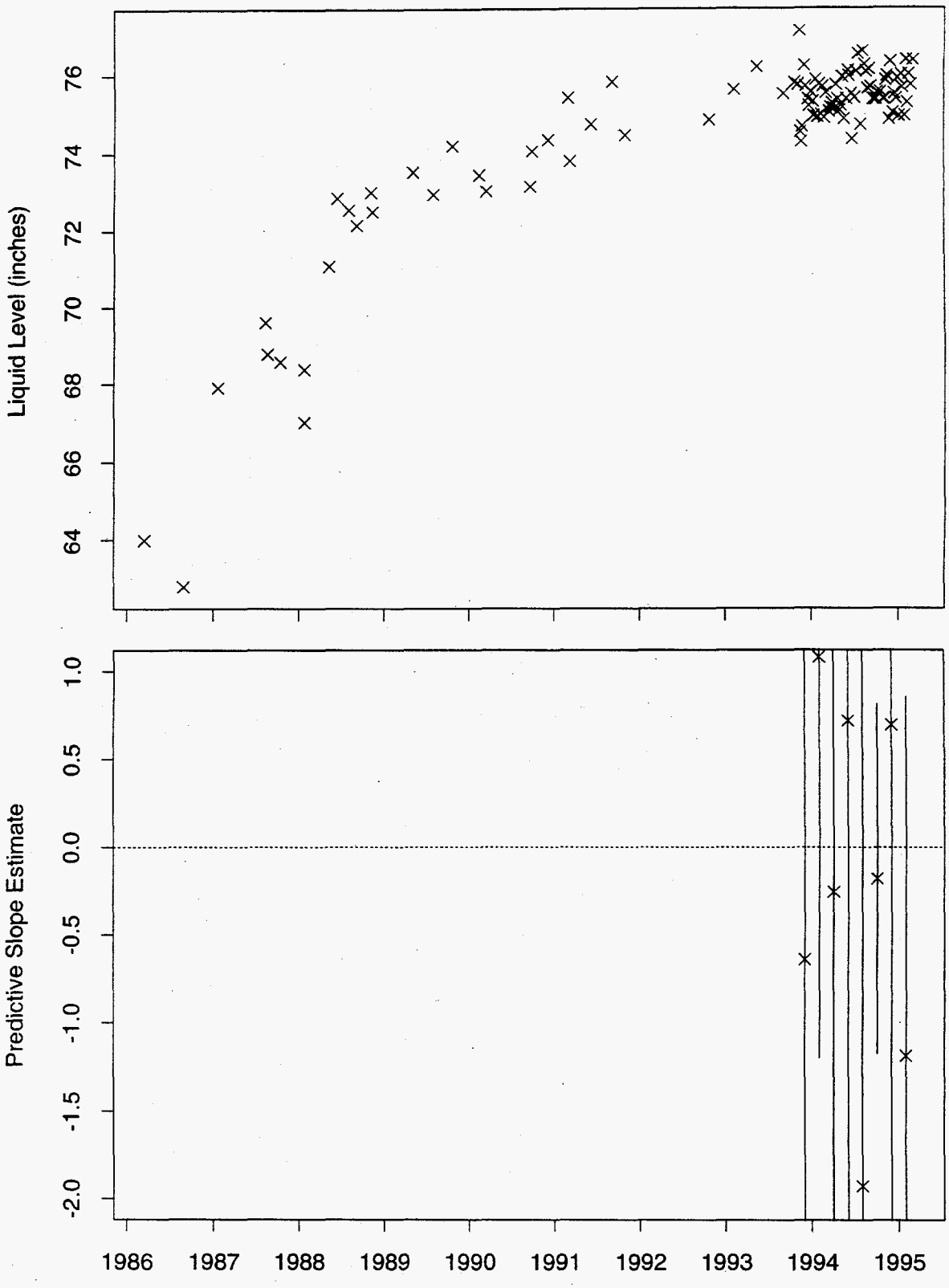

Figure 279: Tank TX-114 Neutron ILL Data

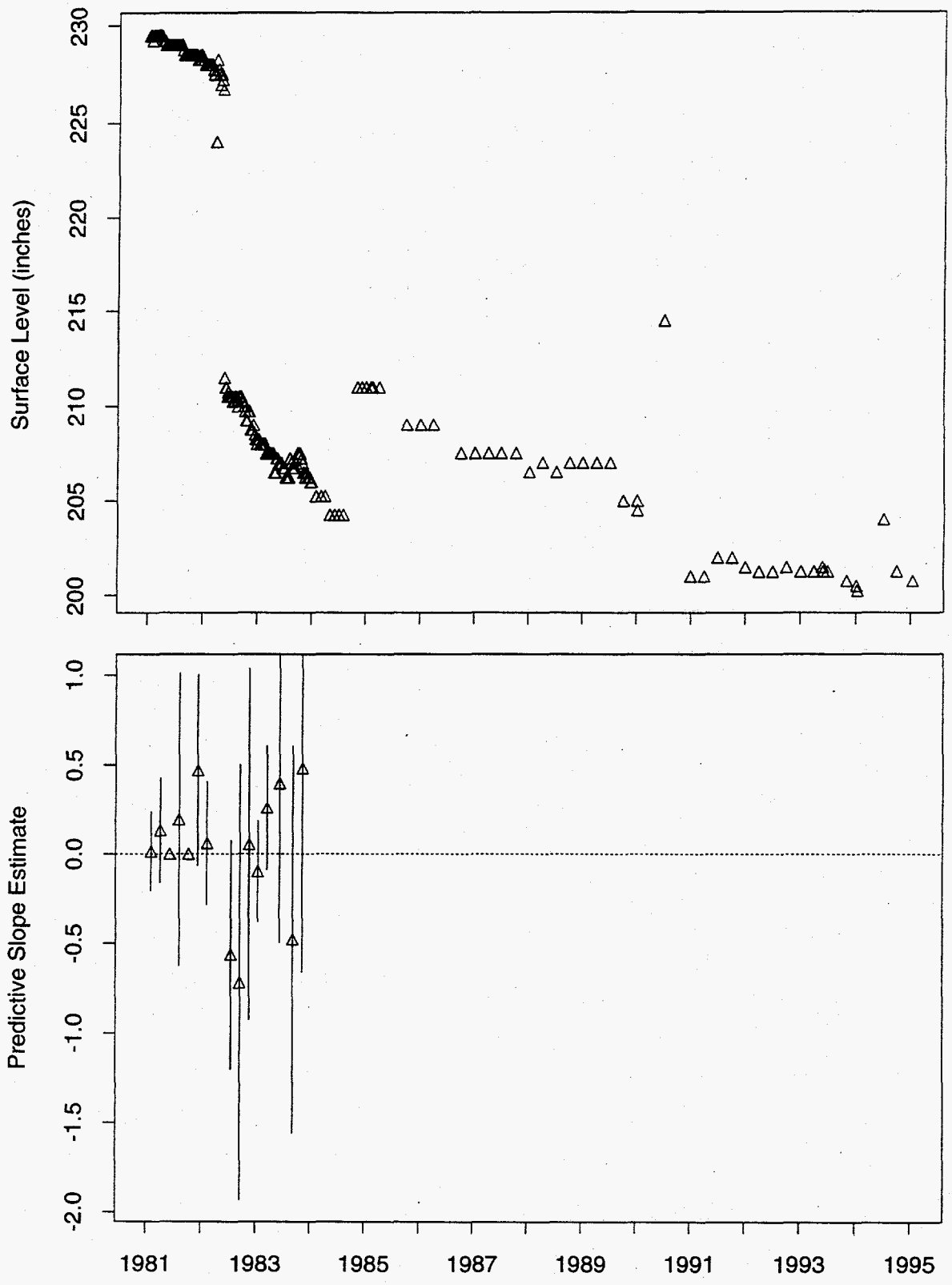

Figure 280: Tank TX–115 MT Data

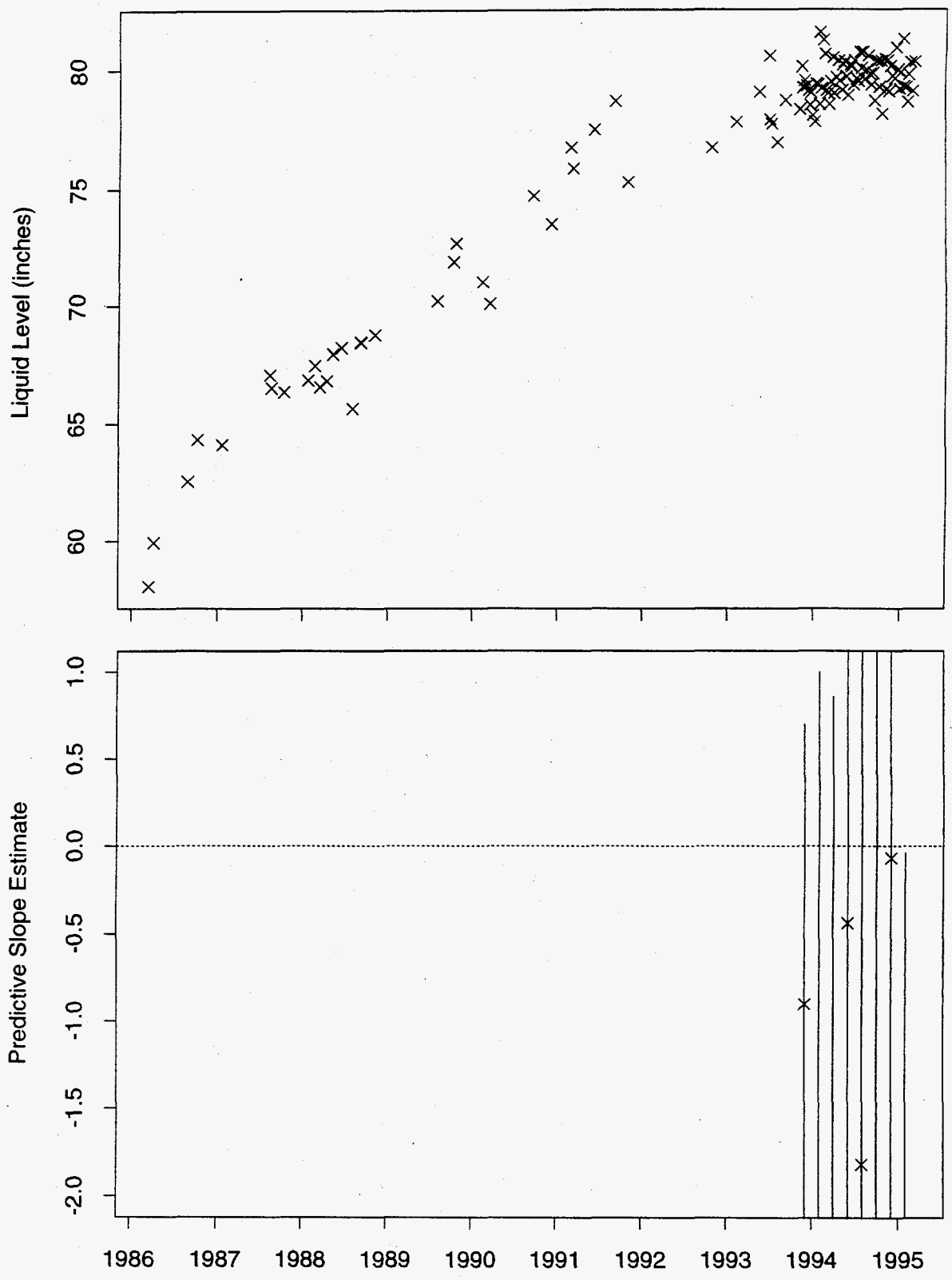

Figure 281: Tank TX–115 Neutron ILL Data

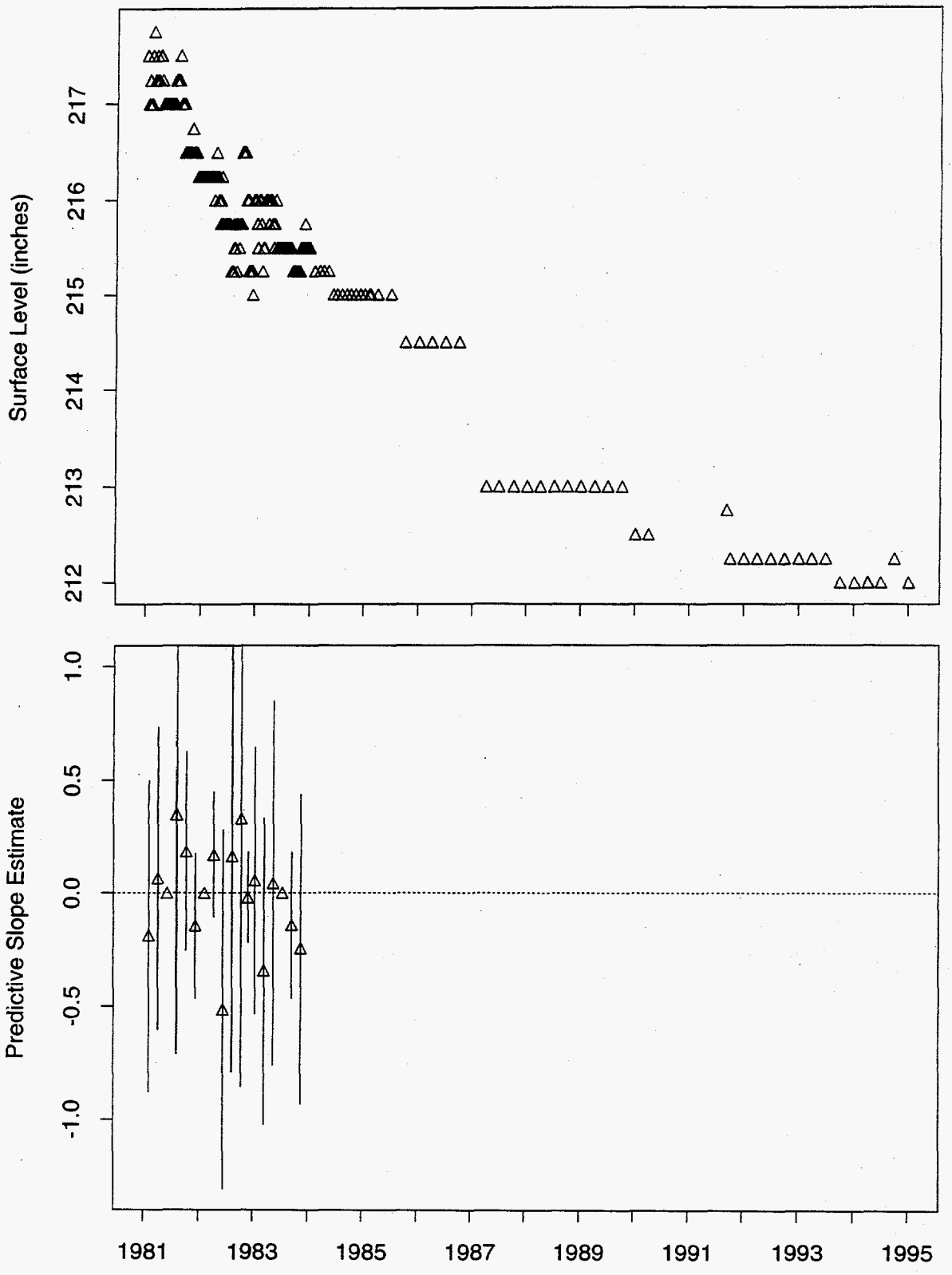

Figure 282: Tank TX–116 MT Data

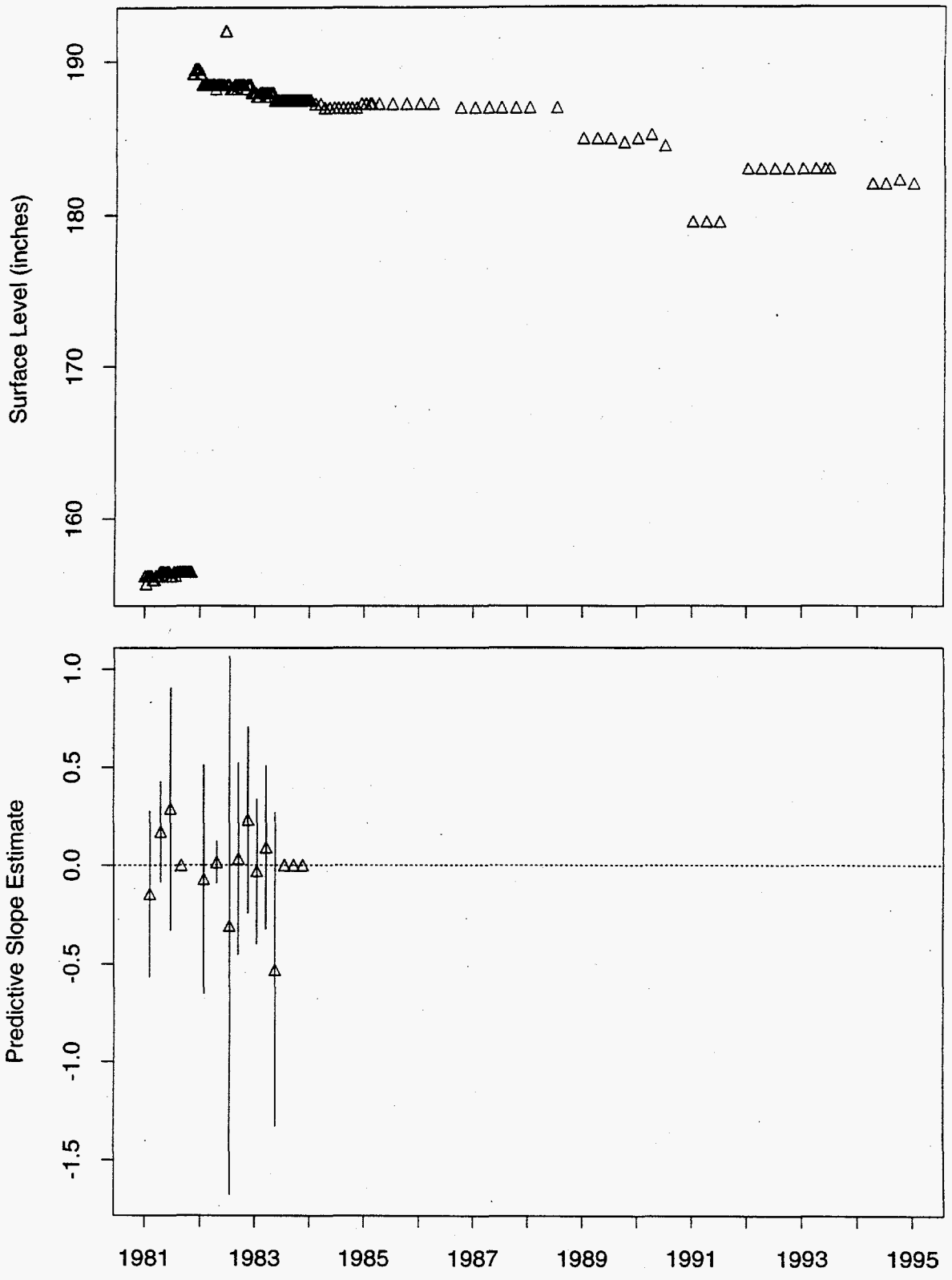

Figure 283: Tank TX–117 MT Data

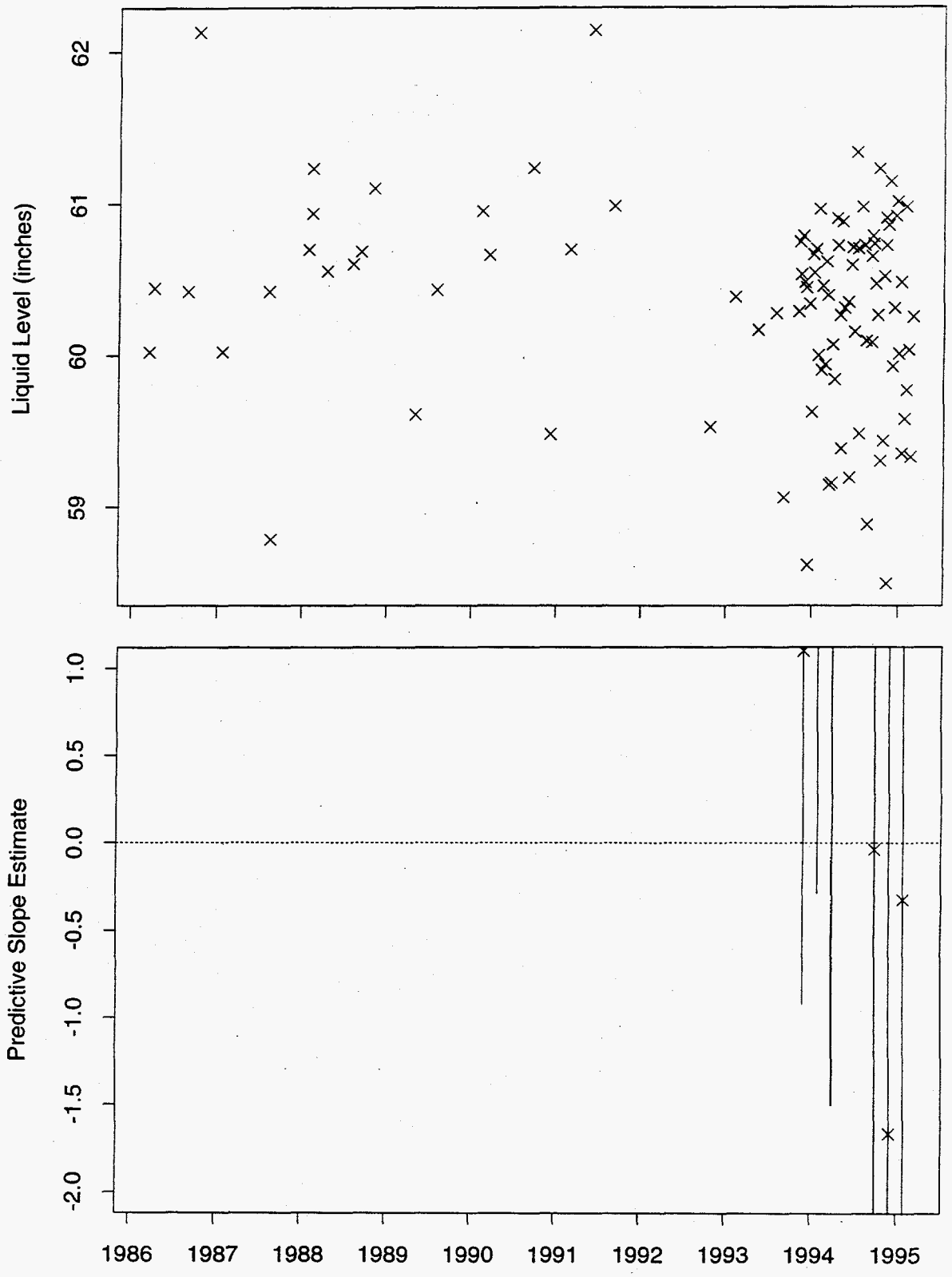

Figure 284: Tank TX-117 Neutron ILL Data

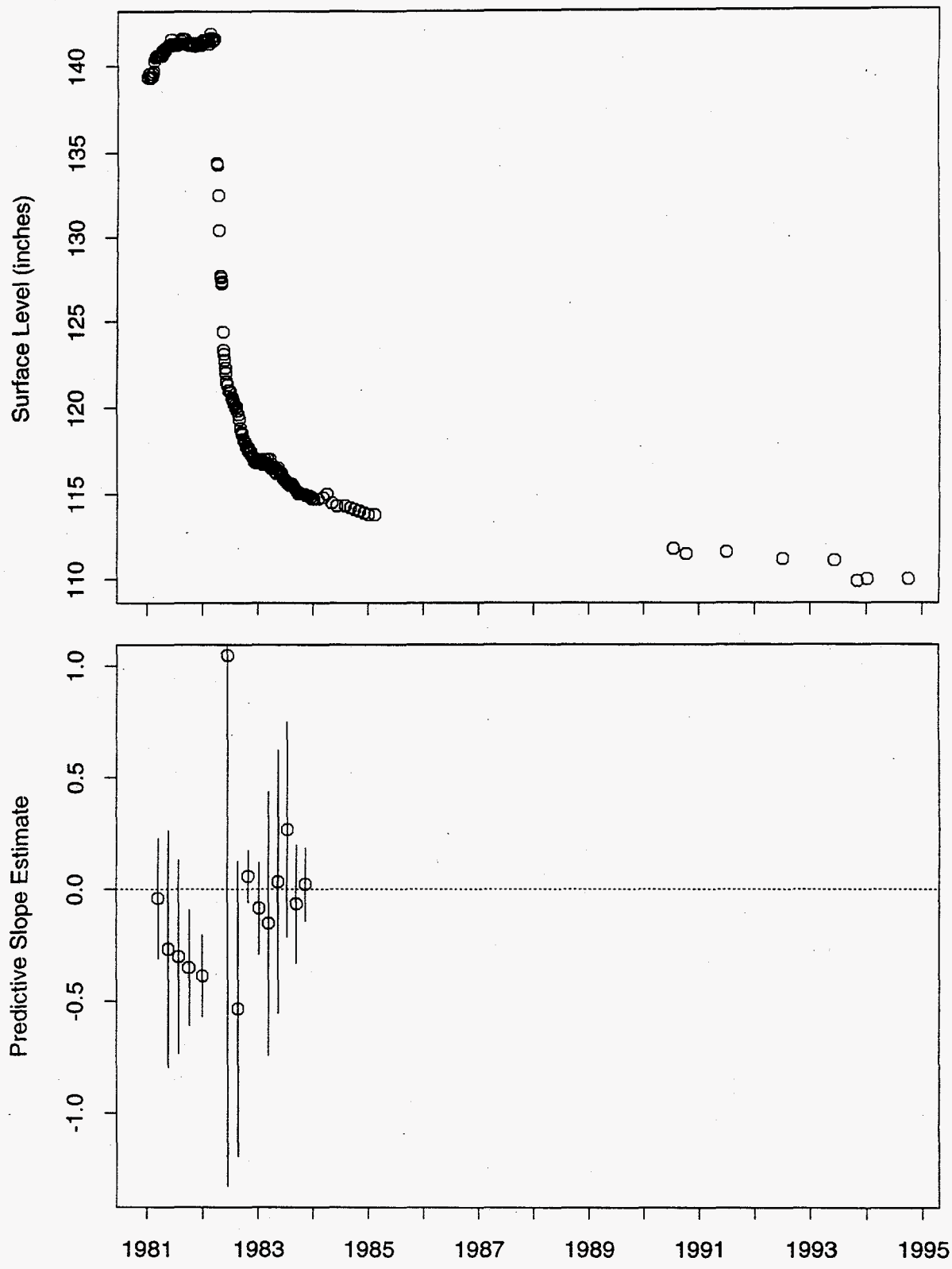

Figure 285: Tank TX–118 FIC Data

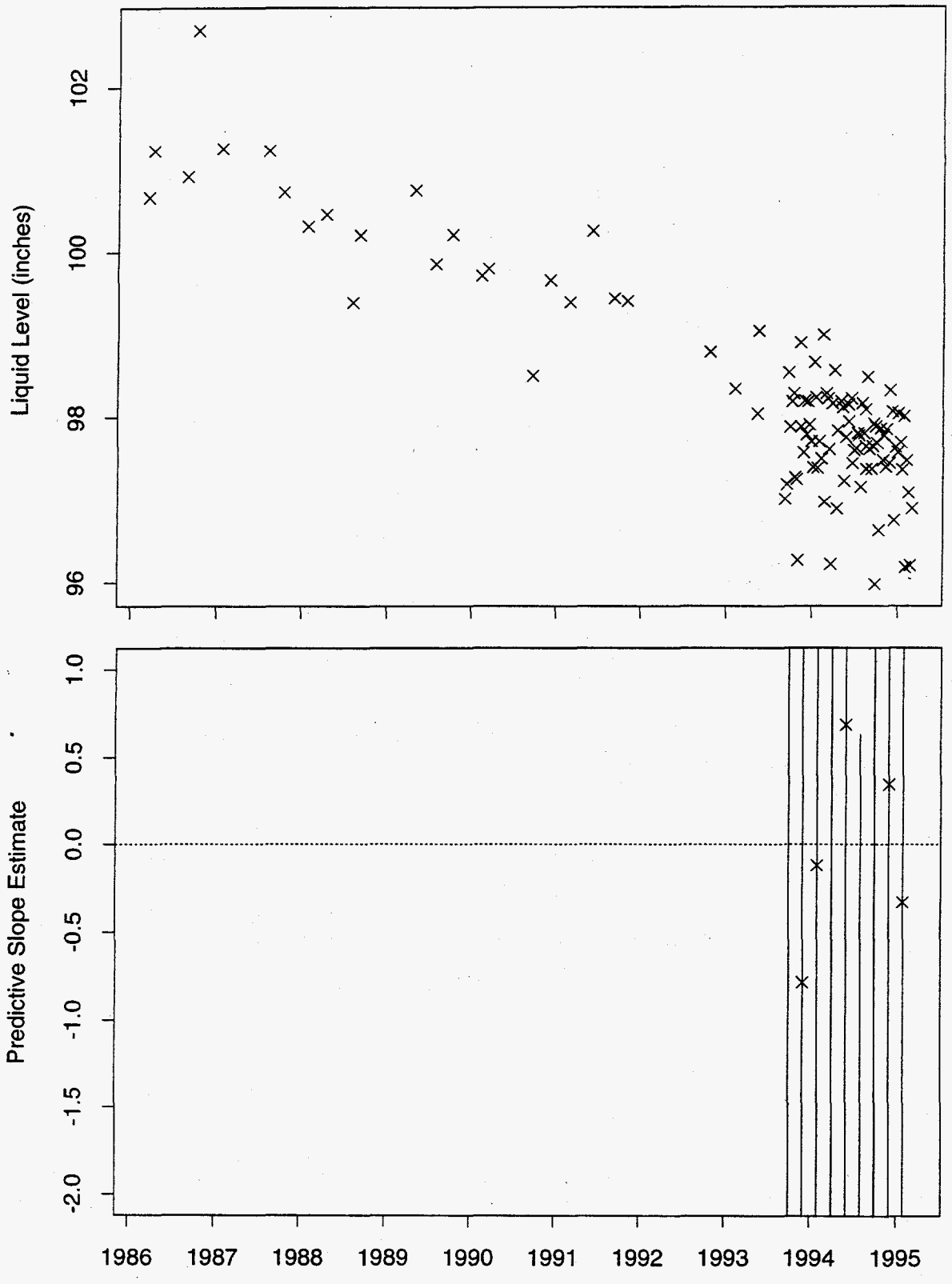

Figure 286: Tank TX–118 Neutron ILL Data

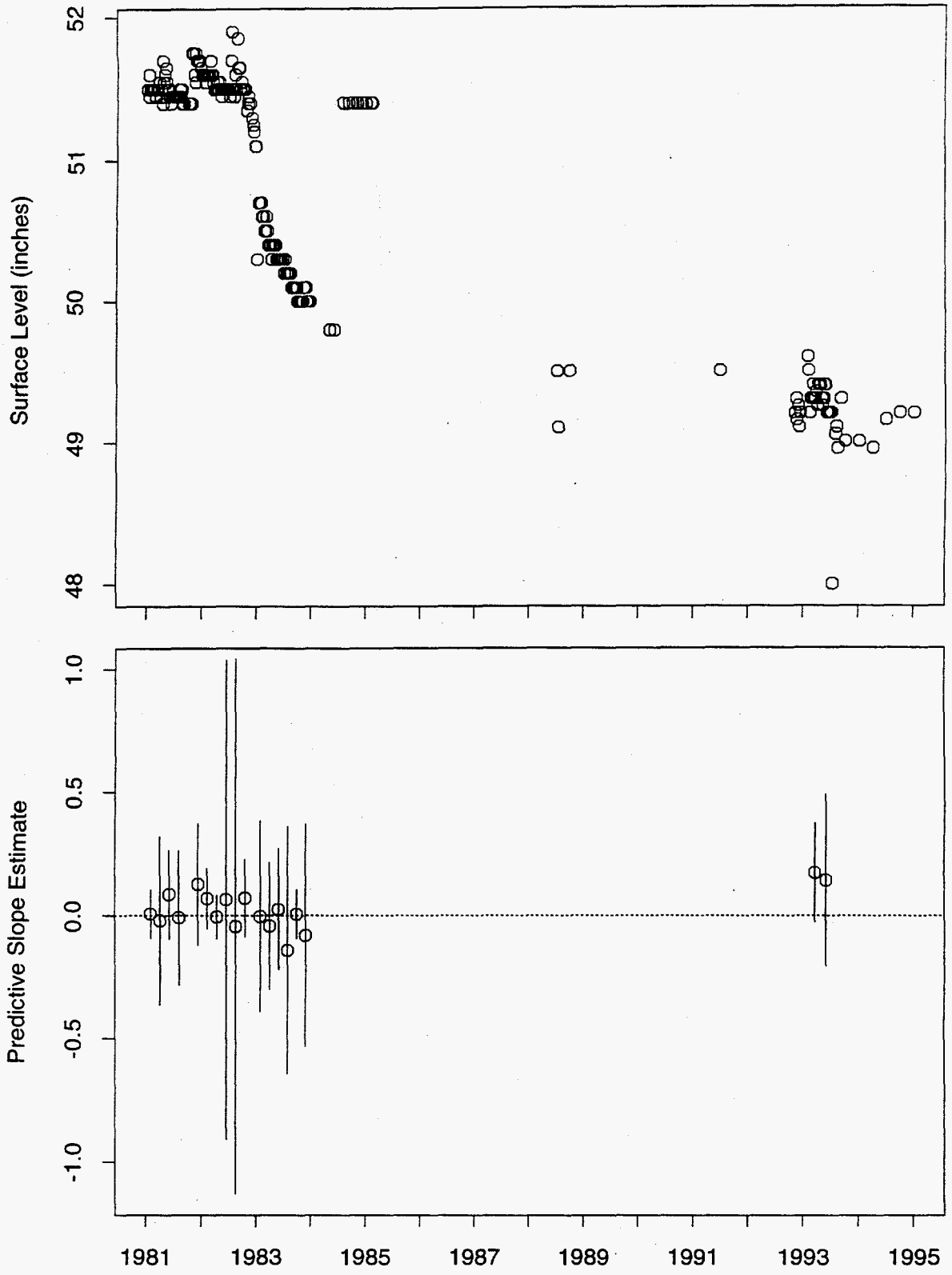

Figure 287: Tank TY-101 FIC Data

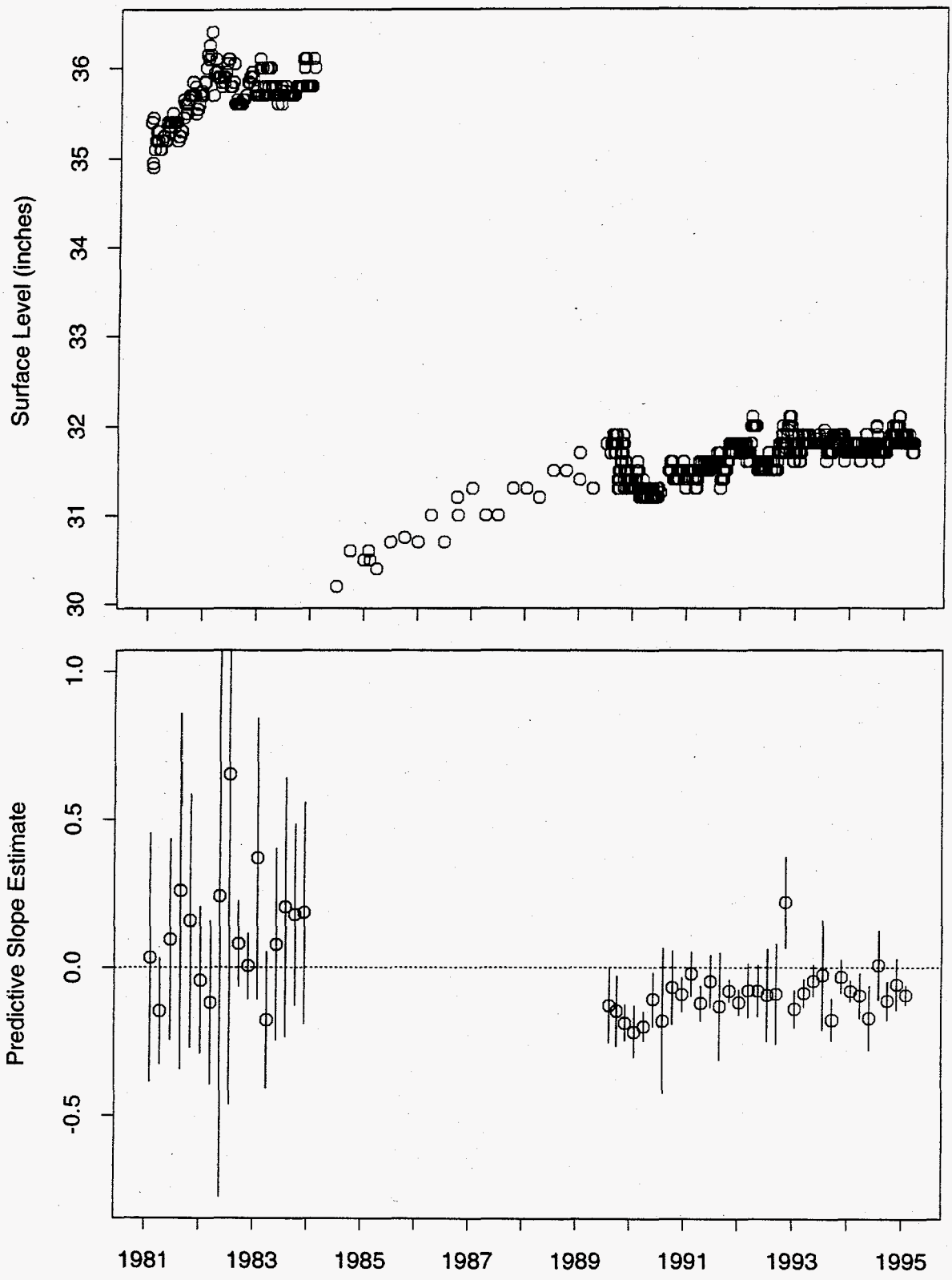

Figure 288: Tank TY–102 FIC Data

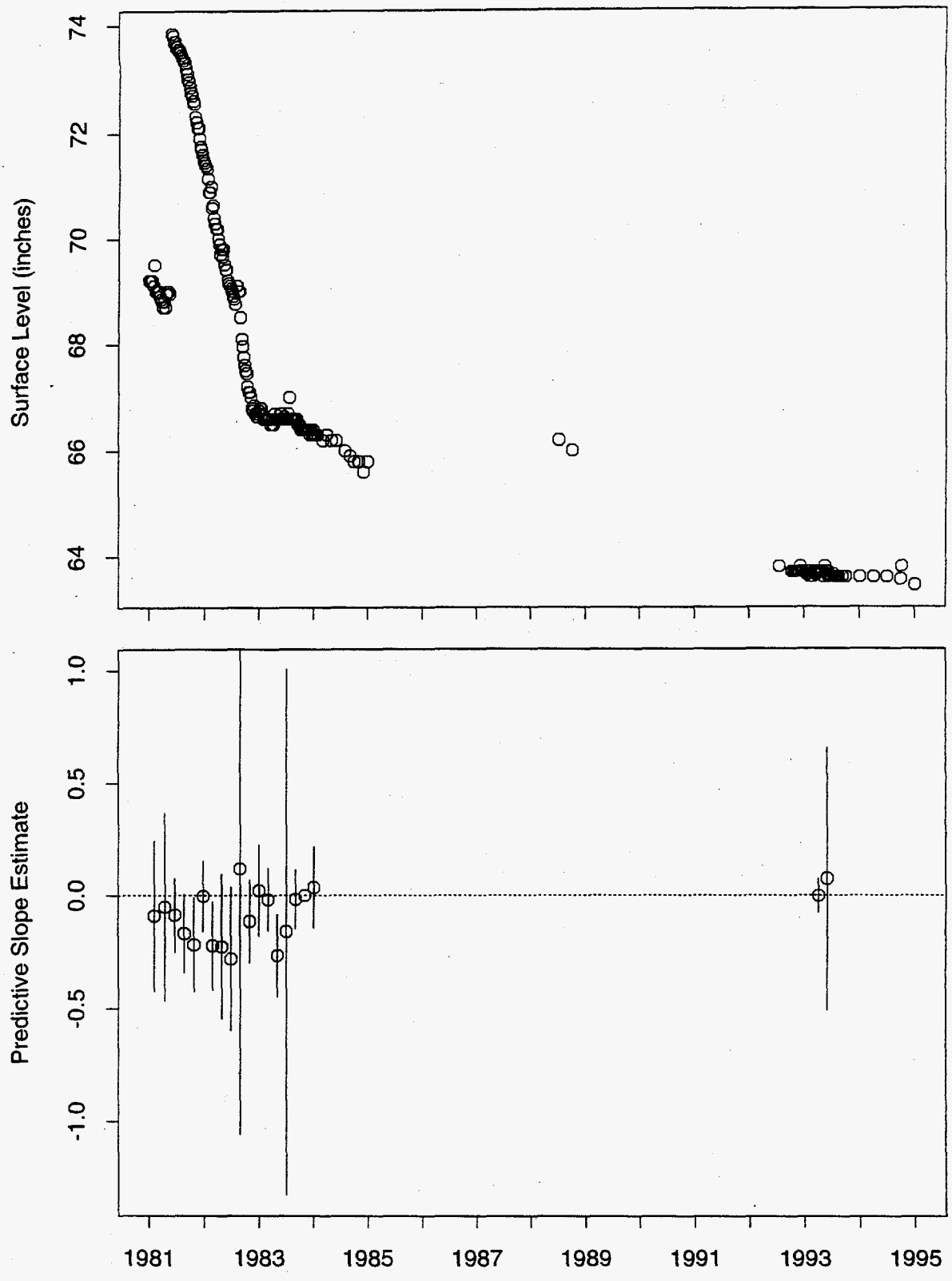

Figure 289: Tank TY–103 FIC Data

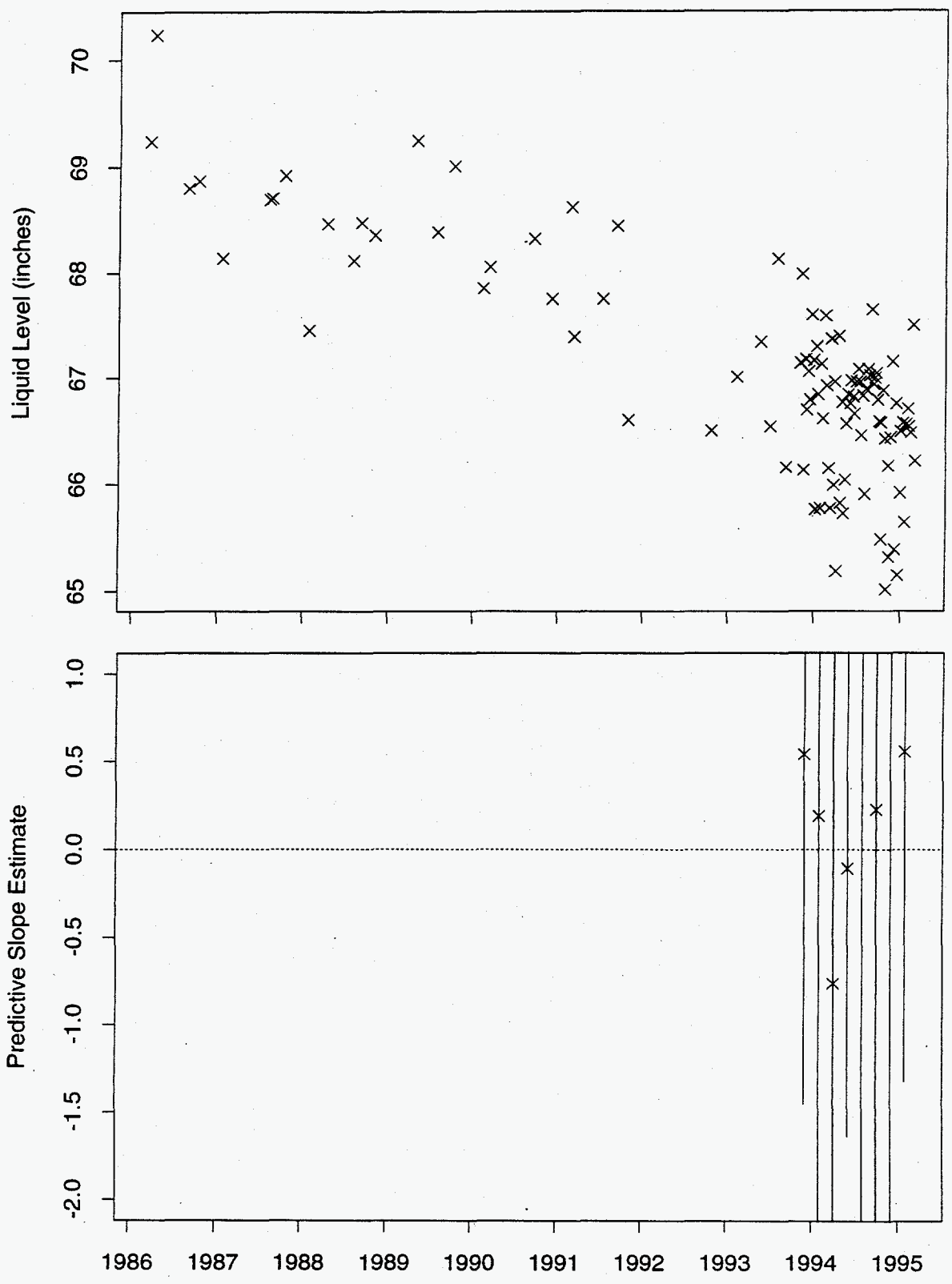

Figure 290: Tank TY–103 Neutron ILL Data

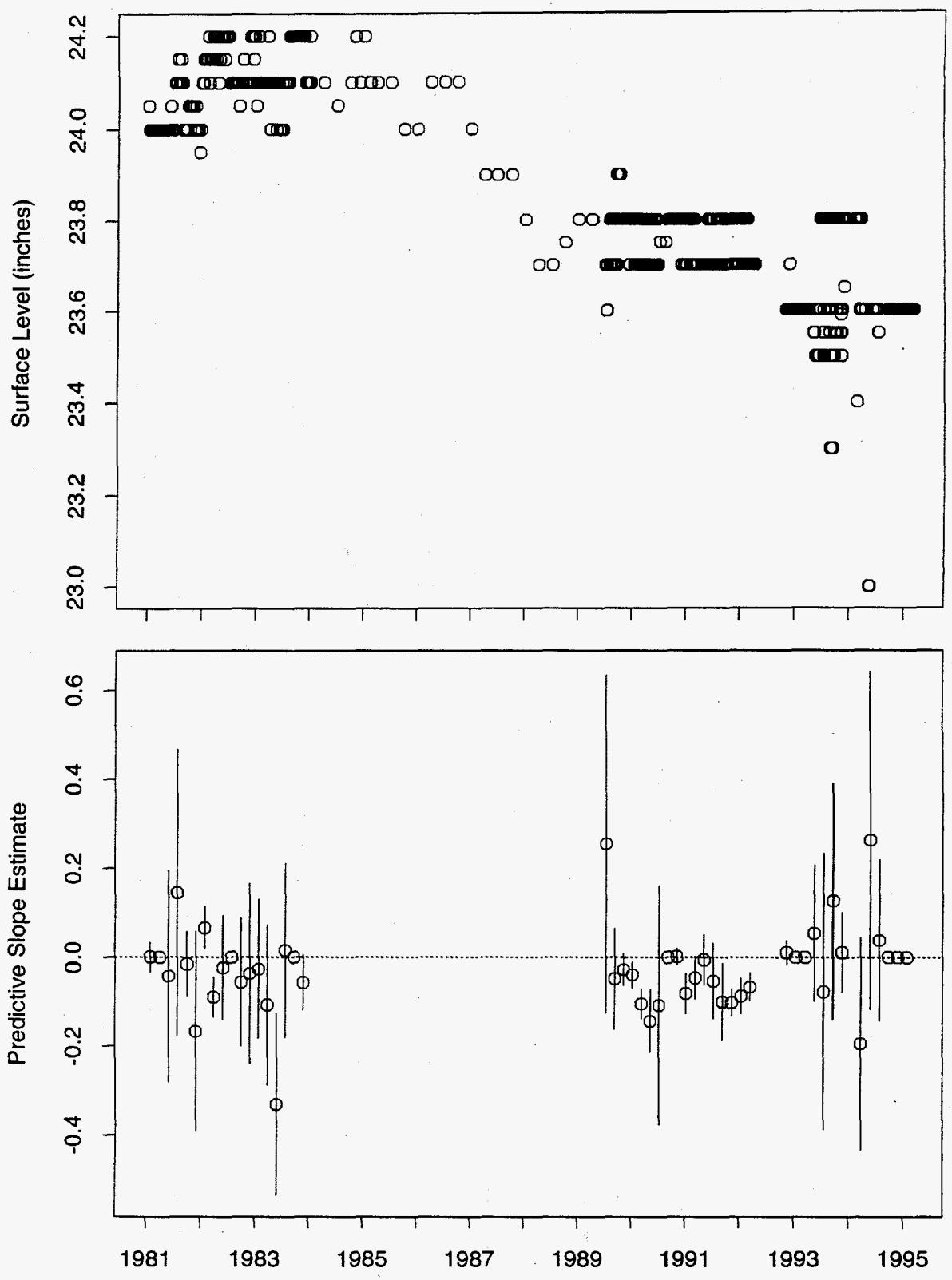

Figure 291: Tank TY-104 FIC Data

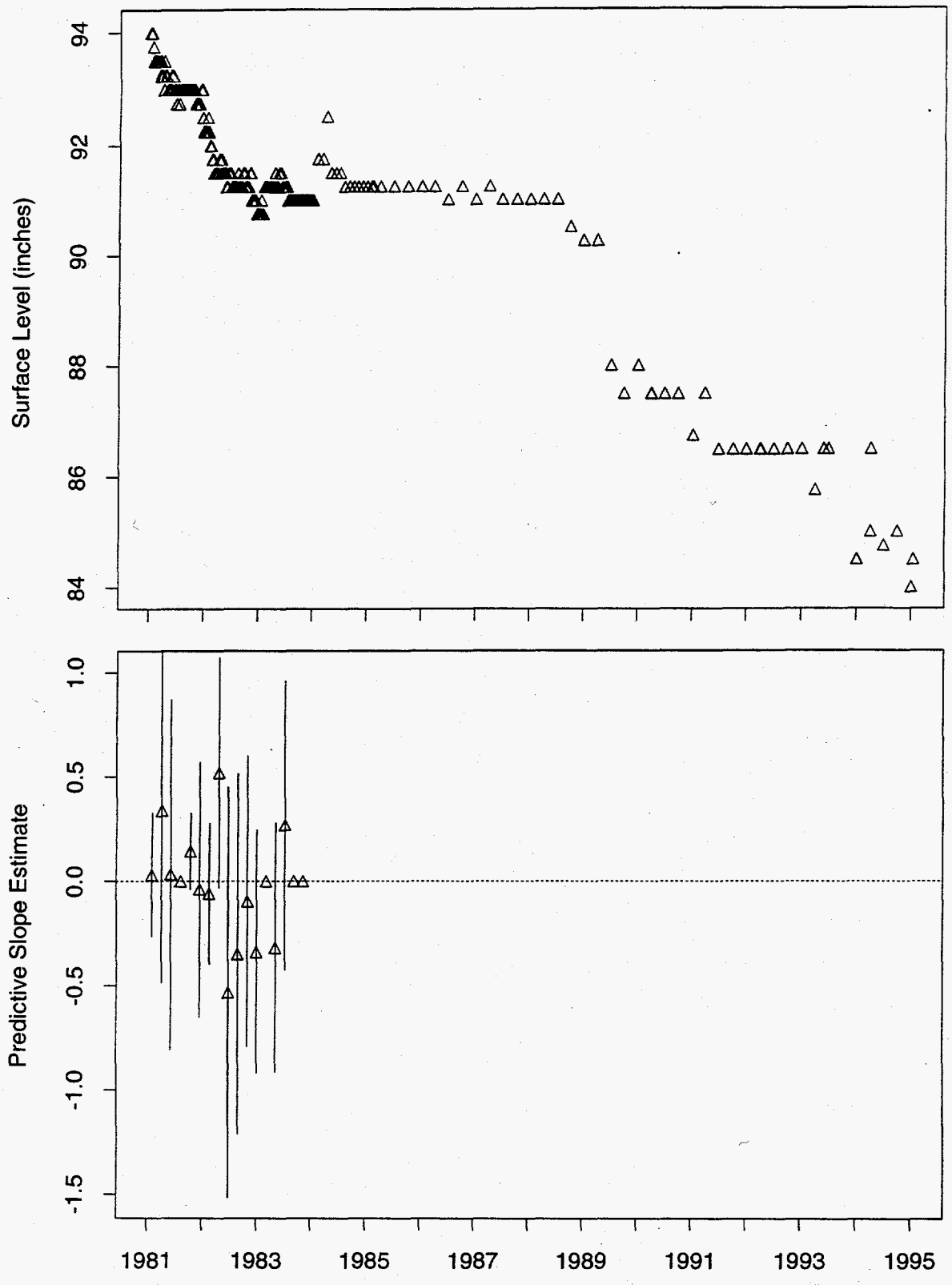

Figure 292: Tank TY-105 MT Data

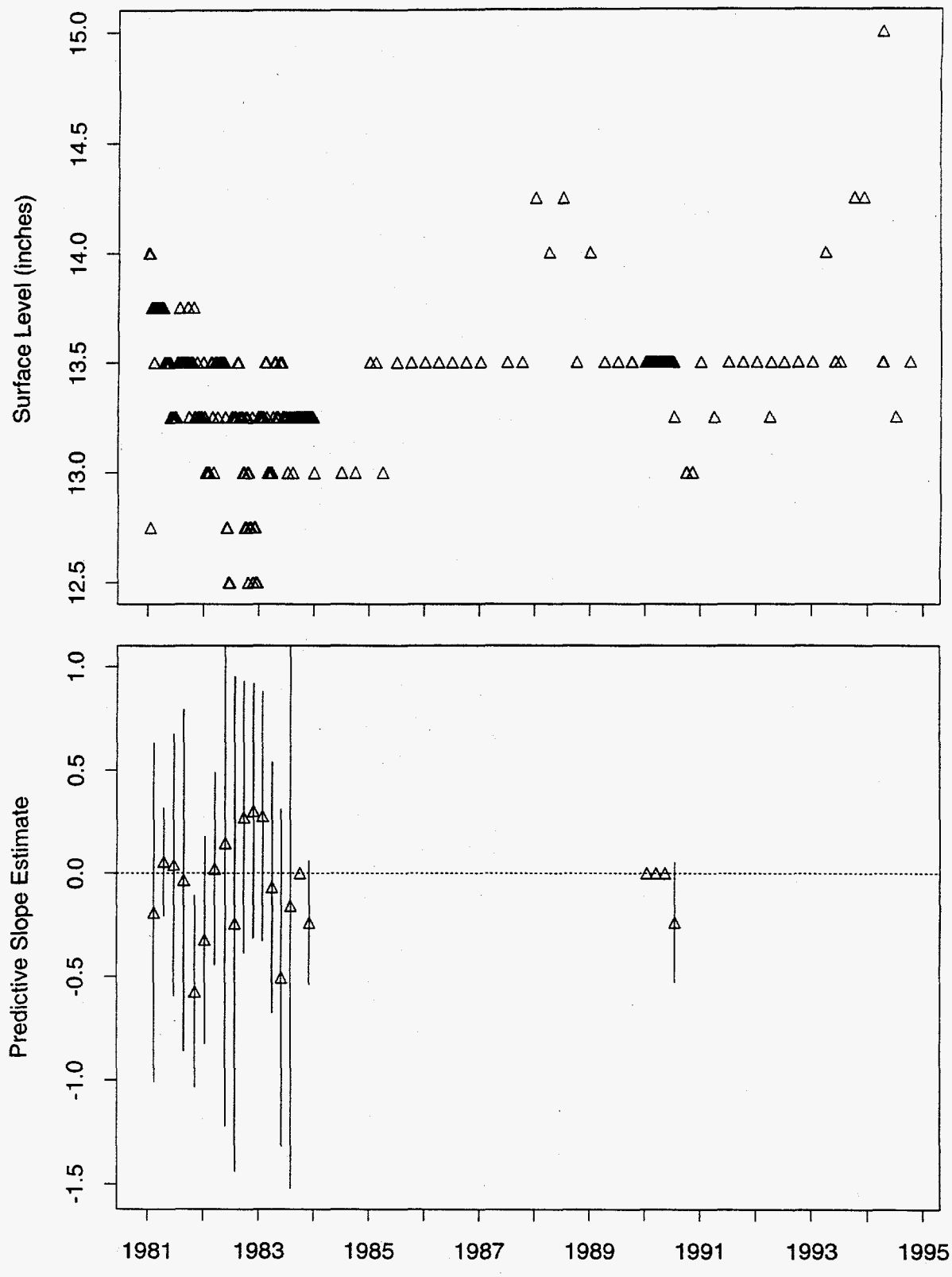

Figure 293: Tank TY–106 MT Data

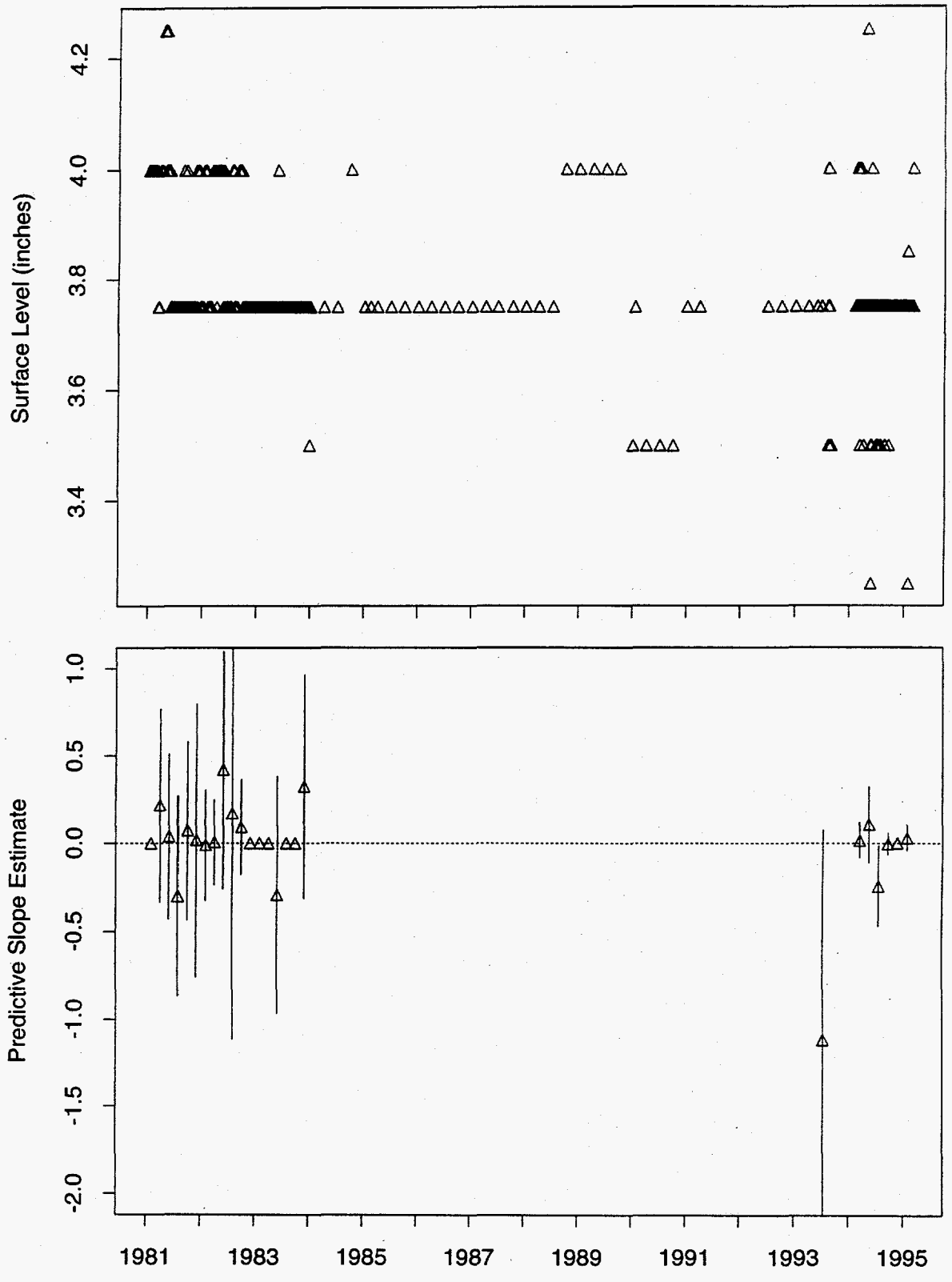

Figure 294: Tank U–101 MT Data

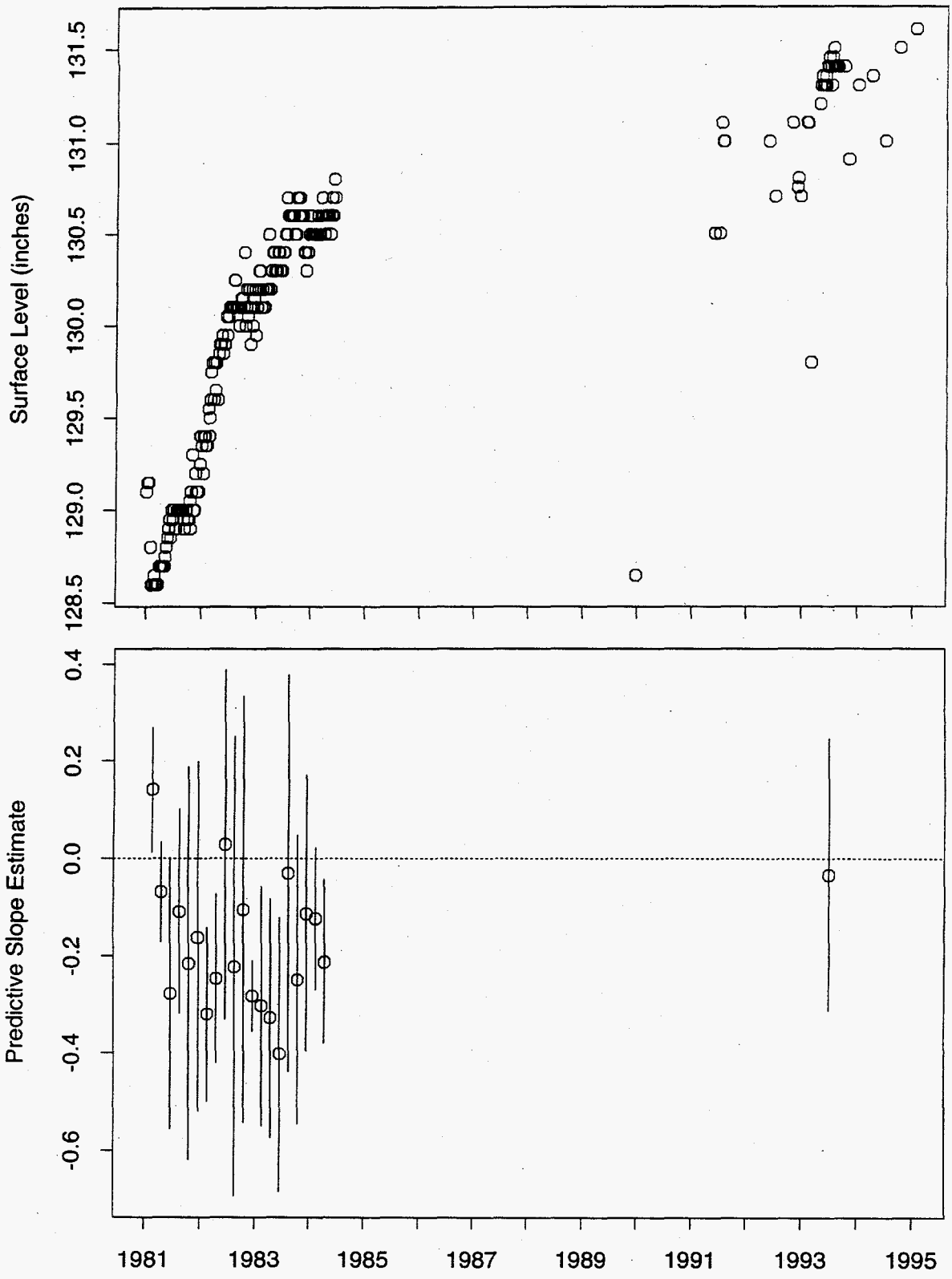

Figure 295: Tank U-102 FIC Data

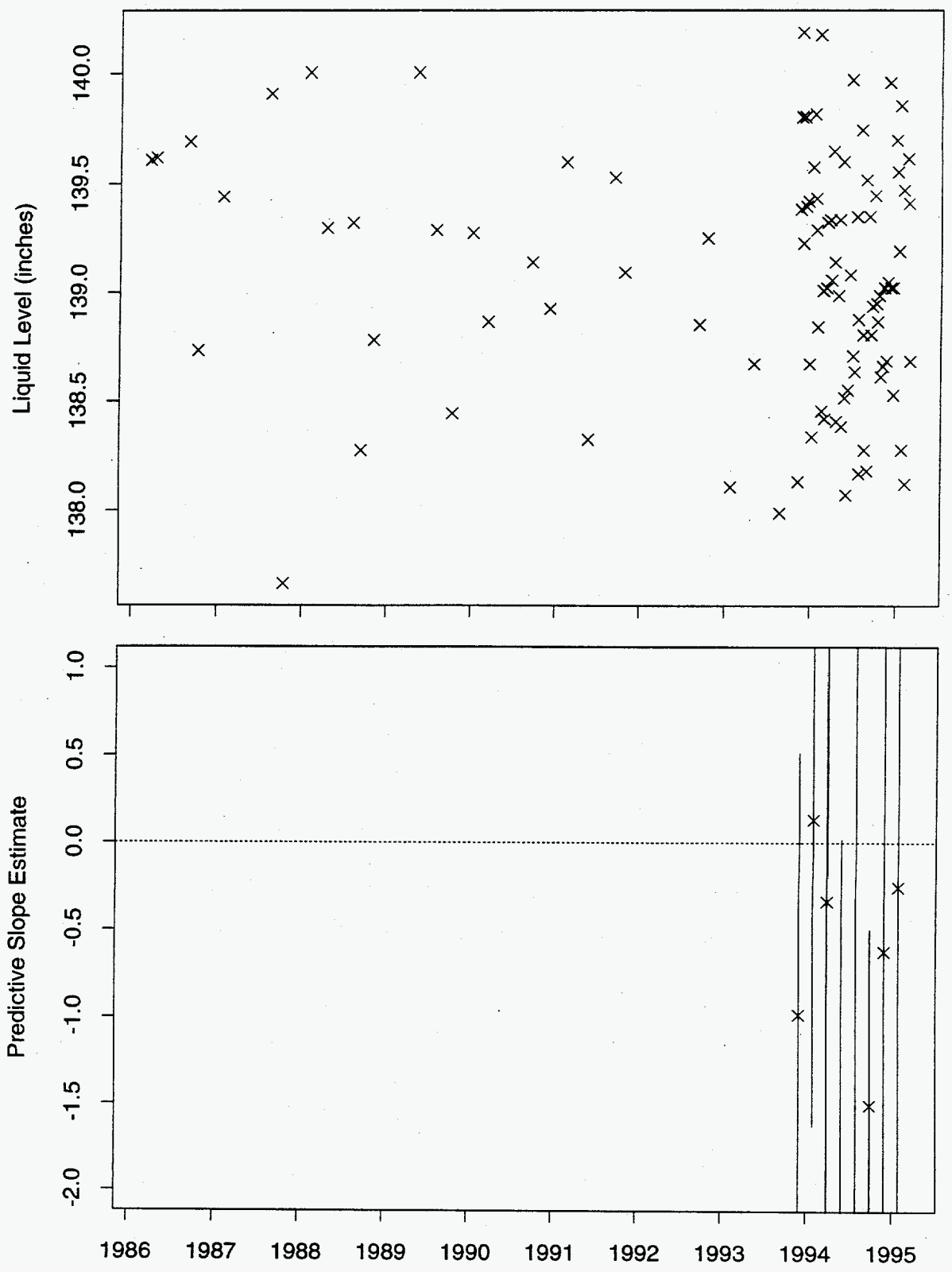

Figure 296: Tank U-102 Neutron ILL Data

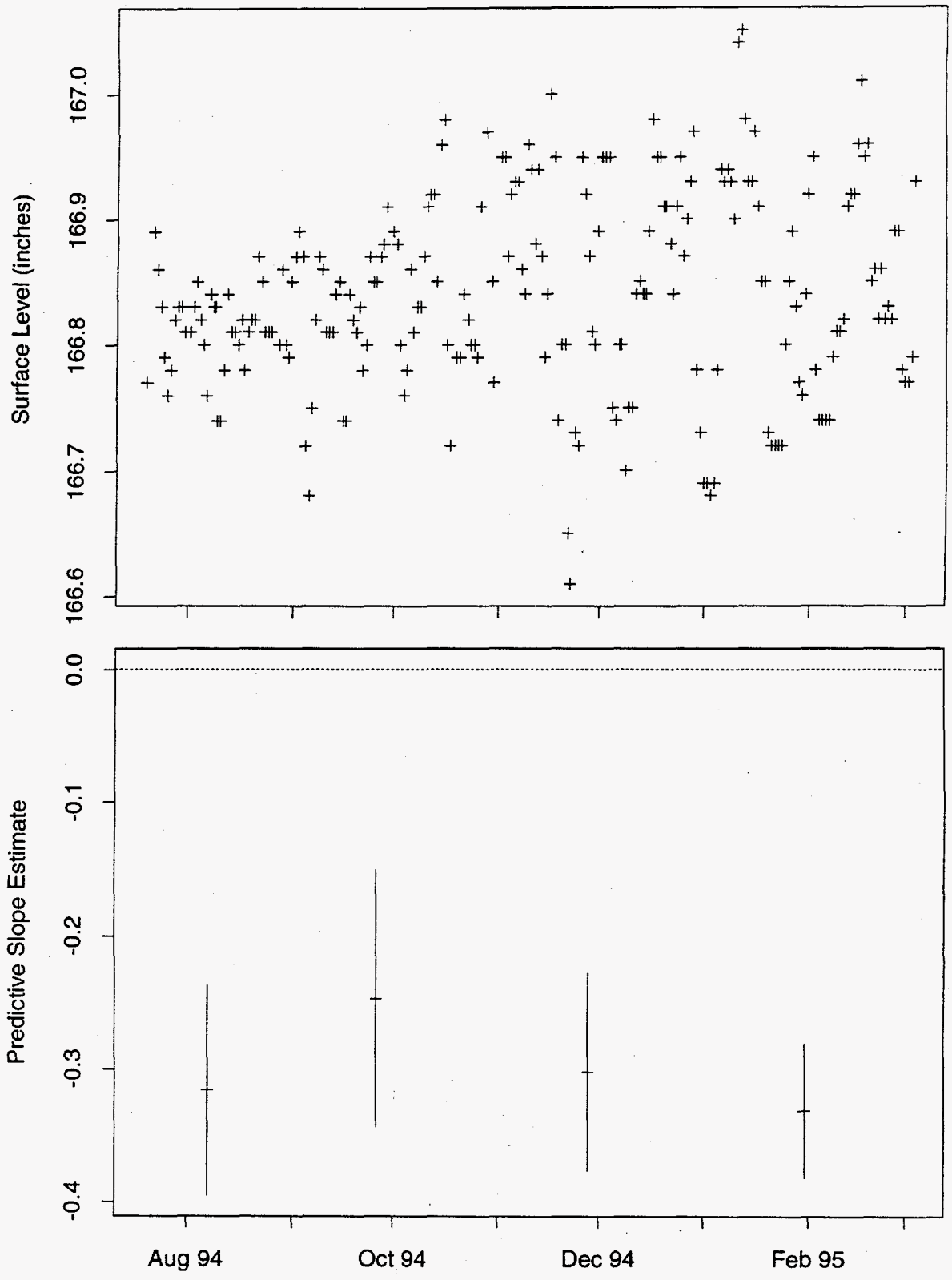

Figure 297: Tank U–103 ENRAF Data

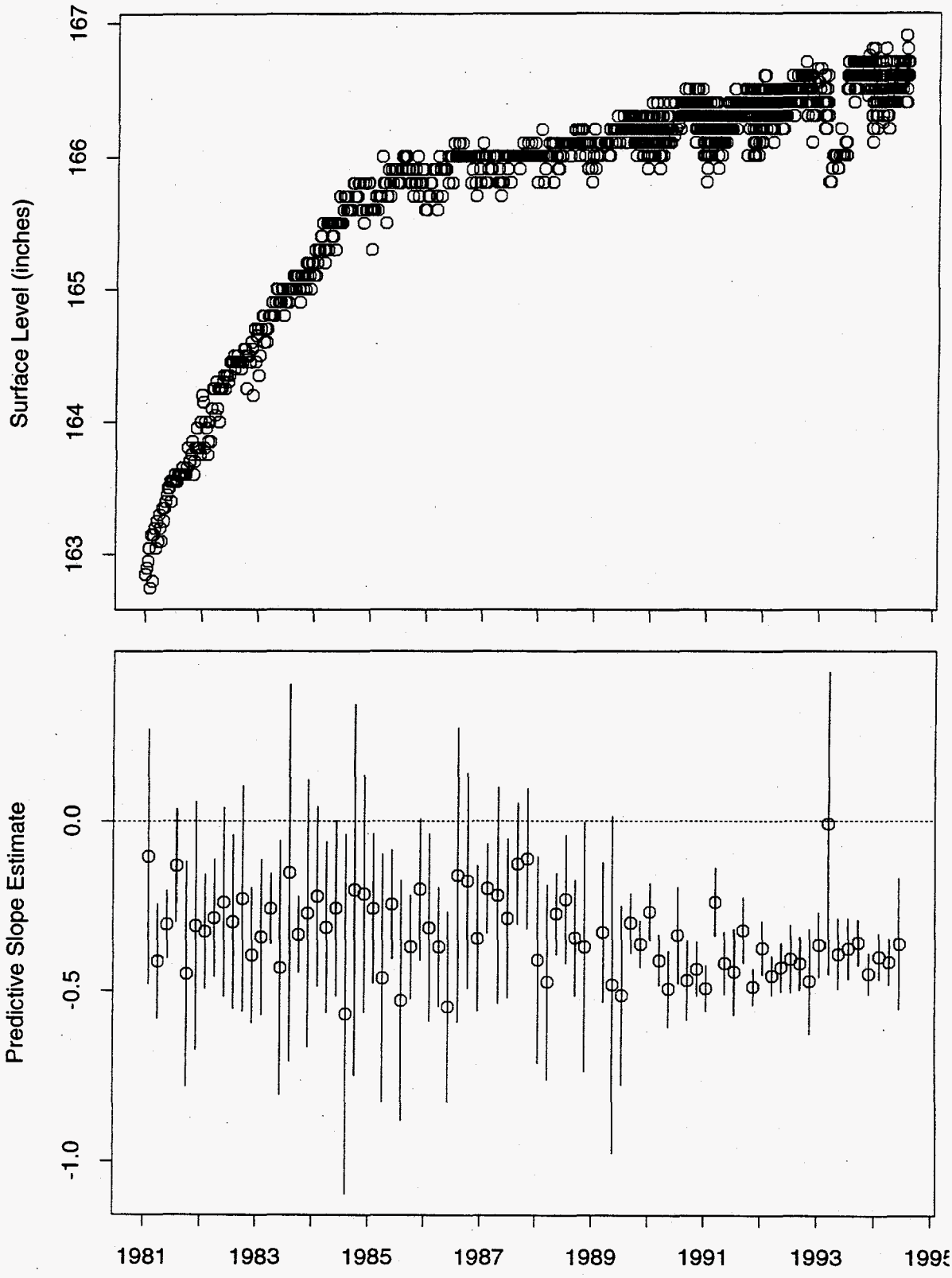

Figure 298: Tank U-103 FIC Data

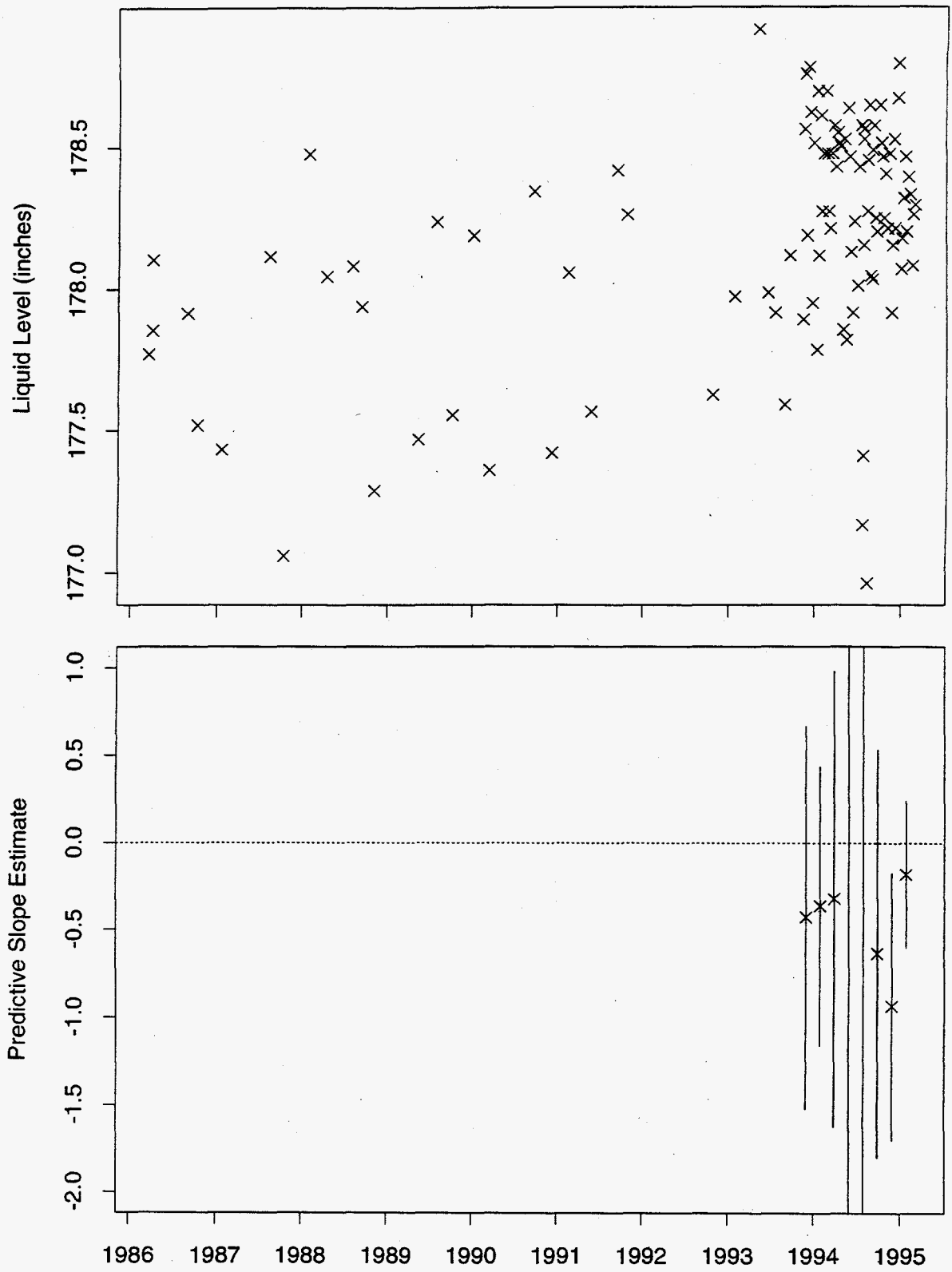

Figure 299: Tank U–103 Neutron ILL Data

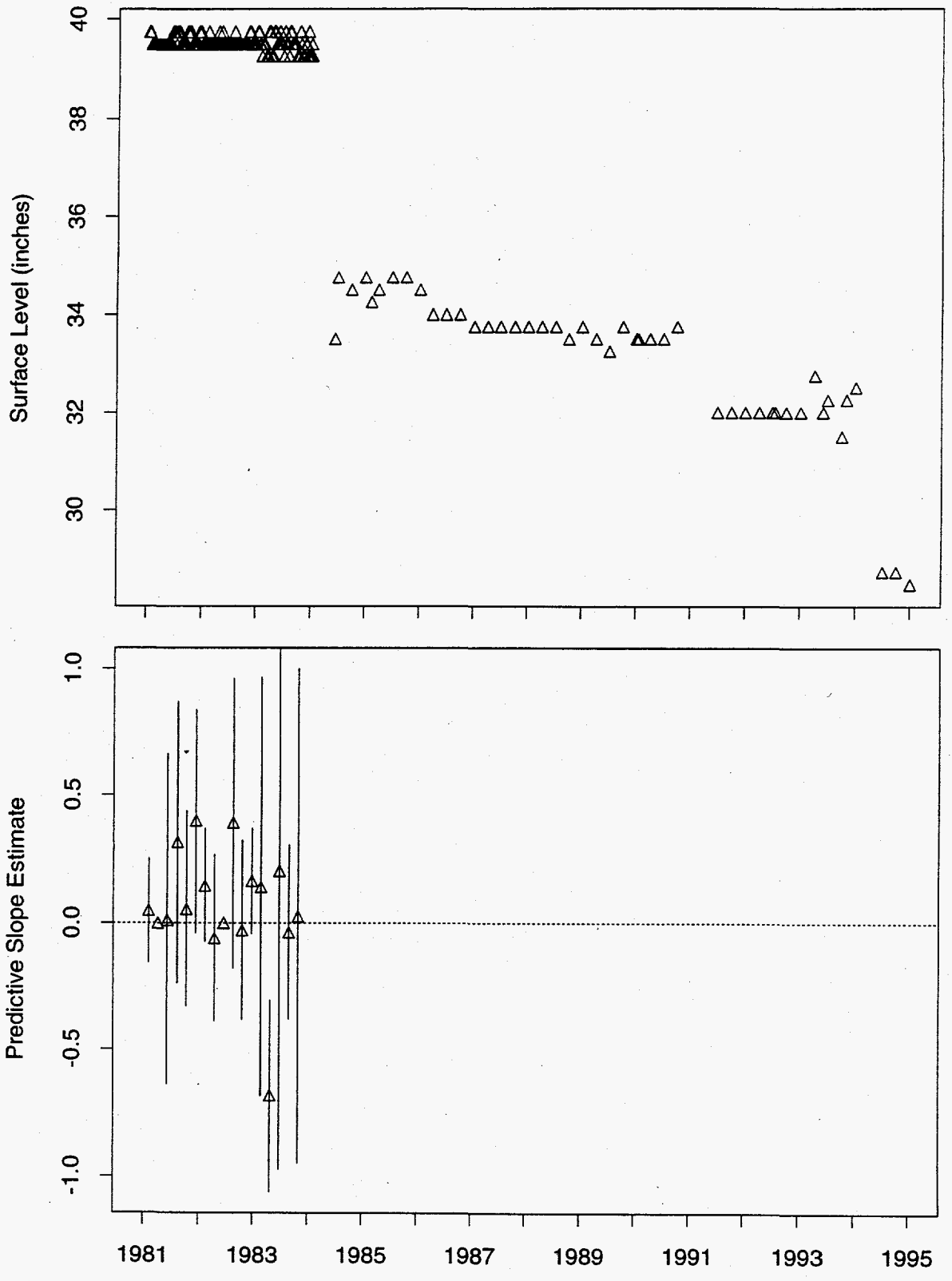

Figure 300: Tank U–104 MT Data

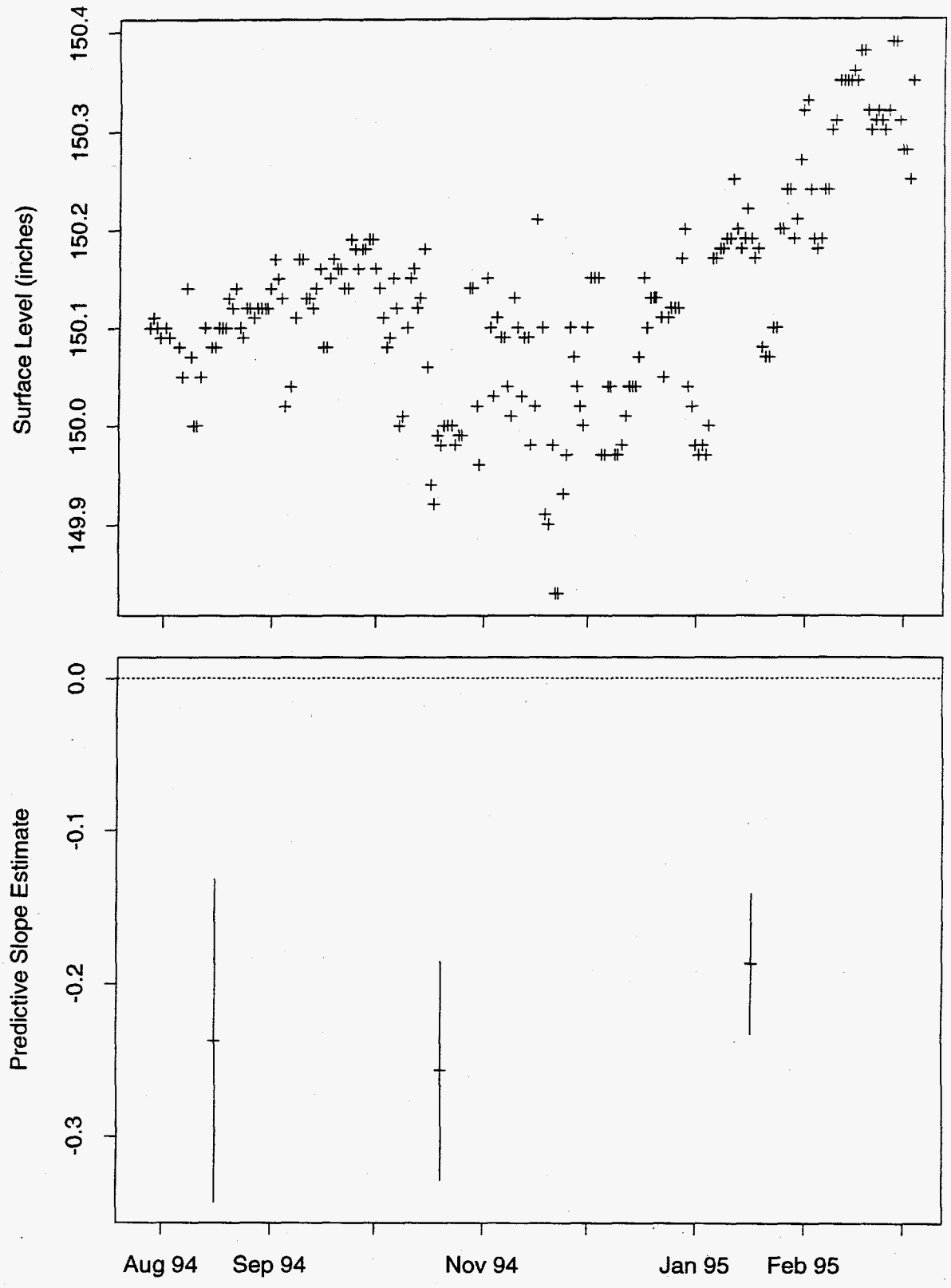

Figure 301: Tank U-105 ENRAF Data

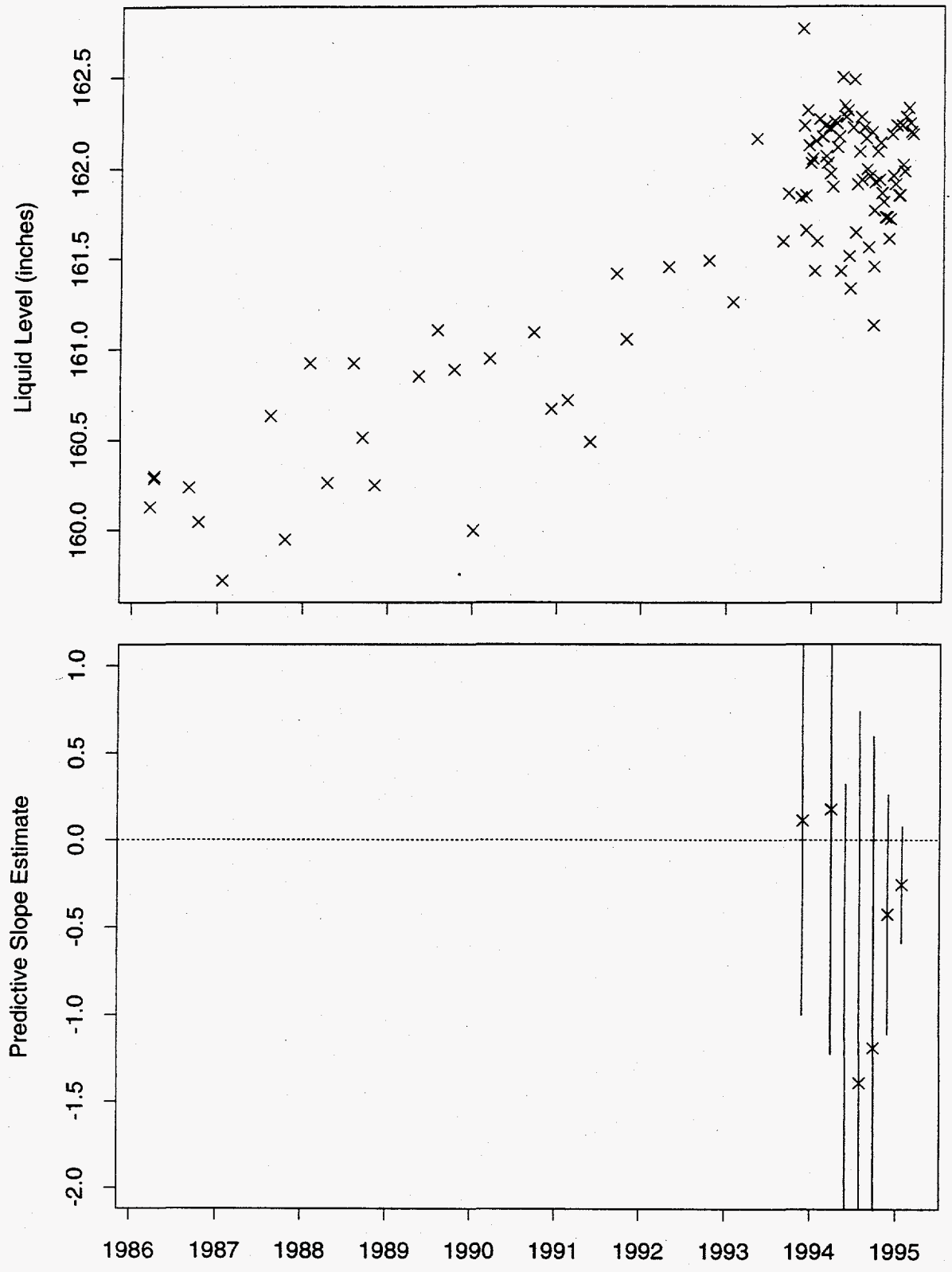

Figure 304: Tank U–105 Neutron ILL Data

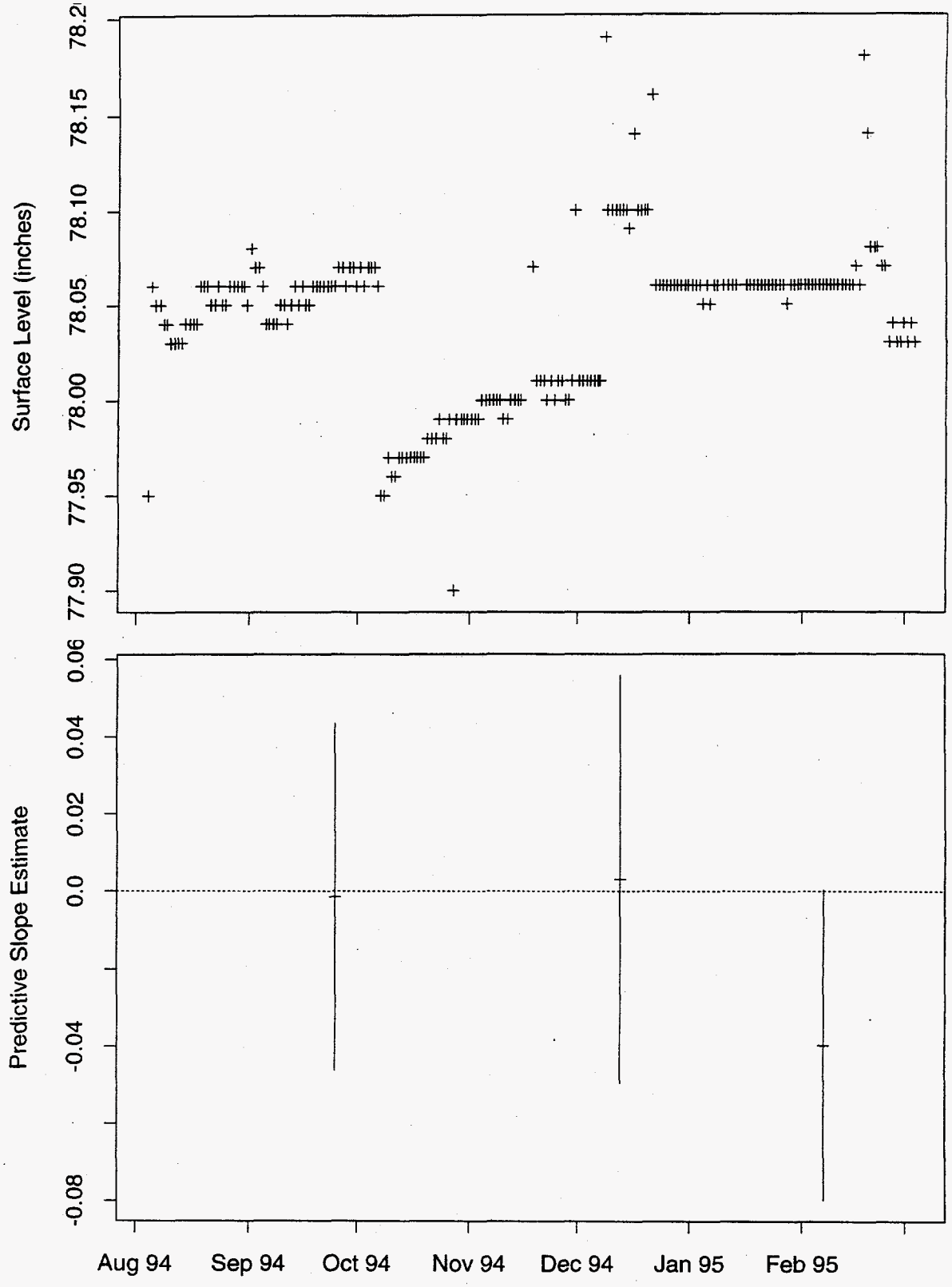

Figure 305: Tank U-106 ENRAF Data

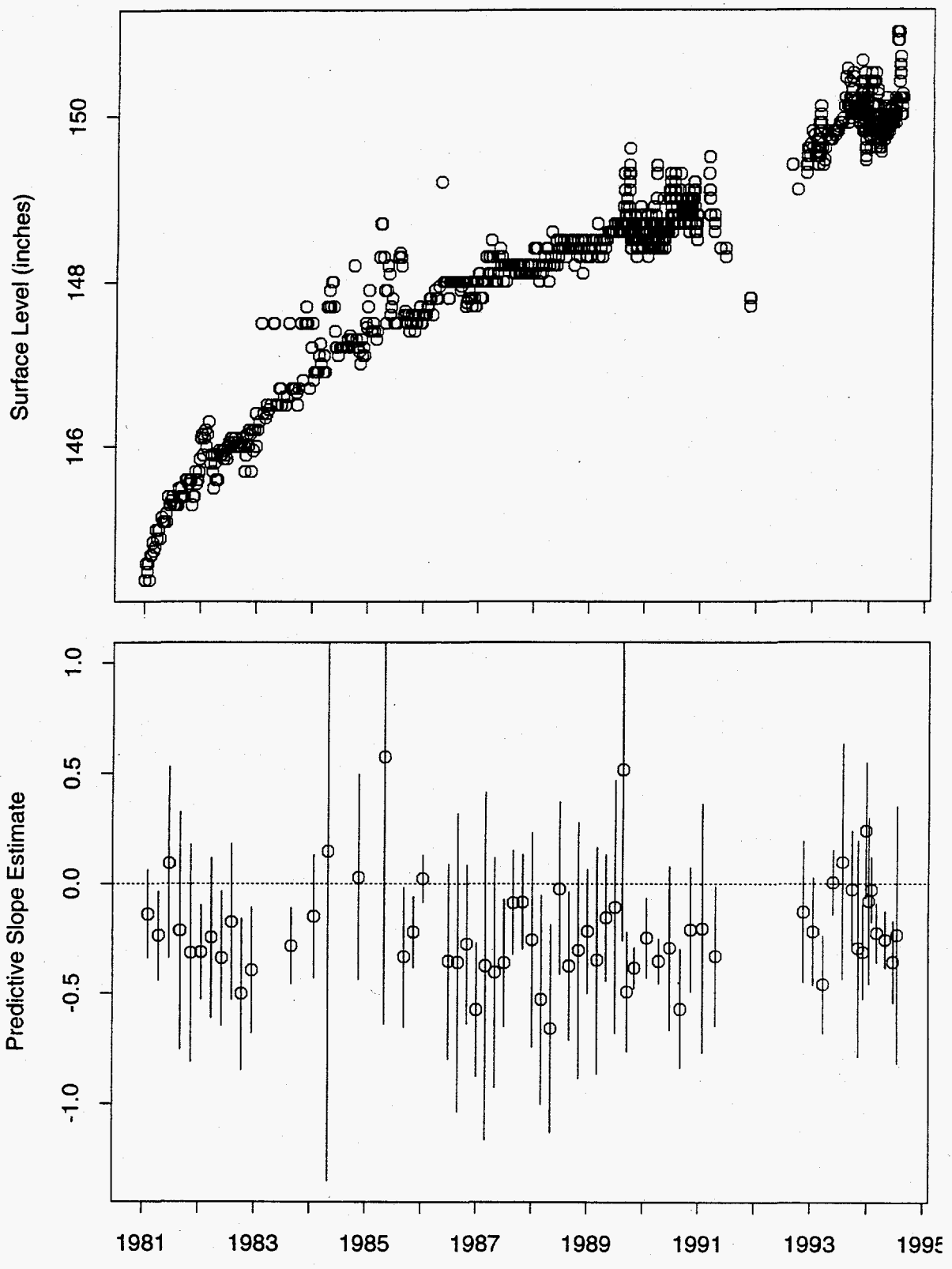

Figure 302: Tank U–105 FIC Data

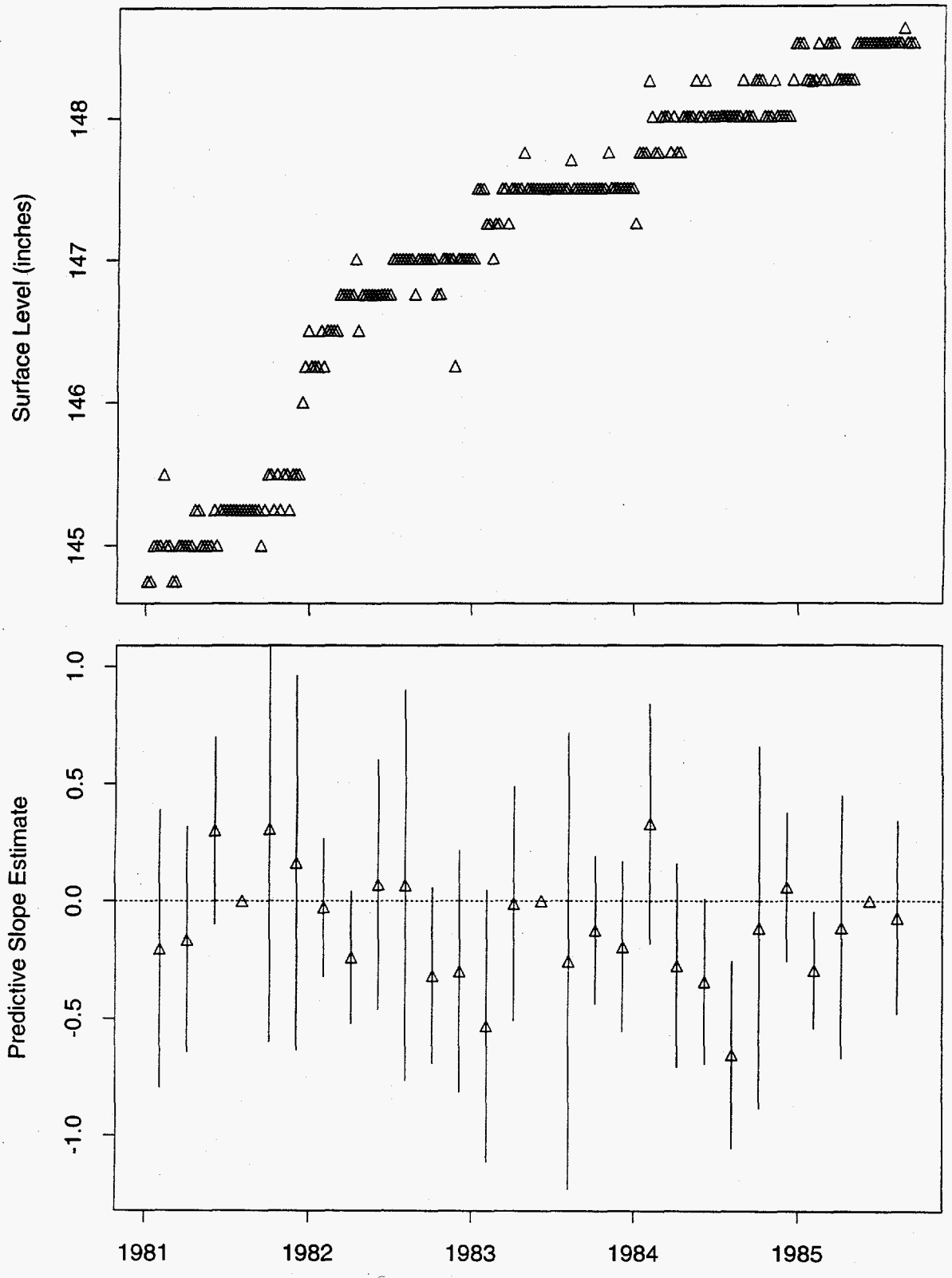

Figure 303: Tank U–105 MT Data

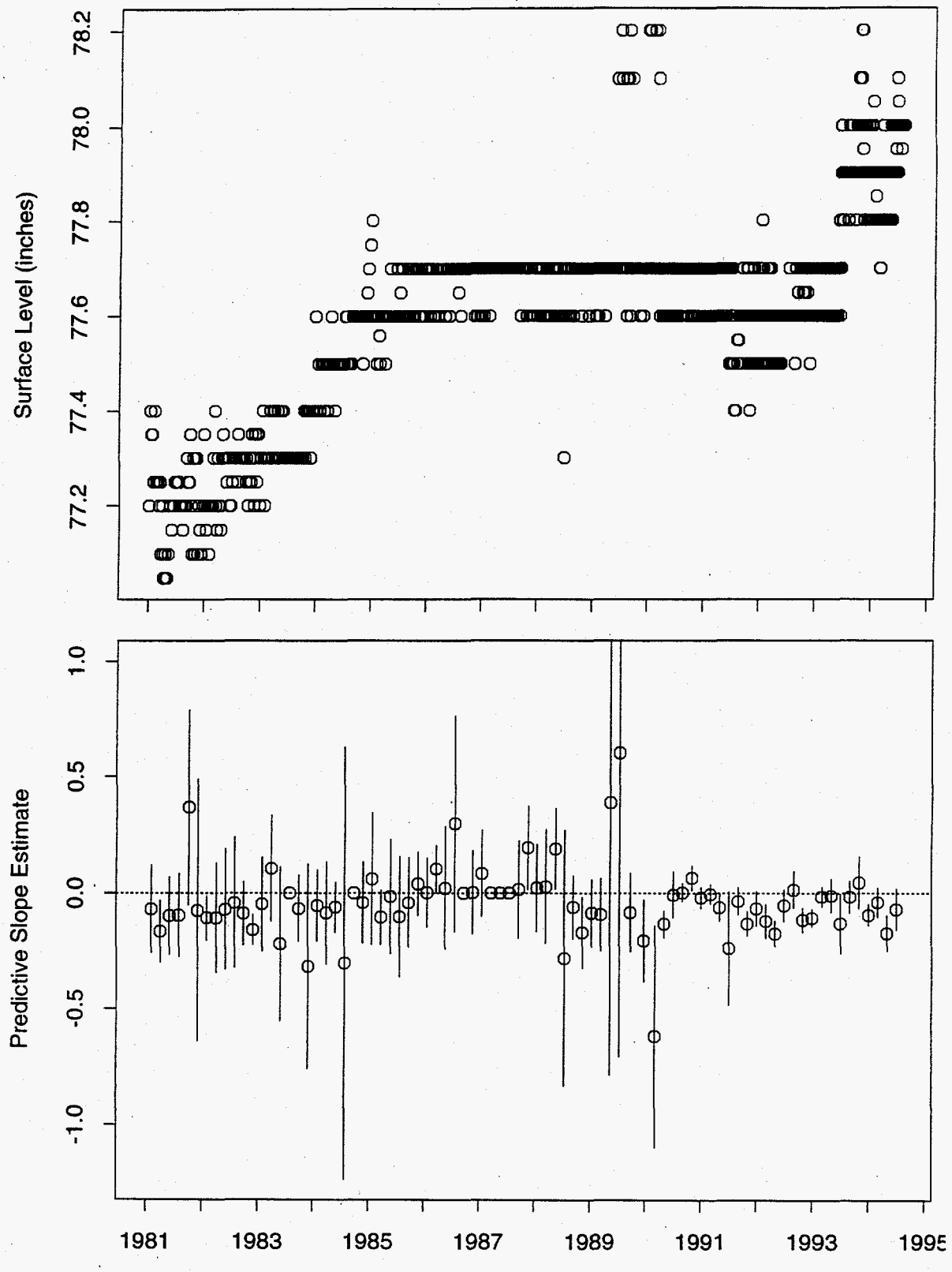

Figure 306: Tank U–106 FIC Data

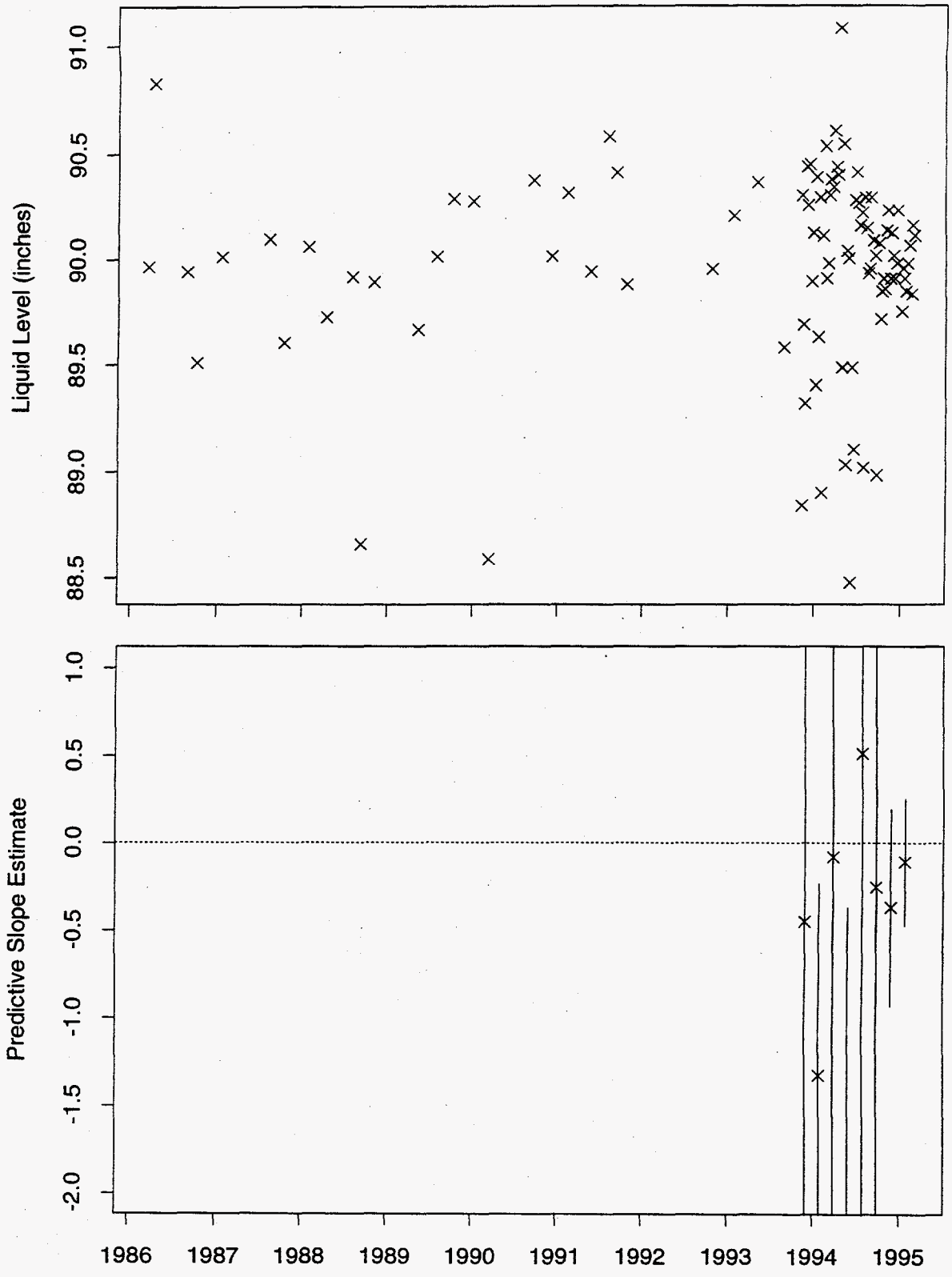

Figure 307: Tank U–106 Neutron ILL Data

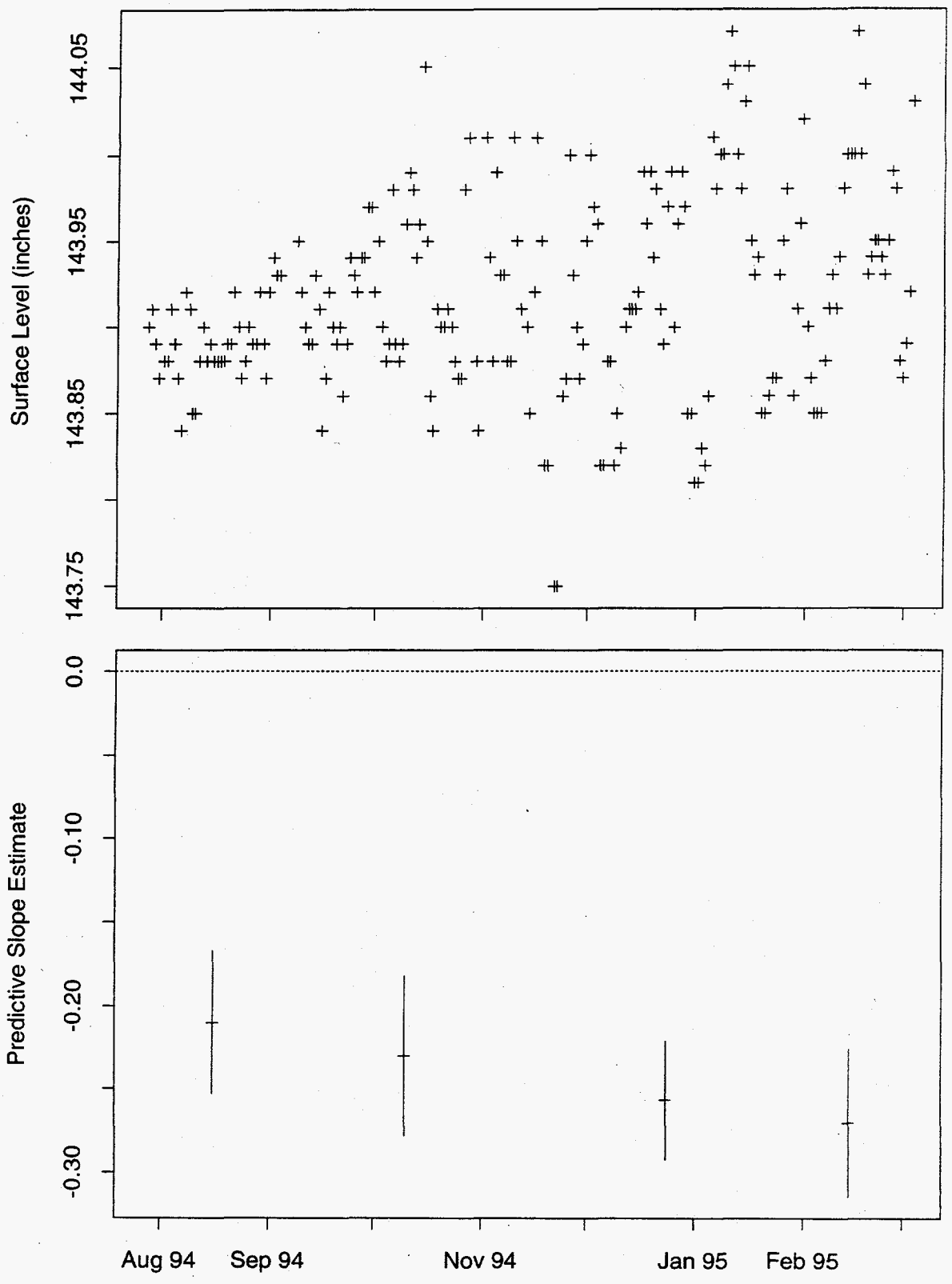

Figure 308: Tank U–107 ENRAF Data

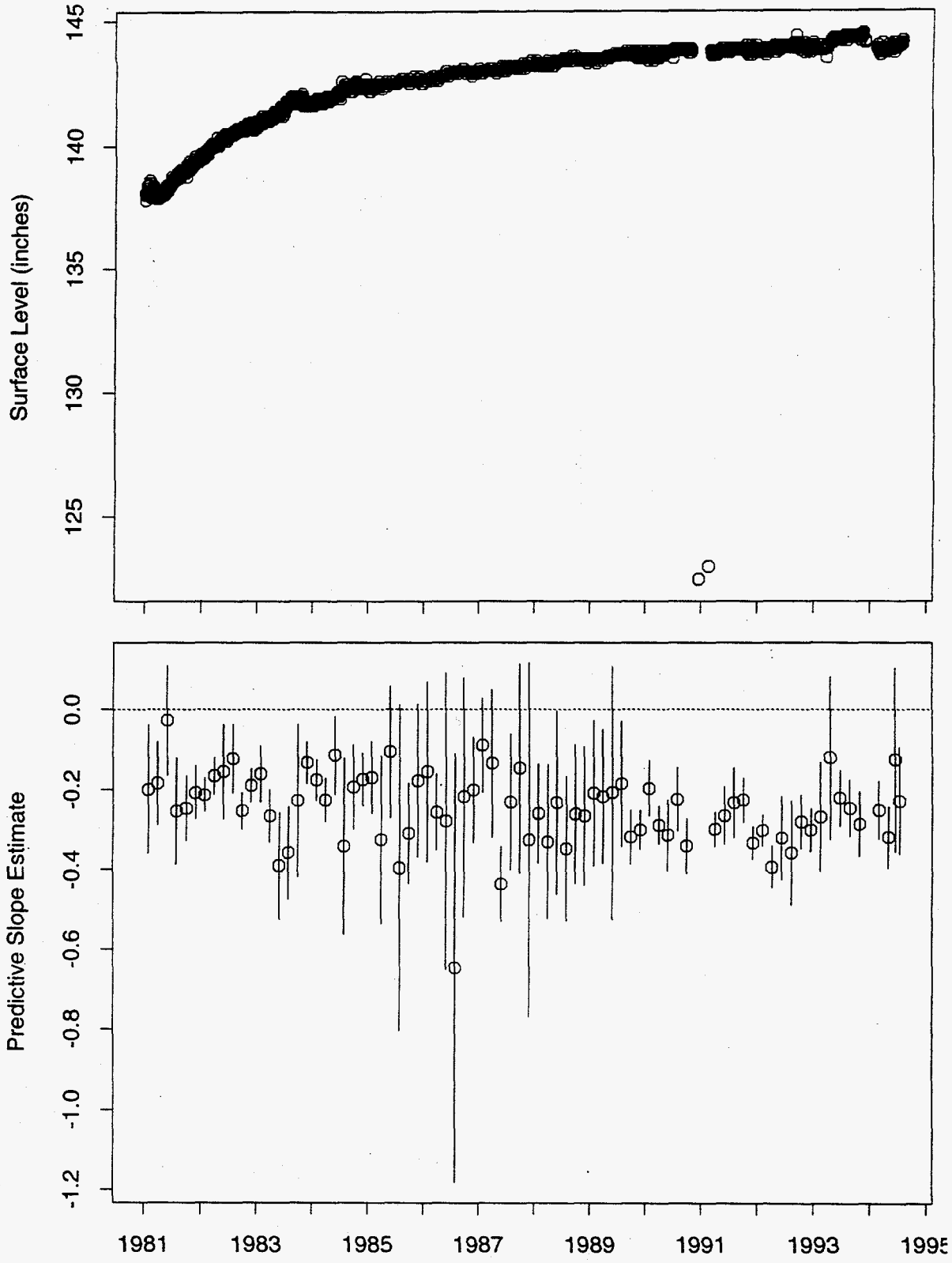

Figure 309: Tank U-107 FIC Data

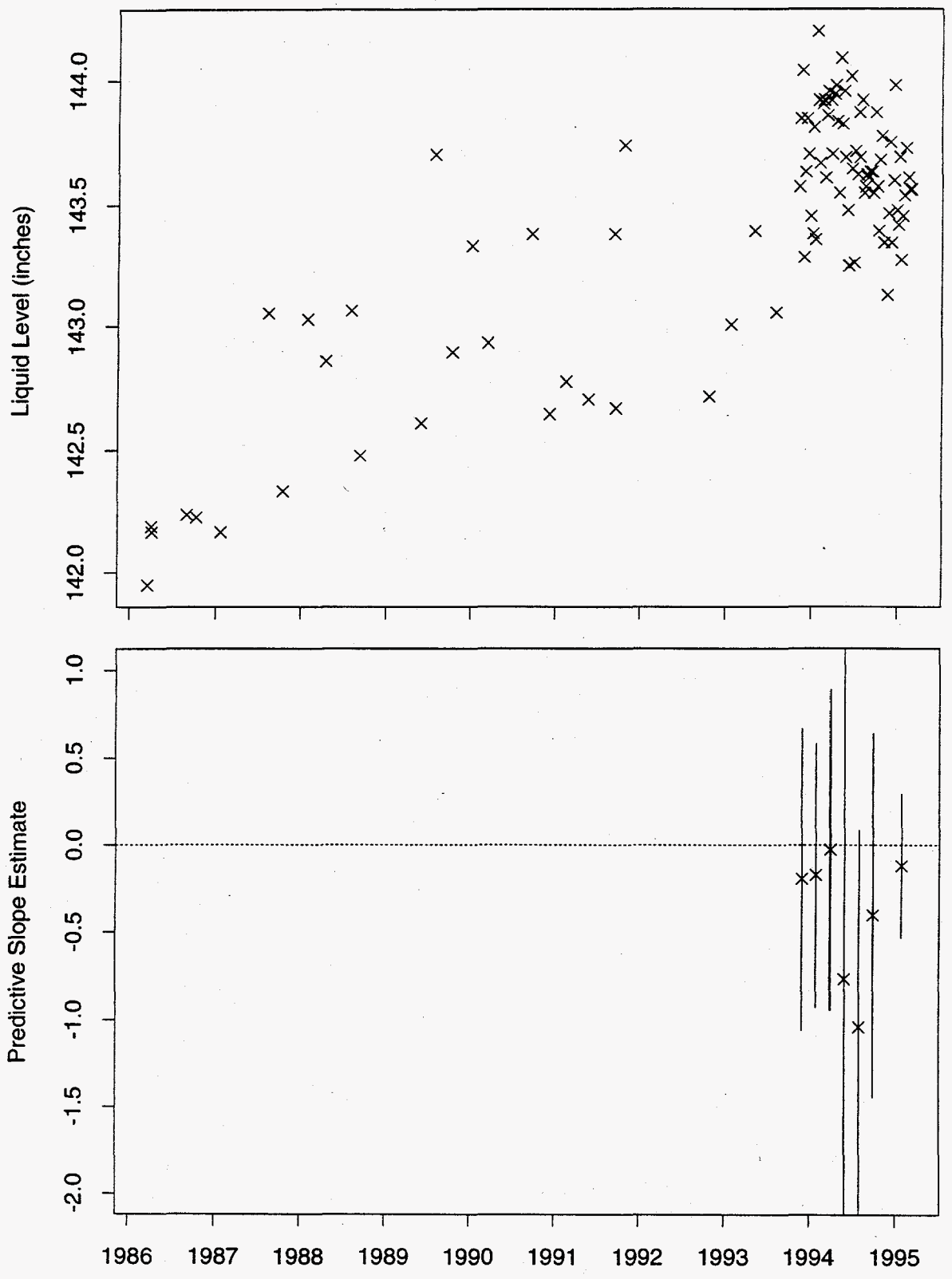

Figure 310: Tank U-107 Neutron ILL Data

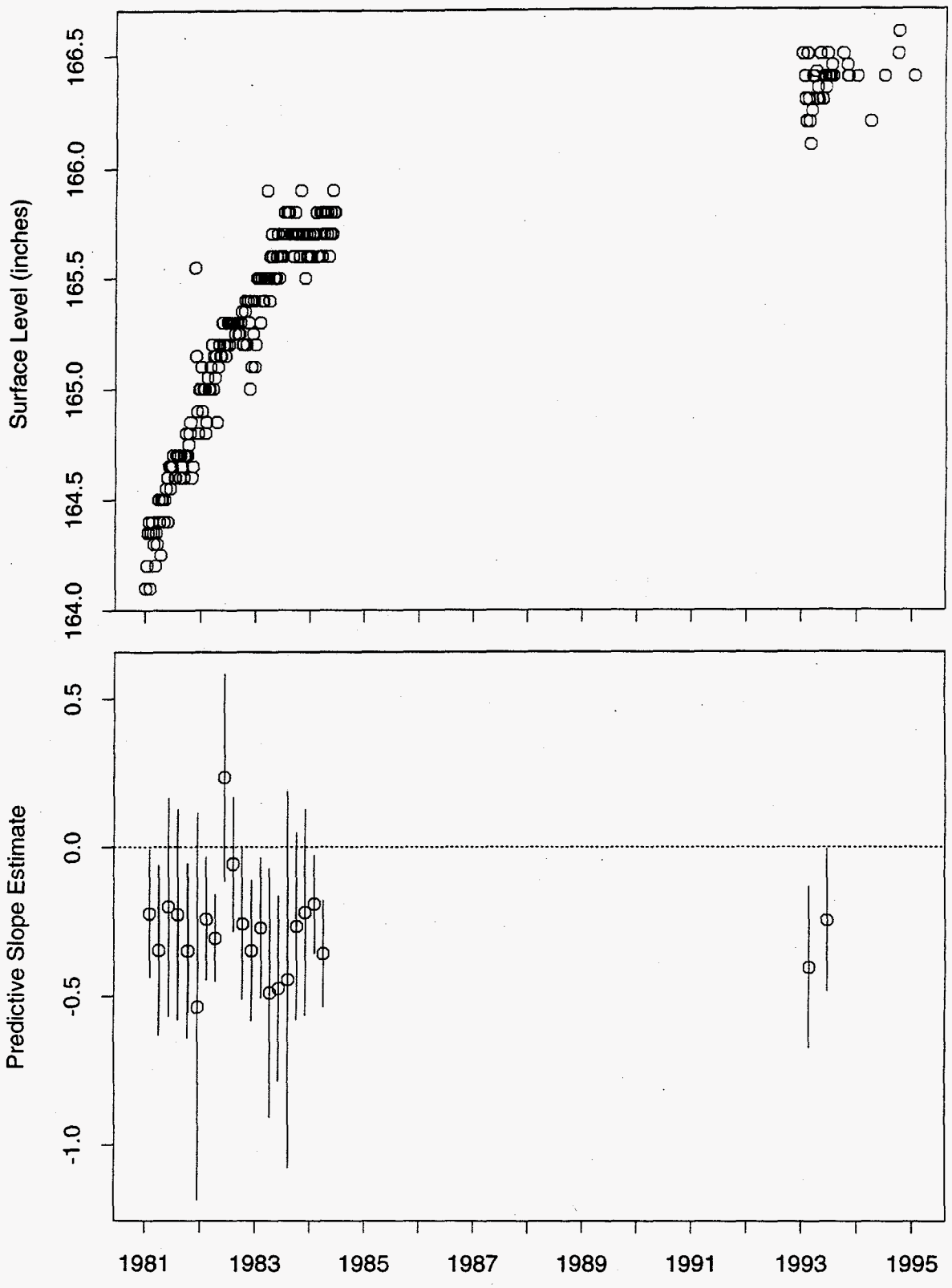

Figure 311: Tank U-108 FIC Data

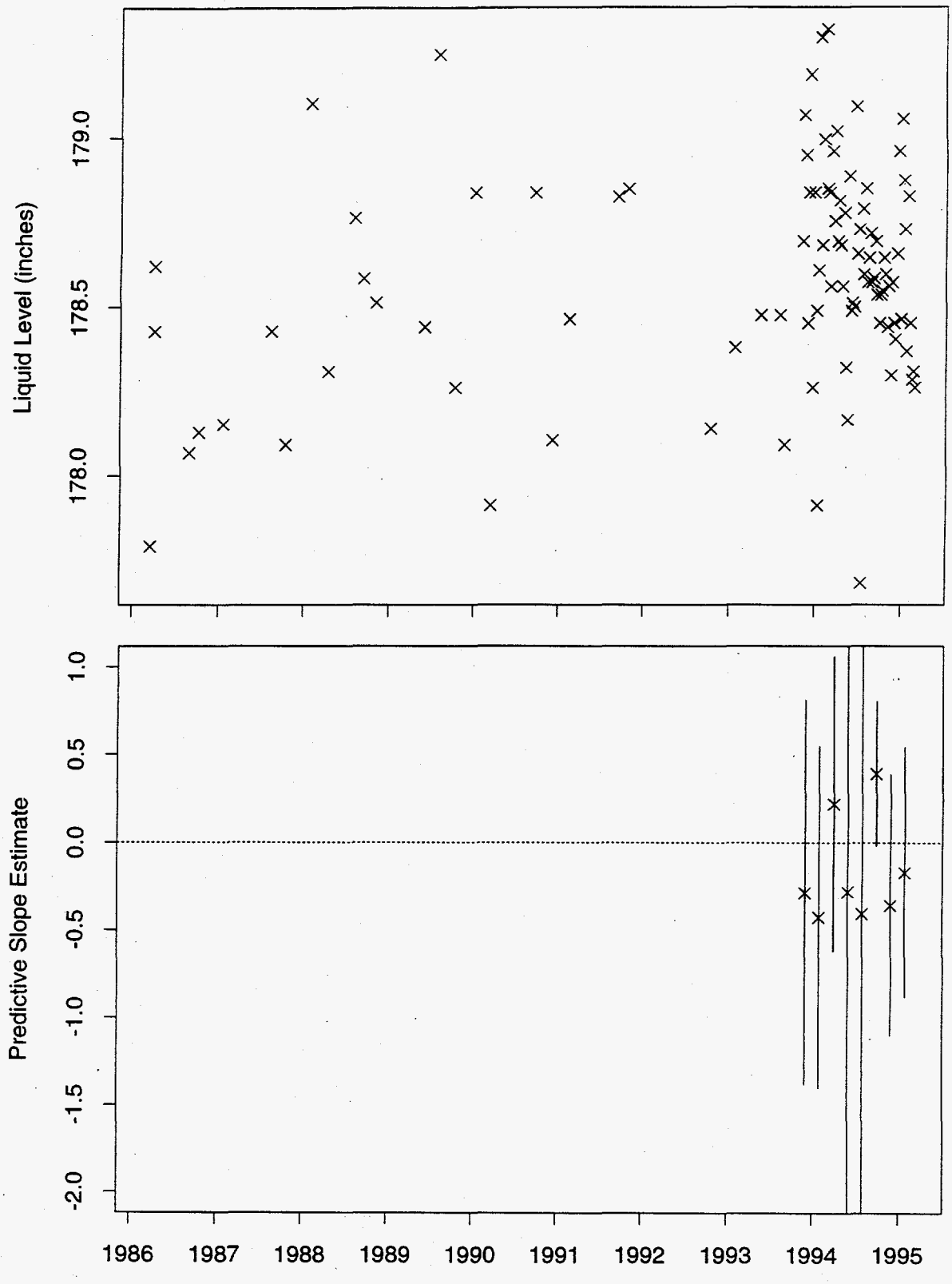

Figure 312: Tank U–108 Neutron ILL Data

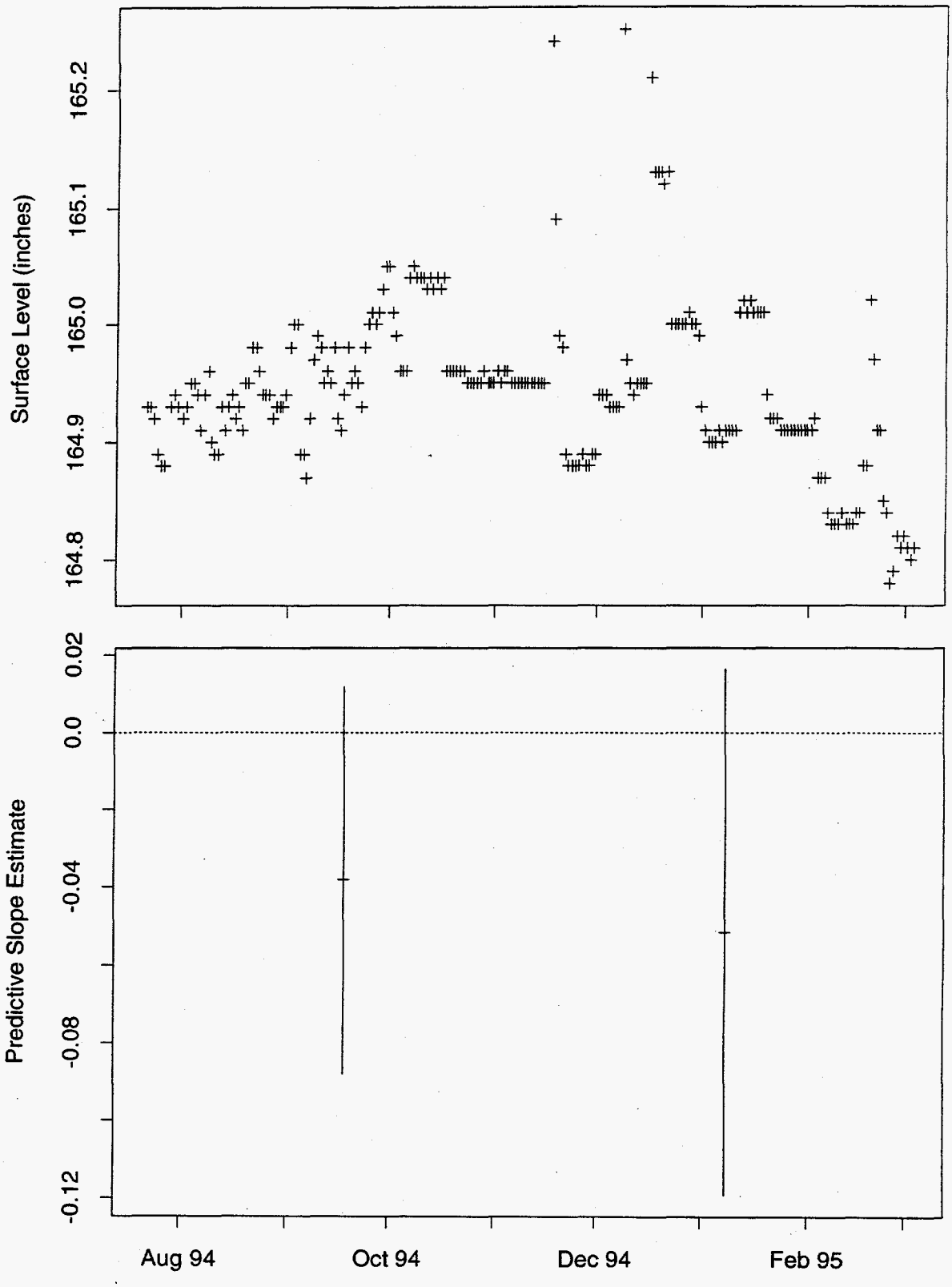

Figure 313: Tank U–109 ENRAF Data

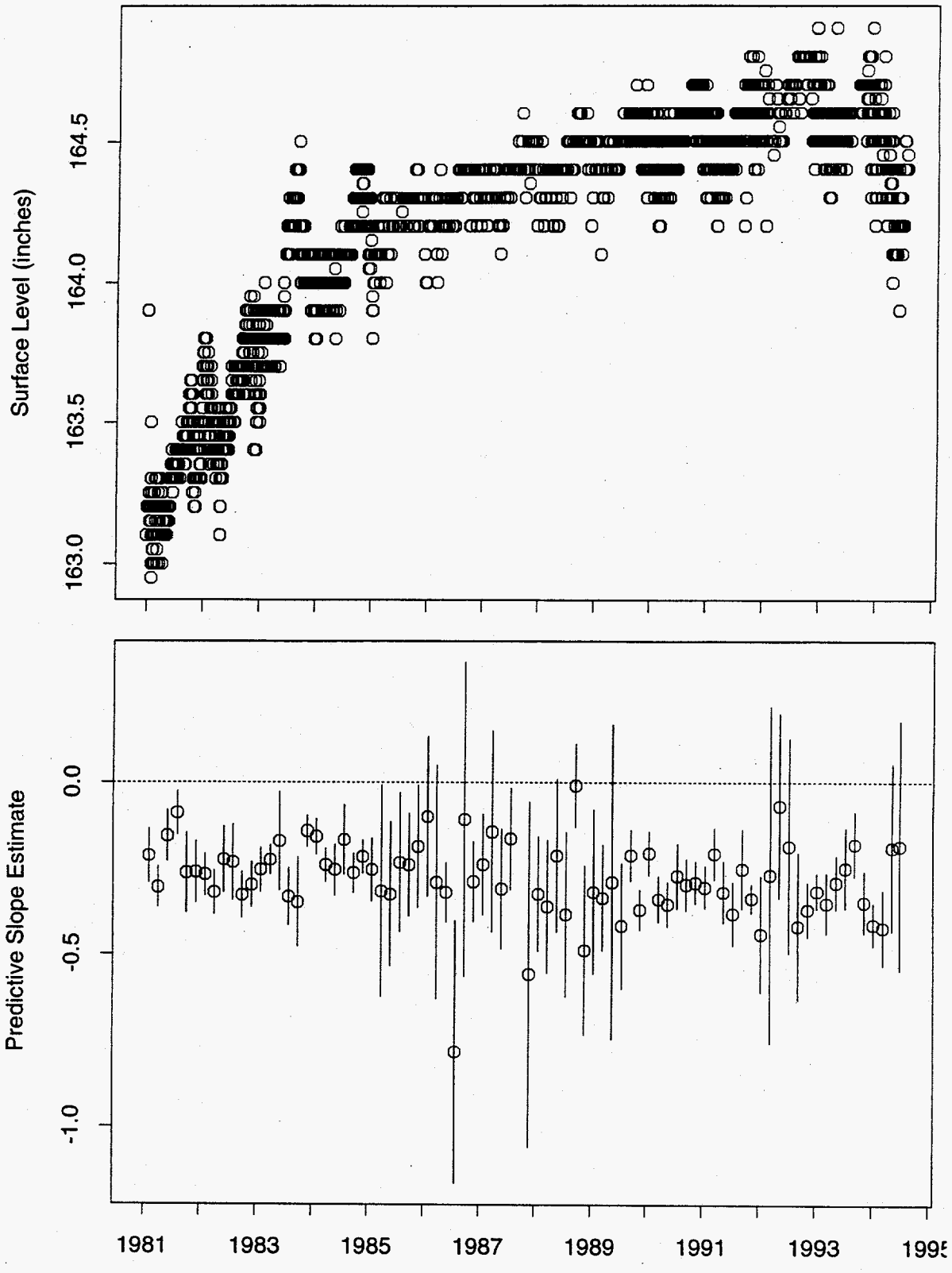

Figure 314: Tank U–109 FIC Data

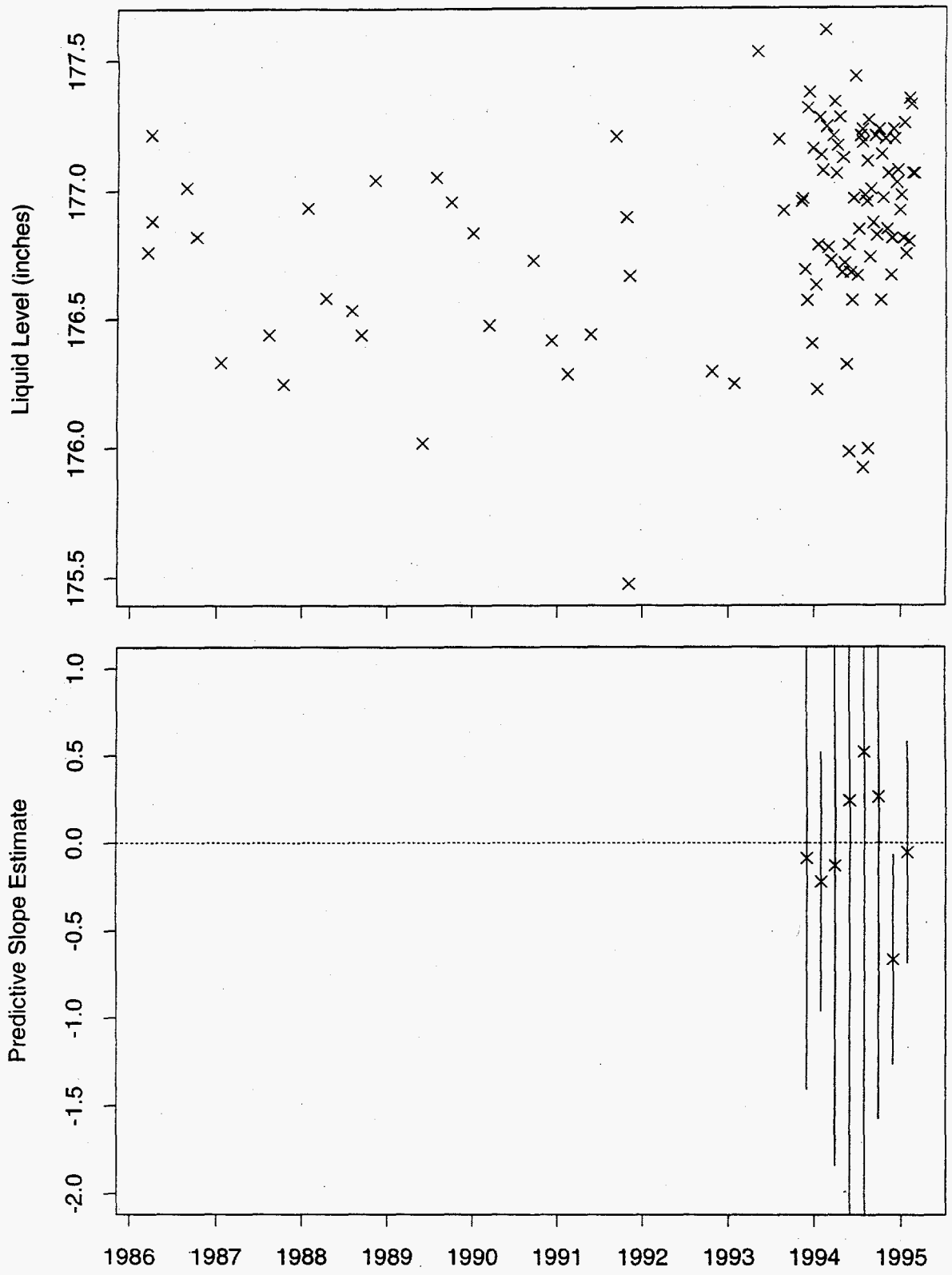

Figure 315: Tank U–109 Neutron ILL Data

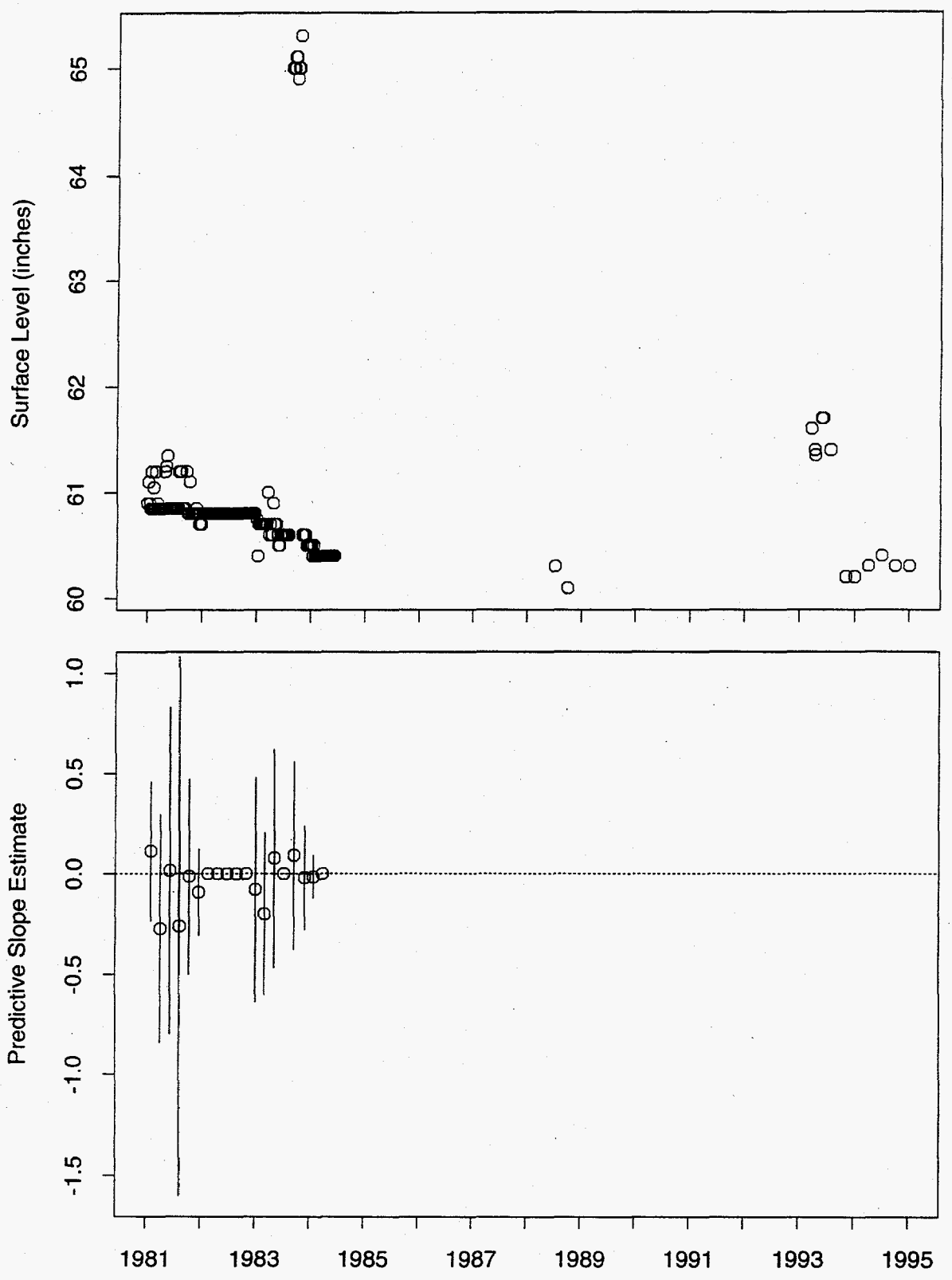

Figure 316: Tank U–110 FIC Data

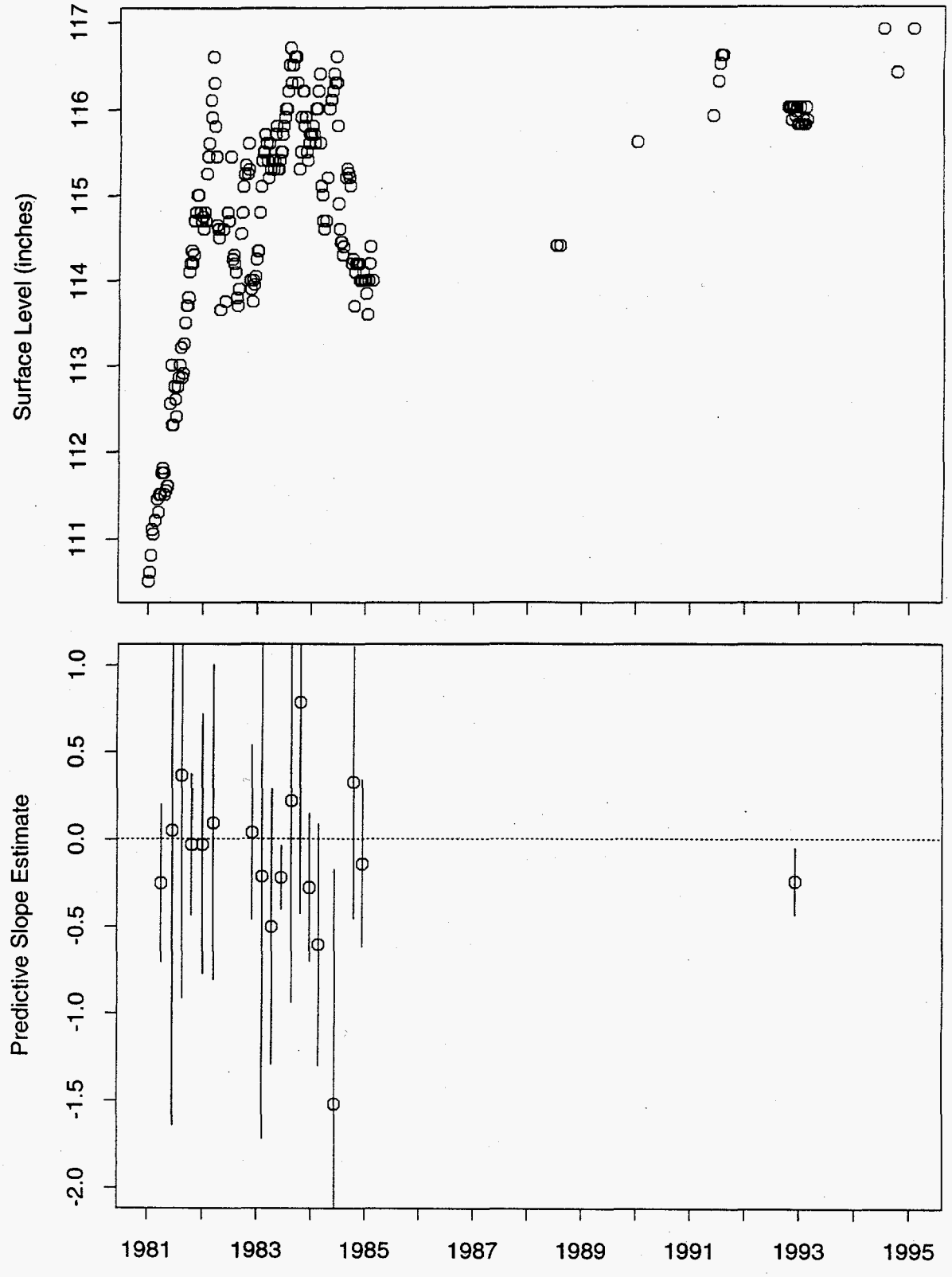

Figure 317: Tank U-111 FIC Data

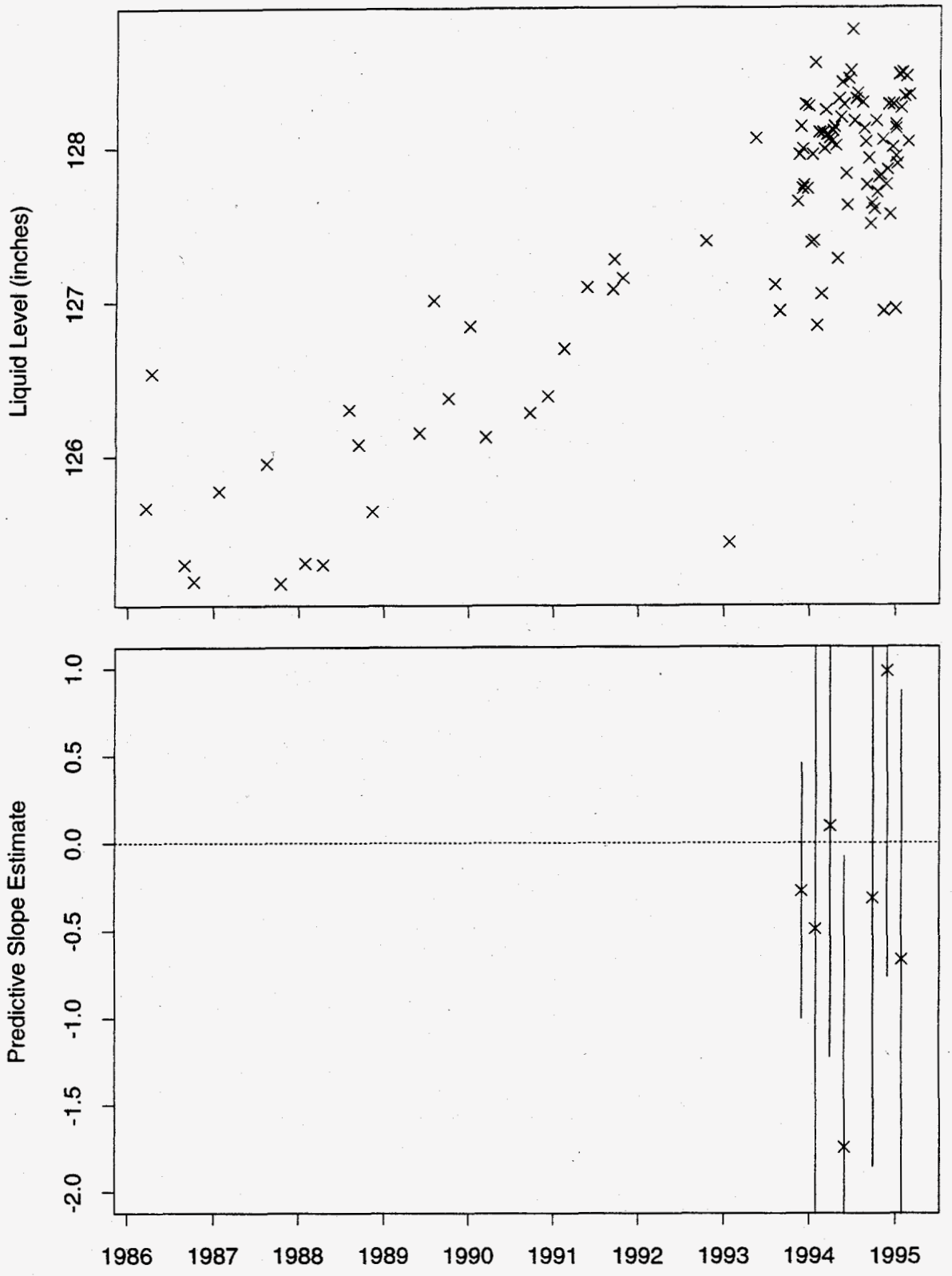

Figure 318: Tank U-111 Neutron ILL Data

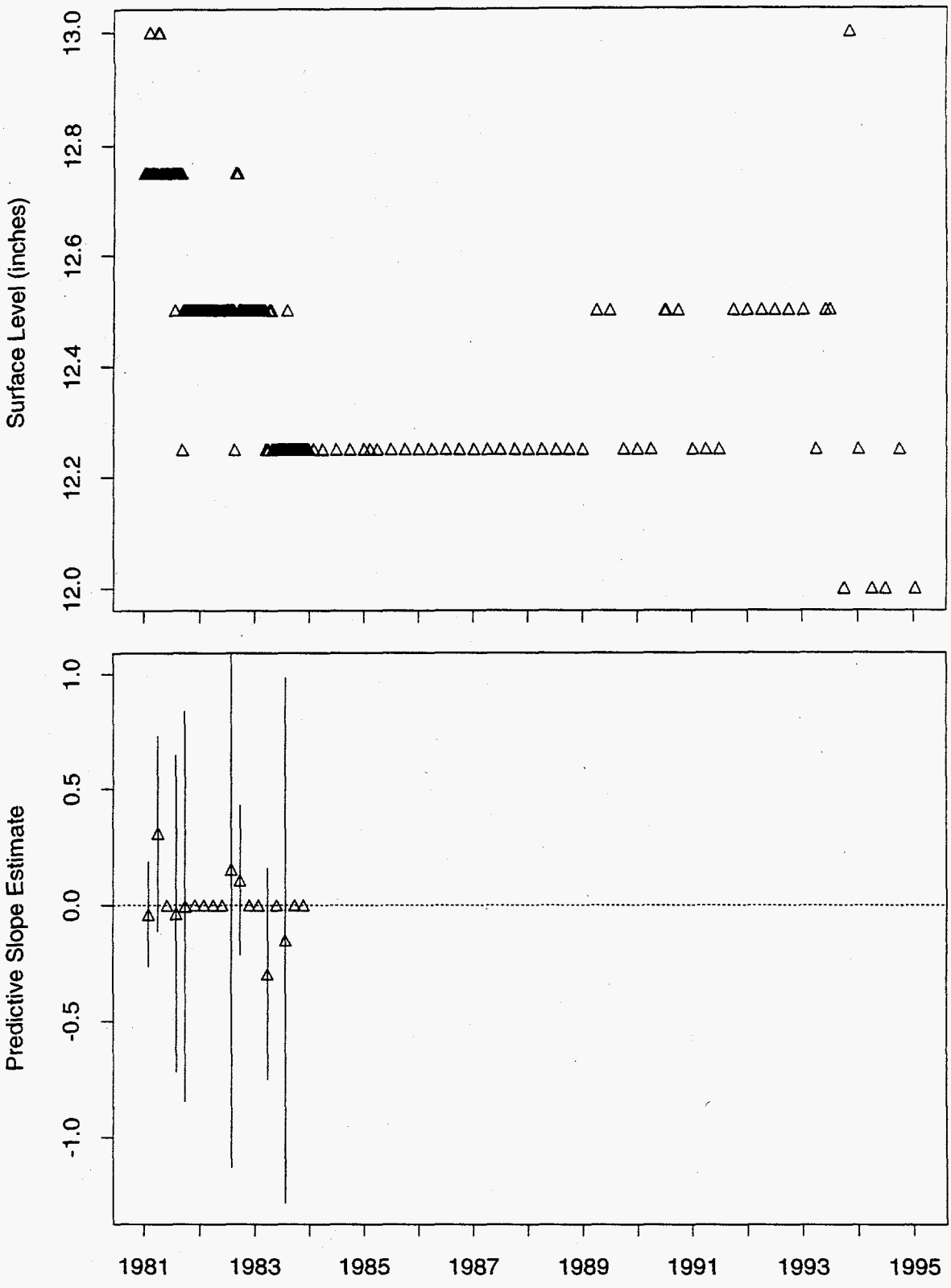

Figure 319: Tank U–112 MT Data

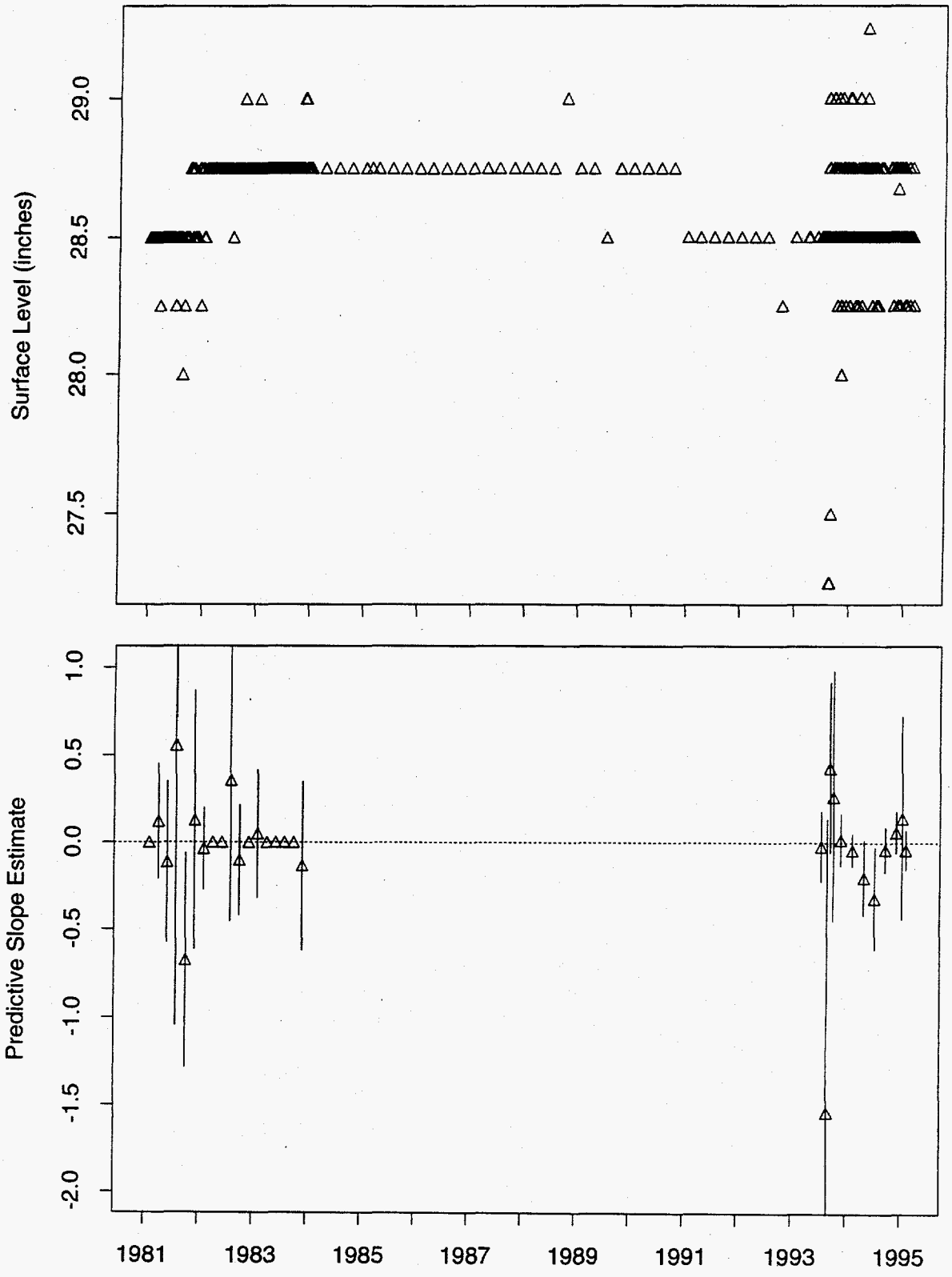

Figure 320: Tank U–201 MT Data

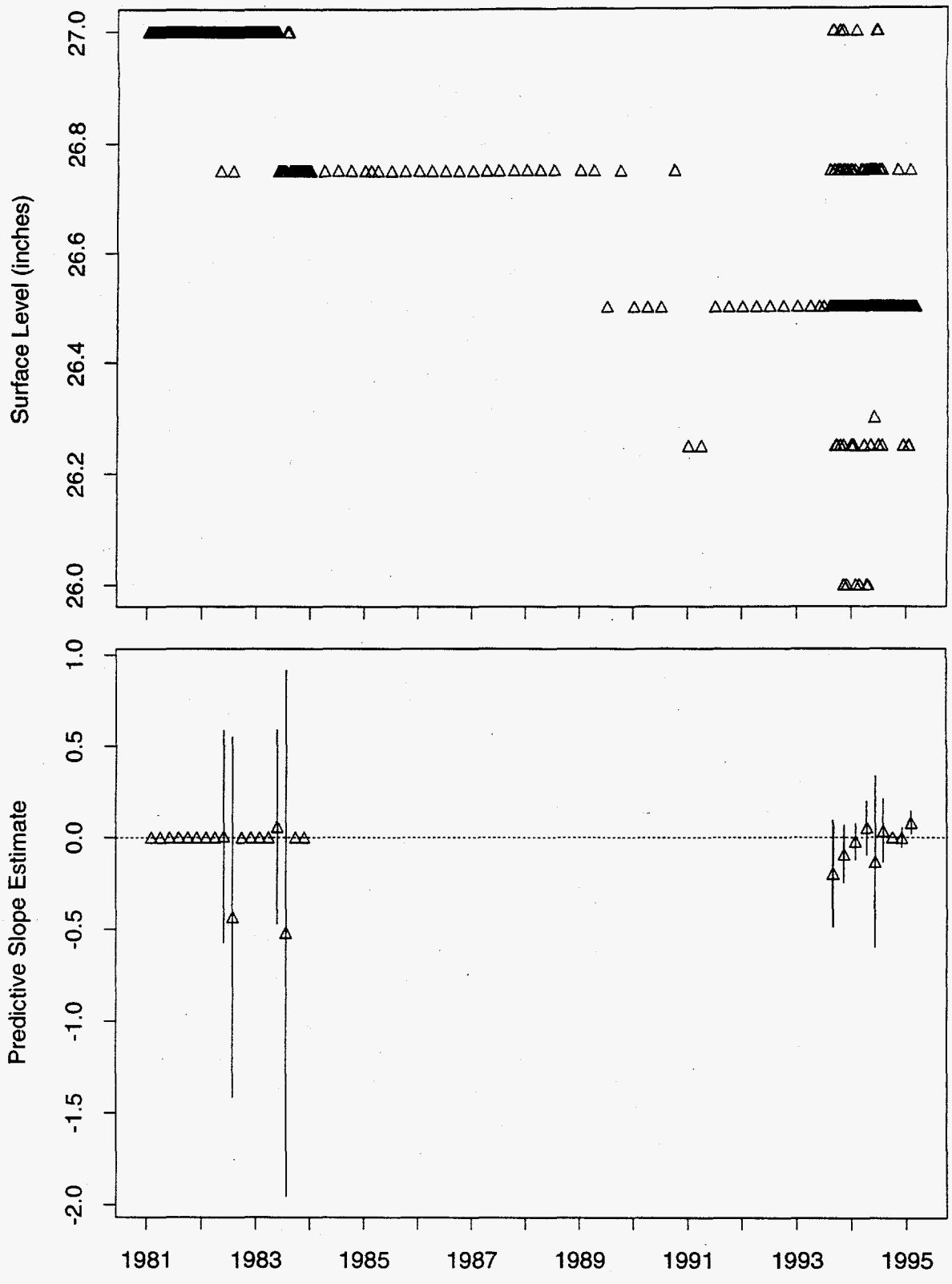

Figure 321: Tank U–202 MT Data

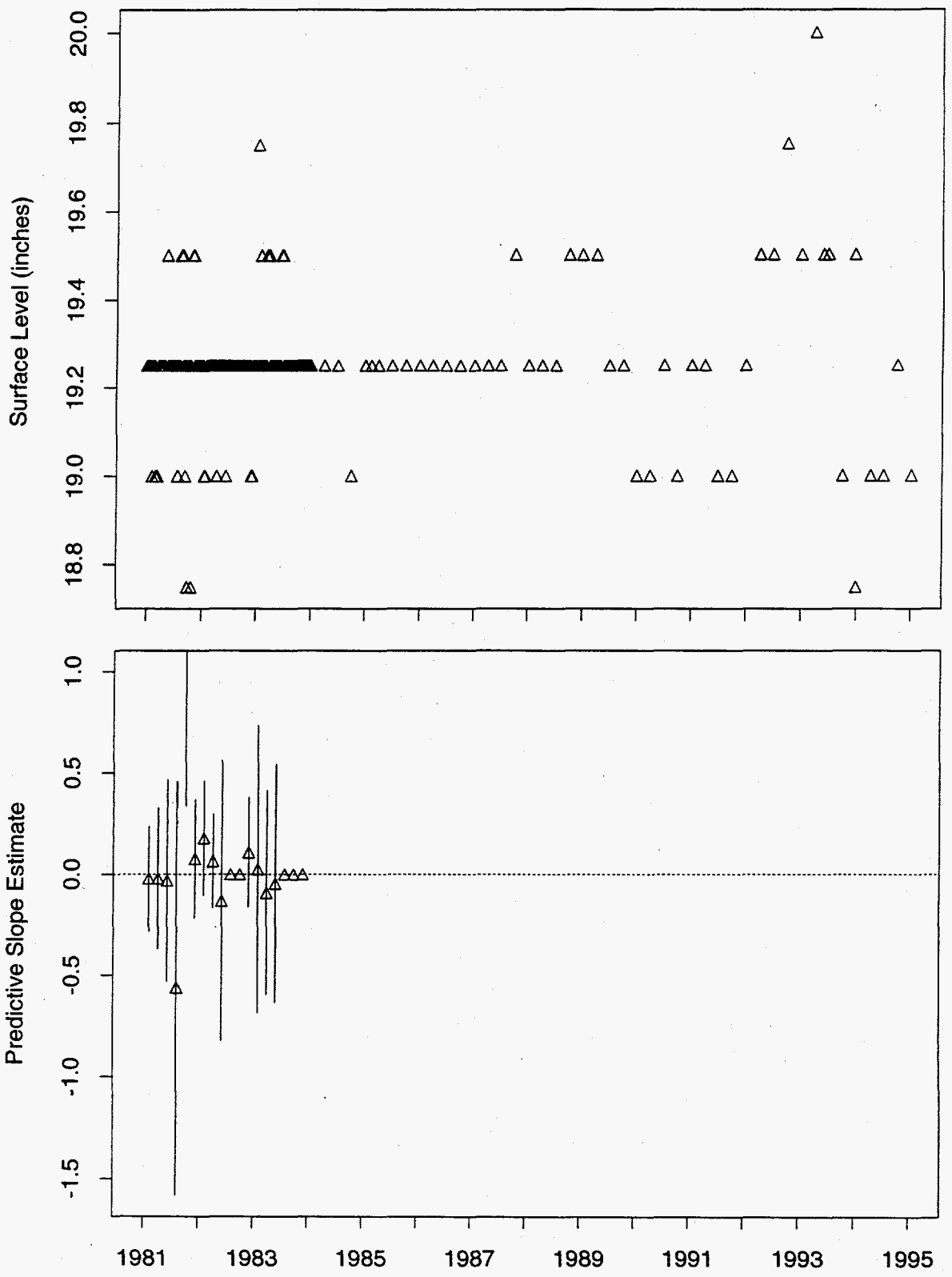

Figure 322: Tank U-203 MT Data

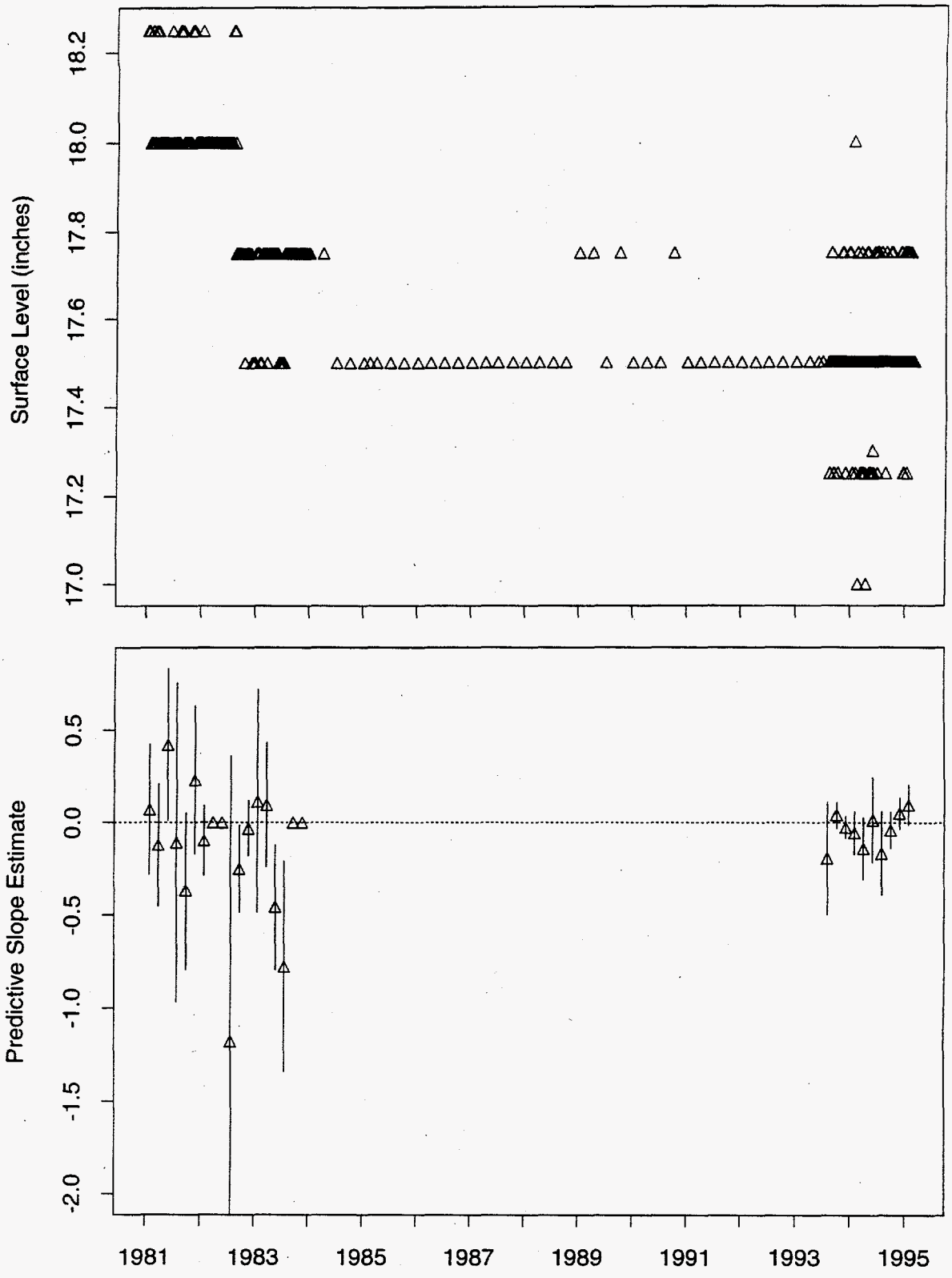

Figure 323: Tank U–204 MT Data

Distribution

No. of Copies

OFFSITE

3 Las Alamos National Laboratory
P.O. Box 1663
Las Alamos, NM 87545
Attn: W.L. Kubic/K575

ONSITE

6 **DOE Richland Operations Office**

R.E. Gerton	S7-54
J.M. Gray	S7-54
M.F. Jarvis	S7-54
G.Z. Morgan	S7-54
G.W. Rosenwald	S7-54
Reading Room	A1-65

33 **Westinghouse Hanford Company**

R.P. Anantatmula	R1-30
H. Babad	S7-30
S.A. Barker	R2-11
W.B. Barton	R2-11
R.J. Cash	S7-15
D.B. Engelman	R1-49
W.G. Farley	H4-65
K.D. Fowler	R2-11
R.L. Guthrie	H4-65
K.M. Hodgson	R2-11
J.D. Hopkins	R2-11
L. Jensen	R2-12
J.R. Jewett	T6-09
G.D. Johnson (5)	S7-15
N.W. Kirch	R2-11
J.A. Lechelt	R2-11
J.W. Lentsch	S7-15
R.M. Marusich	H5-65
N.G. McDuffie	S7-15
J.E. Meacham	S7-15
D.M. Ogden	H0-34
J.C. Person	T6-09
P.E. Peistrup	S7-14
T.E. Rainey	R2-54
R.E. Raymond	S7-12
D.A. Reynolds	R2-11
G.R. Sawtelle	H4-65
R.J. Van Vleet	H4-63
S.R. Wilmarth	R2-12

41 **Pacific Northwest Laboratory**

Z.I. Antoniak	K7-15
J.M. Bates	K7-15
J.W. Brothers (5)	K5-22
S.A. Bryan	P7-25
J.A. Campbell	P8-08
J.B. Colson	K5-10
P.A. Gauglitz	P7-41
R.J. Hall	K8-28
R.T. Hallen	P8-38
P.G. Heasler	K5-12
J.D. Hudson	K7-15
A.M. Liebetrau	K5-12
J.D. Norton	K2-44
L.R. Pederson	K2-44
B.A. Pulsipher	K5-12
F.M. Ryan	K7-70
G.F. Schiefelbein	P8-38
C.W. Stewart	K7-15
D.S. Trent	K7-15
H.H. Van Tuyl	P7-22
P.D. Whitney (10)	K5-12
Information Release Office(7)	K1-06